THE UNIVERSITY OF

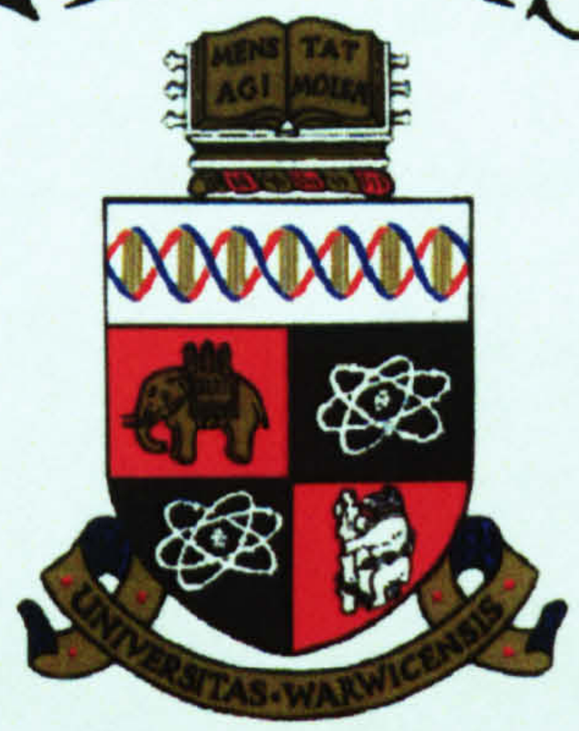

WARWICK

Testosterone as a delivery vector for platinum(II) metallodrugs

Martin Huxley

Submitted in partial fulfilment of the requirements for the degree of
Philosophiae Doctor

University of Warwick

Department of Chemistry
September 2006

PAGE

MISSING

IN

ORIGINAL

Table of Contents (Chapters)

Table of Contents (Detailed Contents)

List of Figures

List of Tables

Abstract

A total of 6 steroidal ligands have been synthesised from simple starting materials using Sonogashira coupling reactions. The ligands are based on testosterone substituted in the 17α-position with ethnynyl-pyridine, ethnynyl-quinoline or ethnynyl-isoquinoline. A range of platinum(II) complexes have been synthesised using these ligands of the type *trans*- and *cis*-$[Pt(NH_3)_2(L)(Cl][NO_3]$, where L is the steroidal ligand, alongside control complexes containing simple aromatic amines for comparison. The addition of the steroid imparted a substantional ability of the steroidal platinum(II) complexes to alter the structure of B-DNA. Furthermore, the steroid imparted cytotoxicity onto the complexes, which were very much more active that the steroidal ligand alone or platinum(II) complexes containing only an aromatic amine. Moreover, forcing the steroidal skeleton closer to DNA using 3-substituted pyridine rings and *cis*-geometries caused greater DNA unwinding, which is likely to relate to direct interactions between the DNA helix and the steroidal skeleton.

Abbreviations

5'-AMP	5'-adenosinemonophosphate
5'-CMP	5'-cytosinemonophosphate
5'-GMP	5'-guanosinemonophosphate
5'-TMP	5'-thyminemonophosphate
A	Adenosine
Amu	Atomic mass unit
AT	Adenine and thiamine DNA base pair
λ	Wavelength
ν	Frequency
C	Cytosine
CC-ET-3-Py	*cis*-[Pt(NH_3)(ET-3-Py)(Cl)][NO_3]
CC-ET-4-IQ	*cis*-[Pt(NH_3)(ET-4-IQ)(Cl)][NO_3]
CC-ET-6-Q	*cis*-[Pt(NH_3)(ET-6-Q)(Cl)][NO_3]
CD_2Cl_2	Deuterated dichloromethane
$CDCl_3$	Deuterated chloroform
CD_3OD	Deuterated methanol
CD_3CN	Deuterated acetonitrile
Cf.	Compare (latin)
COSY	Correlated spectroscopy
δ	Chemical shift (NMR spectra) measured in parts per million (ppm)
ct-DNA	Calf thymus DNA
DMSO	Dimethylsulfoxide
DMSO-d_6	Deuterated dimethylsulfoxide
DNA	Deoxyribonucleic acid
ε	Extinction coefficient
EB	Ethidium Bromide

ESI	Electrospray ionisation (mass spectrometry)
Et	Ethyl
ET-2-Py	17α-pyridin-2-ylethynyl-testosterone
ET-3-Py	17α-pyridin-3-ylethynyl-testosterone
ET-4-Py	17α-pyridin-4-ylethynyl-testosterone
ET-3-Q	17α-quinolin-3-ylethynyl-testosterone
ET-4-IQ	17α-isoquinolin-4-ylethynyl-testosterone
ET-6-Q	17α-quinolin-6-ylethynyl-testosterone
GC	Guanine and cytosine DNA base pair
HMQC	Heteronuclear multiple quantum coherence
IR	Infra red
w	weak
m	medium
s	strong
vs	Very strong
J	Coupling constant in NMR, measured in Hz
LD	Linear dichroism
MLCT	Metal to ligand charge transfer
Me	Methyl
M	mol dm^{-3}, mol L^{-1}
μM	micro molar, 10^{-6} M
mM	milli molar, 10^{-3} M
M/P	Descriptors for the rotation in helices
m/z	Mass over charge ratio (mass spectrometry)
NMR	Nuclear magnetic resonance
s	singlet
d	doublet
t	triplet

TC-ET-3-Py	*trans*-[Pt(NH_3)(ET-3-Py)(Cl)][NO_3]
TC-ET-4-Py	*trans*-[Pt(NH_3)(ET-4-Py)(Cl)][NO_3]
TC-ET-3-Q	*trans*-[Pt(NH_3)(ET-3-Q)(Cl)][NO_3]
TC-ET-6-Q	*trans*-[Pt(NH_3)(ET-6-Q)(Cl)][NO_3]
TC-ET-4-IQ	*trans*-[Pt(NH_3)(ET-4-IQ)(Cl)][NO_3]
Et_3N	Triethylamine
UV/Vis	Ultraviolet/visible

Declaration

The work presented in this thesis is original (except where otherwise stated). No portion of the work submitted in this thesis has been submitted in support of an application for another degree or qualification at this or any other University or institute of learning.

Acknowledgements

So many people to acknowledge! So we'll start with Mike Hannon and Alison Rodger and the entire cast of the Hannon and Rodger group members, past and present; I hear a roll-call…Dazza, Chris, Jessica, Laura, Jackie, Rosa, Phil, Matt, Martin and how could anyone forget Raul. Carmen Narrarro-Ranninger and Adoricion Gomez-Quiroga from UAM also deserve huge thanks. All those fabulous people including Guy Clarkson (X-Ray crystallography), John Bickerton (mass spectrometry) and Adam Clarke (NMR spectroscopy) deserve huge thanks too.

BLANK IN ORIGINAL

In memoriam Mary Huxley

1931-2005

BLANK IN ORIGINAL

Chapter One - Platinum(II) Metallodrugs

1.1. Prologue

The anticancer drug cisplatin is a DNA damaging agent based on the metal platinum; it is licenced for clinical use throughout the Western world and represents an important line of treatment in a number of cancers.[1] As a cure its only substantial success is treatment of germ-cell testicular cancer.[2] The mortality resulting from other cancers is merely delayed, whilst a large number of tumour types are insensitive to treatment regimes from the very beginning.[3]

One of many problems in the treatment regimes of cisplatin is a lack of tissue specificity; there is no differentiation between normal and malignant cells. The work contained in this thesis outlines an attempt to overcome this problem (and others). Chapter One introduces the concept of chemotherapy which may be defined as 'the use of chemicals for the treatment of cancer'. One of the most important chemotherapy drugs, cisplatin, is highlighted with emphasis on its discovery and ability to bind the DNA. The biological consequences of DNA binding and subsequent changes to cellular mechanisms are reviewed, together with biological consequences of new, post-cisplatin drugs based on platinum.

1.2. Introduction

Malignant disease is a major cause of human mortality across the world. Currently, malignant disease is responsible for 25 % of worldwide human mortality, equating to >150,000 deaths in the UK per year.[4, 5] Breast, colorectal, lung and prostate represent 50% of diagnosed cases, the remainder comprising over 200 different types of disease.[6-8] Current 5-year survival rates are 30% for men and 43% for women but variations between tumour types are well established. For example 5-year survival rates for testicular cancer are 95 %[2, 9, 10] but only 3 % for lung cancers.[4]

Chemotherapy began in the 1940's (selected agents are shown in Table 1.1) with the introduction of alkylating compounds such as melphalan and cyclophosphamide. Around the same time other groups of drugs, the antimetabolites and anti-tumour antibiotics found use in the clinic. Both groups of compounds interfere with the correct functioning of DNA via direct or indirect mechanisms involving physical interaction between the agent and

DNA. Later hormone treatments such as tamoxifen helped treat breast cancers but these do not act at a DNA level.

The platinum(II) complex cis-diamminedichloroplatinum(II) (cisplatin) was licenced in the early 1970s and possesses useful therapeutic valve in ovarian, head and neck and lung tumours[1]. It forms metal-ligand bonds to nitrogen containing bases on DNA as a pre-requisite for cytotoxicity. Further developments led to carboplatin, a less toxic complex with very similar results to cisplatin.

Table 1.1. Selected chemotherapy agents.

Class of chemotherapy	Mechanism of action	Examples[a]
Alkylating agents 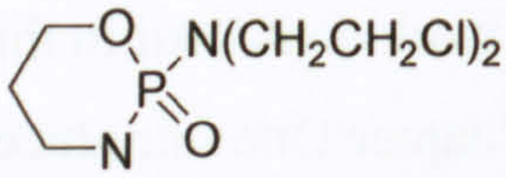 Cyclophosphamide	Covalently bind to DNA obstructing replication.	(a) Melphalan[11] (b) Cyclophosphamide[12, 13]
Antimetabolites 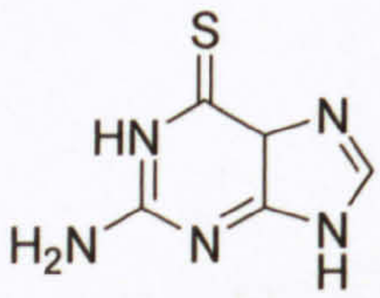 Thioguanine	(a) Impedes DNA synthesis by inhibiting or hampering thymidylate synthesis and becoming fraudulent nucleoside. (b) Interfering with thymidylate synthesis. (c) Used as a fraudulent nucleoside in DNA synthesis. (d) Acts as a fraudulent nucleoside.	(a) Flurouracil[14-17] (b) Methotrexate[18-21] (c) Thioguanine[18, 22-24] (d) Mercaptopurine[18, 22, 25, 26] 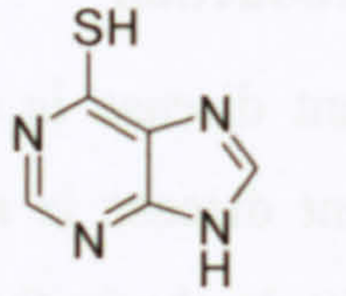 6-mercaptopurine
Antibiotics	(a) Causes break-up of DNA backbone via metal dependent oxidative cleavage of deoxyribose. (b) Acts as an alkylating agent.	(a) Bleomycin[27-32] (b) Mitomycin[28] (c) Dactinomycin (Actinomycin D)[33] (d) Doxorubicin[34, 35]

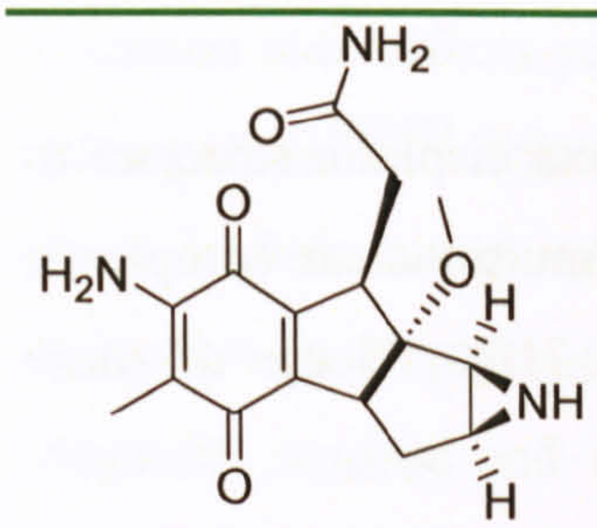

Mitomycin C

(c) Impedes DNA synthesis by interfering with the topoisomerase II pathway.

(d) Intercalates with DNA between guanine residues. Inhibits DNA transcription.

Hormone-based

(a) Interferes with the correct functioning of the androgen receptor.

(b) Selective estrogen receptor modulator (SERM) and blocks uptake of estrogen by the estrogen receptor.

(a) Anti-androgens and inhibitors[36-40]

(b) Tamoxifen[41-44]

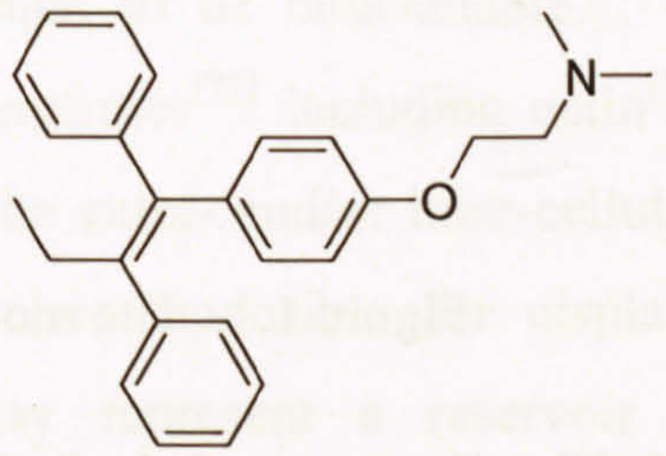

Tamoxifen

Platinum-based[1, 45-51]

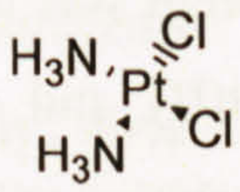

cisplatin

All form covalent bonds to DNA inhibiting cellular process involving DNA.

(a) Cisplatin

(b) Carboplatin

(c) Nedaplatin

(d) Oxaliplatin

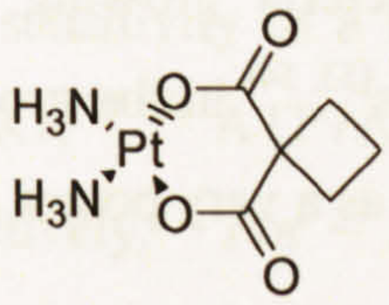

carboplatin

Platinum-based chemotherapeutics have moved beyond the classical cisplatin structure to encompass new ligands: 1,2-diaminocyclohexane in oxaliplatin, multinuclear complexes (e.g., BBR3464) and orally active Pt(IV) complexes (e.g., JM-216). Some of these structures are shown in Figure 1.1 and will be discussed later.

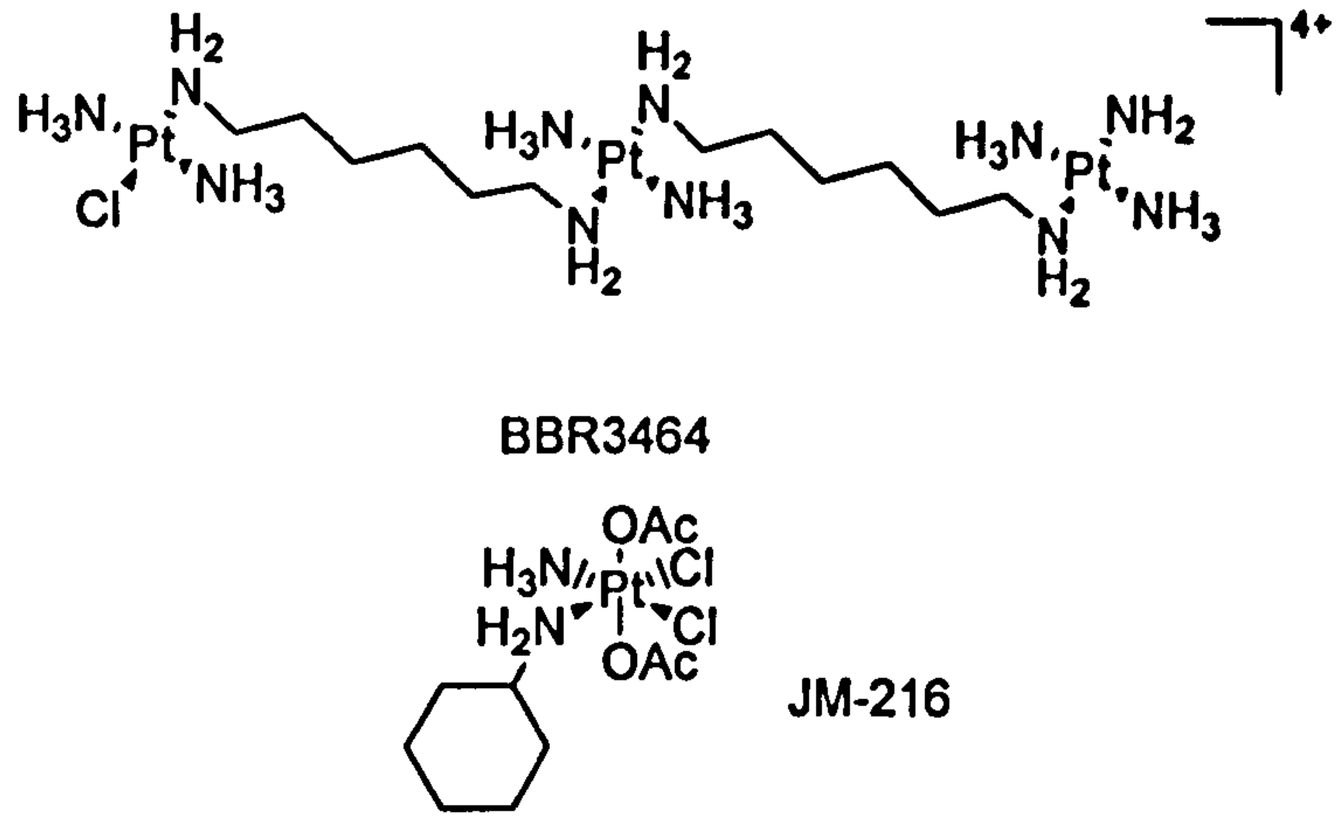

Figure 1.1. The molecular structures of selected chemotherapy agents.

1.3. The discovery of cisplatin

The first recorded synthesis of cisplatin by Peyrone in 1844 led to cis-diamminedichloroplatinum(II) being known as Peryone's Chloride[52] and its biological activity was discovered in 1965. It was observed that cell division of Escherichia coli (E. coli) was inhibited and filamentous growth occurred when an electric current was applied across bacteria growing in culture[53] caused by the formation of Pt(II) and Pt(IV) complexes[53, 54] in the growth media (Figure 1.2). Cis-diamminedichloroplatinum(II) was identified as a very potent antitumour agent whilst the trans isomer was not.[55]

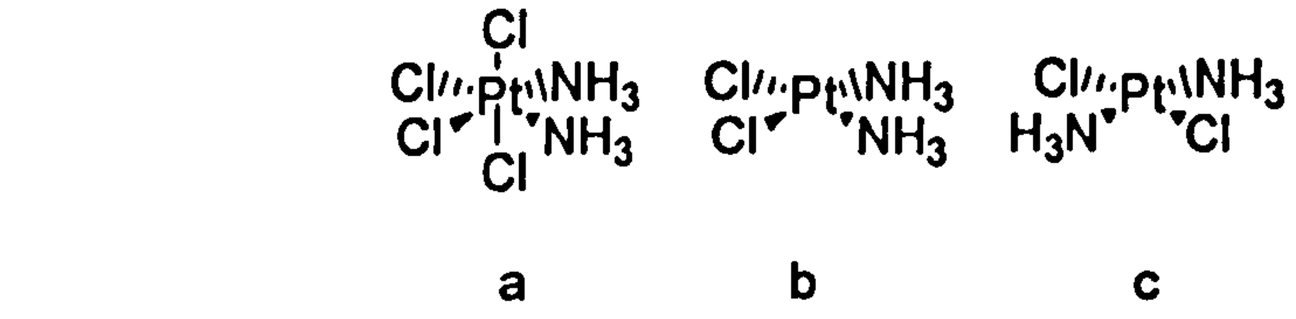

Figure 1.2. Molecular structures of platinum complexes discovered by Rosenberg *et al.*[53]
a) trans-diamminetetrachloro(IV); b) cis-diamminetetrachloroplatinum(II); c) trans-diamminedichloroplatinum(II).

The initial trials of cisplatin were almost abandoned due to kidney toxicity (nephrotoxicity)[56-58], later treated with pre-hydration therapy[59] and diuretics.[60] Other

common side effects relate to hearing damage (ototoxicity),[61] nerve damage (peripheral neuropathy),[62-68] hypomagnesemia[69] and hypocalcemia[70] and procedures to aliviate these include using sulphur containing dithiocarbamates[71] to reduce cytotoxicity by a reduction in cisplatin-protein binding levels. In addition to side-effects, resistance to cisplatin, aquired and intrinsic, is a major obstacle to the clinical efficacy of cisplatin. Tumours are, or become resistant to cisplatin (and often to a wide range of chemotherapy). Patients initially respond to treatment but the majority of tumours progress to a refractory state.

1.4. The biological targets of cisplatin

Intravenous administration of cisplatin prevents substantial levels of hydrolysis due to chloride concentration (approx. 100 mM). In the blood, cisplatin binds to plasma proteins,[72-74] some allowing a small proportion of platinum to be bioavailable.[75, 76] Cisplatin binds to many other biological targets such as enzymes[77] including actin[78], proteinases[79] and also albumin,[79, 80] some of which may be extra- and/or inter-cellular. Binding to sulphur containing molecules is believed to be responsible for cisplatin deactivation[81] although sulphur-platinum conjugates may represent a reservoir of platinum for future reactions.[82-85]

Passage through cell membrane enables cisplatin to interact with lipids and interspersed proteins,[86, 87] however uptake is linear and not saturable up to millimolar concentrations,[88-92] a result suggesting passive diffusion into cells. However, very recently, three copper transporters were found to regulate the sensitivity of a number of cell lines to cisplatin and similar analogue. The proteins CTR1,[93-96] ATP7A[97, 98] and ATP7B[98-103] regulate uptake, accumulation and efflux, respectively. For ~ 30 years a diffusion mechanism has been accepted as likely and it now appears both passive and active transport of platinum(II) drugs can occur across cell membranes.

Once inside the cell, the widely accepted view is that hydrolysis products of cisplatin, caused by low intracellular chloride concentration (3 - 30 mM), bind preferentially to DNA. This viewpoint is backed up by a large range of studies finding:-

1. DNA damaging agents such as UV radiation produce the same effects (*e.g.* cell death) as cisplatin in bacteria and are known inhibitors of DNA synthesis.[104]
2. More platinum is bound to DNA, per mole, than RNA and proteins in cells treated with cisplatin.[105]

3. DNA synthesis is selectively inhibited compared to the synthesis of RNA and proteins[106, 107] and the trans-isomer does not have this effect.[107]
4. Cultured cells deficient in DNA repair mechanisms exhibit greater sensitivity to cisplatin compared to the wild type in eukaryotic[108-111] and prokaryotic[112-119] cells. Such correlations are not found with transplatin[113-115, 118] or [Pt(dien)Cl]Cl.[114]

1.4.1. Cisplatin-DNA adducts

The complex structures that DNA can adopt are discussed in depth in Chapter 4. However to understand binding of cisplatin and analogues it is necessary first to appreciate the structure of B-DNA. DNA possesses a rich source of sites for binding metals ions and/or complexes.[120-122] Briefly it consists of two strands consisting of alternating substituted versions of the 4 nucleobases, guanine (G), adenine (A), cytosine (C) and thymine (T), shown in Figure 1.3, joined together with a sugar ring-phosphate backbone. Between each base is a sugar ring and a phosphate group as shown in Figure 1.4. Each base is capable of hydrogen bonding to another (G bonds to C and A bonds to T).

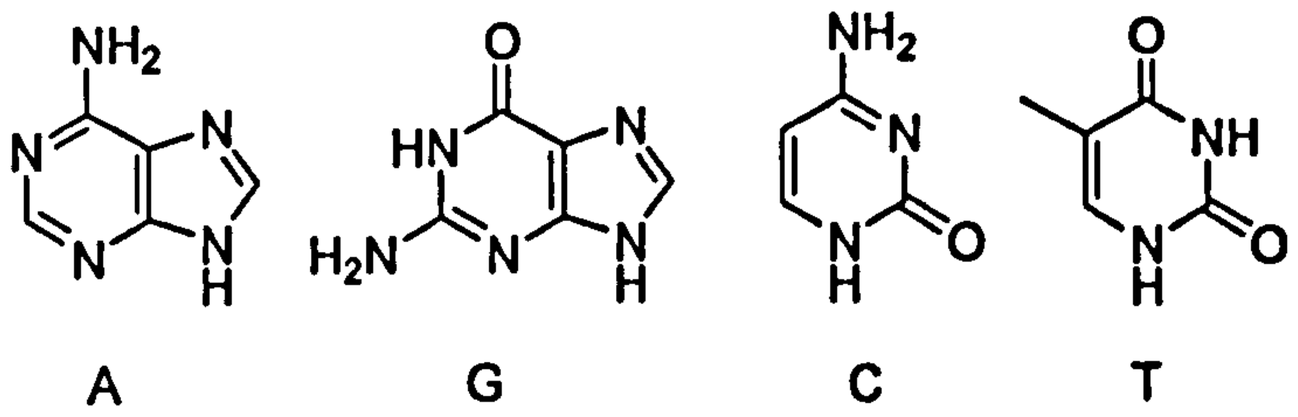

Figure 1.3. The 4 nucleobases of DNA.

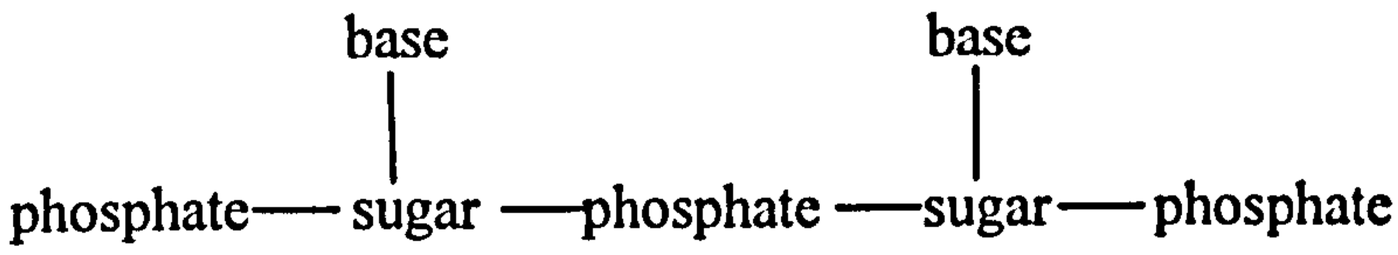

Figure 1.4. The bonding arrangement between sugar, phosphate and nucleobase moieties in a single strand of DNA.

Hydrogen bonding between the bases on strand 1 and strand 2 bind the two strands together. This bonding arrangement forms a helix and the bases stack one above the other in the helical structure, shown in Figure 1.5.

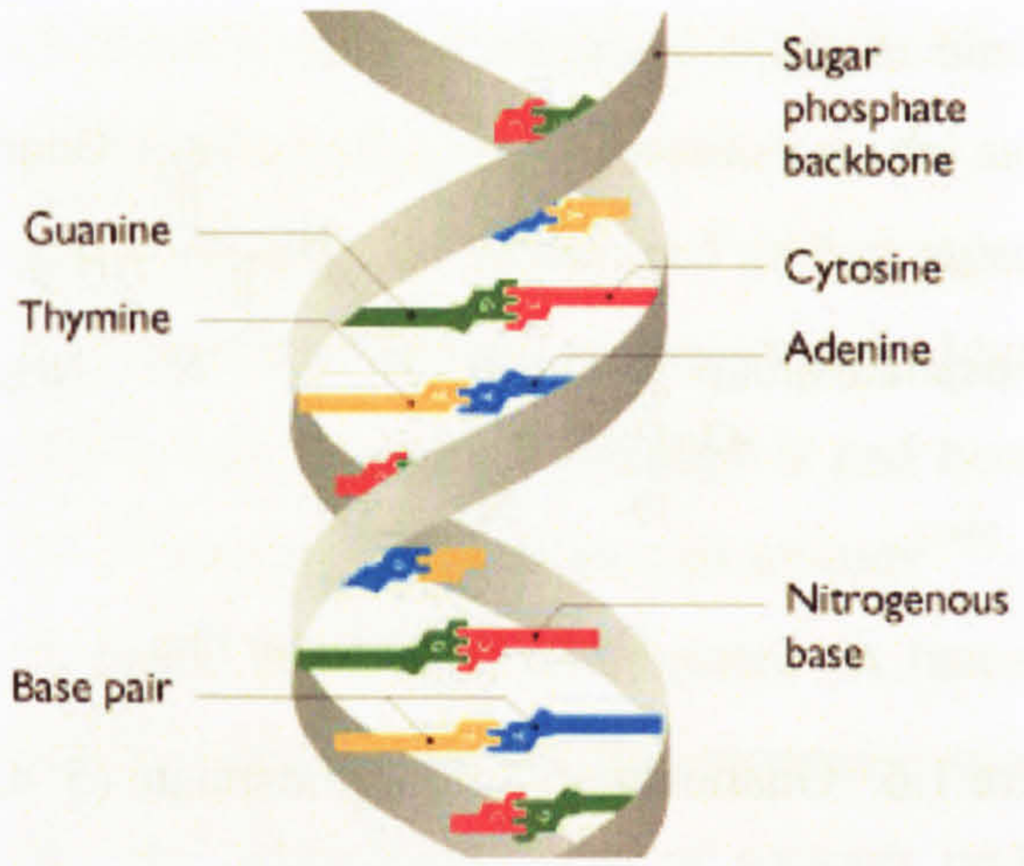

Figure 1.5. The structure of DNA showing the helix and base pair stacking.

Ultraviolet spectrophotometry studies suggest an interaction between nucleobases and cisplatin rather than the phosphate backbone.[123] Furthermore, interaction is specific to DNA rich in GC pairs,[116, 124-126] or areas containing tracts of (dG)n.[127-130] It is known the N7 atom of G is often the site of attack by alkylating agents to which cisplatin is often compared.[131]

The nomenclature used to represent DNA in the following sections is exemplified by the DNA sequence d(GpApTpC). The letter d denotes deoxyribose, the sugar ring between phosphate groups that the nucleobases are covalently bonded too. It is used in front of the sequence to remove the necessity to continuously quote dB, where B represents a nucleobase. The p represents the phosphate group linking sugar-base groups together. Thus d(GpApTpC) is a shorthand for dGpdApdTpdC which is a short length of DNA with the bases in order GATC linked by phosphor-deoxyribose groups. When platinum is bound to a length of DNA the site of binding is indicated by a letter and superscript number in parentheses after the base, i.e. N7. Thus cis-$[Pt(NH3)_2\{d(ATG(N7)pG(N7)pTpC\}]$ represents a platinum atom with two cis ammonia groups bound to 2 adjacent guanines using the N7 atoms in the sequence d(ApTpGpGpTpC).

It is now known that 90% of platinum atoms bound to DNA do so by forming metal-ligand bonds to adjacent N7 atoms of guanine and / or adenine residues on the same strand of DNA.[132, 133] Before the binding site of cisplatin was established studies found cisplatin or $[Pt(en)_2Cl_2]$ bound to G, C, A in model nucleobases such as 5'-GMP (Figure 1.6). In the case of thymine, often little or no binding was observed,[126, 134-137] indicating thymine is substantially un-reactive towards cisplatin.

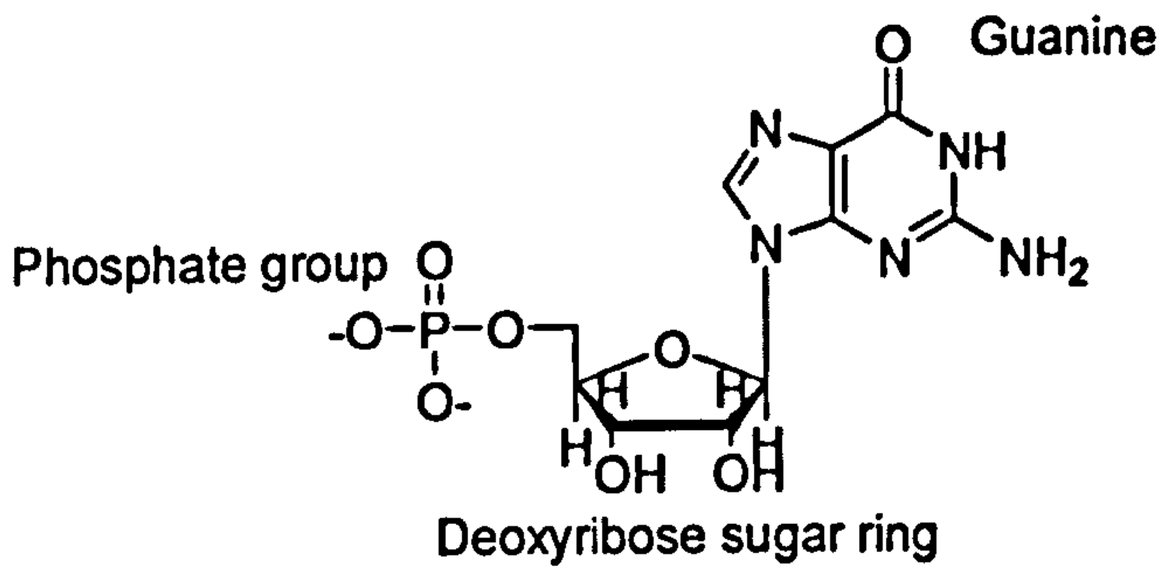

Figure 1.6. Guanosine-5'-monophosphate (5'-GMP)

Studies found Pt(II) binding sites to be the N^7 atom of G[135, 138-141], the N^1 atom and N^7 atom of A[135, 136, 139] and the N^3 atom of C[135, 137, 139] and bi-functional adducts of the type cis-$[Pt(NH_3)_2\{G(N^7)G(N^7)\}]$, cis-$[Pt(NH_3)_2\{A(N^7)A(N^7)\}]$, cis-$[Pt(NH_3)_2\{G(N^7)A(N^7)\}]$ and cis-$[Pt(NH_3)_2\{G(N^7)A(N^1)\}]$ are reportedly formed.[139] Interestingly no bi-functional adducts with C are formed even when cytidine was attached to a G moiety to which Pt(II) was bound [142] and no adducts of the type cis-$[Pt(NH_3)_2\{A(N^1)A(N^1)\}]$ are observed.

From the early 1980's research turned to determining the actual adducts formed on DNA. Identification and characterisation of cisplatin-DNA and transplatin-DNA adducts was successfully carried out using enzyme digests of platinated DNA followed by chromatographic separation.[132, 133, 143-145] The major cisplatin-DNA adducts (totalling 85 % - 90 % of all adducts) were those bonded to the N^7 atoms of adjacent guanine and adenine residues on the same strand of DNA.[132, 133] These adducts, cis-$[Pt(NH_3)_2\{d(GpG)\}]$ (cis-GG) comprising 60 - 65% of all adducts and cis-$[Pt(NH_3)_2\{d(ApG)\}]$ (cis-AG) which formed approximately 20 % are labelled 1,2-intrastrand adducts. Only the cis-AG adduct is formed and no cis-GA, a fact which may be explained by geometry.[146] The abundance of the cis-$[Pt(NH_3)_2\{d(GpG)\}]$ indicates a preference in cis-GG adduct formation. Additional work using tritium (^3H) labelled cisplatin and $Pt(en)Cl_2$ (Figure 1.7) confirmed the previous results[143] that both complexes form the same adducts.

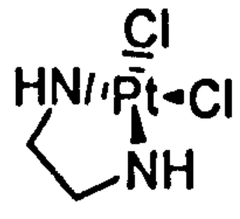

Figure 1.7. The molecular structure of $Pt(en)Cl_2$

Two other adducts were identified; mono-functional cisplatin binding to guanine and cis-$[Pt(NH_3)_2\{d(GMP)_2\}]$, resulting from linking of guanines on the same strand and separated by at least one nucleobase. The latter 1,3-intrastrand adduct represents around 6% of the total number of adducts.[145] A further adduct, an interstrand adduct, formed by binding to G residues on opposing DNA was identified, although it had been discovered previously using DNA[105, 123, 143, 147, 148] and in mammalian cell culture[149] and forms ~ 1 % of all adducts. A very similar range of adducts is reported in hamster ovary cells,[150] the leukaemia cell line L1210[151] (using antibodies that recognise specific adducts)[152] and in isolated DNA, cell culture and white blood cells of patients undergoing treatment for a range of tumours with cisplatin.[153-157] It is noteworthy that adducts formed on native DNA *in vitro* and extracted from patients *in vivo* are comparable. Finally, small proportions of intermolecular adducts are observed including glutathione-Pt-DNA[81] and protein-Pt-DNA[158, 159] cross-links. The structure of the reduced form of glutathione is shown in Figure 1.8. Glutathione is a common molecule present within cells.

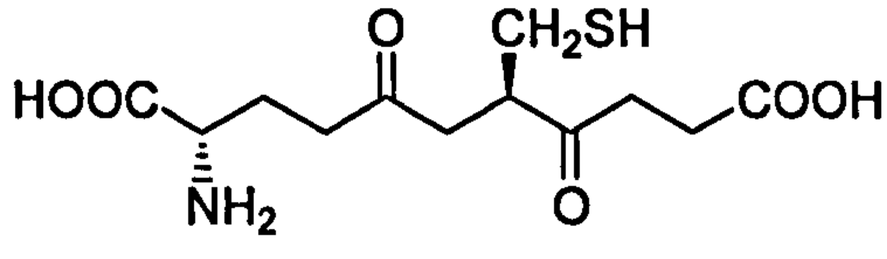

Glutathione (reduced form)

Figure 1.8. The molecular structure of the reduced form of glutathione.

A summary of adducts found on DNA caused by cisplatin are shown in Figure 1.9.

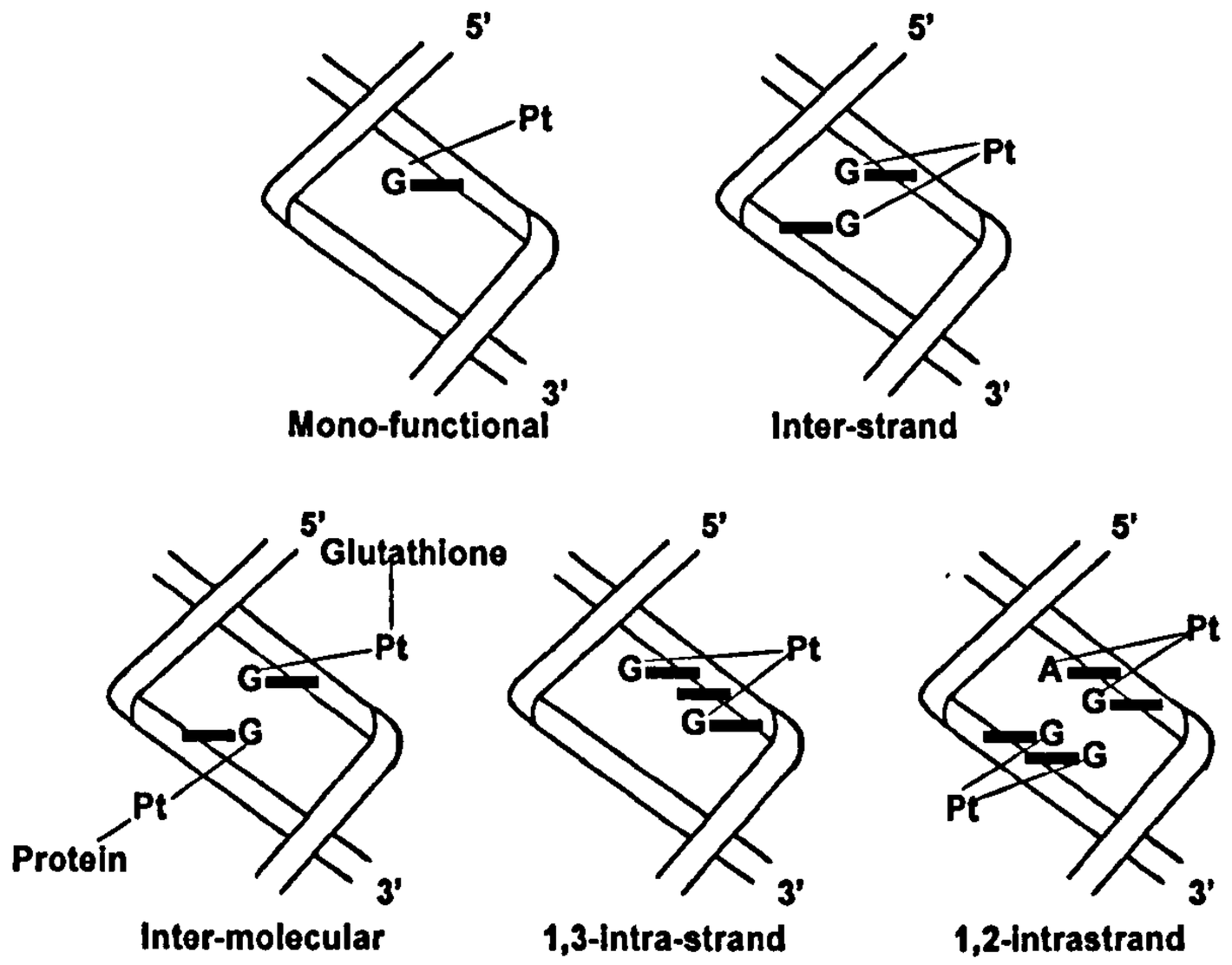

Figure 1.9. The type of adducts formed when cisplatin is bound to DNA.

1.4.2. The effect of cisplatin adducts on DNA structure

There are many parameters that are used to describe DNA structure. Three of these parameters relevant to the effect of Pt(II) complexes on DNA are unwinding, bending and melting. In B-DNA there are 10 base pairs per 1 turn of the helix, giving a helical twist of 36° and DNA unwinding may be defined as the degree to which the helical twist has changed from 36°. DNA bending is the angle produced when the helical axis is bent at a given point. DNA melting is the temperature at which enough interstrand hydrogen bonds have been broken so that DNA exists as single stranded and doubled stranded in a 50:50 ratio.

Some early crystal structures contained a cis-$[Pt(NH_3)_2]^{2+}$ moiety linked to the small fragments d(pGpG),[160, 161] as shown in Figure 1.10. Each structure shows evidence of large distortions to the bases away from the structure they occupy in free DNA including a complete disruption of base stacking.

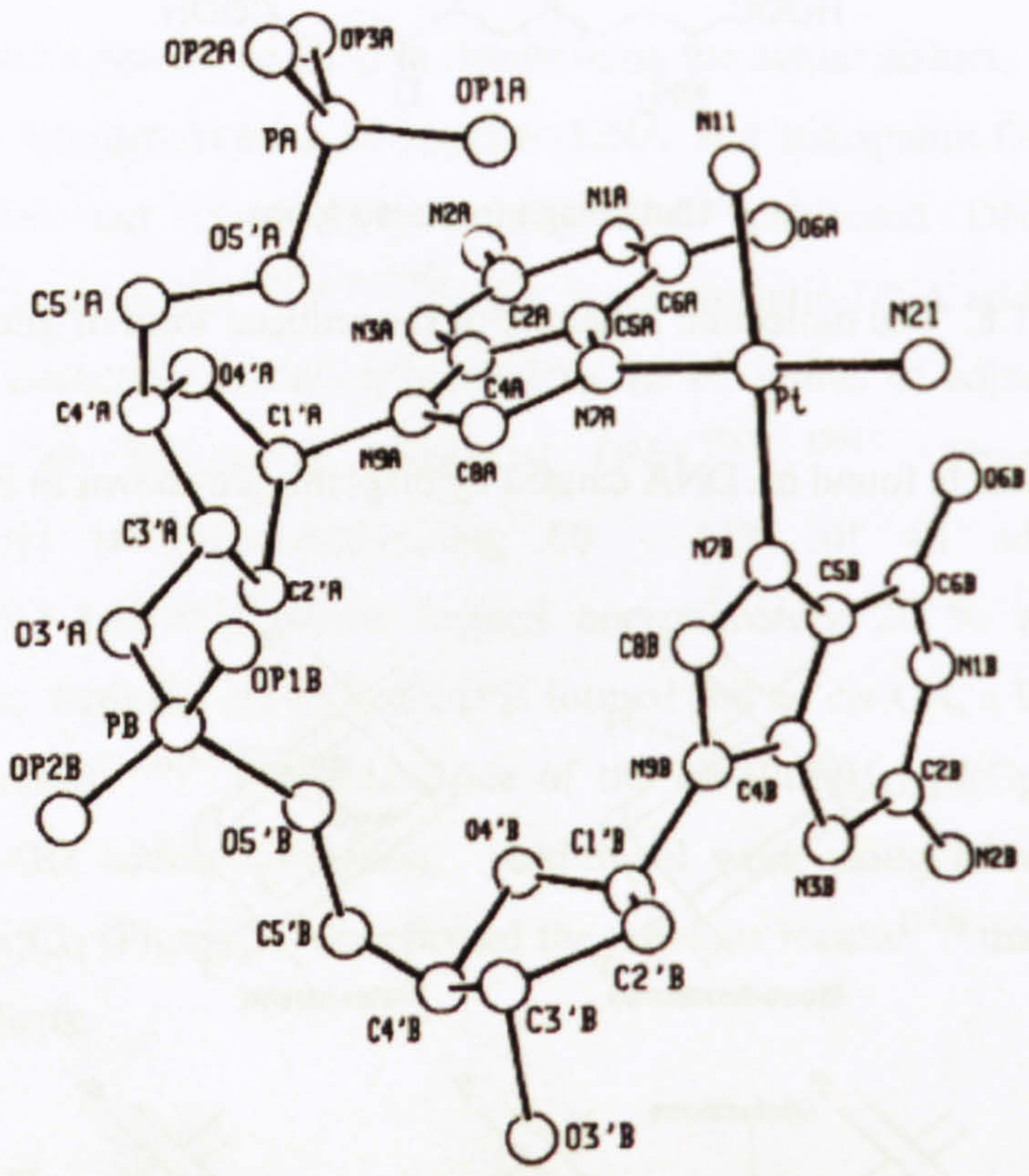

Figure 1.10. The crystal structure of a cis-$[Pt(NH_3)_2\{d(pGpG)\}]$[160]

The effect of the cis-GG adduct on the thermal stability of DNA is to reduce it between 8 and 10°C.[123, 162-164] and the evidence to date suggests a 1,2-intrastrand GG adduct can be found in the major groove causing significant bending of the helix whilst maintaining

hydrogen bonding (Table 1.2). Comparing the adducts formed using the small fragment d(GpA(N^7)pG(N^7) and a cis-GG cross-link, similar changes to the DNA structure are observed.[146, 165] Immunohistochemically, cis-GG and cis-AG are also very similar[166] although recognition is less specific for the cis-AG adduct *Cf.* cis-GG. At the molecular level the adducts are dissimilar as shown by reactivity towards chemical probes.[167]

Table 1.2. The Effect on DNA structure of various cisplatin-DNA adducts

Adduct	Oligonucleotide	Unwinding Angle	Bending Angle	Techniques(s)
1,2-intrastrand cis-GG	d(CpCpU^{Br}pCpTpG*pG*pTpCpTpCpC)·d(GpGpApGpApCpCpApGpApGpG)		32-40°	X-Ray[168, 169]
	d(CpCpU^{Br}pCpTpG*pG*pTpCpTpCpC)·d(GpGpApGpApCpCpApGpApGpG)		78°	NMR[170]
	d(CpTpCpTpCpG*pG*pTpCpTpC)·		80°	NMR[171]
	d(GpApGpApGpCpCpApGpApG)			
	d(CpCpTpG*pG*pTpCpC)·d(GpGpApCpCpApGpG)	19°	58°	NMR[172]
	d(CpCpTpG*pG*pTpCpC)·d(GpGpApCpCpApGpG)	21°	58°	Vibrational circular dichroism[173]
	d(TpCpTpCpG*pG*pTpCpTpC)·d(ApGpApGpCpCpApGpApG)		50-61°	Molecular modelling and extended NMR[174-178]
	d(TpCpTpCpCpTpTpCpTpTpG*pG*pTpTpCpTpCpTpTpCpTpC)·d(ApGpApGpApGpGpApApGpApApCpCpApApGpApApG)		40°	Gel electrophoresis[179]
	d(TpCpTpCpCpTpTpCpTpTpG*pG*pTpTpCpTpCpTpTpCpTpC)·d(ApGpApGpApGpGpApApGpApApCpCpApApGpApApG)		~32°	Gel electrophoresis[180]

1,2-intrastrand cis-AG	d(TpCpTpCpCpTpTpCpTpTpA*pG*pTpTpCpTpCpTpTpCpTpC)·d(ApGpApGpApGpGpApApGpApApTpCpApApGpApGpApApG)		~34°	Gel electrophoresis[180]
1,3-intrastrand cis-GXG	d(TpCpTpCpCpTpTpCpTpTpG*pTpG*pTpCpTpCpTpTpCpTpC)·d(ApGpApGpApGpGpApApGpApCpApCpApGpApGpApApG)		35°	Gel electrophoresis[180]
	d(CpTpCpCpTpCpTpTpCpTpG*pTpG*pTpCpTpTpCpTpG)·d(ApGpGpApGpApApGpApCpApCpApGpApApGpApApGpG)		25-30°	Gel electrophoresis[181]
	d(CpTpCpTpG*pTpG*pTpC pTpC)·d(GpApGpApCpApCpApG pApG)		30°	NMR[182]
	d(CpTpCpTpApG*pTpG*pC pTpCpApC)·d(GpApGpApTpCpApCpG pApGpTpG).		20°	NMR[183]
Interstrand adducts	d(CpCpTpCpG*pCpTpCpTpC)·d(GpGpApGpCpG*pApGpApG)	80°	47°	NMR[184]
	d(CpCpTpCpG*pCpTpCpTpC)·d(GpGpApGpCpG*pApGpApG)	80°	40°	NMR[185]
	d(CpApTpApG*pCpTpApT	80°	20°	NMR[186]

pG)· d(GpTpApTpCpG*pApTpA pC)				
d(CpTpTpCpTpCpCpTpTp G*pCpTpCpTpCpCpTpTpC pTpTpC)· d(GpApApGpApGpGpApA pCpG*pApGpApGpGpApA pGpApApG)		55°		Gel electrophoresis[187]
Several d(TpG*pCpT)·(ApCpG*pT) sequence	with	~79°	~45°	Gel electrophoresis[188]

The binding of cis-$[Pt(NH_3)_2]^{2+}$ to the N^7 of guanine residues forming a 1,3-intrastrand adduct causes the central cytidine residue to become extra-helical and no longer take part in stacking interactions,[189] a result confirmed using 1onger duplexes[180-182, 190] and chemical probes.[191] The thymine residue did not participate in the stacking arrangement (Figure 1.11) and the loss of 2 hydrogen bonds, in part, may explain the destabilisation of the duplex with a 26°C reduction in melting temperature (13°C Cf. 39°C in the unplainated duplex). Van Garderen and van Houte[183] report no extra-helical thymine residue, however a re-interpretation by Teuben *et al*[182] leads to a similar structure proposed by many other studies. A 1,3-intrastrand adduct causes larger and perhaps more significantly, different structural changes to the DNA helix cf. 1,2-intrastrand adducts.

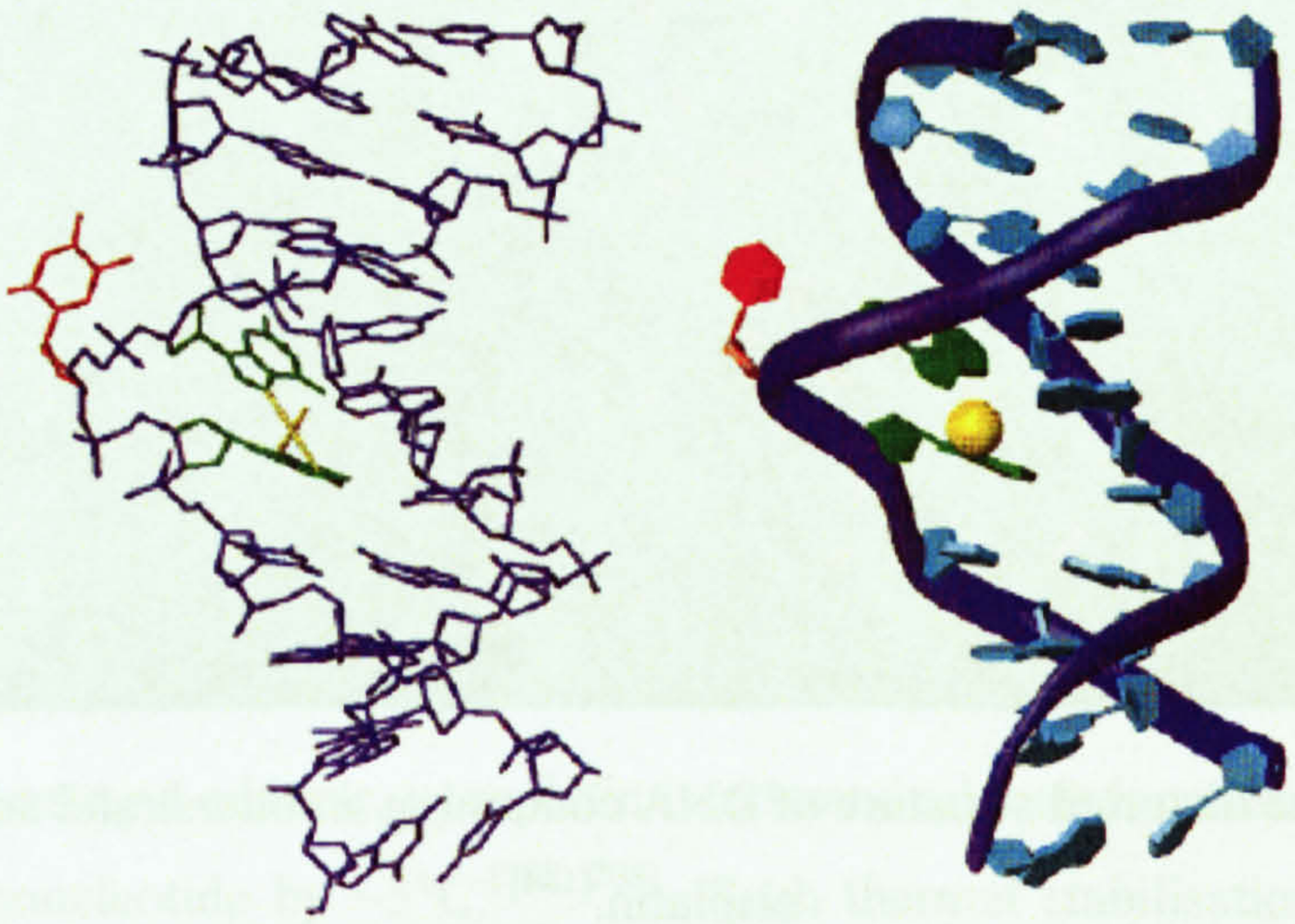

Figure 1.11. The distortion to DNA structure caused by a 1,3-intrastrand adduct[182]

Interstrand adducts are found to stabilises the DNA by 9°C and with the exception of Malinge *et al*[188], report the hydrogen bonds joining the GC pairs disrupted and the cytidine residue no longer takes part in stacking interactions in the helix and is exposed to the solvent (Figure 1.12). The interstrand adduct results in considerable structural aberrations and despite it only representing ~1 % of the total number of adducts on DNA, such large changes may cause serious problems to the correct functioning of DNA.

Whilst exact magnitudes of bending and unwinding angles may not fully agree it is clear there exists considerable differences between the structures of intrastrand and interstrand adducts. Such DNA damage is unlikely to go unnoticed by the biological machinery and it is likely that interstrand and intrastrand adducts cause different biological responses.

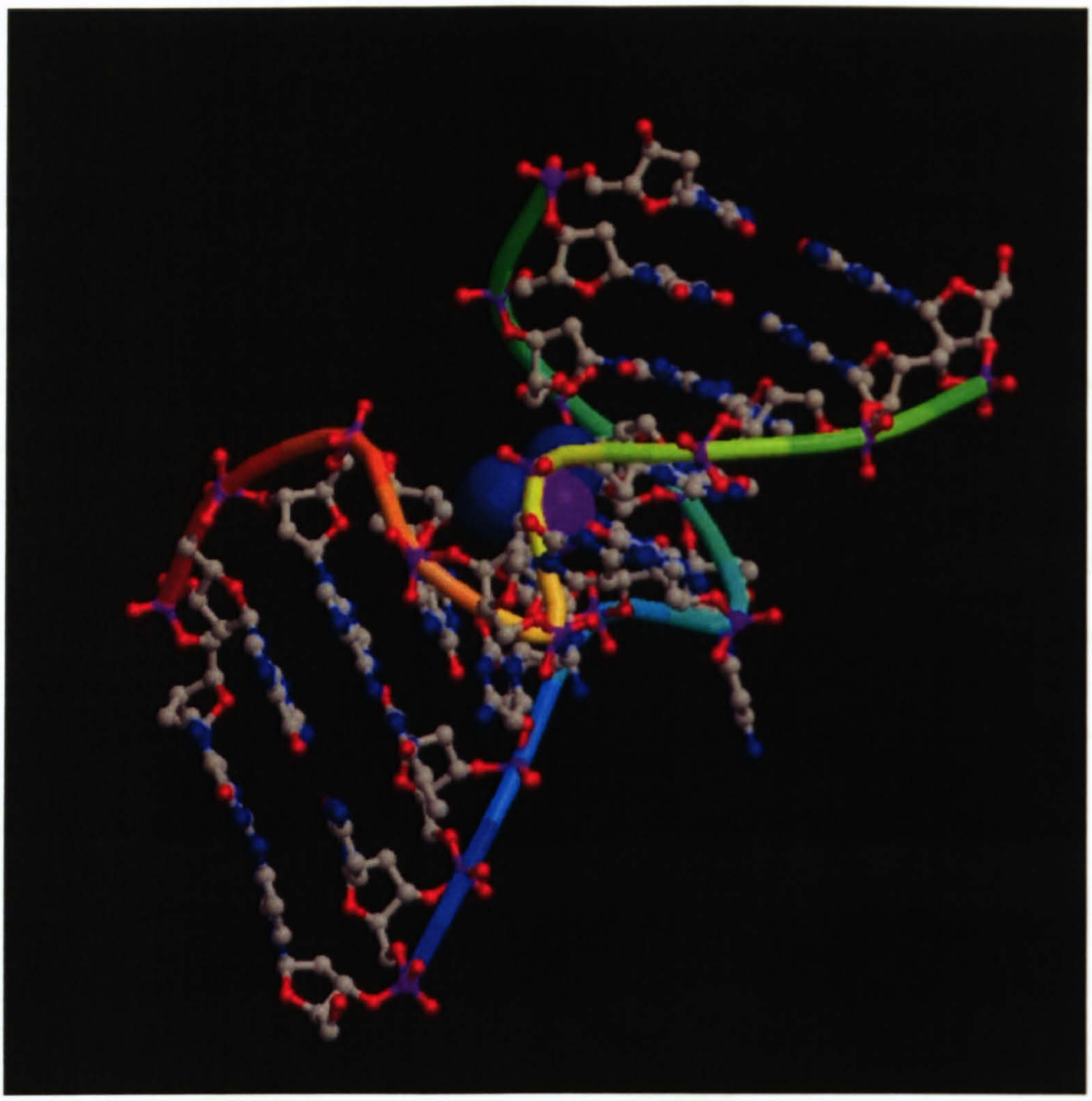

Figure 1.12. The distorted structure of DNA containing an interstrand adduct caused by cisplatin.[184]

1.4.3. Transplatin-DNA Adducts

Similar experiments used to identify cisplatin-DNA adducts find transplatin-DNA digests consisting of trans-[$Pt(NH_3)_2${d(GMP)}{d(AMP)}], trans-[$Pt(NH_3)_2${$(dGMP)_2$}] and trans-[$Pt(NH_3)_2${d(GMP)}{d(CMP)}] forming 10 %, 40 % and 50 % respectively,[192] representing intrastrand and interstrand adducts. Of particular note is that the trans stereochemistry prevents the formation of 1,2-intrastrand cross-links due to steric constraints[128, 193]. Also of note is the relatively high amount, approximately 85 %, of monofunctional adducts remaining after 2 hours.[194] Cisplatin produces 15% monofunctional adducts after 2 hours reducing to 4 % in an hour.[145] Transplatin also forms protein-Pt-DNA and interstrand adducts[158, 159]. Like cisplatin, transplatin retains similar preferences and prefers to binds to the N^7 of guanine residues. The major interstrand adduct, the interstrand trans-GC corresponds to 10 - 20 % of the total number and the work of Eastman[192] suggests the 30 - 40 % of dG - Pt - dC adducts are intrastrand in nature. The 1,3-intrastrand trans-CNG adduct has been formed[195-199] and small oligonucleotide studies suggest transplatin adducts are metastable[200, 201] which, in large

oligonucleotides, result in re-arrangement to 1,4-intrastrand adducts[195-197], although this may be related to the annealing processes used[202] and is not seen in all cases.[203] In contrast, Boudvillian *et al*[202] reports only interstrand and monofunctional adducts when reacting transplatin with native DNA and Brabec *et al*[204] report the interstrand trans-GC adduct is preferentially formed. Similar to some 1,3-intrastrand cisplatin-DNA adducts in 1,3-intrastrand transplatin-DNA adducts the central bases is extra-helical (Figure 1.12).[198, 199] It appears the actual proportions of adducts caused by transplatin on double-stranded DNA are not fully quantified and comparison to cisplatin is difficult.

1.4.4. The effect of transplatin adducts on DNA structure

The effect of transplatin adducts on the structure of DNA are substantially less known than cisplatin. Gel electrophoresis has shown a 1,3-intrastrand trans-GTG adduct caused a 26° bend (towards the major groove) and 45° unwinding on DNA.[202] Later work by Brabec *et al*[205] agreed reporting bending towards the major groove of 26 - 27° using gel mobility assays, chemical probes and molecular mechanics. The structure of the major interstrand adduct trans-GC has been solved using NMR techniques revealing a ~20° bend towards the minor groove with no discernable unwinding, although gel electrophoresis suggest 12°.[206] Such a bend is very much smaller than those reports for cisplatin interstrand adducts.

Like cisplatin interstrand adducts, transplatin interstrand adducts increase the melting point of a 20 bp oligonucleotide by ~5°C.[207, 208] Such thermal stabilisation originates from entropic effects, i.e. the two strands cannot be totally separated. The overall stability of the duplex is much reduced as structural perturbations caused by the adduct result in enthalpic effects, reducing the overall DNA stability; however base pairing is reportedly maintained,[205] unlike in cisplatin interstrand adducts. The differences between cisplatin and transplatin adducts in terms of DNA structure may, in part, be responsible for the differing cytotoxicities observed. Since transplatin is highly toxic, important studies such as those identifying adducts formed in vivo are not available but comparisons with cisplatin suggestions in vitro adducts formed by transplatin are similar to those that would be found in vivo.

1.4.5. The mechanism(s) of adduct formation

In a significant experiment, during the first 2 hours of treating cells with radiolabelled cisplatin none was found bound to genomic DNA.[106] The authors suggested cisplatin is not the active agent and is converted into an activated species and that ~2 hours is required before sufficient concentration(s) of active agent is achieved. Several authors have reported partial hydrolysis is required for cisplatin (and its analogues) to bind to DNA.[123,

[209, 210] and kinetic analyses show the initial binding of cisplatin (and transplatin) is kinetically controlled by the rate of hydrolysis[125, 211]. From these reports it is reasonable to suggest hydrolysis products are almost certainly active metabolites towards DNA in aqueous solution and that cisplatin is not.

It is possible to follow the reaction between cis-$[Pt(NH_3)_2Cl(H_2O)]^+$ and DNA using ^{195}Pt NMR[212] and cisplatin initially forms mono-functional adducts closing to bi-functional adducts with no evidence of aquated products observed. The step-wise formation of bi-functional adducts is illustrated in Figure 1.13, although this evidence does not agree with that of Eastman and Barry,[194] who found a much slower rate of conversion between monofunctional and bifunctional adducts.

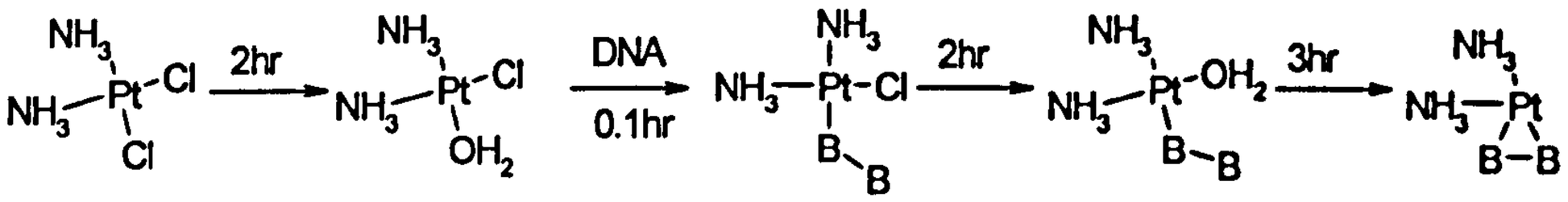

Figure 1.13. The step-wise platination of DNA by cisplatin via a mono-aqua moiety. B represents nucleobases from the double helix of DNA. The half life is given for each step.

Using more biologically relevant DNA concentration than used in ^{195}Pt experiments, Johnson *et al*[211] found cis-$[Pt(NH_3)_2Cl(H_2O)]^+$ and cis-$[Pt(NH_3)_2(H_2O)_2]^{2+}$ were significant in relation to DNA binding and trans-$[Pt(NH_3)(H_2O)Cl]^+$ for transplatin. Both cisplatin and transplatin form hydroxo-complexes where a bound water molecule looses a proton to form, for example, the neutral species cis-$[Pt(NH_3)_2Cl(OH)]$ and cis-$[Pt(NH_3)_2(OH)(H_2O)]^+$ and these being as reactive towards DNA as the diaqua. *Kozelka et al*[213] suggest that the active species towards DNA is the couple cis-$[Pt(NH_3)_2(OH)(H_2O)]^+$ / cis-$[Pt(NH_3)_2(H_2O)_2]^{2+}$ rather than cis-$[Pt(NH_3)_2Cl(H_2O)]^+$. The relevance of these to the intracellular environment in vitro and in vivo remains to be proven and is doubtful given in human ovarian 2008 and C13 cell lines a substantial reduction in intracellular chloride concentration by substitution with nitrate has no effect on the cytotoxicity or the platination of cellular DNA.[214] A previous study found cells treated with 34 - 2400 fold increased levels of aquated species had a 1.9 fold increase in levels of platination of DNA.[215] The two studies suggest the composition of aquated species in the cytoplasm are not relevant to those found in vicinity of DNA. Individually, results regarding adduct formation are clear but taken as a whole package of evidence they do not agree on several points: the relative important of cisplatin metabolites and if chloride concentration is relevant in vivo. Biological studies on cells are likely more relevant given that dilute

solutions of DNA resemble very little the tightly coiled and packed structure of genomic DNA but more experiments are needed before more definite conclusions may be reached.

1.5. The consequences of cisplatin on DNA function

1.5.1. In vivo distribution of cisplatin adducts

Once a certain level of platination of DNA has occurred a cell will die and this is thought (in bacterial cells) to occur around 1.8-7.5 nmoles Pt / g DNA[109, 216], corresponding to a single bound platinum atom per 80,000 – 550,000 nucleotides. Oshita and Eastman[217] report growth inhibition occurring when a single platinum binding event per 250,000 nucleotides occurs in the leukaemia cell line HL-60, representing ~48,000 adducts per cell. Using previously established adduct distributions the 48,000 adducts may be split between 29,000 cis-GG, 14,000 cis-AG, 4,000 cis-GNG and interstrand GG, 500 mono-functional and DNA-protein or –thiol cross-links. Assessing the relative potency of each adduct(s) is a great challenge and to this date the efficacy of each adduct is uncertain.

1.5.2. The effect of cisplatin adducts on DNA function

The primary functions of DNA involve its replication and transcription. Replication is required for cell division and transcription for correct production of messenger RNA for protein synthesis. These two processes occur at different times in the cycle of a cell. The cell cycle consists of 4 phases, namely gap phase 1 (G1), synthesis phase (S), gap phase 2 (G2) and mitosis. Transcription occurs in the G2 phase and replication occurs in the synthesis (S) phase and investigation of these two phases give indications of the ability of cisplatin, or any platinum drug, to interfere with these processes.

1.5.3. The effect of cisplatin adducts on DNA replication

DNA replication involves unravelling DNA from its chromatin structure, separation of strands, synthesis of new strands of DNA using the old strands as templates using a vast array of co-factors proteins and DNA polymerases including polymerase T7 (shown in Figure 1.14). Harder *et al*[218] reported inhibition of several polymerases, although up to 7 fold higher levels of platination of transplatin are required compared to cisplatin.[219] Inhibition (using polymerase I) occurs chiefly at $(dG)_n$ sites ($n \geq 2$) in cisplatin treated DNA[220, 221] and d(GpNpG) sites for transplatin abeit with lower specificity and indicates the possibility of 1,3-intrastrand adducts on viral DNA.[220] Villani *et al*[222] report the prokaryotic DNA polymerase I and eukaryotic polymerase α were blocked at $(dG)_n$ sites, d(GpG), d(ApG) and d(GpApG) sites indicating cis-GG, cis-AG and cis-GAG adduct can block DNA replication and Hoffmann *et al*[223] found inhibition of DNA synthesis in the

order than the cis-GG > cis-AG, although small levels (>5 %) of replication still occurred in both cases. Monofunctional adducts did not prevent replication and were bypassed in the majority of cases. Replicative bypass occurred for in all adducts studied by Comess *et al*[224] including, cis-GG (2-6 % bypass), cis-AG (2-19 %) and cis-GCG (4-27 % bypass) and the 1,4-intrastrand trans-CGCG (39-90 % bypass. Despite being blocked, inhibition of DNA synthesis does not account fully for the antitumour properties of cisplatin and several studies using L1210 leukemia cells report inhibition of DNA synthesis does not correlate with cytotoxicity.[225-227] Another mechanism must be responsible (at least in part) for cisplatin cytotoxicity.

Figure 1.14. The crystal structure of T7 polymerase / DNA complex.[228]

1.5.4. The effect of cisplatin adducts of DNA transcription

The results reported by Sorenson and Eastman[225, 226] suggest inhibition of DNA transcription due to cisplatin adducts rather than replication possesses an important role. A slow progression of the cells through the S phase of the cell cycle before growth arrest in G2 in low concentrations of cisplatin before growth restarting may be interpreted as cells

repairing DNA damage in the S phase before attempting transcription resulting in arrest in G2 which, at higher concentrations of cisplatin, becomes permanent and cells die. Several studies[229, 230] in simplified transcription systems found cis-GG, cis-AG, cis-GTG, trans-GTG, cisplatin interstrand crosslinks and monofunctional adducts [Pt(dien)Cl]Cl provided blocks to DNA transcription, although trans-GTG and monofunctional adducts were primarily bypassed. Conditions perhaps possessing greater biological relevance were used by Cullinane *et al*[231] who found cis-GTG adduct inhibited RNA polymerase activity by 80% whilst the 1,2-intrastrand cis-GG adduct was bypassed in He-La and GM8437A cellular extracts, an unexpected result given previous reports. Later reports in model systems found cis-GG and cis-GTG adducts blocked transcription by RNA polymerase II[232] and T7 RNA polymerase.[233] It appears the source of RNA polymerases (which often differ between experiments) may be a factor in determining the propensity of adducts to inhibit transcription. As such the results, while interesting and informative, are difficult to envisage occurring *in vivo* with substational levels of confidence, even perhaps when using cellular extracts.

Whilst the action of individual adducts is important, the effect of large numbers of adducts was ascertained by Mello *et al*[234] in perhaps the nearest experiment conditions *in vitro* to real biological conditions. Up to 3-fold higher levels of transcription of the plasmid occurs in cell treated with transplatin compared to cisplatin and 4-fold more transplatin adducts were required for similar levels of transcription blockage caused by cisplatin. Only 0 - 16% of cisplatin adducts and 60 - 76% of transplatin adducts are bypassed. To date this represents the most relevant and as such, the most persuasive piece of research on cisplatin and transplatin adducts and DNA transcription.

1.6. Cisplatin and gene expression

The fact cisplatin interferes with DNA transcription suggests differences in the expression of genes may result. This may occur as a direct result of inhibiting transcription of genes encoding essential proteins or binding and interfering with the correct functioning of transcription factors (proteins involved in transcription) and has been reviewed in depth recently.[235-239]

1.7. Cisplatin and apoptosis

The evasion of apoptosis is a peculiarity of most if not all cancers.[240] Apoptosis is a mechanism by which internal cellular signals caused by one or more factors instruct a cell to die.[241] Apoptosis is characterised, although not exclusively, by cell shrinkage, chromatin condensation and subsequent endonuclease cleavage in 180 base pair

multimers.[242] Apoptosis is a consequence of the mechanism (DNA binding) of cisplatin[243], although other, non-DNA binding events leading to apoptosis should not be ruled out.[244]

1.8. The recognition and processing of cisplatin-DNA adducts

It is established DNA binding is an essential first step in the cytotoxicity of cisplatin and apoptosis is the last.[245] The biological events between the two end-points have attracted considerable interest in attempting to fully explain the mechanism of action of cisplatin and are likely to require recognition of DNA damage by cellular proteins to activate mechanisms mediating the cellular response. The DNA damaged caused by cisplatin is recognised by a wide range of often unrelated proteins that may to split into two groups; those preferentially binding to cisplatin-damaged DNA and those whose binding site(s) is similar to cisplain-damaged DNA.[246] Some of the protein groups that recognise cisplatin-DNA adducts are listed below:[247-250]

1. Nucleotide excision repair (NER)
2. Recombinant repair (RR)
3. Mismatch repair (MMR)
4. High mobility group (HMG)
5. Trans-lesion synthesis (TLS)
6. DNA-dependent protein kinases (DNA-PK)

In this section how cells respond to DNA adducts will be elucidated, i.e. attempt repair and how such repairs may be modulated by proteins specifically recognising DNA adducts.

1.8.1. Nucletide excision repair, recombinant repair and trans-lesion synthesis pathways

The primary mechanism for the repair of cisplatin adducts is thought to occur by NER[251, 252] and involves an incision at either end of the damaged DNA, removal of the adduct and ligation to form and bond the new section of strand to the exisiting helix.[253-255] Two other pathways, the RR and TLS modulate cisplatin cytotoxicity in yeast and lung tumour cells in vitro[256] and strains of S. cerevisiae lacking the RR and TLS pathways are hypersensitive to cisplatin,[257, 258] suggesting a significant role of the RR and TLS pathways in addition to the NER mechanism in repairing cisplatin-DNA adducts. Infact intrastrand cross-links are found to be repaired by NER, RR and TLS pathways, whereas repairing interstrand cross-links results in a double strand breaks in DNA[259] indicating the RR mechanism although it requiries functioning NER. The RR pathway repairs DNA

whilst TLS allows DNA polymerase to bypass the adduct creating mutated DNA and possible genetic damage.

1.8.2. Interaction between HMG proteins and the NER pathway

High mobility group proteins comprise a large array of polypeptides intrinsically entwined in the integral functioning of DNA related activities including, amongst others, DNA repair,[260] transcription and gene regulation[261] and chromatin structure.[262, 263] HMG-box proteins HMG1 and HMG2 (now referred to as HMGB1 and HMGB2) bind to cisplatin (but not transplatin) damaged DNA.[264, 265] In the same year Pil and Lippard[266] identified recombinant rat HMGB1 binds specifically to 1,2-intrastrand cis-GG and cis-AG adducts and not transplatin adducts or 1,3-intrastrand cis-GTG adducts. The affinity of HMGB1 for cisplatin-damaged DNA correlates with the amount of damaged DNA[267] and crystal structure of the A domain of HMGB1 bound to a 1,2-intrastrand cis-GG adduct has given much additional information (Figure 1.15).[268]

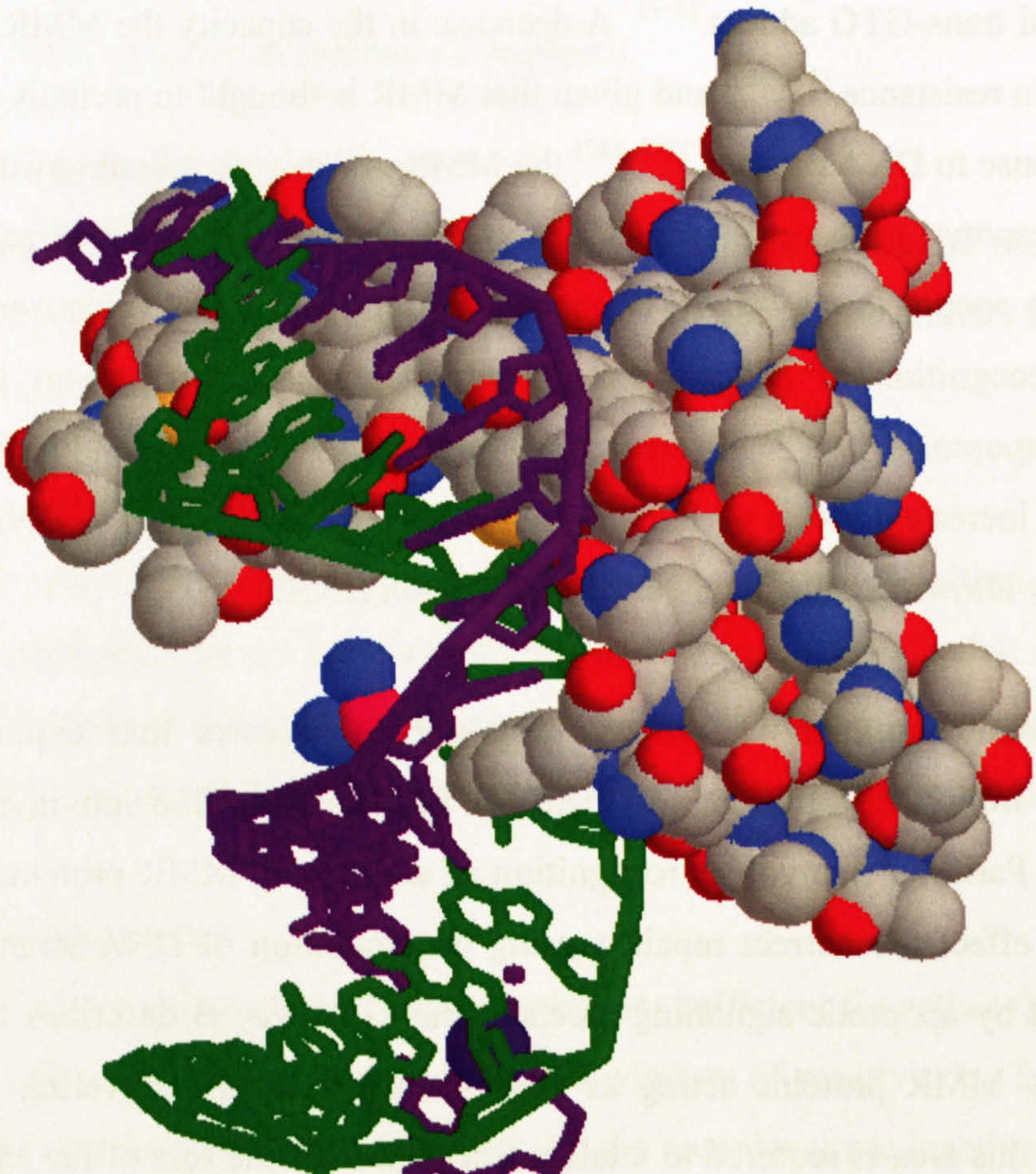

Figure 1.15. The crystal structure of domain A of HMGB1 bound to a 1,2-intrastrand cis-GG adduct,[268] drawn using protein explorer[269]

The cis-GG adduct has been found refractory to repair[270] and using whole cell extracts[271] 1,3-intrastrand adducts are repaired 15 - 20 fold more than 1,2-intrastrand adducts. Specific binding of HMG proteins to cis-AG or cis-GG adducts inhibited excision repair of DNA[272] in line with other reports.[268, 273, 274] Unfortunately *in vivo* data regarding the protective ability of HMG proteins remains absent but the existing reports make a strong case for 1,2-intrastrand adducts being shielded from repair by members of the HMG-box protein family.

1.8.3. MMR Pathway

The mismatch repair (MMR) mechanism recognises and corrects mismatched nucleotides in newly synthesised DNA and consists of more than 13 individual proteins which take part in the recognition and repair of DNA and if required signal apoptosis.[275] The MMR protein hMSH2 specifically recognises cis-GG adducts and shows affinity for other cisplatin adducts but not those of transplatin or [Pt(dien)Cl]Cl.[276] Another MMR protein, hMutSα displays a similar affinity profile, binding to cis-GG adducts but not 1,3-intrastrand trans-GTG adduct.[277] A decrease in the capacity the MMR pathway can lead to cisplatin resistance.[278-280] and given that MMR is thought to partially mediate apoptosis as a response to DNA damage,[281, 282] the MMR is likely, to an unknown extent, determine a cell's response to the cisplatin adducts it recognises. This links directly cisplatin-DNA adducts to apoptosis via the MMR mechanism and is unusual, most routes are circuitous protein recognition of adducts simply activates many downstream signalling factors, effecting apoptosis.[283, 284] Errors in the MMR proteins hMutSα and hMutLα are proposed to lead to increased levels of TLS, preventing MMR recognition of DNA damage[285] and very likely allowing genetic mistakes to persist on DNA.

Kartalou and Essigman[286] propose 2 possible pathways that explaining the events occurring from the formation of cisplatin adducts to cell death involving the MMR pathway. Pathway A involves recognition of adducts by MMR proteins but the MMR is unable to effect the correct repair causing accumulation of DNA strand breaks that are recognised by apoptotic signalling mechanisms. Pathway B describes the recognition of adducts by MMR proteins acting as DNA-damage sensors activating apoptosis. More reseach in this area is required to attain a full picture of the role of the MMR in mediating cisplatin toxicity. Should the MMR proteins be found acting as 'apoptotic sensors' it will signal another area in which research should investigate further.

1.9. Mechanisms of resistance to cisplatin

Several mechanisms have been proposed to account for resistance and have been reviewed in depth recently:[49, 248, 287-290]

a) Decreased uptake / increased efflux of cisplatin from the cell.
b) Increased levels of sulphur containing proteins/compounds that bind to platinum and render inactive (such as glutathione).[291, 292]
c) Enhanced DNA repair by the NER mechanism.[293]
d) Loss of MMR activity (reduced recognition of DNA damage).[294]
e) Defective elements of the apoptosis mechanism.[295]
f) Altered expression of significant genes, e.g., p53, bcl-2.[296, 297]
g) Altered expression of important proteins.[298, 299]

The identification of mechanisms of resistance to cisplatin in cells allows chemists to selectively design compounds targeting single or multiple mechanims involved in cisplatin resistance. These new complexes, in addition to those overcoming clinical ineffectiveness may be called the 'next generation' platinum complexes.

1.10. Next generation platinum complexes

Post-cisplatin complexes have been synthesised in an attempt to overcome the problems associated with cisplatin treatment. In designing these compounds chemists have taken into account structure-activity relationships of Pt(II) complexes.

1.10.1. Structure - activity relationships

Structure-activity relationships (SAR) regarding cisplatin are by definition empirical. Rosenberg[53-55] found only the cis isomers and not trans isomers were active and Cleare and Hoeschele[300] using systematic ligand replacement in platinum(II) complexes and Sarcoma 180 mice and suggested that for antitumour activity a platinum(II) complex should possess:

a) Electrical neutrality.
b) A pair of cis leaving groups (necessary but not sufficient for activity).
c) The leaving groups should 'fall within a window of reactivity'. Too reactive and the complexes are toxic. To inert and the complexes are inactive.
d) Non-leaving groups should be trans to leaving groups and consist of inert amine type systems.

In apparent contradiction to earlier findings, Braddock *et al.*[301] concluded no systematic pattern of structure activity relations exists when investigating a range of platinum(II) and platinum(IV) complexes. However, the SAR of Cleare and Hoeschele has guided research from the early 1970's onwards with thousands of cisplatin analogues being produced. Some notable successes have been achieved and now two other platinum(II) complexes, carboplatin and oxaliplatin are used in the clinical setting. The SAR described by Cleare and Hoeschele have been 'broken' a substational number of times and such rules may be considered somewhat redundant and whether these rules really informed research or narrowed its view is a valid debate.

1.10.2. Carboplatin

Carboplatin (Figure 1.16) was developed by a collaboration of Johnson Matthey and the Institute for Cancer Research, UK and was designed to reduce the severe toxicity encountered with cisplatin in the clinical setting by using a less labile leaving group. As a result, carboplatin possesses a much reduced toxicity profile compared to cisplatin although myleosupression (suppression of bone marrow production of red and white blood cells) is increased[302] and determines the maximum dose tolerated by the patient. It is active in the same tumours as cisplatin and unfortunately retains a similar resistance profile as cisplatin despite having different proportion of DNA adducts.[182]

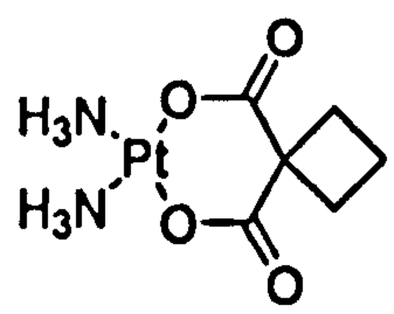

Figure 1.16. The molecular structure of carboplatin

1.10.3. Oxaliplatin

Oxaliplatin, (trans-R, R)1,2-diamminocyclohexaneoxalatoplatinum(II) is shown in Figure 1.17. It has a different spectrum of activity compared to cisplatin and carboplatin and is active in cisplatin-refractory tumours (tumours that no longer respond to cisplatin treatment).[303] Oxaliplatin acts in synergy with other chemotherapy drugs (cisplatin, carboplatin and others) in colorectal and ovarian cancer, two types of maliganant disease commonly resistant to cisplatin.[304]

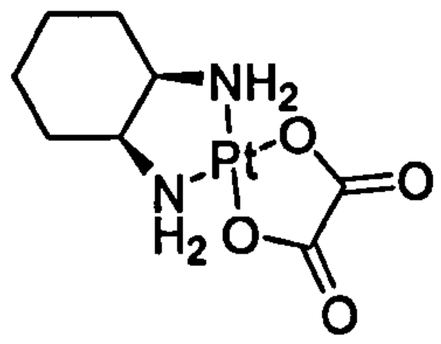

Figure 1.17. The molecular structure of oxaliplatin.

Oxaliplatin DNA-adducts are 60 – 65 % cis-GG, 25 – 4 0% cis-AG, 5 – 10 % cis-GNG and a few percent interstrand adducts (similar to cisplatin).[305-307] Oxaliplatin adducts are differentially recognised by cellular repair proteins belonging to the MMR mechanism differently to cisplatin (but the same in the RR and TLS pathways).[48] Such differential recognition (due perhaps to the non-leaving group) is likely to form part of the explanation for its activity in cisplatin-resistant tumours.[308] Oxaliplatin has recently been granted approval for clinical use in the USA in treatment of metastatic carcinoma of the colon and rectum.[309]

1.10.4. Multi-nuclear platinum complexes

If the activity of platinum drugs is based on the recognition and processing of DNA adducts then complexes producing different adducts may be recognised and processed differently. This may lead to complexes with broader anti-cancer activity and lacking cross-resistance with currently licensed drugs. This idea has lead to the development of dinuclear and trinuclear complexes (Figure 1.18).

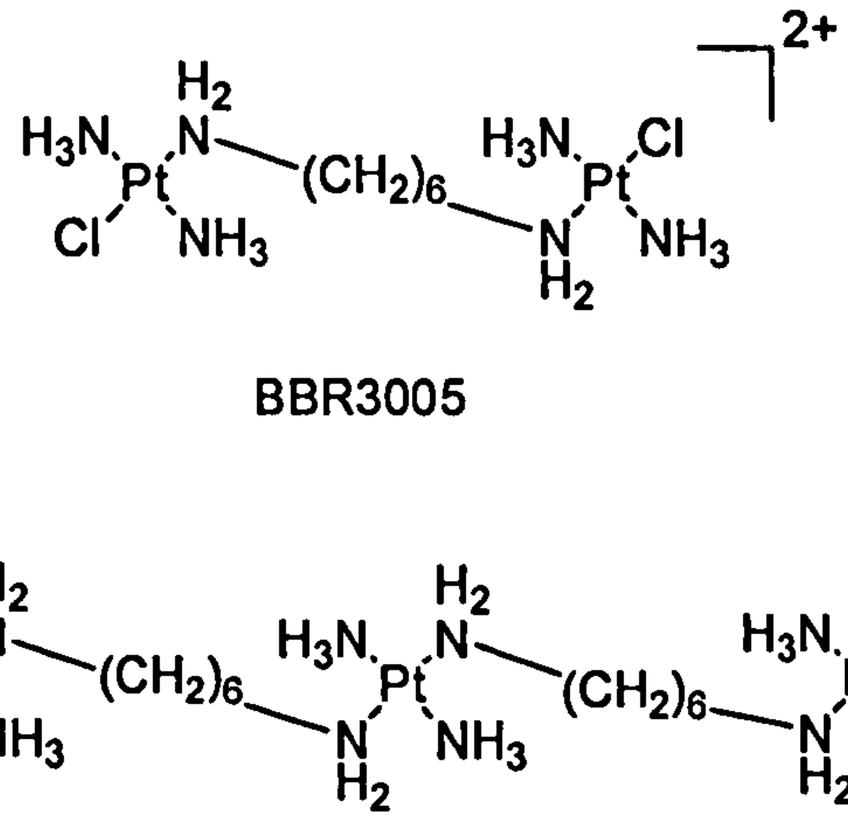

BBR3005

BBR3464

Figure 1.18. The chemical structures of dinulcear BBR3005 and trinuclear BBR3464.

Farrell and co-workers investigate "non-classical" structures and are of the opinion that "future discovery of clinically useful platinum agents is likely to arise from 'non-classical' structures".[302] The structures are very different from cisplatin and are not consistant with the SAR suggested by Cleare and Hoeschele.[300] The aim was to produce complexes possessing 'activity in cisplatin-resistant cells and a broader profile of antitumour activity'.[310] A large range of dinuclear and trinuclear complexes have been synthesised and assessed for biological activity and this work has been recently reviewed.[311] The complexes display activity *in vitro* and *in vivo* comparable to cisplatin and often at 10 fold less concentrations in cisplatin-resistant tumours.[310] The complex BBR3464 binds to DNA and the profile is significantly different from cisplatin with 20% of DNA adducts being interstrand (cisplatin ~ 1 - 3 %) and capable of spanning 6-8 base pairs.[312] The study also found antibodies recognising cisplatin adducts did not recognise adducts formed by BBR3464 suggesting structural features that would not be recognised by those proteins binding specifically to cisplatin adducts.

The 1,2-, 1,3- and 1,5-intrastrand adducts caused by BBR3464 on DNA are repaired by the NER pathway more efficiently than 1,2-intrastrand cisplatin adducts and are not recognised by the HMG-domain proteins.[313] Further work identified the effect of interstrand adducts of BBR3464 on the structure of DNA and found 1,2-, 1,4- and 1,6-interstrand adducts and are not recognised by HMGB1 or HBGB2.[314] Significantly 1,4-interstrand adducts are not repaired by NER and may remain on DNA for an unknown length of time. BBR3464 also exhibits increased levels of intracellular accumulation compared to cisplatin.[315] This is perhaps surprising as neutrality is a requirement of the early SAR for cisplatin. It now appears increased charge may correlate with enhanced uptake as the +8 complex is uptaken faster than the +6.[316] The complex (Figure 1.19) is unusual as it possesses no chlorides and is likely to bind electrostatically. It is possible it represent a future class of platinum based anti-cancer drugs possessing only the ability to bind electrostatically to DNA.

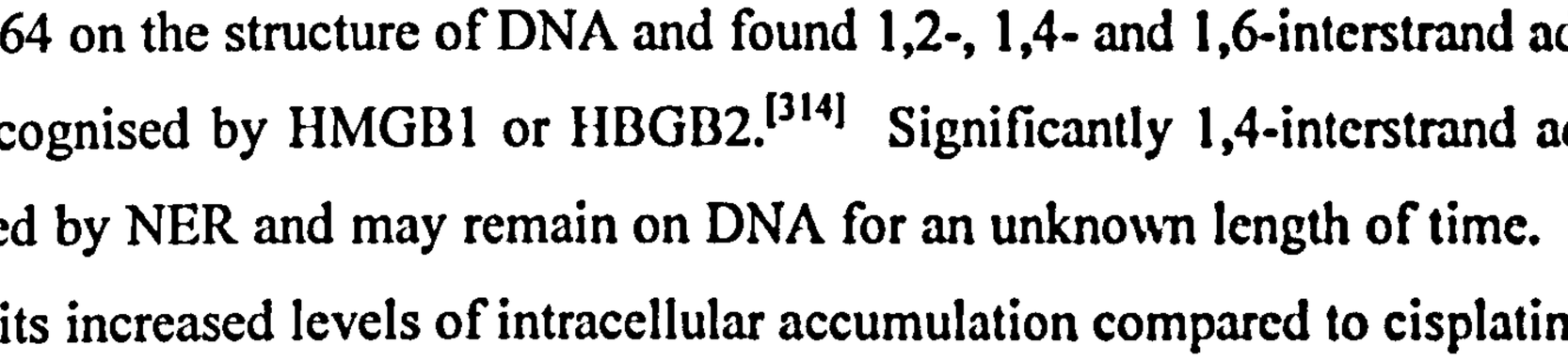

Figure 1.19. The latest trinuclear complex from Farrell and co-workers.

1.10.5. Sterically hindered platinum complexes (ZD0473)

ZD0473, shown in Figure 1.20, was specifically designed by Johnson Matthey and the Cancer Research Campaign, UK to inhibit detoxification by sulphur containing cellular components and be active in cisplatin resistant tumours.

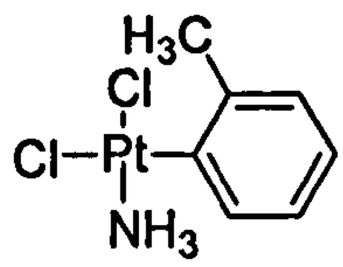

ZD0473

Figure 1.20. The chemical structure of ZD0473

Inhibiting detoxification is via creation of axial steric crowding (caused by 2-methyl group) hindering substitution of chloride groups. As may be expected, slower rates of hydrolysis are reported[317] and reduced rates of detoxification by sulphur containing biomolecules without significant loss of DNA binding ability and retention of cytotoxicity are observed.[318] In ovarian and colon cancer cell lines resistant to oxaliplatin[319] and cisplatin[320, 321] ZD0473 is not cross-resistant. As of November 2005, ZD0473, now known commercially as picoplatin received orphan drug designation by the U.S. Food and Drug Administration.[322]

1.10.6. Trans-activation and other non-classical platinum complexes

The current status of platinum complexes possessing *trans* stereochemistry has been reviewed in detail recently where more detailed information is present.[323-325] The intial SAR suggest trans complexes are inactive, although only 7 complexes of the formula trans-$[Pt(L)_2Cl_2]$ where L is NH_3, $MeNH_2$ or $MeEt_2$ were tested. More recently the group of Farrell discovered 'activation' of the trans geometry by replacing the ammonia groups of transplatin by pyridine or 4-methylpyridine; these complexes exhibit greater activity than cis counterparts.[326] Replacement of a single amine group of transplatin by a planar aromatic ligand to yield the formula trans-$[PtCl_2(quinoline)(NH_3)]$ or an additional substitution by DMSO such as trans-$[PtCl_2(quinoline)(DMSO)]$ resulted in biologically active trans complexs.[327, 328] These complexes are shown in Figure 1.21. An inversion of cytoxicity was observed as the trans-complexes were more cytotoxic in L1210 tumour cells than the cis counterparts.

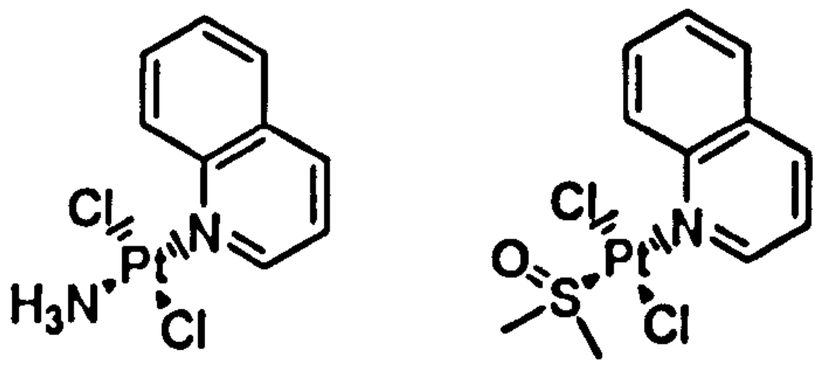

Figure 1.21. The trans-complexes developed by Farrell and co-workers.

Other active trans complexes such as those with the formula trans-$Pt[Cl_2(amine)(isopropylamine)]$[329], trans-$Pt[Cl_2(4\text{-methylpyridine})(piperizine)]$[330] and trans-$Pt[Cl_2(iminoether)_2]$[331] as shown in Figure 1.22 as A, B and C respectively, are also active. It may be suggested rather than transplatin epitomising the trans geometry by its lack of cytotoxicity it is infact the exception to the rule and that trans complexes are generally active.

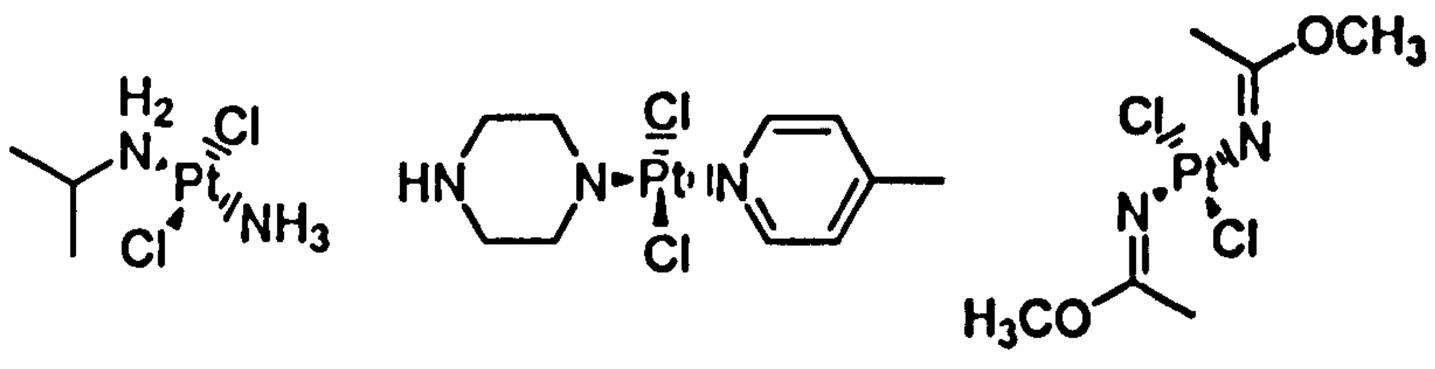

A B C

Figure 1.22. Active trans complexes

Charged complexes based on the structure in Figure 1.23, where L was a range of substituted pyridine, purine and pyrimidine ligands are found to be cytotoxic.[332] In vivo testing in mice found 12 out of 32 complexes more active in S180a tumours in mice than cisplatin and the origin of the cytotoxic was reported due to the formation of monofunctional adducts.[333]

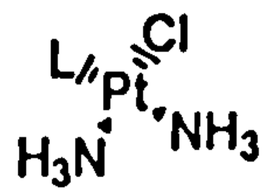

Figure 1.23. Cytotoxic complexes based on $[Pt(NH_3)_2(L)Cl][X]$

Such trans complexes, neutral and also charged represent a very important line of investigation in the search for new complexes for use in the clinic.

1.11. Epilogue

Chapter One has introduced the concept of chemotherapy: the use of chemicals in the treatment of cancer. Platinum(II) complexes, the best example of which is cisplatin act via binding to DNA and disrupting cellular pathways. There are several modes whereby cisplatin binds to DNA of which 1,2-intrastrand adducts form the majority. Each adduct type is not equivalent in terms of causing structural changes to the DNA helical structure each is differentially recognised by cellular proteins. It is this differential recognition that is likely to result in the degree of biological response of the cell.

Platinum(II) drugs, via DNA binding, are effective in treating a limited range of tumours and such treatments have many problems including high levels of toxicity, lack of tissue specificity and eventually cells become resistant.

BLANK IN ORIGINAL

Chapter Two - Targeting cancer with steroidal conjugates

2.1. Prologue

The attempt to overcome the lack of tissue specificity in current anticancer drugs such as cisplatin involves the use of a transport mechanism common to many tissues in the body but found to be enhanced in malignant tissue; the localisation of steroids into the DNA containing nucleus of cells by steroid receptors.

Through attaching a steroid based on testosterone to a platinum centre known to be cytotoxic,[334, 335] it may be possible to transport a steroidal platinum complex direct into the cell nucleus. A large number of tumour types tend to express high levels of steroidal receptors; for example ~80 % of breast tumours overexpress the androgen receptor which binds many substrates based on testosterone.[336-338] The hypothesis on which this work is based is that using the steroidal transport system, steroidal platinum complexes might be selectively localised in the nucleus of tumour cells leaving normal tissue less affected.

In this chapter combinations of steroids with anticancer compounds are discussed and the role of steroids in malignant disease evaluated. The design of such agents is also reviewed. Finally the epilogue unites these themes together.

2.2. Approaches for targeting of cancer with steroids and mimics

Conjugating a suitable cytotoxic moiety and active bio-ligand may cause improved transport of a compound into targeted cells and / or a synergistic effect. This has been attempted many times in pursuit of targeting DNA binding drugs such as cisplatin to the nucleus of cells, using a number of different delivery vectors tethered to platinum(II) and platinum(IV) complexes. Examples include attaching platinum(II) to DNA intercalators such as doxorubicin,[339, 340] anthraquinones,[341-343] ethidium bromide[344] and acridine derivatives,[345-348] anticipating increased localisation of the drug in the vicinity of genomic DNA. Others groups have attached sucrose[349] and antitrypanosomatid[350] drugs but overall the attempts have produced mixed results and no clinical progress. Other groups have targeted sex steroid receptors by linking steroids to cytotoxic agents and it is this aspect of targeting that will be concentrated on.

2.2.1. Steroid conjugates with alkylating agents

Early efforts with 3-substituted steroids (Figure 2.1) exhibited no binding affinity for their respective receptor (progesterone receptor) or therapeutic activity.[351-353]

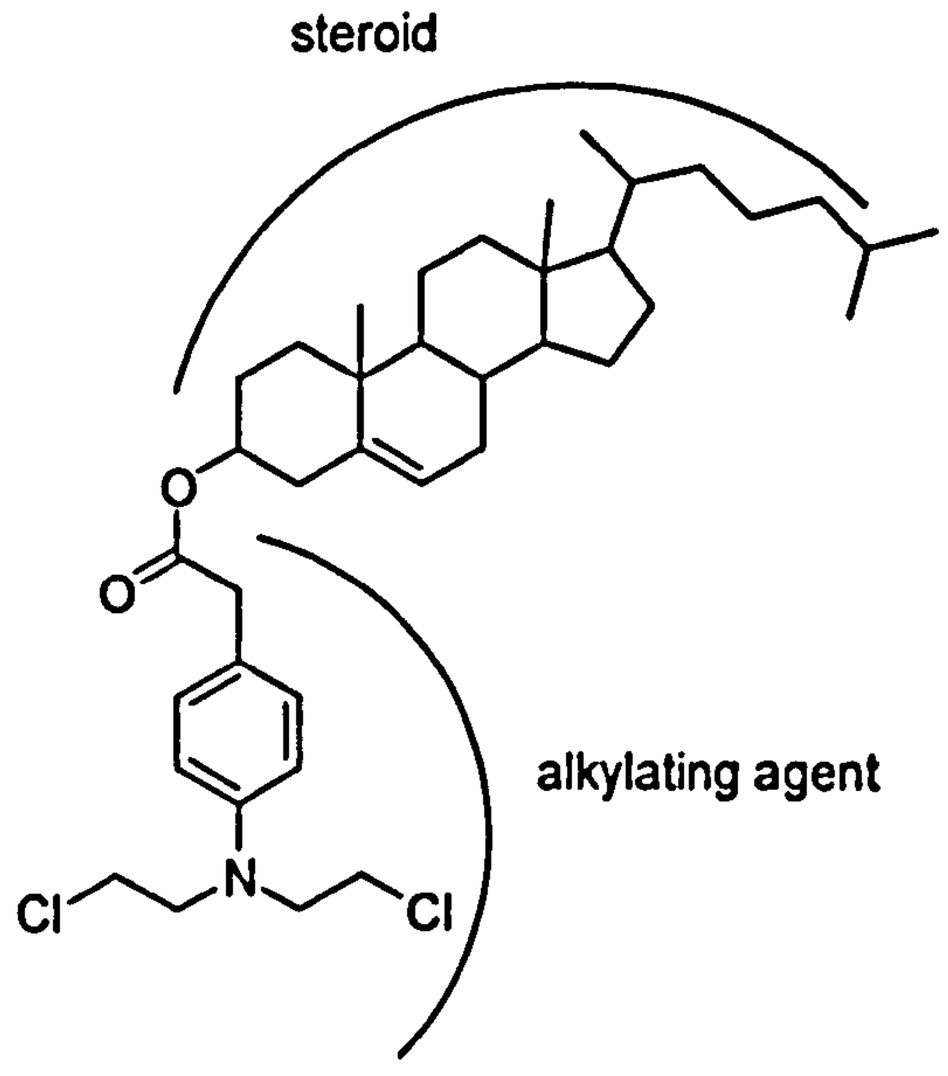

Figure 2.1. The structure of 3β-hydroxy-5-cholestene p-[N, N-bis-(chloroethyl)amino]phenylacetate.

Later work by Leclercq produced compounds with strong binding affinity for the estrogen receptor but bereft of cytotoxicity[354] and one is shown in Figure 2.2.

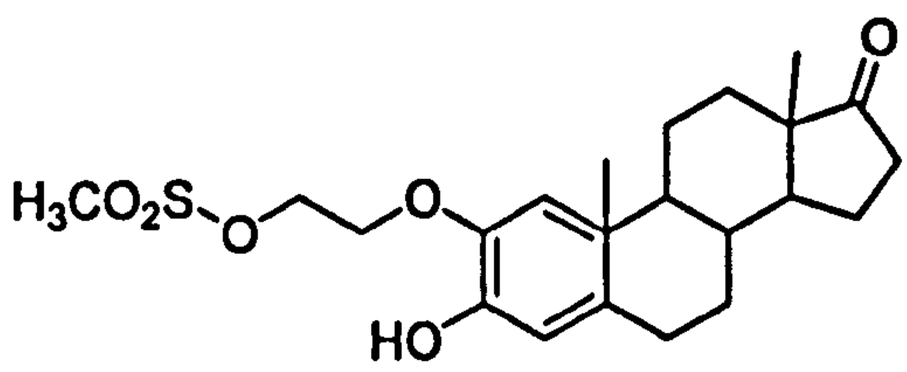

Figure 2.2. A mesylate derivative of the estrogen estrone.

The group of Leclercq turned to synthetic estrogens as vehicles for cytotoxic agents using hexestrol- and diethylstilbestrol-linked to alkylating agents. Hexestrol (Hex) and diethylstilbestrol (DES), whose structures are shown in Figure 2.3, have affinity for the estrogen receptor. Substituted Hex and DES compounds in many cases showed acceptable receptor binding but exhibited proliferative effects in the breast cancer cell line MCF-7.[355-358]

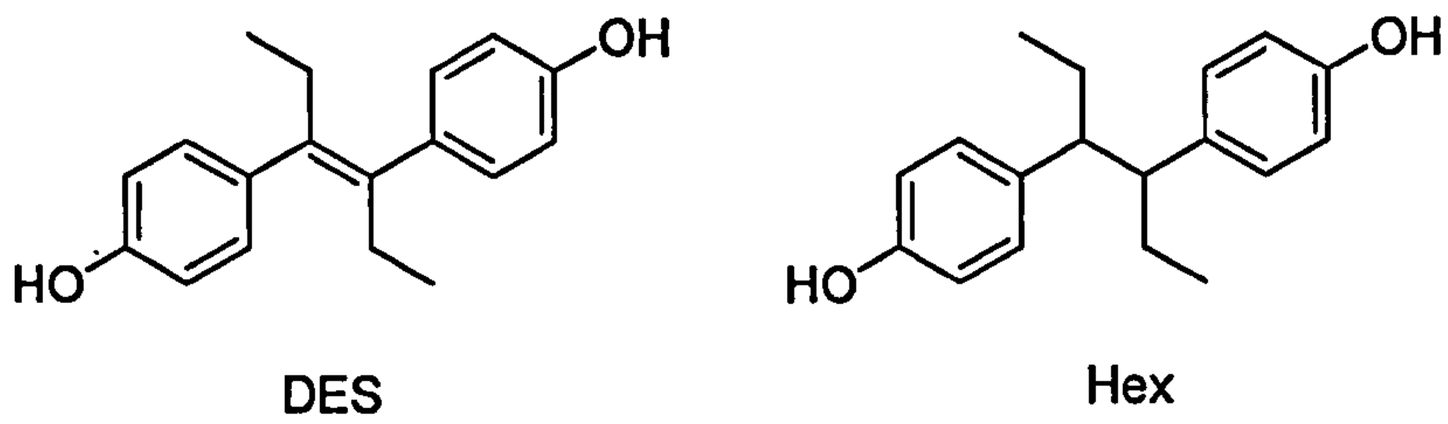

Figure 2.3. The chemical structures of Hex and DES.

2.2.2. Targeting steroid receptors with metal centres

More recently, structures with affinity for the estrogen receptor conjugated to a metal centres by many different groups have been synthesised and are reviewed below. The research possesses two distinct aims; the first as complexes useful for imaging agents and the second as complexes for targeted chemotherapy. Both aims require complexes to be selectively uptaken by estrogen receptors in tumour cells.

For use as imaging agents the group of Katzenellenbogen have used Rhenium(V) and Technetium(V) complexes as mimics for steroids based on androgens, oestrogens and progesterones. The radiopharmaceutical ^{99}Technetium may be used in medical imaging technologies and in these systems part of the steroid is replaced with a chelated metal as shown in Figure 2.4.

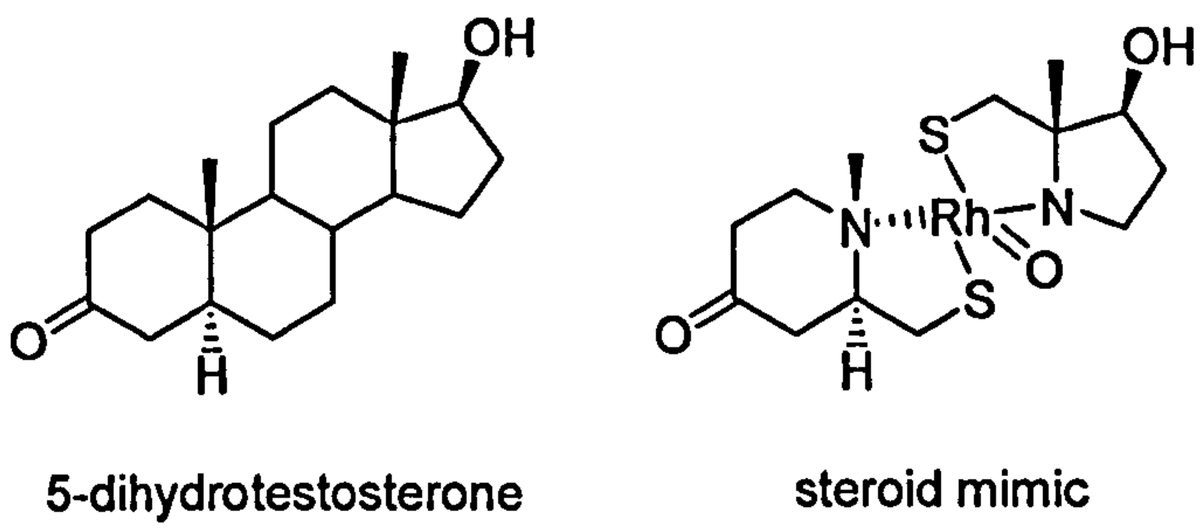

Figure 2.4. Design of a metal complex mimic of the steroid 5-dihydrotestosterone.

In addition to androgens[359, 360] (the family of male steroids based on testosterone), metal complex mimics of the steriods estradiol[361, 362] and progesterone[363] have been reported. This type of design has resulted in unstable complexes and poor affinity for the respective receptors.

Another approach is appending a chelating ligand to a steroid skeleton capable of binding selected metals. Good binding affinities of complexes using steroid skeletons substitued with a rhenium or technetium chelating system with the bound metal been reported targeting the estrogen[364-376], progesterone[377-379] and androgen receptors.[380] The group

of Jaouen has been very active in this area using steroidal estrogens and non-steroidal estrogens, such as tamoxifen, that are capable of binding metals. This creates radiopharmaceuticals with potential usage as imaging agents or due to cytotoxic properties, for chemotherapy.

These include those based on ruthenium[381-384] and iron[385-392] primarily as cytotoxicity agents and rhenium / technetium[384, 393-400] and metal (Co, Mo, Cr, Os) carbonyls primarily as radiopharmaceuticals for imaging.[384, 401-417] A steroid-linker conjugate is also reported to bind the metals Pt, Pd, Ni, Zn and Re[418]. The structure-activity rules for some steroidal metal complexes have been reviewed recently.[419]

2.2.3. Targeting steroid receptors with steroid-platinum conjugates

Whilst much of the research into steroidal metal complexes has focussed on radioimaging, the possibility of using a steroid as a means of transporting a cytotoxic metal, such a platinum(II) was reported in 1986. The complex uses a 2-amino estradiol, shown in Figure 2.5, as a steroidal ligand capable of binding to platinum. Once bound to platinum(II) the complex exhibits moderate relative binding affinity (RBA) of 8.5% toward the estrogen receptor in MCF-7 cells compared to estradiol (by definition RBA = 100%).[420]

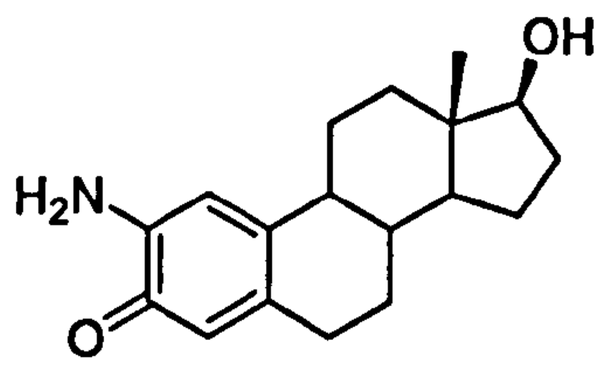

Figure 2.5. A 2-amino substituted oestrogen ligand capable of coordinating platinum.

Georgiadis and Haroutounian[421] report mixed results binding platinum to oestrogen, progesterone and testosterone skeletons. Only one complex achieved activity comparable to cisplatin *in vivo*, depicted in Figure 2.6 with an LD_{50} (the concentration which kills 50% of mice) of 35 mg / kg compared to 15-20 mg / kg for cisplatin.

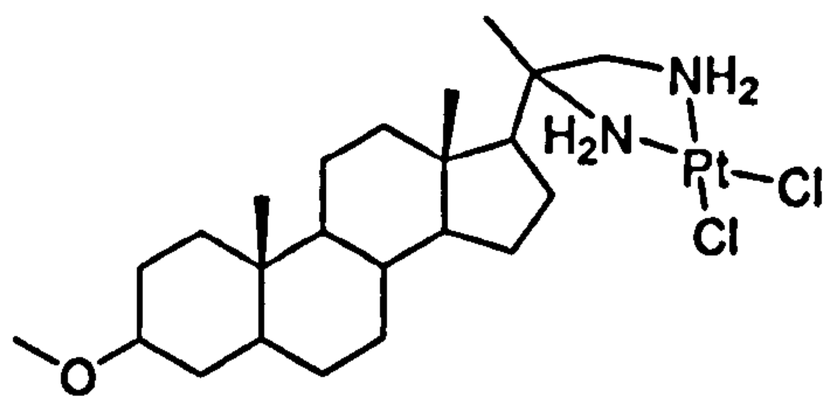

Figure 2.6. A platinum complex based on progesterone designed to bind to the progesterone receptor.

The use of 3-substituted estrone and estradiol steroid skeletons resulted in binding affinities of 0.98 % and 0.57 % for the complexes A and B in Figure 2.7.[422] Despite such poor RBA values, the cytotoxicity of the estrone derivative was comparable to cisplatin in the MCF-7 cell line.

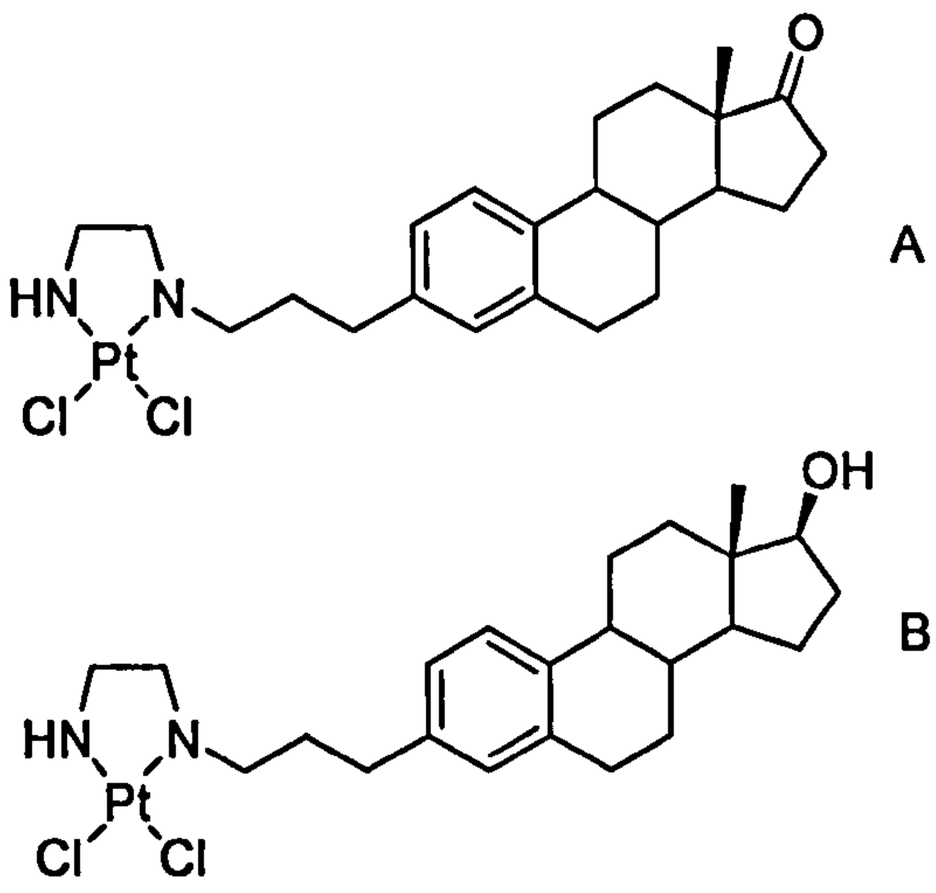

Figure 2.7. The estrogen-derivatised platinum complexes, A based on estrone and B based on estradiol.

Attempts to append a platinum group from the 17 position of estradiol resulted in low binding affinities.[393] These complexes exhibited RBA values of 0.2 % (left) and 0.05 % (right) in Figure 2.8. Cytotoxic testing *in vitro* was not conducted on the basis of these RBA values.

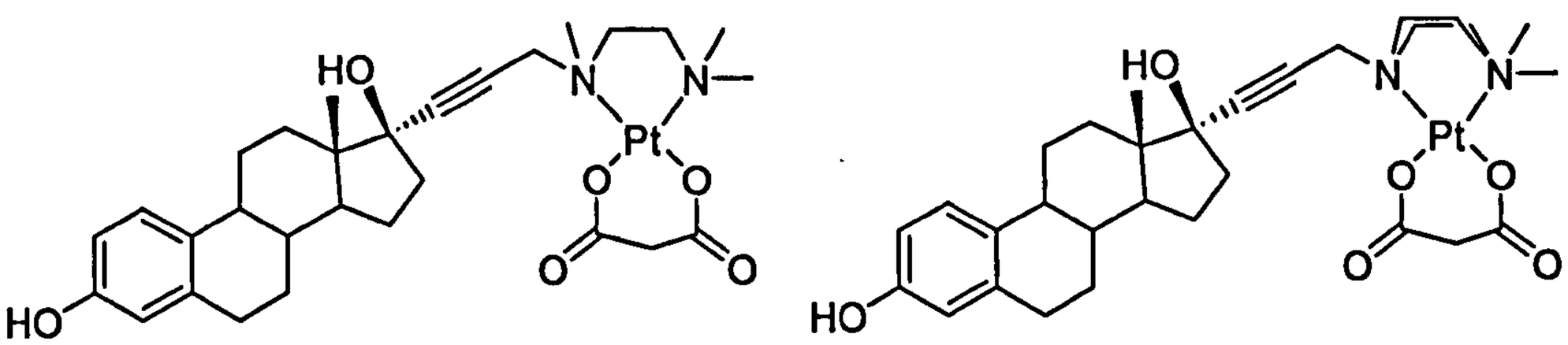

Figure 2.8. Platinum(II) complex with 17 substituted estrogens as ligands.

Very recently, during the course of this thesis, modification at the 16 position of estradiol has resulted in a set of complexes displaying high affinity for the estrogen receptor. The structure, based on a 2-aminopyridine chelating group joined via an alkyl chain to the 16 position of estradiol is shown in Figure 2.9.

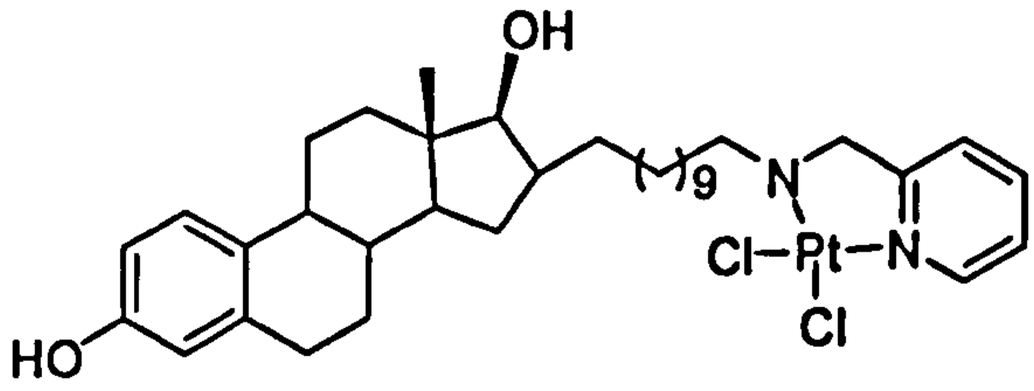

A

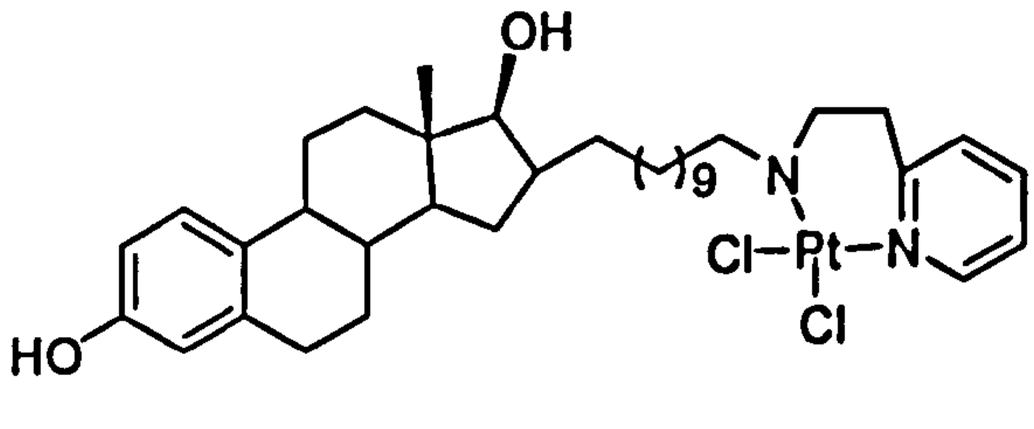

B

Figure 2.9. Steroidal platinum complexes based on oestrogen showing high affinity for the ER.

Complex B in Figure 2.9 was found to possess a high affinity for the alpha form of the estrogen receptor and has 20 – 32 (~ 0.5 μM) fold greater cytoxicity than cisplatin and tamoxifen in MCF-7 cells. Complex A in Figure 2.9 exhibits 2 - 3 fold higher toxicity in MCF-7 (5.9 μM) cells compared to cisplatin and tamoxifen.[334] The high level of receptor binding by complex B may relate to the observed levels of cytotoxicity but further work is required to prove this hypothesis. Additional work led to the development of the structure shown in Figure 2.10. The addition of a CH_2OH group in the 16 position of the steroid is shown by molecular modelling to facilitate extra hydrogen bonding interactions between the steroid and receptor possibly increasing receptor binding affinity which is greater than estradiol.[335]

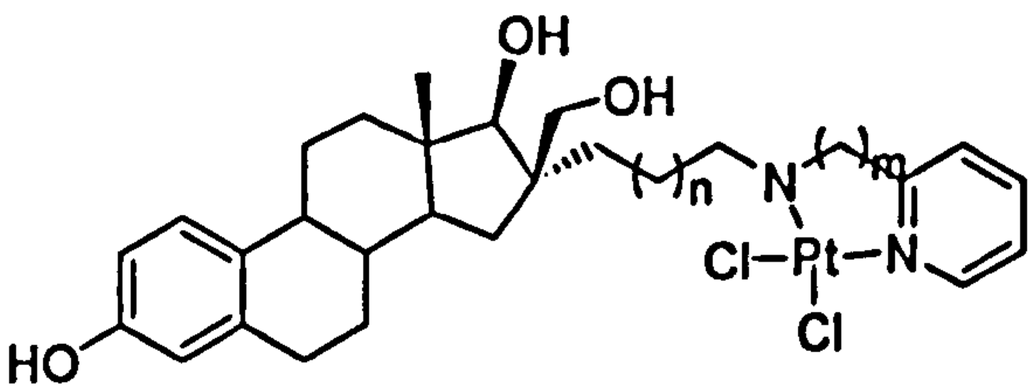

Figure 2.10. A steroidal platinum complex based on oestrogen and targeting the estrogen receptor.

The complex in Figure 2.10 is active against a range of breast cancer lines and the activity is best when n=8 and m=2 and exceeds that of cisplatin;[423] *in vivo* testing is planned.

The group of Schönenberger designed complexes based on synthetic non-steroidal oestrogens and antioestrogens. In a derivatised hexestrol (Figure 2.11) cytotoxicity reportedly begins at concentrations of the order 100 μM in the MCF-7 cells.[424] However, when tested in rat mammary tumours rich in oestrogen receptors the complex is better tolerated than cisplatin and displays higher efficacy. Moreover levels of platinum in the tumour compared to blood plasma were 10.6 fold high compared to cisplatin. A further study on the breast cancer cell lines MCF-7 (ER+) and MDA-MB231 (ER-) showed the complex possessed a poor RBA (0.35 %) and no selectivity for ER+ cells was observed.

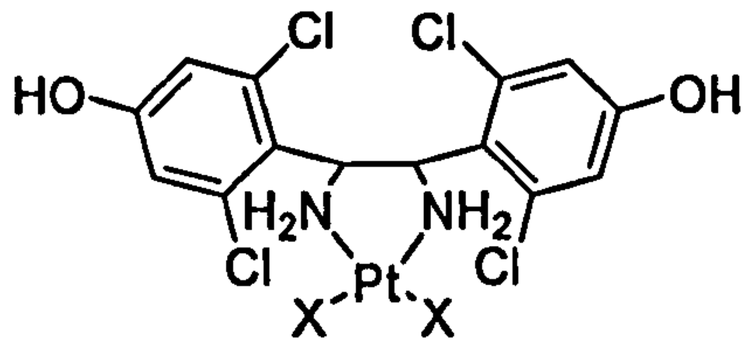

Figure 2.11. A nonsteroidal platinum complex designed to target the oestrogen receptor.

The antioestrogen 5-hydroxy-2-(4-hydroxylphenol)-3-methylindole was linked (via a variable length chain) to a cisplatin-analogue using the indole nitrogen shown in Figure 2.12 (left) in an attempt to target the oestrogen receptor. Selective cytoxicity was observed in oestrogen positive tumours compared to estrogen negative tumours.[424-426] The complex was more cytotoxic than an equimolar dose of the free ligand.

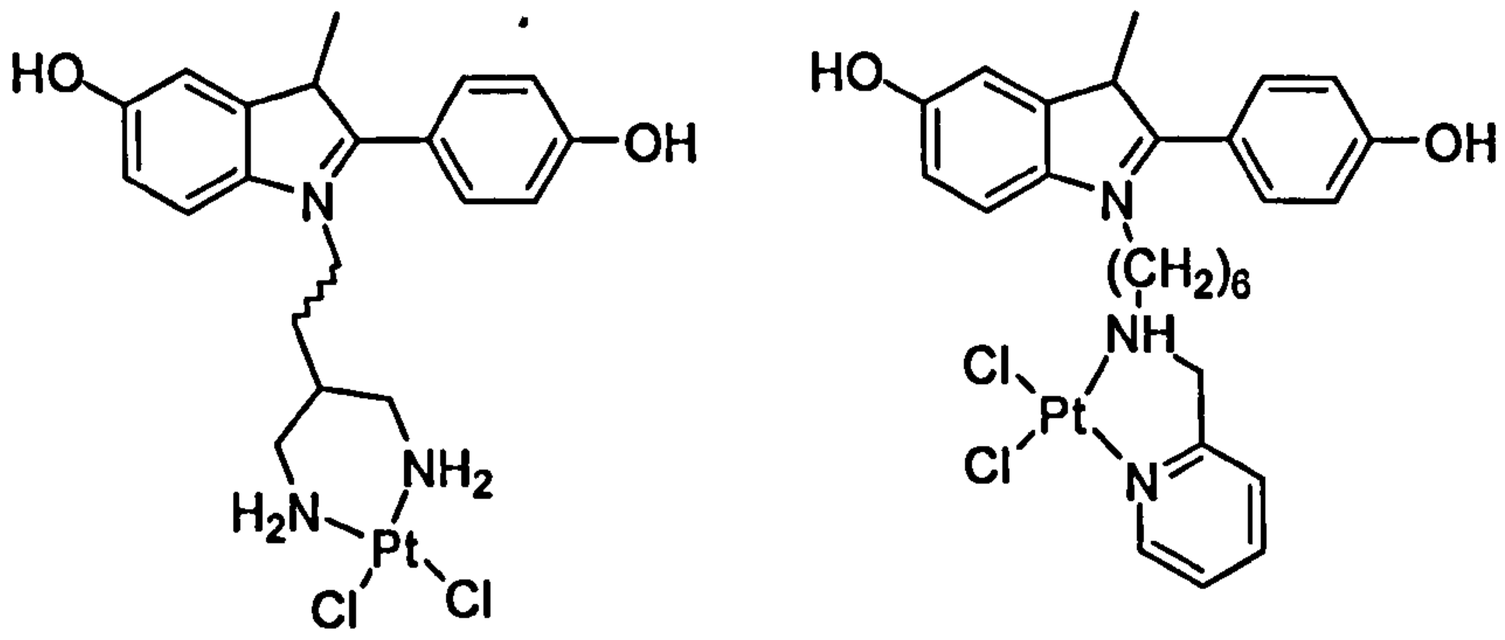

Figure 2.12. Antiestrogen-platinum conjugates displaying cytotoxicity, selective to ER+ tumours.

The complex in Figure 2.12 (right) also shows affinity for the estrogen receptor (RBA= 32 %) and reduces the growth in ER+ mammary tumours *in vitro* and is more potent *in vivo*.[427]

An attempt to conjugate an oxaliplatin analogue to the estrogen receptor ligand tamoxifen was attempted by the group of Jaouen. The complex, pictured in Figure 2.13, have RBA values of 6.4 % (R = OH) and 0.5 % (R = H) and possessed inhibitory effects on MCF-7 cells at concentration of 1 - 10 μM.[428] The cytoxicity of the complex was higher than oxaliplatin. This was attributed to the anti-proliferative properties of the organic ligands and the platinum components produced no measurable effect.

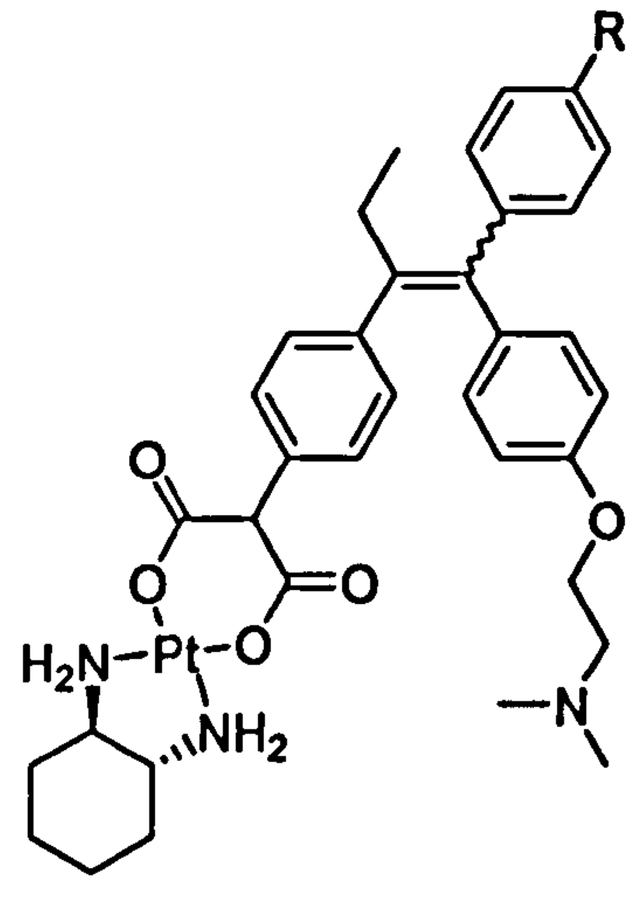

Figure 2.13. A tamoxifen-oxaliplatin conjugate.

Approaches to using steroids have taken many different routes and the lack of *in vivo* testing is particulary noteworthy as extending results from *in vitro* testing to a truly biological enviroment is fraught with difficulty. Despite this since mid-1980 when platinum was conjugated to steroid skeletons, this design has provided complexes with excellent affinity for their respective receptor. Such 'steroidal reagents' may be viewed as the most promising and a review of such complexes follows.

2.3. Steroidal reagents

Steroidal reagents may be defined as "multifunctional compounds based on steroids where one function is non-steroidal in nature". The ability of the steroidal platinum compound to be transported via steroid receptors, in this case the AR, relies on suitably altering the steroidal skeleton and incorporating a binding site for platinum. Unfortunately research into the differential binding affinities for modified testosterones toward androgen receptor is extremely limited. However, structure-function relationships exist between modified oestrogen and the ER and limited data regarding progesterone and its receptor.

The structure of testosterone is very similar to that of oestrogen with the major difference being in the steroid A-ring, phenolic in oestrogen and an α,β-unsaturated ketone in testosterone. Full structural and numerical notations are shown in Figure 2.14.

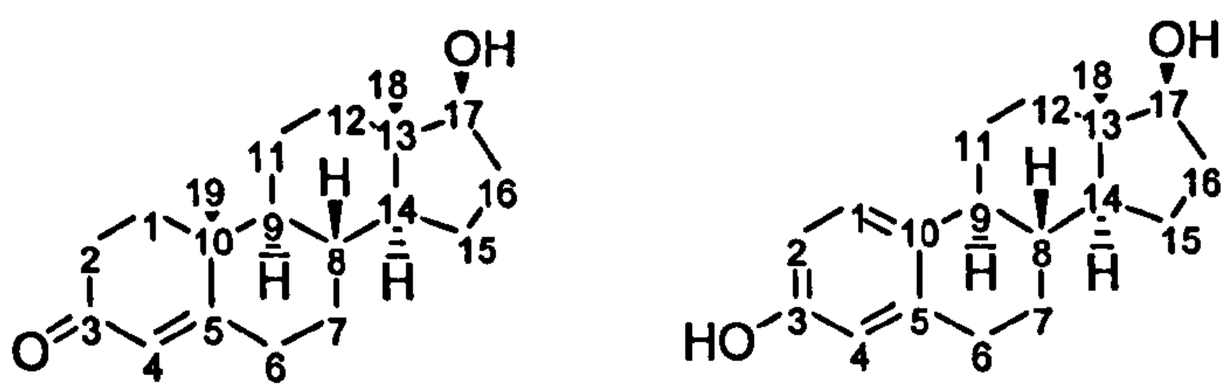

testosterone oestradiol

Figure 2.14. The full structural notation of testosterone and oestadiol; by convention the angular methyl groups 18 and 19 define the upper side or β-face of the molecule. The opposite face or lower side is the α-face.

Structure activity relationships between oestradiol and the ER were reviewed in 1997[419] and report the importance of the phenolic-OH, aromatic A-ring and 17β-hydroxyl in substrate binding. Substitution in the 3 and 17 positions by a methyl ester reduces the RBA to 0.06 %[429] and 7 %[430] in rat ER at 0-4°C indicates the importance of the 3- and 17β-hydroxyl functional groups. From crystal structure evidence presented later regarding the androgen receptor, weak hydrogen bonding interactions are found between amino acid residues and 3-keto and 17β-hydroxyl functionalities. It is likely modification of 3-keto and 17β-hydroxyl groups in testosterone will be detrimental to the RBA of modified testosterones. Anstead *et al*[419] suggests positions on the skeleton tolerating small substituents and those that tolerate larger groups. Small hydrophobic groups are tolerated in the 4, 12β, 14α and 16α positions whilst larger groups are tolerated at 7α, 11β and 17α (Figure 2.15)

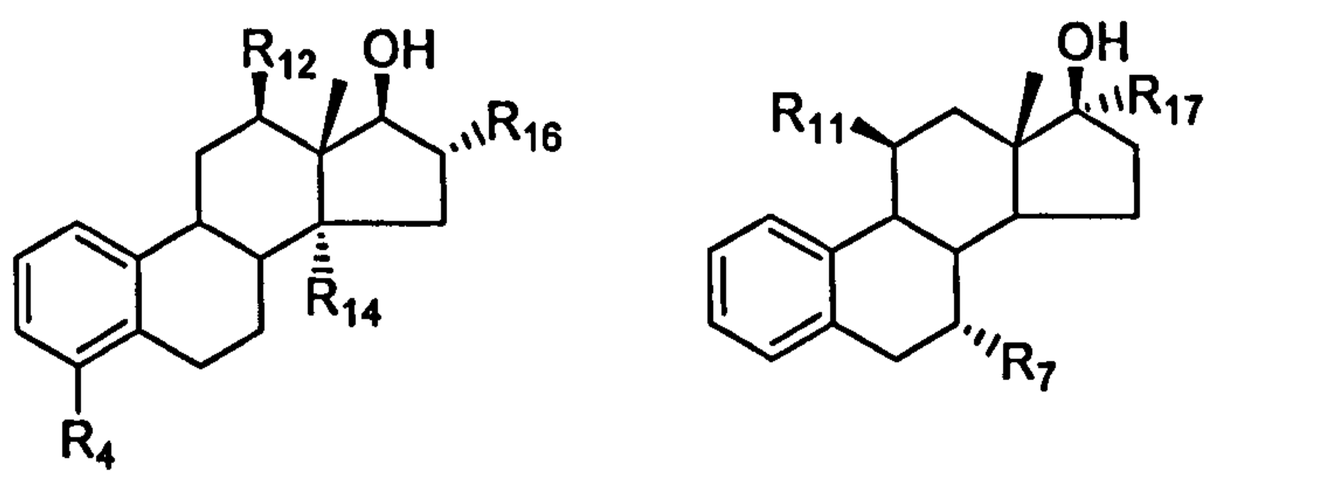

Small substituents tolerated Large substituents tolerated

Figure 2.15. Modifications to the oestradiol skeleton that are tolerated by the oestrogen receptor

The A ring of oestradiol has been modified in attempting to create organometallic chromium carbonyl complexes. Although not related to testosterone, as it does not possess an aromatic A-ring, modifications indicate steric bulk in tolerated reasonably well below the α-face and not tolerated on the β face.[403] It may be suggested 17α and 7α positions represent a promising position in which to append a platinum moiety. Large substituents are tolerated at these positions in addition to the α-face accommodating steric bulk, characteristics likely attributed to an appended platinum group. Since testosterone has no hetroatoms able to coordinate platinum, a suitable group must be appended to the testosterone skeleton. This logically leads to a 3 compartment design to a steroidal platinum agent; a steroidal domain (for receptor binding), a platinum domain (for DNA binding) and a linker domain (joining steroidal and platinum domains together). Out of the three positions reported to accommodate bulky substituents: 7α, 17α and 11β, modifications to the 7α and 17α position will be considered in terms of the RBA value of respective receptors (little data on 11β modification exists). It is approximated that an RBA of >1% is required to observe selective uptake is receptor positive tissues.[431]

2.3.1. 7α substitution

Skaddan *et al*[369] successfully targeted the oestrogen receptor substituting at the 7α position of oestradiol with metal binding sites at the end of an alkyl chain. The relative binding affinities of the compounds ranged from 8-45 % and are shown in Table 2.1. Rhenium is used as a surrogate for ^{99m}Technitium, actually used in radioimaging but expensive to produce and presenting difficulties in handling.

Table 2.1. The relative binding affinity of a selection of modified oestrogens for the oestrogen receptor.

7-alpha substituent	RBA (25°C)	
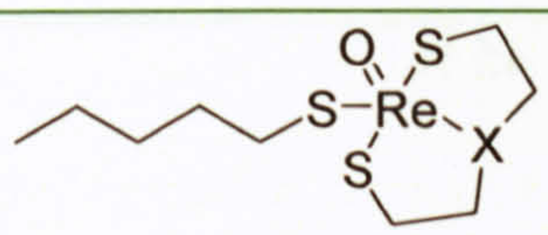	21 %	X=S
	20 %	X=O
	45 %	X=NMe
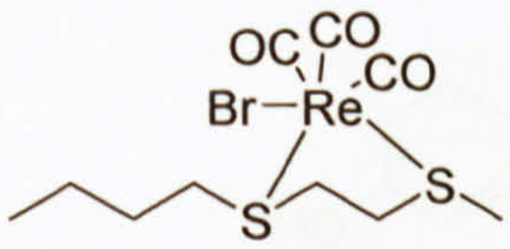	15 %	
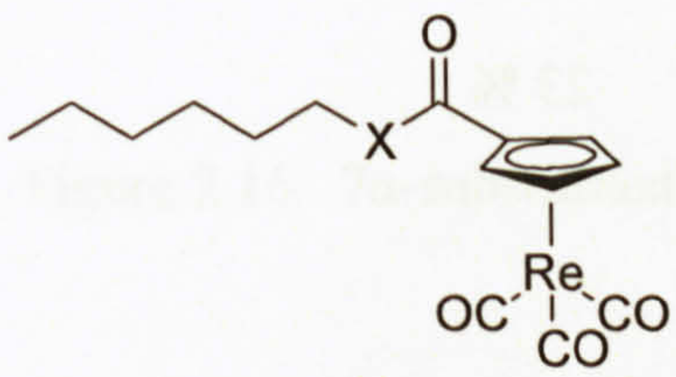	8 %	X=O
	24 %	X=NH
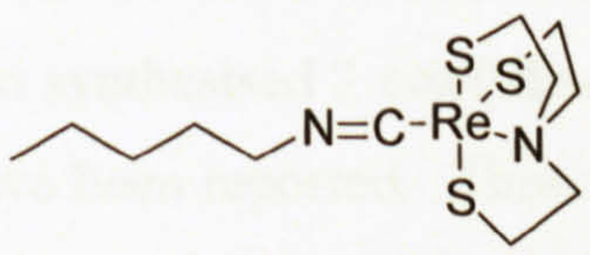	15 %	
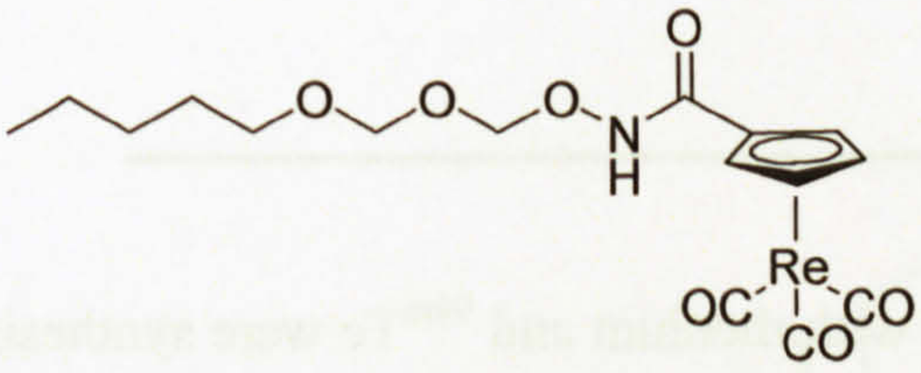	23 %	
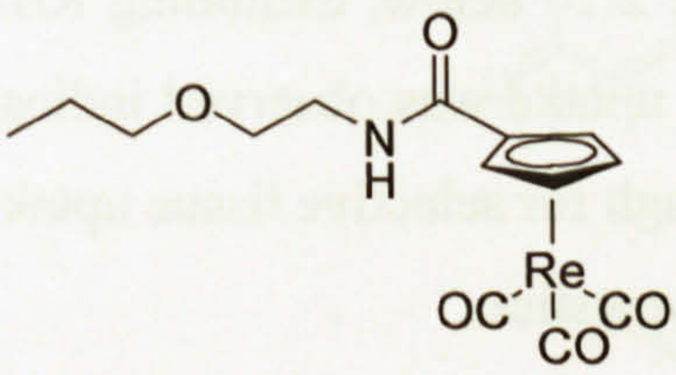	20 %	

Skaddan *et al*[376] report further 7α-substituted oestrogens resulting in RBA values for the oestrogen receptor between 20-45%. The authors describe the use of ^{99m}Tc in place of rhenium in the four complexes in Table 2.2 and the tissue distribution profile. Low levels of uptake were observed in rats for all four ^{99m}Tc complexes and the authors report, despite good RBA values, the observed uptake was not receptor mediated.

Table 2.2. The structures and RBA of several rhenium complexes for the oestrogen receptor.

7α-substituent	RBA (25°C)
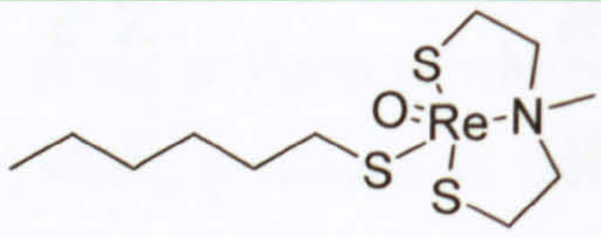	45 %
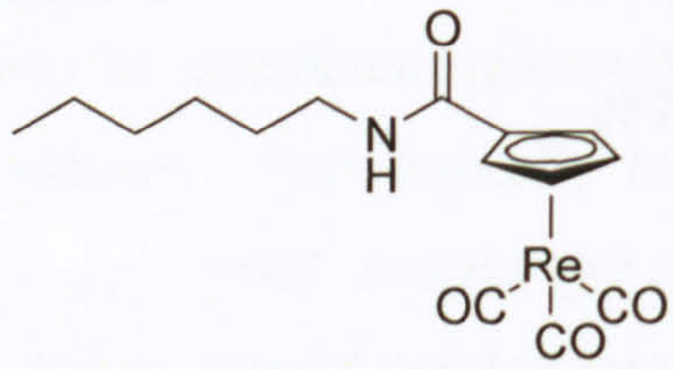	24 %
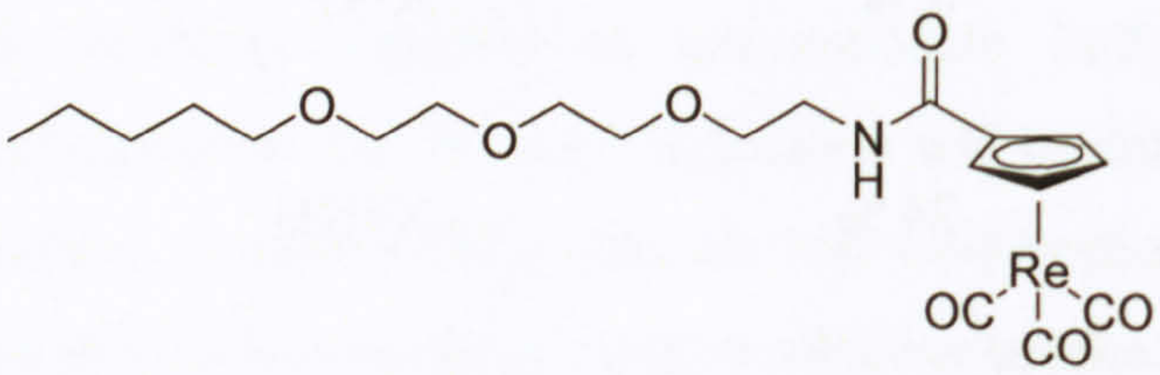	23 %
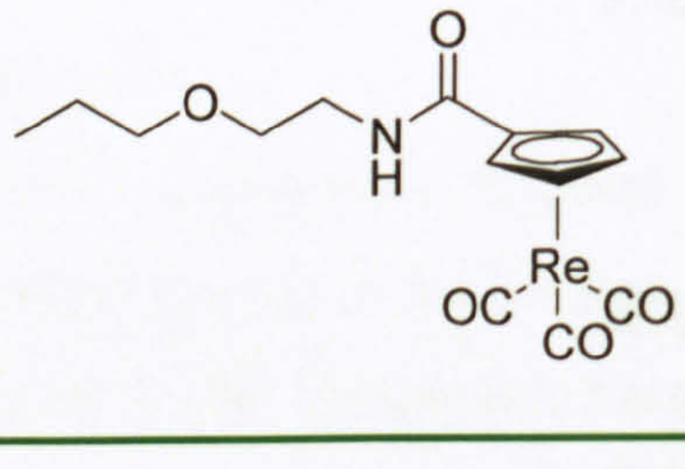	20%

Two further 7α-substituted oestradiol complexes with rhenium and ^{94m}Tc were synthesised by Luyt *et al*[372] with compounds A and B, in Figure 2.16 below, exhibiting RBA values of 18 % and 1.9 % respectively. No tissue selective uptake was observed indicating that good affinity for respective receptors alone is not enough for selective tissue uptake. What other indicators hold prognostic value remains a valid question.

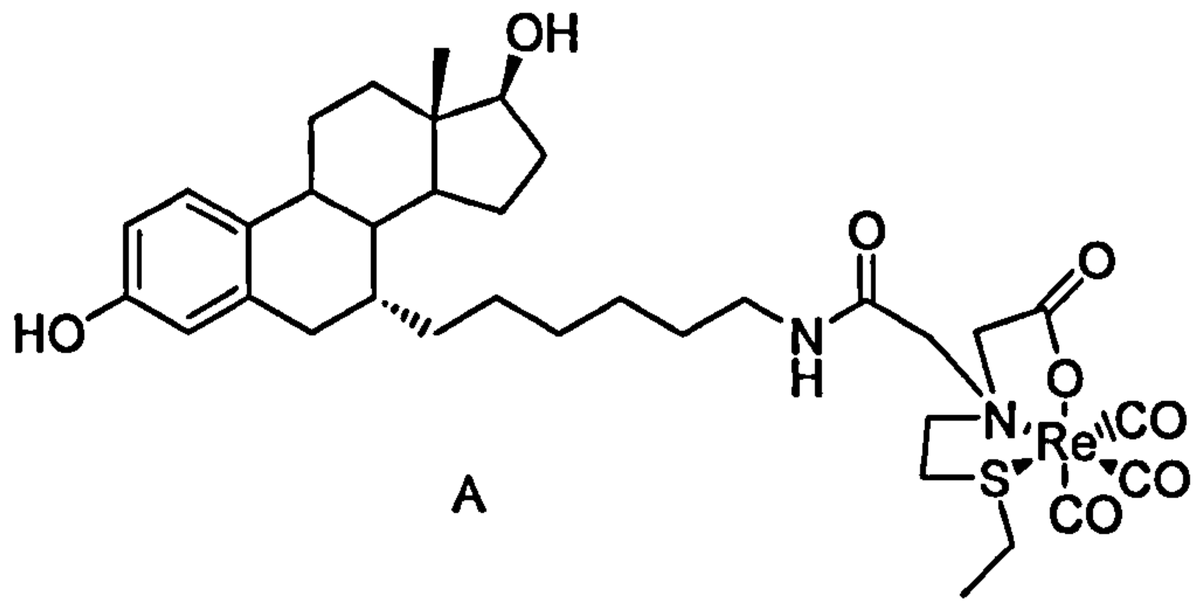

A

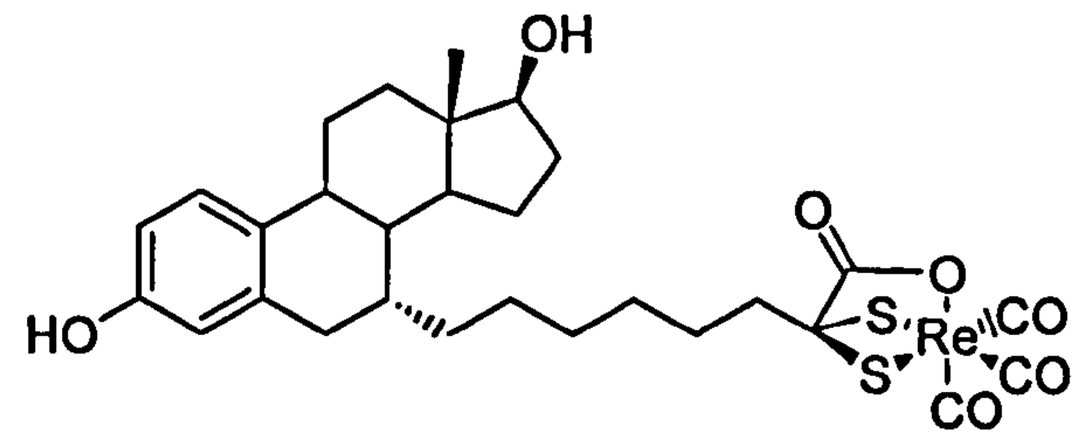

B

Figure 2.16. 7α-substituted oestradiol compounds complexed to rhenium.

Rhenium complexes of testosterone, modified at the 7α-position are reported by Wüst *et al*[380] who synthesised 2 complexes, shown in Figure 2.17 below. Unfortunately no RBA values have been reported. These are the only 7α-substituted testosterones to the author's knowledge.

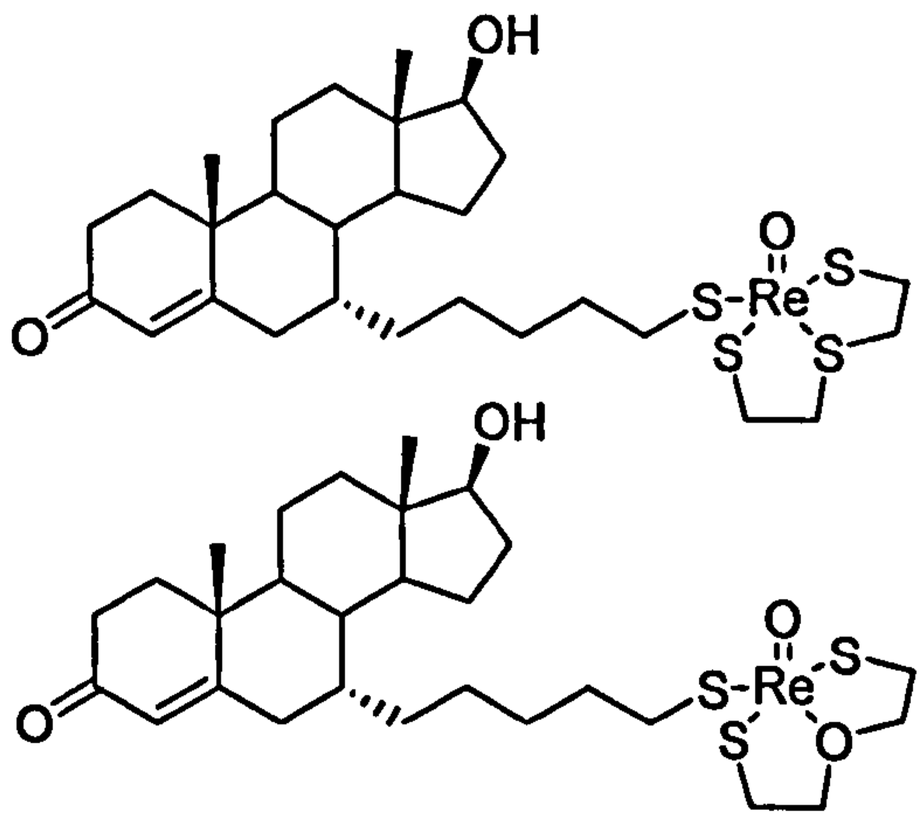

Figure 2.17. Rhenium complexes with 7α-modified testosterone as a ligand

Modification of the 7α-position of the steroid skeleton with an alkyl chain and chelating group has shown itself to be an excellent method in forming steroidal metal complexes with good affinity for the target receptor. Several problems exist when substituting at this position. Such modification is synthetically time consuming and often requires >8 steps to achieve the final product and despite good RBA values no selective uptake in target tissue

(breast for example) has been noted. One possible cause of this is the lipophilicity of steroidal metal compounds. The compounds tend to have a greater lipophilicity that oestradiol. Relatively high lipophilicity is thought responsible for non-specific tissue uptake.

2.3.2. 17α substitution

Salman *et al*[432, 433] reports on the affinity of 31 compounds, based on 17α-substituted oestradiol, for the oestrogen receptor derived from rats. Some of the highest RBA's were reported for rigid groups such as ethynyl spacers and the lowest for less rigid motifs. RBA of selected substituents are given in Table 2.3.

Table 2.3. The RBA of selected compounds, modified at the 17α-position, for the oestrogen receptor.

17α-Group	RBA (%)
	4.9
	4.7
	<0.1
	<0.1
	<0.1
	0.2
	<0.1
	32
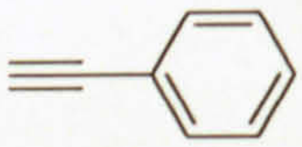	5.8
	7.1
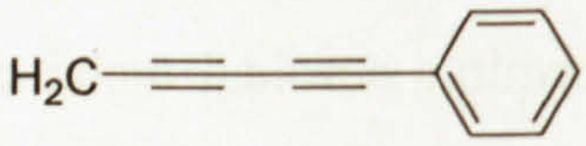	0.4

The data suggests good RBA values are achieved by rigid substituted groups, such as alkyne groups originating at the 17-carbon of oestradiol and this too may be the case for testosterone. Since the reports by Salman *et al*[432, 433] much work has focused on modification of steroids at the 17-carbon in the α position. For possible use in medicinal imaging Luyt *et al*[372] modified oestradiol at the 17-carbon with a ligand chelating Re and ^{94m}Tc with two different spacers. The RBA toward the oestrogen receptor were 0.25 % and 0.14 % for complex A and B, in Figure 2.18 respectively.

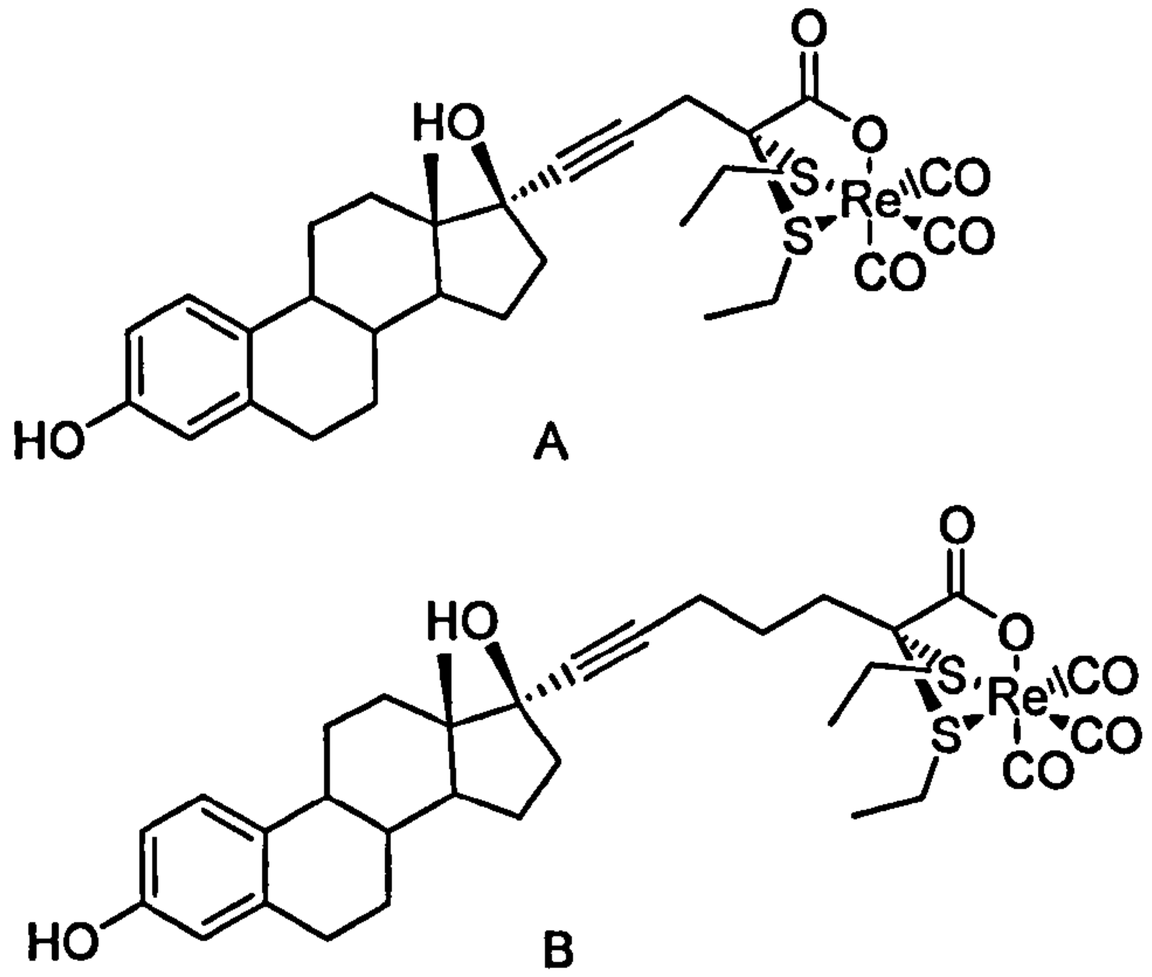

Figure 2.18. The Re complexes synthesised by Luyt *et al*[372].

A large number of ligand and complexes based on modified steroidal skeletons have been reported by the group of Jaouen at carbon 17. Vessieres *et al* modified the ligand in Figure 2.19 which possesses RBA's of 389 % and 251 % for the progesterone and glucocorticoid receptors, respectively. Substrates for the glucocorticoid receptor are adrenal hormones often involved in metabolism of carbohydrate, protein and fat.

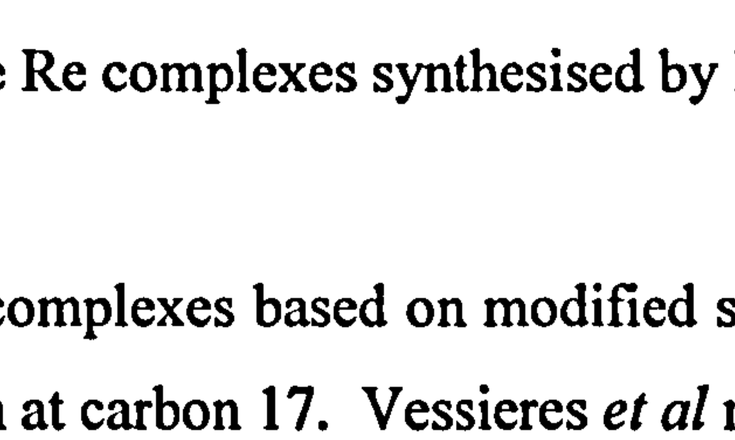

Figure 2.19. The chemical structure of mifepristone or RU 486.

Synthesis of organometallic mifepristones results in dramatically reduced affinity for the oestrogenreceptor. Coordination of $Co_2(CO)_4$ and Mo(cyclopentadiene)$_2(CO)_4$ to the ethnynyl and benzene groups result in RBA values falling from 389 % to 10-20% for the PR and from 251 % to 8-29% for the GR. Whilst the drops are substantial the actual RBA values of 8-29% are higher than the 1 % thought enough for selective tissue uptake.[431]

Further investigations by Amouri *et al*[384] showed 17α-substitutions of oestradiol by rigid allyl groups allows retention of a acceptable affinity for the oestrogen receptor. The coordination of $Cr(CO)_3$ had little effect on the RBA of the steroidal chromium complex (Table 2.4)

Table 2.4. Rigid substituents at the 17α-position and the RBA for the oestrogen receptor

17α-substituent	RBA (25°C, lamb cytosol)
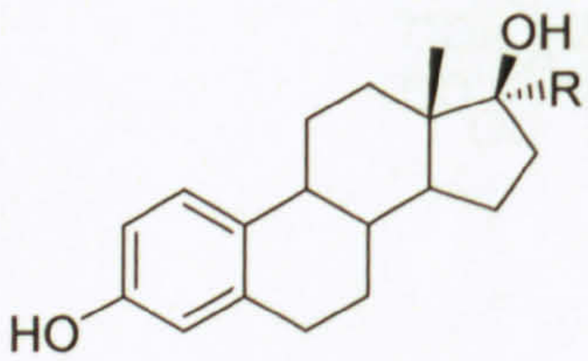	25 %
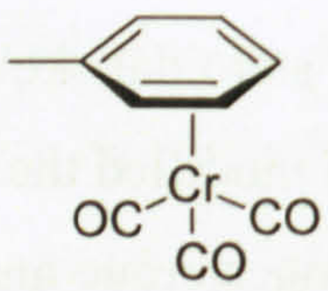	11 %
	27 %
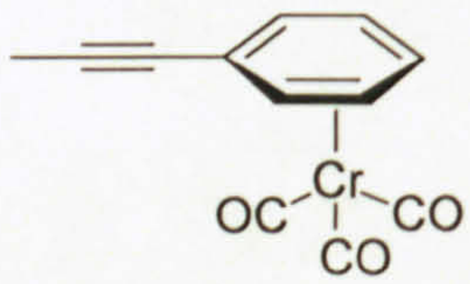	24 %

Use of rigidity in 17α-modified oestradiols has resulted in further compounds with good RBA for the oestrogen receptor. Top *et al*[399] report the use of 17α-cyclopentadiene for cooridination of Mo and Re proving modification by ethnynyl based groups at the 17α-position can result in good affinity for the respective receptors, shown in Table 2.5.

Table 2.5. The RBA of selected modified oestradiols.

17α-substituent	RBA (25°C, lamb uterus)
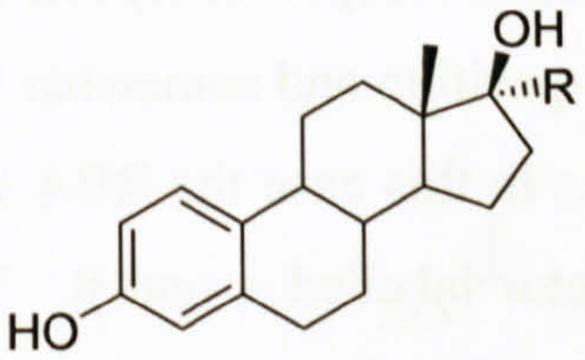	15 %
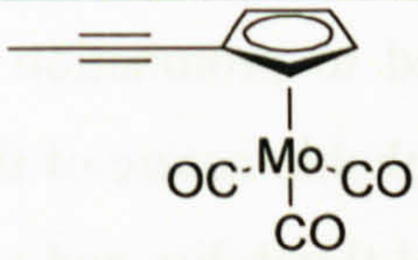	16 %
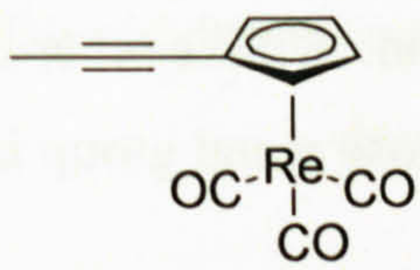	

Binding a metal direct to the 17α-ethnynyl group can result in similar binding affinities to those observed using ethnynyl-pyridine and ethnynyl-cyclopentadiene as metal cooridination sites. For example $Mo_2(Cp)_2(CO)_4$ bound to 17α-ethnynylestradiol, shown in Table 2.6 has a binding affinity of 16 %. This RBA value is significantly reduced from the RBA of 17α-ethnynylestradiol itself (70%).

Table 2.6. The RBA of selected modified oestrogens

17α-substituent ([M])	RBA (25°C, lamb uterus)
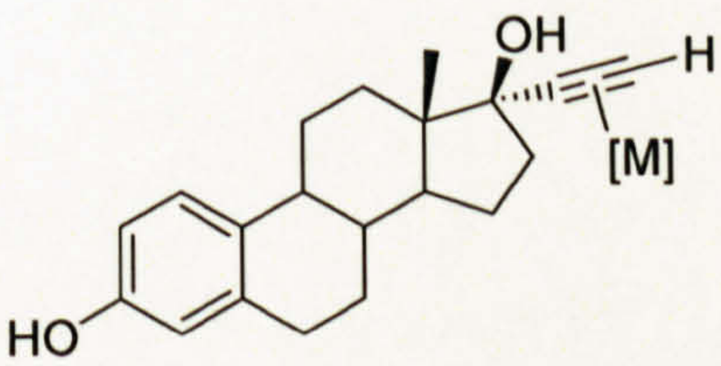	70 %
[M]=$Co_2(CO)_6$	5 %
[M]=$Mo_2(Cp)_2(CO)_4$	16 %
[M]=$Os_3(CO)_{10}$	0.5 %

There are examples of poorer RBA using 17α-modified oestradiol and Osella *et al*[396] reports on 3% affinity for the oestrogen receptor of the complex shown in Figure 2.20 despite the rigid linker used. Even poorer affinity for the oestrogen receptor is reported by Cassino *et al*[393], again using a rigid ethnynyl group at the 17α-position and somewhat less rigid moieties for binding platinum(II), shown in Figure 2.21. In this case the RBA was determined for the two different types of the oestrogen receptor labelled α and β. The uncoordinated ligands achieved RBA of ≤0.15 % and between 0.04-0.16 % for the platinum(II) complexes. The poor binding was attributed to protonation of the amino group, likely detrimental to binding, considering the hydrophobic nature of the LBD of the oestrogen receptor. The use of an -C≡C-CH_2- group caused flexibility and relatively close proximity of the platinum(II) centre to the oestrogen skeleton. Unlike other steroidal metal complexes with higher RBA for the respective receptor, whose metal group is further away from the steroid skeleton.

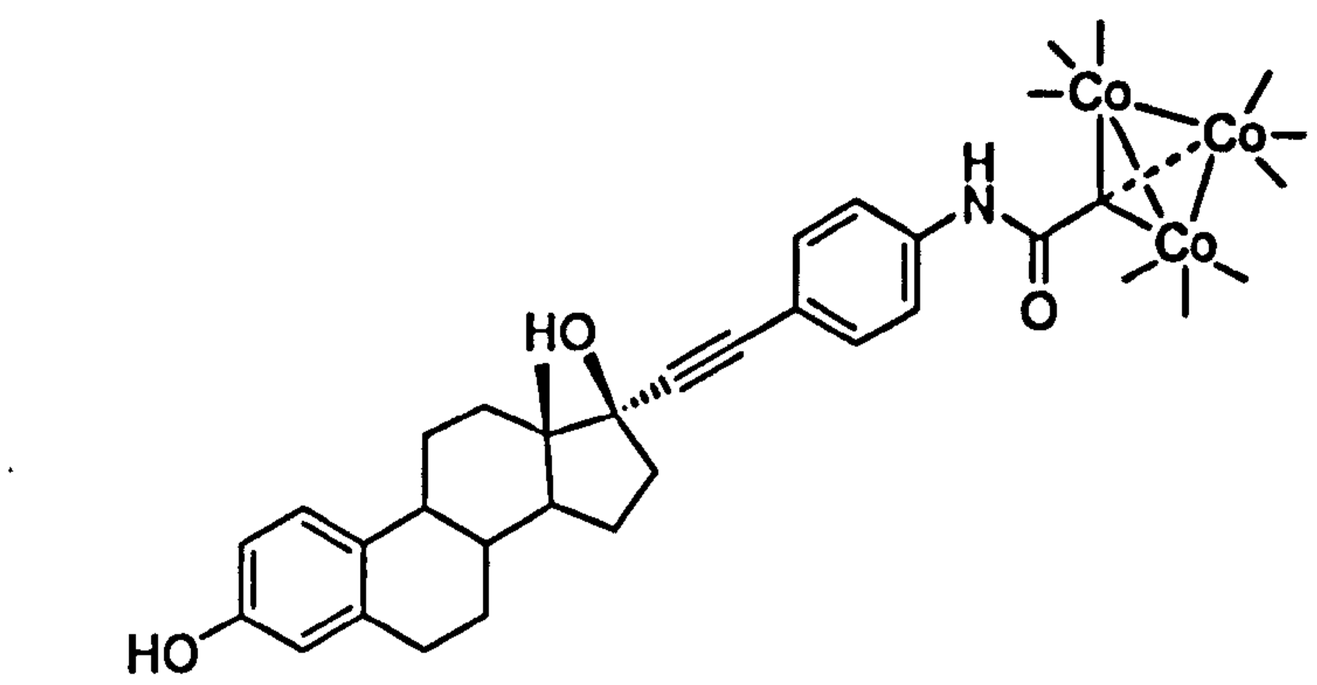

Figure 2.20. An organometallic oestrogen-based colbalt complex with an RBA towards the oestrogen receptor of 3 %.

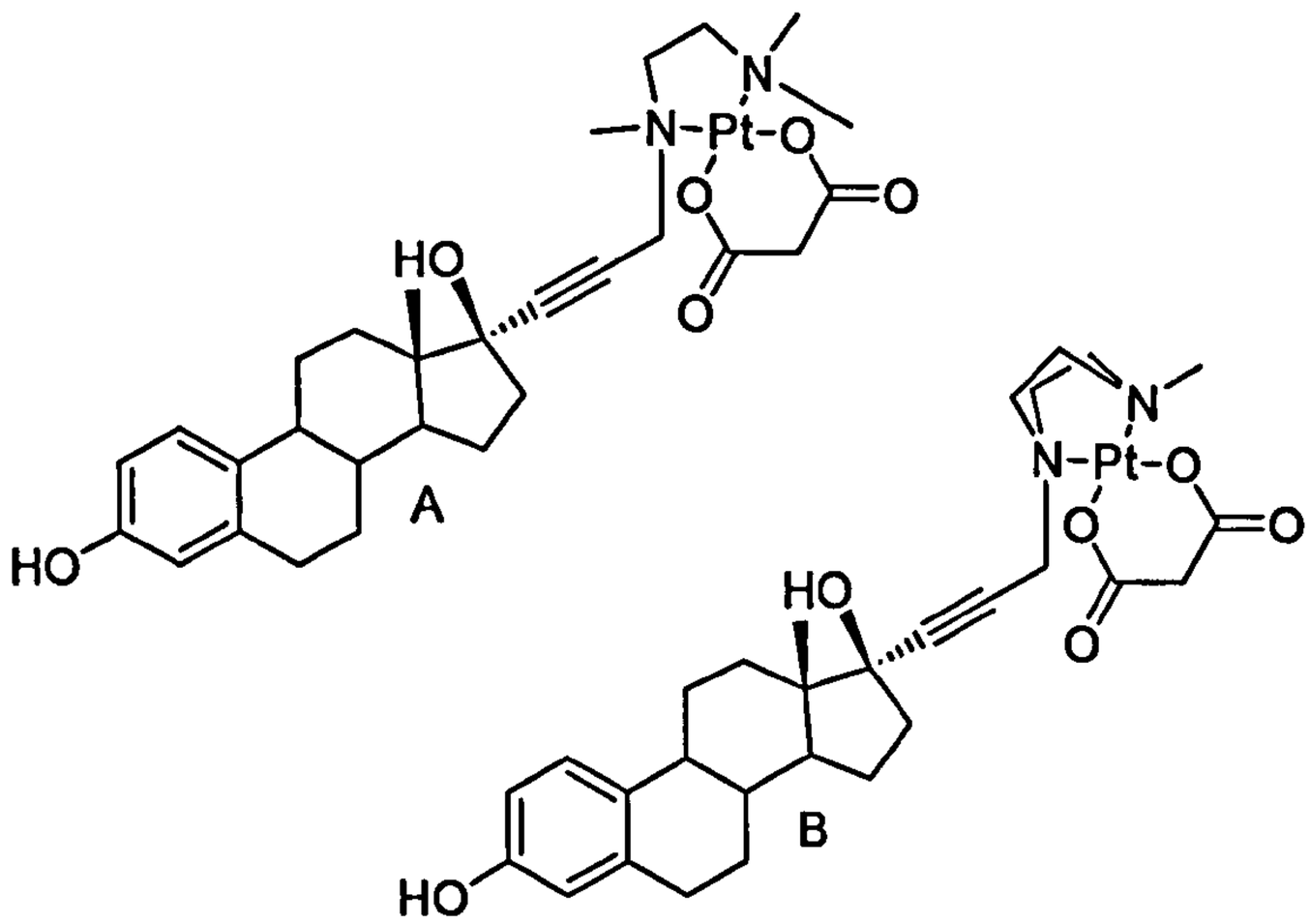

Figure 2.21. Steroidal platinum(II) complexes based on oestradiol using bidentate nitrogen donors and malonato leaving group.

The use of an rigid ethnynyl group followed by a less rigid thioether was used by Wust *et al.*[364] to attach rhenium to an estradiol skeleton as shown in Table 2.7. No *in vitro* testing was conducted on this compound.

The studies of interaction of the oestrogen receptor with substrates allows an idea to be formed of those modifications to the steroid skeleton in testosterone based systems that result in substrates having, to first approximations, an excellent chance of possessing a high enough RBA to be potentially therapeutically useful.

Table 2.7. The RBA of a group of 17α-substituted estradiols

17α-substituent	RBA (25°C, lamb uterus)	
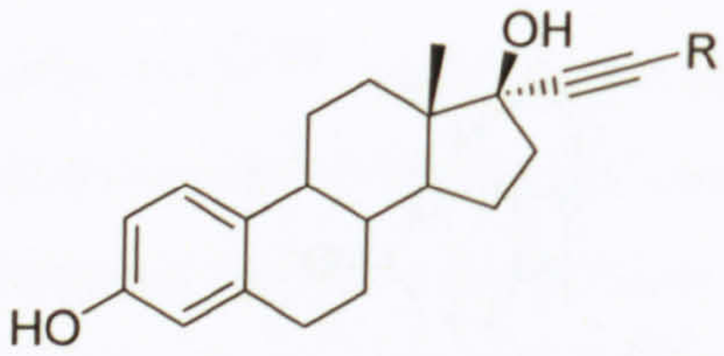		
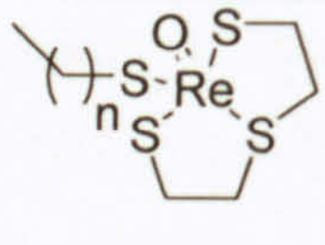	2.3 %	n=1
	7.4 %	n=2
	14.1 %	n=3
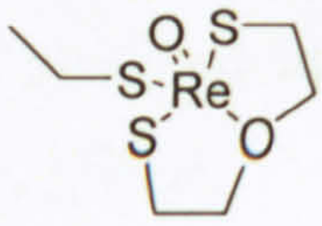	3.6 %	n=1
	7.4 %	n=2
	10.5 %	n=3
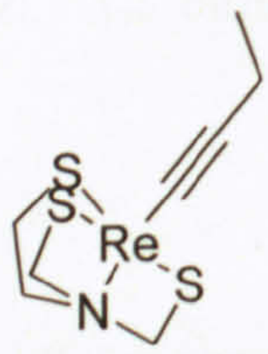	0.6 %	
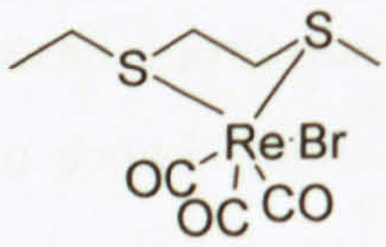	2.1 %	

2.4. Androgens, the androgen receptor and malignant disease

The terms 'androgen' encompasses the male sex hormones or steroids in vertebrates that control or maintain masculine characteristics. The production facilities of androgens are the testes and ovaries (women produce smaller amounts of androgens) producing gonadol androgens, the adrenal cortex adjacent to the kidney producing adrenal androgens and localised production in selective tissues. Testosterone is the major androgenic steriod circulating in plasma and is synthesised using two possible pathways shown in Figure 2.22.[434] Approx 60 % of circulating testosterone is bound to the sex hormone binding globulin (SHBG), 40 % is bound to serum albumin and 1-2 % is circulating freely.[435] The bio-available androgens are found localised in specific tissues including breast, ovarian and prostate.[436] The main function of the androgen receptor is to allows a relatively simple molecule, such a testosterone, once bound to the AR, to control many different biochemical pathways simultaneously resulting in a wide variety biological effects.

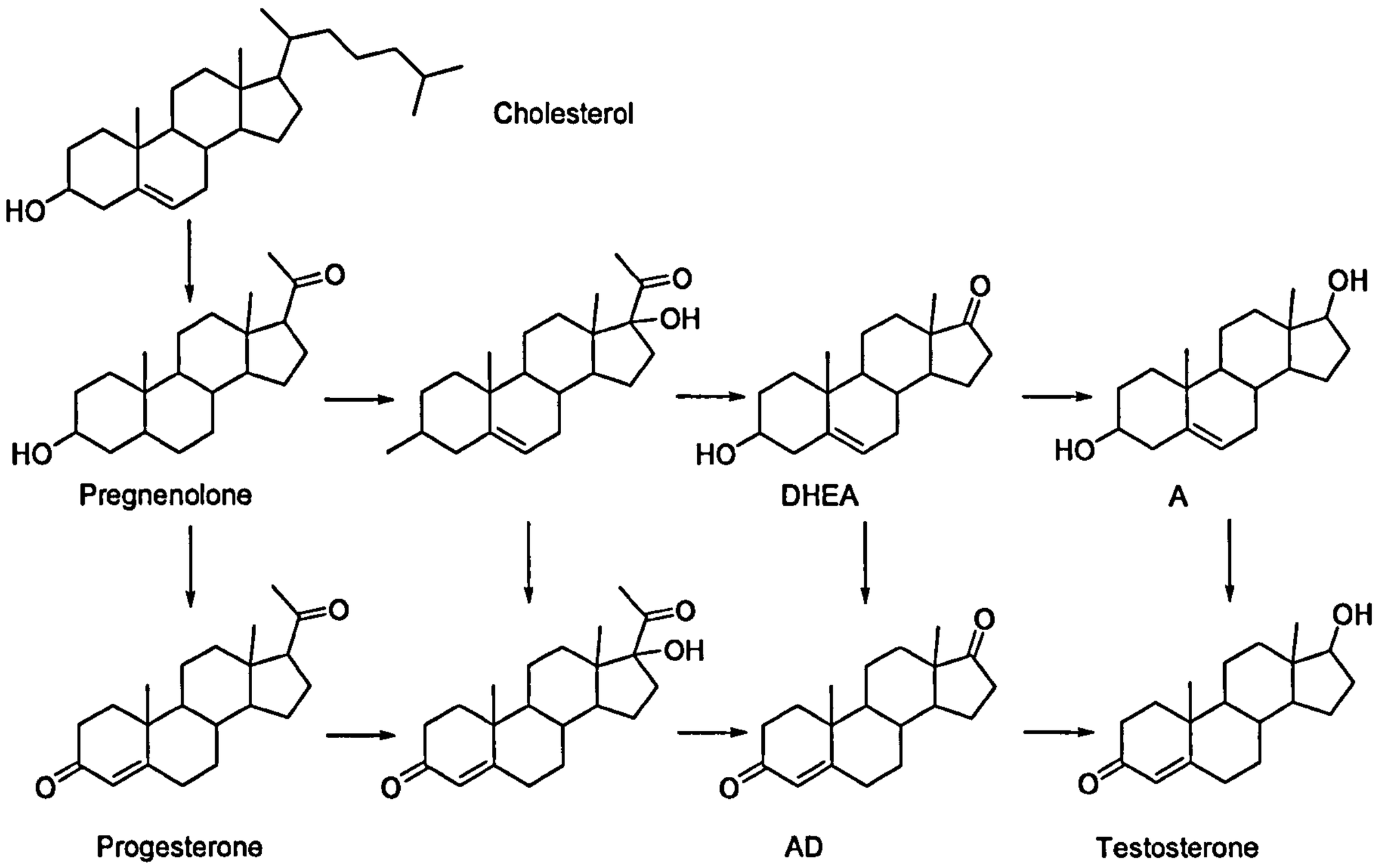

Figure 2.22. The pathways from cholesterol in the biosynthesis of testosterone.

2.4.1. The structure of the androgen receptor

The androgen receptor primarily binds testosterone and its metabolite (via the 5α-reductase enzyme), dihydrotestosterone. Prior to establishing the structure of the AR, the structural details of two of its substrates are required and are shown in Figure 2.23. T and DHT are based on the steroid skeleton comprising the A, B, C and D rings

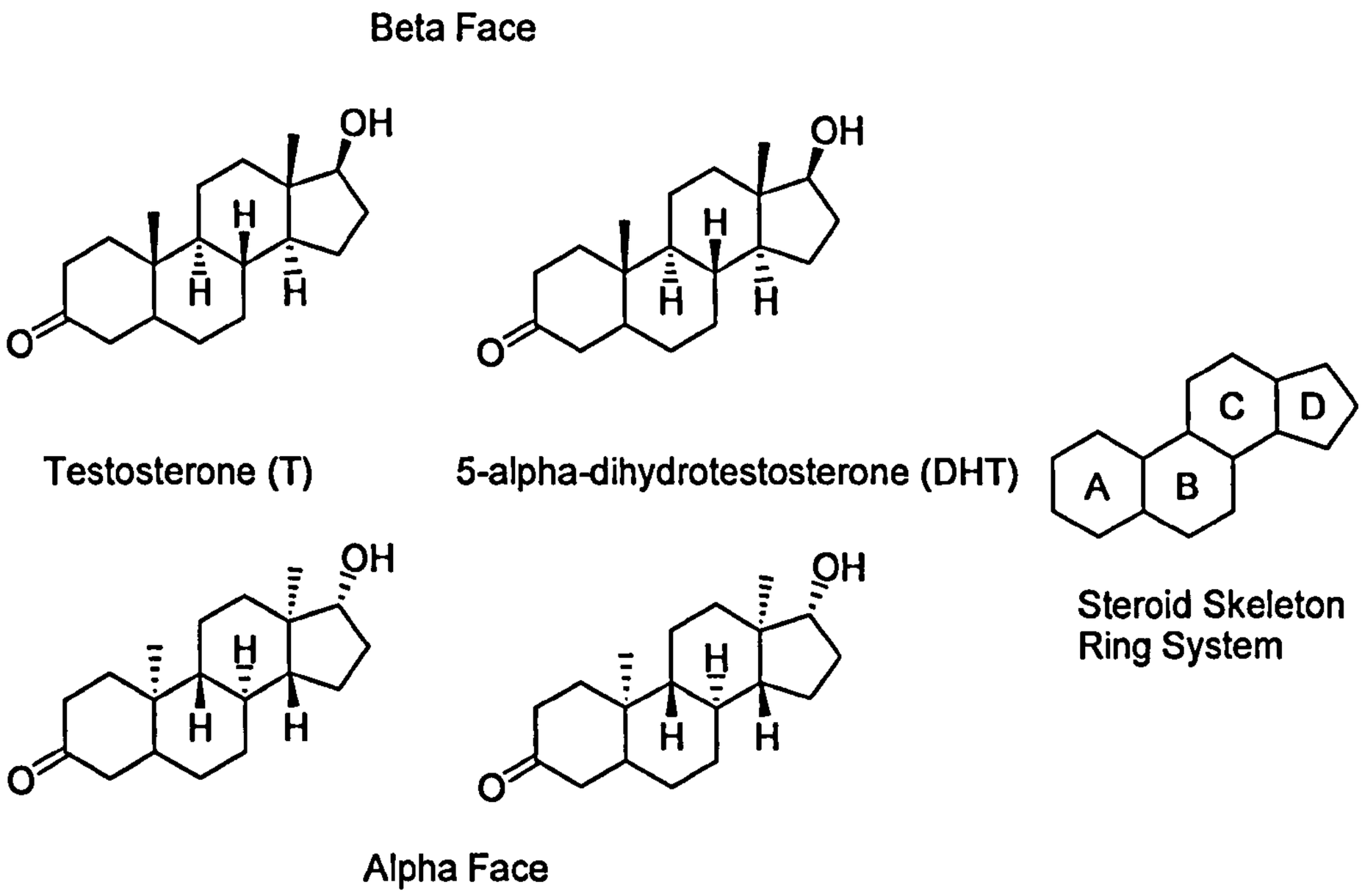

Figure 2.23. The molecular structures of testosterone and dihydrotestosterone showing the two faces of the molecule and the steroid ring system.

The androgen receptor is a ligand dependent nuclear transcription regulator whose gene of 8 exons is located on the long arm of the X chromosome (Xq11-12) and encodes a protein (the AR) approximately 920 amino acids long[437] depending on the number of polyglutamine / polyglycine repeats.[438] Similar to other members of the nuclear receptor family it consists of 3 domains, the NH_2-terminal domain, DNA binding domain (DBD) containing a hinge region and ligand-binding domain (LBD).[439, 440] The NH_2-terminal domain contains a region known as an activation function (AF-1) which activates the receptor for transcription. The DBD is a 68-amino acid highly conserved region and consists of two zinc fingers (loops of amino acids joined by a sulphur-sulphur bridge between cysteine residues) that recognise and bind to DNA.[441] Also in the DBD is a hinge region which signals the requirement for nuclear localisation of the receptor-substrate complex for DNA binding.[442, 443] The structure of the unliganded retinoid X receptor LBD (RXR-LBD), shown in Figure 2.24 is comprised of 12 alpha helixes and 4 strands.[444] The LDB contain an activation function, AF-2 and is transcription inactive in the unbound state. Although no structure of unliganded AR LBD exists, the LBD of nuclear receptors is remarkably similar and RXR-LBD is considered a prototype for all receptor LBDs.[445] Also in Figure 2.24 is the crystal structure of the AR LBD bound with the synthetic androgen metribolone[446] (structure in Figure 2.25) and is similar to the crystal structure of the rat AR LBD bound with DHT.[447]

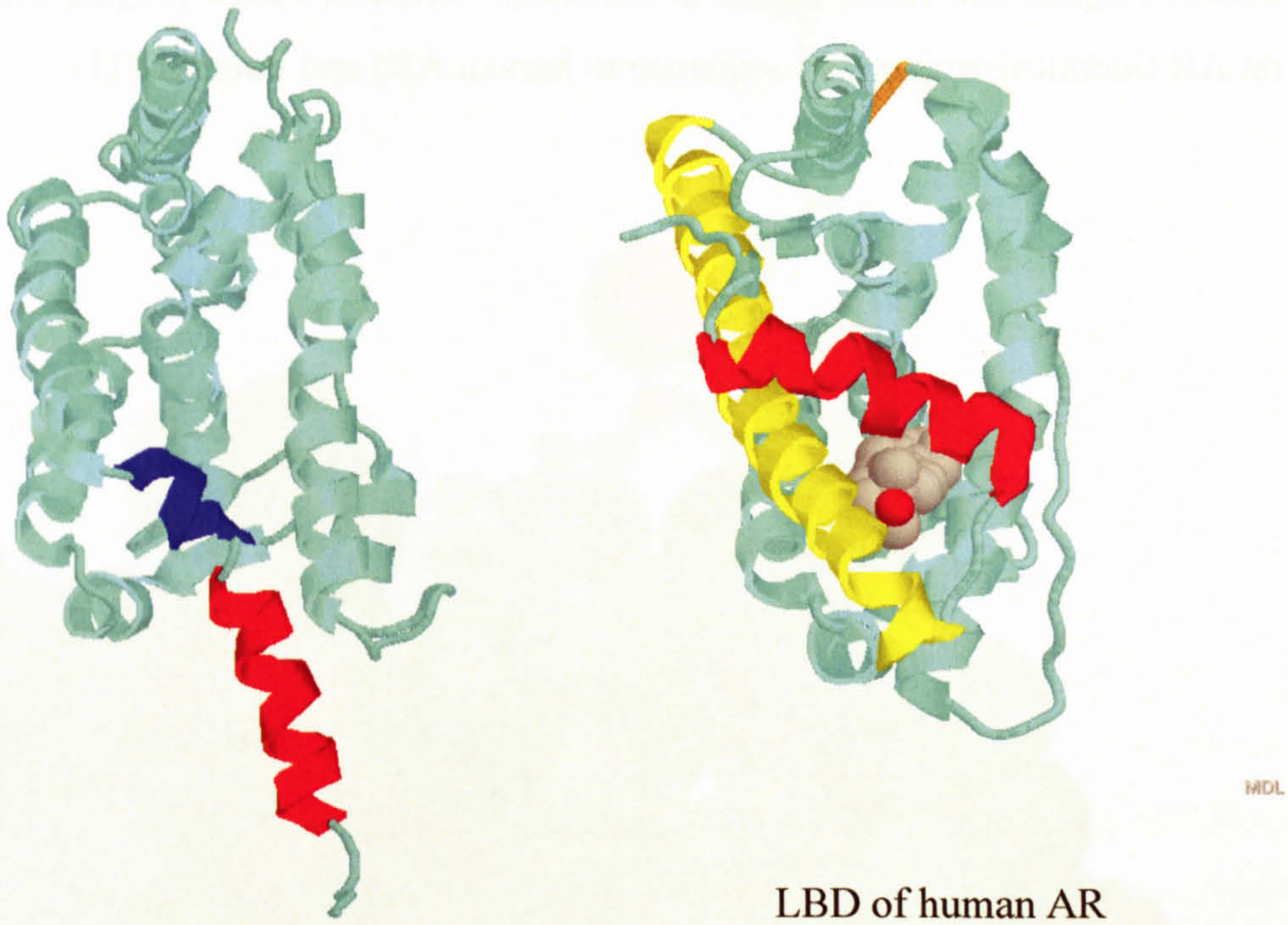

Unliganded LBD
retinoid X receptor

LBD of human AR
binding metribolone

Figure 2.24. The crystal structures of the retinoid X receptor LBD and the AR LBD.[445, 446] Structures have been drawn using Protein Explorer.[269]

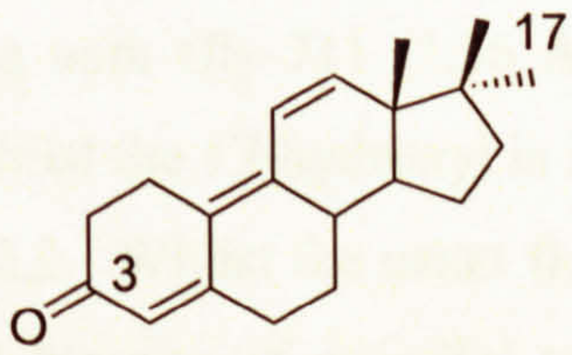

Figure 2.25. The chemical structure of metribolone highlighting the 3 and 17 positions.

In the absence of ligand, helix-12 (red) in Figure 2.24 (left), containing the inactive AF-2 region is found directed away from the LBD and helix-11 partially fills the LBD. Upon binding helix-12 folds back over the LBD, trapping the androgen. Helix-11 is now parallel to helix-10 and formed a single helix with segmentation between helix-10 and helix-11 (yellow). These and other structural changes form the ligand binding pocket in the LBD (shown in Figure 2.26) and aids protein interactions with co-activators of transcription.[448]

The LBP of the human AR is hydrophobic in character. Of the 19 residues interacting with metribolone, 12 are hydrophobic and the remaining 7 polar/charged residues are mostly concentrated around the 3 and 17 positions and involved in electrostatic interactions

between ligand and LBD, shown in the crystal structure below (Figure 2.26 and 2.27) with rat AR (identical amino acid sequence to human AR) and bound DHT.

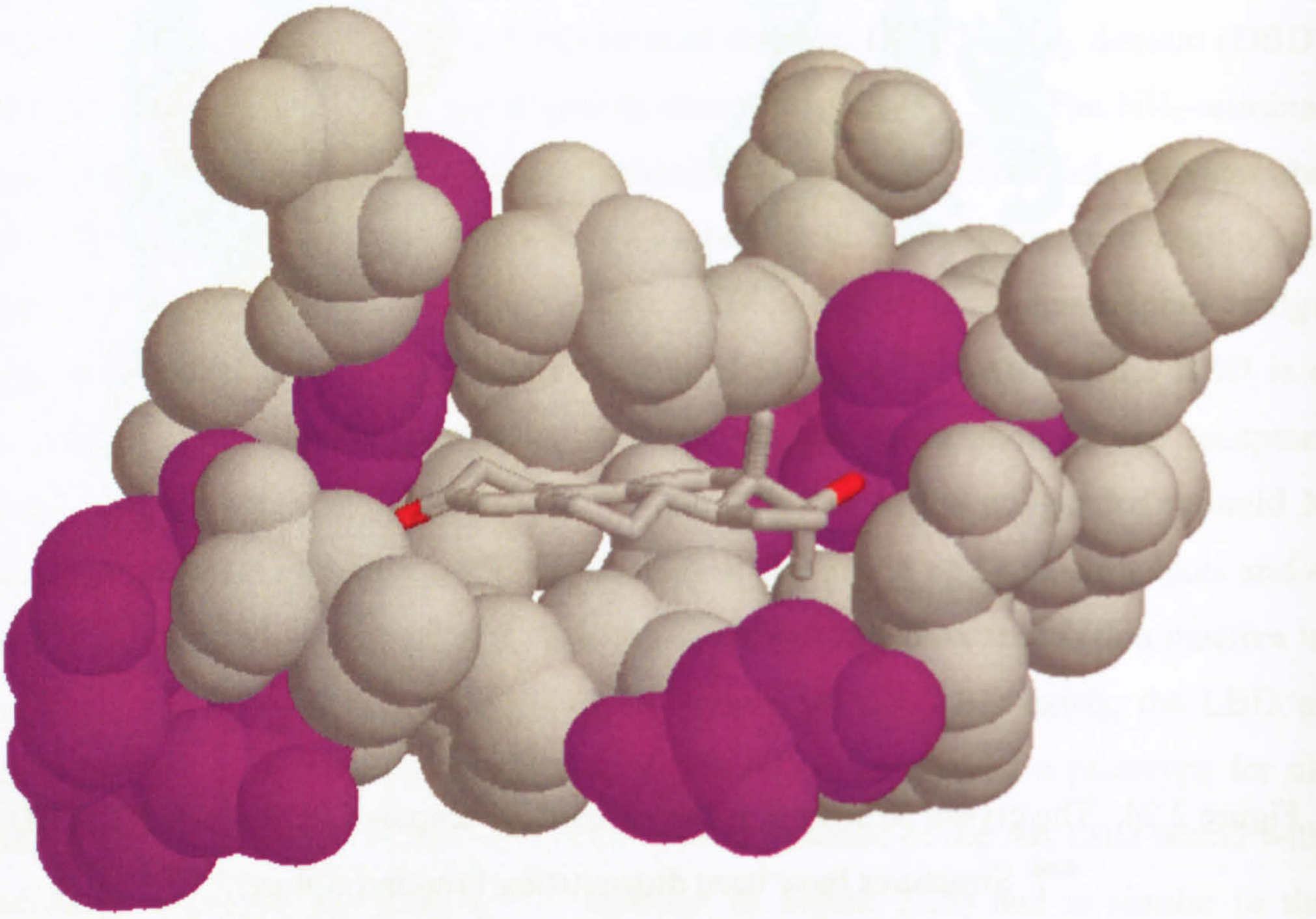

Figure 2.26. The ligand binding pocket (LPB) of the LBD domain of the human AR receptor and bound metribolone.[446] Grey represents hydrophobic residues and purple those residues that are polar/charged in nature.[269]

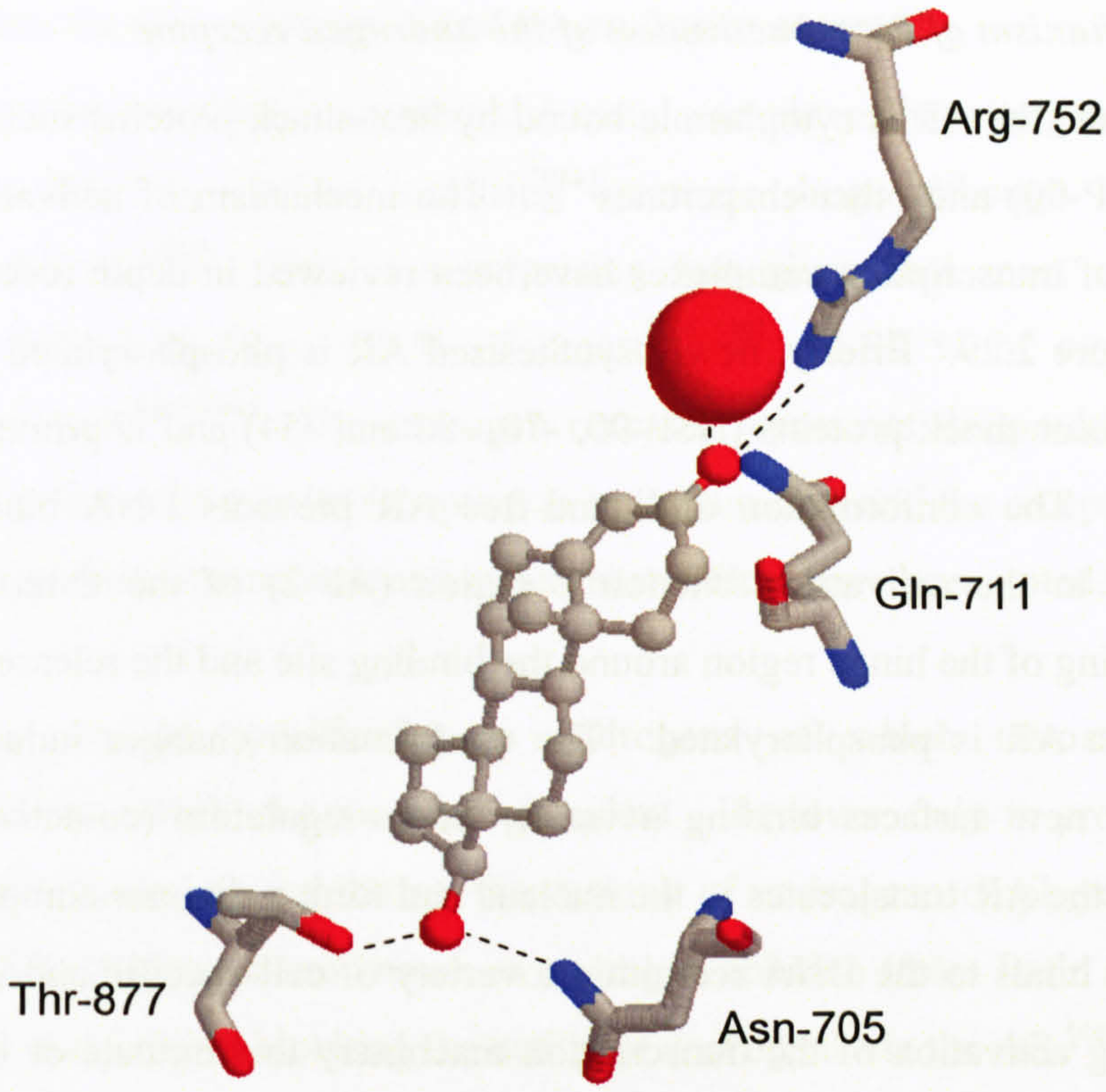

Figure 2.27. The electrostatic interactions between 3-ketone and 17-hydroxyl of DHT and the LBD of the AR.[446]

The 3-ketone group is interacting with Gly-711 (3.36 Å distance) and Arg-752 (2.89 Å) and a water molecule (3.46 Å) whilst the 17-hydroxyl is interacting with Asn-705 (2.80 Å) and Thr-877 (3.36 Å) in Figure 2.2. Whilst the exact free energies are not known for the binding of androgens to the AR binding of estradiol to the estrogen receptor α, with a similar LBD to the AR is known. The free energy contributed by the 3 and 17 functionalities of estradiol, shown in Figure 2.28 are approximately 1.9 kcal mol^{-1} and 0.6 kcal mol^{-1}.[419]

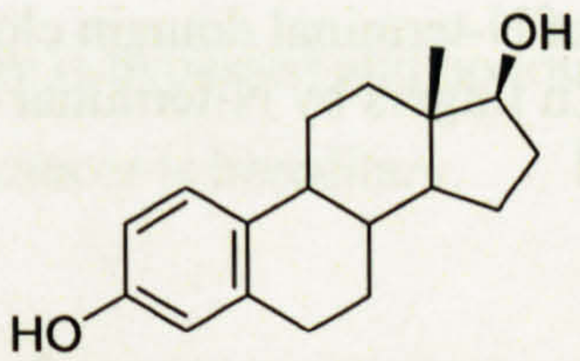

Figure 2.28. The molecular structure of estradiol.

2.4.2. The mechanism of ligand activation of the androgen receptor

Without substrate, the AR is cytoplasmic bound by heat shock proteins such as heat shock protein 90 (HSP-90) and other chaperones[449]. The mechanism of activation of the AR and formation of transcription complexes have been reviewed in depth recently[450-453] are depicted in Figure 2.29. Briefly, newly synthesised AR is phosphorylated and stabilised via binding of heat shock proteins (HSP-90, -70, -56 and -54) and is primarily located in the cytoplasm. The conformation of ligand-free AR prevents DNA binding. Ligand binding occurs in the activation function 2 region (AF-2) of the C-terminus domain facilitating closing of the hinge region around the binding site and the release of heat shock proteins and the AR is phosphorylated. The conformation changes induced by ligand binding expose new surfaces binding a variety of co-regulators (co-activators and co-repressors) and the AR translocates to the nucleus and form a dimmer complex. The AR-AR homodimer binds to the DNA recruiting a variety of cell specific and ubiquitous co-factors, allowing activation of the transcription machinery to stimulate or inhibit gene(s) transcription. This induces the synthesis of a variety of gene products dependent not only on AR-ARE interactions but the levels of co-activators and co-repressors. These gene products are likely to initiate or involve other biological pathways associated with the proliferation and maintenance of malignant disease.

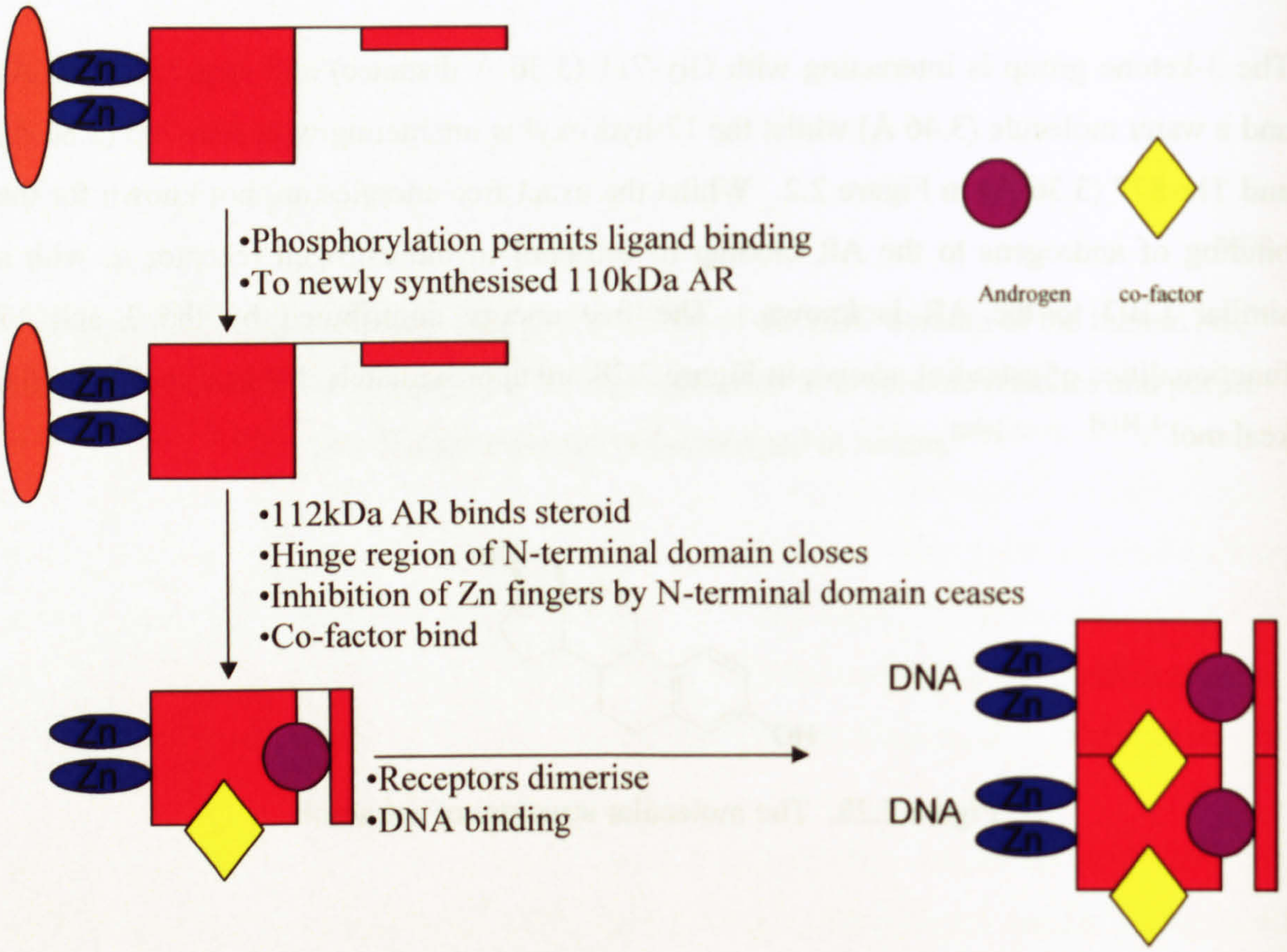

Figure 2.29. A schematic of the steps from AR synthesis to DNA binding.

2.4.3. Malignant disease, androgens and the androgen receptor

To the authors best knowledge no steroidal metal complexes have targeted the androgen receptor (AR) with the aim of localising cytotoxic drugs although it has been for radiopharmaceuticals.[380] This is a surprising fact given that most cancers may be described as AR+ including ~80 % of breast[336-338], 74-90 % of ovarian[454-457] and virtually all prostate.[458-460] The androgen receptor represents the predominant receptor expressed of the three sex steroid receptors in many tumours and the receptor pathways are often not independent, interactions and synergistic effects have been noted.[461]

Many cancers depend specifically on androgens of which testosterone (T) and dihydrotestosterone (DHT) are the most abundant. However, only in prostate cancer are endocrine-based treatments inhibiting the actions of androgens employed, as shown in Figure 3.30. The treatments are known as androgen ablation (from Latin *ablatus* meaning *to carry away)* and involve blocking the action of androgens via the AR.[462] Initial tumour response rates vary between 80-90% but almost all progress to androgen refractory states resulting in mortality occurs. Androgen ablation remains the mainstay treatment for cancer of the prostate although combination therapies involving carboplatin are under investigation.[463]

The AR and its substrates are intrinsically linked with the formation of prostate cancer from normal tissue and mutations and over-expression of the AR are possible candidates.[464] Several mechanisms are proposed for the transition and propagation of refractory tumours and this subject has been reviewed in general recently.[465-471] Proposed pathways for the development of refractory tumours include:

1. AR levels amplified.
2. Overexpression of co-factors involved in AR pathway.
3. Relaxing of ligand specificity (by gene mutation) allows promiscuous activation of the AR by non-androgens.
4. The AR signalling pathway is bypassed and no longer required for cell survival.
5. Susceptibility to prostate cancer is hereditary.

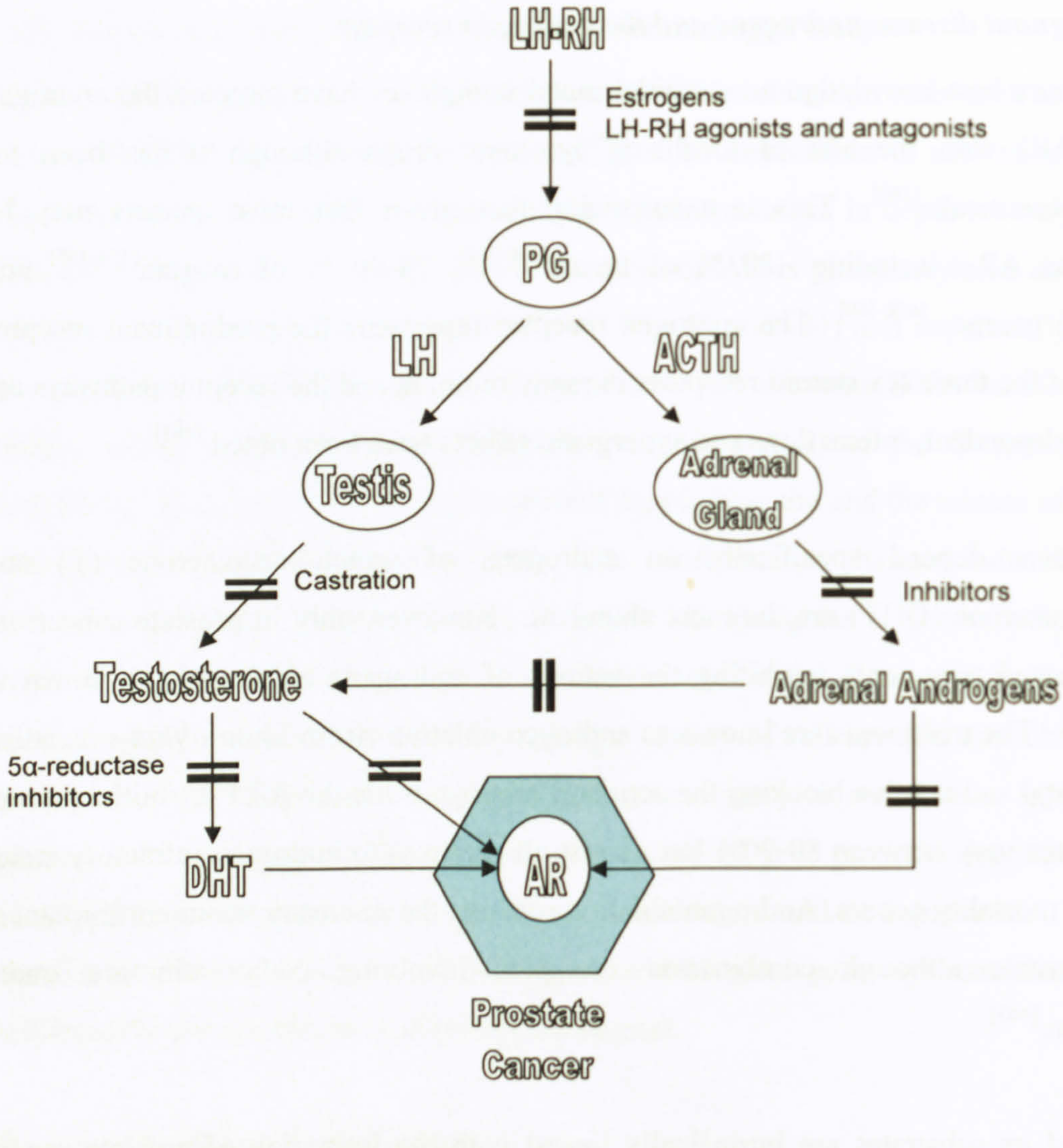

Figure 3.30. Targets used in endocrine therapy in prostate cancer. Lutenising hormone-releasing hormone (LH-RH) is released from the hypothalamus acting on the pituitary gland (PG) which releases lutenising hormone (LH) and adrenocorticotropin hormone (ACTH). Double lines represent current and possible endocrine treatments interfering or inhibiting the connecting pathways and activation of the AR

Despite progression to refractory disease the AR continues to be expressed in substantially all prostate tumours and none of the above pathays reduce the applicability of using the AR as a transporter of cytotoxic drugs. This fact makes the androgen receptor in prostate malignancies a target for steroidal platinum complexes.

The role of androgens in relation to breast cancer has been reviewed recently by Liao and Dickson[472] who suggest several mechanisms (the issue has been reviewed additionally[473, 474]) of carcinogenesis/cartinomatosis in breast tissue:

1. Androgens cause growth stimulation in breast epithelia (membrane tissue covering breast tissue) and breast cancer by biotransformation to oestrogens via aromatase enzymes.[475, 476] This results in an excess of oestrogen resulting in growth stimulation of breast tissue.
2. Low levels of adrenal androgens stimulate breast cancer cell proliferation via binding to the ER in low oestrogens levels situations, i.e. postmenopausal women.

The treatment of breast tumours generally involves endocrine treatments blocking the oestrogen receptor[477] such as tamoxifen or preventing oestrogen biosynthesis such as aromatase inhibitors.[478] Platinum-based chemotherapy is generally not used due to toxicity[479] except in metastatic maligancies.[480] The AR remains a viable target in breast tissue.

Ovarian epithelium tissue, the membrane like tissue coving the ovaries is reported to respond to androgen treatment in primary cell cultures from patients[481] which are the origin of 90% of ovarian cancers.[482] The study demonstrated that treatment with androgens lead to decreased cell death or increased proliferation in 7 out of 9 cell cultures. The role of androgens, in addition to oestrogens, are reportedly involved and are risk factors for developing ovarian cancer[482-484] with possible synergistic effects occurring between oestrogens and androgens.[485] Endocrine treatments are not used in ovarian cancers but many ovarian cancers are treated by surgical removal of malignant tissue followed by carboplatin but most patients eventually relapse.[486, 487] Here too the AR may be used as a transporter of cytotoxic complexes.

2.5. Eplilogue

In cancer chemotherapy few drugs specifically target tumours over normal tissue. Platinum drugs such as cisplatin and newly licensed metal-based cancer therapeutic arsenic trioxide may hardly be called targeted. One of the problems with cisplatin is a lack of tissue specificity. If a cytotoxic drug is designed to specifically target malignant tissue the possibility of overcoming poor tissue specificity of platinum(II) drugs may be addressed.

Since the primary target of chemotherapy is DNA, using an existing cellular mechanism to transport a cytotoxic platinum(II) complex directly to DNA is very appealing. Achieving

targeted metal therapeutics requires hijacking an active transport mechanism present in higher levels in tumour tissue compared to normal tissue. Such a methodology permits many different types and configurations of moieties to be transported using the same vector and the most active selected in pre-clinical trials.

Using the steroid transport system to localise platinum(II) complexes in the vicinity of DNA may result in drugs that target both specific tissue and are also recognised differentially by cellular proteins overcoming several type of resistance mechanisms observed in cells treated with platinum(II) drugs.

Chapter Three - Synthesis and characterisation of steroidal ligands and platinum(II) complexes

3.1. Introduction

3.1.1. Platinum - an introduction

Platinum, from the Spanish *plata* meaning 'silver plate' was discovered in 16th century Columbia and belongs to the family of noble metals that includes palladium. The chemistry of platinum was subject to intense study after its arrival in Europe in the 1740's and the 1st organometallic derivative of platinum known as Zeise's Salt, in Figure 3.1, $K[Pt(C_2H_4)Cl_3].H_2O$ was reported in the 1820s.[488-490]

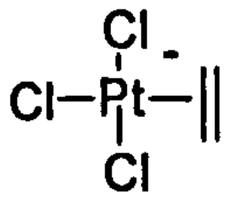

Figure 3.1. The structure of Zeisse's Salt

Platinum exhibits a large range of oxidation states. It exhibits every oxidation state from formal negative oxidation states in carbonyl anion clusters ($[Pt_3(CO)_3(\mu\text{-}CO)_3]_n^{2-}$) to the VI state in PtF_6.[491] The most common oxidation states are II and IV and the II (d^8) state is by far the commonest. The II state is heavily studied, partly due to the ease of forming complexes with a large range of ligands whose donor atoms come from most groups of the periodic table and a number of reviews have been published[492-501]. The most interesting oxidation states, from a chemotherapeutic viewpoint, are Pt(II) and Pt(IV) as both have proven anti-tumour properties.

The +II state exhibits varied coordination numbers from 4 to 6 but 4 coordination represents the vast majority of d^8 complexes (cordination numbers of 5[502-506] or 6[507-509] are known but rare) and exhibits square planar geometry. The square planar structure arises as the most stable configuration for d^8 low spin metals. The approximate relative energies of the 5 d orbitals in several crystal fields are shown in Figure 3.2. In the square planar ligand field the 8 d electrons of Pt(II) occupy stabilised orbitals, leaving the high energy $d_{x^2-y^2}$ orbital unfilled. These relative energy levels are only approximate and from spectral studies of $[PtCl_4]^{2-}$ the d_{z^2} orbital lies below that of d_{xy} and d_{xz} and often depends on the nature of the ligands for a given metal in a square planar configuration.[510]

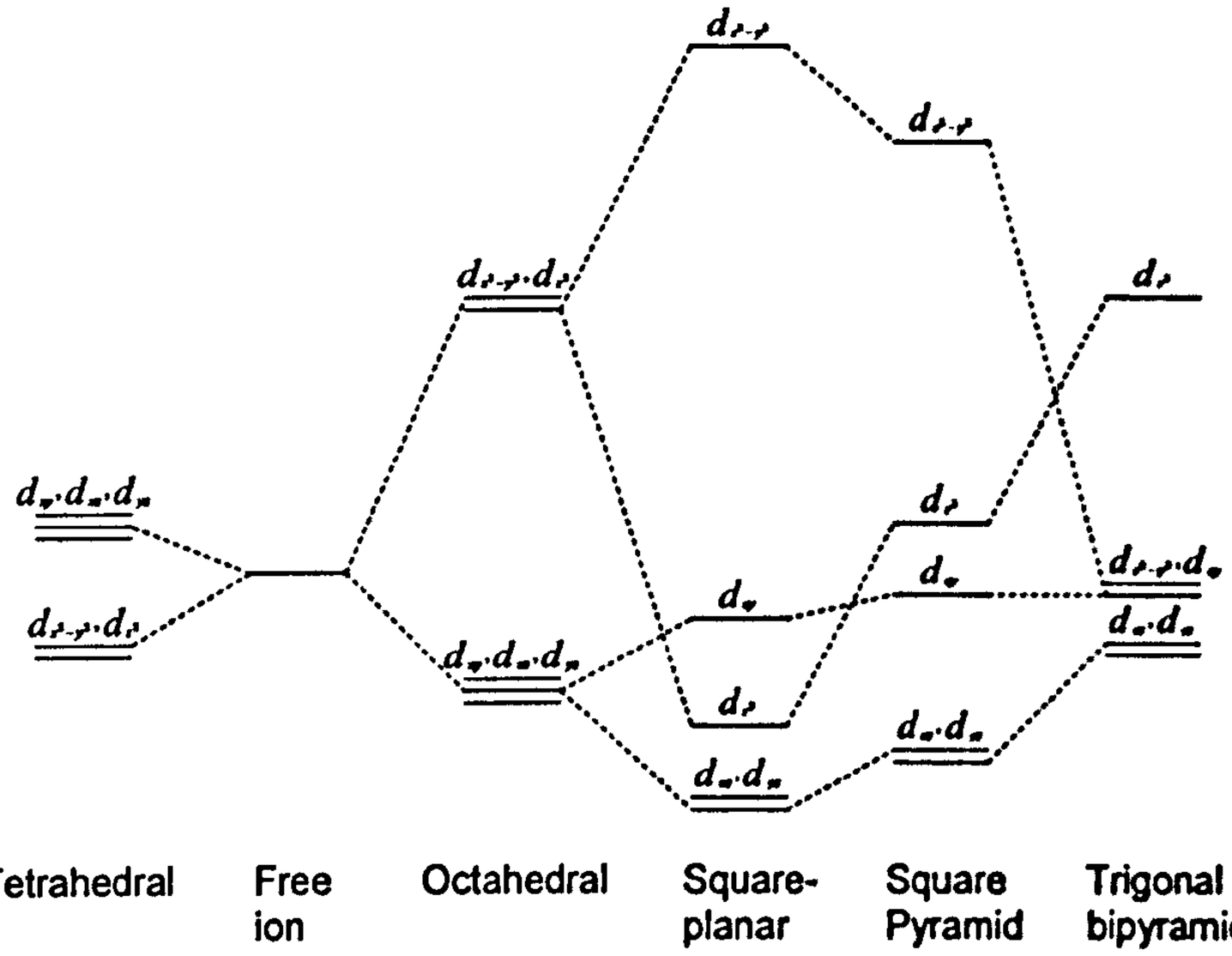

Figure 3.2. The approximate relative energies of d-orbitals in differing crystal field environments.

The most important Pt(II) complex from a medical viewpoint is cisplatin, first reported synthesised by Peyrone in 1844.[52] Its structure was correctly assigned by Alfred Werner who in 1893 proposed structures for the α (cis) and β (trans) forms of diamminedichloroplatinum(II).[511] In 1913 for 'his work on the linkage of atoms on molecules...' he was awarded the Nobel Prize for Chemistry.

3.1.2. The molecular design of steroidal platinum complexes

The conjugation of steroids and platinum(II) logically follows a design containing 3 distinct moieties. The first is a steroid, in this case testosterone, as to the author's knowledge, this has not been attempted for targeted cytotoxic drugs. The second is a platinum centre and one with only a single leaving group and/or a DMSO ligand satisfies a requirement to be non-conventional. The third is a suitable linking group and a mono-functional aromatic amine such as pyridine or quinoline. Figure 3.3 shows the three moieties or domains.

The design of a steroidal metal complex will contain the following features:

1. Attachment of planar aromatic amine to testosterone skeleton should allow good receptor binding.
2. The groups coordinated to platinum(II) must allow covalent DNA binding.
3. The synthesis should be relatively facile.
4. The platinum centre should be positively charged to enhance water solubility (very important due to the hydrophobic steroid).
5. The platinum domain should be 'non-classical' in terms of the ligand arrangement, e.g. monofunctional and containg ligand such as DMSO.

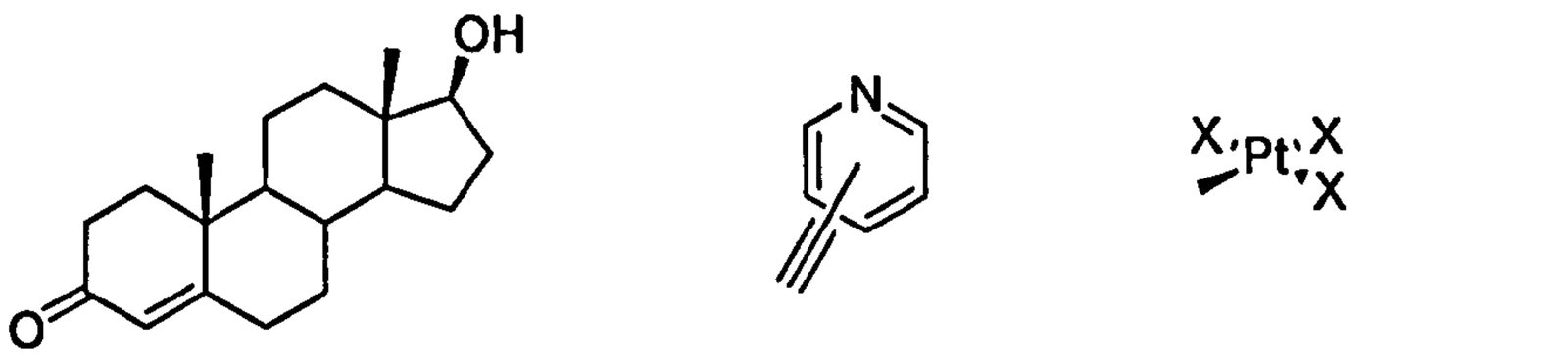

steroid domain linker domain platinum(II) domair

Figure 3.3. The design of steroidal platinum complexes.

Features 4 and 5, regarding the platinum centre are very important; since 1969 much synthesis has focussed on the structure activity rules proposed in the early 1970's and it's essencial that new complexes move away from those rigid rules if truly novel-acting complexes are to be developed. The ethnynyl-pyridyl or ethynyl-quinyl group will be used to link to testosterone and is capable of coordinating platinum(II), leaving three vacant coordination sites on Pt(II), giving rise to the possibility of a very large number of different combinations of ligands and geometries unlike bidentate ligands. Figure 3.4 shows the 5 combinations of geometries and ligands which will be made. The labels given to each type of coordination sphere, *i.e.* trans-cationic = TC will be used from now on.

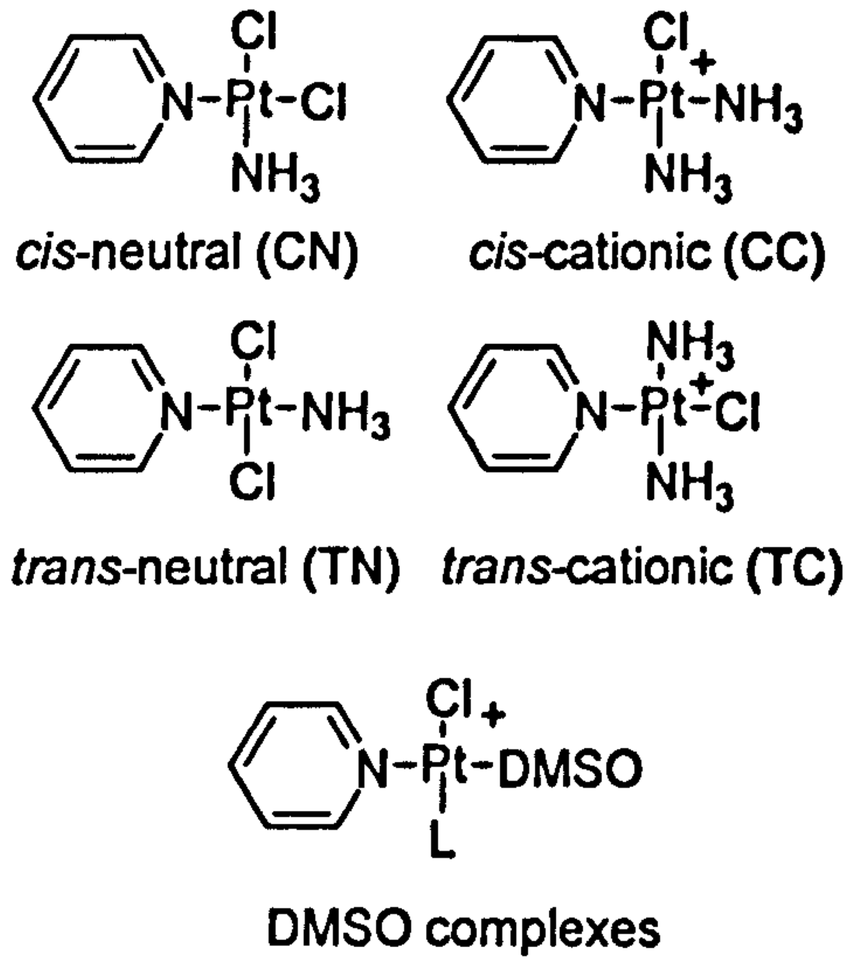

Figure 3.4. The geometry of 5 different types platinum(II) complexes. The steroid-linker ligand is replaced by pyridine for clarity.

Trans- and cis-cationic (TC and CC) and those containing DMSO are non-conventional. All are positively charged to aid water solubility and reduce the high lipophilicity often associated with steroidal metal complexes. The design results in complexes similar to that shown in Figure 3.5, using a 4-ethynynl-pyridine to link the steroid and platinum moieties together. The molecular design primarily focuses on using testosterone to deliver a platinum complex with the ability to bind to DNA and overcome the problem of decreased uptake found is some cisplatin resistant cells. The complex is also designed to have less systemic toxicity through two methods; firstly, the compound is more targeted so less is required for treatment and secondly, using less complex for treatment will result in less toxicity. The complex is designed to overcome other mechanisms of resistance. Where the platinum centre and steroidal group are close together, when using 2 and 3 ethynyl-pyridine linker domains for example, it is entirely likely that decreased levels of inactivation by sulphur containing bio-molecules may occur due to steric crowding. Finally the design is a large departure from 'classical' platinum drugs and as such, cross-resistance with cisplatin and carboplatin is not expected to occur.

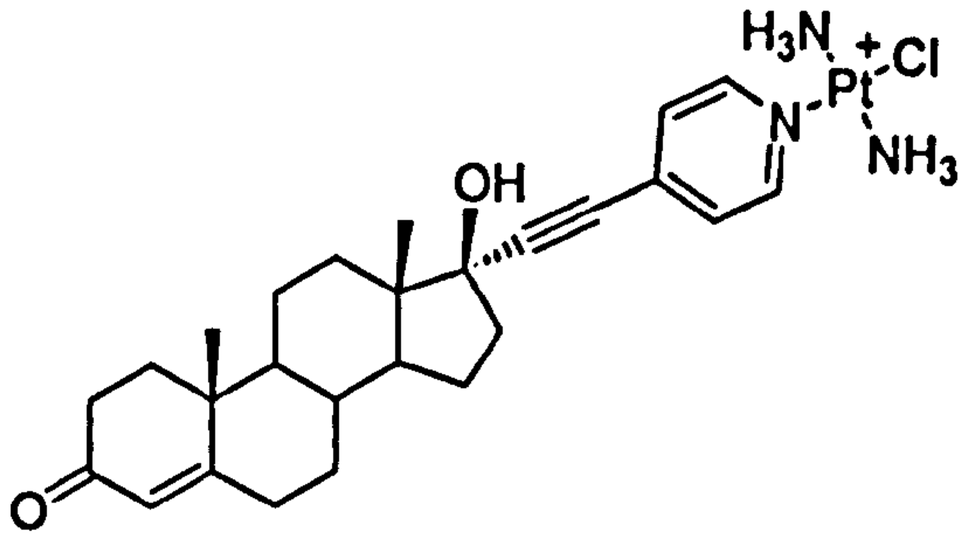

Figure 3.5. An example of a steroidal metal complex.

3.1.3. Synthetic routes to organic ligands

The route chosen to produce modified testosterone is via Sonogashira coupling due to the commercial availability of inexpensive bromo-pyridines, quinolines, isoquinolines and 17α-ethynyltestosterone in addition to the relative ease of separation of the desired products.

A Sonogashira coupling is a palladium catalysed reaction between an acetylinic group (*i.e.* 17α-ethnynyltestosterone) and a halogenated group[512] (*i.e.* 2-bromopyridine), an example of which is shown in Figure 3.6. A copper(I) salt is used to reduce Pd(II) to catalytically active Pd(0) *in situ* and requires inert conditions as copper(I) salts catalyse homo-coupling of the acetylinic groups in a Glaser coupling.[513] To remove the acetylinic proton the reaction was originally conducted in an organic base.

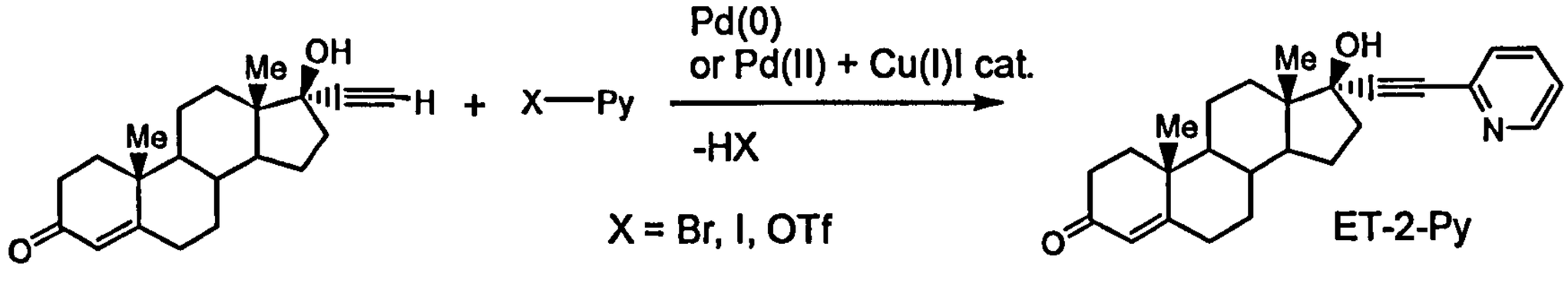

Figure 3.6. The Sonogashira coupling between ethisterone and 2-bromopyridine.

The proposed catalytic cycle of the Sonogashira reaction is presented in Figure 3.7 and in addition to the product, a protonated base is the major by-product of the reaction.

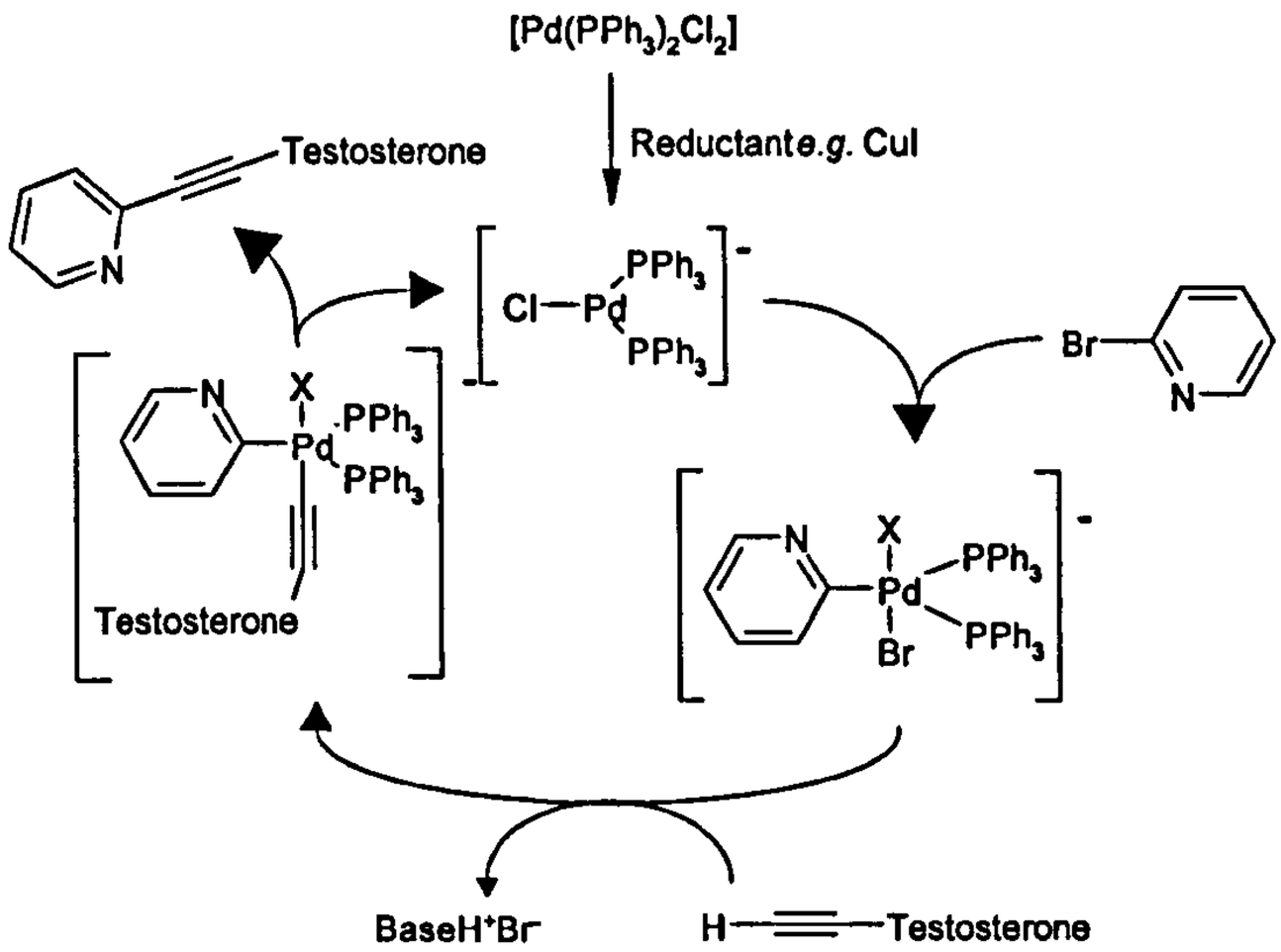

Figure 3.7. The proposed catalytic cycle for the palladium catalysed Sonogashira cross-coupling reaction.[512, 514-516]

The catalytic cycles involves reduction of Pd(II) to Pd(0) by Cu(I) and insersion into a Ar-Br bond and the formation of a Pd-C bond after the deprotonation of ethisterone by a base, *i.e.* triethylamine. The protonated base precipitates out from solution and a 1,2-insertion reaction at the Pd centre completes the reaction to form the desired product.

Another route to steroid-linker ligands involves a nucleophilic attack of a lithiated ethnynyl-pyridine nucleophile create a new stereocentre at the 17-carbon, shown in Figure 3.8. This nucleophilic attack possesses facial selectivity but diasteroisomers inevitably occur, requiring addition purification steps and is unlikely to be attempted.

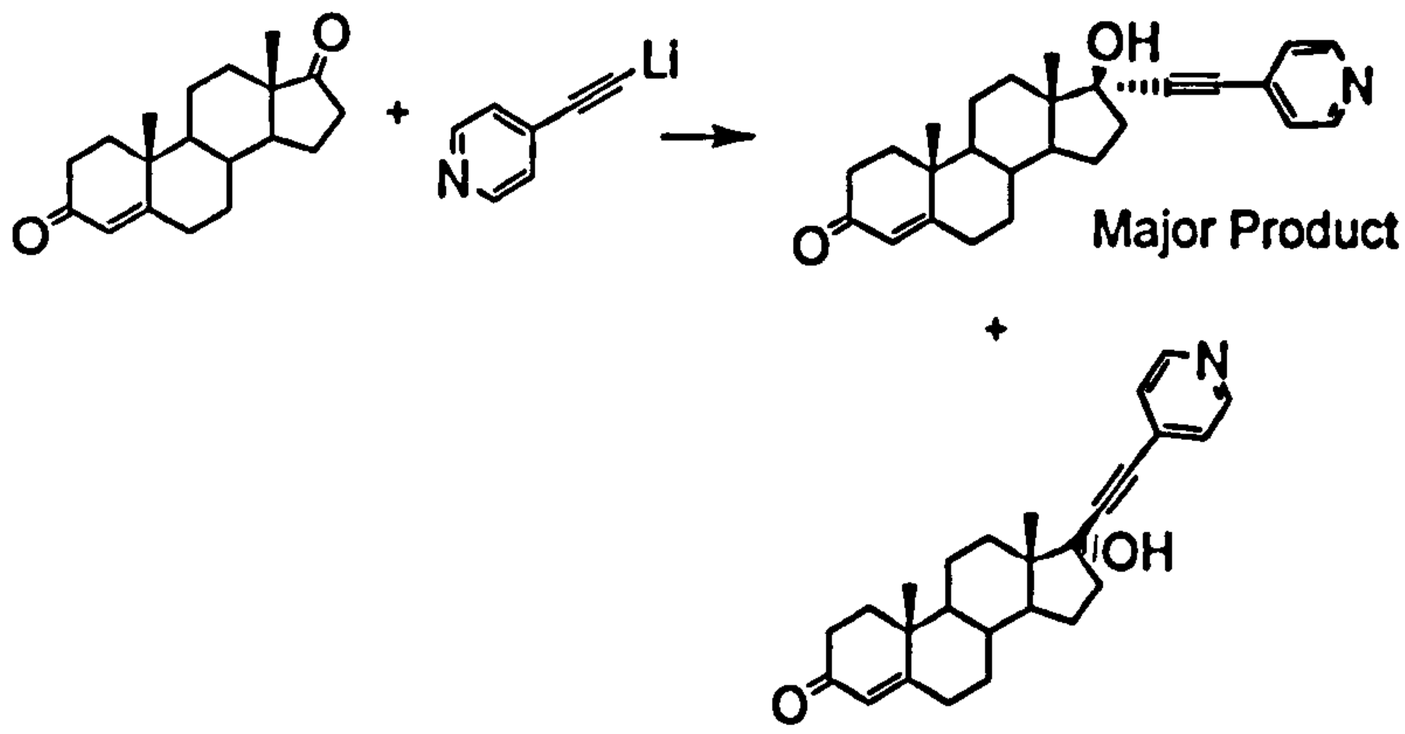

Figure 3.8. The nucleophilic attack by a lithiated species, possessing facial steroselectivity, creating a 17α-pyridylethynyl-substituted testosterone.

3.1.4. Synthetic routes to steroidal metal complexes

The five different co-ordination spheres will require 4 different synthetic routes. Trans-cationic (TC) and cis-cationic (CC) complexes are synthesised using the same synthetic method, removal of a chloride ion from transplatin (for TC complexes) or cisplatin (for CC complexes) by a silver nitrate and binding of the solvent (DMF) to the vacant ligand site forming the complex $[trans\text{-}Pt(NH_3)_2(DMF)Cl]^+$.[332, 333] The labile DMF ligand is substituted by the organic ligand to form the complex, shown in Figure 3.9.

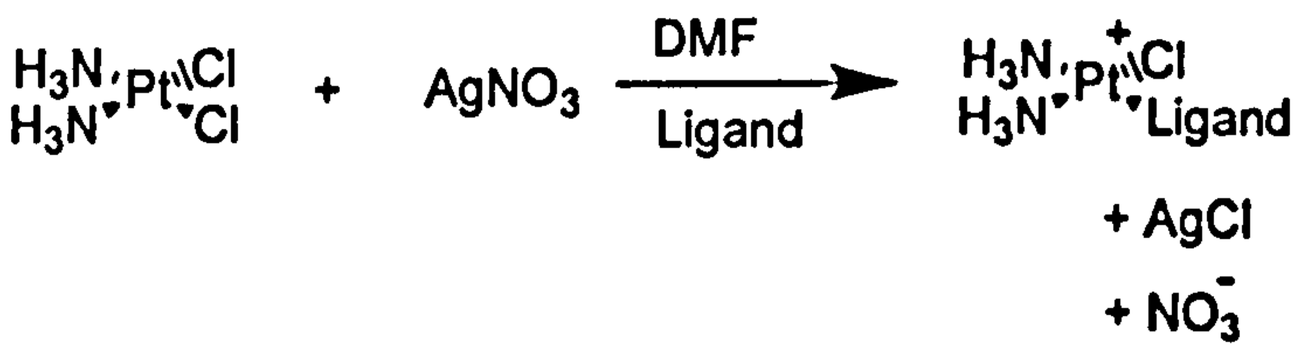

Figure 3.9. Synthetic route to TC complexes.

Trans-neutral complexes will be synthesised using the main synthetic route to this type of complexes; substitution of two chlorides forming 'solvento species' before substitution by steroidal ligands (Figure 3.10). Treatment with hydrochloric acid, due to the trans-effect results in a trans geometry.

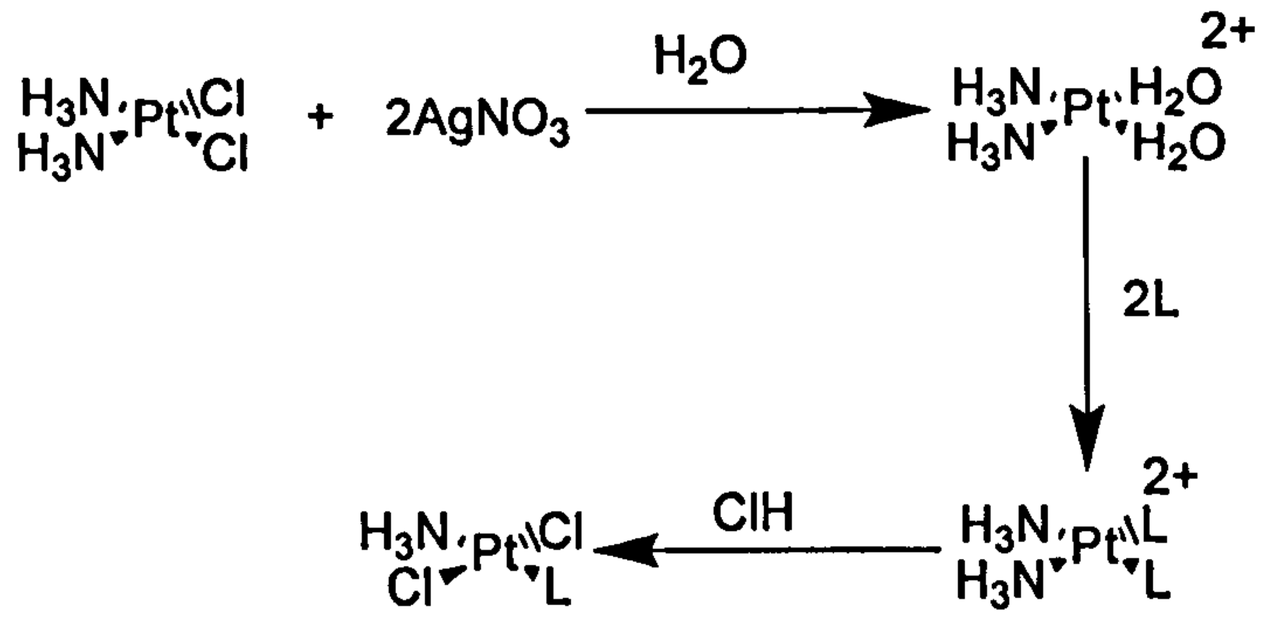

Figure 3.10. Synthesis of trans-neutral complexes.

Synthesis of complexes (cis-neutral) with the molecular formula cis-$Pt(NH_3)(L)(Cl)_2$ may follow two routes. The first route is via the reactive intermediate $[Pt(NH_3)(Cl)_3]^-$ and treating this with an amine ligand, L, to form cis-$Pt(NH_3)(L)(Cl)_2$. Syntheses by Abrams and co-workers have produced several different salts of $[Pt(NH_3)(Cl)_3]^-$ for use in a range of solvents in addition to water (Figure 3.11).[517]

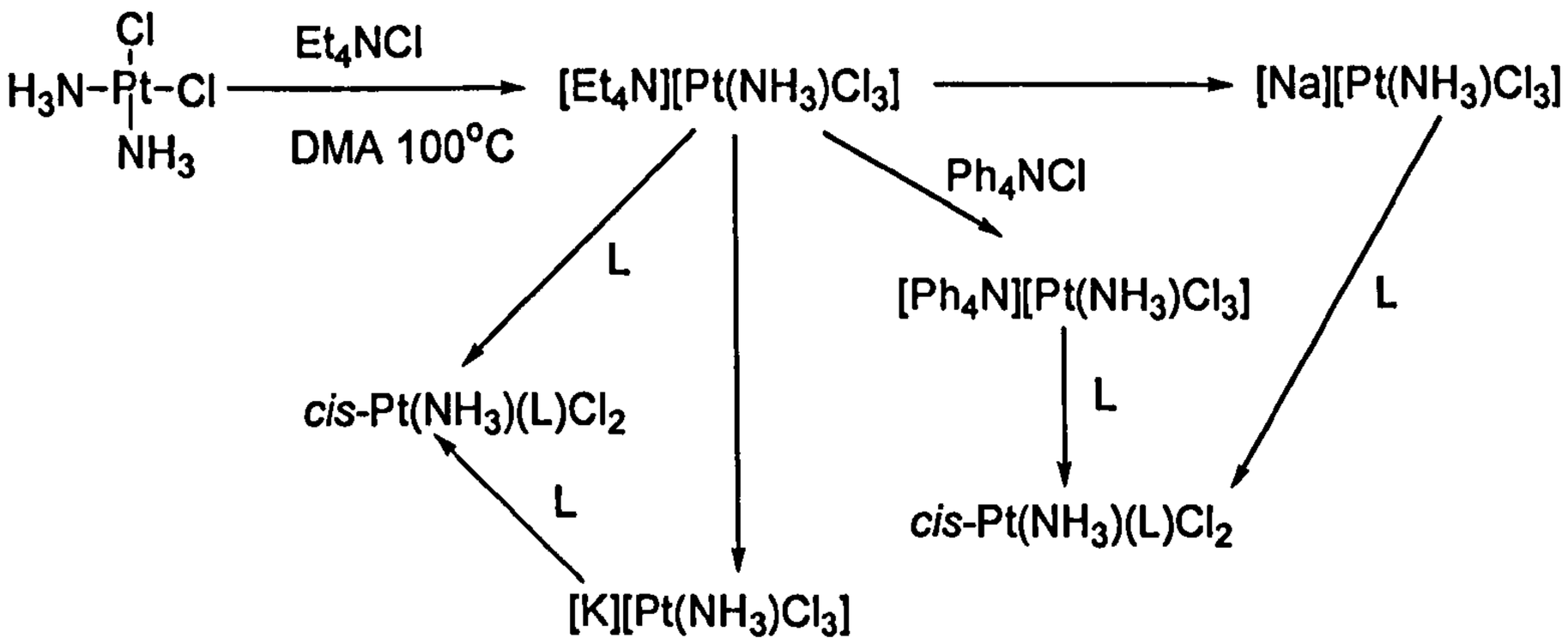

Figure 3.11. The routes to platinum complexes with the molecular formula cis-$Pt(NH_3)(L)(Cl)_2$.

Regarding complexes containing DMSO, the substitution of a DMSO ligand from cis-$Pt(DMSO)_2Cl_2$ by amines has been known for over 30 years.[518] Farrell and co-workers investigated amine and DMSO containing complexes thoroughly during the 1980's and assigned the reaction products as trans and reported several crystal structures.[519-522]

Farrell also proposed a mechanism for the reaction between an anitrogen containing ligand and cis-$Pt(DMSO)_2Cl_2$ shown in Figure 3.12.[519]

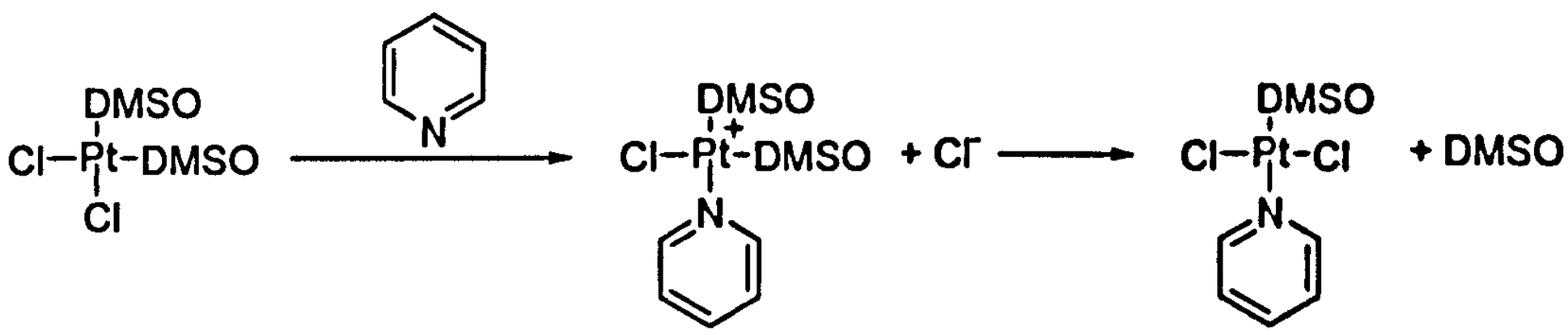

Figure 3.12. The proposed mechanism for the reaction of a ligand with cis-$Pt(DMSO)_2Cl_2$ using pyridine as an example.

Once the last complex (Figure 3.12) has been formed, removal of chloride using silver nitrate, addition of a planar amine such as pyridine and subsequent purification should yield a complex of the formula $Pt(L)(Pyridine)(DMSO)Cl^+$.

3.2. Results and discussion

Whilst all characterisation data is referred to in this section, much is to be found in the appendices and these are referred to, for example, Figure A.2.3., meaning Figure 2.3 in Appendix 2)

3.2.1. The synthesis of 17α-subsituted testosterones

The only problem encountered using the Sonogashira reaction was the requirement for inert conditions. Failure to observe strict inertness resulted in varying degrees of Glaser coupling, visible in the ^1H NMR spectrum as a deviation of 1:1 ratio between steroidal and pyridine hydrogens and in the mass spectrum (ESI-MS, +ve) at $m/z = 623$, corresponding to (Ethynyl-testosterone)$_2$.

3.2.2. The synthesis of ligands $L_1 - L_6$

Using readily available commercial reagents six ligands were synthesised (Figure 3.13) in good to high yield with the majority requiring only simple purification steps such as re-crystallsation. Only ET-3-Py and ET-4-Py required flash column chromatography to separate out the desired product. The compound structure was confirmed using a range of spectroscopic techniques. In general the molecular formulae were confirmed using elemental analysis and the ^1H NMR spectra used confirm the ratio of steroidal skeleton and aromatic group and ^{13}C DEPT NMR spectroscopy was used to establish that no changes to the steroidal skeleton occurred, *i.e.* quaternary. Infrared spectroscopy confirmed the presence of the major functional groups including an α,β-unsaturated carbonyl, hydroxyl

and aromatic ring. Vibrational bands relating to the ethnynyl group were not always present.

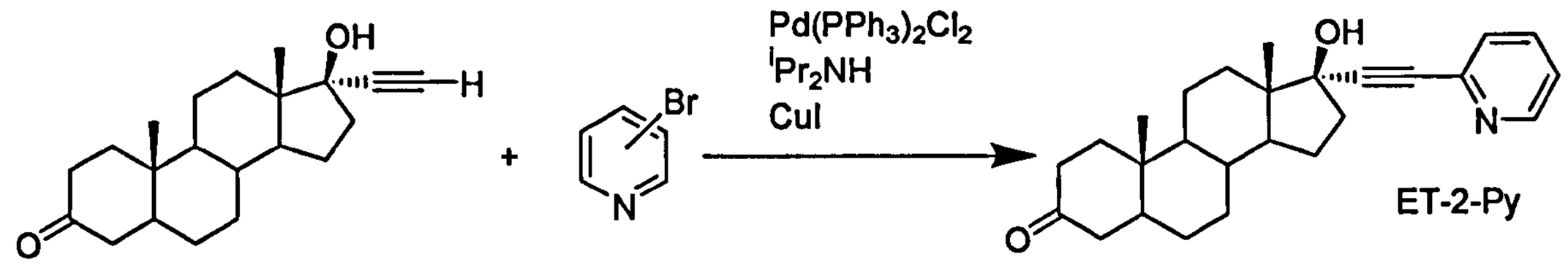

Figure 3.13. The molecular structures of ligand L_1 - L_6

The 6 ligands (Figure 3.13) are identified by shortened acronyms. A pyridine with 17α-substitured testosterone at the 2 position full nomenclature name is (8R,9S,10R,13S,14S,17S)-17-Hydroxy-10,13-dimethyl-17-pyridin-2-ylethynyl-1,2,6,7,8,9,10,11,12,13,14,15,16,17-tetradecahydro-cyclopenta[a]phenanthren-3-one although here the steroid skeleton will be referred to as testosterone and the ligand as 17α-pyridin-2-ylethynyl-testosterone or ET-2-Py. This nomenclature is repeated for all the ligands and subsequent complexes.

3.2.2.1. Ligand L_1: 17α-pyridin-2-ylethynyl-testosterone (ET-2-Py)

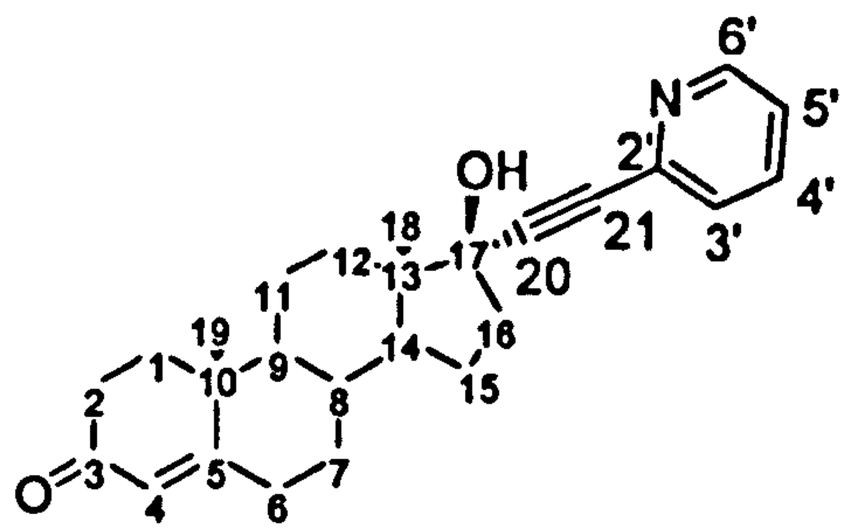

$C_{26}H_{31}NO_2$

The Sonogashira cross-coupling reaction between ethisterone and 2-bromopyridine afforded the product 17α-pyridin-2-ylethynyl-testosterone in excellent yield and requiring only simple purification. The product was soluble in chloroform, dichloromethane, methanol, DMF and DMSO, partially soluble in acetonitrile, barely soluble in diethyl ether and insoluble in water. Purification of the crude product involved two steps: a) washing with water to remove diisopropylamine and copper salts; b) recrystallisation to remove palladium complexes (determined by their orange / yellow colour) together with small amounts of ethisterone and product that remain dissolved. The product began to crystallise almost immediately after the cooling period was initiated and this was complete in 24 hours.

The white solid was analysed by elemental analysis and mass spectroscopy whose results are consistent with the proposed structure. The mass spectrum (Appendix A.1.1) corresponds to $C_{26}H_{31}NO_2 + H^+$ and has the correct isotope distribution pattern.

The ^1H NMR spectrum (Figure 3.14) shows a steroidal skeleton and pyridine ring in a 1:1 ratio with a loss of acetylene resoance ca. 2.55 ppm indicating a reaction at that centre. The α,β-unsaturated carbonyl proton (H4) and methyl resonances appear with little shifting compared to ethisterone as would be expected due to the distance from the pyridine ring.

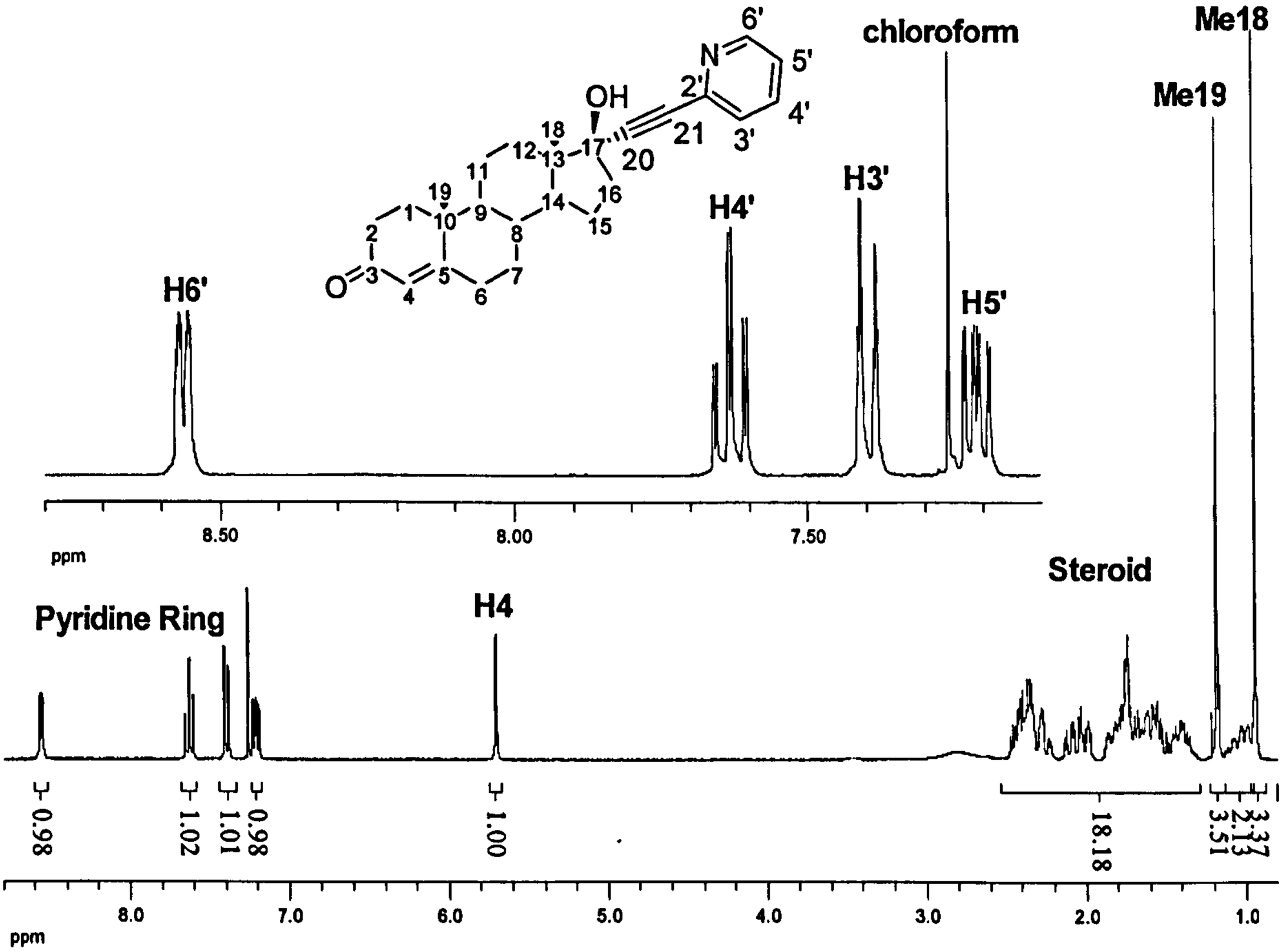

Figure 3.14. ^{1}H NMR spectrum of ET-2-Py in $CDCl_3$.

The assignment of the pyridine resonances may be made from inspection of the coupling constants and was confirmed by a COSY spectrum (Figure A.1.2). The COSY spectrum clearly shows ^{3}J and ^{4}J coupling allowing assignments in conjunction with the 1D ^{1}H-NMR spectrum. Cross coupling of H6' with a triplet at 7.63 ppm shows this is H5'. Coupling of H5' to a doublet at 7.40 ppm and coupling of this doublet with a ddd signal at 7.21 ppm allows the assignment of H3' and H5' respectively.

The ^{13}C DEPT NMR spectrum (Figure 3.15) contains 26 signals, with the correct amounts of C / CH_2 and CH / CH_3 groups. The pyridine carbons, C2, C4, C18 and C19 are assigned in association with a ^{1}H-^{13}C HMQC spectrum (Figures A.1.3 and A.1.4.). The signal of highest chemical shift at 200 ppm is assigned to the ketone carbon, C3. The signal around 171 ppm is assigned to C5 which is β to an α,β-unsaturated carbonyl and the 143 ppm resonance is assigned to C2'. The close signals at 123.8 ppm and 122.9 ppm may be assigned to C4 and C5' respectively using the cross coupling peak locations in the HMQC spectrum. The three resonances at 93.0 ppm, 85.3 ppm and 79.8 ppm may be assigned either of the three quaternary carbons C17, C20 and C21. The three remaining signals of CH type carbons at 53.2 ppm, 50.1 ppm and 38.8 ppm may be assigned to either of three carbons C8, C9 and C14.

The IR spectra (Figure A.1.5) show bands of the most characteristic functional groups. The steroid skeleton is represented in the spectrum with υO-H, υC-H, υC≡C and υC=O stretches. The weak band at 2219 cm^{-1} and strong band at 1665 cm^{-1} are assigned to a υC≡C and an α,β-unsaturated ketone υC=O stretch, respectively. The pyridine ring exhibits several bands, aromatic υC-H stretches between 3150 cm^{-1} and 3180 cm^{-1} and υC-H out of plane ("oop") at 765 cm^{-1}. The 765 cm^{-1} band is indicative of a 2-substituted pyridine ring. The yield is 76 %. The combined spectroscopy data is in agreement with the structure of ET-2-Py.

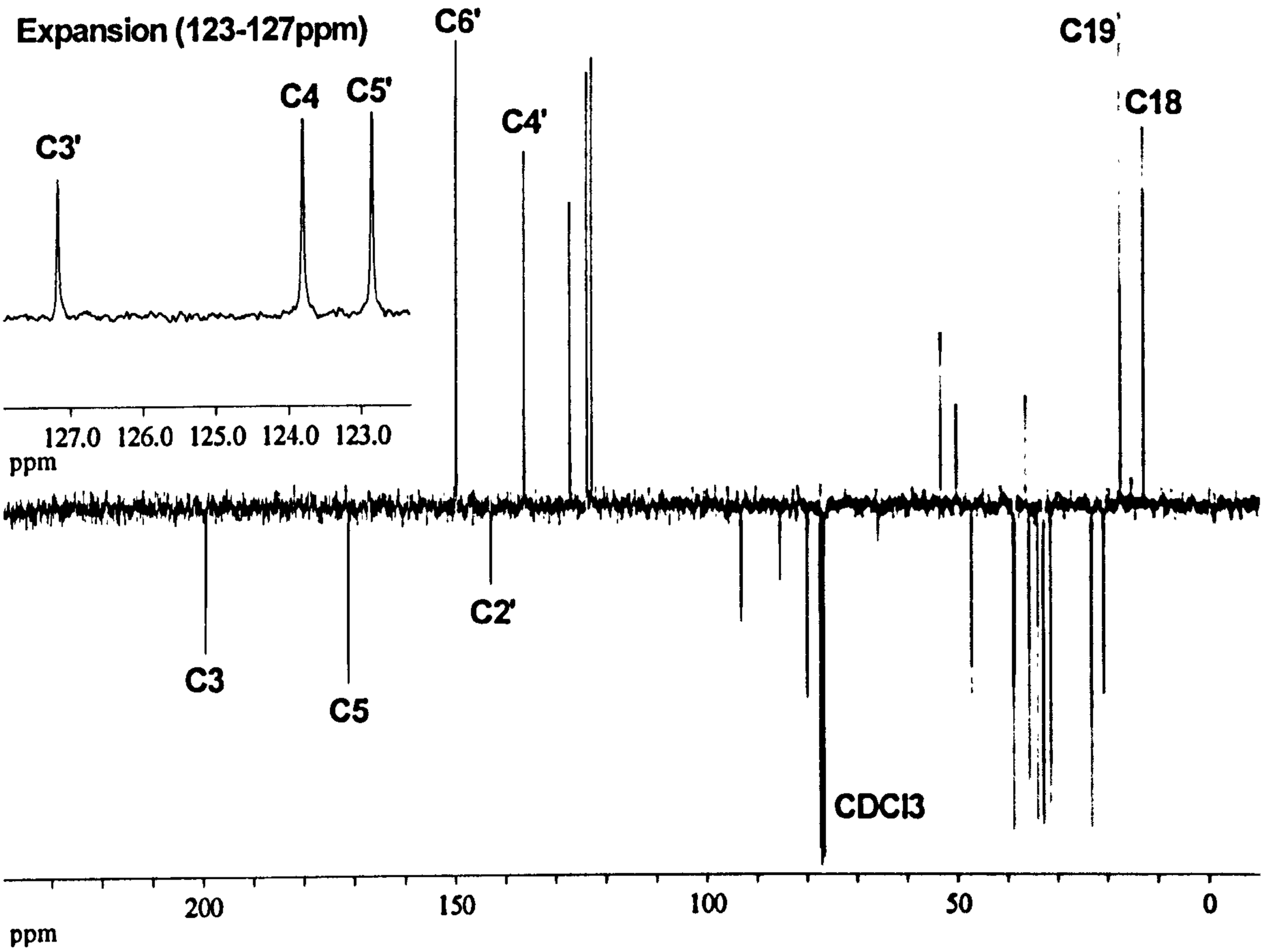

Figure 3.15. The ^{13}C spectrum of ET-2-Py with selected assignments.

3.2.2.2. Ligand L_2: 17α-pyridin-3-ylethynyl-testosterone (ET-3-Py)

$C_{26}H_{31}NO_2$

The coupling of 3-bromopyridine and 17α-ethynyltestosterone afforded the product 17α-pyridin-3-ylethynyl-testosterone in good yield. The product was soluble in chloroform, dichloromethane, methanol, acetonitrile, DMF and DMSO, partially soluble in diethylether and insoluble in water. Purification was primarily by flash column chromatography although washing a chloroform solution of crude product with water removed proportions of protonated base and copper salts. Column chromatography separated the product from the remaining impurities using silica gel.

The molecular formula of ET-3-Py was confirmed by elemental analysis and the parent ion peak in ESI-MS at *m/z* = 390 may be attributed to protonated ET-3-Py (Figure A.1.6.). The ^{1}H NMR spectrum (Figure 3.16) reveals resonances assigned to a 3-substituted pyridine ring and steroidal skeleton in a 1:1 ratio. There is no evidence of an acetylene proton ca. 2.54 ppm, observed in ethisterone, indicating the reaction took place completely. The assignment of the pyridine resonances may be made from inspection of the coupling constant of the 7.73 ppm resonance and the cross-peaks in the COSY spectrum of ET-3-Py (Figure 3.17). The origin of broadness of the 3 aromatic protons is unknown.

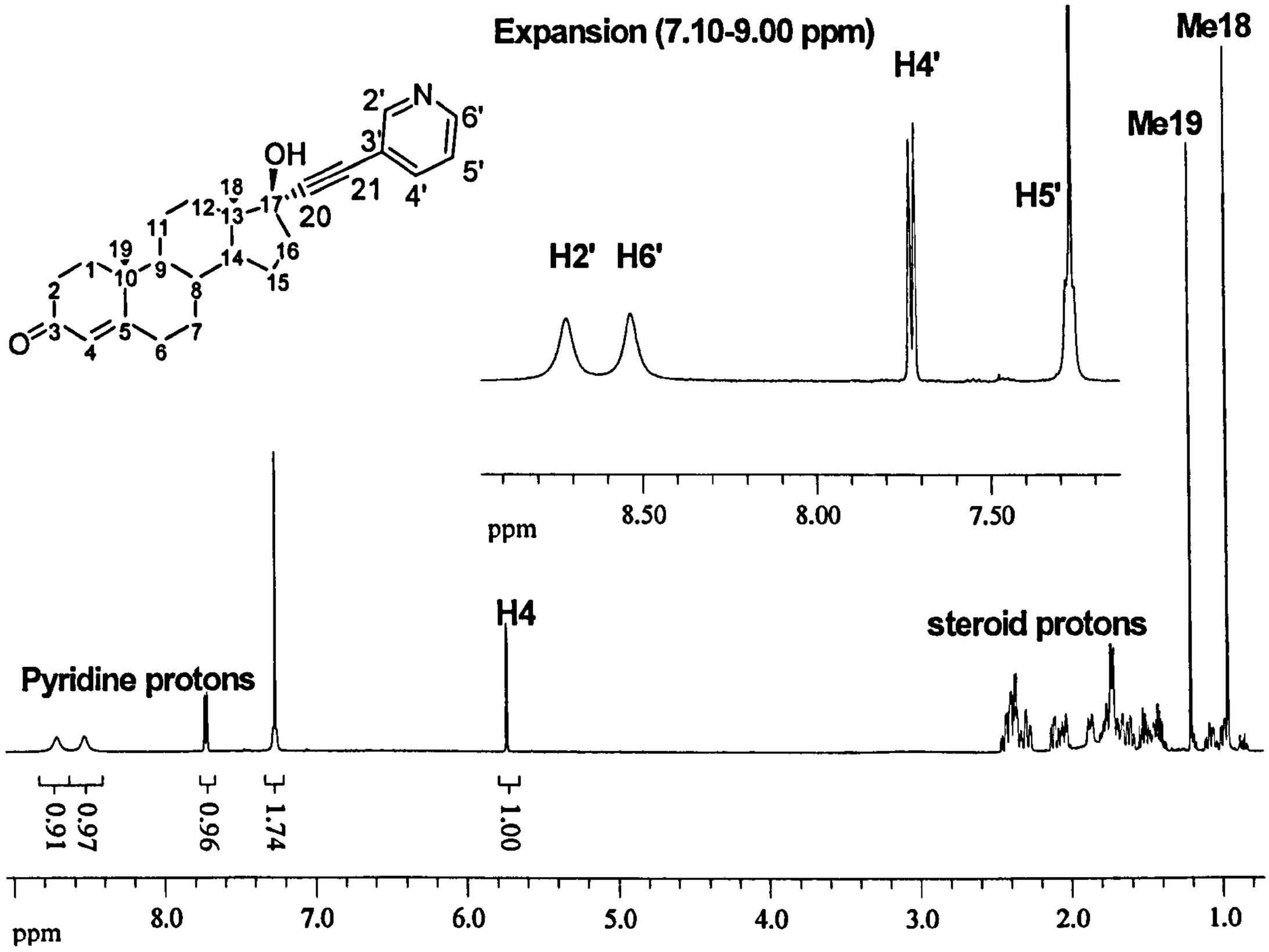

Figure 3.16. The ^{1}H NMR spectrum of ET-3-Py in $CDCl_3$.

Inspection of the COSY spectrum, cross-peaks may be observed between the doublet at 7.73 ppm and singlet at 8.53 and multiplet (overlapping with $CHCl_3$) at 7.27 ppm. This permits assignment of H5' and H6'. The remaining signal at 8.72 ppm may be assigned to H2' which shows no evidence of coupling to any other proton and being α to the pyridine nitrogen is expected at higher chemical shift than some other pyridine protons.

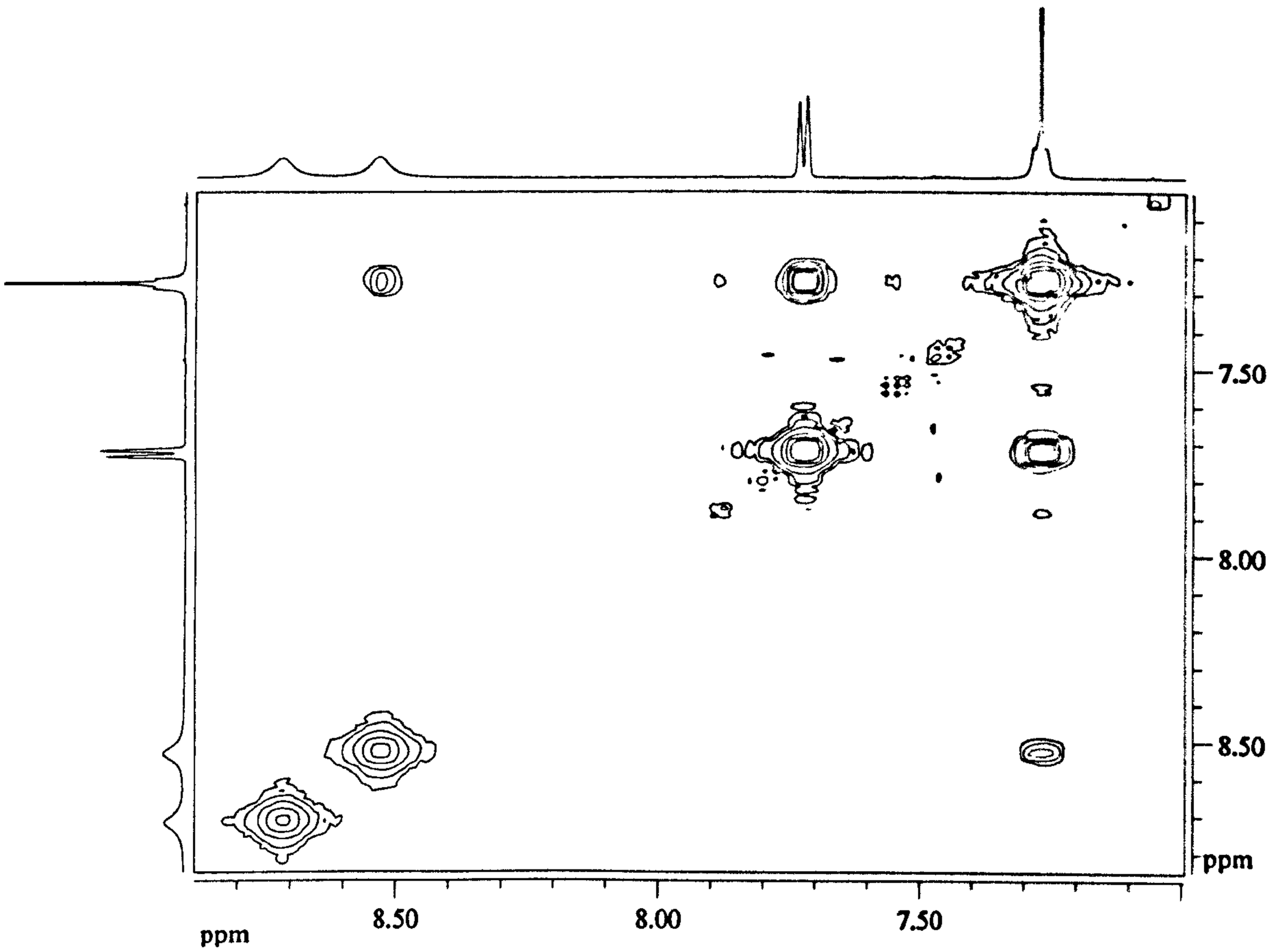

Figure 3.17. The COSY spectrum of ET-3-Py in $CDCl_3$.

The IR spectrum (Figure A.1.7) shows the fundamental vibrations characteristic of functional groups in ET-3-Py. The steroid is represented by *υ*O-H, *υ*C-H, *υ*C=O stretches whilst the pyridine *υ*C=C stretch as shoulders to the *υ*C=O vibration and *υ*C-H out of plane bend at lower wavenumbers. The yield is 68 %. The spectroscopic data confirm the structure of ET-3-Py.

3.2.2.3. Ligand L_3: 17α-pyridin-4-ylethynyl-testosterone (ET-4-Py)

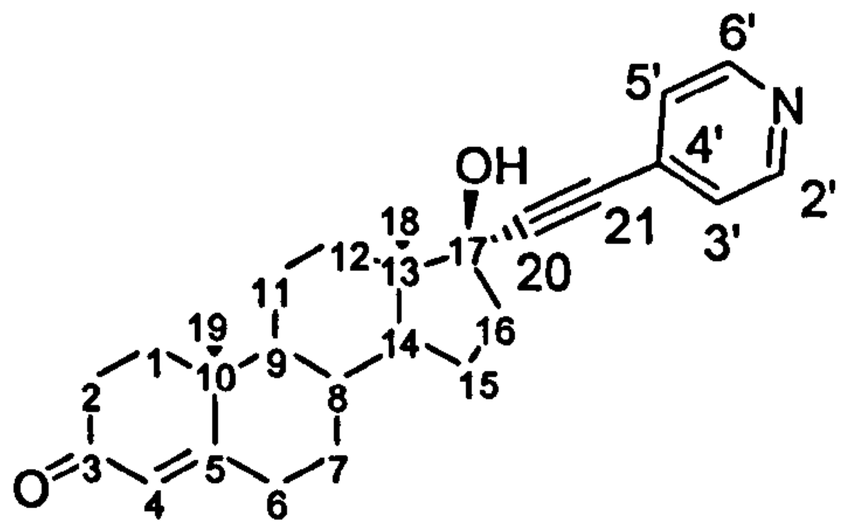

$C_{26}H_{31}NO_2$

The reaction between 4-bromopyridine and ethisterone using bis(triphenylphosphine)dichloropalladium(II) as a catalyst in the presence of copper iodide and diisopropylamine produced the desired product ET-4-Py in reasonable yield. Purification required several steps: a) removal of diisopropylamine by washing with chloroform and reduction *in vacuo*; b) removal of diisopropylamine salt by selective precipitation and washing; c) flash column on silica to separate the ET-4-Py from palladium salts. The product is a white fluffy solid very soluble in DMSO, DMF, chloroform, dichloromethane, methanol and acetonitrile, partially soluble in diethylether and insoluble in water.

Elemental analysis confirmed the chemical formula and mass spectroscopy confirmed the parent ion is 390.3, corresponding to protonated ET-4-Py with the correct isotope distribution (Figure A.1.8). The ^{1}H NMR (Figure 3.18) indicates the presence of a steroidal skeleton and 4-substitited pyridine ring in a 1:1 ratio. No evidence is present of acetylinic protons such as that seen in ethisterone indicating the reaction took place completely. The integrations of all protons in the ^{1}H NMR spectrum accounts for all steroidal and pyridine protons except for 17β hydroxyl group. The assignment of pyridyl protons assumes hydrogens closer to the nitrogen atom are at higher chemical shifts than those at greater distance. The broadness of the pyridine signals indicates the ring is spinning on the NMR timescale. H4 may be assigned due to its chemical shift and Me18 and Me19 from comparison with estradiol which posses an identical D ring but no Me19 in its structure.

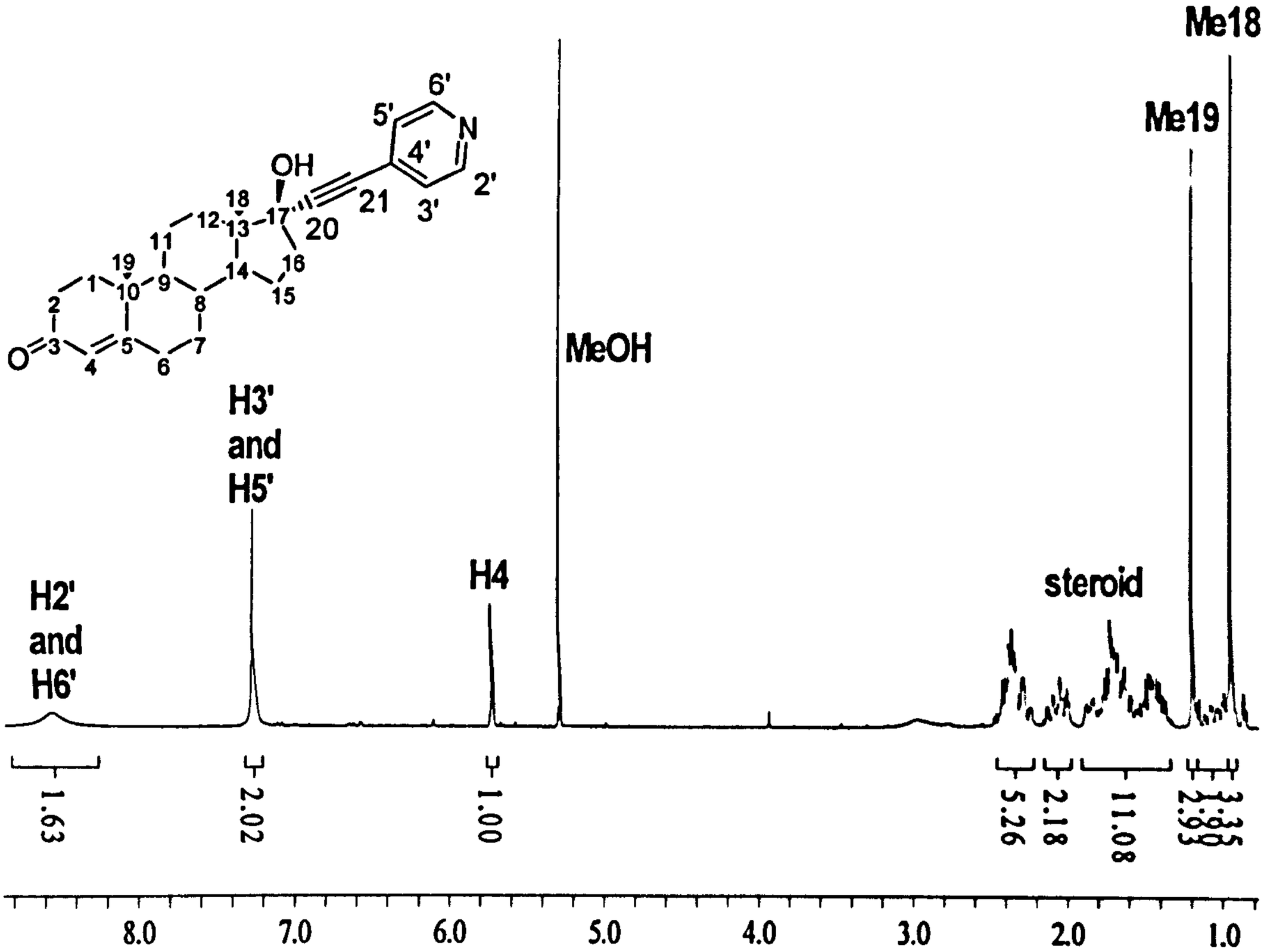

Figure 3.18. The ^{1}H NMR of ET-4-Py in CD_3OD.

The infrared spectrum (Figure A.1.9) shows several bands characteristic of functional groups in the proposed structure. Bands due to the steroid skeleton υO-H, υC-H and υC=O stretching modes are present in the spectrum. The weak band at 2220 cm^{-1} may be assigned to υC≡C stretch whilst the band at 824 cm^{-1} is υC-H bending. The position of the 824 cm^{-1} agrees with that expected from a 4 substituted pyridine ring. The yield is 68 %. The spectroscopic data is fully in agreement with the production of ET-4-Py.

3.2.2.4. Ligand L_4: 17α-quinolin-3-ylethynyl-testosterone (ET-3-Q)

$C_{30}H_{33}NO_2$

The cross-coupling of ethisterone and 3-bromoquinoline afforded ET-3-Q in 80 % yield, using simple purification methods. The final re-crystallisation from acetonitrile resulted in

the formation of a bright white crystalline solid. The ligand was very soluble in DMF, DMSO, chloroform, dichloromethane and THF, partially soluble in methanol, ethanol and acetonitrile and insoluble in diethylether and water. Purification of the crude product involved separating ET-3-Q from the copper, palladium and diisopropylammonium salts (Br^- or I^-). The first and latter were removed by treating the crude product with water and palladium salts by slow crystallisation from acetonitrile. The black precipitate observed in the re-crystallisation steps may possibly be decomposed palladium salts which were filtered off.

The ^1H NMR spectrum (Figure 3.19) and ESI-MS spectrum and elemental analysis indicate a successful reaction. Signals originating from a steroid skeleton (H4, Me18 and Me19) and substituted quinoline are present in the ^1H NMR spectrum in a 1:1 ratio. No acetylene proton from ethisterone is apparent indicating the reaction took place at this centre. The assignment of the quinoline resonances may be completed by combined analysis of the 1D and 2 D ^1H NMR (Figure A.1.10) spectra. The highest resonance at 8.99 ppm results from H2', on account of its coupling constant and proximity to the nitrogen atom; H4' is assigned from its coupling constant. Other assignments are best guesses from the resonance structure of quinoline. A NOE differential or NOESY NMR spectrum is required for a complete assignment. All steroid protons are accounted for including the broad resonance at 3.81 ppm which may be assigned to the 17α-hydroxyl group as well as H4 (5.72 ppm) and the steroidal methyls C19 and C18. The steroidal skeleton hydrogens are, in some cases, well resolved and coupling patterns of individual hydrogens may be distinguished.

The carbon spectra may be assigned from 1D and 2D NMR spectra. The ^{13}C DEPT NMR (Figure 3.20) contains all resonances except that only two resonances are seen of C8, C9 and C14 in the 30-50 ppm region. The quinoline signals may be assigned using ^{13}C-^1H HMQC spectrum (Figure A.1.11). The signal at 200 ppm may be assigned to C3. The resonance around 170 ppm was assigned to the quaternary carbon C5 due to it's β proximity an α,β-unsaturated ketone. Since C10' is α to a nitrogen its resonance will be higher that C5' whose position is β and both are assigned accordingly.

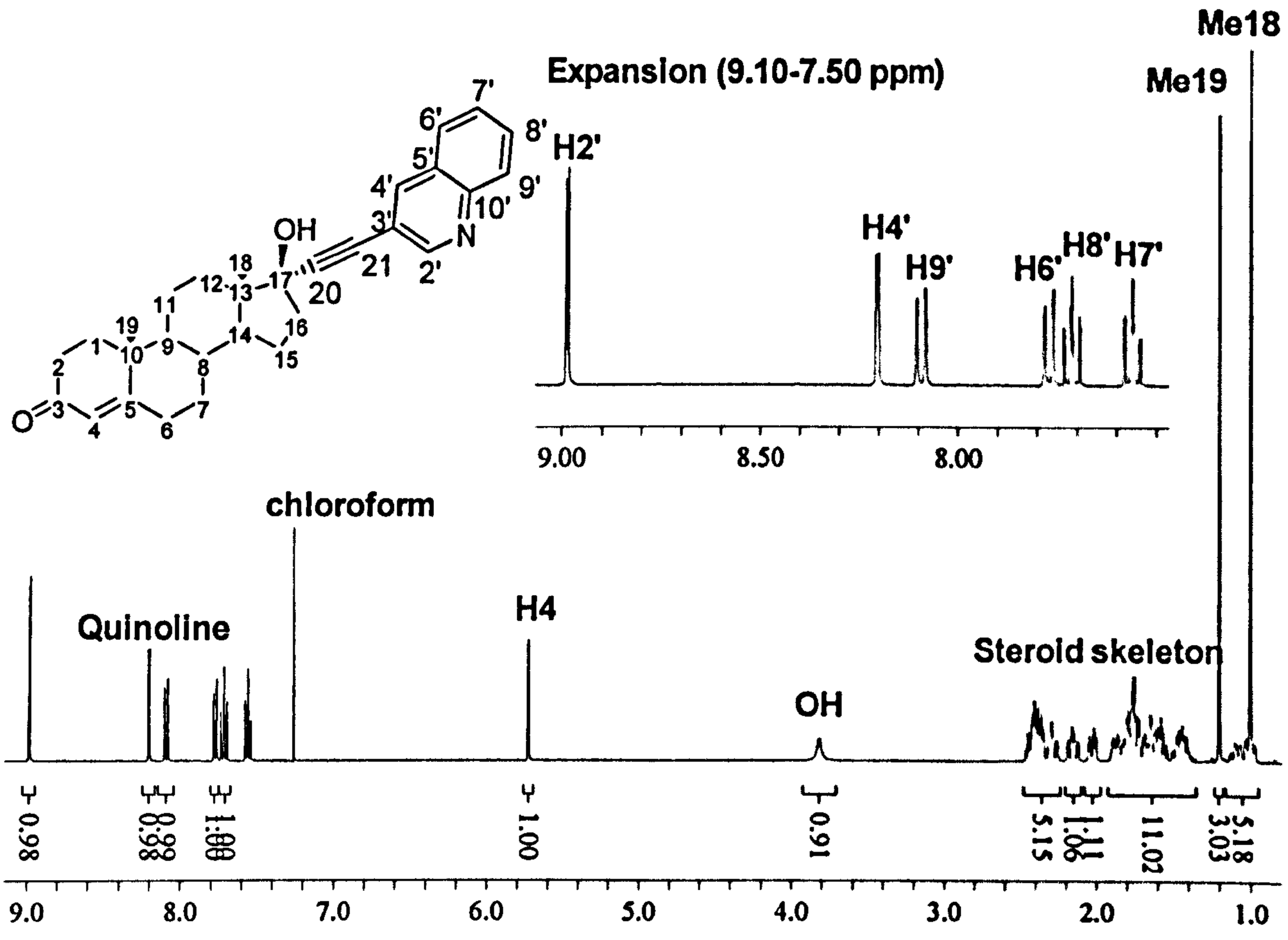

Figure 3.19. The ^{1}H NMR spectrum of ET-3-Q in $CDCl_3$.

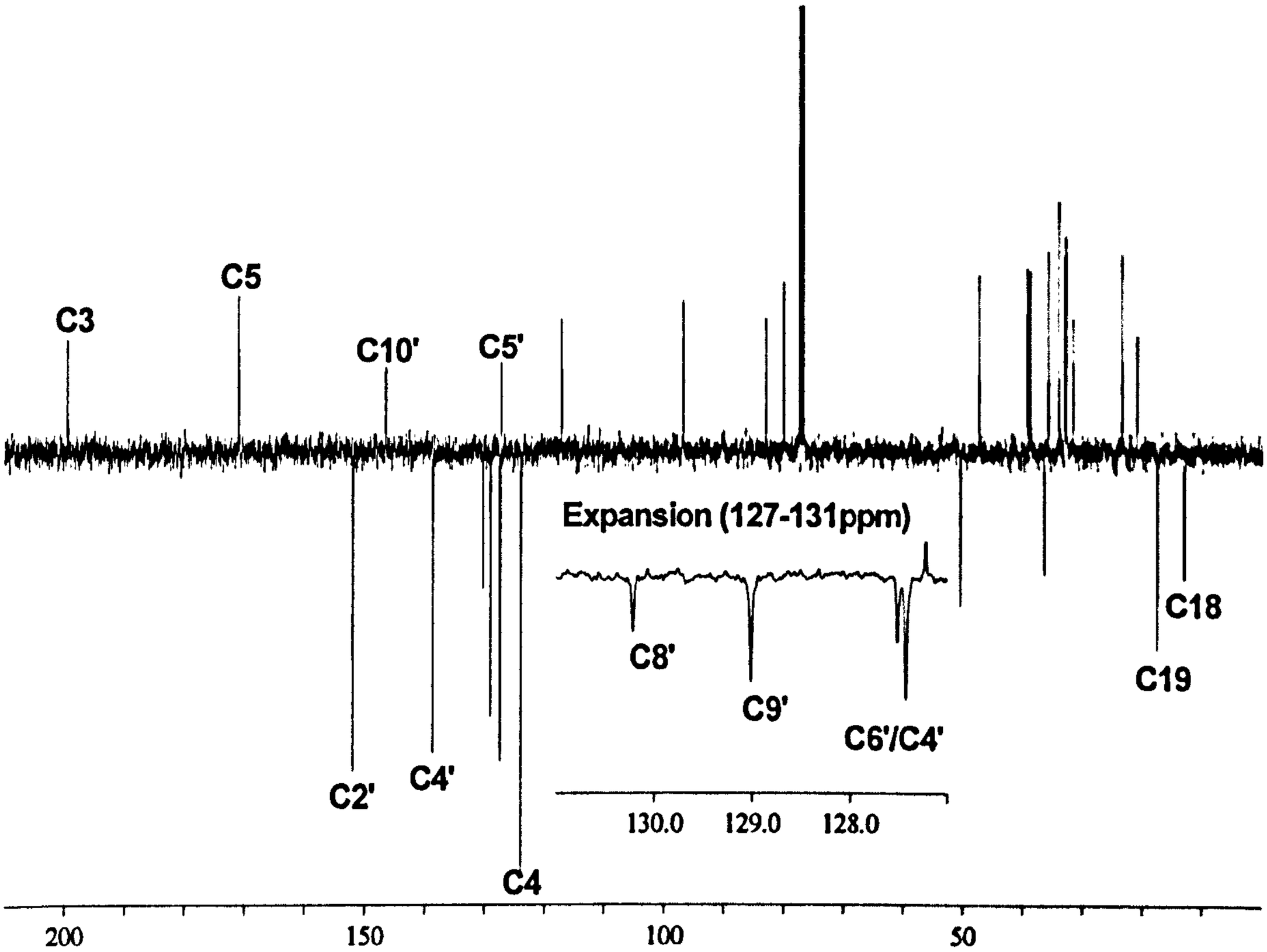

Figure 3.20. The ^{13}C DEPT NMR spectrum of ET-3-Q in $CDCl_3$.

The IR spectroscopy (Figure A.1.12) shows several bands characteristic of the functional groups of ET-3-Q. The υO-H stretch at 3210 cm^{-1} is assigned to the 17β-hydroxyl group of the steroidal skeleton. Bands around 2800-2950 cm^{-1} and at 1668 cm^{-1} result from υC-H and υC=O stretches. Often υC≡C stretching modes are too weak a band to observe but in the case of ET-3-Q weak band at 2215 cm^{-1} may be assigned to this vibrational mode. The yield is 80 %. The combined data prove ET-3-Q was successfully synthesized in high yield.

3.2.2.5. Ligand L_5: 17α-isoquinolin-4-ylethynyl-testosterone (ET-4-IQ)

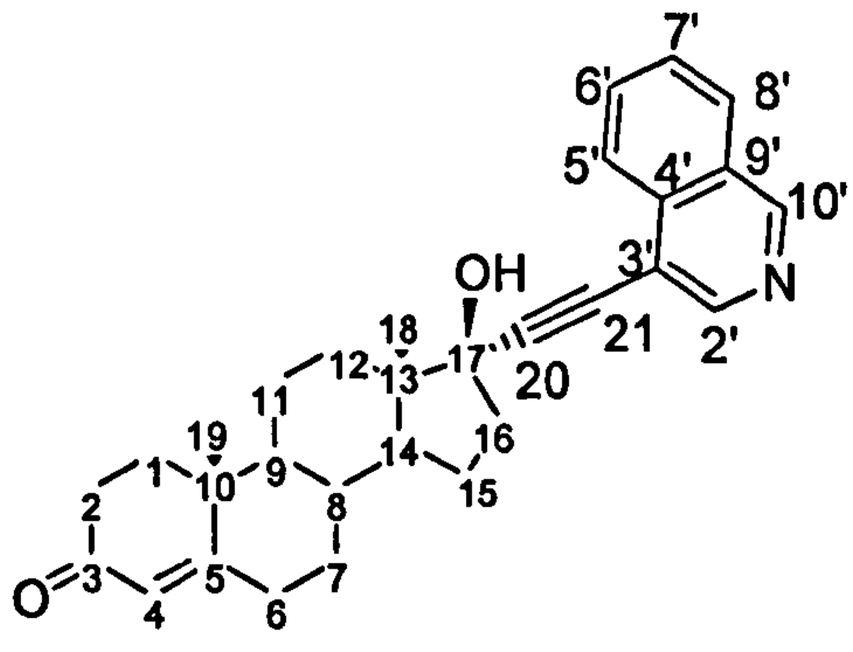

$C_{30}H_{33}NO_2$

The Sonogashira palladium cross-coupling of ethisterone and 4-bromoisoquinoline successfully formed the desired product in high yield and only simple purification techniques, yield a slightly off white crystalline solid. The molecular formula of $C_{30}H_{33}NO_2$ was confirmed by elemental analysis and the appearance of 441 *m/z* ion in ESI-MS corresponds to this formula. ^{1}H and COSY NMR techniques confirm the expected substitution pattern of the isoquinoline group of 2 singlets, 2 doublets and 2 triplets. The signal at 9.14 ppm (Figure 3.21) may be assigned to H2' by comparison to the ligand, ET-3-Py, and H8' by its proximity to the nitrogen atom; following on from this assignment H5', H6', H7' and H10' may be assigned. However, an NOE differential spectrum would confirm the assignment of H2' and H10' and is required for a full assignment.

The loss of the acetylene proton at ca. 2.55 ppm in the ^{1}H NMR demonstrates the reaction took place completely. The α, β-unsaturated ketone proton (H4) is evident at 5.72 ppm and broad 17β-hydroxyl resonance at 4.72 ppm. The ^{13}C DEPT NMR (Figure 3.22) shows a carbonyl resonance at 199.45 ppm in addition to it's infrared stretching mode at 1645 cm^{-1} (Figure A.1.6). The quinoline resonances in addition to C4, Me18 and Me19 have been assigned using ^{13}C-^{1}H HMQC techniques (Figures A.1.14 and A.1.15) although C5' and C6' peaks are too close together to accurately assign. Higher field (0-60 ppm) resonances

from CH and CH_3 groups from the steroid skeleton are present with one exception. The methyl carbons C18 and C19 are present but only two signals remain for the chiral carbons C8, C9 and C14. This may be due to the relative insensitivity of ^{13}C NMR.

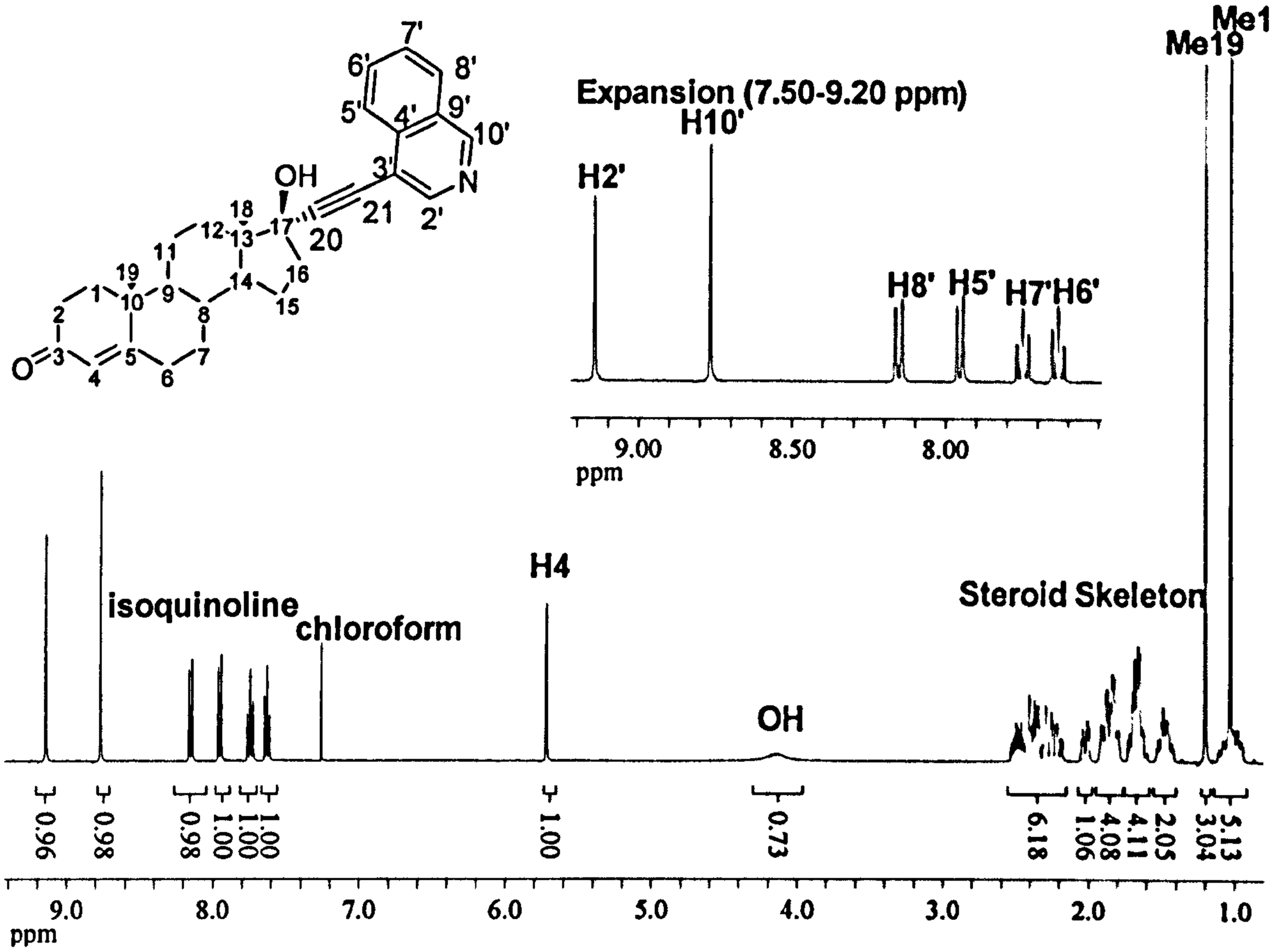

Figure 3.21. The ^1H NMR spectrum of ET-4-IQ in $CDCl_3$.

The infrared spectrum (Figure A.1.16) contains all the fundemental bands characteristic of the functional groups present in ET-4-IQ with the expection of ET-4-IQ with the exception of the $\upsilon C{\equiv}C$ stretch around 2215 cm^{-1}. Given that $\upsilon C{\equiv}C$ stretches are weak and often not observed the lack of a vibrational mode is unsurprising. The $\upsilon C{=}O$ stretch position at 1645 cm^{-1} is consistant with a α,β-unsaturated carbon. The yield is 89 %. The above data is conclusive evidence for the successful synthesis and purification of ET-4-IQ.

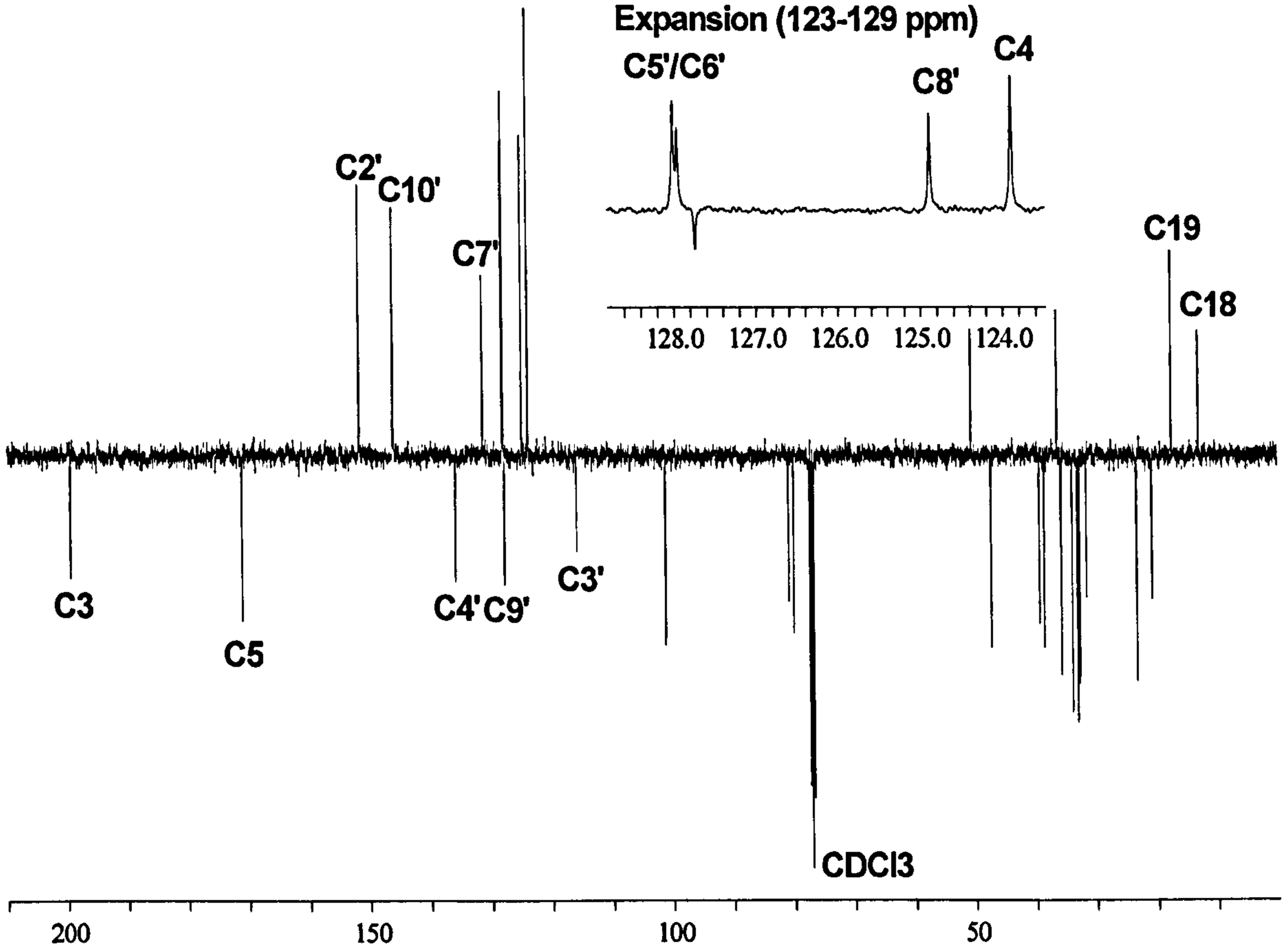

Figure 3.22. The ^{13}C NMR spectrum of ET-4-IQ in $CDCl_3$.

3.2.2.6. Ligand L_6: 17α-quinolin-6-ylethynyl-testosterone (ET-6-Q)

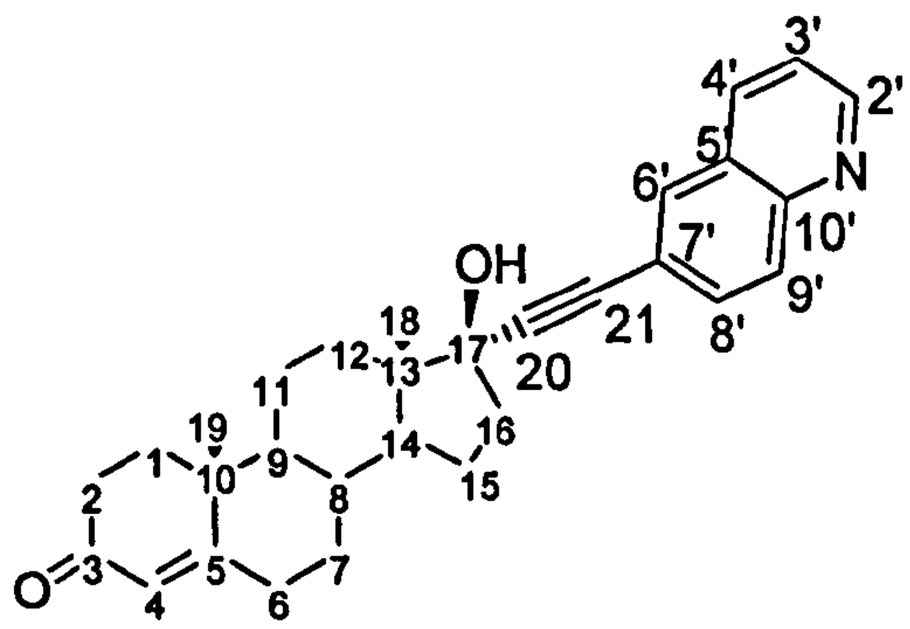

$C_{30}H_{33}NO_2$

The reaction between 6-bromoquinoline and ethisterone using the Sonogashira coupling reaction afforded the desired product in good yield and requiring only simple purification techniques. The product was soluble in chloroform dichloromethane, methanol, DMF and DMSO, partially soluble in acetonitrile, barely soluble in diethylether and insoluble in water. Purification involved 2 steps: a) the removal of copper salts and protonated diisopropylamine with water; b) recrystallisation to remove palladium salts. The product required 72hrs to fully crystallise.

Elemental analysis confirmed the chemical formula of the compound and the parent ion peak at *m/z* = 440 in the ESI-MS corresponds to the mass of protonated ET-6-Q (Figure A.1.17). The ^{1}H NMR spectrum (Figure 3.23) shows two large sets of protons, aromatic and aliphatic in a 1:1 ratio in addition to a peak at 5.65 ppm which may be assigned to H4. The aliphatic region may not be assigned using the current data beyond that of Me18 and Me19 and confirming the correct number of hydrogen atoms (26). The 17α-hydroxyl proton is not observed, probably due to proton exchange. The aromatic resonances, from quinoline, may be assigned in part from examination of the coupling constants and confirmed by a COSY spectrum (Figure A.1.18). H2' may be assigned from its position at the highest chemical shift due to it's proximity to the nitrogen atom and the $^{3}J_{(H-H)}$ and $^{4}J_{(H-H)}$ coupling forming a double of doublets. H6' may be assigned from $^{4}J_{(H-H)}$ coupling from H8'. H3' is assigned from the coupling pattern (doublet of doublets). The splitting pattern expected from H9' is a doublet with no $^{4}J_{(H-H)}$ coupling observed, hence assignment of the 7.97 ppm resonance. The assignment of H4' and H8' is confirmed by cross-coupling peaks in the COSY spectrum.

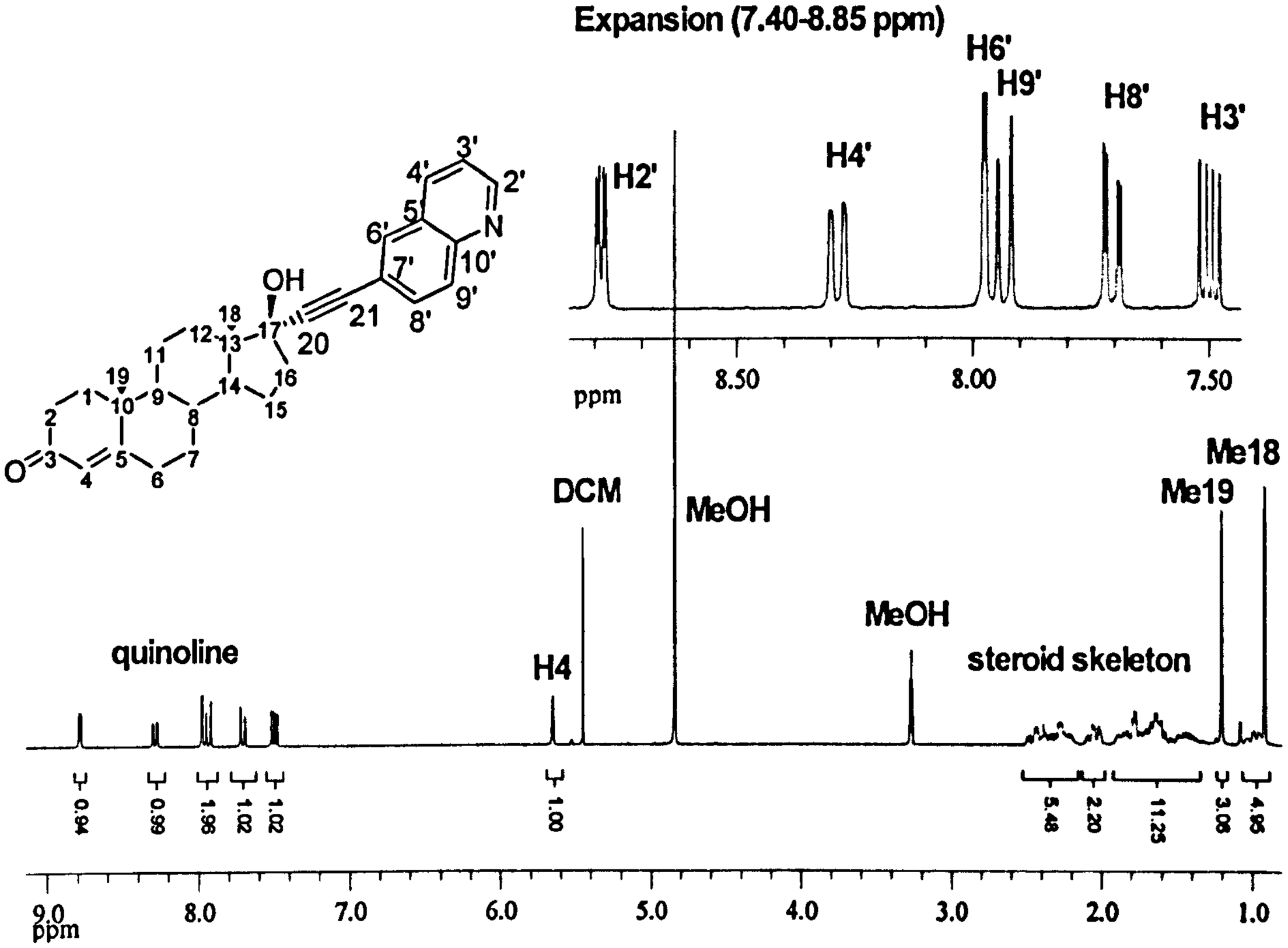

Figure 3.23. The ^{1}H NMR spectrum of ET-6-Q in CD_3OD

The IR spectrum (Figure A.1.19) of the product exhibits several bands characteristic of the fundamental vibration of several functional groups. Bands due to *υ*O-H, *υ*C-H and *υ*C=O

stretches may be observed at 3156, 2938 and 1673 cm^{-1} respectively. No band due the υC≡C stretch mode is seen although these are often too weak to observe. The yield is 60 %. The combined spectroscopy is in agreement with the structure of ET-6-Q.

3.2.3. The synthesis of steroidal platinum(II) complexes: trans-cationic (TC)

Trans-cationic complexes from herein are described as TC-X where X is the steroidal ligand, *i.e.* ET-6-Q or a simple ligand such as pyridine (TC-Py) or quinoline (TC-Q). Attempts to form TC complexes with quinoline ligands often resulted in mixtures of trans-$[Pt(NH_3)_2(L)Cl]^+$ and $[Pt(NH_3)_2(L)_2]^{2+}$ in ratios of sometimes 8:1 respectively. The $[Pt(NH_3)_2(L)_2]$ ion may be observed using mass spectroscopy (ESI, +ve) and ^{1}H NMR spectroscopy. In some cases in mass spectroscopy the $[M-H]^+$ is observed and in others the M^{2+} ion is observed where M = $[Pt(NH_3)_2(L)_2]$. The use of decolourising charcoal in these situations aided isolation of the desired product. However, in the case of TC-IQ isolation of the desired product did not result in success. The complexes were characterised using a range of spectroscopic techniques (^{1}H NMR and mass spectroscopy are examples) and elemental analysis. Evidence for platinum bonded to the hetrocyclic nitrogen atom is presented using NMR evidence, including platinum satellites, downfield shifts of aromatic resonances and in some cases ^{195}Pt NMR spectroscopy.

2.2.3.1. Trans-$[Pt(NH_3)_2(Py)Cl][NO_3]$: TC-Py

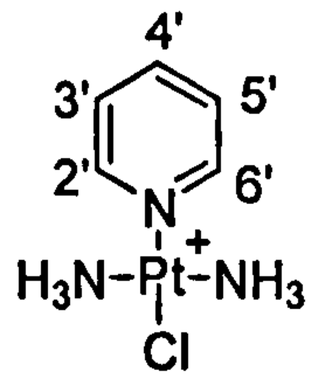

$[C_5H_{11}ClN_3Pt][NO_3]$

The desired product was formed relatively easily between the reaction of trans-$[Pt(NH_3)_2(DMF)Cl]^+$ and pyridine. Purification consisted of several re-crystallisations to achieve the desired purity level of the product. The mass spectrum shows a peak at *m/z* = 343 whose isotope distribution pattern matches that of $[Pt(NH_3)(Py)Cl]^+$ (Figure A.2.1). Elemental analysis is consistant with proposed formula of $[C_5H_{11}ClN_3Pt][NO_3]$. The ^{1}H NMR spectrum (Figure 3.24) may be assigned by inspection of the integration and coupling constants. Platinum satellites either side of the signal assigned to H2'/ H6' are clearly visible and provide excellent evidence for a Pt-N bond. The chemical shifts move downfield compared to pyridine (Figure A.2.2); Downfield shifts of 0.28, 0.22 and 0.14 ppm are observed for the hydrogen atoms, H2'/H6', H4' and H3'H5', respectively. The

^{195}Pt NMR chemical shift is in the region expected for the complexes of the type $[Pt(L)_3Cl]^+$ where L = nitrogen containing ligand. The yield is 20 % and the data presented is in agreement with the proposed structure of TC-Py.

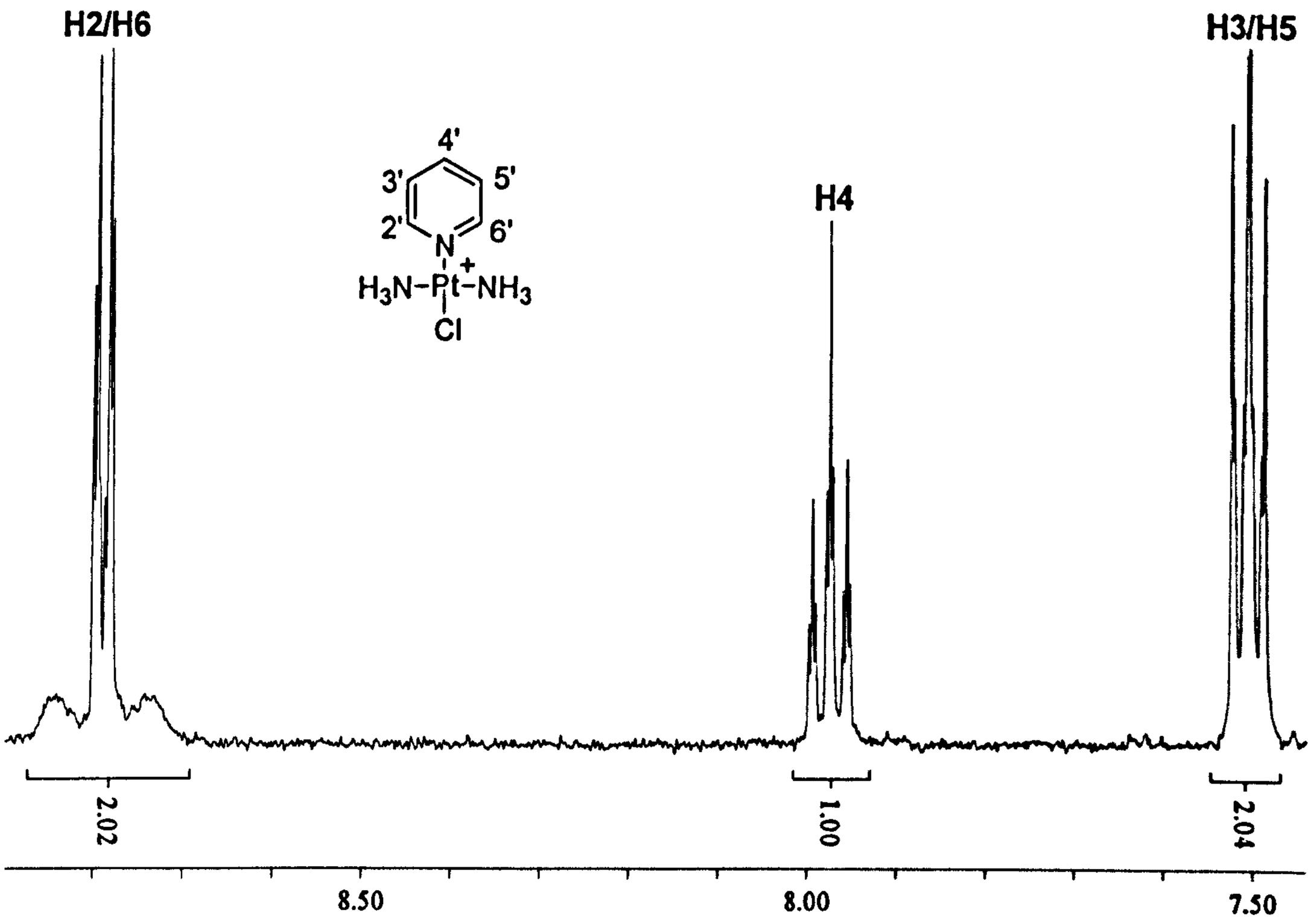

Figure 3.24. The aromatic region of the ^1H NMR spectrum of TC-Py in CD_3OD.

3.2.3.2. Trans-[Pt(NH$_3$)$_2$(Quinoline)Cl][NO$_3$]: TC-Q

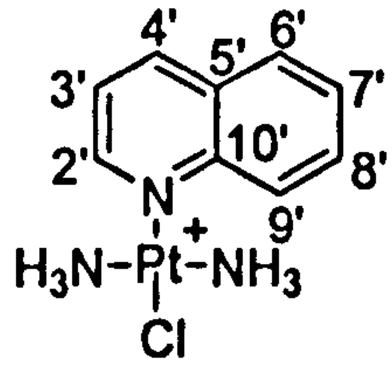

$[C_9H_{13}N_3Pt][NO_3]$

The reaction of transplatin and quinoline via the intermediate trans-$[Pt(NH_3)_2(DMF)Cl]^+$ produced crude trans-$[Pt(NH_3)_2(Quin)Cl]^+$ in high yield which due to purification by selective precipitation and re-crystallisation was substantially reduced by > 50 %. The complex was very soluble in DMSO and DMF, soluble in water, partially soluble in methanol and insoluble in diethylether and chloroform.

The mass spectrum (Figure A.2.3) is consistant with the chemical formula $[Pt(NH_3)_2(DMF)Cl]^+$ and elemental analysis confirmed the proposed chemical formula of $[C_9H_{13}N_3Pt][NO_3]$. The ^1H NMR spectrum (Figure 3.25) may be assigned from the coupling constants and comparison with unbound quinoline. A full assignment requires NOE differential or NOESY NMR techniques and assignment are based on the unbound ligand. All the chemical shifts move downfield between 0.3 (H7') and 1.68 (H9') compared to quinoline. Although no platinum satellites are observed around H2' due to the poor solubility of TC-Q in CD_3OD the downfield shifts of the hydrogen resonances is evidence for platinum binding to the quinoline nitrogen atom. The binding requires donation of electron density from the nitrogen atom to platinum, making the nitrogen increasingly electropositive and itself withdrawing electron density from the aromatic rings causing the dowfield shift. The chemical shift in ^{195}Pt NMR is characteristic of the ligand arrangement $[PtL_3Cl]^+$ where L is a nitrogen containing ligand.

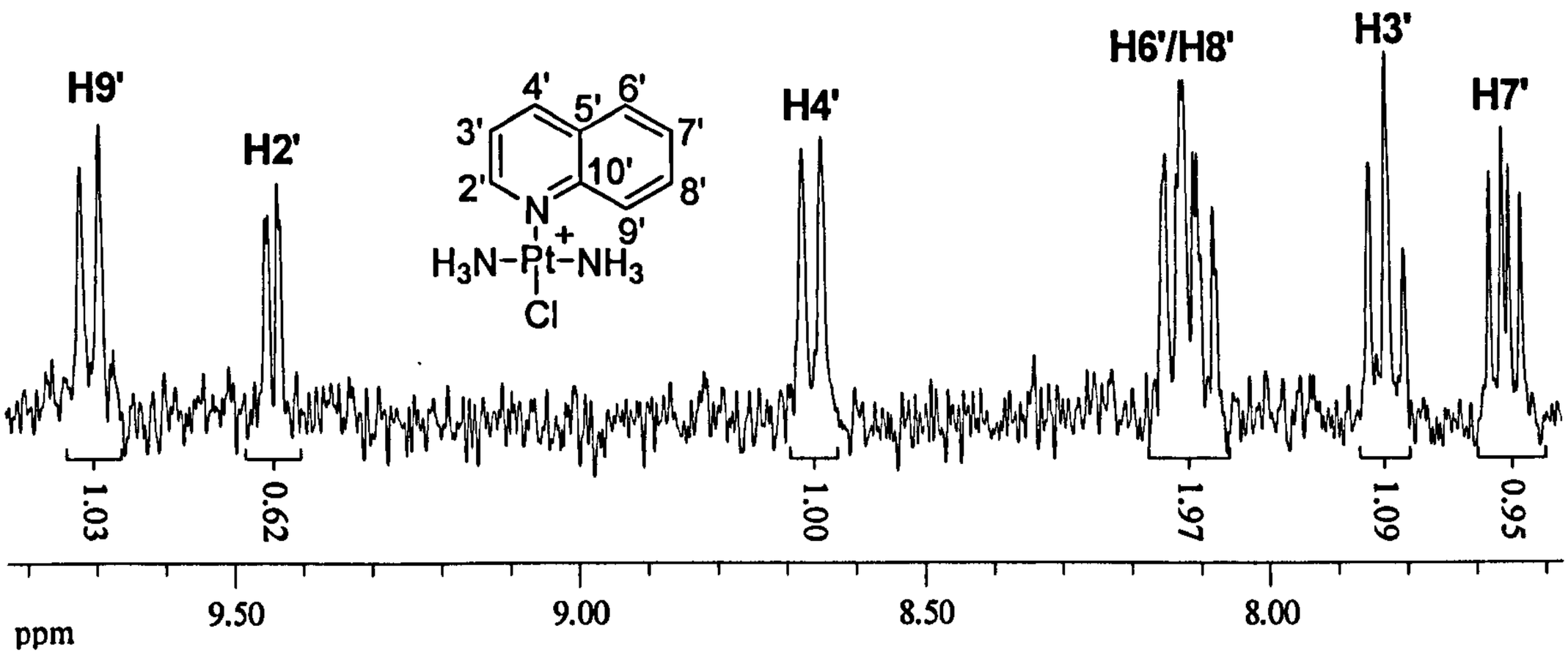

Figure 3.25. The ^1H NMR spectrum of TC-Q in CD_3OD.

The IR spectrum (Figure A.2.4) shows fundamental bands characteristic of the functional groups present within TC-Q. Bands assigned to υN-H stretch are observed at 3266 cm^{-1} whilst the strong broad band centred around 1330 cm^{-1} may be assigned to υN-O stretch and υN-H deformations overlapping and is evidence for the nitrate counter ion. The yield is 15 % and the spectroscopic data presented above is consistent with the proposed structure of TC-Q.

3.2.3.3. Trans-[Pt(NH$_3$)$_2$(ET-3-Py)Cl][NO$_3$]: TC-ET-3-Py

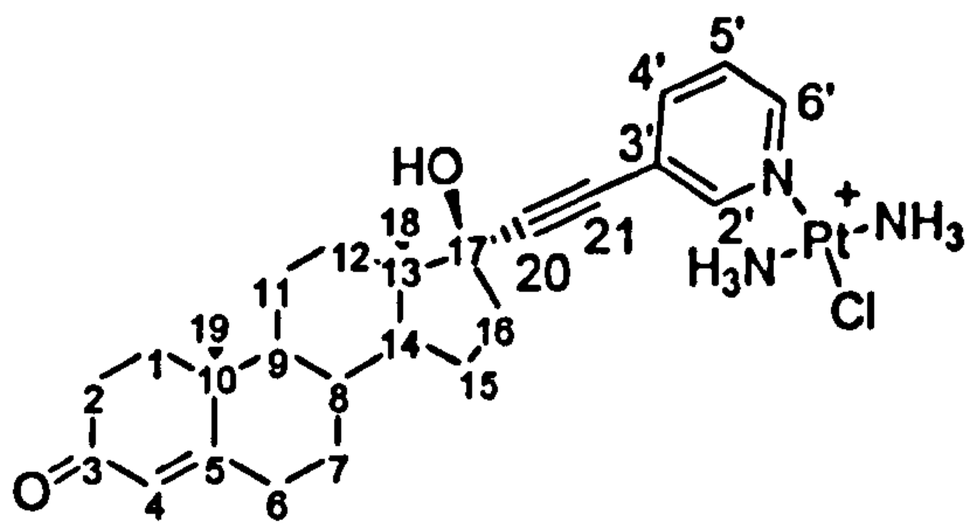

$[C_{26}H_{37}ClN_3O_2Pt][NO_3]$

TC-ET-3-Py was formed by reacting trans-$[Pt(NH_3)_2(DMF)Cl]^+$ with one equivalent of ET-3-Py in DMF and purified using decolourising charcoal and repeated recrystallisations from methanol. The products was a white fluffy solid, soluble in DMSO, DMF, less so in methanol and water and insoluble in diethylether and chloroform.

Elemental analysis confirmed the chemical formula as that expected and the mass spectrum (ESI, +ve) found a single peak at *m/z* = 654 corresponding to the platinum complex $[Pt(NH_3)_2(ET\text{-}3\text{-}Py)Cl]^+$. The aromatic region of ^{1}H NMR spectrum (Figure 3.26) may be assigned by inspection of the coupling constants and confirmed by a COSY spectrum (Figure A.2.5). The resonance of highest chemical shift may be assigned to H2' due to the small coupling constant (1.8 Hz) and H6' by its splitting pattern, a doublet of doublets (^{3}J and ^{4}J coupling). Finally H5' is assigned by the coupling constants, doublet of doublets (^{3}J coupling) leaving the remaining signal assigned to H4'. Of particular note is the baseline broadness around the signals assigned to H2' and H6' and is very suggestive of platinum satellies (and hence platinum binding to the pyridine nitrogen) although no distinct satellites may be observed. The other signals are assigned by the chemical shift and on the case of Me19 by comparison with estradiol, a steroid with an identical D ring but no Me19. The steroidal skeleton may not be fully assigned but the correct integration is observed. Additional evidence of the ligand bound to platinum comes from the downfield shifts observed when compared to the free ligand (Figure A.2.6). Shifts of 0.42, 0.23, 0.17 and 0.36 ppm are observed for H2', H4', H5' and H6' respectively and these are of lesser magnitude with increasing distance from the pyridine nitrogen.

The IR spectrum (Figure A.2.7) displays many bands including those at 2943, 1645 and 1330 cm^{-1} and may be assigned to υC-H str, υC=O str and υN-H def/υN-O str respectively. The spectroscopy confirms the expected structure of the desired product and the yield is 28 %.

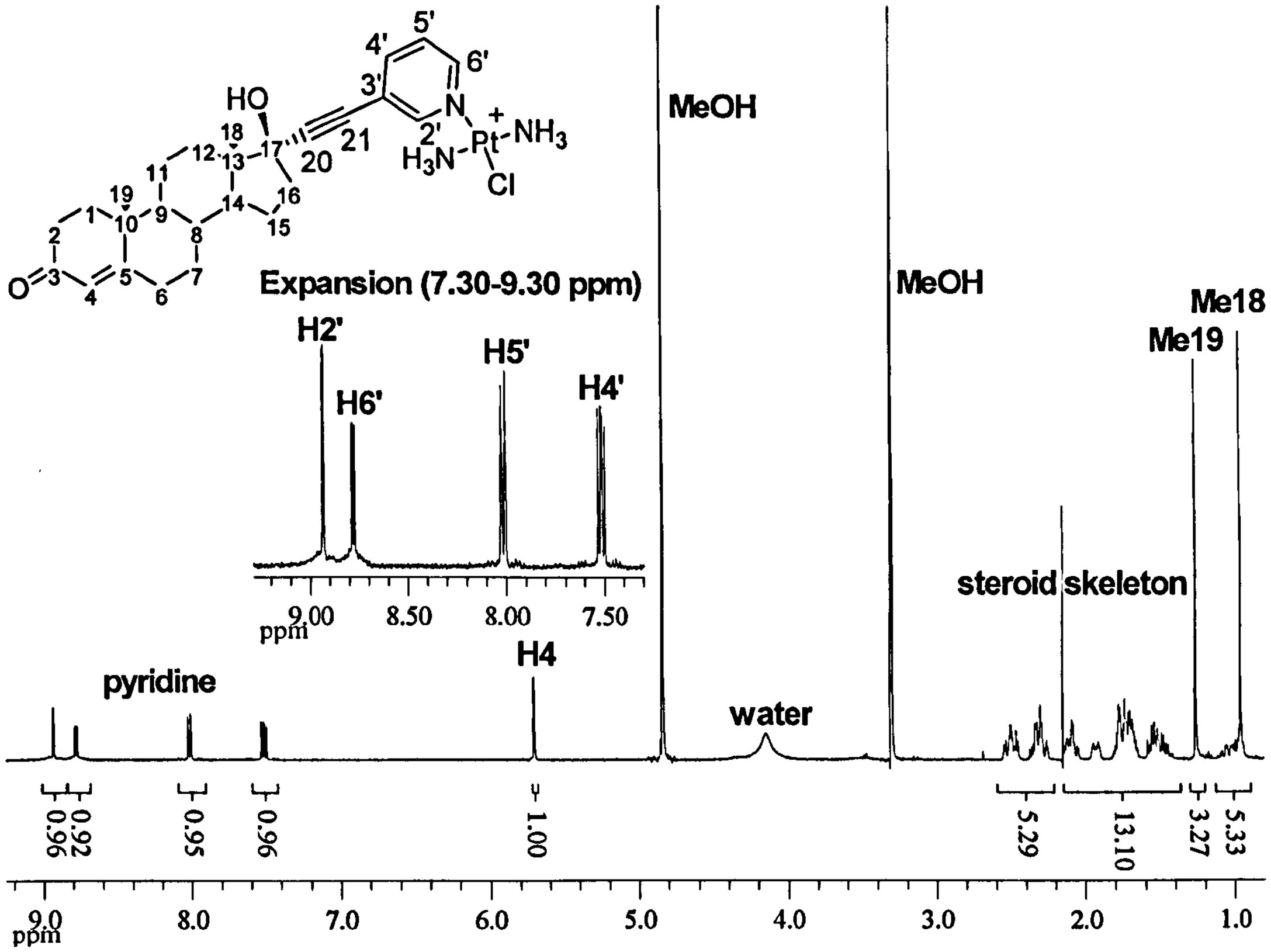

Figure 3.26. The ^{1}H NMR spectrum of TC-ET-3-Py in CD_3OD.

3.2.3.4. Trans-[Pt(NH$_3$)$_2$(ET-4-Py)Cl][NO$_3$]: TC-ET-4-Py

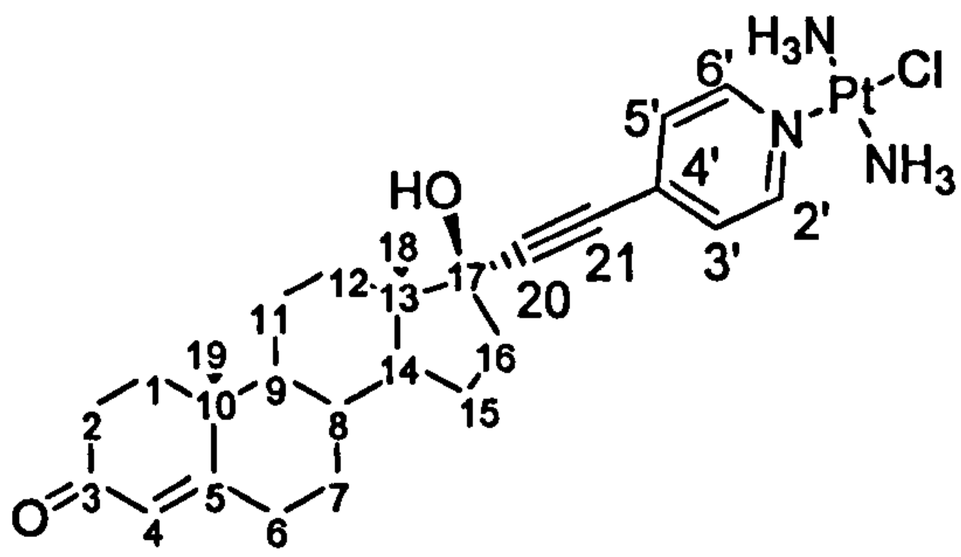

$[C_{26}H_{37}ClN_3O_2Pt][NO_3]$

The reaction between transplatin and ET-4-Py via a reactive intermediate resulted, after purification, in a bright white solid that was very soluble in DMSO and DMF, less so in methanol and water and insoluble in diethylether. Purification was by repeated recrystallisations.

Elemental analysis confirmed the proposed chemical formula and mass spectrometry (ESI, +ve) where the parent peak of $m/z = 654$ corresponds to $[Pt(NH_3)_2(ET\text{-}4\text{-}Py)Cl]^+$ (Figure A.2.8). In the ^{1}H NMR spectrum (Figure 3.27) the chemical shifts of the pyridine proton

pairs H2'/H6' and H3'/H5' are shifted downfield by 0.28 and 0.12 ppm, respectively, compared to the free ligand (Figure A.2.9).

The downfield shift in TC-ET-4-Py *Cf.* ET-4-Py may be rationalised by the withdrawal of electron density from the pyridine ring due to an increasingly electropositive nitrogen atom as a result of donating its non-bonding electron pair for covalent bonding to platinum. The closer proximity of H2'/H6' to the pyridine nitrogen atom accounts for its larger shift downfield compared to H3'/H5' after binding to platinum(II).

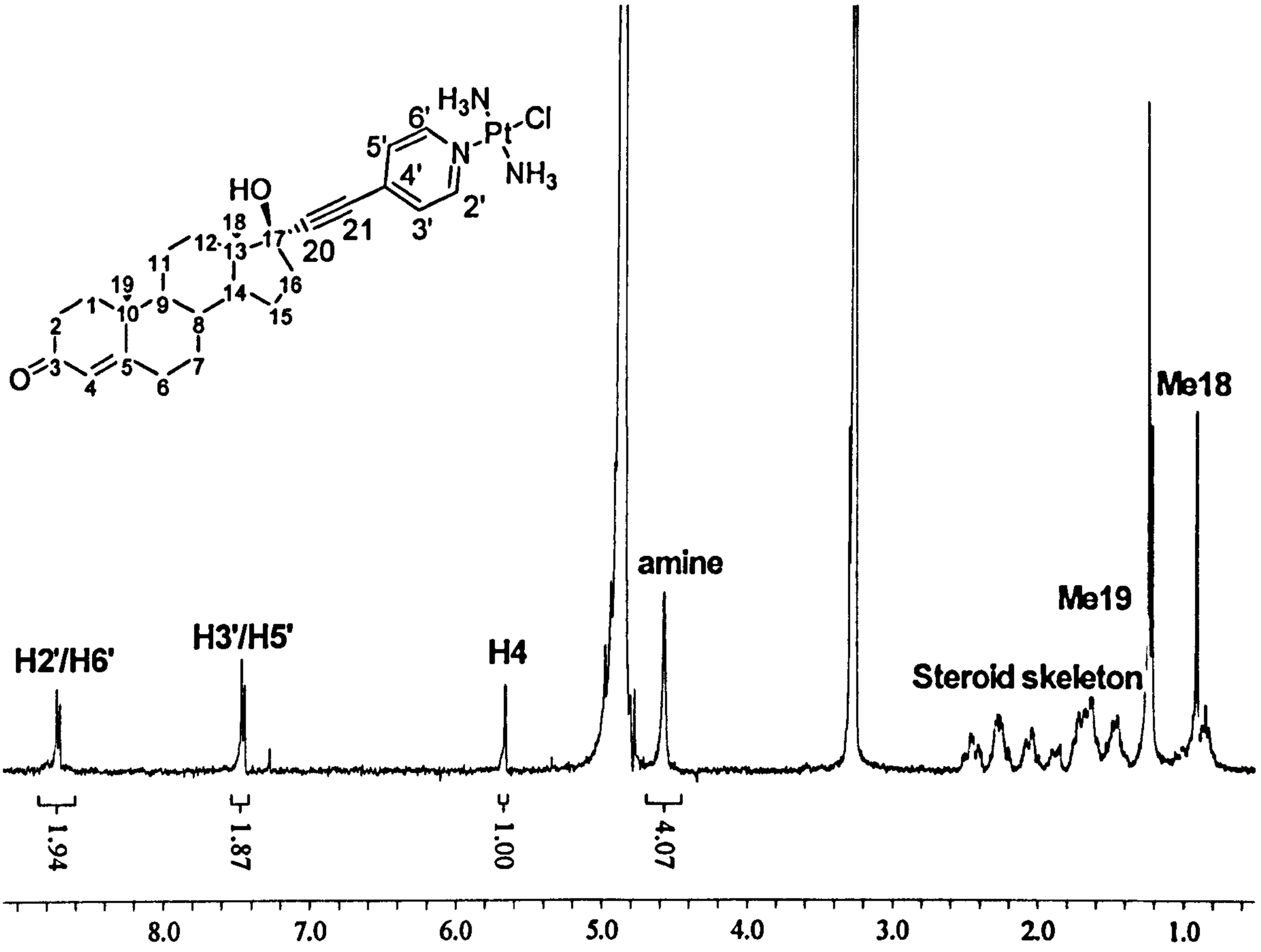

Figure 3.27. The ^{1}H NMR spectrum of TC-ET-4-Py in CD_3OD.

The infrared spectrum (Figure A.2.10) shows several vibrational modes characteristic of the functional groups present in TC-ET-4-Py. The ligand ET-4-Py is represented in the spectrum by bands assigned to υO-H, υC-H, υC≡C and υC=O stretches. The NH_3 groups of the complex show characteristic absorptions around 3210 and 1300 cm^{-1} corresponding to υN-H stretch and υN-H deformation respectively. The υN-O stretch expected from the nitrate salt likely contributes to the broad band around 1300-1400cm^{-1} in addition to the other bands mentioned. The band at 825 cm^{-1} may be assigned to υC-H out of plane deformation and is characteristic of a 2-substituted pyridine ring. The spectroscopic

evidence presented here is in agreement with the proposed structure of TC-ET-4-Py and the yield is 22 %.

3.2.3.5. Trans-[Pt(NH$_3$)$_2$(ET-3-Q)Cl][NO$_3$]: TC-ET-3-Q

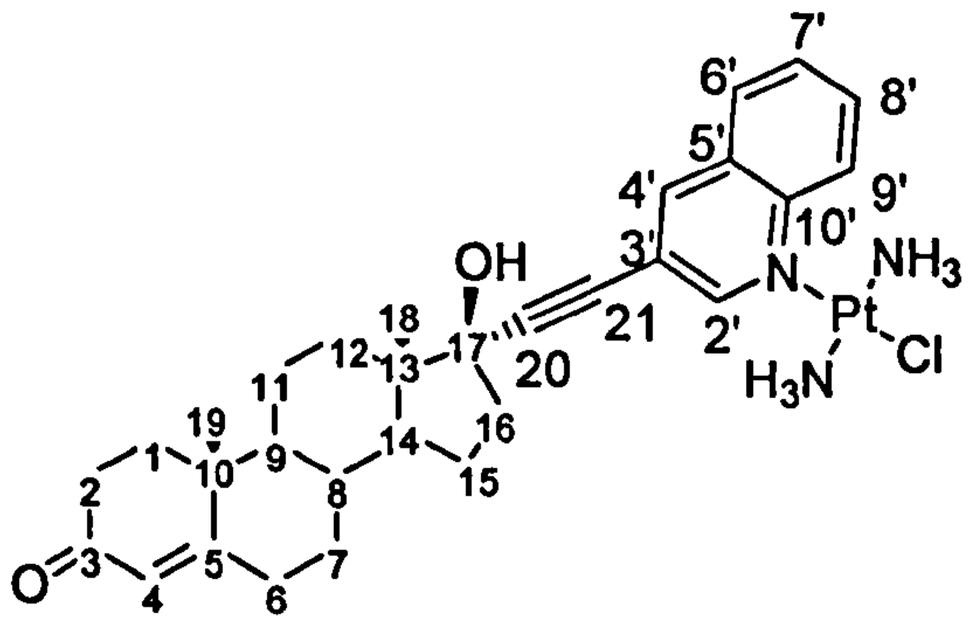

$[C_{30}H_{39}ClN_3O_2Pt][NO_3]$

The reaction between trans-$[Pt(NH_3)(DMF)Cl]^+$ and ET-3-Q yielded the desired product in low yield. The purification involved filtration of DMF insoluble silver chloride and selective precipitation / adsorption on charcoal in isolating the main product from DMF and unreacted transplatin, trans-$[Pt(NH_3)(DMF)Cl]^+$ and the disubstituted complex $[Pt(NH_3)_2(ET\text{-}3\text{-}Q)_2]^{2+}$.

Elemental analysis confirmed the chemical formula and ESI-MS parent ion peak at *m/z* = 704.2 corresponds to the ion $[Pt(NH_3)_2(ET\text{-}3\text{-}Q)Cl]^+$ (Figure A.2.11) whose experimental isotope distribution pattern matches that predicted for $[Pt(NH_3)_2(ET\text{-}3\text{-}Q)Cl]^+$ (Figure A.2.12). The ^{1}H NMR spectrum (Figure 3.28) is that of the bound ligand ET-3-Q and assignment are as for the free ligand. The spectrum may be assigned by observation of the coupling constants, COSY spectrum (Figure A.2.13) and comparison with ET-3-Q. There is no clear evidence of platinum satelites either side of the H2' signal but small signals can be differentiated from the baseline. No evidence of NH_3 groups is present possibly due to proton exchange. Compared to the ^{1}H NMR spectrum of the free ligand, in the spectrum of TC-ET-3-Q the aromatic proton resonances have shifted downfield and in general the closer the proton to the nitrogen atom, the greater the shift (Figure A.2.14). The resonances of the protons H2', H4', H6', H7' and H8' are shifted downfield by 0.68, 0.29, 0.15, 0.18, 0.03 ppm respectively. The signal from H9' is shifted 1.97 ppm downfield and such a large downfield shift may represent a direct interaction between H9' and platinum.

The IR spectrum of TC-ET-3-Q (Figure A.2.15) exhibits several broad bands from overlapping characteristic vibrational modes of groups within TC-ET-3-Q. Overlapping

υO-H, υC-H and υN-H stretches are centred around 3256 cm^{-1} and bands corresponding to υC=O is seen at 1645 cm^{-1} and υN-H deformation and υN-O stretch from the NH_3 ligand and NO_3^- counter-ion overlap around 1332 cm^{-1}. The combined spectroscopic data is in agreement with the structure of TC-ET-3-Q and the yield is 28 %.

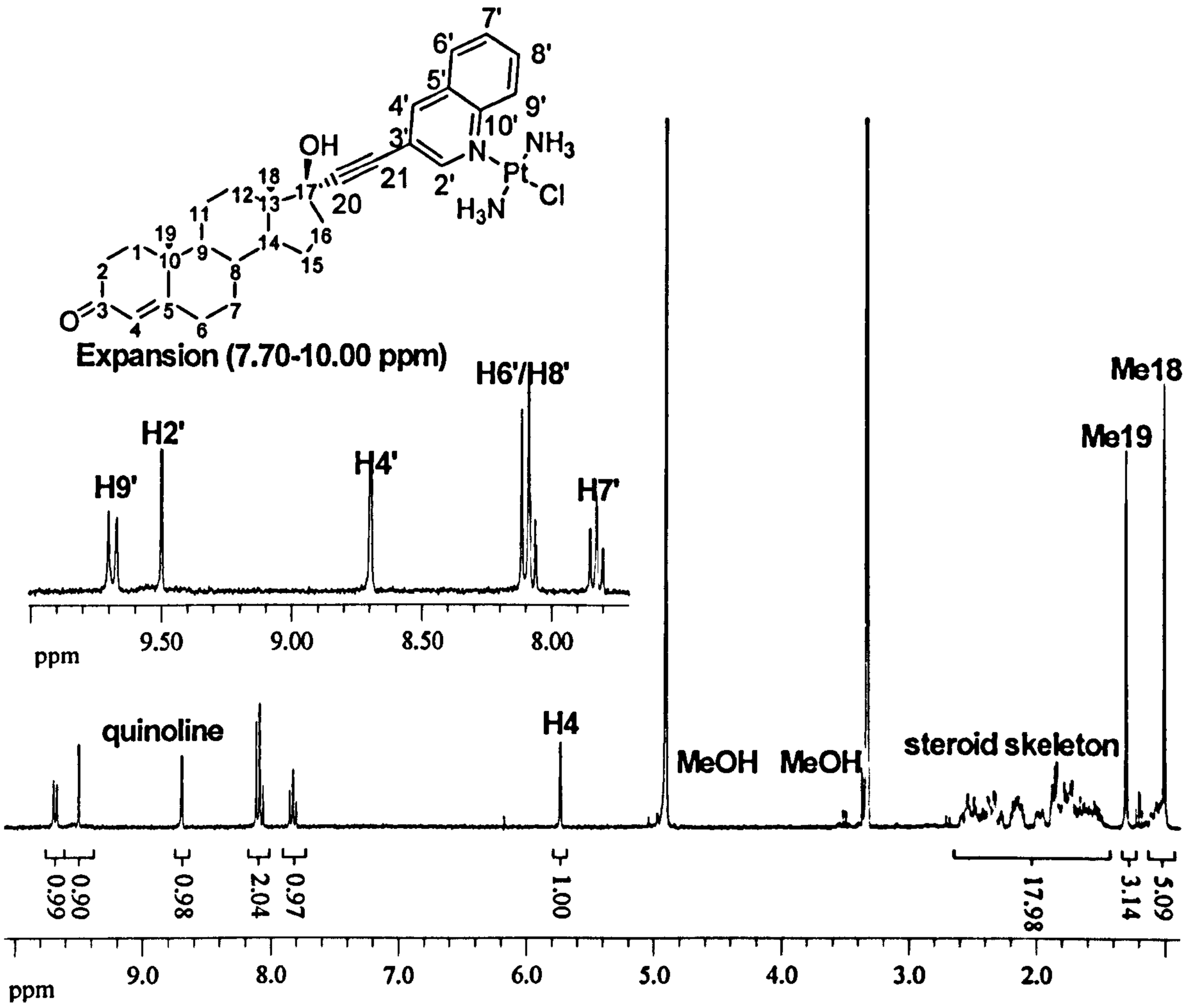

Figure 3.28. The ^1H NMR spectrum of TC-ET-3-Q in CD_3OD.

3.2.3.6. Trans-[Pt(NH$_3$)$_2$(ET-4-IQ)Cl][NO$_3$]: TC-ET-4-IQ

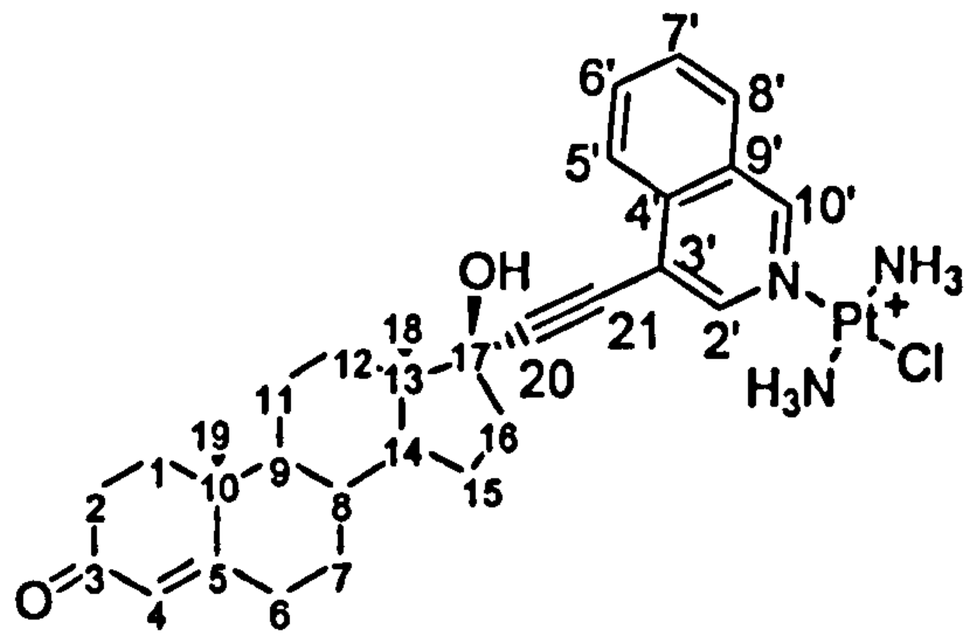

$[C_{30}H_{39}ClN_3O_2Pt][NO_3]$

The reaction between trans-$[Pt(NH_3)_2(DMF)Cl]^+$ and ET-4-IQ produced two main products, trans-$[Pt(NH_3)_2(ET\text{-}4\text{-}IQ)Cl]^+$ and $[Pt(NH_3)_2(ET\text{-}4\text{-}IQ)_2]^{2+}$, presumably trans, in

an approximate 8:1 ratio by ^{1}H NMR (Figure A.2.16). The complex $[Pt(NH_3)_2(ET\text{-}4\text{-}IQ)_2]$ was observed as the monocation, presumably loosing H^+ (Figure A.2.17). The ratio was not dependent on the ratio of starting materials: up to an 5 fold excess of ET-4-IQ over transplatin nor if ET-4-IQ was added slowly to the solution containing trans-$[Pt(NH_3)_2(DMF)Cl]^+$. Purification of the crude mixture was achieved in several steps: a) selective precipitation of steroidal platinum complexes to separate from un-reacted starting materials; b) selection adsorbtion onto charcoal of disubstituted complexes compared to monosubstituted, presumably due to charge differences; c) selective dissolving in methanol (the complex crystals are more soluble than ET-4-IQ). The product was soluble in DMF, DMSO and methanol, less so in water and insoluble in diethylether and chloroform.

The use of charcoal had two effects on the relative proportions of the reaction products. Whilst ET-4-IQ, trans-$[Pt(NH_3)_2(ET\text{-}4\text{-}IQ)Cl]^+$ and $[Pt(NH_3)_2(ET\text{-}4\text{-}IQ)_2]^{2+}$ adsorbed onto the charcoal, ET-4-IQ adsorbed more slowly than trans-$[Pt(NH_3)_2(ET\text{-}4\text{-}IQ)Cl]^+$ which in turn adsorbed slower than $[Pt(NH_3)_2(ET\text{-}4\text{-}IQ)_2]^{2+}$. The effect of removing $[Pt(NH_3)_2(ET\text{-}4\text{-}IQ)_2]^{2+}$ lead to increased relative amounts of ET-4-IQ compared to trans-$[Pt(NH_3)_2(ET\text{-}4\text{-}IQ)Cl]^+$ which were later separated. The final product was analysed by mass spectroscopy whose m/z = 704.2 corresponds to the platinum complex $[Pt(NH_3)_2(ET\text{-}4\text{-}IQ)Cl]^+$ (Figures A.2.18 and A.2.19) with comparable experimental and theoretical isotope distribution pattern. Elemental analysis matches the proposed chemical formula.

The ^{1}H NMR spectrum (Figure 3.29) may be assigned by the coupling constants and comparison with the spectrum of ET-4-IQ. The assignment are as for ET-4-IQ but require NOE differential or NOESY NMR spectroscopy to fully assign. The NH_3 groups are not visible possibly due to hydrogen exchange. Broadening of the signals assigned to H2' and H10' may be attributed to platinum satellites although no discernable peaks are visible either side of the main peak. Other NMR evidence for the ligand bound to platinum is the chemical shifts of the aromatic protons of TC-ET-4-IQ are shifted downfield compared to ET-4-IQ (Figure A.2.20). The downfield shifts are 0.85, 0.45, 0.39, 0.26, 0.30, 0.30 ppm for H2', H10', H8', H5', H7' and H6' respectively.

The infrared spectrum of TC-ET-4-IQ (Figure A.2.21) shows bands characteristic of the functional groups present in the TC-ET-4-IQ. The broad bands around 3200 cm^{-1} may be assigned to υO-H, υC-H and υN-H stretching modes overlapping. The broad band at 1657 cm^{-1} likely originates from the υC=O stretching vibrational modes overlapping other bands, whilst the large broad band around 1350 cm^{-1} may be assigned to υN-H

deformations and υN-O stretch from the NH_3 ligand and $[NO_3]^-$ counter-ion respectively. The yield is 25 % and the spectroscopic evidence presented confirms the proposed structure for TC-ET-4-IQ.

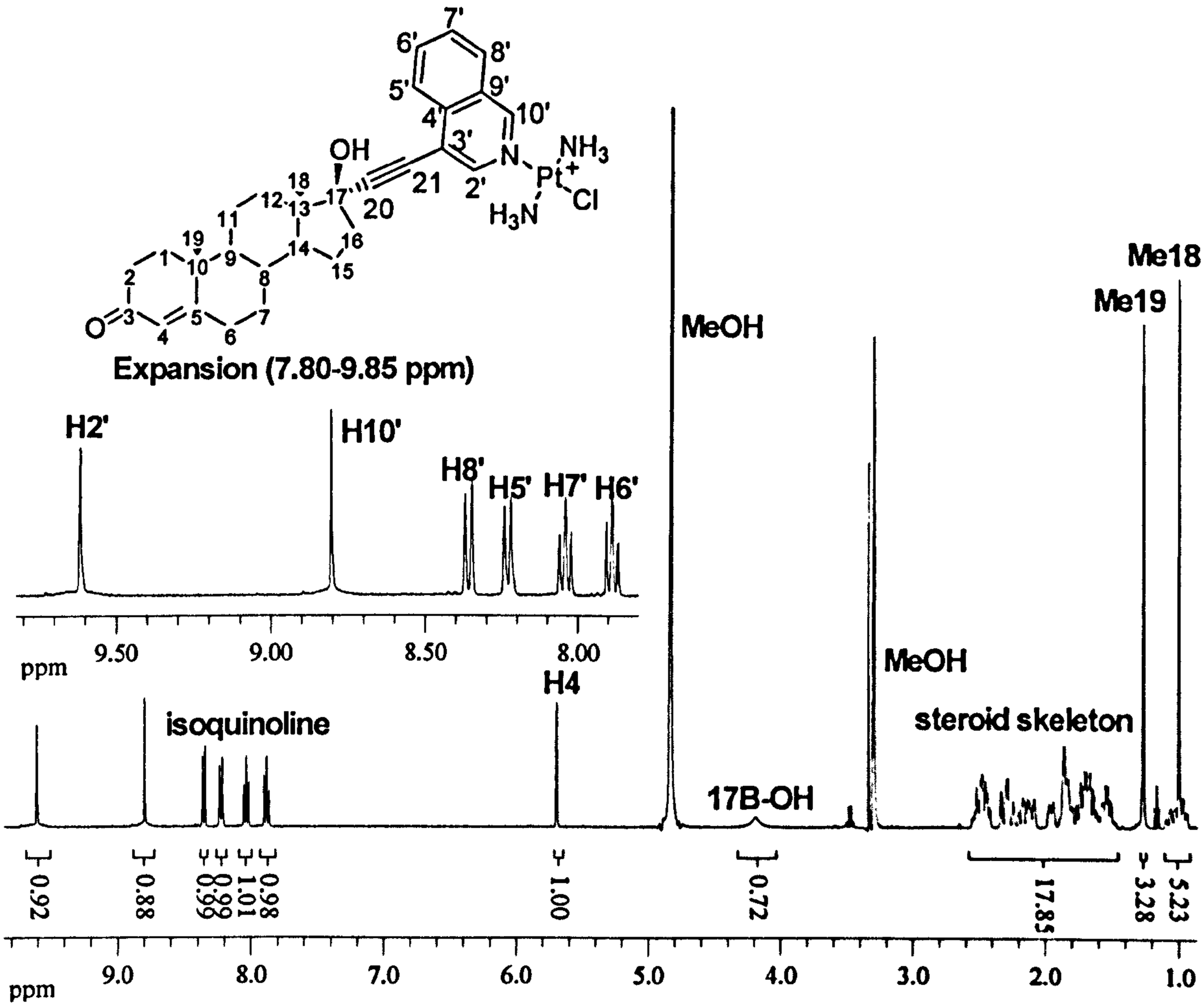

Figure 3.29. The ^{1}H NMR spectrum of TC-ET-4-IQ in CD_3OD.

3.2.3.7. Trans-[Pt(NH$_3$)$_2$(ET-6-Q)Cl][NO$_3$]: TC-ET-6-Q

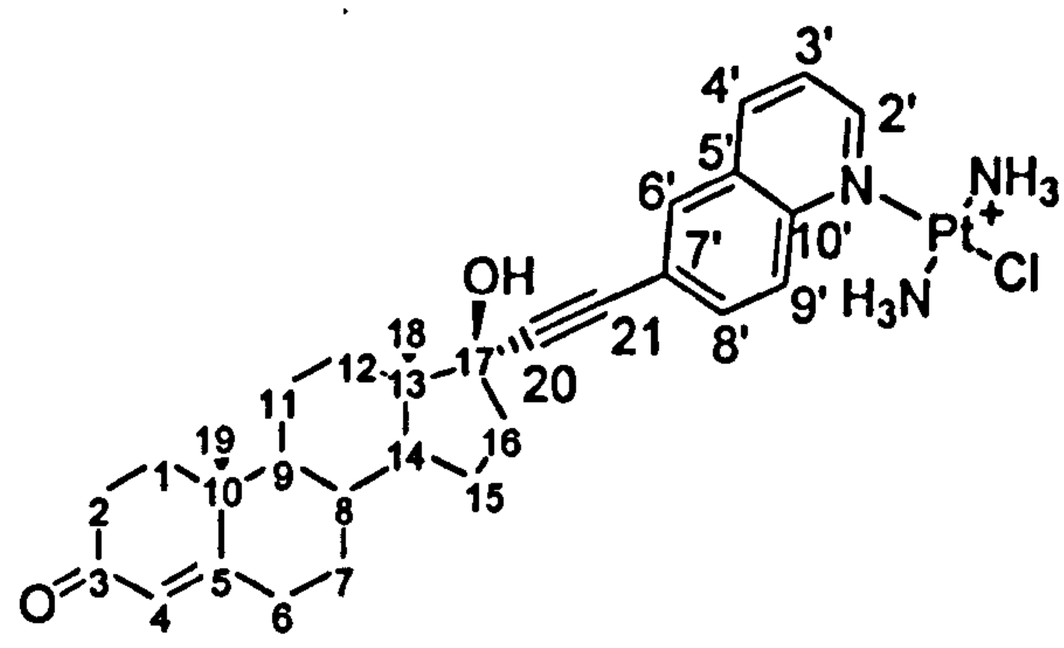

$[C_{30}H_{39}ClN_3O_2Pt][NO_3]$

The reaction between trans-$[Pt(NH_3)_2(DMF)Cl]^+$ and ET-6-Q yielded the desired product after purification by selective precipitation to remove residual DMF, ET-6-Q and

transplatin. The product was a white fluffy solid, soluble in DMF and DMSO, less so in methanol and water and insoluble in chloroform and water.

The chemical formula of the product was confirmed by elemental analysis to be $[C_{30}H_{39}ClN_3O_2Pt][NO_3]$. The parent ion peak at m/z = 704.2 corresponds to the platinum complex $[Pt(NH_3)_2(ET\text{-}6\text{-}Q)Cl]^+$ and the theoretical and experimental isotope distribution patterns match (A.2.22). The ^1H NMR (Figure 3.30) is essentially that of the ligand ET-6-Q, the NH_3 groups are not observed possibly due to proton exchange. All hydrogen atoms are accounted for with the exception of the 17β-hydroxyl hydrogen atom which isn't observed in the free ligand perhaps due to proton exchange. The quinoline resonances may be assigned by inspection of the coupling constants and comparison with the free ligand ET-6-Q.

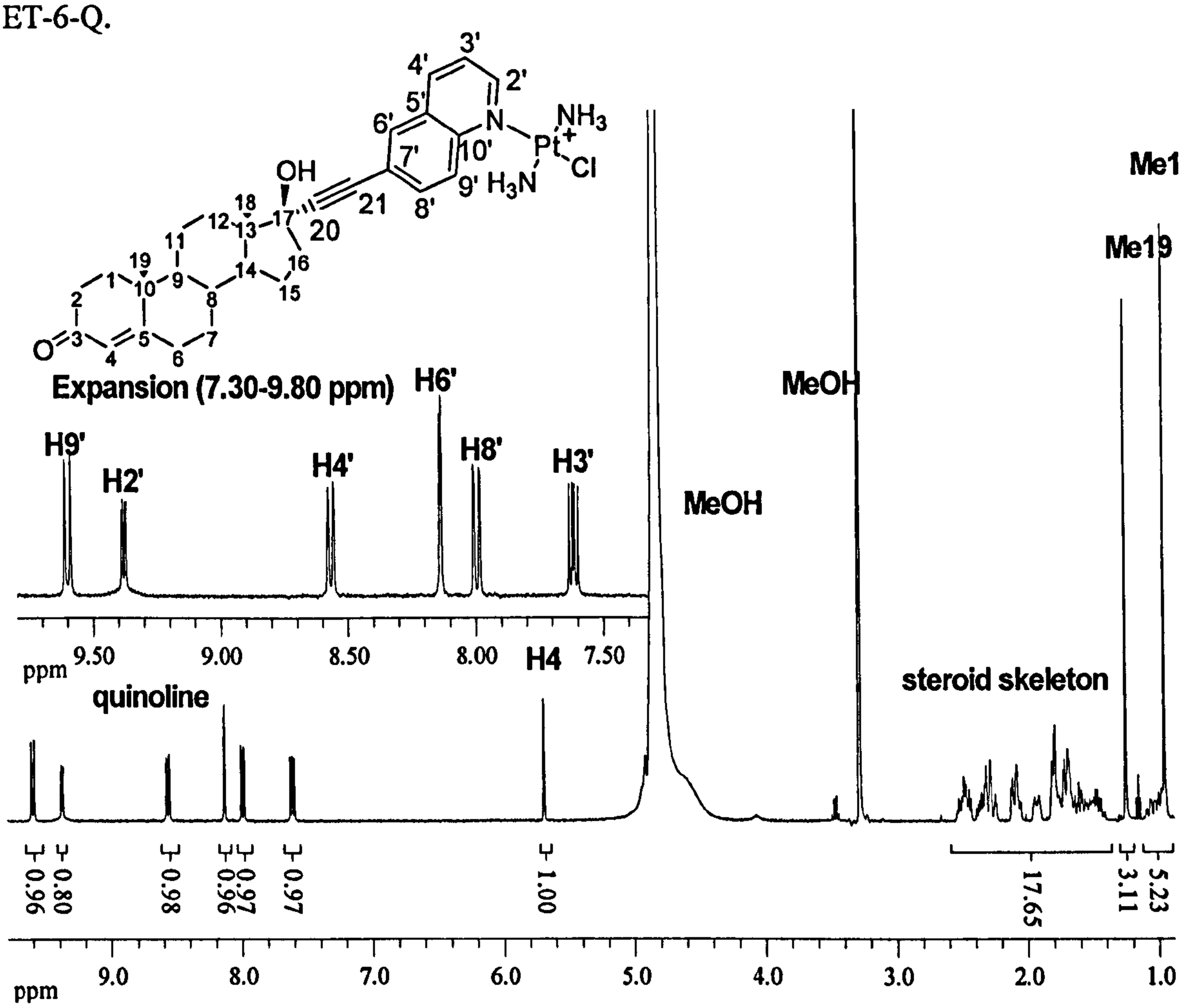

Figure 3.30. The ^1H NMR spectrum of TC-ET-6-Q in CD_3OD.

There are two differences between the ^1H NMR spectrum and that of ET-6-Q. Whilst clear platinum satilites are not observed either side of the resonance assigned to H2', broadening of the baseline can clearly be seen indicating that platinum is bound to the nitrogen atom of the quinoline ring. As may be expected there is a downfield shift in all the aromatic hydrogen resonances with some greater than others (A.2.23). Shifts of 0.59, 0.12, 0.30,

0.17, 0.30 and 1.67 ppm are observed for atoms H2', H3', H4', H6', H8' and H9' respectively. The magnitude of the shift decreases with decreasing distance away from the nitrogen atom. The large shift of H9' is perhaps due to direct interaction with the platinum(II) metal.

The IR spectrum (A.2.24) shows several bands characteristic of the functional groups present in TC-ET-6-Q. Around 3300 cm^{-1} several overlapping bands may be observed and assigned to υC-H, υN-H and υO-H stretching vibrations. Aliphatic υC-H stretching modes from the steroidal skeleton are clearly observed between 2830 and 2974 cm^{-1} as is the υC=O stretch at 1666 cm^{-1}. The large broad band centred around 1325 cm^{-1} may be assigned to overlapping bands from υN-H deformations of NH_3 ligands and υN-O stretching from the nitrate counter ion. The above data is evidence for the proposed structure of TC-ET-6-Q and the yield was 38 %.

3.2.4. The synthesis of steroidal platinum(II) complexes: cis-cationic (CC)

In the case of CC complexes cisplatin was used as a starting material to result in *cis* complexes. Of particular note was the light sensitivity of some of the CC complexes and decomposition was accompanied by the complexes turning from white to grey / green. The complex CC-ET-3-Q decomposed whilst the crude product was being filtered as did CC-ET-4-Py. The other complexes were much more robust and required only storage in dark conditions. Without this the complexes shows signs of decomposition within one week. Light sensitivity is not new in platinum complexes; an aqueous solution of cisplatin will decompose within days if not stored in the dark. The complexes were analysed using a range of techniques including elemental analysis and NMR spectroscopy. ^{195}Pt NMR spectroscopy was attempted on the complexes and despite the low sensitivity of the technique signals were observed in many of the complexes and commensurate with the formula $[Pt(NH_3)_2(L)Cl]^+$ where L is a nitrogen containing ligand.

3.2.4.1. Cis-$[Pt(NH_3)_2(Py)Cl][NO_3]$: CC-Py

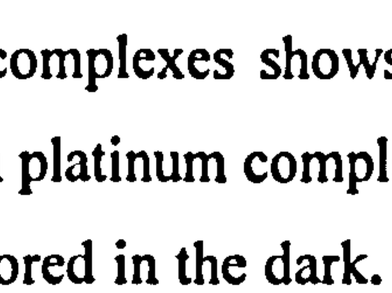

$[C_5H_{11}ClN_3Pt][NO_3]$

Synthesis of the crude complex was easily achieved and the pure complex after several recrystallisation procedures. The complex was identified using several techniques

including elemental analysis, ESI-MS, IR and ^{1}H and ^{195}Pt NMR spectroscopy. Elemental analysis is consistant with the formula $[C_5H_{11}ClN_3Pt][NO_3]$ and the mass spectroscopy (ESI, +ve) spectrum shows a parent ion peak at *m/z* = 344 and isotope distribution matching $[C_5H_{11}ClN_3Pt]^+$ (Figure A.3.1).

The ^{1}H NMR spectrum (Figure 3.31) shows the aromatic hydrogen atoms of the pyridine ring in the product. Three signals are observed due to symmetry with H2/H6 having the highest chemical shift due to it position relative to nitrogen. The H2/H6 protons are split by H3/H5 into a doublet but the smaller signals at each side of the signal are due to $^{3}J_{(Pt\text{-}H)}$ coupling with a coupling constant of 21.6 Hz. The magnitude of the splitting observed is consistent with that expected from ^{195}Pt. The chemical shifts of all 5 hydrogen atoms of the pyridine are shifted relative to free pyridine as shown in Figure A.3.2. H2/H6, H4 and H3/H5 are shifted downfield by 0.32 ppm, 0.19 ppm and 0.14 ppm respectively. This is consistent with bonding arrangements between platinum and pyridine where the nitrogen sp^2 lone pair is donated to the platinum centre making the nitrogen more electropositive and withdrawing electron density from the aromatic ring system. The ^{195}Pt NMR resonance is in agreement with that expected of a complex of the type $[Pt(NH_3)_2(L)Cl]^+$ where L is a nitrogen containing ligand.

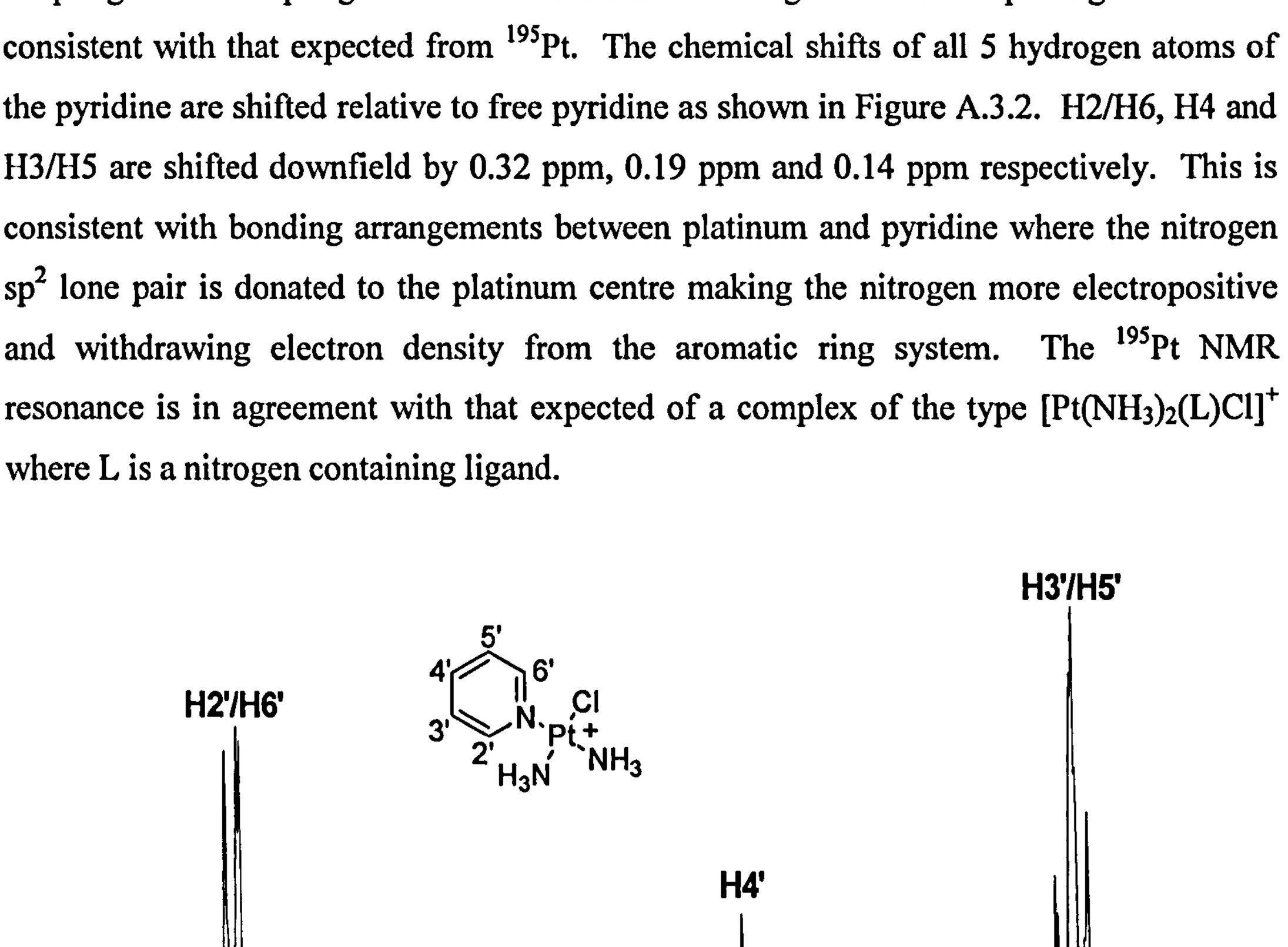

Figure 3.31. The ^{1}H NMR spectrum of CC-Py in CD_3OD.

The IR spectrum (Figure A.3.3) shows several bands, many of which may be attributed to υN-H and υC-H stretching and bending modes. The broad strong peak at around 1340 cm^{-1} may be attributed to an overlapping υN-H deformation mode and υN-O stretching mode. The 1st υN-O stretching mode in nitrate ions exhibit a single band in the 1350 cm^{-1}-1380 cm^{-1} region whilst the υN-H deformation is between 1280 cm^{-1} and 1300 cm^{-1} in cisplatin and transplatin and the two appear overlapping. This gives evidence for the nitrate counter ion and NH_3 groups present within the structure. Further evidence of a pyridine ring may be found due to υC-H out of place deformations found at 760 cm^{-1} and 687 cm^{-1} and are those expected for a pyridine ring. The spectroscopic data is in agreement with the product being CC-Py and the yield is 23 %.

3.2.4.2. Cis-[Pt(NH$_3$)$_2$(ET-3-Py)Cl][NO$_3$]: CC-ET-3-Py

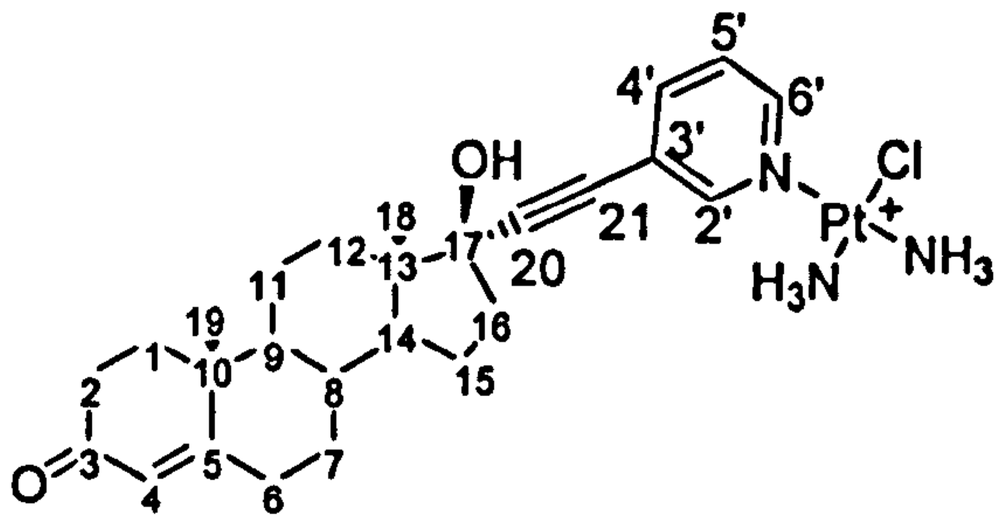

$[C_{26}H_{37}ClN_3O_2Pt][NO_3]$

The substitution of a chloride in cisplatin by DMF aided by silver chloride and further substitution of DMF by ET-3-Py produced the desired product in low yield due the large number of purification steps required. Multiple re-crystallisations resulted in a bright white solid soluble in DMSO, DMF, partially soluble in water and methanol and insoluble in chloroform and diethylether. The chemical formula of the product matches that of $C_{26}H_{37}ClN_4O_5Pt$ and the m/z = 654 corresponds to the complex $[Pt(NH_3)_2(ET\text{-}3\text{-}Py)Cl]^+$.

The ^{1}H NMR (Figure 3.32) is essentially that of ET-3-Py and the correct integration ratio is observed between the pyridine ring and steroidal skeleton. The methyl groups of the skeleton ring, Me18 and Me19 are assigned by comparison with estradiol, an oestrogen based steroid with an identical D ring to ethisterone but without Me19 on the A/B ring interface. In this case it appears the 17β-hydroxyl hydrogen is seen. The remaining spectrum may be assigned by inspection of the coupling constants observed for the pyridine ring. The highest ppm resonance is assigned to H2' due to its position and coupling constant (1.8 Hz), whilst H6' is assigned to the second highest resonance due to it's proximity to the nitrogen atom of the pyridine ring and it being a doublet. The signal

around 7.4 ppm is assigned to H5' as a doublet of doublets is predicted from this hydrogen. The remaining signal is assigned to H4' and the coupling constant further confirms this.

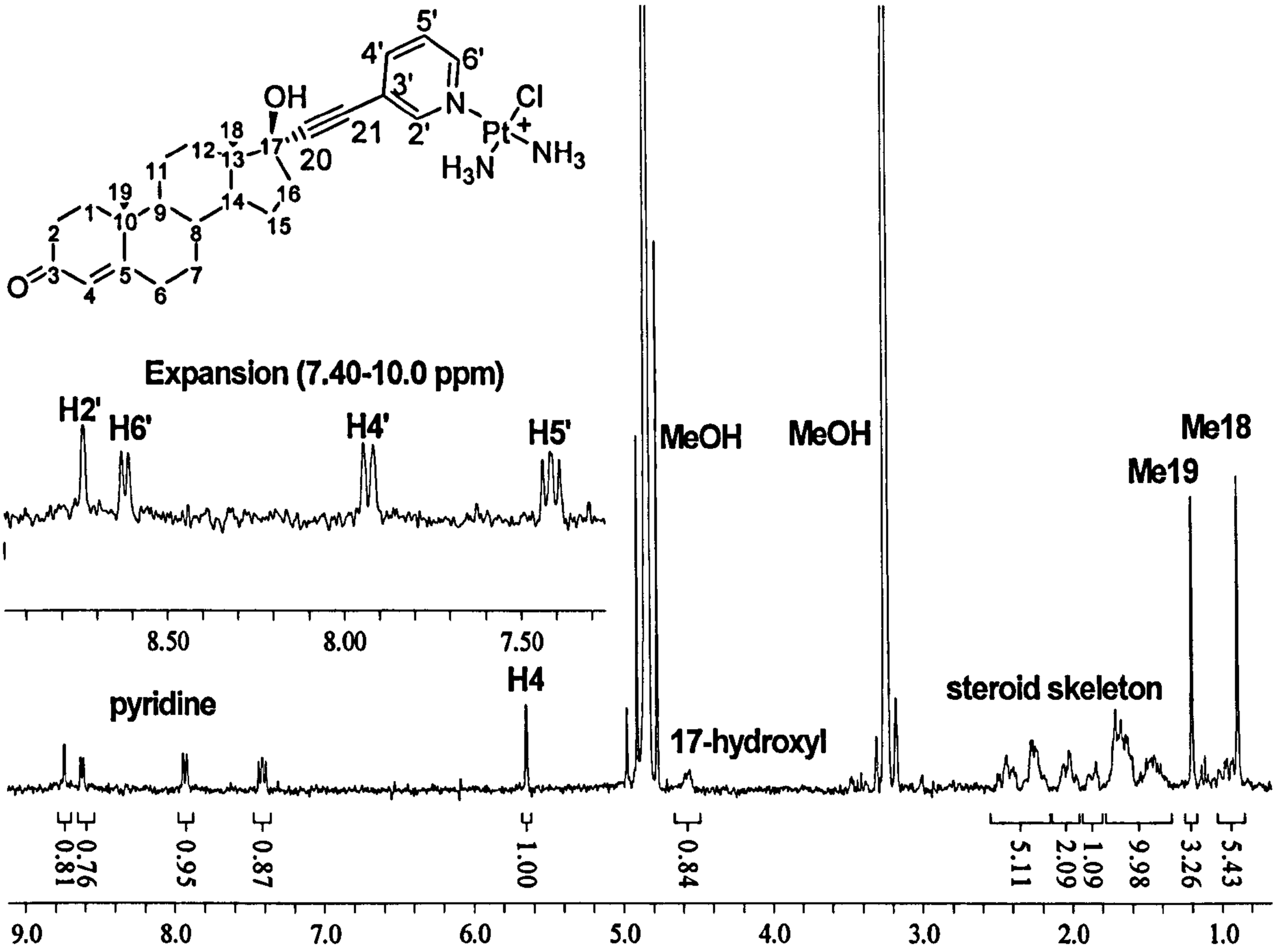

Figure 3.32. The ^{1}H NMR spectrum of CC-ET-3-Py in CD_3OD.

No discernable platinum satellites are observed in the ^{1}H NMR spectrum due to the low concentration in CD_3OD. However the ^{195}Pt NMR resonance is commensurable with a platinum complex of the formula $[Pt(NH_3)_2(L)Cl]^+$ where L is a nitrogen containing ligand. The downfield shift of the aromatic hydrogens H2', H4', H5' and H6' resonances by approximately 0.23, 0.14, 0.06 and 0.20 ppm indicates the ET-3-Py is bound to platinum (Figure A.3.4). The IR spectrum (Figure A.3.5) contains viubrational bands assigned to υN-H (3281 cm^{-1}), υC-H (2940 cm^{-1}) and υC=O (1644 cm^{-1}stretching modes. The spectroscopy confirms the predicted structure of CC-ET-3-Py and the yield is 12 %.

3.2.4.3. *Cis-[Pt(NH$_3$)$_2$(ET-4-IQ)Cl][NO$_3$]: CC-ET-4-IQ*

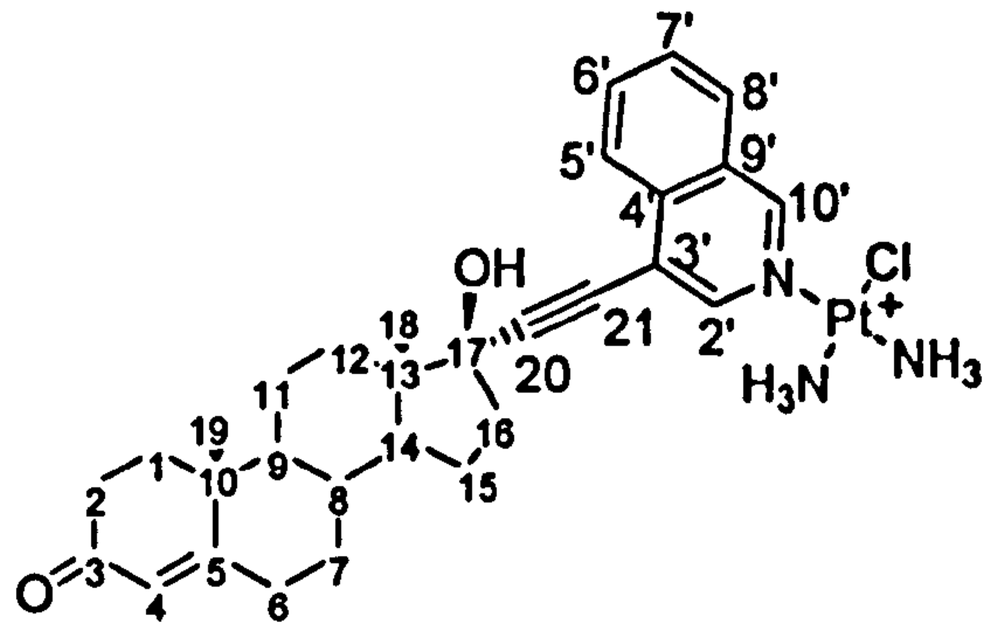

$[C_{30}H_{39}ClN_3O_2Pt][NO_3]$

The reaction to produce the CC-ET-4-IQ resulted in the formation of the desired product and also a complex where 2 ET-4-IQ ligands appear bound to platinum forming a disubstituted species in an approximate ration of 8:1 (Figure A.3.6). Purification involved extensive stirring of a methanolic solution of the crude product with decolourising charcoal to which the disubstituted appeared more attracted and hence removed from solution at a faster rate than the desired product. This charcoal treatment also had the effect of removing DMF but increasing the relative proportions of the free ligand, ET-4-IQ which was removed later via repeated recrystallisations procedures.

The desired product was isolated as a bright white solid, soluble in DMSO, DMF and methanol, less so in water and insoluble in diethylether. The elemental composition matches that expected of the desired products and the *m/z* =704 matches the complex $[Pt(NH_3)_2(ET\text{-}4\text{-}IQ)Cl]^+$ (Figure A.3.7) with the correct isotope distribution pattern (Figure A.3.8). The ^{1}H NMR spectrum (Figure 3.33) is that of bound ET-4-IQ and is assigned as the ligand. It may be assigned by inspection of the coupling constants, comparison with the free ligand ET-4-IQ and a COSY spectrum (Figure A.3.9). The broadness baseline around the signals assigned to H2' and H10' indicate that ET-4-IQ is bound to platinum but no distinct satellites may be observed.

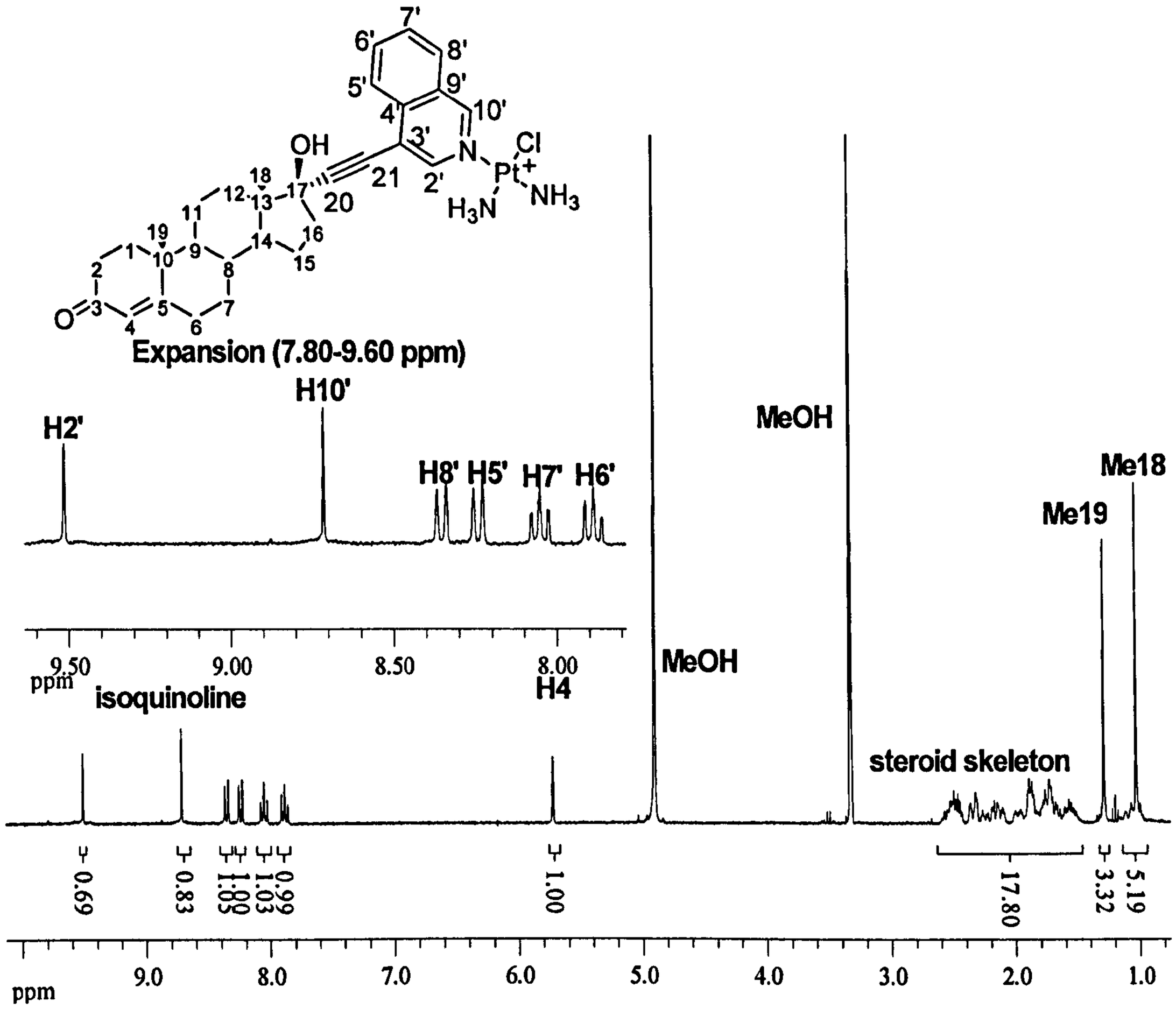

Figure 3.33. The ^{1}H NMR spectrum of CC-ET-4-IQ in CD_3OD.

Evidence for the ligand bound to platinum comes from the ^{195}Pt NMR resonance, that is in line with that expected from a complex of the formula $[Pt(NH_3)_2(L)Cl]^+$ where L is a nitrogen containing ligand. Further evidence is the downfield shifts of the resonances from the hydrogens of the isoquinoline ring system (Figure A.3.10). Each hydrogen, H2', H5', H6', H7', H8' and H10' are shifted downfield by 0.75, 0.33, 0.36, 0.29, 0.36 and 0.33 ppm respectively and is commensurate with the effect of withdrawing electron density from the isoquinoline ring for binding to platinum. The IR spectrum (A.3.11) shows several bands expected from the proposed structure, including υC=O and υC-H stretching modes. The strong broad band around 1330 cm^{-1} is likely arising from overlapping υN-H deformation and υN-O stretching modes indicating the presence of the nitrate counter ion. The spectroscopy is in agreement with the structure propsed for CC-ET-4-IQ with a yield of 27%.

3.2.4.4. Cis-[Pt(NH$_3$)$_2$(ET-6-Q)Cl][NO$_3$]: CC-ET-6-Q

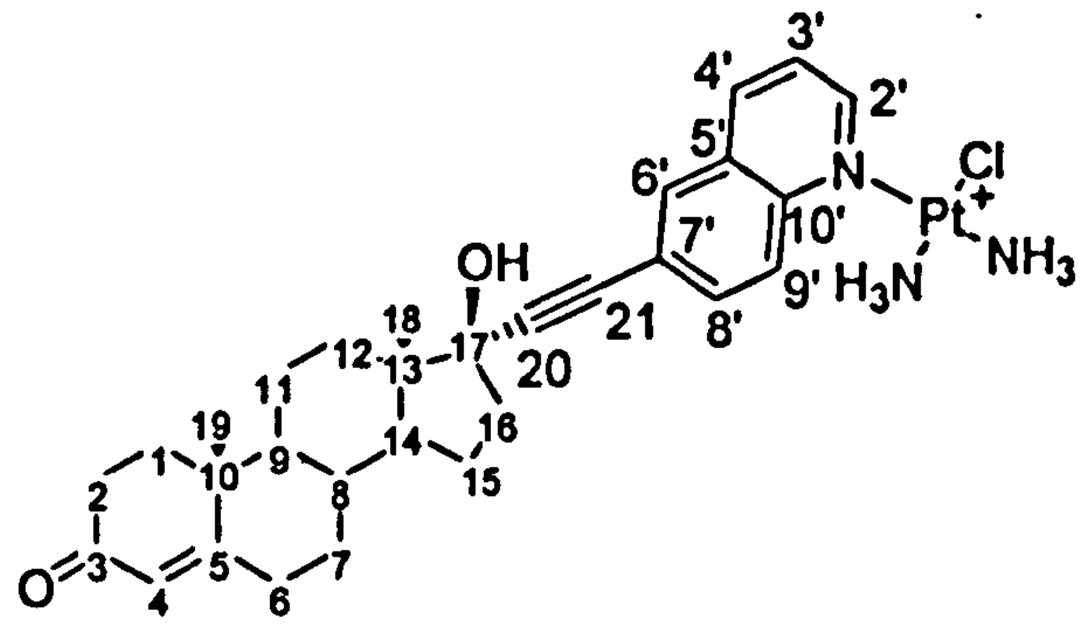

$[C_{30}H_{39}ClN_3O_2Pt][NO_3]$

The synthesis of CC-ET-6-Q proceeded smoothly. However, in common with some other reactions it produced a disubstituted complex, $[Pt(NH_3)_2(ET\text{-}6\text{-}Q)_2]^{2+}$, as identified by mass spectroscopy (A.3.12 and A3.13). Unusually for a steroidal platinum complex the ESI mass spectrum exhibits the 2+ charged ion, rather than the ion $[M\text{-}H]^+$ which is usually found, where M = $[Pt(NH_3)_2(ET\text{-}6\text{-}Q)_2]$. This impurity was removed in a similar way to the reactions synthesising TC-ET-4-IQ and CC-ET-4-IQ, by using charcoal, to which the higher charged complexes adsorbed more quickly than those of less charge, *i.e.* the 2+ disubstituted complexes were selectively removed solution leaving only cis-$[Pt(NH_3)_2(ET\text{-}6\text{-}Q)Cl]^+$ and residual free ligand (removed by recrystallisation). The complex was soluble in DMSO and DMF, less so in methanol and water and insoluble in diethylether and chloroform.

The mass spectrum produced a single peak at *m/z* = 704 corresponding to the complex $[Pt(NH_3)_2(ET\text{-}6\text{-}Q)Cl]^+$ (Figure A.3.14) with the correct isotope distribution (Figure A.3.15) and elemental analysis confirmed the predicted molecular formula. The ^{1}H NMR (Figure 3.34) may be assigned by analysing the coupling constants and comparison with the unbound ligand. Similar to all complexes with quinoline the chemical shift of H9' is further downfield (by 1.63 ppm) than all the other signals compared to the free ligand (Figure A.3.16.). This may represent an interaction between H9' and the platinum atom. The other hydrogen atoms, H2', H3', H4', H6' and H8' are also shifted downfield by 0.42, 0.04, 0.23, 0.09 and 0.19 ppm indicating that the ligand is bound to platinum. No platinum satellites are observed due to the low concentration of the complex in methanol.

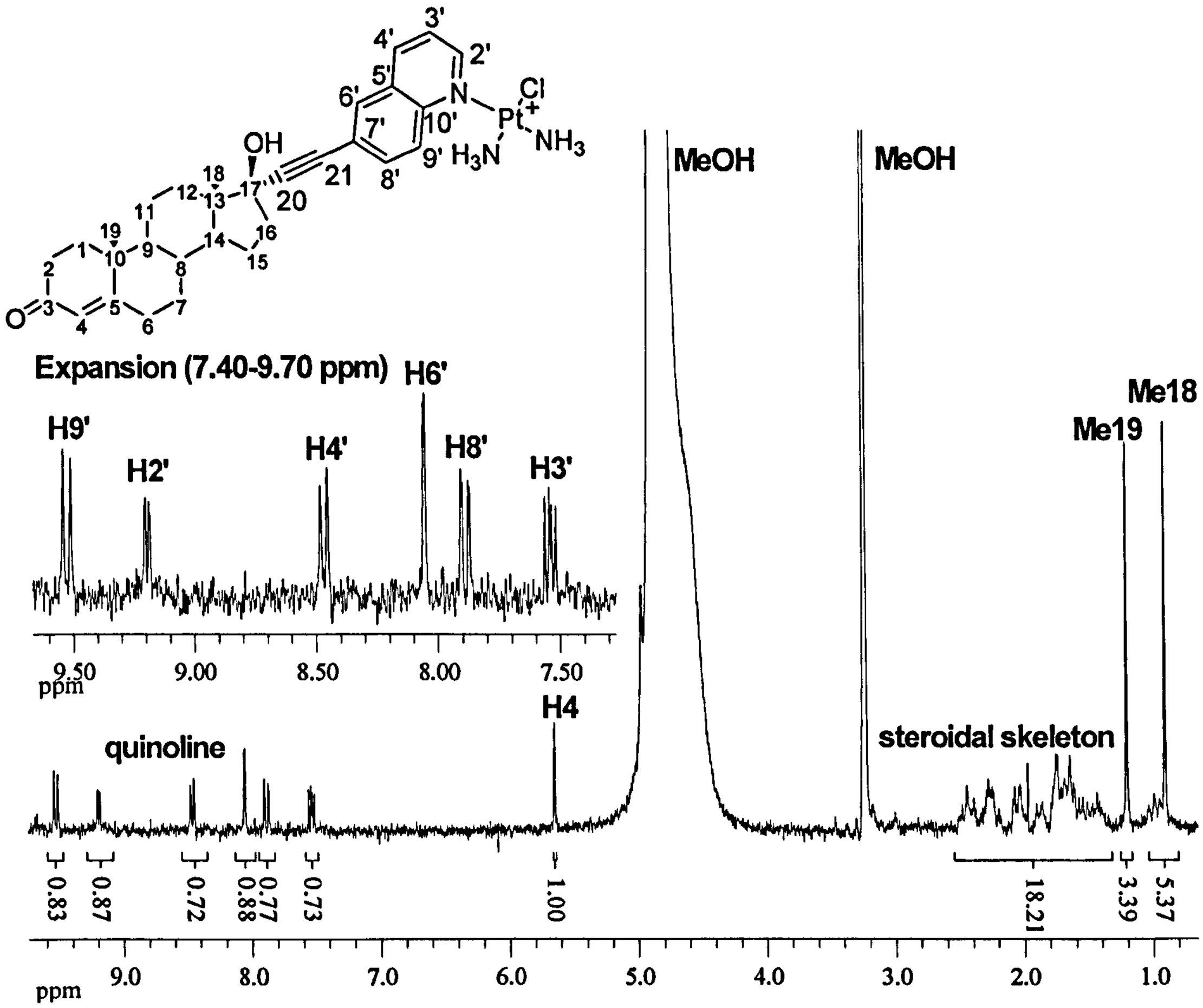

Figure 3.34. The ^{1}H NMR spectrum of CC-ET-6-Q in CD_3OD.

The infrared spectrum (Figure A.3.17) reveals several vibrational bands in agreement with the proposed structure of CC-ET-6-Q. Bands assigned to υN-H, υC-H and υC=O stretches may be observed at 3284, 2939 and 1646 cm^{-1} respectively. A broad band is observed round 1330 cm^{-1} and may be assigned to overlapping υN-H def and υN-O stretching modes indicating the presence of the nitrate counter-ion. The spectroscopy agrees with the proposed structure of CC-ET-6-Q and the yield is 24 %.

3.2.5. Geometry of cis-cationic and trans-cationic complexes

There exists no direct evidence of the geometric arrangement in TC and CC complexes, *i.e.* a structure solved by X-ray crystallography. The evidence presented does support the ligands bound to platinum(II), *i.e.* 2 NH_3 groups, a steroidal ligand and a single chloride. From the reaction scheme used, it may be reasonably expected that the complexes products from transplatin are trans and those from cisplatin are *cis*. Given the ligands, only two geometric arrangements can be reasonably expected; whereby the NH_3 groups are cis and where NH_3 groups are trans. The only technique fully used that is sensitive to this

arrangement is ^{1}H NMR spectroscopy. The chemical shifts of the hydrogen atoms of the pyridine, quinoline and isoquinoline rings are dependent, to an extent, on the bonding of aromatic rings to the platinum atom whose bonding is affected, primarily, by the ligand trans to the aromatic amine. It is also reasonable to postulate if the ligand trans is different, then the chemical shifts of the aromatic hydrogen atoms will also be different. Comparing the chemical shifts of the 8 complexes, cis and trans-cationic containing the ligands pyridine, ET-3-Py, ET-4-IQ and ET-6-Q reveals that in all cases the chemical shifts of aromatic hydrogen atoms are found at higher ppm values in the complexes labelled trans to those labelled cis (Figures A.4.1 to A.4.4). This indicates there is less electron density in the aromatic ring(s) in one set of complexes (labelled trans) than another set (labelled cis). This gives evidence that one set of complexes using cisplatin as a starting material has a different trans ligand than those using transplatin as a starting material and from this is it reasonable to suggest that one set of complexes is cis and another trans.

3.2.6. The synthesis of steroidal platinum(II) complexes: trans-neutral (TN)

The poor solubility of steroid-linker ligands caused problems in attempts at this reaction scheme. For example, the use of 50:50 water:ethanol to aid solubility of ET-4-Py resulted in an orange solution after 96 hours at 65°C. The ^{1}H NMR spectrum showed two sets of peaks, those of the free steroid and presumably those of trans-$[Pt(NH_3)_2(ET\text{-}4\text{-}Py)_2]^{2+}$ at lower field. The addition of concentrated HCl with heat resulted in an orange solid after 24 hours at 80°C. The orange solid did not contain the steroidal ligand (by ^{1}H NMR) and neither did the filtrate and presumably the steroidal ligand decomposed. Further reactions were attempted but without success; firstly in gaining acceptable yield of complexes with the formula trans-$[Pt(NH_3)_2(ET\text{-}4\text{-}Py)_2]^{2+}$ and secondly the use of hydrochloric appeared to decompose the organic material. Attempts to form trans-$Pt(NH_3)$(3-bromopyridine)Cl_2 were successful but subsequent reactions attempting a Sonogashira coupling with 17α-ethnynyltestosterone (using K_2CO_3 as a base) failed even using molar percentage ratios of catalyst from 4-50%. All attempts to synthesise trans-neutral complexes were not successful.

3.2.7. The synthesis of steroidal platinum(II) complexes: cis-neutral (CN)

The use of this reaction scheme did not result in the successful synthetic of complexes of the type cis-$[Pt(NH_3)(L)Cl_2]$ where L is a range of steroidal ligands. Even the dichloromethane soluble salt, $[Ph_4N][Pt(NH_3)Cl_3]$ did not react with ligand L_1-L_3. Forming cis-$[Pt(NH_3)(Py)Cl_2]$ required 75°C for a 28 % yield so the difficulties with L_1-L_6 are perhaps unsurprising. Using this reaction cis-$[Pt(NH_3)$(3-bromopyridine)$Cl_2]$ was synthesised successfully but this did not react with 17α-ethnynyltestosterone under

Sonogashira conditions, even with high catalyst loading (up to 50 molar percent) and using various solvents.

3.2.8. The synthesis of steroidal platinum(II) complexes containing DMSO as a ligand

Unlike other reactions in this chapter forming *trans* geometries the complex *trans*-Pt(ET-2-Py)(DMSO)Cl_2 formed with ease, despite the sterically hindered ligand. The formation of the desired products was monitored using several techniques. In some cases elemental analysis confirmed the chemical formulae, whilst in all cases peaks at *m/z* values corresponding to protonated complexes were observed by mass spectrometry (ESI, +ve). ^{1}H NMR spectroscopy was used to further aid confirmation of the structure and chemical shifts relative to the free ligands and platinum satellites were used to confirm the DMSO is not only bound to platinum, but bound via the sulphur. Sulphur binding is also strongly suggested by an increase, to higher wavenumbers, of the IR band assigned to the fundamental υS=O stretching mode.[523] Interestingly, the chemical shift of the DMSO methyl hydrogens, technically diastereotopic, appears dependent on the NMR solvent with a singlet in some solvents and a doublet in others. ^{195}Pt NMR spectroscopy was also employed with ease due to excellent complex solubility and the chemical shift in all cases corresponded to that expected from a complex of the formula Pt(L)(DMSO)Cl_2 where L is a nitrogen containing ligand. ^{1}H NMR spectroscopy suggests the stereochemistry is trans, due to the platinum satellites accompanying the DMSO methyl hydrogens signal. In the case of Pt(Quinoline)(DMSO)Cl_2 and Pt(ET-2-Py)(DMSO)Cl_2 an X-ray crystal structure is reported and in both cases the stereochemistry is trans.

3.2.8.1. Trans-Pt(Py)(DMSO)Cl_2

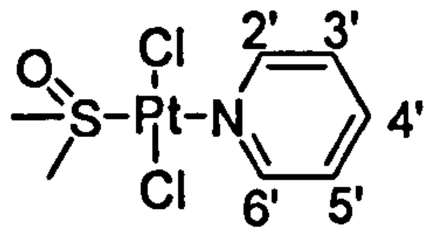

$C_7H_{11}Cl_2NOPtS$

The reaction between cis-Pt(DMSO)$_2Cl_2$ and 1 equivalent of pyridine in methanol resulted in a fine yellow powder requiring only washing to remove DMSO. The solid was soluble in DMSO and DMF, partially soluble in chloroform and methanol and insoluble in water and diethylether.

Elemental analysis confirmed the predicted chemical formula of $C_7H_{11}Cl_2NOPtS$ and the ^{195}Pt NMR signal is consistent with the formula type [Pt(DMSO)(L)Cl_2] where L is a

nitrogen containing ligand confirming the trans nature of the complex. The ^{1}H NMR spectrum (Figure 3.35) may be assigned by observation of the coupling constants and integrations. Platinum satellites are visible either side of the resonances assigned to H2' (8.79 ppm) and the DMSO methyl hydrogens resonance (3.52 ppm). This provides evidence for platinum being bound to the nitrogen pyridine and via the sulphur as $^3J_{(Pt\text{-}H)}$ coupling occurs in sulphur bound and $^4J_{(Pt\text{-}H)}$ in oxygen bound DMSO. The shift to higher wavenumbers of the υS=O stretch at 1150 cm^{-1} in the IR spectrum (Figure A.5.1) provides additional evidence for sulphur bound DMSO.[523] Vibrational bands relating υC-H stretching and υC-H deformations of the DMSO methyls and pyridine are observed at 2995 / 2913 and 765 and 691 cm^{-1} respectively. The spectroscopic evidence is in agreement with the proposed structure of trans-Pt(DMSO)(Py)Cl_2 and the yield is 95 %.

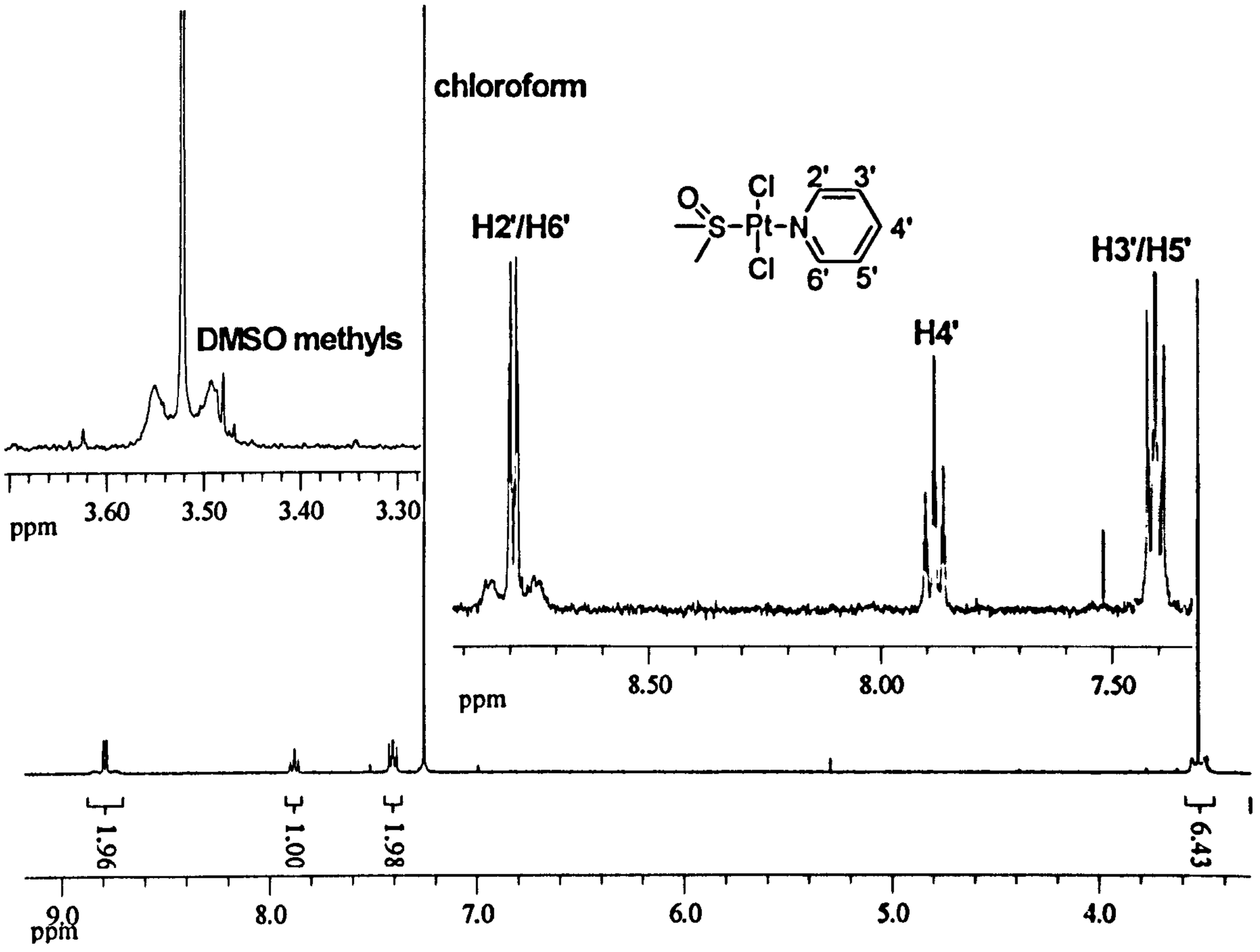

Figure 3.35. The aromatic region in the ^{1}H NMR spectrum of trans-Pt(DMSO)(Py)Cl_2.

3.2.8.2. Trans-Pt(Quin)(DMSO)Cl_2

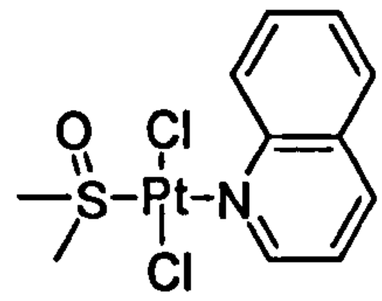

$C_{11}H_{13}Cl_2NOPtS$

The reaction between cis-bis(dimethylsulphoxide)dichloroplatinum(II) and quinoline produced a fine, bright yellow powder. The ^{195}Pt NMR spectra resonance is in agreement with the structure Pt(L)(DMSO)Cl_2 where L is a nitrogen containing ligand whilst the peak at $m/z = 474$ corresponds to protonated Pt(Quin)(DMSO)Cl_2. The ^{1}H NMR (Figure 3.36) may be assigned by examination of the coupling constants; however, some assignments are best guesses given the resonance structure of quinoline and NOE differential and / or NOESY NMR spectroscopy is required to confirm the assignment. Clear platinum satellites are visible on either side of the signals at 9.01 and 3.45 ppm assigned to H2' and the DMSO methyl's respectively with respective ^{3}J coupling constants of 15.2 and 8.8 Hz. In addition to downfield shifts of aromatic hydrogen resonances using ^{1}H NMR spectroscopy compared to quinoline and movement to higher wavenumbers of the υS=O stretching fundamental vibration in the IR spectrum (Figure A.5.2) this provides evidence of the both quinoline and DMSO bound to platinum.[523]

A smaller set of quinoline peaks is observed downfield from those of trans-Pt(Quin)(DMSO)Cl_2 and may be assigned to either of the disubstituted complexes Pt(Quin)$_2Cl_2$ or $[Pt(Quin)_2(DMSO)Cl]^+$, both observed in the mass spectrum as small peaks at $m/z = 567$ ($[Pt(Quin)_2(DMSO)Cl]^+$) and $m/z = 525$ $[H(Pt(Quin)_2Cl_2)]^+$.

The infrared spectrum (Figure A.5.2) shows signals that may be assigned to quinoline and DMSO ligands. In particular the υS=O, υC-S (asym) and υC-S (sym) stretching bands at 1132 / 1124, 739 and 698 cm^{-1} of the DMSO and υC-H 'oop' deformation bands at 811 and 779 cm^{-1} of the quinoline are very evident. The overall spectroscopy is in agreement with the structure proposed and a yield of 98% is achieved.

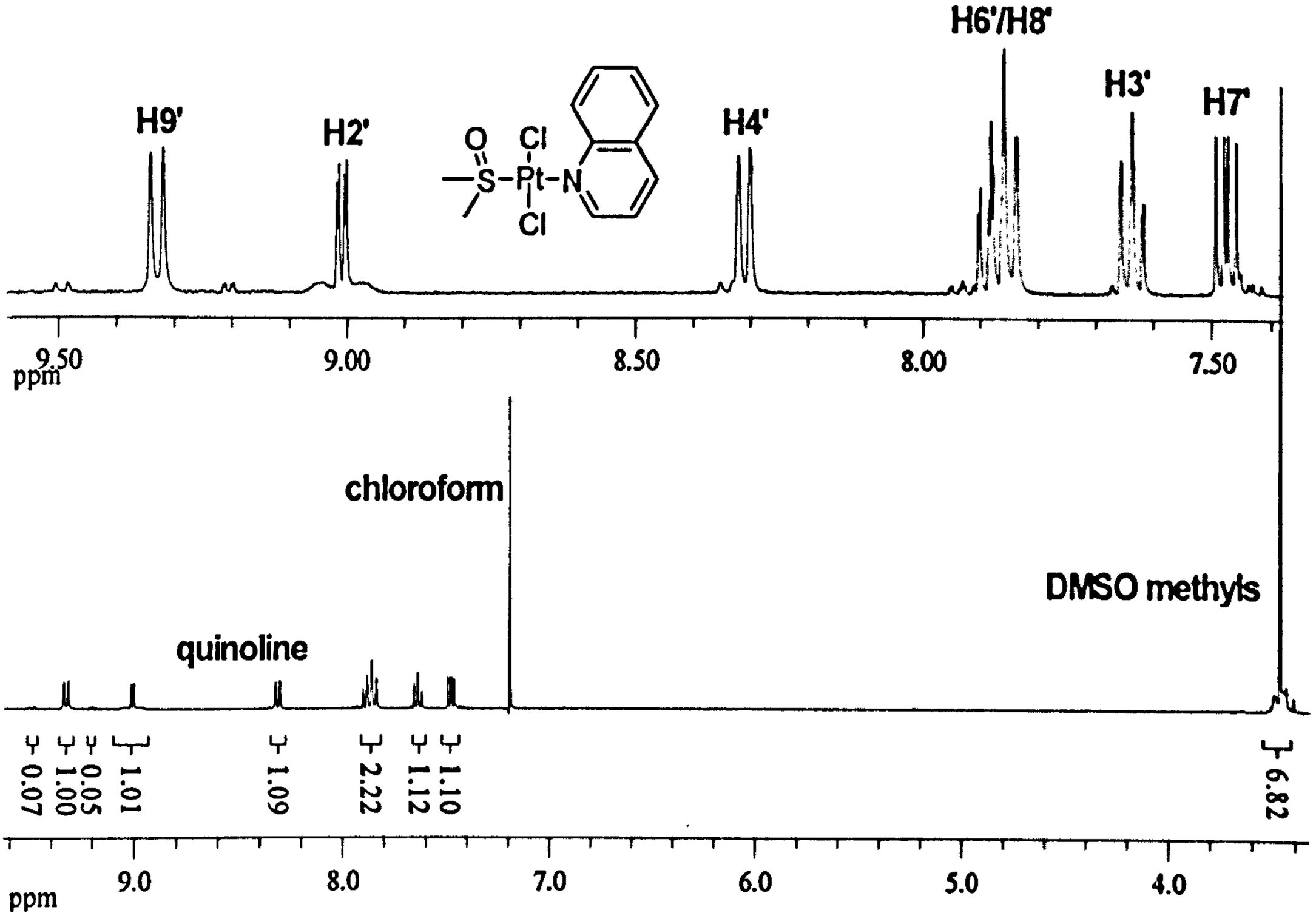

Figure 3.36. The ^{1}H NMR of trans-[Pt(Quin)(DMSO)Cl_2] in $CDCl_3$.

3.2.8.3. Trans-Pt(ET-2-Py)(DMSO)Cl_2

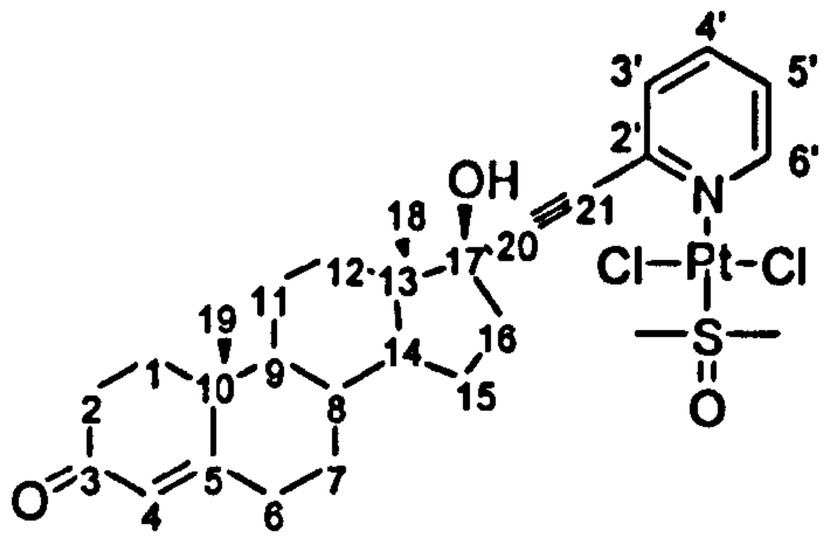

$C_{28}H_{37}Cl_2NO_3PtS$

Mixing of the complex cis-[Pt(DMSO)Cl_2] with ET-2-Py in methanol afforded the crude complex in quantitative yield. The main impurities in the crude product were identified by NMR and ESI-MS as Pt(ET-2-Py)$_2Cl_2$ and Pt(ET-2-Py)$_2$(DMSO)(Cl) in a ratio with Pt(ET-2-Py)$_2Cl_2$ of ~2 : 98. The formation of side produces is not reduced with slower addition of ligand or excess of ligand (up to 5-fold). The compound could be purified by flash column chromatography as the mono-substituted main product eluted slightly faster than the di-substituted products and collecting the first half of the single yellow band did that not contain disubstituted products.

$Pt(ET\text{-}2\text{-}Py)(DMSO)Cl_2$ was partially soluble in methanol and insoluble in diethylether and water. The solid was highly soluble in DMSO, chloroform, dichloromethane, acetone, acetonitrile and ethyl acetate. Such unusual solubility, given a neutral platinum(II) complex and steroidal ligand, may be attributed to the coordinated DMSO. Insolubility in water and diethylether may be attributed to the neutrality of the complex and the steroidal ligand. The reaction is complete in 24 hours produces.

Mass spectroscopy (ESI, +ve), ^{1}H NMR spectroscopy and elemental analysis confirmed the identity of this complex. The ^{1}H NMR spectrum (Figure 3.37) clearly shows 4 pyridine hydrogen signals together with a singlet of the DMSO methyl hydrogens. The baseline around the resonances at 8.53 and 3.44 ppm is broadened due to ^{195}Pt coupling but no distinct satellites are observed. The broadening of the 3.44 ppm signal is explained by $^{3}J_{(Pt\text{-}H)}$ cross coupling and is strong evidence of sulphur binding the Pt rather an oxygen. Oxygen bound implies a $^{4}J_{(Pt\text{-}H)}$ coupling arrangement and baseline broadening is likely less pronounce. The 1.2 ppm downfield shift indicates a loss of electron density on the sulphur of the DMSO ligand compared to free DMSO and is consistent with electron donation from the sulphur to platinum(II).

The assignment of the pyridine protons may be made from inspection of the coupling constants and confirmed by a COSY spectrum (Figure A.5.3). The resonance at 5.72 pm is assigned to H4 and those at 1.20 ppm and 0.97 ppm to the steroidal methyl groups from the chemical shifts and integrations. The ^{13}C NMR spectrum DEPT spectrum (Figure 3.38), run in deuterated acetone to gain a concentrated sample show the DMSO methyl carbons chemically non-equivalent similar to that of the methyl protons in ^{1}H NMR spectrum. All carbons are accounted for in the spectrum and assignments are aided by ^{1}H-^{13}C HMQC spectrum (Figure A.5.4). The effect of platination on the pyridine ring was assessed by the shift in the ^{1}H NMR resonances. Every resonance of the pyridyl hydrogens is shifted. H3', H4' and H5' resonances shift downfield by 0.15, 0.16 and 0.17 ppm respectively confirming binding induces deshielding of these protons (Figure A.5.5). The H6' resonance is different and a small shift of 0.03ppm upfield suggesting a small shielding effect.

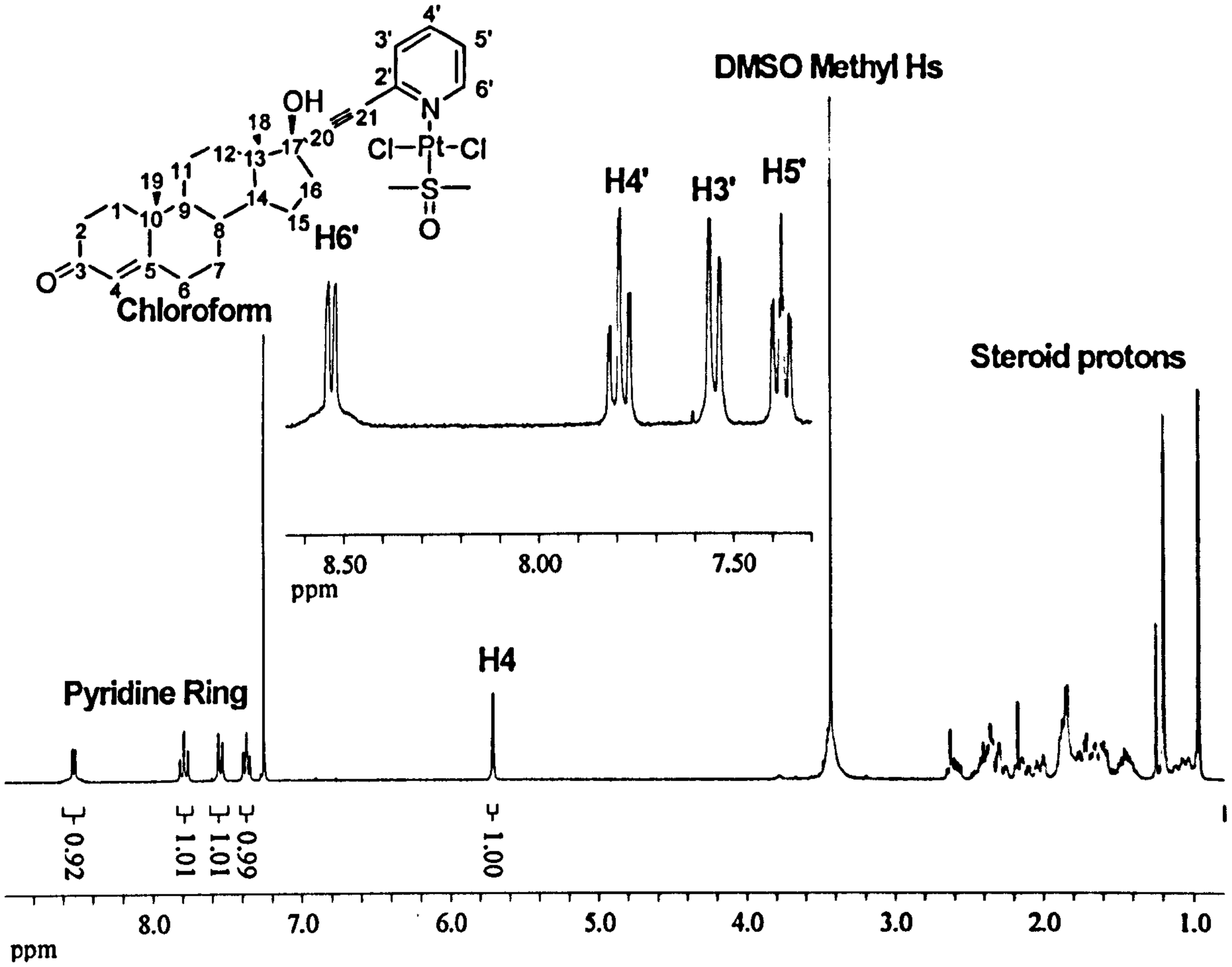

Figure 3.37. The ^{1}H NMR spectrum of trans-Pt(ET-2-Py)(DMSO)Cl_2 in $CDCl_3$.

The infrared spectrum (Figure A.5.6) is very informative regarding the functional groups and bonding arrangement in the complex. The steroidal ligand dominates the infrared spectrum with the υO-H, υC-H, υC≡C, and υC=O stretches. The υC≡C is clearly visible at 2227 cm^{-1} and the 3-keto υC=O stretch is at 1657 cm^{-1}. The υC-H out-of-plane ('oop') deformation at 747 cm^{-1} is indicative of a 2-substituted pyridine ring and is likely to overlap somewhat with υC-S asymmetric and symmetric stretching modes of the DMSO ligand. The bonding between Pt and sulphur of the DMSO are elucidated in the split υS=O band at 1147 cm^{-1} and 1127 cm^{-1} which is approx 100 cm^{-1} higher than free DMSO (1042 cm^{-1}) and strongly suggests sulphur binding.[523] The ESI peak of m/z = 734.5 agrees with that expected from protonated trans-Pt(ET-2-Py)(DMSO)Cl_2.

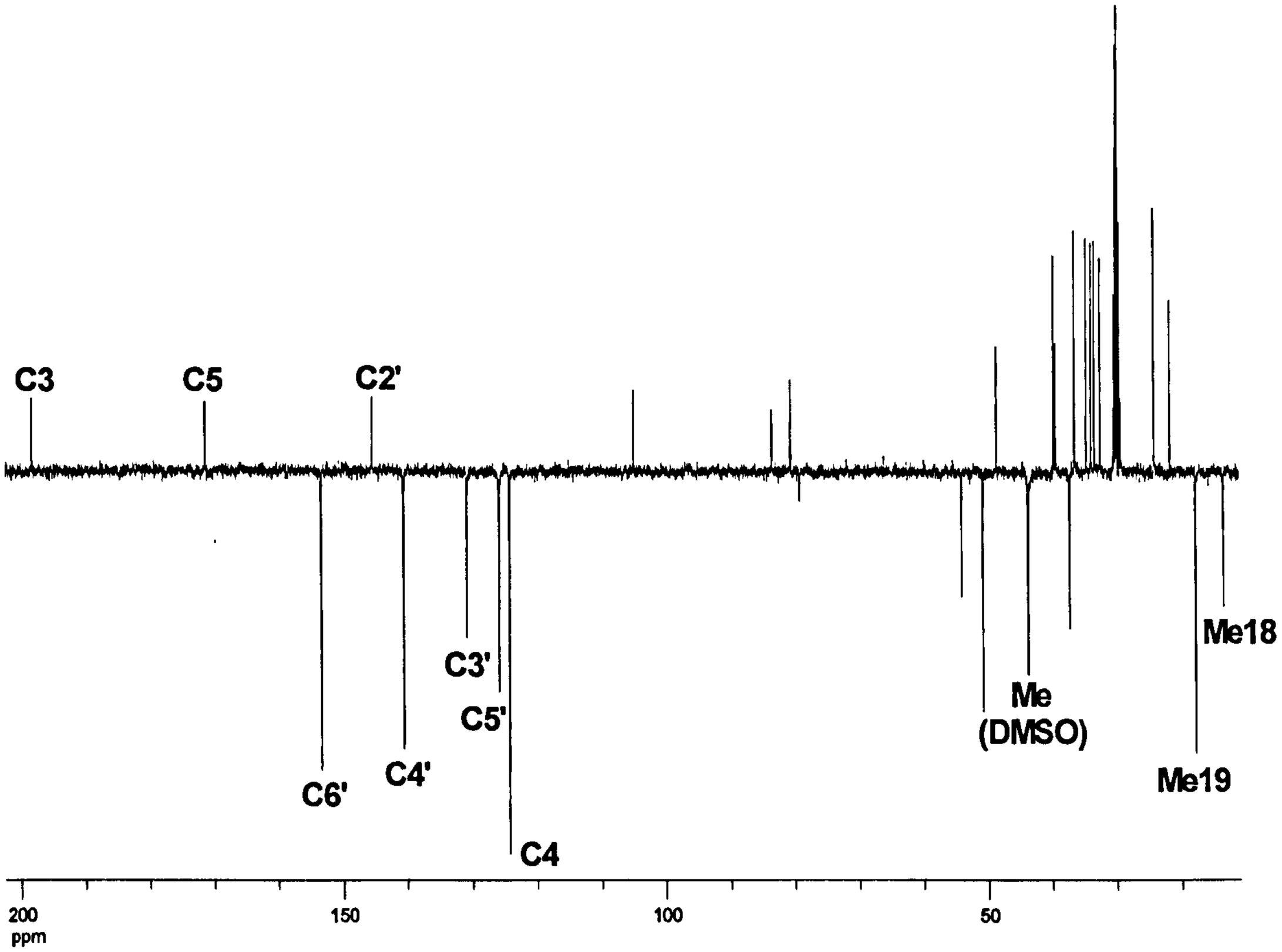

Figure 3.38. The ^{13}C DEPT NMR spectrum of trans-Pt(ET-2-Py)(DMSO)Cl_2 in $(CD_3)_2CO$.

The methyl groups of platinum bound DMSO exhibit a single band in the ^1H NMR spectrum. This is not the case in non-chlorinated solvents where the band is split into a doublet as shown in Figure 3.39, with a splitting of 5.4 Hz, 5.7 Hz and 7.0 Hz for deuterated acetonitrile, methanol and acetone respectively. If the non-chlorinated solvents are removed *in vacuo* and replaced with $CDCl_3$ (far right spectrum) the signal is a singlet strongly suggesting this is a solvent effect of unknown origin.

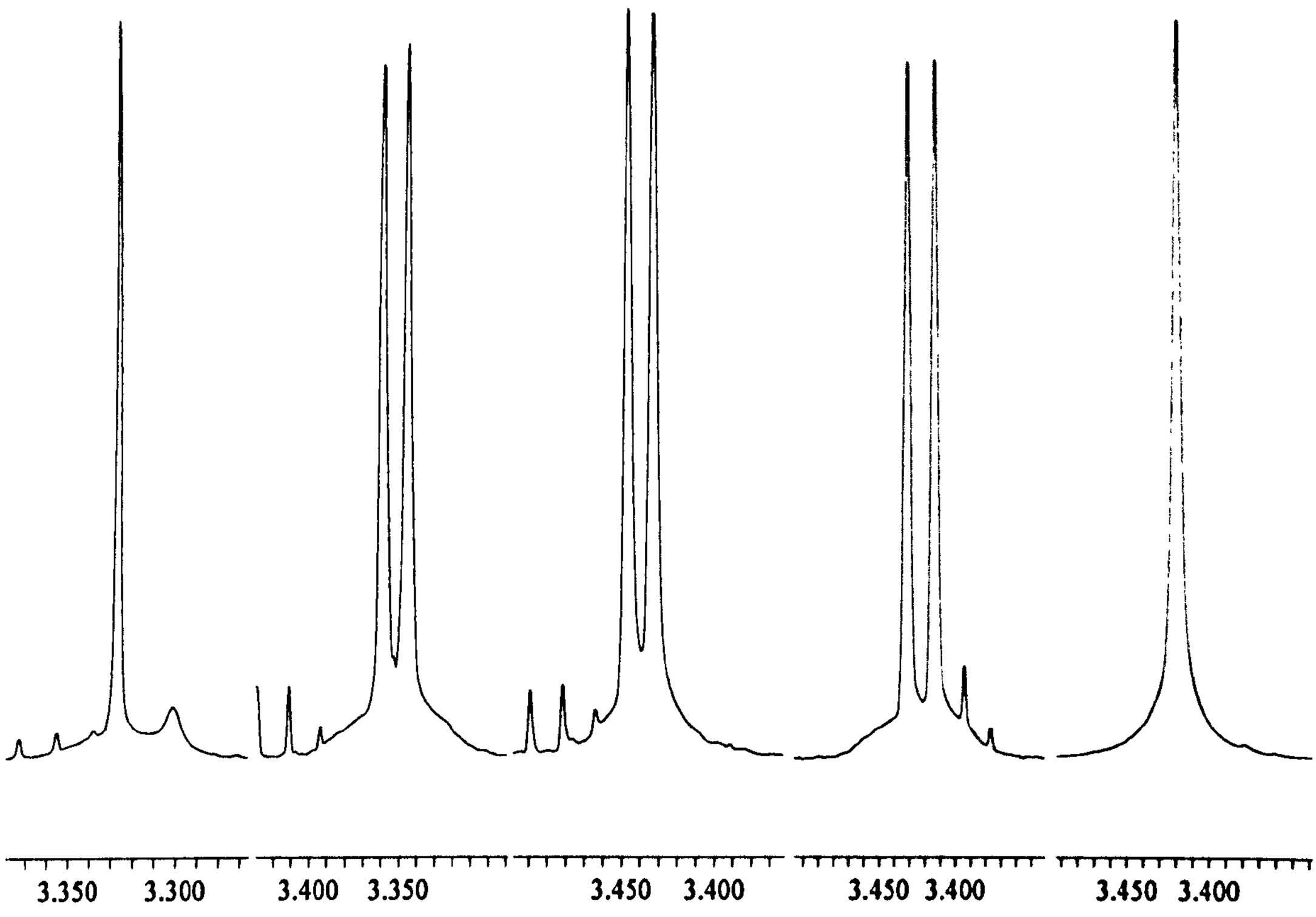

Figure 3.39. The ^{1}H NMR of DMSO methyl proton resonances in various solvents.

The reaction requires <24 hrs for completion and may be monitored via NMR. The ^{1}H NMR spectra of 2 hr and 6 hr aliquots of the reaction mixture are shown in Figures 3.40 and 3.41. After 2 hours approximately 28% of the ET-2-Py is co-ordinated to platinum which increases to 93% after 6 hours. In the ^{1}H NMR spectra at 2 hours and 6 hours there are 2 proton resonances around 3.45 ppm. The resonance at 3.44 ppm is the final product whilst the lower field resonance at 3.47 ppm appears to be an intermediate in the reaction whose integration relative to the 3.45 ppm signal is equal to that of 3.47 ppm after 2 hours, lower after 6 hours and is not observed in the final product. In the aromatic region there still appears to be only one environment for the pyridine ring protons. This is also found in ^{13}C NMR, where the DMSO methyl carbon resonances, confirming using cross coupling peaks from HMQC spectra are split into 2 signals (around 0.1ppm difference) in those solvents where doubles are observed around 3.45 ppm in ^{1}H NMR spectra and singlets where singlets are observed in ^{1}H NMR spectra.

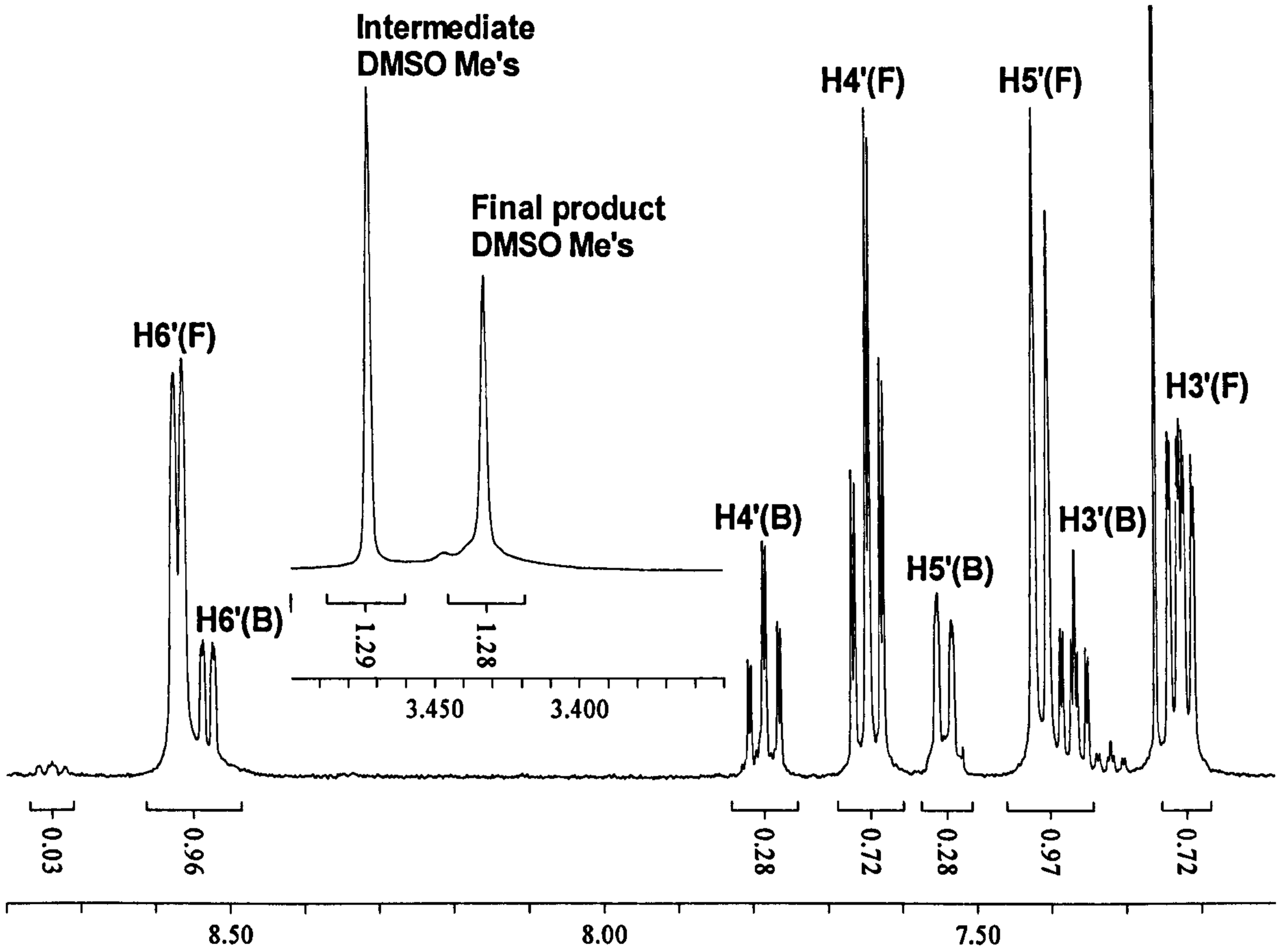

Figure 3.40. The ^{1}H NMR spectrum of an aliquot of the reaction between cis-$Pt(DMSO)_2Cl_2$ and ET-2-Py after 2 hours at 25°C in $CDCl_3$.

Purification entailed separation of the major product from impurities totalling approx 2% (by NMR). Several species and fragments were identified by mass spectrometry (ESI, +ve) including $Pt(ET\text{-}2\text{-}Py)(DMSO)Cl_2$, $Pt(ET\text{-}2\text{-}Py)_2(Cl)_2$ and Pt(ET-2-Py)(DMSO)(Cl) and were all observed as monocations (Figure 3.42 and Table 3.1). The peak at m/z = 1123 may be a 5-coordinate Pt complex, $Pt(DMSO)(ET\text{-}2\text{-}Py)_2Cl_2$ in a protonated form; given the relatively slow kinetics of platinum chemistry, such a 5-coordinate intermediate may exist at a high enough concentration to be sensitive to ESI-MS.

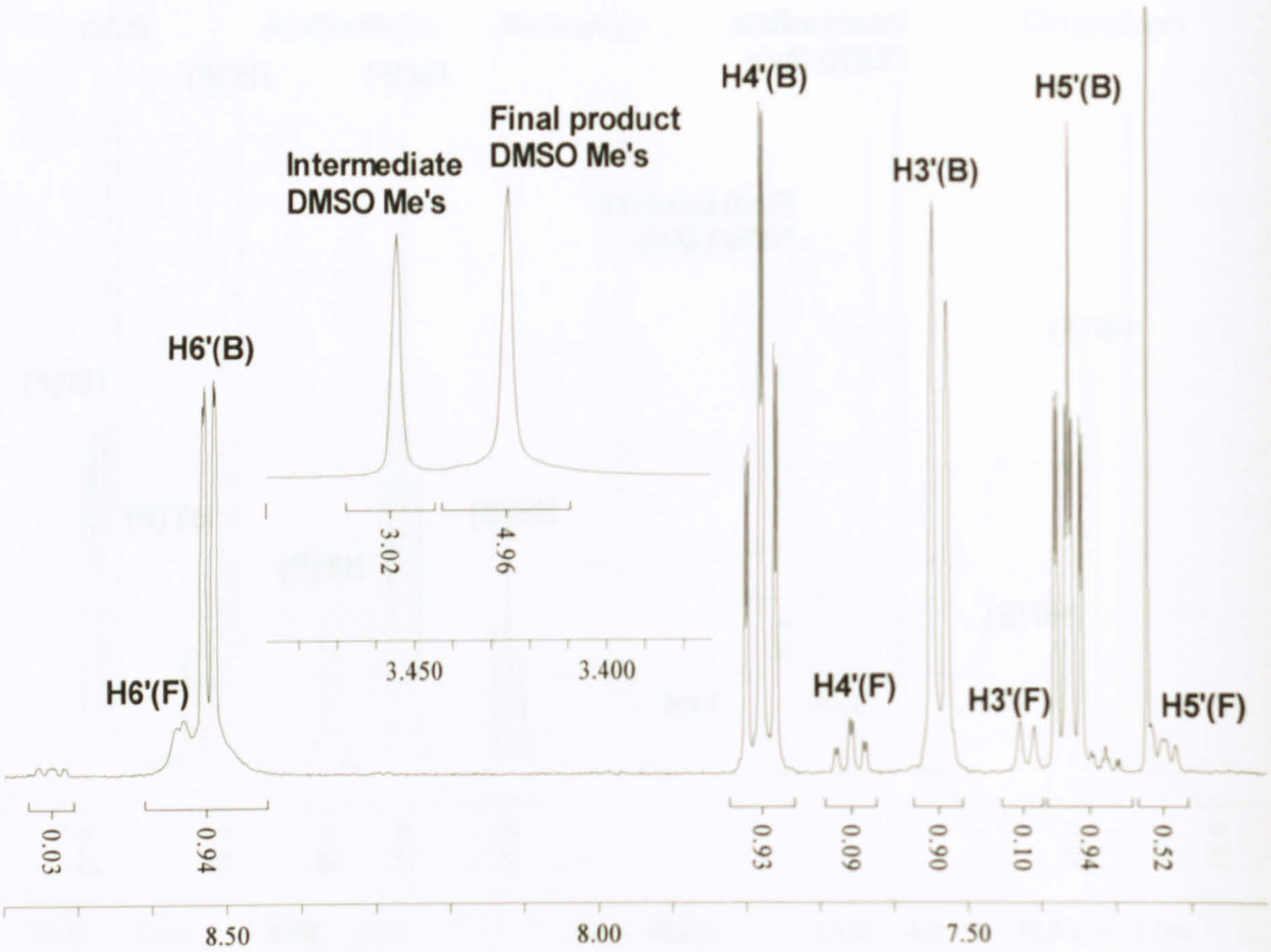

Figure 3.41. The reaction between cis-$Pt(DMSO)_2Cl_2$ and ET-2-Py monitored by ^1H NMR after 6 hours at 25°C in $CDCl_3$. Approximately 7% of ET-2-Py remains unbound to platinum.

Table 3.1. Selected assignments from the reaction of cis-$Pt(DMSO)_2(Cl)_2$ and ET-2-Py in methanol at 25°C

Peak Label	Observed m/z	Assignment
	583.5	$H[Pt(ET\text{-}2\text{-}Py)_2]^+$
	734.5	$H[Pt(ET\text{-}2\text{-}Py)(DMSO)Cl_2]^+$
A	1045.5	$H[Pt(ET\text{-}2\text{-}Py)_2(Cl)_2]^+$
B	1087.5	$[Pt(ET\text{-}2\text{-}Py)(DMSO)(Cl)]^+$
C	1123.5	$H[Pt(ET\text{-}2\text{-}Py)_2(Cl)_2(DMSO)]^+$

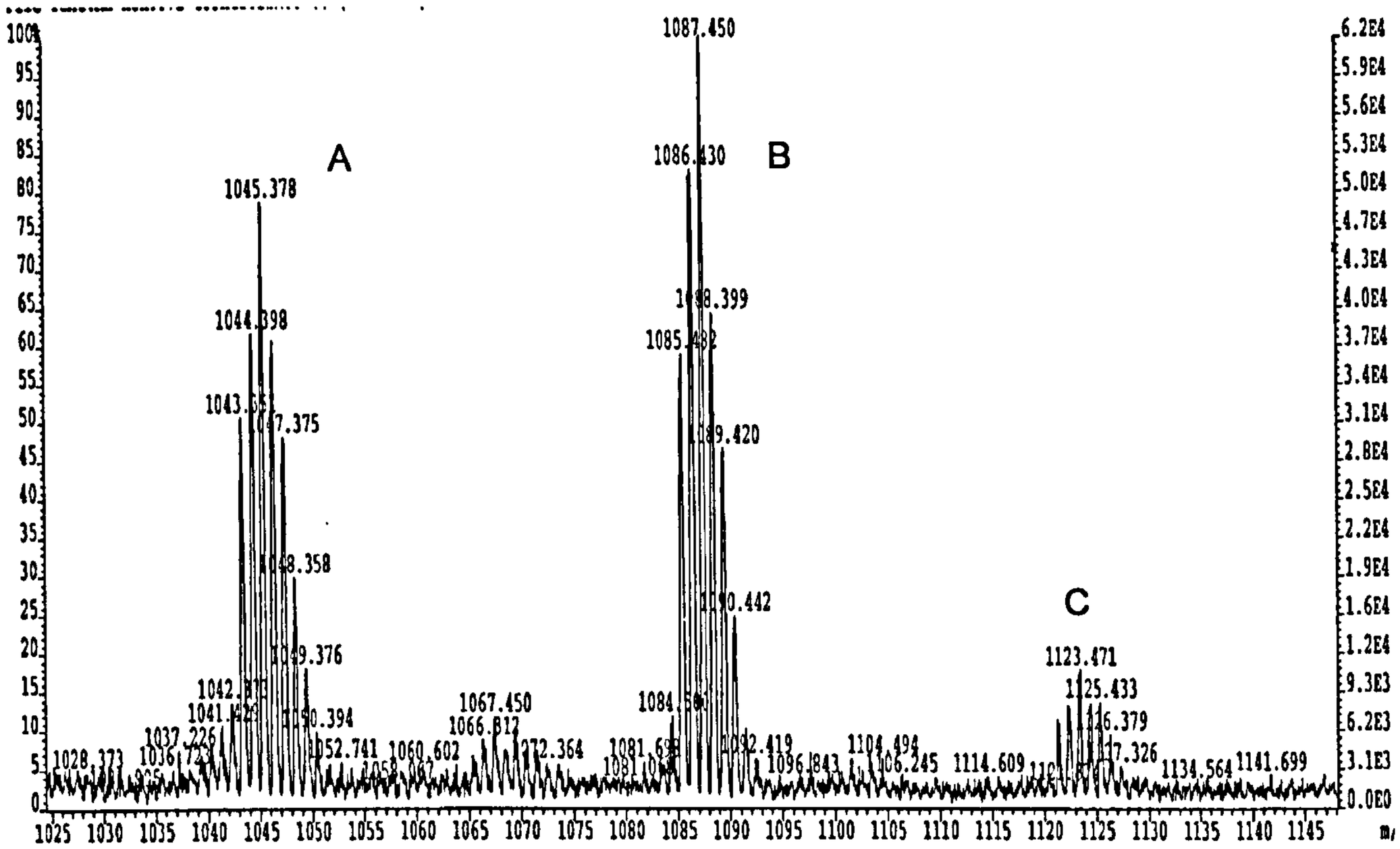

Figure 3.42. A selected range of *m/z* in the FAB mass spectrum of crude Pt(ET-2-Py)(DMSO)Cl_2] showing peaks A, B and C.

Trans-Pt(ET-2-Py)(DMSO)Cl_2 is purified using a long (1 m) column eluted with a 98:2 dichloromethane:methanol mixture. The first half of the single yellow band contains trans-Pt(ET-2-Py)(DMSO)Cl_2 whilst the second half trans-Pt(ET-2-Py)(DMSO)Cl_2 and the impurities which are shown around 8.90 ppm in Figure 3.43 and are seen as 2 doublets with broadening indicating $^3J_{(Pt-H)}$ coupling. A smaller third doublet may be observed at 8.80 ppm.

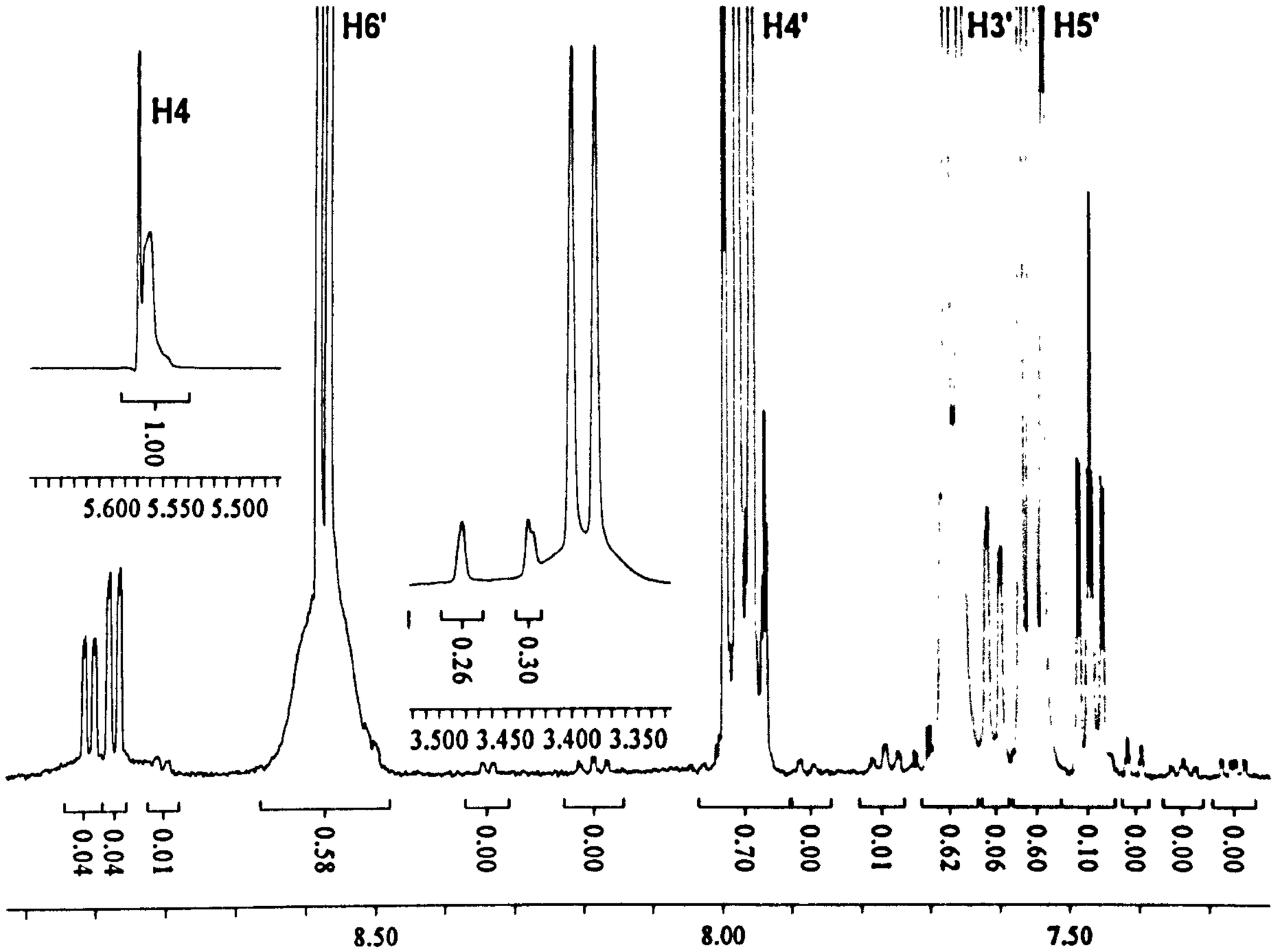

Figure 3.43. The 2nd half of the single yellow band from the purification of trans-Pt(ET-2-Py)(DMSO)Cl_2 using column chromatography.

A COSY spectrum shows the two singlets around 8.90 ppm are coupled to the signal at 7.48 ppm. The 7.48 ppm signal is coupled to a resonance under the large signal at 7.96 ppm which in turn is coupled to the 7.60 ppm signals. From this data it appears there are two different environments for the pyridine in the impurities although their identity has not been confirmed. The overall data suggests the trans-Pt(ET-2-Py)(DMSO)Cl_2 has been successfully synthesised and purified. The trans stereochemistry was confirmed by single crystal X-Ray crystallography (Figure 3.44).

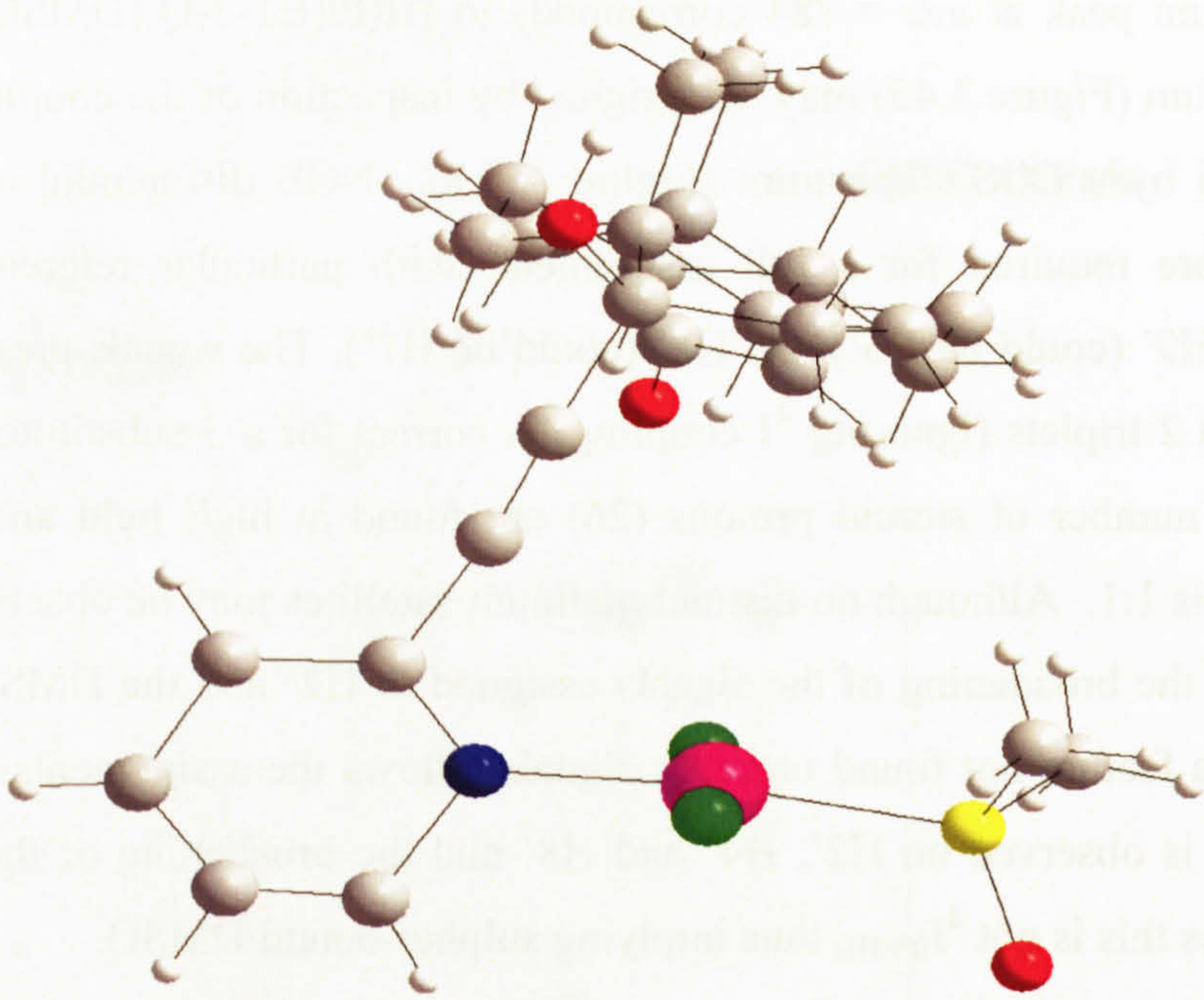

Figure 3.44. The X-ray crystal structure of trans-Pt(ET-2-Py)(DMSO)Cl_2 showing trans chloride ligands.

3.2.8.4. Trans-Pt(ET-3-Q)(DMSO)Cl_2

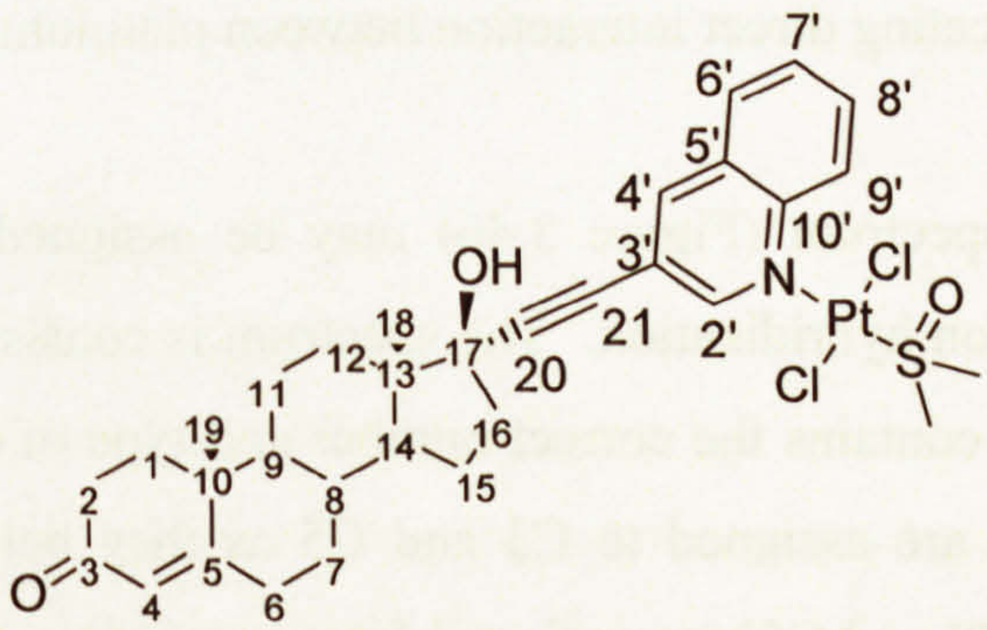

$C_{33}H_{39}Cl_2NO_3PtS$

Reacting cis-bis(dimethylsulphoxide)dichloroplatinum(II) and ET-3-Q in methanol gave the desired product in excellent yield and required flash column chromatography to separate platinum(II) complexes of the type PtL_2X_2 and $[Pt(L)_2(X)(DMSO)]^+$ where L = ET-3-Q and X = Cl and ET-3-Q as identified by mass spectroscopy (ESI, +ve) as monocations and ^1H NMR (Figure A.5.7). The compound was soluble in most organic solvents, although partial solubility was observed in methanol. The compound is insoluble in diethylether and water.

Elemental analysis shows the chemical formula expected for the desired products and the mass spectrum peak at *m/z* = 784 corresponds to $[H(Pt(ET\text{-}3\text{-}Q)(DMSO)Cl_2)]^+$. The ^1H NMR spectrum (Figure 3.45) may be assigned by inspection of the coupling constants and is confirmed by a COSY spectrum (Figure A.5.8). NOE differential or NOESY NMR techniques are required for a full assignment, with particular reference to the peaks assigned to H9' (could be H6') and H8' (could be H7'). The signals present, 2 singlets, 2 doublets and 2 triplets (ignoring ^4J coupling) is correct for a 3-substituted quinoline ring. The correct number of steroid protons (26) are found at high field and the quinoline : steroid ratio is 1:1. Although no distinct platinum satellites may be observed either side of any peak(s), the broadening of the signals assigned to H2' and the DMSO methyl proton resonances, a feature not found on other signals, allows the assignments to be confirmed. Some $^4J_{(H\text{-}H)}$ is observed on H2', H4' and H8' and the broadening of the DMSO methyl peak indicates this is not $^4J_{(Pt\text{-}H)}$, thus implying sulphur bound DMSO.

Further evidence of platinum binding is found by comparison with the chemical shifts of ET-3-Q (Figure A.5.9). In every case a downfield shift is observed, consistant with electron donation from nitrogen to platinum(II) making the aromatic ring system more electron poor and the hydrogens resonate at higher chemical shifts. Downfield shifts of 0.20, 0.14, 0.12, 0.11 and 0.09 ppm are observed compared to ET-3-Q for H2', H4', H6', H7' and H8'. In common with other complexes, the H9' resonance is shifted 1.32 ppm downfield, possibly indicating direct interaction between platinum and H9'.

The ^{13}C DEPT NMR spectrum (Figure 3.46) may be assigned by examination of the chemical shifts and carbon hybridization. The spectrum is consistant with the structure of the desired product at it contains the correct number and type of carbon atom resonances. The 2 low field signals are assigned to C3 and C5 as they belong to an α,β-unsatured ketone. The carbons C10' and C6' are assigned from inspection of the signals and the fact that C10' is α to the nitrogen atom of quinoline and C6' is γ. The other aromatic signals, C4 and the DMSO carbons are assigned by inspection of the HMQC spectrum (Figures A.5.10 and A.5.11).

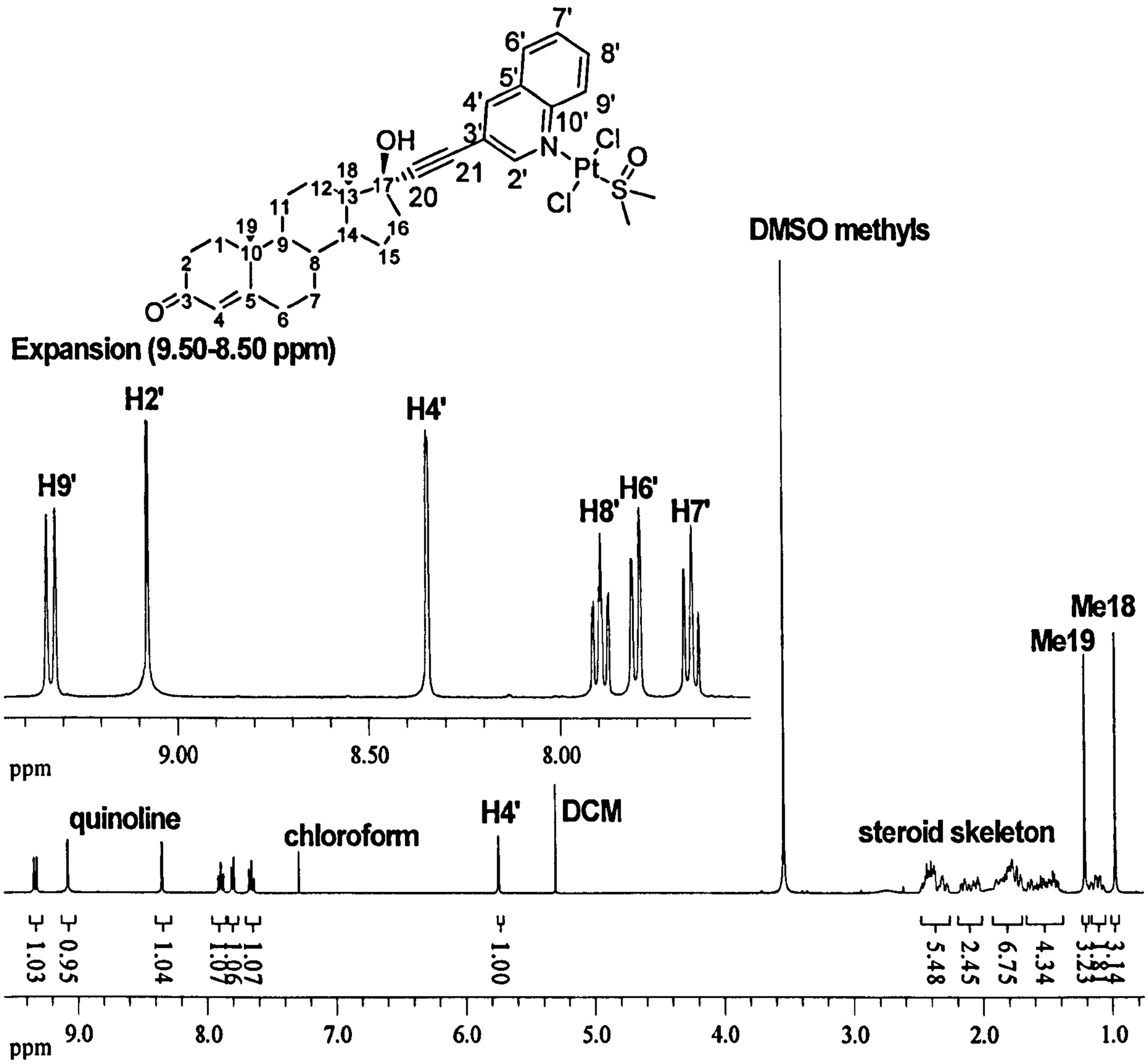

Figure 3.45. The ^{1}H NMR spectrum of trans-Pt(ET-3-Q)(DMSO)Cl_2.

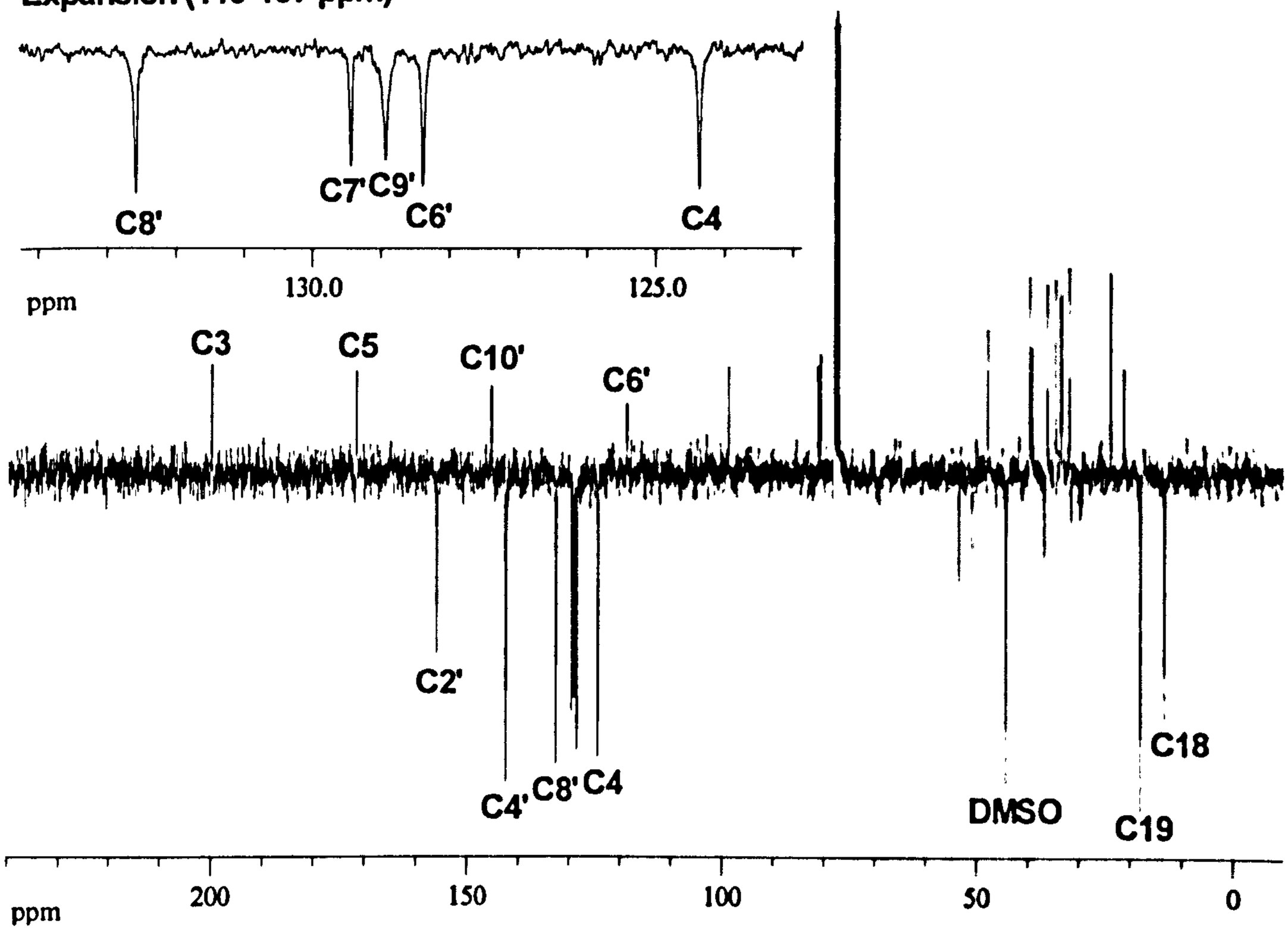

Figure 3.46. The ^{13}C NMR spectrum of trans-Pt(ET-3-Q)(DMSO)Cl_2 in $CDCl_3$.

In addition to NMR spectroscopy the infrared spectrum (Figure A.5.12) suggests sulphur bound DMSO by the position of the υS=O stretching frequency which relative to DMSO has increased in wavenumbers. The infrared spectrum (Figure A.4.12) shows the υS=O fundamental stretching vibrational band is at 1124 cm^{-1} compared to 1042 cm^{-1} in free DMSO and is consistant with sulphur bound DMSO.[523] All the data is consistent with the structure of trans-Pt(ET-3-Q)(DMSO)Cl_2 and the yield is 70 %.

3.2.9. The syntheses of platinum(II) starting materials

The syntheses of the platinum(II) starting materials cis-Pt$(NH_3)_2I_2$[524], *cis*-Pt$(NH_3)_2Cl_2$[524], trans-Pt$(NH_3)_2Cl_2$[525] and cis-Pt$(DMSO)_2Cl_2$[526] are from published methods and were identified by colour, infrared spectroscopy (Figures A.6.1 to A.6.4), ^1H NMR spectroscopy (Figure A.6.5) and elemental analysis. Yields were in line with those expected from literature reports.

3.2.10. Conclusions and further investigations

In total 11 platinum(II) complexes have been synthesised which will be used for further investigations. These may be split into three groups and are shown in Table 3.2 and will from this point on be known by their shorthand designations, *i.e.* CC-ET-3-Py.

Table 3.2. Platinum(II) complexes that are to be used in further investigations

Non-steroidal or control complexes	Trans-cationic	Cis-cationic
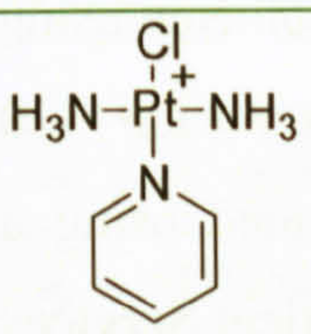 TC-Py	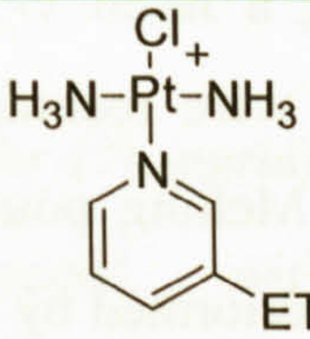 TC-ET-3-Py	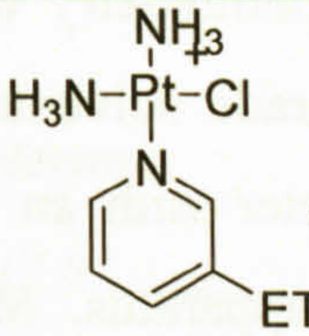 CC-ET-3-Py
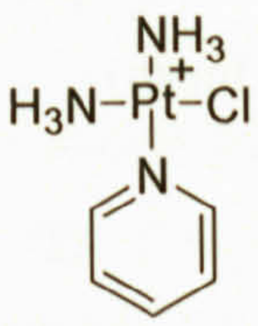 CC-Py	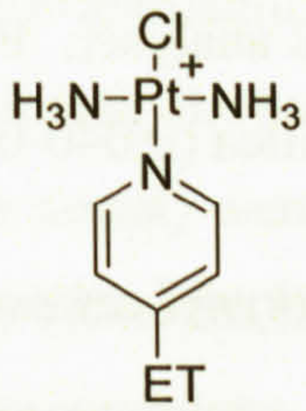 TC-ET-4-Py	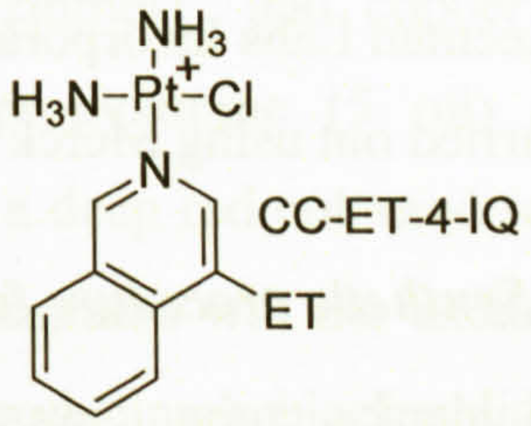 CC-ET-4-IQ
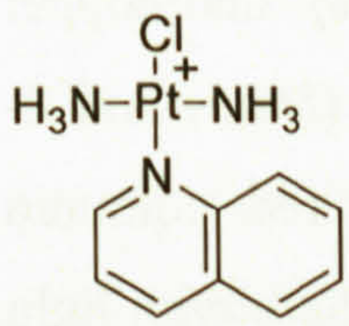 TC-Q	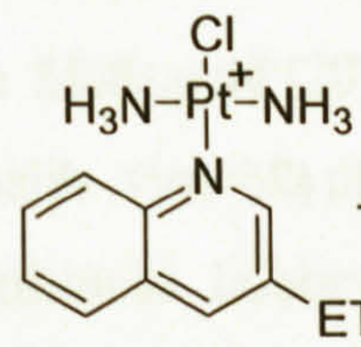 TC-ET-3-Q	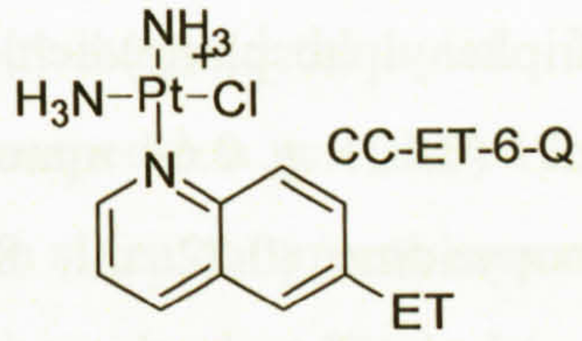 CC-ET-6-Q
	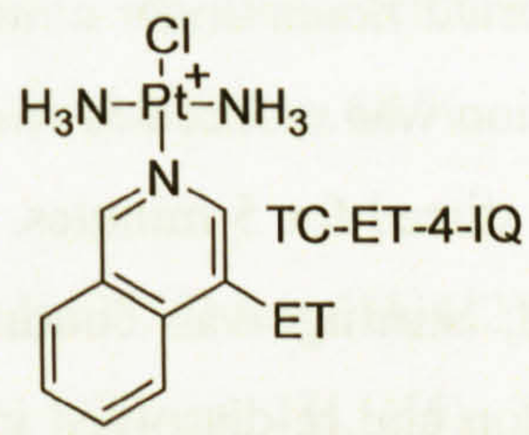 TC-ET-4-IQ	
	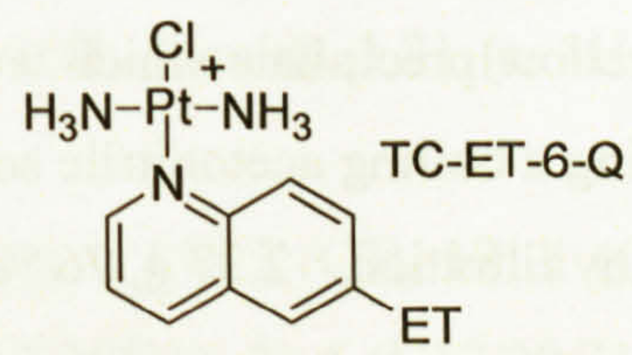 TC-ET-6-Q	

3.3. Experimental Details

All Sonogashira reaction reagents were fully dried before use and solvents degassed and followed the original protocol with the exception of using THF as a solvent.[512] 17α-ethnynyltestosterone, copper(I) iodide, dimethylsulphoxide and silver nitrate were obtained from Aldrich. Bis(triphenylphosphine)dichloropalladium(II), 2-bromopyridine, 3-bromopyridine, 4-bromopyridine hydrochloride, 3-bromoquinoline, 4-bromoisoquinoline, diisopropylamine and potassium tetrachloroplatinate(II) were obtained from Avocado. Potassium chloride, potassium iodide and all common organic solvents were obtained from Fisher Scientific.

^{1}H NMR and ^{13}NMR spectra were recorded on Brucker DPX300 or AMX400 spectrometers operated in fourier transform mode. ^{195}Pt NMR and Far IR spectra were

obtained by Dr Adoracion Gomez Quiroga at the UAM, Madrid, Spain. Chemical shifts were referenced to tetramethylsilane or H_2PtCl_6 as an internal standard or to residual solvent peaks. ESI mass spectra were recorded on a Brucker esquire 2000. Ultraviolet and visible spectrophotometry was performed using a Jasco V-570 spectrophotometer using spectroscopy grade solvents. Infrared spectra were recorded on a Nicolet Avatar 320 spectrophotometer with an ATR attachment. Melting points were determined using a Sturat SMP 10 apparatus. Microanalyses were performed by Warwick Analytical Services on a Leeman Labs Incorporated CE440 elemental analyser. Flash column chromatography was carried out using Merck 9385 Kieselgel 60 silica (0.040-0.063mm, 230-400 mesh).

3.3.1. Synthetic procedure for 17α-pyridin-2-ylethynyl-testosterone

A Schlenk tube was charged with ethisterone (2.5 g, 8 mmol), bis(triphenylphosphine)dichloropalladium(II) (0.224 g, 0.32 mmol, 4 mol%) and copper iodide (0.121 g, 0.64 mmol, 8 mol%). THF (25 ml), diisopropylamine (5 ml) and 2-bromopyridine (0.82 ml, 8.4 mmol) were added resulting in a deep red coloured suspension. The reaction was stirred for 72 hours under a nitrogen atmosphere with light exclusion. The resulting yellow suspension was reduced *in vacuo* to a paste. Methanol (20 ml) was added and the suspension was stirred for 5 minutes. Upon the addition of water (200 ml) a yellow precipitate formed; stirring was continued for 30 minutes. The precipitate was then collected by filtration and re-dissolved in 20 ml of methanol. Water (200 ml) was added resulting in a yellow precipitate which was collected by filtration and re-crystallised twice by slowly cooling a boiling acetonitrile solution to -20°C yielding fine white needles which were collected by filtration. 2.37 g, 76 % yield.

^{1}H-NMR (300 MHz, $CDCl_3$): δ 8.56 (ddd, 1H, J = 4.9, 1.7, 0.9 Hz, H6'), 7.63 (dt, 1H, J = 7.7, 1.8 Hz, H4'), 7.40 (td, 1H, J = 7.9, 1.0 Hz, H3'), 7.21 (ddd, 1H, J = 7.6, 4.9, 1.2 Hz, H5'), 5.71 (s, 1H, H4), 2.50-1.30 (m, 18H, steroid), 1.18 (s, 3H, Me19), 1.15 – 0.98 (m, 2H, steroid), 0.94 (s, 3H, Me19).

^{13}C-NMR (100 MHz, $CDCl_3$): δ 199.5 (C3), 171.2 (C5), 149.8 (C6'), 142.9 (C2'), 136.2 (C4'), 127.7 (C3'), 123.8 (C4), 122.9 (C5'), 93.0, 85.3, 79.8, 53.2, 50.1, 47.2, 38.8, 38.6, 36.2, 35.6, 33.9, 32.8, 32.7, 31.4, 23.2, 20.7, 17.4 (C19), 12.8(C18).

IR: υ 3200m (O-H str), 3175m (C-$H_{aromatic}$ str), 2932m (C-H str), 2878m (C-H str), 2856m (C-H str), 2219w (C≡C str), 1665s (C=O str), 1615m, 1585m, 1560m, 1497w, 1467m, 1427m, 1382m, 1358m, 1332m, 1273m, 1233m, 1189m, 1149m, 1149m, 1126m, 1062s, 1026m, 999m, 968m, 950m, 920m, 890m, 868m, 840w, 820w, 768s (C-H 'oop'), 742m, 700m, 677m cm^{-1}.

Mass spectrum (ESI, +ve): $m/z = 390$ $[H(C_{26}H_{31}NO_2)]^+$.

MP (uncorr.): 253-255°C.

Elemental analysis: Calculated for $C_{26}H_{31}NO_2$; C, 80.2; H, 8.0; N, 3.6. Found C, 80.05; H, 7.98; N, 3.52.

3.3.2. Synthetic procedure for 17α-pyridin-3-ylethynyl-testosterone

A Schlenk was charged with ethisterone (2.5 g, 8.00 mmol), bis(triphenylphosphine)dichloropallladium(II) (0.224 g, 0.32mmol) and copper iodide (0.121 g, 0.64 mmol). Tetrahydrofuran (40 ml), diisopropylamine (5 ml) and 3-bromopyridine (0.82 ml, 8.4 mmol) were added resulting in a deep red coloured solution. The reaction was stirred for 72 hours under a nitrogen atmosphere wth the exclusion of light. The resulting black mixture was reduced *in vacuo* producing a black solid which was collected by filtration. Methanol (20 ml) was used to re-suspend the solid. Water (200 ml) was added resulting in a brown precipitate and the suspension was stirred for 1hr and filtered to collect a brown solid. This was purified using a silica column to remove the first yellow band (eluent dichloromethane) and the product (eluent 98:2 dichloromethane:methanol). Yield 2.05 g, 68 %.

^{1}H-NMR (300 MHz, $CDCl_3$): δ 8.72 (m, 1H, H2'), 8.53 (s, 1H, H6'), 7.73 (d, 1H, J = 7.9 Hz, H4'), 7.27 (s, 1H, H5'), 5.73 (m, 1H, H4), 2.48-2.25 (m, 5H, steroid), 2.15-2.05 (m, 2H, steroid), 1.90-1.37 (m, 10H, steroid), 1.21 (s, 3H, Me19), 1.13-0.98 (m, 2H, steroid), 0.96 (s, 3H, Me18).

^{13}C-NMR (100 MHz, $CDCl_3$): δ 198.2 (C3), 171.1 (C5), 151.5 (C2'), 147.5 (C6'), 138.7 (C4'), 123.5 (C4), 97.5 (C17/20/21), 81.6 (C17/20/21), 79.1 (C17/20/21), 53.2 (C8/9/14), 50.0 (C8/9/14), 47.0, 38.8, 38.3, 36.0 (C8/9/14), 35.5, 35.3, 33.6, 32.7, 32.5, 31.2, 30.7, 23.0, 20.5, 17.1 (C19), 12.8 (C18).

IR: υ 3351m (O-H str), 2941m (C-H str), 2894m (C-H str), 1657s (C=O str), 1614m, 1475m, 1444m, 1425m, 1408m, 1381m, 1375m, 1352m, 1274m, 1232m, 1188m, 1125m, 1061m, 1025m, 948m, 866m, 807m, 700s cm^{-1}.

Mass spectrum (ESI, +ve): $m/z = 390$ $[H(C_{26}H_{31}NO_2)]^+$.

Elemental analysis: calculated for $C_{26}H_{31}NO_2$; C, 80.2; H, 8.0; N, 3.6. Found C, 80.01; H, 8.21; N, 3.38.

3.3.3. Synthetic procedure for 17α-pyridin-4-ylethynyl-testosterone

A Schlenk tube was charged with ethisterone (2.50 g, 8.00 mmol, bis(triphenylphosphine)dichloropalladium(II) (0.224 g, 0.16 mmol), copper iodide (0.121 g, 0.64 mmol) and 4-bromopyridine hydrochloride (1.64 g, 8.4 mmol). Tetrahydrofuran

(25 ml) and diisopropylamine (10 ml) were added resulting in a red / brown coloured solution. The reaction was stirred for 72 hours at room temperature under a nitrogen atmosphere in the absence of light. The resulting yellow / brown solution was reduced *in vacuo* to a brown solid. Methanol (20 ml) was added and the mixture stirred for 5 minutes before water (200 ml) was added resulting in a yellow flocculent precipitate which was collected by filteration. The solid was dissolved in chloroform (40 ml) and this solution was washed with water (15 x 20 ml). The chloroform solution was reduced *in vacuo* to ca. 5 ml and purified using a silica column (elutent dichloromethane:methanol, 98:2) to separate the desired product from palladium salts. 2.12 g, 68 % yield.

^{1}H-NMR (300 MHz, CD_3OD): δ 8.44 (s, 1H, H2'& H6'), 7.35 (d, 1H, J = 5.6 Hz, H3' & H5'), 5.66 (s, 1H, H4), 2.42 (m, 2H, steroid), 2.25 (m, 3H, steroid), 2.03 (m, 2H, steroid), 1.86 (m, 1H, steroid), 1.79-1.30 (m, 10H, steroid), 1.21 (s, 1H, steroid), 1.10-0.85 (m, 5H, steroid).

IR: υ 3189m (O-H str), 2932m (C-H str), 2886m (C-H str), 2856m (C-H str), 2220w (C≡C str), 1663s (C=O str), 1614m, 1596m 1540w, 1492m, 1467m, 1436m, 1417m, 1383m, 1356m, 1333m, 1291m, 1269m, 1231m, 1215m, 1187m, 1149m, 1126m, 1058m, 1027m, 1002m, 962m, 921m, 889m, 963m, 824s (C-H 'oop' bend), 775m, 747m, 699m, 678m, 664m cm^{-1}

UV / Visible (methanol): 242nm (ε = 30800 mol^{-1} dm^3 cm^{-1})

Mass spectrum (ESI, +ve): 390.3 $[H(C_{26}H_{31}NO_{2})]^+$

Elemental Analysis: calculated for $C_{26}H_{31}NO_2$; C, 80.2; H, 8.2; N, 3.6. Found C, 80.05; H, 8.01; N, 3.48

3.3.4. Synthetic procedure for 17α-quinolin-3-ylethynyl-testosterone

A Schlenk tube was charged with ethisterone (2.5 g, 8 mmol), bis(triphenylphosphine)dichloropallladium(II) (0.112 g, 0.16 mmol and copper iodide (0.060 g, 0.32 mmol). Tetrahydrofuran (25 ml), diisopropylamine (5 ml) and 3-bromoquinoline (0.82 ml, 8.4 mmol) were added resulting in a deep red colour solution. The reaction was stirred for 48 hours under a nitrogen atmosphere with the exclusion of light. The resulting reaction suspension was reduced to a paste *in vacuo* and methanol (20 ml) added. The addition of water (200 ml) resulted in a brown precipitate. The suspension neutralised with several drop of concentrated hydrochloric acid. The brown solid was filtered and acetonitrile (300 ml) added to the solid. The mixture was heated to boiling for 30 minutes until a black solid precipitated from the orange / yellow solution. The precipitate was filtered off through celite and the filtrate reduced in volume to ca. 200 ml.

This mixture was cooled quickly to -20°C and the precipitated crude ET-3-Q was immediately filtered, dissolved in chloroform (50 ml) and extensively washed with water (15 x 15 ml). The solution was dried over $MgSO_4$ and reduced to a solid *in vacuo*. The slightly yellow solid was crystallized slowly from boiling acetonitrile twice to yield large bright crystals which were collected by filtration, 2.81g, 80% yield.

^{1}H-NMR (400 MHz, $CDCl_3$): δ 8.99 (d, 1H, J = 2.1 Hz, H2'), 8.20 (d, 1H, J = 2.0 Hz, H4'), 8.09 (d, 1H, J = 8.5 Hz, H9'), 7.77 (d, 1H, J = 8.1 Hz, H6'), 7.56 (ddd, 1H, J = 8.1, 7.0, 1.1 Hz, H8'), 7.71 (ddd, 1H, J = 8.4, 6.9, 1.4 Hz, H7'), 5.72 (s, 1H, H4), 3.81 (s, 1H, 17α-OH), 2.55-2.25 (m, 5H, steroid), 2.16 (ddd, 1H, J = 13.9, 11.9, 3.9 Hz, steroid), 2.03 (ddd, 1H, J = 13.4, 11.9, 4.9 Hz, steroid), 1.95-1.35 (m, 11H, steroid), 1.20 (s, 3H, Me19), 1.15-0.95 (m, 5H, steroid).

^{13}C-NMR (100 MHz, $CDCl_3$): δ 199.5 (C3), 171.0 (C5), 151.9 (C9'), 146.4 (C10'), 138.6 (C4'), 130.2 (C8'), 129.0 (C9'), 127.5 (C6'/C7'), 127.4 (C7'/C6'), 127.2 (C5'), 123.9 (C4), 117.1 (C3'), 96.8, 83.0, 79.9, 50.4, 47.3, 39.1, 38.6, 36.3, 35.7, 33.9, 33.0, 32.8, 31.5, 23.3, 20.8, 17.4 (C19), 13.0 (C18).

IR: *υ* 3210m (O-H str), 2943m (C-H str), 2883m (C-H str), 2862m (C-H str), 2837m (C-H str), 2215w (C≡C str), 1667s (C=O), 1610m, 1570m, 1491m, 1448m, 1429m, 1385m, 1343m, 1286m, 1273m, 1240m, 1231m, 1150m, 1130m, 1072m, 1002m, 964m, 949m, 922m, 871m, 863m, 837w, 787s, 760s, 725m, 691m, 673m cm^{-1}.

Mass spectrum (ESI, +ve): *m/z* = 440 $[H(C_{30}H_{33}NO_2)]^+$.

MP (uncorr.): 223 – 224 °C.

Elemental analysis: calculated for $C_{30}H_{33}NO_2$; C, 82.0; H, 7.6; N, 3.2. Found C, 81.61; H, 7.19; N, 3.23.

3.3.5. Synthetic procedure for 17α-isoquinoline-4-ylethynyl-testosterone

A Schlenk was charged with ethisterone (4.00 g, 12.8 mmol), bis(triphenylphosphine)dichloropalladium(II) (0.359 g, 0.51 mmol) and copper iodide (0.195 g, 1.02 mmol) and 4-bromoisoquinoline (3.13 g, 15 mmol). THF (35 ml) and diisopropylamine (10 ml) were added resulting in a deep red coloured solution. The reaction was stirred for 72 hours under a nitrogen atmosphere excluding light. The resulting yellow / brown solution was reduced to a paste *in vacuo*. The paste was dissolved in chloroform (50 ml) and extensively washed with water (15 x 25 ml). The chloroform layer was reduced to a solid *in vacuo*, acetonitrile (500 ml) added and the mixture heated to boiling for 30 min until the solution was orange. It was then reduced in volume to ca. 200 ml. This solution was cooled quickly to -20°C and precipitated crude

ET-4-IQ was immediately filtered. The slightly yellow solid was slowly re-crystallised twice from boiling methyl cyanide to yield a bright white crystalline material which was collected by filtration, 5.03 g, 89% yield.

^{1}H-NMR ($CDCl_3$, 400 MHz): δ 9.14 (s, 1H, H2'), 8.77 (m, 1H, H10'), 8.15 (d, 1H, J = 8.3 Hz, H8'), 7.75 (ddd, 1H, J = 8.1, 7.1, 0.9 Hz, H5'), 7.63 (t, 1H, J = 7.5 Hz, H7'), 7.52 (t, 1H, J = 7.6 Hz, H6'), 5.72 (s, 1H, H4), 4.15 (s, 1H, 17α-OH), 2.55-2.15 (m, 6H, steroid), 2.02 (m, 1H, steroid), 1.92-1.75 (m, 4H, steroid), 1.70-1.55 (m, 4H, steroid), 1.55-1.40 (m, 4H, steroid), 1.20 (s, 3H, Me19), 1.10-0.9 (m, 5H, steroid).

^{13}C-NMR (125 MHz, $CDCl_3$): δ 199.5 (C3), 171.0 (C5), 151.5 (C2'), 146.0 (C10'), 135.7 (C4'), 131.3 (C7'), 128.0 (C5'/C6'), 128.0 (C5'/C6'), 127.7 (C9'), 124.9 (C8'), 123.9 (C4), 115.9, 101.2, 80.9, 80.0, 50.5, 47.3, 39.4, 38.6, 36.3, 35.7, 33.9, 33.1, 32.7, 31.6, 23.3, 20.8, 17.4 (C19), 13.0 (C18).

IR: υ 3326m (O-H str), 2940m (C-H str), 2916m (C-H str), 2892m (C-H str), 2854m (C-H str), 1645s (C=O str), 1607m, 1562m, 1497w, 1442m, 1416w, 1389m, 1362m, 1332m, 1285m 1263m, 1253m, 1233m, 1221m, 1192m, 1155w, 1130m, 1118m, 1069m, 1056m, 1045m, 1031m, 1009m, 1000m, 970w 948m, 921w, 897m, 880m, 838w, 797m, 785s, 760s, 717m, 767m cm^{-1}.

MP (uncorr.) : 213 – 215 °C.

Mass spectrum (ESI, +ve): m/z = 440 $[H(C_{30}H_{33}NO_2)]^+$.

Elemental analysis: calculated for $C_{30}H_{33}NO_2$; C, 82.0; H, 7.6; N, 3.2. Found C, 82.06; H, 7.32; N, 3.27.

3.3.6. Synthetic procedure for 17α-quinoline-6-ylethynyl-testosterone

A Schlenk tube was charged with ethisterone (2.5 g, 8 mmol), bis(triphenylphosphine)dichloropalladium(II) (0.112 g, 0.16 mmol and copper iodide (0.060 g, 0.32 mmol). Tetrahydrofuran (25 ml), diisopropylamine (10 ml) and 6-bromoquinoline (0.82 ml, 8.4 mmol) were added resulting in a deep red colour solution. The reaction was stirred for 48 hours under a nitrogen atmosphere with the exclusion of light. The resulting reaction suspension was reduced to a paste *in vacuo* and methanol (20 ml) added. The addition of water (200 ml) resulting in a brown / yellow precipitate and the suspension neutralised with several drop of concentrated hydrochloric acid. The brown / yellow solid was collected by filtration and acetonitrile (300 ml) added to the solid. The mixture was heated to boiling for 30 minutes until a black solid precipitated from the orange / yellow solution. The precipitate was collected by filtration through celite and discarded. Filtrate reduced in volume to ca. 200 ml and cooled quickly to -20°C and the

precipitated crude ET-6-Q immediately collected filtration, dissolved in chloroform (50 ml) and extensively washed with water (15 x 15 ml). The solution was dried over $MgSO_4$ and reduced to a solid *in vacuo*. The slightly yellow solid was crystallized slowly from boiling acetonirile twice and the large bright white crystals collected by filtration, 2.10 g, 60 % yield.

^{1}H-NMR (300 MHz, CD_3OD): δ 8.79 (dd, 1H, J = 1.7 Hz, J = 4.3 Hz, H2'), 8.29 (dd, 1H, J = 8.5, 1.0 Hz, H4'), 7.97 (d, 1H, J = 1.7 Hz, H6'), 7.93 (d, 1H, J = 8.8 Hz, H9'), 7.70 (dd, 1H, J = 8.8, 1.8 Hz, H8'), 7.50 (dd, 1H, J = 8.4, 4.3 Hz, H3'), 5.65 (s, 1H, H4), 2.52-2.16 (m, 5H, steroid), 2.12-1.98 (m, 2H, steroid), 1.94-1.30 (m, 11H, steroid), 1.20 (s, 3H, Me19), 1.05-0.88 (m, 5H).

IR: υ 3156m (O-H + C-H str), 2938m (C-H str), 2858m (C-H str), 1673s (C=O str), 1614m, 1571m, 1492m, 1435m, 1417m, 1378m, 1342m, 1284m, 1271m, 1231m, 1187m, 1148m, 1125m, 1067m, 1010m, 999m, 960m, 946m, 910m, 865m, 836m, 785s, 753s, 724m, 689m, 671m cm^{-1}.

Mass spectrum (ESI, +ve): m/z = 440 $[H(C_{30}H_{33}NO_2)]^+$.

Elemental analysis: calculated for ($C_{30}H_{33}NO_2$); C, 82.0; H, 7.6; N, 3.2. Found C, 81.79; H, 7.52; N, 3.00.

3.3.7. Synthetic procedure for trans-[Pt(NH3)$_2$(Py)Cl][NO$_3$]

To a solution of trans-diamminedichloroplatinum(II) (0.200 g, 0.667 mmol) in DMF (1 ml) was added a silver nitrate (0.111 g, 0.653 mmol) in DMF (1 ml) and stirred over night at 40 C in the absence of light. Silver chloride was removed by filration through celite yielding a pale yellow solution. The solution was cooled to -18 C and pyridine (54 µl, 0.053g, 0.667 mmol) added with a micro syringe with stirring. The solution was allowed to reach room temperature over 4 hours and the mixture stirred overnight. The slow addition of diethylether (200ml) yielded an off-white precipitate that was collected by filtration. The precipitate was dissolved in warm methanol (10 ml) and diethylether (10 ml) slowly added resulting in a small amount of off-white precipitate and this was collected by filtration and discarded. Diethylether (100 ml) was added to the remaining filtrate resulting in a white precipitate and this was collected by filtration. This procedure was repeated 3 times further and the final bright white precipitate collected by filtration and washed with diethylether (2 x 5 ml) and dried over phosphorus pentoxide. 0.058g, 20% yield.

^{1}H-NMR (400 MHz, CD_3OD): δ 8.79 (ddt, 2H, $J_{(Pt-H)}$ = 22.12 Hz, $J_{(H-H)}$ = 5.1 Hz, 1.45 Hz, H2'/H6'), 7.97 (tt, 1H, J = 7.8, 1.5 Hz, H4'), 7.51 (ddd, 2H, J = 7.7, 5.2, 1.4 Hz, H3'/H5').

IR: 3271m, 3124m, 1611m, 1586m, 1488w, 1457m, 1343s, 1306s, 1241m, 1162m, 1078m, 1048m, 1021m, 981m, 932m, 871m, 825m, 761m, 688m cm^{-1}.

Mass spectrum (ESI, +ve): *m/z* = 343 $[Pt(NH_3)_2(Py)Cl]^+$.

Elemental analysis: calculated for $C_5H_{11}ClN_4O_3Pt$; C, 14.8; H, 2.7; N, 13.8; Cl, 8.7. Found C, 15.15; H, 2.90; N, 13.92; Cl, 8.89.

3.3.8. Synthetic procedure for trans-[Pt(NH3)$_2$(Quinoline)Cl][NO$_3$]

To a solution of trans-diamminedichloroplatinum(II) (0.200 g, 0.67 mmol) in DMF (1 ml) was added a silver nitrate (0.11 g, 0.65 mmol) in DMF (1 ml). The mixture was stirred over night in the absence of light. Silver chloride was removed by filtration through celite resulting in a pale yellow solution. The solution was cooled to -18 C and quinoline (79 µl, 0.087g, 0.67 mmol) added with a micro syringe with stirring. The solution was stirred, reached room temperature and stirred overnight. The slow addition of diethylether (200ml) yielded an off-white precipitate that was filtered off. The precipitate was dissolved in warm methanol (10 ml) and diethylether (10 ml) slowly added resulting in a small amount of off-white precipitate and this was collected by filtration and discarded. Diethylether (100 ml) was added to the remaining filtrate resulting in a white precipitate and this was collected by filtration. This procedure was repeated 3 times further and the final bright white precipitate was collected by filtration and washed with diethylether (2 x 5 ml) and dried over phosphorus pentoxide. 0.045g, 15% yield.

^{1}H-NMR (300 MHz, CD_3OD): δ 9.71 (d, 1H, J= 8.6 Hz, H9') 9.44 (dd, 1H, J = 5.2, 1.2 Hz, H2'), 8.66 (d, 1H, J = 8.3 Hz, H4') 8.12 (m, 2H, H6'/H8'), 7.83 (t, 1H, J = 7.4 Hz, H3'), 7.66 (dd, 1H, J = 8.3, 5.4 Hz, H7').

IR: υ 3266m, 2781m, 1743m, 1622m, 1590m, 1509m, 1458w, 1338s, 1314s, 1262m, 1207m, 1163m, 1139m, 1128m, 1040m, 978m, 924s, 871m, 829m, 813s, 777s, 751m cm^{-1}

Mass spectrum (ESI, +ve): *m/z* = 394 $[Pt(NH_3)_2(Quin)Cl]^+$.

Elemental analysis: calculated for $C_9H_{13}ClN_4O_3Pt$; C, 23.7; H, 2.9; N, 12.3; Cl, 7.8. Found C, 23.41; H, 2.83; N,12.20; Cl, 7.58.

3.3.9. Synthetic procedure for trans-[Pt(NH3)$_2$(ET-3-Py)Cl][NO$_3$]

To a solution of trans-diamminedichloroplatinum(II) (0.200 g, 0.67 mmol) in DMF (1 ml) was added a silver nitrate (0.11 g, 0.65 mmol) in DMF (1 ml). The mixture was stirred overnight in the absence of light. Silver chloride was removed by filtration through celite resulting in a pale yellow solution. The solution was cooled to -18°C and 17α-pyridin-3-

ylethynyl-testosterone (0.254 g, 0.653 mmol) added with stirring. The solution reached room temperature and the mixture stirred for a further 8 hours. The slow addition of diethylether (200 ml) yielded a white precipitate which was collected by filtration off. The crude product was dissolved in warm methanol (25 ml), decolourising charcoal (0.02 g) was added and the resulting suspension stirred for 10 minutes. The charcoal was removed by filtration through celite and the filtrate reduced *in vacuo* to ca. 10 ml. The addition of diethylether (10 ml) resulted in a small amount of yellow precipitate which was discarded. Diethylether (100 ml) was added to the remaining filtrate resulting in a white precipitate and this was collected by filtration. This procedure was repeated 3 times further and the final bright white precipitate was washed with diethylether (2 x 5 ml) and dried over phosphorus pentoxide. 0.125 g, 28% yield.

^{1}H-NMR (400 MHz, CD_3OD): δ 8.93 (d, 1H, J = 1.8 Hz, H2'), 8.78 (dd, 1H, J = 5.8, 1.1 Hz, H6'), 8.02 (td, 1H, J = 8.0, 1.6 Hz, H4'), 7.52 (dd, 1H, J = 8.0, 5.8 Hz, H5'), 5.71 (s, 1H, H4), 2.60-1.40 (m, 18H, steroid), 1.26 (s, 1H, Me19), 1.15-0.90 (m, 5H, steroid).
IR: υ 3279m, 2944m (C-H str), 2876m (C-H str), 1644m (C=O str), 1474m, 1330s, 1233m, 1190m, 1125m, 1059m, 947m, 868m, 812m, 691m cm^{-1}.
Mass spectrum (ESI, +ve): m/z = 654 $[Pt(NH_3)_2(ET\text{-}3\text{-}Py)Cl]^+$.
Elemental analysis: calculated for $C_{26}H_{37}ClN_4O_5Pt$; C, 43.6; H, 5.2; N, 7.8; Cl, 5.0. Found C, 43.25; H, 5.25; N, 7.85; Cl, 5.20.

3.3.10. Synthetic procedure for trans-[Pt(NH3)$_2$(ET-4-Py)Cl][NO$_3$]

To a solution of trans-diamminedichloroplatinum(II) (0.200 g, 0.67 mmol) in DMF (1 ml) was added silver nitrate (0.11 g, 0.65 mmol) in DMF (1 ml) and the mixture stirred overnight in the absence of light. Silver chloride was collected by filtration through celite and discarded. The solution was cooled to -18°C and 17α-pyridin-4-ylethynyl-testosterone (0.254 g, 0.653 mmol) added with stirring. The solution reached room temperature and the mixture stirred for a further 8 hours. The slow addition of diethylether (200 ml) yielded a white precipitate and this was collected by filtration. The crude product was dissolved in warm methanol (25 ml). Decolourising charcoal (0.05 g) was added and the resulting suspension stirred for 5 minutes. The charcoal was discarded after filtration through celite and filtrate reduced *in vacuo* to ca. 5 ml. The addition of diethylether (10 ml) resulted in a small amount of yellow precipitate which was discarded. Diethylether (100 ml) was added to the remaining filtrate resulting in a white precipitate which was collected by filtration and this procedure repeated twice. The final precipitate was collected by filtration, washed with diethylether (2 x 5 ml) and dried over phosphorus pentoxide. 0.104 g, 22% yield.

^{1}H-NMR (300 MHz, CD_3OD): δ 8.72 (d, 1H, J = 6.7 Hz, H2'/H6'), 7.46 (d, 1H, J = 6.6 Hz, H3'/H5'), 5.66 (s, 1H, H4), 2.6-1.4 (m, 18H, steroid), 1.21 (s, 3H, Me19), 0.91-0.81 (m, 5H, steroid).

^{195}Pt-NMR (64 MHz, CD_3OD) : δ -2874 ppm.

IR: υ 3350m (O-H str), 3281m (N-H and C-H str), 2940m (C-H str), 2227w (C≡C str), 1669m (C=O str), 1615m, 1493w, 1416s, 1377s, 1307vs, 1231m, 1184m, 1148w, 1125m, 1069m, 106m, 1044m, 1027m, 1013m, 950m, 921w, 868m, 825m (C-H 'oop'), 780w, 730w, 680w cm^{-1}.

UV / Visible (Methanol): 242nm (ε = 20500 mol^{-1} dm^3 cm^{-1}).

Mass spectrum (ESI, +ve): *m/z* 654 $[Pt(NH_3)_2(ET\text{-}4\text{-}Py)Cl]^+$.

Elemental analysis: calculated for $C_{26}H_{37}ClN_4O_5Pt$; C, 43.6; H, 5.2; N, 7.8; Cl, 4.9. Found C, 43.78; H, 5.00; N, 7.89; Cl, 4.96

3.3.11. Synthetic procedure for trans-[Pt(NH3)$_2$(ET-3-Q)Cl][NO$_3$]

To a solution of trans-diamminedichloroplatinum(II) (0.200 g, 0.67 mmol) in DMF (1 ml) was added silver nitrate (0.11 g, 0.65 mmol) in DMF (1 ml) and the mixture stirred overnight in the absence of light. Silver chloride was discarded after filtration through celite leaving a pale yellow filtrate. The solution was cooled to -18°C and 17α-quinolin-3-ylethynyl-testosterone (0.287 g, 0.65 mmol) added with stirring. The solution reached room temperature and the mixture stirred for a further 8 hours. The slow addition of diethylether (200 ml) yielded a white precipitate which was collected by filtration. The crude product was dissolved in warm methanol (50 ml), decolourising charcoal (0.1 g) was added and the resulting suspension stirred for 5 minutes. The charcoal discarded after filtration through celite and filtrate reduced *in vacuo* to ca. 15 ml. The addition of diethylether (15 ml) resulted in a small amount of yellow precipitate which was discarded after filtration through celite. Diethylether (100 ml) was added to the remaining filtrate resulting in a white precipitate and this was collected by filtration. This procedure was repeated 3 times further and the final bright white precipitate was washed with diethylether (2 x 10 ml) and dried over phosphorus pentoxide. 0.128 g, 28% yield.

^{1}H-NMR (300 MHz, CD_3OD): δ 9.62 (d, 1H, J = 8.5 Hz, H9'), 9.44 (d, 1H, J = 1.8Hz, H2'), 8.63 (d, 1H, J = 1.2 Hz, H4'), 8.02 (m, 2H, H6'/H8'), 7.76 (t, 1H, J = 7.6 Hz, H7'), 5.67 (s, 1H, H4), 2.55-1.40 (m, 18H, steroid), 1.23 (s, 1H, Me19), 1.10-0.90 (m, 5H, steroid).

IR: υ 3255m, 2938m (C-H str), 1646s (C=O str), 1496m, 1332vs, 1243m, 1125m, 1059m, 1026m, 947m, 869m, 835m, 779m, 754m, 677m, 667m cm^{-1}.

Mass spectrum (ESI, +ve): *m/z* = 704.2 $[Pt(NH_3)_2(ET\text{-}3\text{-}Q)Cl]^+$.

Elemental analysis: calculated for $C_{30}H_{39}ClN_4O_5Pt$; C, 47.0; H, 5.1; N, 7.3; Cl, 4.6. Found C, 48.39; H, 5.25; N, 7.32; Cl, 4.93.

3.3.12. Synthetic procedure for trans-[Pt(NH3)$_2$(ET-4-IQ)Cl][NO$_3$]

To a solution of trans-diamminedichloroplatinum(II) (0.200 g, 0.67 mmol) in DMF (1 ml) was added a silver nitrate (0.11 g, 0.65 mmol) in DMF (1 ml) and the mixture stirred overnight in the absence of light. The removal of silver chloride by filtration through celite yielded a pale yellow filtrate. The solution was cooled to -18°C and 17α-isoquinolin-4-ylethynyl-testosterone (0.287 g, 0.65 mmol) added with stirring. The solution reached room temperature and the mixture stirred for a further 8 hours. The slow addition of diethylether (200 ml) yielded a white precipitate which was filtered off. The crude product was dissolved in warm methanol (50 ml), decolourising charcoal (0.1 g) was added and the resulting suspension stirred for 5 minutes. The charcoal was filtered off using celite and filtrate reduced *in vacuo* to ca. 15 ml. The addition of diethylether (15 ml) resulted in a small amount of yellow precipitate which was collected by filtration and discarded. Diethylether (100 ml) was added to the remaining filtrate resulting in a white precipitate and this was collected by filtration. This procedure was repeated 3 times further and the final bright white precipitate which was collected by filtration and washed with diethylether (2 x 10 ml) and dried over phosphorus pentoxide. 0.128 g, 28% yield.

^{1}H-NMR (300 MHz, CD_3OD): δ 9.62 (d, 1H, J = 8.5 Hz, H9'), 9.44 (d, 1H, J = 1.8Hz, H2'), 8.63 (d, 1H, J = 1.2 Hz, H4'), 8.02 (m, 2H, H6'/H8'), 7.76 (t, 1H, J = 7.6 Hz, H7'), 5.67 (s, 1H, H4), 2.55-1.40 (m, 18H, steroid), 1.23 (s, 1H, Me19), 1.10-0.90 (m, 5H, steroid).

IR: υ 3255m, 2938m (C-H str), 1646s (C=O str), 1496m, 1332vs, 1243m, 1125m, 1059m, 1026m, 947m, 869m, 835m, 779m, 754m, 677m, 667m cm^{-1}.

Mass spectrum (ESI, +ve): *m/z* = 704.2 $[Pt(NH_3)_2(ET\text{-}3\text{-}Q)Cl]^+$.

Elemental analysis: calculated for $C_{30}H_{39}ClN_4O_5Pt$; C, 47.0; H, 5.1; N, 7.3; Cl, 4.6. Found C, 48.24; H, 5.12; N, 7.5; Cl, 4.89.

3.3.13. Synthetic procedure for trans-[Pt(NH3)$_2$(ET-6-Q)Cl][NO$_3$]

To a solution of trans-diamminedichloroplatinum(II) (0.20 g, 0.67 mmol) in DMF (1 ml) was added a silver nitrate (0.11 g, 0.65 mmol, 0.98 eq.) in DMF (1 ml) and the mixture was stirred overnight in the absence of light. The silver chloride precipitate was collectred by

filtration and discarded leaving a pale yellow solution filtrate. The solution was cooled to -18°C and 17α-quinolin-6-ylethynyl-testosterone (0.254 g, 0.653 mmol) added with stirring. The solution reached room temperature and the mixture stirred overnight. The slow addition of diethylether (200ml) yielded a white / yellow precipitate which was collected by filtration. The solid was dissolved in methanol (50 ml) and decolourising charcoal (0.2 g) was added and the mixture stirred for 20 minutes. The decolourising charcoal was removed by filtration through celite and filtrate reduced *in vacuo* to approximately 5 ml. The addition of diethylether (10 ml) resulted in a small amount of yellow precipitate which was filtered off. Diethylether (100 ml) was added to the remaining filtrate resulting in a white precipitate which was collected by filtration. The solid was dissolved in warm methanol (15 ml) and diethylether was added (150 ml) resulting in a white precipitate which was collected by filtration and the procedure repeated twice before the final precipitate was collected by filtration, washed with diethylether (5 x 5 ml) and dried over phosphorus pentoxide. 0.151 g, 34 % yield.

^{1}H-NMR (400 MHz, CD_3OD): δ 9.60 (d, 1H, J = 9.0 Hz, H9'), 9.38 (dd, 1H, J = 5.3, 1.8Hz, H2'), 8.57 (d, 1H, J = 8.3 Hz, H4'), 8.14 (d, 2H, J = 1.6 Hz, H6'), 8.80 (dd, 1H, J – 9.0, 1.8 Hz, H8'), 7.62 (dd, 1H, J = 8.4, 5.3 Hz, H3'), 5.69 (s, 1H, H4), 2.50-1.40 (m, 18H, steroid), 1.25 (s, 1H, Me19), 1.10-0.88 (m, 5H, steroid).

IR: *v* 3298m, 2974m, 2945m, 2858m, 2830m (C-H str), 1666m(C=O str), 1616m, 1590m, 1504m, 1435m, 1332s, 1326s, 1309s, 1271m, 1231m, 1187m, 1147m, 1129m, 1060m, 1028m, 1014m, 998m, 962m, 933m, 892m, 855m, 835m, 825m, 762m, 673m cm^{-1}.

Mass spectrum (ESI, +ve): *m/z* = 704.2 $[Pt(NH_3)_2(ET\text{-}6\text{-}Q)Cl]^+$.

Elemental analysis: calculated for $C_{30}H_{39}ClN_4O_5Pt$; C, 47.0; H, 5.1; N, 7.3; Cl, 4.6. Found C, 48.36; H, 5.00; N, 7.45; Cl, 4.28.

3.3.14. Synthetic procedure for cis-[Pt(NH3)$_2$(Py)Cl][NO$_3$]

To a solution of cis-diamminedichloroplatinum(II) (0.200 g, 0.67 mmol) in DMF (1 ml) was added silver nitrate (0.111 g, 0.63 mmol) in DMF (1 ml) and the mixture was stirred over night at 40°C in the absence of light. Silver chloride was removed by filtration and discarded leaving a pale yellow filtrate. The solution was cooled to -18 C and pyridine (54 µl, 0.053g, 0.67 mmol) added with stirring. The solution reached room temperature the mixture stirred overnight. The slow addition of diethylether (200ml) to the solution yielded an off-white precipitate that was collected by filtration. The precipitate was dissolved in warm methanol (10 ml) and diethylether (10 ml) slowly added resulting in an off-white precipitate which was collected by filtration and discarded. Diethylether (100

ml) was added to the remaining filtrate resulting in a white precipitate which was collectred by filtration. This procedure was repeated 3 times, the final bright white precipitate was collected by filtration, washed with diethylether (2 x 5 ml) and dried over phosphorus pentoxide. 0.065g, 23% yield.

^{1}H-NMR (400 MHz, CD_3OD): δ 8.68 (dd, 1H, $J_{(Pt-H)}$ = 21.6 Hz, $J_{(H-H)}$ = 5.4 Hz, H2'/H6'), 7.92 (t, 1H, J = 7.8 Hz, H4'), 7.43 (t, 1H, J = 7.0 Hz, H3'/H5').
^{195}Pt-NMR (65 MHz, CD_3OD): δ -2375.
IR: υ 3256m, 3187m, 3123m, 1655w, 1611m, 1586m, 1488w, 1456m, 1345s, 1305s, 1241m, 1213m, 1162m, 1124m, 1078m, 1049m, 1021m, 978m, 870m, 824m, 760s, 687s cm^{-1}.
Mass spectrum (ESI, +ve): m/z = 343 $[C_6H_{15}ClN_3Pt]^+$.
Elemental analysis: calculated for $C_5H_{11}ClN_4O_3Pt$; C, 14.8; H, 2.7; N, 13.8; Cl, 8.7 Found C, 15.00; H, 2.84; N, 13.79; Cl, 8.62.

3.3.15. Synthetic procedure for cis-[Pt(NH3)$_2$(ET-3-Py)Cl][NO$_3$]

To a solution of cis-diamminedichloroplatinum(II) (0.400 g, 1.14 mmol) in DMF (3 ml) was added silver nitrate (0.22 g, 1.13 mmol) in DMF (1 ml) and this mixture was stirred overnight in the absence of light. The silver chloride precipitate was removed by filtration leaving a pale yellow filtrate. To the filtrate was added 17α-pyridin-3-ylethynyl-testosterone (0.508 g, 0.1.14 mmol) and the solution stirred overnight. The slow addition of diethylether (200 ml) to the solution yielded a white precipitate which was filtered off. The crude product was dissolved in warm methanol (25 ml), decolourising charcoal (0.05 g) was added and the resulting suspension stirred for 5 minutes. The charcoal was collected by filtration through celite and discarded. The filtrate was reduced *in vacuo* to ca. 10 ml and the addition of diethylether (15 ml) resulted in a small amount of yellow precipitate which collected by filtration and discarded. Diethylether (100 ml) was added to the remaining filtrate resulting in a white precipitate and this was collected by filtration and procedure repeated twice. The final precipitate, after collection by filtration was washed with diethylether (2 x 5 ml) and dried over phosphorus pentoxide. 0.110 g, 12% yield.

^{1}H-NMR (300 MHz, CD_3OD): δ 8.74 (s, 1H, H2'), 8.62 (d, 1H, J = 5.6 Hz, H6'), 7.93 (d, 1H, J = 8.3 Hz, H4'), 7.41 (dd, 1H, J = 7.8, 6.2 Hz, H5'), 5.65 (s, 1H, H4), 4.57 (s, 1H, 17β-OH), 1.20 (s, 1H, steroid), 2.51-1.30 (m, 20H, steroid), 1.20 (s, 3H, Me19), 1.05-0.95 (m, 5H, steroid).
^{195}Pt-NMR (65 MHz, CD_3OD) : δ -2280 ppm.

IR: υ 3281m, 2940m, 1644m, 1357s, 1293m, 1233m, 1124m, 1048m, 927m, 869m, 834m, 807m, 691m cm^{-1}.

Mass spectrum (ESI, +ve): 654 $[Pt(NH_3)_2(ET\text{-}3\text{-}Py)Cl]^+$.

Elemental analysis: calculated for $C_{26}H_{37}ClN_4O_5Pt$; C, 43.6; H, 5.2; N, 7.8; Cl, 5.0. Found C, 43.28; H, 5.22; N, 7.82; Cl, 5.15

3.3.16. Synthetic procedure for cis-[Pt(NH3)$_2$(ET-4-IQ)Cl][NO$_3$]

To a solution of cis-diamminedichloroplatinum(II) (0.20 g, 0.67 mmol) in DMF (1 ml) was added a silver nitrate (0.11 g, 0.65 mmol) in DMF (1 ml) and the mixture stirred overnight in the absence of light. The silver chloride precipitate was removed by filtration through celite. The pale yellow filtrate was cooled to -18°C and 17α-isoquinolin-4-ylethynyl-testosterone (0.254 g, 0.653 mmol) added with stirring. The solution reached room temperature and the mixture stirred overnight. The slow addition of diethylether (200ml) yielded a yellow precipitate which was collected by filtration. This was dissolved in methanol (15 ml) and the suspension immediately filtered and the white / yellow solid discarded. The addition of diethylether (10 ml) to the methanolic solution resulted in a small amount of yellow precipitate which was collected by filtration and discarded. Diethylether (100 ml) was added to the filtrate and the precipitate collected by filtration. The solid was dissolved in warm methanol (15 ml) and diethylether was added (150 ml) resulting in a white precipitate which was collected by filtration and the procedure repeated twice. The solid was then dissolved in methanol (50 ml) and decolourising charcoal (0.5 g) was added and the suspension stirred for 35 minutes. Charcoal was removed by filtration through celite and discarded. The colourless solution was reduced *in vacuo* to ca. 15 ml and the addition of diethylether (10 ml) caused a yellow precipitate which, after collection by filtration was discarded. Addition of diethylether (200 ml) to the filtrate caused white precipitate which was collected by filtration, dissolved in methanol (20 ml) and the solution filtered through celite. To the filtrate was added diethylether (100 ml) and the white precipitate was collected by filtration and dried over phosphorus pentoxide. 0.85 g, 27 % yield.

^{1}H-NMR (300 MHz, CD_3OD): δ 9.45 (s, 1H, H2'), 8.65 (s, 1H, H10'), 8.29 (d, 1H, J = 8.4 Hz, H8'), 8.18 (d, 1H, J = 8.2 Hz, H5'), 7.99 (ddd, 1H, J = 1.2 Hz, J = 7.0 Hz, J = 8.3 Hz, H7'), 7.82 (ddd, 1H, J = 1.0 Hz, 7.1 Hz, 8.1 Hz, H6'), 5.66 (s, 1H, H4), 2.60-1.40 (m, 18H, steroid), 1.23 (s, 3H, 1.22 (s, 3H).

^{195}Pt-NMR (65 MHz, CD_3OD): δ -2283 ppm.

IR: υ 3284m, 2939m, 2875m, 1646m (C=O str), 1329m, 1233m, 1161m, 1127m, 1068m, 1043s, 960s, 907s, 872s, 834m, 780m, 754m cm^{-1}.

Elemental analysis: calculated for $C_{30}H_{39}ClN_4O_5Pt$; C, 47.0; H, 5.1; N, 7.3; Cl, 4.6. Found C, 46.68; H, 5.21; N, 7.58; Cl, 4.76.

3.3.17. Synthetic procedure for cis-[Pt(NH3)$_2$(ET-6-Q)Cl][NO$_3$]

To a solution of cis-diamminedichloroplatinum(II) (0.20 g, 0.67 mmol) in DMF (1 ml) was added a silver nitrate (0.11 g, 0.65 mmol) in DMF (1 ml) and the mixture stirred overnight in the absence of light. The silver chloride precipitate was removed by filtration through celite resulting in a pale yellow filtrate. The filtrate was cooled to -18°C and 17α-quinolin-6-ylethynyl-testosterone (0.254 g, 0.65 mmol) added with stirring. The solution reached room temperature and the mixture stirred overnight. The slow addition of diethylether (200ml) yielded a yellow precipitate which was collected by filtration. This was dissolved in methanol (15 ml) and immediately filtered through celite. The addition of diethylether (10 ml) to the methanolic solution resulted in a small amount of yellow precipitate which was discarded after being collected by filtration. Diethylether (100 ml) was added to the remaining filtrate resulting in a white precipitate which was collected by filtration. The solid was dissolved in warm methanol (15 ml) and diethylether added (150 ml) resulting in a white precipitate which collected by filtration and this procedure repeated twice. The precipitate was collected by filtrationd, dissolved in methanol (50 ml) and decolourising charcoal (1.0 g) added. The suspension stirred was for 45 minutes and decoloursing charcoal removed by filtration through celite and discarded. The colourless solution was reduced *in vacuo* to ca. 15 ml and the addition of diethylether (10 ml) caused a yellow precipitate which was collected by filtration and discarded. Addition of diethylether (200 ml) to the filtrate caused white precipitate which was collected by filtration, re-dissolved in methanol (20 ml) and filtered again through celite. To the filtrate was added diethylether (100 ml) and the white precipitate was collected by filtration and dried over phosphorus pentoxide. 0.72 g, 24 % yield.

^{1}H-NMR (300 MHz, CD_3OD): δ 9.53 (d, 1H, J = 9.0 Hz, H9'), 9.20 (dd, 1H, J = 1.2Hz, J = 5.2 Hz, H2'), 8.47 (d, 1H, J = 8.2 Hz, H4'), 8.06 (d, 1H, J = 1.3 Hz, H6'), 7.89 (dd, 1H, J = 1.8 Hz, 8.9 Hz, H8'), 7.54 (dd, 1H, J = 5.3 Hz, 8.5 Hz, H3'), 5.65 (s, 1H, H4), 2.54-1.30 (m, 18H, steroid), 1.21 (s, 3H, Me19), 1.10-0.85 (5H).

IR: υ 3284m, 2939m, 2876m, 1646m, 1329m, 1233m, 1161m, 1127m, 1043s, 960s, 906s, 872s, 779m, 754m cm^{-1}.

Mass spectrum (ESI, +ve): m/z = 704 $[Pt(NH_3)_2(ET\text{-}6\text{-}Q)Cl]^+$.

Elemental analysis: calculated for $C_{30}H_{39}ClN_4O_5Pt$; C, 47.0; H, 5.1; N, 7.3; Cl, 4.6. Found C, 46.61; H, 5.01; N, 7.36; Cl, 4.82.

3.3.18. Synthetic procedure for trans-Pt(Py)(DMSO)Cl_2

A suspension of cis-bis(dimethylsulphoxide)dichloroplatinum(II) (0.350 g, 0.83 mmol) in methanol (20 ml) was stirred for 10 minutes. Pyridine (67 µl, 0.065 g, 0.83 mmol) was added via a microsyringe and stirring continued for 8 hours. The resulting suspension was reduced *in vacuo* to ca. 2 ml and diethylether (50 ml) added. The precipitate was collected by filtration, washed with methanol (2 x 5 ml) and diethylether (3 x 5 ml), resulting in a bright yellow solid, 0.33 g, 95 % yield.

^{1}H-NMR (400 MHz, $CDCl_3$): δ 8.79 (ddd, 2H, $J_{(Pt-H)}$ = 20.3 Hz, $J_{(H-H)}$ = 6.6, 1.5 Hz, H2'/H6'), 7.88 (tt, 1H, J = 7.7, 1.5 Hz, H4'), 7.41 (ddd, 2H, J = 7.7, 5.2, 1.4 Hz, H3'/H5'), 3.52 (d, 6H, $J_{(Pt-H)}$ = 11.9 Hz).
^{195}Pt-NMR (65 MHz, CD_3OD): δ -2902 ppm
IR: υ 2995w (C-H str), 2913w (C-H str), 1609m, 1483w, 1447m, 1422wm 1402w, 1349w, 1317w, 1240w, 1211w, 1150s (S=O str), 1072m, 1028m, 981m, 944m, 924m, 765s, 734m, 691s cm^{-1}.
Elemental analysis: calculated for $C_7H_{11}Cl_2NOPtS$; C, 19.9; H, 2.6; N, 3.3; Cl, 16.8. Found C, 19.89; H, 2.60; N, 3.25; Cl, 16.85.

3.3.19. Synthetic procedure for trans-Pt(Quinoline)(DMSO)Cl_2

A suspension of cis-bis(dimethylsulphoxide)dichloroplatinum(II) (0.350 g, 0.83 mmol) in methanol (20 ml) was stirred for 10 minutes. Quinoline (98µl, 0.107g, 0.83 mmol) was added via a microsyringe and stirring continued overnight. The resulting yellow suspension was reduced *in vacuo* to ca 10 ml and diethylether (50 ml) added. The precipitate was collected by filtration, washed with ethanol (2 x 10 ml) and diethylether (2 x 10 ml) resulting in a bright yellow solid. 0.38 g, 98 % yield.

^{1}H-NMR (400 MHz, $CDCl_3$): δ 9.33 (dd, 1H, $J_{(Pt-H)}$ = 15.2 , 8.8 Hz, H9'), 9.01 (dd, 1H, J = 5.3, 1.5 Hz, H2'), 8.31 (d, 1H, J = 8.2 Hz, H4'), 7.87 (m, 2H, H8'/H6'), 7.64 (ddd, 1H, J = 8.1, 7.0, 1.4 Hz, H3'), 7.48 (dd, 1H, J = 8.3, 5.3 Hz, H7'), 3.45 (d, 6H, $J_{(Pt-H)}$ = 8.8 Hz) DMSO methyls).
^{195}Pt-NMR (65 MHz, $CDCl_3$): δ -3035.
IR: υ 3057w (C-H str), 2997w (C-H str), 2915w (C-H str), 1588m, 1507m, 1459m, 1437m, 1411m, 1393m, 1379m, 1311m, 1232m, 1210m, 1150m, 1132s (S=O str), 1124s (S=O).

1061m, 1016s, 977m, 956m, 933m, 913m, 868m, 811s (C-H oop), 779s (C-H oop), 739s (C-S str), 698 (C-S str) cm^{-1}.

Mass spectrum (ESI, +ve): *m/z* = 474 $[H(Pt(Quin)(DMSO)Cl_2]^+$

3.3.20. Synthetic procedure for trans-Pt(ET-2-Py)(DMSO)Cl_2

To a stirring suspension of cis-bis(dimethylsulphoxide)dichloroplatinum(II) (0.5 g, 1.18 mmol) in methanol was added, in 10 portions, solid 17α-pyridin-2-ylethynyl-testosterone (0.5 g, 1.13 mmol) over an 8 hr period. Stirring was continued for a further 24hrs resulting in a bright yellow precipitate which was collected by filtration. The product was purified on a 1 m long silica column, using dichloromethane : methanol, 98:2 as eluent and the first half of the single yellow band was collected, 0.635 g 72 % yield.

^{1}H-NMR (300 MHz, $CDCl_3$): δ 8.53 (d, 1H, J = 5.1 Hz, H6') 7.79 (dt, 1H, J = 1.5 Hz, 7.8 Hz, H4') 7.55 (d, 1H, J = 7.9 Hz, H3') 7.38 (ddd, 1H, J = 7.4, 5.8, 1.4 Hz, H5') 5.72 (s, 1H, H4) 3.44 (s, 6H, DMSO-Methyls) 2.70-1.30 (m, 18H, steroid) 1.20 (s, 3H, Me19) 1.18-1.00 (m, 2H, steroid) 0.97 (s, 3H, Me18) ppm

^{13}C-NMR (101 MHz, $CDCl_3$): δ 199.6 (C3), 171.2 (C5), 152.2 (C6'), 144.3 (C2'), 138.9 (C4'), 129.1 (C3'), 124.6 (C5'), 123.8 (C4), 104.4, 80.3, 53.2, 50.4, 47.5, 43.5 (DMSO Methyls), 38.6, 38.4, 36.3, 35.6, 33.9, 33.1, 32.8, 31.4, 23.3, 20.8, 17.4 (Me19), 12.8 (Me18) ppm

^{195}Pt-NMR (64 MHz, $(CD_3)_2CO$): δ -3106.6

IR : υ 3428m(O-H), 2939m(C-H str), 2858m(C-H str), 2227m(C≡C str), 1657s(C=O str), 1615w, 1599m, 1562w, 1476s, 1450m, 1433m, 1418m, 1379m, 1358m, 1331m, 1292m, 1231m, 1187m, 1147s(S=O str), 1127s(S=O str), 1060m, 1023s(C=O bend), 972m, 948m, 919m, 889m, 866m, 839m, 840m, 821m, 747s(C-H oop), 694m, 679m, 665m cm^{-1}

ESI-MS m/z = 734.5 $[H(Pt(ET\text{-}2\text{-}Py)(DMSO)Cl_2)]^+$

3.3.21. Synthetic procedure for trans-Pt(ET-3-Q)(DMSO)Cl_2

A suspension of cis-bis(dimethylsulphoxide)dichloroplatinum(II) (0.500g, 1.18 mmol) in methanol (20 ml) was stirred for 10 minutes before ET-3-Q (0.520 g, 1.18 mmol) was added and stirred for 24 hours resulting in a yellow suspension. The yellow solid was collected by filtration and purified on a silica column (eluent dichloromethane : methanol 98:2) collecting the first half of the single yellow band, 0.575 g, 62 % yield.

^{1}H-NMR (400 MHz, $CDCl_3$): δ 9.30 (d, 1H, J = 8.7 Hz, H9'), 9.05 (d, 1H, J = 1.8 Hz, H2'), 8.31 (d, 1H, J = 1.4 Hz, H4'), 7.86 (ddd, 1H, J = 8.6, 7.0 Hz, H8'), 7.77 (d, 1H, J = 8.2 Hz, H6'), 7.62 (t, 1H, J = 7.5 Hz, H7'), 5.71 (s, 1H, H4'), 3.05 (s, 6H, DMSO methyls),

2.47-1.36 (m, 18H, steroid), 1.18 (s, 3H, Me19), 1.16-1.02 (m, 2H, steroid), 0.94 (s, 3H, Me18).

^{13}C-NMR (124 MHz, $CDCl_3$): δ 200.0 (C3), 171.5 (C5), 155.9 (C2'), 145.0 (C10), 142.3 (C4'), 132.6 (C8'), 129.4 (C7'), 128.9 (C9'), 128.4 (C6'), 124.4 (C4), 118.6, 98.8, 81.2, 80.7, 53.5, 50.8, 47.7, 44.3 (DMSO Methyls), 39.5, 39.1, 36.7, 36.0, 34.4, 33.4, 33.2, 31.8, 23.7, 21.1, 17.8 (C19), 13.3 (C18).

^{195}Pt-NMR (65 MHz, $CDCl_3$): δ -3042.

IR: 2940m (C-H str), 2858m (C-H str), 2226w (C≡C str), 1707m, 1660s (C=O str), 1615m, 1570w, 1497m, 1450m, 1434m, 1416m, 1361m, 1294m, 1273m, 1231m, 1222m, 1146s (S=O str), 1057m, 1023s, 965m, 947m, 915m, 865m, 839m, 802m, 778s, 751s, 734m, 694m, 677m cm^{-1}.

Mass spectrum (ESI, +ve): m/z = 785 [H(Pt(ET-3-Q)(DMSO)Cl_2)].

Elemental analysis: calculated for $C_{33}H_{39}Cl_2NO_3PtCl$; C, 49.0; H, 5.0; N, 1.8; Cl, 9.0. Found C, 49.22; H, 4.99; N, 1.78; Cl, 9.21.

3.3.22. Synthetic procedure for cis-diamminediiodoplatinum(II)

According to the procedure of Dhara,[524] potassium iodide (5 g, 30 mmol) was added to potassium tetrachloroplatinate(II) (2.75 g, 6.60 mmol) in water (50 ml) resulting in a change from light red to dark red solution almost instantanously and was stirred for 30 minutes. Ammonium hydroxide as a 25 % solution (1.03 ml, 13.26 mmol) was added over a period of 10 minutes with stirring which continued for a further 30 minutes resulting in a dark yellow / brown precipitate which was collected by filtration, washed with ice cold water (2 x 10 ml), ethanol (2 x 10 ml) and diethylether (10 ml) and air dried. 3.15 g, 99 % yield.

IR: υ 3274m (N-H str), 3212m (N-H str), 3166m (N-H str), 1594m (N-H def), 1514m (N-H def), 1288s (N-H def), 1271s(N-H def), 752s (N-H def) cm^{-1}.

Elemental analysis: calculated for for $PtN_2H_6I_2$; H, 1.3; N, 5.8; I, 52.6. Found H, 1.10; N, 5.53; I, 52.48.

3.3.23. Synthetic procedure for cis-diamminedichloroplatinum(II)

Following the procedure of Dhara,[524] to a suspension of *cis*-diamminediiodoplatinum(II) (2 g, 4.15 mmol) in water (50 ml) was added silver nitrate (1.376 g, 8.1 mmol) in water (10 ml) and the mixture stirred at 40°C for 48 hours in the absence of light resulting in a yellow suspension and a clear solution. Silver iodide was removed by filtration through celite. Potassium chloride (0.340 g, 4.57 mmol) was added and dissolved with brief stirring. The solution was left to stand at room temperature for 24 hrs in the dark and

bright yellow crystals formed. The mixture was cooled to 0°C and the bright yellow / orange crystals collected by filtration, washed with ice-cold water (10 ml), ethanol (15 ml) and diethylether (15 ml) and air dried. 1.18g, 95% yield.

IR: υ 3284m (N-H str), 3204m (N-H str), 1623m (N-H def), 1539m (N-H def), 1317m (N-H def), 1293s (N-H def), 798s (N-H def) cm^{-1}.
Elemental analysis: calculated for $PtN_2H_6Cl_2$; H, 2.0; N, 9.3; Cl, 23.6. Found H, 2.10; N, 9.36; Cl, 23.62.

3.3.24. Synthetic procedure for trans-diamminedichloroplatinum(II)

Following the reaction scheme of Kauffman and Cowan,[525] a solution of potassium tetrachloroplatinate(II) (2 g, 4.82 mmol) in water (40 ml) was acidified with concentrated hydrochloric acid (1.25 ml) and heated to boiling in a large diameter vessel. 6 M aqueous ammonia (1.5ml) was added dropwise immediately above the boiling solution in aliquots (0.2 ml) allowing 10 minutes between each addition whilst continuing heating and topping up with water to maintain 40 ml volume. A further portion of 6 M aqueous ammonia (13.5ml) was added dropwise over a period of 30 minutes with continued boiling for 2 hours. The mixture was kept to 40 ml volume by the addition of water. Faster addition of ammonia led to precipitation of $[Pt(NH_3)_4][PtCl_4]$ (Magnus Green salt) as a green precipitate. The resulting clear colourless solution was evaporated to ca. 20 ml and 6 M hydrochloric acid (200ml) was added and the solution boiled and reduced to 15 ml – 20 ml whereas a fine yellow power is deposited. The solution was refrigerated overnight and a fine yellow power was collected by filteration, washed with ice-cold water (2 x 10 ml), ethanol (15 ml) and diethylether (15 ml). A further crop was obtained by adding 6 M hydrochloric acid (200 ml) to the filtrate and boiling until reduced to ca. 20 ml and cooled until a fine yellow deposited. The compound was recrystallised from 0.1 M hydrochloric acid. 1.16g, 80% yield.

IR: υ 3287m (N-H str), 3203m (N-H str), 1634m (N-H def), 1544m (N-H def), 1289s (N-H def), 810s (N-H def) cm^{-1}.
Elemental analysis: calculated for $PtN_2H_6Cl_2$; H, 2.0; N, 9.3; Cl, 23.6. Found H, 1.83; N, 9.13; Cl, 23.83.

3.3.25. Synthetic procedure for cis-bis(dimethylsulphoxide)dichloroplatinum(II)

Following the synthesis of Wayland *et al*[526], dimethylsulphoxide (1.142 g, 14.46 mmol) in water (5 ml) was added to a solution of potassium tetrachloroplatinate(II) (2 g, 4.82 mmol) in water (5 ml) and the mixture allowed to stand. Over a period of an hour the red solution

becomes clear and overnight fine yellow needle-like crystals form. The material was collected by filtration, washed with ice cold water (2 x 10 ml), ethanol (10 ml) and diethylether (10 ml) and air dried. 0.8275 g, 81 % yield.

^{1}H-NMR (400 MHz, $CDCl_3$): δ3.52 (s, 12H) $^{3}J_{Pt-H}$ = 21.6 Hz

IR: υ 3037m (C-H str), 3010m (C-H str), 2990m (C-H str), 2926m (C-H str), 2917m (C-H str), 2906m (C-H str), 1412m, 1400m, 1384m, 1315m, 1305m, 1299m, 1250m, 1154s (S=O str), 1131s (S=O str), 1018s, 982m, 941m, 920m, 736m, 690m cm^{-1}.

Elemental analysis: calculated for $C_4H_{12}Cl_2O_2PtS_2$; C, 11.4; H, 2.9; Cl, 16.8; S, 15.2. Found C, 11.29; H, 2.76; Cl, 17.03; S, 15.10.

3.4. Attempted syntheses

3.4.1. Attempted synthesis of cis and trans-[Pt(NH3)$_2$(Isoquinoline)Cl][NO$_3$]

The synthetic method is identical to that of trans-[$Pt(NH_3)_2$(Quinoline)Cl][NO_3] using transplatin to produce trans complexes and cisplatin to produce *cis* complexes. The reaction produced mixtures of cis- and trans-[$Pt(NH_3)_2$(Isoquinoline)Cl]$^{+}$ and [$Pt(NH_3)$(Isoquinoline)$_2$]$^{2+}$ that could not be purified to obtain the desired product.

3.4.2. Attempted synthesis of cis-[Pt(NH3)$_2$(Quinoline)Cl][NO$_3$]

The synthetic method is identical to that of trans-[$Pt(NH_3)_2$(Quinoline)Cl][NO_3] using cisplatin instead of transplatin as the intial starting material. Despite many different solvent combinations the products stubbornly remained as an oil and could not be seperated as a solid.

3.4.3. Attempted synthesis of cis and trans-[Pt(NH3)$_2$(ET-2-Py)Cl][NO$_3$]

Following the synthetic method of trans-[$Pt(NH_3)_2$(ET-3-Py) the compounds identified at the end were the platinum starting material (cisplatin or transplatin) and the ligand ET-2-Py. No binding of ET-2-Py to platinum was evident

3.4.4. Attempted synthesis of cis-[Pt(NH3)$_2$(ET-4-Py)Cl][NO$_3$]

Following the synthetic method of trans-[$Pt(NH_3)_2$(ET-3-Py) the product turned from white to grey upon attempting to isolate using filtration.

3.4.5. Attempted synthesis of cis-[Pt(NH3)$_2$(ET-3-Q)Cl][NO$_3$]

Following the synthetic method of trans-[$Pt(NH_3)_2$(ET-3-Py) the product turned from white to grey upon attempting to isolate using suction filtration.

3.4.6. Attempted synthesis of trans-Pt(ET-4-IQ)(DMSO)Cl$_2$

Following the synthetic method of trans-[Pt(ET-3-Q)(DMSO)Cl$_2$ the reaction product was contaminated with trans-[Pt(ET-4-IQ)$_2$Cl$_2$] and the desired product could not be isolated.

3.4.7. Attempted Sonogashira reactions to produce TC, CC, TN and CN complexes

Attempts were made to react the TC, CC, TN and CN complexes with 3-bromopyridine as a ligand with ligands L_1 - L_6 under varied Sonogashira conditions using potassium carbonate as a base. All solvents used were anhydrous and included tetrahydrofuran, acetone, chloroform, DMF and DMA. Catalyst loading varied from 4 mole % to 50 mole %. No coupling was observed in all cases.

3.4.8. Conclusions

A range of 6 ligands combining a steroidal domain and linker domain have been synthesised by the Sonogashira palladium cross-coupling reaction in good to high yields. All required simple purification techniques. The 6 ligands were designed to have affinity for the testosterone based on literature reports whilst also possessing a hetroatom (nitrogen) having a good affinity for platinum(II). In the platinum domain 5 different coordination spheres were proposed and 2 of these proved successful, leading to the possibility of 18 complexes to be synthesised. Despite synthetic problems and light-sensitivity issues a total of 11 platinum complexes were synthesised, including some containing pyridine or quinoline ligands as positive controls to compare to the steroidal counterparts. Complexes of the type trans-[Pt(L)(DMSO)Cl$_2$] where L is an aromatic amine were synthesised successfully but aqueous insolubility precluded biological testing. Aiming to increase solubility by a substitution reaction to synthesise [Pt(L)(L')(DMSO)Cl]$^+$ where L is pyridine or quinoline and L' ligand L_1 - L_6 proved elusive. Also proving elusive was the successful synthesis of trans- and cis-neutral complexes using very standard procedures which work well for ligands such as pyridine or quinoline but not for steroidal ligands. Attempts to use other methods, *i.e.* forming TN and CN complexes with 3-bromopyridine and then substituting the bromine for an ethnynyltestosterone via Sonogashira coupling also proved unsuccessful. Despite this, should the complexes have been synthesised they would be electrically neutral with a large hydrophobic ligand. These two characteristics are likely to have made the complex unattractive from a clinical point of view due to the likely poorly water solubility. The complexes likely relatively high lipophilicity would be too high for tissue selective uptake.

Despite the synthetic challenges, two ranges of complex have been synthesised, trans- and cis-cationic with a variety of steroidal ligands and those containing pyridine or quinoline, to act as positive controls.

Chapter Four – Hydrolysis and binding to nucleo bases

4.1. Introduction

Steroidal metal complexes reported herin have been designed specifically for ultimate use *in vivo* which involves an aqueous environment of pH 7.4 and a temperature of 37°C. The *in vivo* behaviour of the clinical platinum(II) drugs is very important; hydrolysis is required for the complexes to develop its clinical potency. Determining the *in vivo* behaviour of cisplatin for example, presents several difficulties that are overcome employing a simplified system. Such systems model the interaction between DNA and a platinum(II) complex, in well defined conditions, using model nucleobases representing DNA. This chapter reports and discusses the behaviour of steroidal platinum(II) complexes in aqueous solution and any interaction occuring between complex and DNA base.

4.1.1. Hydrolysis of platinum(II) complexes

Platinum(II) complexes frequently undergo solvolysis reactions and their behaviour in aqueous solution has been thoroughly investigated. The $[PtCl_4]^{2-}$ ion undergoes reversible hydrolysis in aqueous acid, water and dilute aqueous NaCl, forming $[PtCl_3(H_2O)]^-$ and $[PtCl_2(H_2O)_2]$.[527] The complex $[Pt(NH_3)Cl_3]^-$ forms $[Pt(NH_3)Cl_2(H_2O)]$ and $[Pt(NH_3)Cl(H_2O)_2]^+$ in aqueous solution;[528, 529] these may be separated using electrophoresis and ion-exchange and monitored using uv-visible spectrophotometry and pH changes. The rate of hydrolysis of cisplatin has been measured using several different techniques including UV / vis. spectrophotometry,[530-535] ion-exchange,[530] HPLC,[536] TLC,[537] eletrophoresis[537] and ^{195}Pt NMR;[530-535, 537] the hydrolysis of newer drugs such as carboplatin have also been researched.[538] The main products depend on pH and $[Cl^-]$ but under physiological conditions are cis-$[Pt(NH_3)(OH_2)Cl]^+$ and cis-$[Pt(NH_3)_2(OH)(Cl)]$.[539]

The pK_a of a H_2O molecule is decreased on bonding to a platinum(II) centre; this favours the formation of hydroxide complexes which may dimerise to form hydroxide-bridged di-nuclear species and even higher order oligomers, whose structures have been investigated using X-ray diffraction.[540, 541] The literature is quite clear: Pt-Cl bonds are labile in the aqueous environment.

4.1.2. Hydrolysis of cisplatin

Dissolving $Pt(en)Cl_2$ (similar to cisplatin) in aqueous solution produces several species as the chloride ions are displaced by water molecules as shown in Table 4.1.

Table 4.1. The approximate relative amounts of hydrolysed species in aqueous solutions of $Pt(en)Cl_2$ where $[Pt(en)(H_2O)Cl]^+ = 100$, as a function of chloride concentration.[542]

Complex	Relative amount in ~ 100 mM chloride	Relative amount in ~ 4 mM chloride
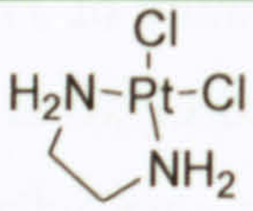	373	145
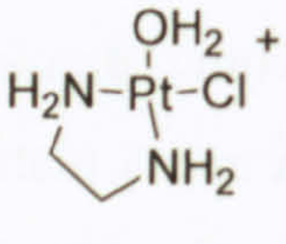	100	100
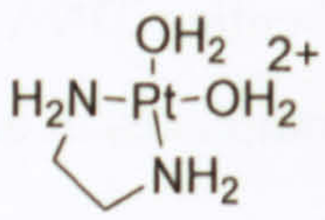	0.1	3.5
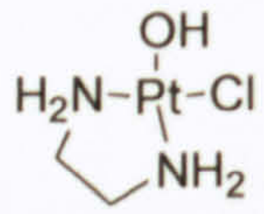	100	100
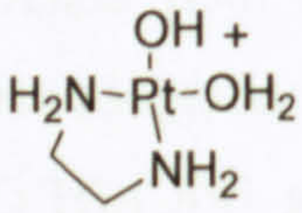	0.5	138
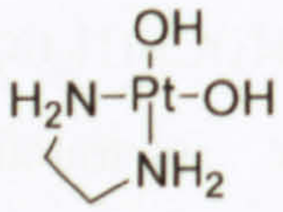	0.3	86

The close relationship between cisplatin and $Pt(en)Cl_2$, suggests results for $Pt(en)Cl_2$ are representative of cisplatin at intracellular and intercellular chloride concentrations. In acidic media – pH ~5 – the formation of hydroxide products is disfavoured and primarily cis-$[Pt(NH_3)_2Cl(H_2O)]^+$ is produced, in a reversible reaction, with very small amount of cis-$[Pt(NH_3)_2(H_2O)_2]^{2+}$ present. The opposite pH range – pH ~9 – results in irreversible hydrolysis to relatively inert cis-$[Pt(NH_3)_2(OH)_2]$, although acidification results in protonation of the hydroxide forming a labile complex.[531]

The most important pH from a biological viewpoint is pH 7.4; in this environment of 100mM chloride, hydrolysis of cisplatin occurs with a half life of approximately 1 hour and an equilibrium of cis-$[Pt(NH_3)_2Cl_2]$, cis-$[Pt(NH_3)_2Cl(H_2O)^+]$ and cis-$[Pt(NH_3)_2(OH)(H_2O)^+]$ exists in 50:20:30 ratios; in the low Cl^- environment of intercellular space, cis-$[Pt(NH_3)_2Cl(H_2O)^+]$ and cis-$[Pt(NH_3)_2(OH)(H_2O)^+]$ are the primary products, in approximately 50:50 ratio in rapid equilibrium with almost no cis-$Pt(NH_3)_2Cl_2$ remaining.[532]

4.1.3. Model systems to probe DNA binding of Pt(II) complexes

In the first instance DNA may be modelled by its components, the nucleobases guanine, adenine, cytosine and thymine. The purine base derivative 9-ethylguanine, shown in Figure 4.1 is modified in the 9 position where in DNA the ribose unit is connected and may be used as a model; guanosine 5'-monophosphate (5'-GMP) is also a model nucleobase, but unlike 9-ethylguanine it contains a ribose and phosphate group; however, 5'-GMP has a free phosphate group not found in DNA.

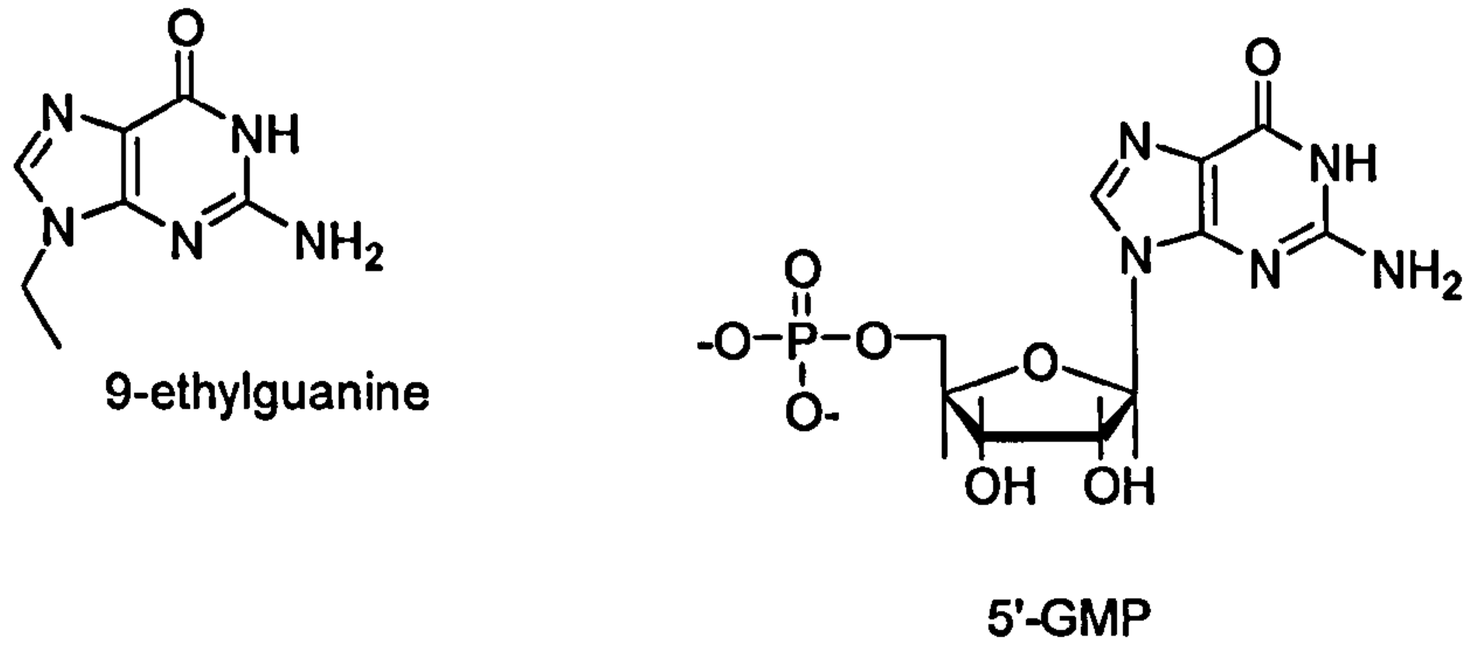

Figure 4.1. The structure of Hmgua and 5'-guanosine-monophosphate.

The benefits of using systems such as 9-ethylguanine and 5'-GMP as models for DNA bases is experimental simplicity, and the interaction between a complex and models for each individual model base (i.e., adenosine 5'-monophosphate, 5'AMP) can be used. The relatively low molecular weight and gram scale quantities available allow application of mass spectrometry and NMR techniques, in addition to UV / vis. spectrophotometry, to observe changes and identify the species involved.

4.2. Results

During characterisation charged platinum(II) complexes proved readily identifiable by ESI-mass spectrometry (ESI-MS); this justifies the use of ESI-MS for analysis of aqueous solutions of such complexes. All the results were collected using the materials and methods described in § 4.5.

4.2.1. Hydrolysis of non-steroidal platinum(II) complexes

A peak at *m/z* = 343 is observed when TC-Py and CC-Py are dissolved in water and incubated for 3 days at 37 °C; when exposed to the same conditions the spectrum of TC-Q displays a peak at *m/z* = *394*; these peaks correspond to those expected from the parent ions. In all three cases small peaks are observed *m/z* = 19 below that ascribed to the parent ion; these correspond to the places where it is expected the aqua or hydroxide complexes

would be found, if created. However, these addition peaks are small, indicating either little hydrolysis has occurred or the newly created complexes have poor sensitivity towards ESI mass spectrometry. A summary of the peaks found is presented in Table 4.2.

Table 4.2. Signals seen in the ESI-MS spectra of control platinum(II) complexes.

Complex	Peaks (*m/z*)	Peak identity	Appendix Figure
TC-Py	343.3	$[Pt(NH_3)_2(Py)Cl]^+$	A.7.1.
	324.2	$[Pt(NH_3)_2(Py)(OH)]^+$	A.7.1.
CC-Py	343.2	$[Pt(NH_3)_2(Py)Cl]^+$	A.7.2.
	324.2	$[Pt(NH_3)_2(Py)(OH)]^+$	A.7.2.
TC-Q	394.2	$[Pt(NH_3)_2(Quin)Cl]^+$	A.7.3.
	375.3	$[Pt(NH_3)_2(Quin)Cl]^+$	A.7.3.

4.2.2. Hydrolysis of TC steroidal platinum(II) complexes

After standing for three days in aqueous solution two sets of peaks may be identified from TC complexes in ESI-MS: those complexes containing a pyridine linker-ligand, *i.e.* TC-ET-3-Py, exhibit two sets of significant, large peaks; the first at $m/z = 654$ and the second at $m/z = 635$. The first corresponds to the parent complex and the second to $[Pt(NH_3)_2(L)(OH)]^+$ where L is a steroidal ligand. Those complexes with a quinoline or isoquinoline containing linker-ligand, *i.e.* TC-ET-3-Q, exhibit sets of peaks at $m/z = 704$ and $m/z = 685$. Like their pyridine-containing counterparts these peaks correspond to the parent complex and $[Pt(NH_3)_2(L)(OH)]^+$, where L is a steroidal ligand.

The pH of the solutions used for ESI-MS analysis were checked and found to be neutral indicating no acid-base chemistry is present. The direct attachment of OH^- to the platinum complex is therefore discounted. Substitution of chloride by water would result in the complex $[Pt(NH_3)_2(L)(OH_2)]^{2+}$, where L is a steroidal ligand; however no 2+ ions are observed. Given the tendency for lowering of the pKa of hydrogen atoms on co-ordinated water molecules, it is reasonable to suggest the parent complexes have had chlorides substituted by water with subsequent loss of H^+, as shown in Figure 4.2, using TC-ET-4-Py as an example. Table 4.3, below, shows the assignment of each peak observed.

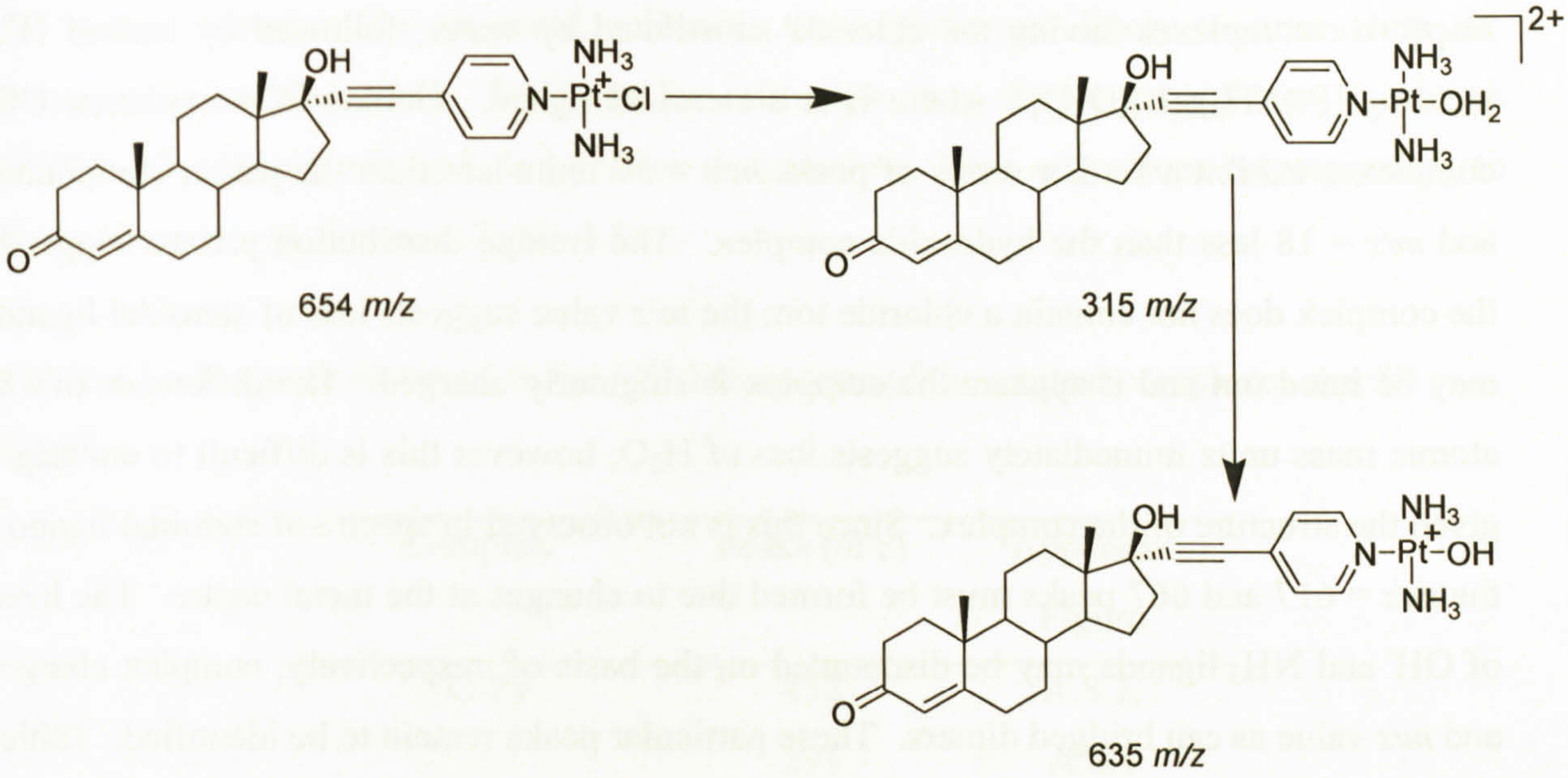

Figure 4.2. The hydrolysis of TC-ET-4-Py with expected *m/z* values.

Table 4.3. Summary of the findings in identifying species during the hydrolysis of TC complexes.

Complex	Peaks (*m/z*)	Peak identity	Appendix Figure
TC-ET-3-Py	654.2	$[Pt(NH_3)_2(ET\text{-}3\text{-}Py)Cl]^+$	A.7.4.
	635.3	$[Pt(NH_3)_2(ET\text{-}3\text{-}Py)(OH)]^+$	A.7.4.
TC-ET-4-Py	654.2	$[Pt(NH_3)_2(ET\text{-}4\text{-}Py)Cl]^+$	A.7.5.
	635.2	$[Pt(NH_3)_2(ET\text{-}4\text{-}Py)(OH)]^+$	A.7.5.
TC-ET-3-Q	704.2	$[Pt(NH_3)_2(ET\text{-}3\text{-}Q)Cl]^+$	A.7.6.
	685.3	$[Pt(NH_3)_2(ET\text{-}3\text{-}Q)(OH)]^+$	A.7.6.
TC-ET-4-IQ	704.2	$[Pt(NH_3)_2(ET\text{-}4\text{-}IQ)Cl]^+$	A.7.7.
	685.3	$[Pt(NH_3)_2(ET\text{-}4\text{-}IQ)(OH)]^+$	A.7.7.
TC-ET-6-Q	704.2	$[Pt(NH_3)_2(ET\text{-}6\text{-}Q)Cl]^+$	A.7.8.
	685.3	$[Pt(NH_3)_2(ET\text{-}6\text{-}Q)(OH)]^+$	A.7.8.

4.2.3. Hydrolysis of CC steroidal platinum(II) complexes

Three cis-cationic complexes (CC-ET-3-Py, CC-ET-4-IQ, CC-ET-6-Q) were analysed using ESI-MS to ascertain their behaviour in aqueous solution. The complex CC-ET-3-Py displays three significant peaks at *m/z* = 654, 635 and 617; the complexes CC-ET-4-IQ and CC-ET-6-Q display three significant peaks at *m/z* = 704, 685 and 667. The highest peaks, in similar fashion to TC complexes are assigned to the parent complex, $[Pt(NH_3)_2(L)Cl]^+$, where L is a steroidal ligand. The peaks at *m/z* = 685 and 635 may be assigned to

respective complexes having the chloride substituted by water; followed by loss of H^+, yielding $[Pt(NH_3)_2(L)(OH)]^+$, where L is a steroidal ligand. Unlike TC complexes, CC complexes exhibit a further series of peaks *m/z* = 37 units less than the parent compound and *m/z* = 18 less than the hydroxide complex. The isotope distribution pattern suggests the complex does not contain a chloride ion; the *m/z* value suggests loss of steroidal ligand may be ruled out and it appears the complex is singularly charged. The difference of 18 atomic mass units immediately suggests loss of H_2O; however this is difficult to envisage given the structure of the complex. Since this is not observed in spectra of steroidal ligand, the *m/z* = 617 and 667 peaks must be formed due to changes at the metal centre. The loss of OH^- and NH_3 ligands may be discounted on the basis of, respectively, complex charge and *m/z* value as can bridged dimers. These particular peaks remain to be identified. Table 4.4 contains a summary of the peaks found.

Table 4.4. A summary of the ESI-MS spectra of cis-cationic complexes.

Complex	Peaks (*m/z*)	Assignment	Appendix Figure
CC-ET-3-Py	654	$[Pt(NH_3)_2(ET\text{-}3\text{-}Py)(Cl)]^+$	A.7.9.
	635	$[Pt(NH_3)_2(ET\text{-}3\text{-}Py)(OH)]^+$	A.7.9.
	617		A.7.9.
CC-ET-4-IQ	704	$[Pt(NH_3)_2(ET\text{-}4\text{-}IQ)(Cl)]^+$	A.7.10.
	685	$[Pt(NH_3)_2(ET\text{-}4\text{-}IQ)(OH)]^+$	A.7.10.
	667		A.7.10.
CC-ET-6-Q	704	$[Pt(NH_3)_2(ET\text{-}6\text{-}Q)(Cl)]^+$	A.7.11.
	685	$[Pt(NH_3)_2(ET\text{-}6\text{-}Q)(OH)]^+$	A.7.11.
	667		A.7.11.

4.2.4. Binding of non-steroidal platinum(II) complexes to model nucleobases

The binding of TC-Py, CC-Py and TC-Q to 5'AMP, 5'-GMP, 5'-TMP and 5'-CMP was ascertained by ESI-MS (Figures A.8.1 – A.8.3); the complex and nucleobase were incubated for 72 hours at 37°C in the presence of TAE buffer as outlined in §4.5. No evidence of unreacted complex is present in the spectrum indicating the complexes have completely reacted. However, no peaks are present corresponding to those expected to arise from an interaction with nucleobases; this is a very surprising result given the affinity of nucleobases for platinum(II), further techniques such as NMR are required to fully investigate the interaction. In the case of TC-Py peaks at *m/z* = 452 and 291 are observed. In relation to the three complexes peaks at *m/z* ~ 110 higher and 52 lower than *m/z* value of

the parent complex are observed. Hence, these peaks are likely to arise from the complexes reacting with TAE buffer although no simple complexes, such as $[Pt(NH_3)(L)(OAc)]$, where L is pyridine or quinoline, have *m/z* values corresponding to those observed, as shown in Table 4.5.

Table 4.5. The peak observed in the ESI-MS spectra of the control complexes and 5'-GMP.

Complex	Peaks (*m/z*)	Appendix Figure
TC-Py	452	A.8.1.
	291	A.8.1
CC-Py	452	A.8.2.
	291	A.8.2.
TC-Q	504	A.8.3.
	321	A.8.3.

4.2.5. Binding of steroidal platinum(II) complexes to model nucleobases

Four model nucleobases, 5'-GMP, 5'-AMP, 5'-CMP and 5'-TMP were assessed in their ability to bind steroidal platinum(II) complexes as described in § 4.5. A summary of the results can be found in Table 4.6 and the spectra are contained in Figures A.8.4 – A.8.12. No signal is observed that may be interpreted as an interaction between the nucleobases 5'-TMP / 5'-CMP and platinum(II) complexed studied. Of particular note is that no sets of peaks corresponding to the parent complex are observed whilst those of the complex $[Pt(NH_3)_2(L)(OH)]^+$, where L is a steroidal ligand are clearly present. This indicates an interaction has occurred with the buffer.

When mixed with 5'-AMP the results were almost identical to that of 5'-TMP / 5'-CMP in that no peaks are observed corresponding to the steroidal platinum(II) complexes reacting with 5'-AMP. In a single case, a significant set of peaks at 964 *m/z* are observed when CC-ET-3-Py and 5'-AMP are mixed and incubated for 3 days. The peak at 964 *m/z* may be ascribed to an adduct formed between 5'-AMP and CC-ET-3-Py with the formula $H[Pt(NH_3)_2(ET\text{-}3\text{-}Py)(5'\text{-}AMP)]^+$. Other complexes apart from CC-ET-3-Py are capable of binding to 5'-AMP. The complexes, TC-ET-3-Q, TC-ET-3-Py and TC-ET-6-Q, when mixed with 5'-AMP produced peaks corresponding to $H[Pt(NH_3)_2(ET\text{-}3\text{-}Q)(5'\text{-}AMP)]^+$ (*m/z* = 1014), $H[Pt(NH_3)_2(ET\text{-}3\text{-}Py)(5'\text{-}AMP)]^+$ (*m/z* = 964) and $H[Pt(NH_3)_2(ET\text{-}6\text{-}Q)(5'\text{-}AMP)]^+$ (*m/z* = 1014), respectively; a high signal to noise ratio precluded definitive results.

The weak signals may indicate the three other complexes bind poorly to 5'-AMP or that once bound or the resulting adduct is not sensitive to ESI mass spectrometry.

Mixing 5'-GMP and steroidal complexes produced a large set of results: all steroidal complexes produced an adduct, $[Pt(NH_3)_2(L)(5'\text{-GMP})]$ as summerised in Table 4.6 and an example of which is shown in Figure 4.3. A set of peaks *m/z* = 16 units below those attributed to the adduct are currently unidentified.

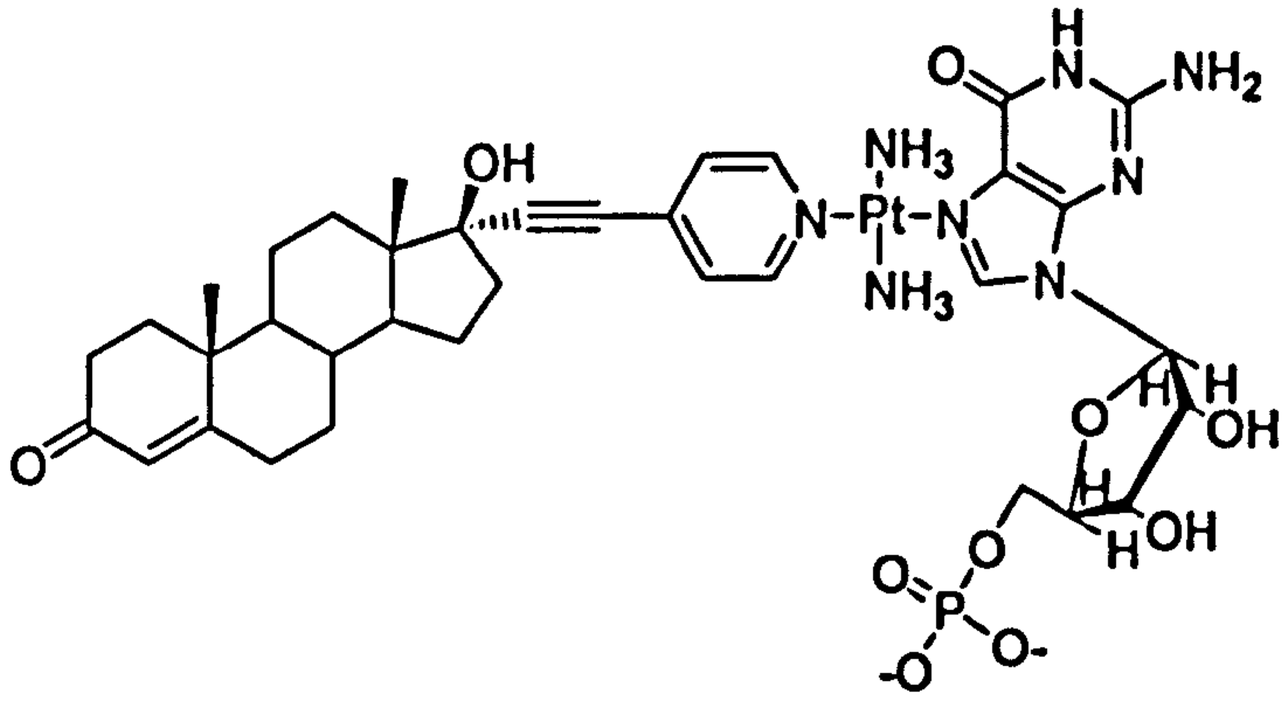

Figure 4.3. The adduct between TC-ET-4-Py and 5'-GMP

In addition to peaks from adducts, peaks corresponding to the parent complex are *not* observed in the spectra. It appears the hydrolysed complex remains in solution whilst the parent complex has reacted. Other peaks are observed at *m/z* ~ 110 and ~ 23 units above the parent complex are likely to rise from reactions of the complexes with buffer. The peak *m/z* ~ 23 units above the parent complex match the isotope distribution pattern of $[Pt(NH_3)_2(L)(OAc)]^+$, where L is a steroidal ligand and an example spectrum is shown in Figure A.8.7. The peaks *m/z* ~ 110 higher are as yet unassigned and do not correspond to a simple co-ordination of the buffer components (Tris, Acetate and EDTA) and complex. Similar peaks, *m/z* ~ 110 higher than the parent complex ion are observed in the case of TC-Py, CC-Py and TC-Q indicating steroidal complexes react slower with the buffer than those without steroid groups.

Table 4.6. Summary of the binding of complexes with model nucleobases.

Complex	Peaks (*m/z*)	Peak identity	Appendix Figure
TC-ET-3-Py + 5'-GMP	981.2	$[Pt(NH_3)_2(ET\text{-}3\text{-}Py)(5'\text{-}GMP]^+$	A.8.4.
	635.3	$[Pt(NH_3)_2(ET\text{-}3\text{-}Py)(OH)]^+$	A.8.4.
TC-ET-4-Py + 5'-GMP	981.3	$[Pt(NH_3)_2(ET\text{-}4\text{-}Py)(5'\text{-}GMP]^+$	A.8.5.
	635.2	$[Pt(NH_3)_2(ET\text{-}4\text{-}Py)(OH)]^+$	A.8.5.
TC-ET-3-Q + 5'-GMP	1030.2	$[Pt(NH_3)_2(ET\text{-}3\text{-}Q)(5'\text{-}GMP)]^+$	A.8.6.
	685.3	$[Pt(NH_3)_2(ET\text{-}3\text{-}Q)(OH)]^+$	A.8.6.
TC-ET-4-IQ + 5'GMP	1030.3	$[Pt(NH_3)_2(ET\text{-}4\text{-}IQ)(5'\text{-}GMP)]^+$	A.8.7.
	727.2	$[Pt(NH_3)_2(ET\text{-}4\text{-}IQ)(OAc)]^+$	A.8.7.
	685.3	$[Pt(NH_3)_2(ET\text{-}4\text{-}IQ)(OH)]^+$	A.8.7.
TC-ET-6-Q + 5'-GMP	704.2	$[Pt(NH_3)_2(ET\text{-}6\text{-}Q)Cl]^+$	A.8.8.
	685.3	$[Pt(NH_3)_2(ET\text{-}6\text{-}Q)(OH)]^+$	A.8.8.
CC-ET-3-Py + 5'GMP	981.2	$[Pt(NH_3)_2(ET\text{-}3\text{-}Py)(5'\text{-}GMP]^+$	A.8.9.
	635.3	$[Pt(NH_3)_2(ET\text{-}3\text{-}Py)(OH)]^+$	A.8.9.
CC-ET-3-Py + 5'-AMP	964.2	$[Pt(NH_3)_2(ET\text{-}3\text{-}Py)(5'\text{-}AMP]^+$	A.8.10.
	635.3	$[Pt(NH_3)_2(ET\text{-}3\text{-}Py)(OH)]^+$	A.8.10.
CC-ET-4-IQ	1030.3	$[Pt(NH_3)_2(ET\text{-}4\text{-}IQ)(5'\text{-}GMP)]^+$	A.8.11.
	685.3	$[Pt(NH_3)_2(ET\text{-}4\text{-}IQ)(OH)]^+$	A.8.11.
CC-ET-6-Q	1030.2	$[Pt(NH_3)_2(ET\text{-}6\text{-}Q)(5'\text{-}GMP)]^+$	A.8.12.

4.3. Discussion

The relative lability of Pt-Cl bonds, seen so often in the literature, is apparent for all the complexes; all form primarily one species when exposed to aqueous solution, a peak 19 amu below that of the original complex and assigned to an hydroxyl-species. This species may be formed by the technique used to analyse the behaviour of the complexes, rather than be actually present in solution, as solutions of all the complexes remain pH neutral.

Interestingly CC complexes exhibit an additional signal – as yet unidentified – that suggests these complexes are less stable than their trans counterparts; this adds additional evidence to that found in Chapter Three, that TC complexes are more stable than their cis counterparts. Information regarding the kinetics of hydrolysis was not investigated, but the endpoint remains clear: the complexes behave in a similar manner in that they all hydrolyse.

The mixing with nucleobases gave several important pieces of information: firstly, all the steroidal platinum complexes bind to 5'-GMP, some bind to 5'-AMP and, none bind to 5'-TMP and 5'-CMP. This appears in-line with that expected from the literature[132, 133] but it is reasonable to suggest, given no evidence of an interaction between, say TC-Py and 5'GMP, that some of the complexes may not be so sensitive to detection using ESI-MS. Secondly, the complexes react with the buffer used as shown by the observation of peaks in the same position relative to the parent compound; and thirdly, when mixed with a buffered solution of nucleobase, the parent ion peak is not observed, *as if all had reacted.* The second point is unsurprising; TAE contains several nucleophiles both capable and likely to react with a platinum(II) centre; one is identified, resulting from the acetate substitution of either chloride or water ligand. One other, ~ 110 *m/z* above the parent complex also arises from an interaction between buffer and complex. In the case of the non-steroidal complexes, the reaction with the buffer is total, no parent ion peaks are not observed and given literature reports that TC-Py and TC-Q react with 5'-GMP and 9-ethylguanine in *cacodylate buffer.*[543] This suggests the reaction with buffer is inhibited in complexes containing the steroid skeleton, as the corresponding peaks (~ 110 *m/z* higher) are seen alongside those complexes bound to the nucleobases, indicating reduced kinetics at the platinum(II) centre due to the presence of the steroid. One of the design briefs – to design complexes that possibly have reduced ability to react with sulphur-containing bio-molecules – may have been fulfilled.

The third point is crucial, it suggests that upon exposure to nucleophiles – those present in the buffer, nucleobase or both – the species primarily reacting is the parent complex and *not* the hydrolysed product, which remains in solution. Substitution at 4-coordinate metal sites can take two pathways: direct substitution by the nucleophile or via a solvento species; here the data suggests the first pathway, very much more than the latter, is in operation. Figure 4.4 illustrates the two pathways.

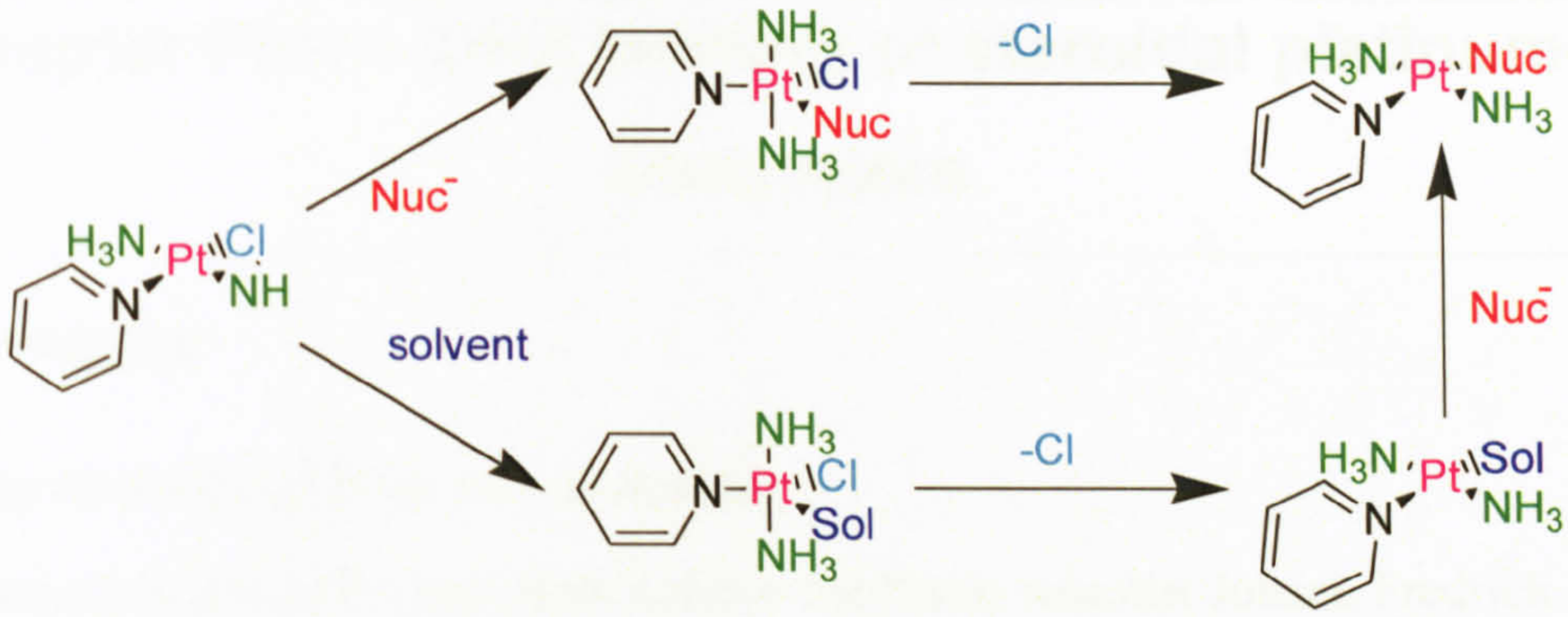

Figure 4.4. The pathways of the nucleophilic substitution reactions at square planar complexes.

It appears the triammine complexes studied, whether containing a steroid or not, proceed *primarily* via direct nucleophilic substitution; this is not unsurprising given the two path system has been identified for platinum(II) complexes containing one leaving group and three inert nitrogen-containing ligands[544-546] and, that direct substitution is thought the pathway these types of compounds take in nucleophilic reactions.[547, 548]

4.4. Conclusion

Using ESI mass spectrometry it is shown that the Pt-Cl bond in cis- and trans-$[Pt(NH_3)(L)(Cl]^+$ is labile in nearly all cases. It is clear the complexes react with the model nucleobase 5'-GMP; although only some appear to react with 5'-AMP; and none react with 5'-TMP or 5'-CMP. Hydrolysis appears to be unnecessary for the complexes to bind to model nucleobases: here direct substitution of a Pt-Cl bond by the incoming nucleophile – likely the N^7 of guanine for example – occurs, leaving only hydrolysed complex in solution. The complexes are shown to react with the buffer medium, a reaction which shows the addition of a steroidal skeleton to the coordinating aromatic amine reduces the rate of substitution at platinum(II) centres, very likely due to steric factors.

4.5. Materials and Methods

5'-GMP was obtained from Sigma (Poole, UK) and stored at 4°C in a dessicator; it was dissolved freshly in 1X TAE buffer before each experiment. Fresh solution of complexes in ultra-pure water were used and mixed with 5'-GMP in a 1:1 ratio. The stock solutions of base and complex were both 1 mM. All the solutions were incubated for three days at 37°C in the dark. ESI-MS spectra were taken on a Bruker Esquire 2000 spectrometer and were recorded in positive mode between 0 and 2000 *m/z* using the low ionisation strength of 20%.

BLANK IN ORIGINAL

Chapter Five – DNA binding of steroidal platinum(II) complexes

5.1. Introduction

5.1.1. The discovery of DNA and its structure

DNA research began in the late 1860's, when the Swiss scientist Johann Fredrich Miescher isolated a crude extract of DNA from the nuclei of pus cells and determined the elemental composition of the weakly acidic substance; high in phosphorus and containing various elements including carbon, hydrogen, oxygen and unlike proteins, no sulphur. Miescher had isolated what he termed 'nuclein' (recently reviewed[549]) and what is now called DNA. The chemical composition of DNA – the nucleic acids – was determined by Albrect Kossel[550] (Nobel Prize 1910) and found to contain 4 bases: adenine and guanine (based on purine) together with cytosine and thymine (based on pyrimidine). In addition to 4 nucleobases, nuclein also contained a 5-membered sugar ring and phosphorus moiety; we now know these, respectively, as dexoyribofuranose and the phosphodiester backbone.

In the 1950s Chargaff and co-workers[551] found the ratio of purine and pyrimidine bases in DNA to be close to 1 and the molar ratios of guanine and cytosine were equivalent as were the molar ratios of adenine and thymine. In 1953 Watson and Crick[552] proposed the now accepted structure of DNA: their paper beginning with the words "We wish to suggest a structure for the salt of deoxyribose nucleic acid (D.N.A.). This structure has novel features which are of considerable biological interest."

DNA is composed of two strands of phosphodiester groups linked covalently to deoxyribofuranose bound to a nucleobase. The two strands are held together by hydrogen bonding between the purine bases (G and A) and the pyrimidine bases (A and T) as shown in Figure 5.1.

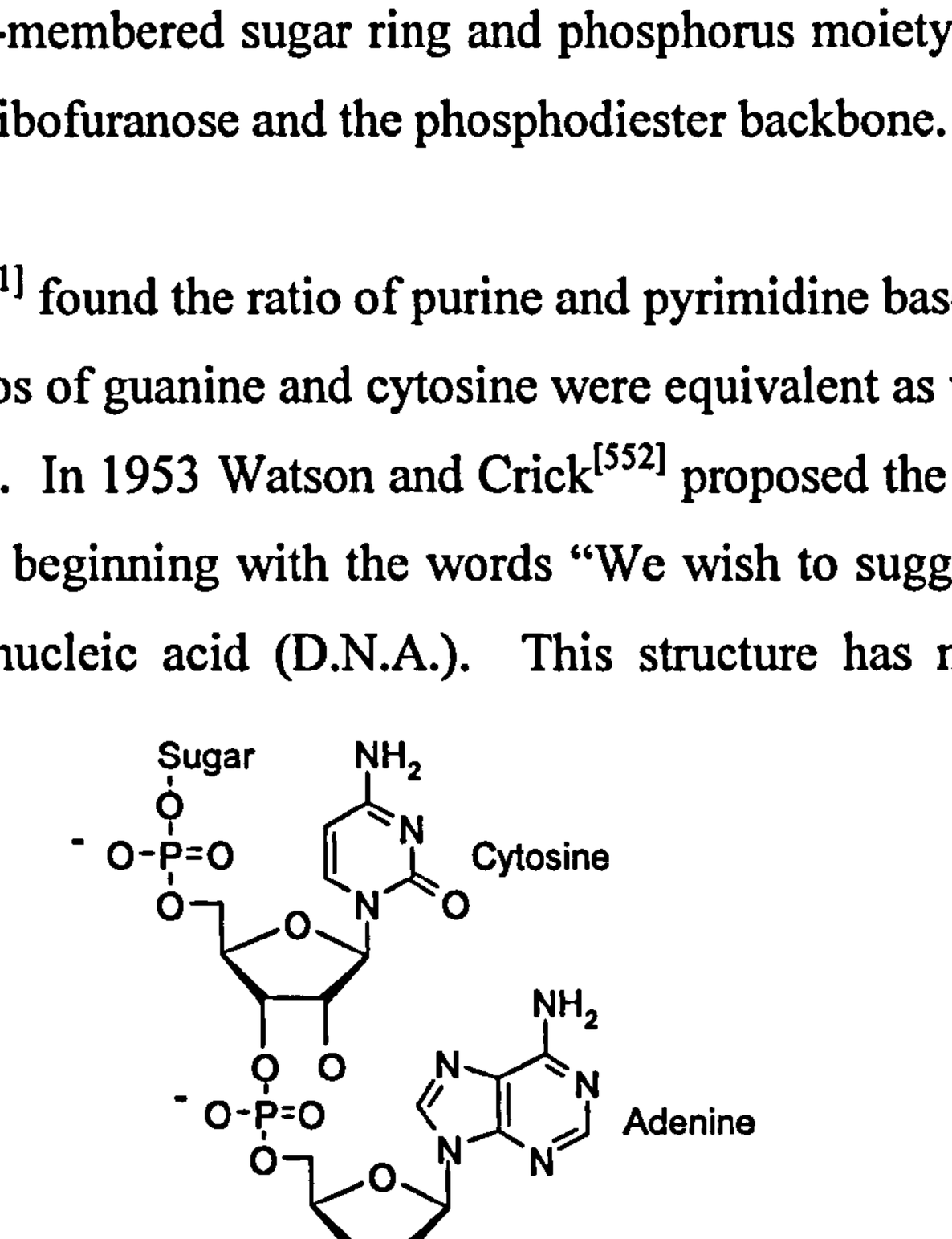

Figure 5.1. The structure of a DNA strand.

Each strand of DNA is made of three elements:

1) Deoxyribofuranose, a 5-membered sugar hetrocylic ring
2) The nucleobases, G, C, A and T covalently bound to the sugar ring
3) The phosphodiester backbone, linking the sugar – base functionalities together in a chain. A single nucleobase, sugar and phosphate are known as a nucleotide.

The DNA strands have directionality; the nucleobases are attached to deoxyribofuranose forming a nucleoside; the nucleosides have a specific direction by being bonded to the phosphate groups; the phosphate groups are linked to the 5' hydroxyl group of one sugar and the 3' hydroxyl group of the next sugar (5' – 3'); and the opposite strand has the reverse directionality (3' – 5').

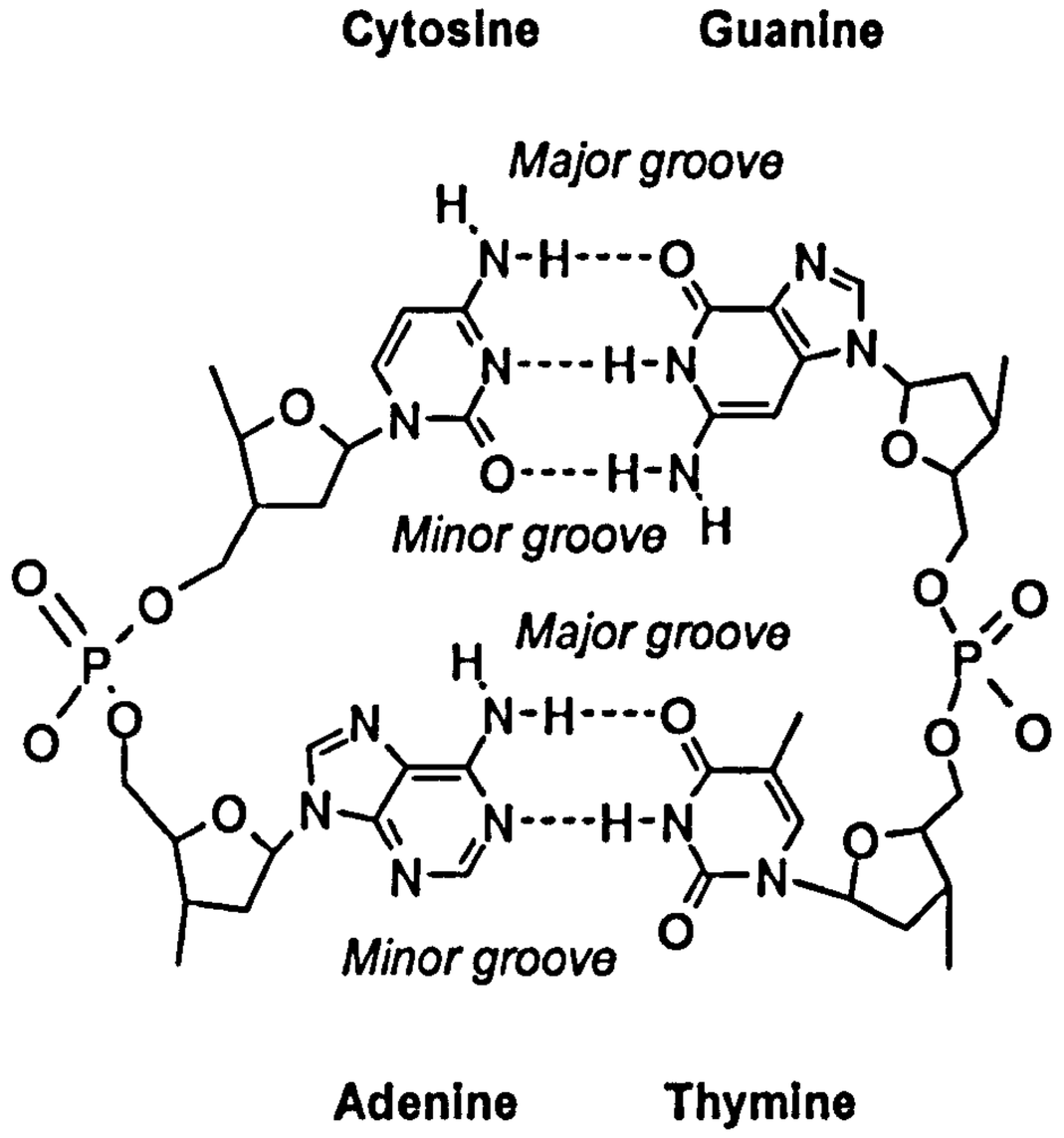

Figure 5.2. The hydrogen bonding arrangement between individual nucleobases in double stranded DNA forming major and minor grooves.

The molecular structure of DNA is a double helix in which guanine always pairs with cytosine and adenine with thymine (Figure 5.2). Primarily, three different forms of DNA are found in the biological arena, A, B and Z; the most common form of DNA is B-DNA and will be discussed. B-DNA is a helix. A helix is mathematically defined as a three-dimensional curve that lies on a cylinder so that its angle to a plane perpendicular to the axis is constant. In the case of DNA the curve is traced by the phosphodiester backbone, the pairs of planar bases approximately 90 degrees to the helical axis; the bases pairs are attached to the sugar-phosphate backbone asymmetrically and the helical structure gives rise to grooves in the DNA of two difference sizes. As shown in Figure 5.3, the major

groove is approximately 12 angstroms wide and the smaller minor groove is approximately 6 angstroms wide.

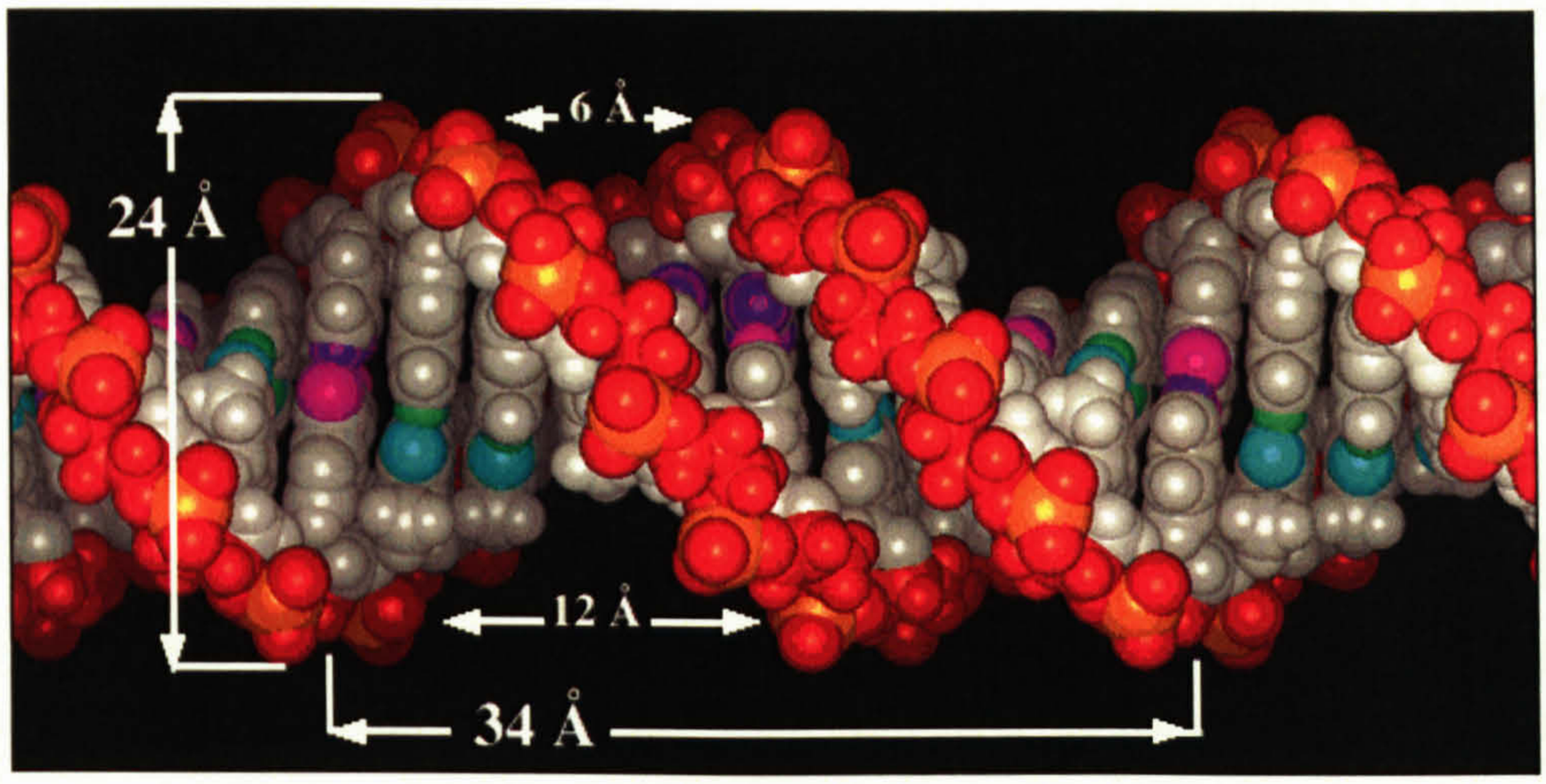

Figure 5.3. The structure of B-DNA.

5.1.2. Techniques

Several techniques are used to investigate the interaction between steroidal platinum(II) complexes and DNA and elucidate their effect. More detailed information regarding the theory of absorbance spectropscopy, supercoiled DNA and linear dichroism may be found is Appendix Nine and will only be very briefly described here.

Absorption spectroscopy is the investigation of the interaction between electromagnetic radiation and molecules. It is used to probe the movement of electrons in a molecule excited by absoption of electromagnetic radiation. The main use of absorption spectroscopy in this thesis is to determine exactly which chromophore(s) (moieties of the molecule absorpting light) are responsible for the absorbance of light at a particular wavelength in a steroidal platinum(II) complex. Following on from this is linear dichroism (*LD*): once a sample is orientated in a specific direction, *e.g.* long strands of DNA forced roughly parallel to each other, the difference in absorption between light linearly polarised parallel and perpendicular to the orientation axis yields an LD spectrum. An LD spectrum may elucidate the global effects a complex being bound to a DNA helix can cause; such as bending. Furthermore, the spectrum is very informative regarding the orientation of a molecule (say a metal complex) bound to DNA. This assumes where the complex (and its components) absorb is known (hence absorption spectroscopy) and that the exact angle of a transition (the precise direction of movement of electrons occuring in a transition) is known from LD obtained of molecules aligned using a stretched film. Finally gel

electrophoresis of supercoiled DNA, once analysed may yield the angle a complex unwinds the DNA helix.

5.2. Results and discussion

In total, the ability of 11 individual complexes to bind to DNA by electrophoresis and linear dichroism was assessed; the effect on the DNA structure due to such binding was investigated with a view to understanding, at the molecular level, the binding of complex and DNA. Of the 11 complexes 8 are steroidal metal complexes and three contain only simple aromatic ligands such as pyridine. All results were collected using the materials and methods as described in § 5.7. The results fall into three categories; those relating to the control complexes, TC-Py, CC-Py and TC-Q; those relating to *trans*-cationic steroidal platinum(II) complexes; and those relating to *cis*-cationic steroidal platinum(II) complexes. However the *superhelicity constant* for the DNA must first be calculated using cisplatin and the plasmid DNA pBR322.

5.2.1. Gel Electrophoresis

5.2.1.1. Cisplatin and pBR322

The plasmid pBR322 is a closed circular DNA containing 4361 base pairs; it is negatively supercoiled and will be used to determine the unwinding angles for steroidal platinum(II) complexes using the methods in § 5.7.1. Further, more detailed information on supercoiled DNA may be found in § A.9.3.5. Briefly, closed circular supercoiled DNA consists of sections of helix wrapped around itself to create an additional layer of coiling. Such DNA can also exist without supercoiled and can often appear as a ring of DNA, otherwise known as relaxed. The superhelicity constant for pBR322 is not known and is determined by treating the plasmid with cisplatin and monitoring the point where the supercoiled and relaxed forms migrate at the same position on the gel. Figure 5.10 shows the electrophoresis gel in which increasing amounts of cisplatin have been bound to pBR322. Two bands are observed, supercoiled and relaxed (refer to Figure 5.4) in untreated plasmid (far left and far right lanes of the gel). As the amount of cisplatin bound to pBR322 increases the mobility of the supercoiled band begins to decrease and it travels less distance in the gel and indicates the amount of supercoiling is reducing. The mobility of the relaxed DNA begins to increase slightly and eventually the point where supercoiled and relaxed DNA travel to in the gel co-inside – this is the co-migration point. At this point all the supercoils in the original plasmid have been removed. The ratio at which this occurs is converted into $r_{b(c)}$, where $r_{b(c)}$ is the inverse of the ratio of the number of bases : platinum(II) atoms at which co-migration occurs. Further cisplatin binding results in the

mobility of supercoiled plasmid increasing, a sign that pBR322 is gaining positive supercoils. In effect, it is observed as the amount of cisplatin bound to pBR322 increases, it unwinds the plasmid before winding the plasmid back up, forming positive supercoils.

The unwinding angle of 13° has already been determined for cisplain[553] and using $r_{b(c)}$ = 0.083 as the co-migration point (from Figure 5.4.), the superhelical density is calculated after rearranging the equation in § A.9.3 to be -0.059; that is the plasmid, on average, contains 26 supercoils in its native state. The negative sign indicates pBR322, similar to nearly all naturally occuring supercoiled DNA's, is negatively supercoiled. This and subsequent experiments require the point at which supercoiled DNA (SC) and relaxed (R) co-migrate to determine the unwinding angle and due to the nature of the experiment this point is subjective. Hence a relatively narrow range of $r_{b(c)}$ values were chosen and the experiment repeated to confirm the values chosen are reproducible.

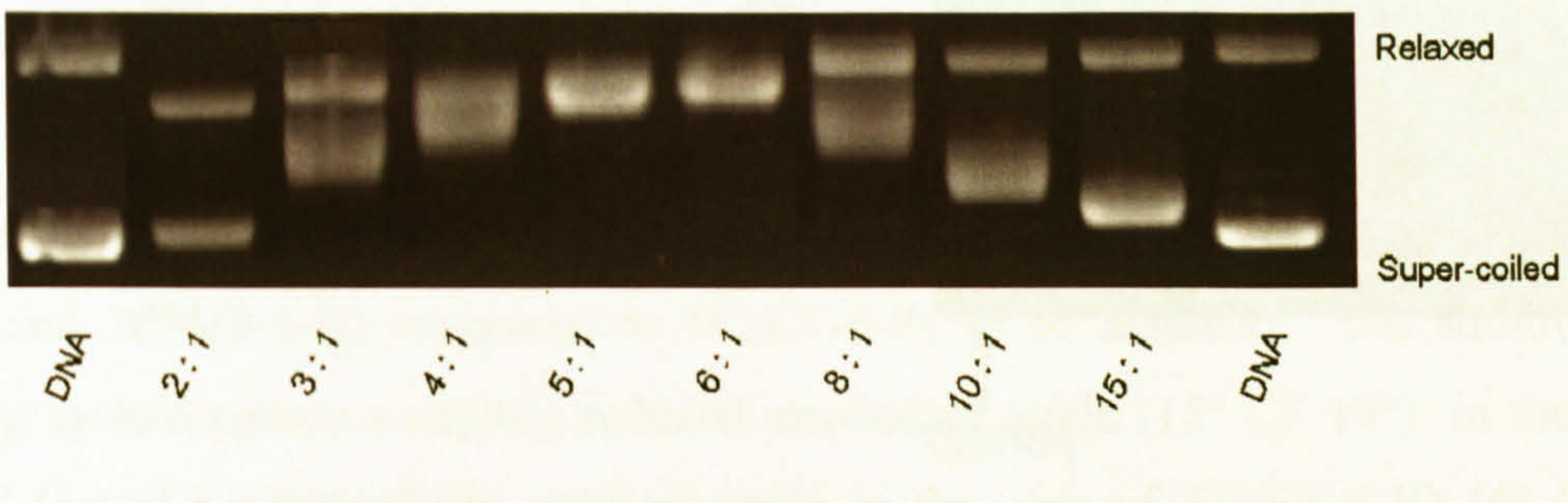

Figure 5.4. Agarose gel of cisplatin and pBR322 at various loadings.

5.2.1.2. Non-steroidal complexes (the control complexes) and pBR322

Treatment of pBR322 with the three non-steroidal complexes resulted in the mobility of the supercoiled plasmid in agarose gel decreasing in proportion to the ratio of DNA:complex as shown for all three in Table 5.1. This is indicative of a loss of the number of supercoils in the plasmid. This strongly suggests the complexes bind to DNA. The loss of supercoils may be explained as a result of the plasmid accommodating local unwinding of the DNA helix at the binding site. Unlike that of cisplatin at the same range of ratios, TC-Py, CC-Py and TC-Q only cause the plasmid to loose supercoils and approach the relaxed conformation (the point of co-migration) and not introduce positive supercoils (Table 5.1). The complex TC-Py (Table 5.1) caused the two types of plasmid to co-migration at $r_{b(c)}$ = 0.5, corresponding to an unwinding angle of 2° ± 1.5°, the large error due to the difference between $r_{b(c)}$ values in adjacent lanes. It is reasonable to suggest the effect on the structure of DNA, in terms of unwinding, is small and unwinding angles are of the order < 3.5° for all three complexes.

Table 5.1. Images of pBR322 treated with TC-Py, CC-Py and TC-Q as measured by ethidium bromide stained gel electrophoresis. Complex loading from right to left, pBR322, 10bp:1, 8bp:1, 6bp:1, 4bp:1, 2bp:1 and 1bp:1. SC = supercoiled and R = relaxed plasmid

Ethidium bromide stained gel of pBR322	Complex
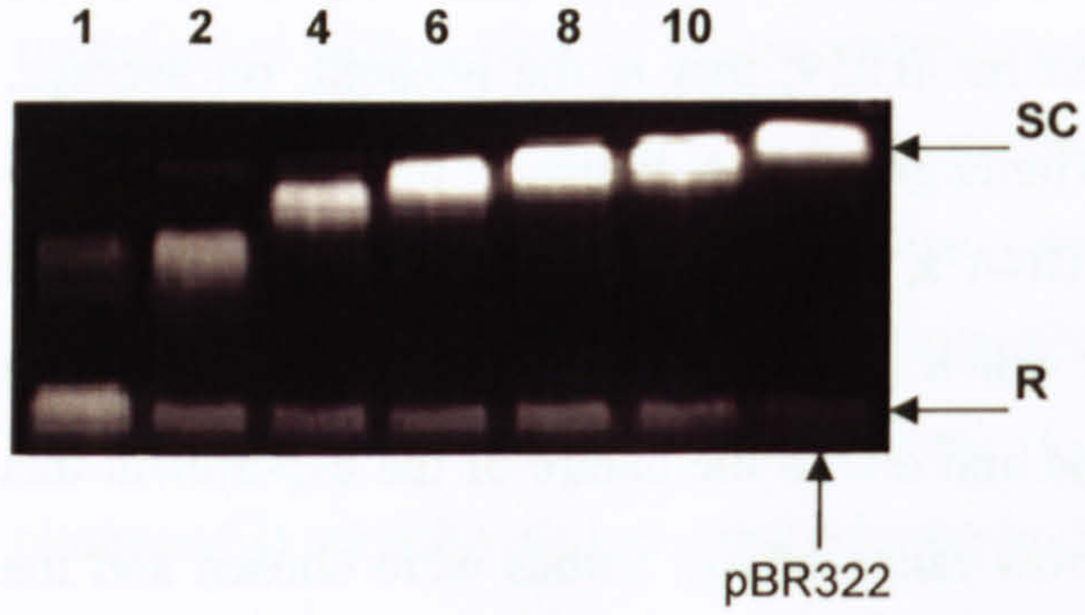	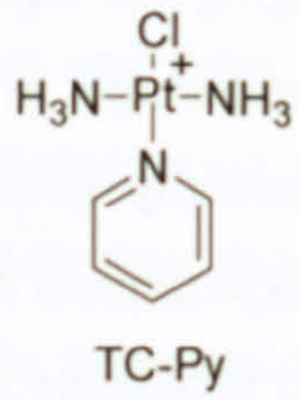 TC-Py
	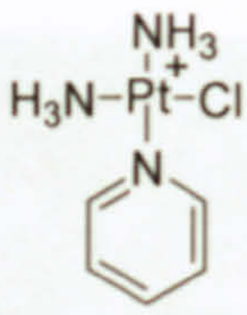 CC-Py
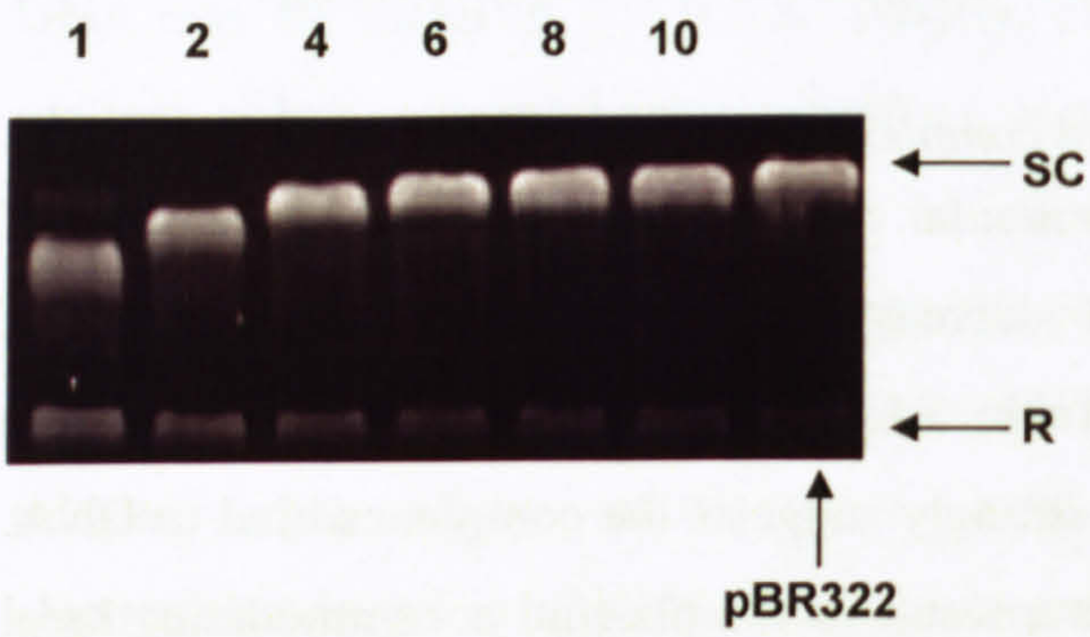	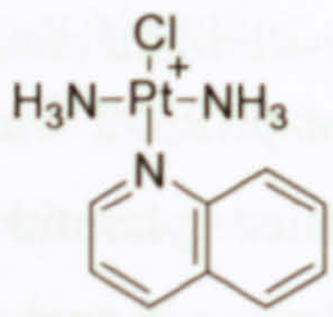 TC-Q

5.2.1.3. Trans-cationic complexes

The effect of five trans-cationic complexes on pBR322 DNA was studied by gel electrophoresis. The complexes are similar to those discussed in *5.2.1.2.* in that they are able to form only a single metal-ligand bond with DNA, except now a steroidal group is attached to the aromatic amine. The effect on the electrophoretic mobility of SC and relaxed plasmid is similar to that of their non-steroidal counterparts, in that primarily the SC plasmid mobility decreases, eventually co-migrating with the relaxed form, which can be ascribed to a loss of supercoiling resulting in 100 % relaxed DNA. At higher complex

loadings (expect in the case of TC-ET-4-Py), the mobility of SC plasmid begins to increase indicating the size of the plasmid is becoming smaller and is commensurate with the induction of positive supercoils. At the very highest loadings in all cases, except TC-ET-4-IQ, such positive supercoiling is replaced by dramatic slowing of the migration of SC and relaxed plasmids. This is a strong indication of DNA aggregation; these structures are poorly stained, presumably due to lack of access of ethidium bromide to the DNA helices.

The presence of the steroid in all five complexes results in an increased ability for those complexes to unwind the DNA helix (as measured by a loss of supercoiling) compared to the control complexes in Table 5.1. In the case of TC-ET-4-IQ, $\phi = 4°$, where ϕ is the angle that the DNA helix is unwould; unwinding angles for all other TC complexes are $\geq 11°$. This provides evidence that the presence of an ethynyl-testosterone group is causing the complex to possess a far greater ability to unwind DNA and the large unwinding angles suggest a direct interaction of the testosterone group and the DNA helix. Within the group of 5 complexes, three may be compared; TC-ET-3-Py; TC-ET-3-Q; TC-ET-4-IQ. Each complex possesses an identical nitrogen containing ring with the steroidal group β to that of the nitrogen donor; this allows the effect of the additional aromatic ring system in TC-ET-3-Q and TC-ET-4-IQ compared to TC-ET-3-Py to be assessed. The addition of an extra ring system causes a slightly reduced unwinding angle (15° *Cf.* 19°) in the case of TC-ET-3-Q and a substantially reduced angle in the case of TC-ET-4-IQ (4° *Cf.* 19°), indicating in the case of 3-substituted pyridines rings, an additional ring is detrimental to DNA unwinding, particularly when located close the ethynyltestosterone substituent. Whilst aromatic amines, such a pyridine and quinoline are capable of intercalation, the presence of an ethynyltestosterone bound to the aromatic ring system precludes this and intercalation can be disregarded as a possible mechanism of binding.

Table 5.2. The effect on pBR322 of steroidal trans-cationic complexes as measured by electrophoresis gels. The numbers refer to DNA bp : complex and supercoiled (SC) and relaxed (R) conformations.

Ethidium Bromide Stained Gel	Complex	Unwinding Angle
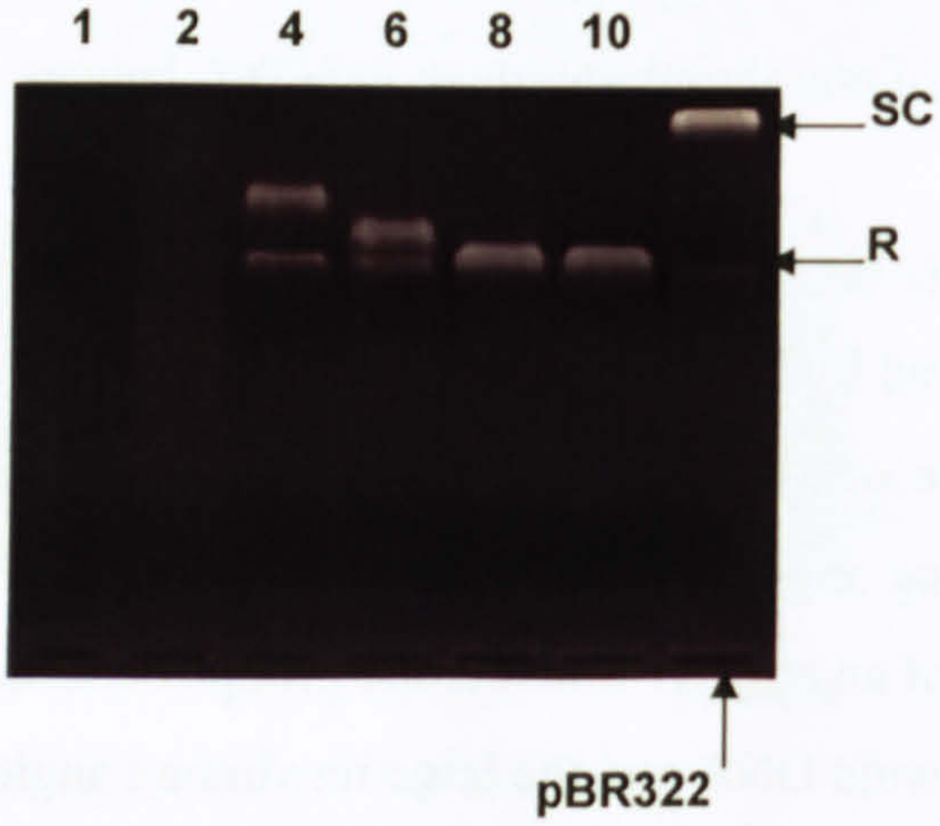	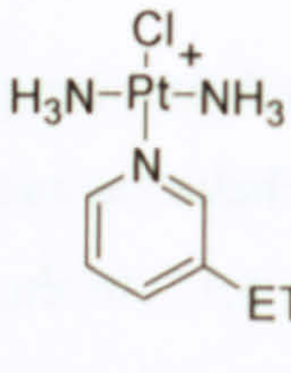 TC-ET-3-Py	19°
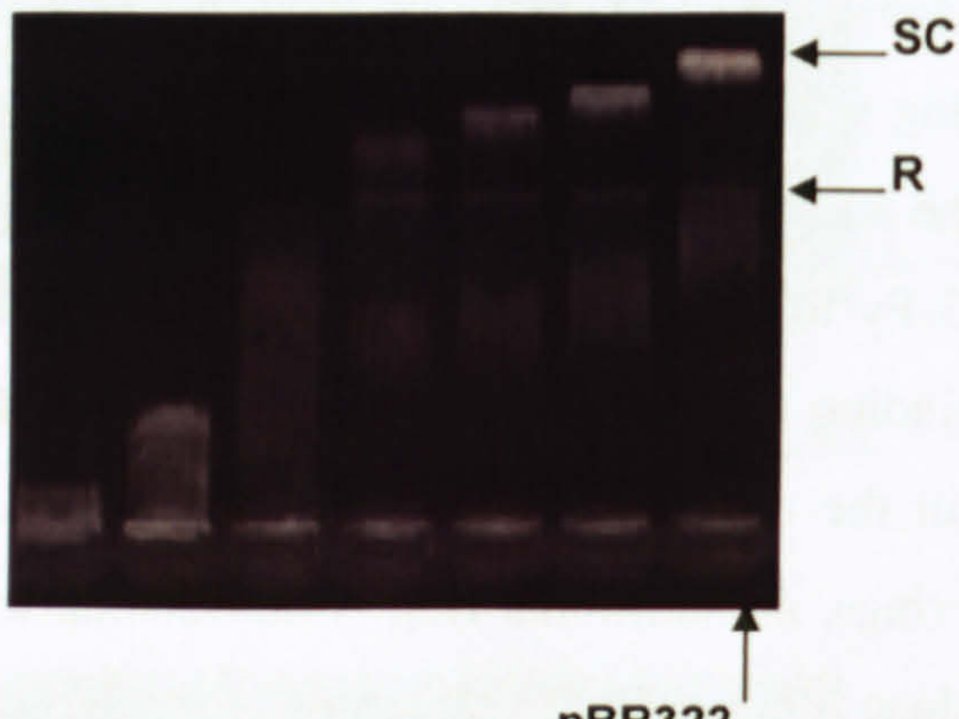	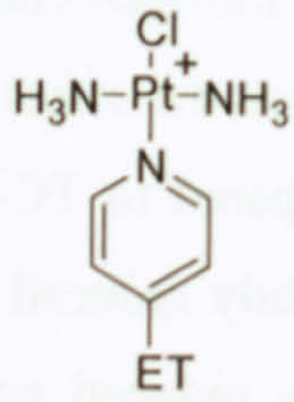 TC-ET-4-Py	11°
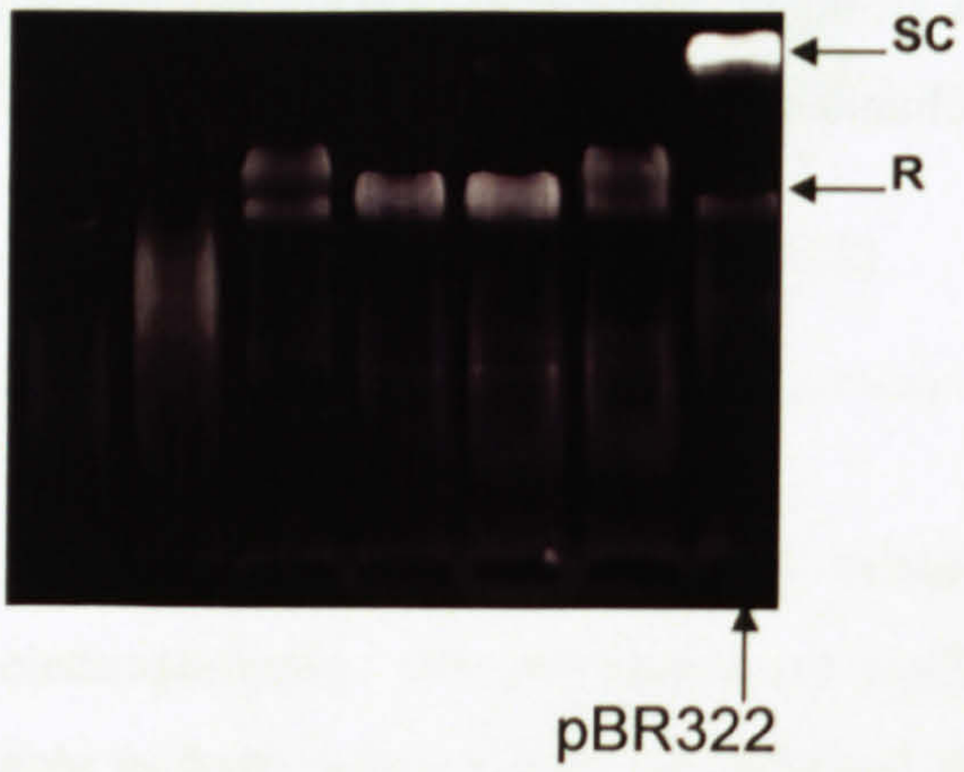	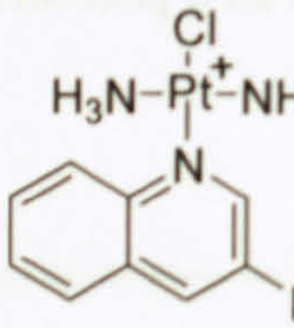 TC-ET-3-Q	15°

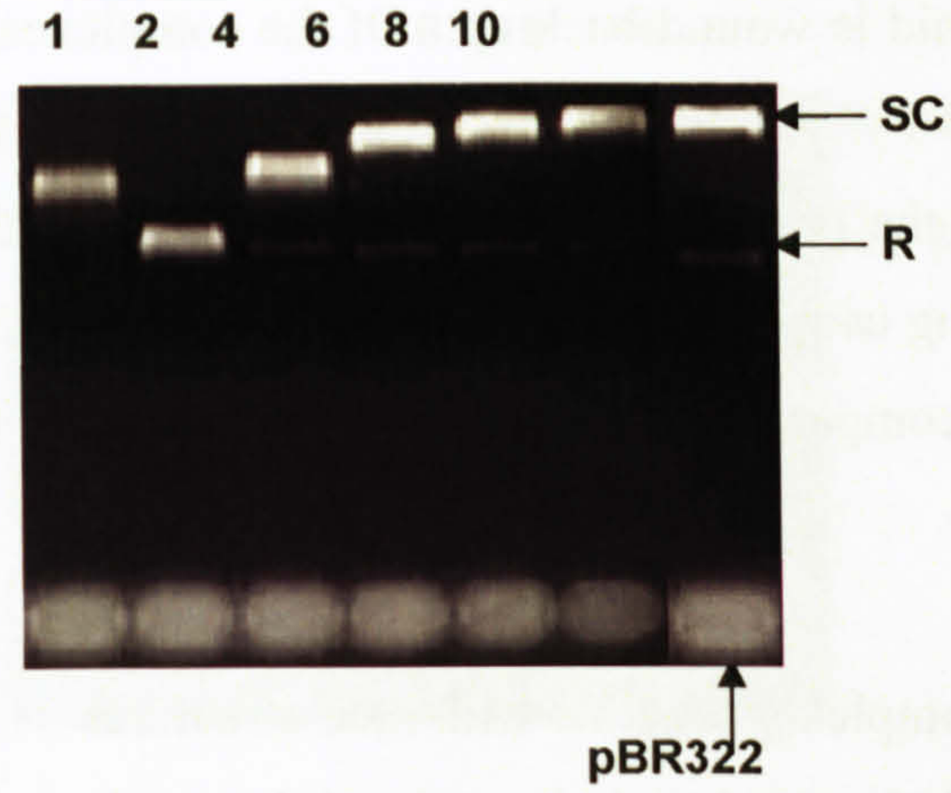

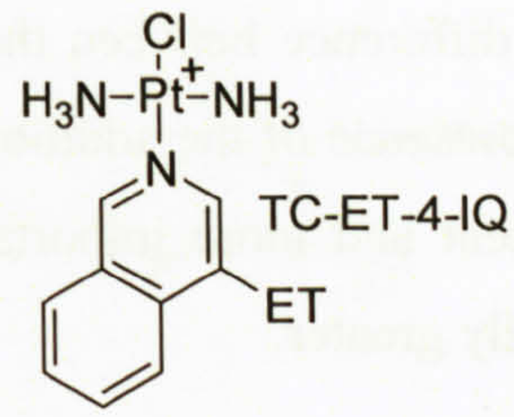

4°

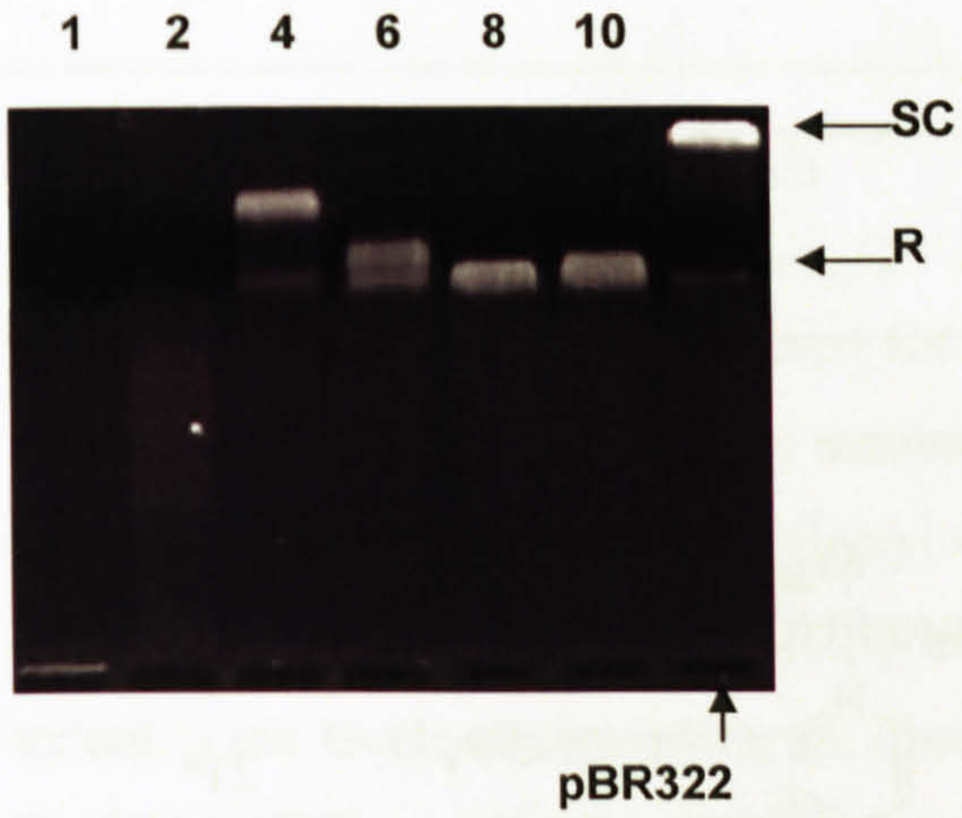

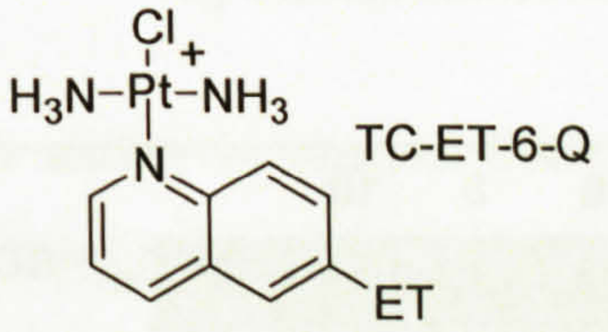

19°

5.2.1.4. Cis-cationic complexes and pBR322

Three *cis*-cationic complexes, CC-ET-3-Py, CC-ET-4-IQ and CC-ET-6-Q were assessed in their capacity to cause a loss of supercoiling in the plasmid pBR322. At the concentrations used the reduced migration of SC plasmid caused by a loss of supercoiling is not seen and the co-migration points for CC-ET-3-Py and CC-ET-6-Q occur towards the lowest complex loadings. What is observed is the plasmid traveling further in the agarose gel, indicating it is getting physically smaller due to the production of positive supercoils. For CC-ET-3-Py and CC-ET-6-Q, $r_{b(c)}$ values of 0.050 and 0.055 respectively are observed yielding respective unwinding angles of 21° and 19°; in the case of CC-ET-4-IQ, SC and R forms co-migrate where $r_{b(c)} \leq 0.05$, giving an unwinding angle of $\geq 21°$.

In the case of CC-ET-4-IQ and CC-ET-6-Q, at the higher loading values electrophoretic migration slows dramatically indicating DNA aggregation, which in the case of CC-ET-6-Q presumably blocks intercalaction of ethidium bromide as no band is observed. The alterations to electrophoretic mobility of SC plasmid are fully consistent with complex binding to DNA, unwinding the negative supercoils at lower loadings as a result of unwinding the DNA helix at a local level; additional local unwinding causes the

introduction of positive supercoils and the plasmid is wound back up. Of the complexes, CC-ET-3-Py and CC-ET-4-IQ and, TC-ET-3-Py and TC-ET-3-Q may be directly compared; the only difference between them is the presence or absence of an additional aromatic ring. The presence of the additional ring caused the complex to unwind DNA to an event greater extent and more importantly compared to the controls, the unwinding angles are substantially greater.

Table 5.3. The 1% agarose gels of cis-cationic complexes together with their structures and unwiding angles. SC and R refer to supercoiled and relaxed plasmid and the numbers refer to the DNA bp : complex ratio

Ethidium Bromide stained gel	Complex	Unwinding Angle
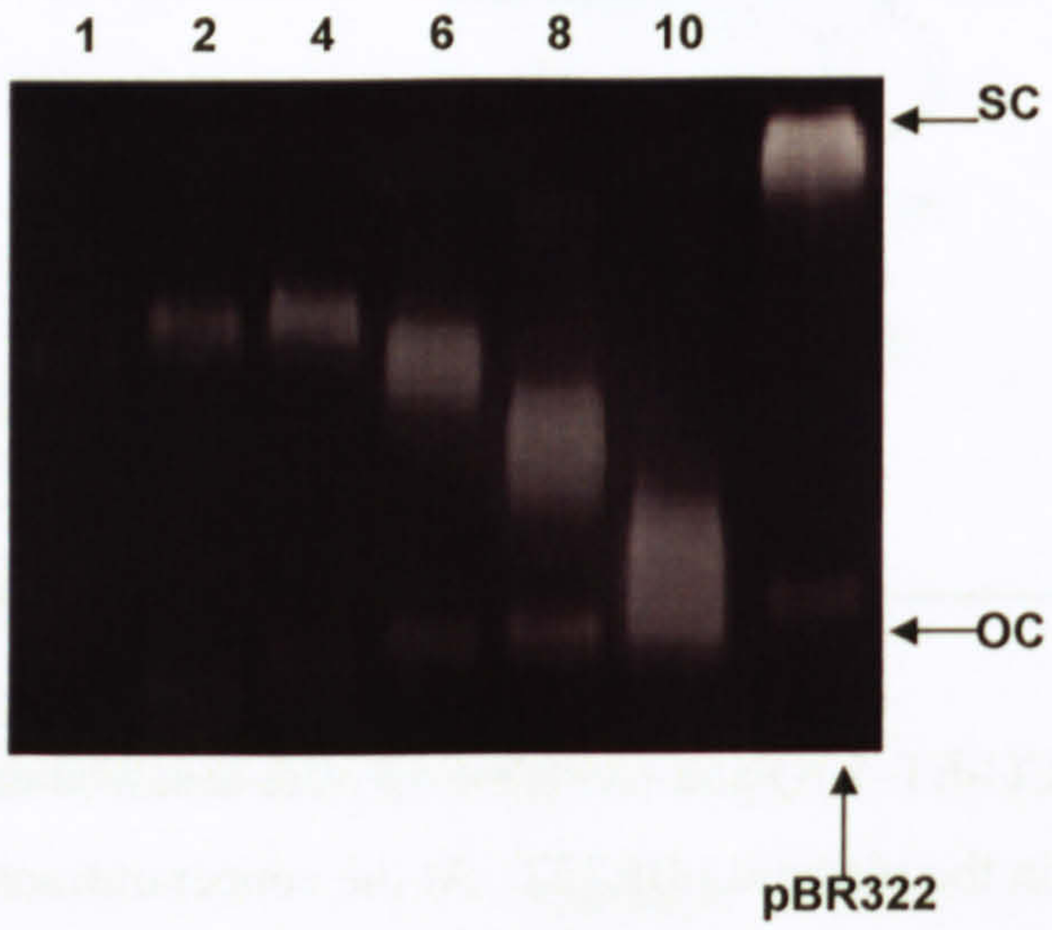	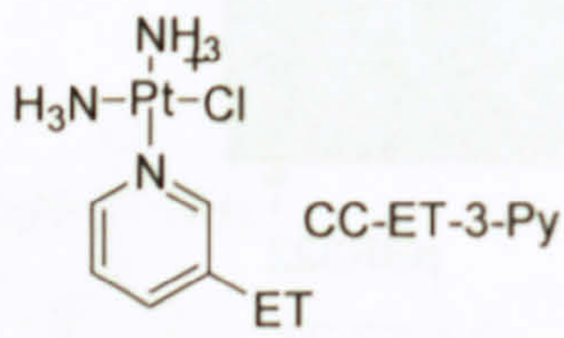 CC-ET-3-Py	21°
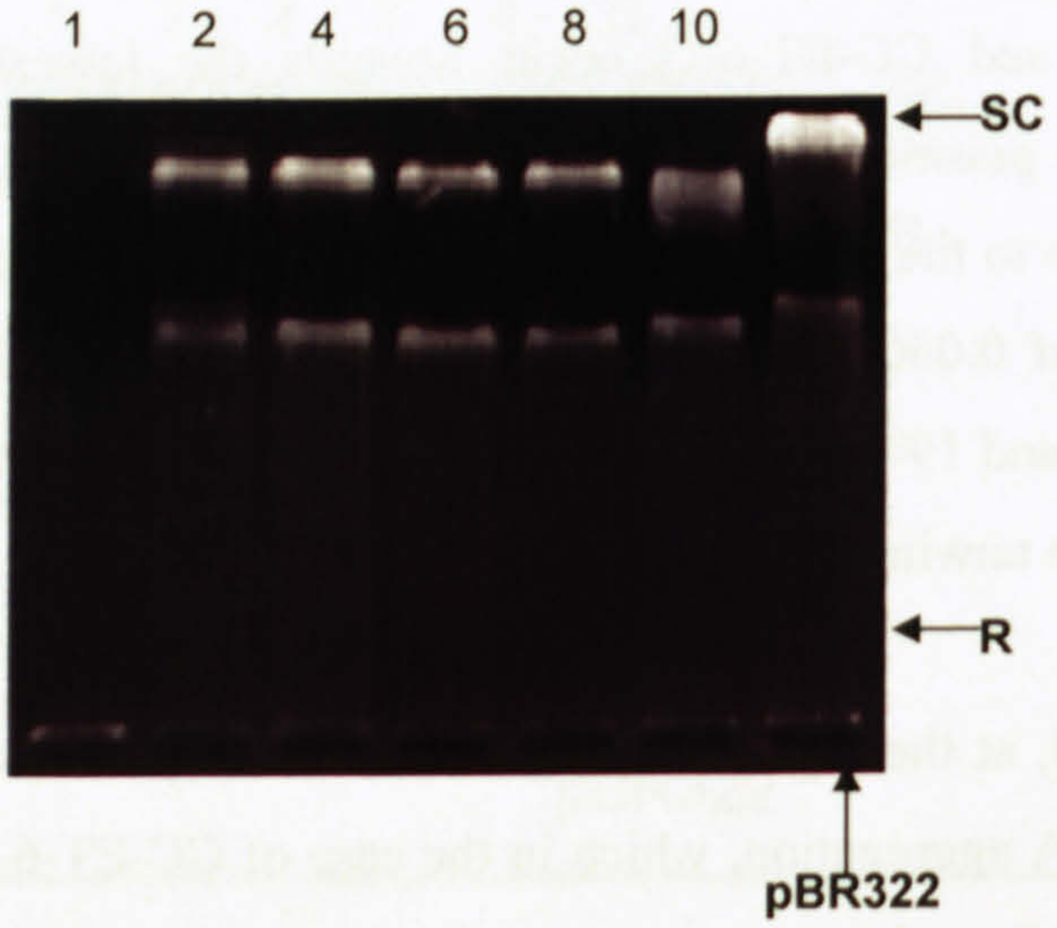	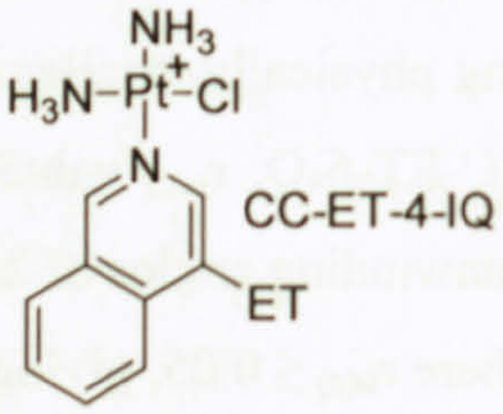 CC-ET-4-IQ	>21°

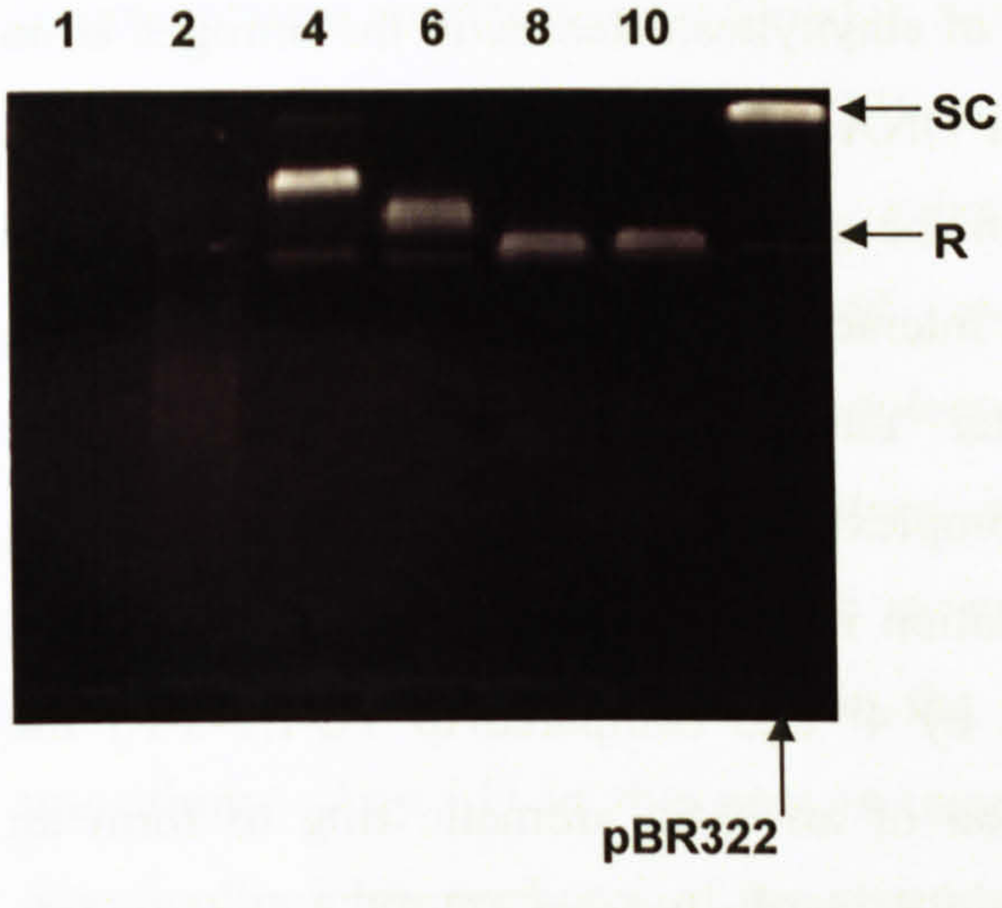

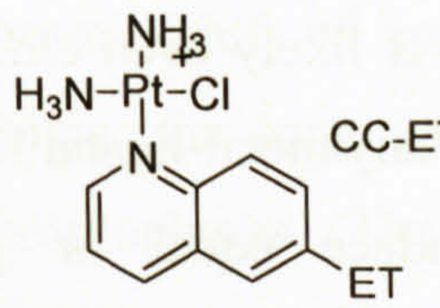

CC-ET-6-Q 19°

5.2.1.5. Gel electrophoresis discussion

When the complexes were assessed for their ability to unwind DNA a wide variety of unwinding angles were found; the amount of unwinding affected primarily by whether the aromatic amine contained an ethynyl-testosterone group, or not. The non-steroidal complexes, TC-Py, CC-Py and TC-Q do not effect unwinding of the helix to any great extent. Low levels of unwinding are observed, a fact not unsurprising given the complexes $[Pt(NH_3)_3Cl]Cl$ and [Pt(dien)Cl]Cl unwind the plasmid pUC 19 by only 6°.[554] It appears that non-steroidal complexes, even with a pyridine ligand cis to any metal-ligand DNA interaction, can be accommodated by the helix without substantional unwinding. It is also unlikely, given the small unwinding angles and steric constraints of the complexes that intercalation forms part of the binding mode to DNA as intercalators tend to cause large unwinding angles, typically > 30°.[555, 556]

Substituting an ethynyltestosterone group onto the aromatic amine, in various positions, induced substantially greater unwinding of the helix compared to TC-Py, CC-Py and TC-Q; this fact holds true for both cis-cationic and trans-cationic complexes. All the complexes are only able to bind to DNA monofunctionally and large unwinding angles compared to the control complexes must be addressed to the presence of a bulky steroidal group; in order for this group to affect the DNA structure, a helix-steroid interaction must occur, a reasonable proposition, given that structure of the complexes means the steroid and DNA must be in proximity to each other. In the case of TC-ET-4-Py, the ethynyltestosterone group is pointing away from the helix but it is reasonable to assume (from the crystal structure data reported in Chapter Three) that an approximate 90° bend at carbon-17 of the steroid may bring the steroidal skeleton into close proximity to DNA; it must be remembered the steroidal skeleton is free to rotate relative to the platinum(II)

centre. In the other complexes, the β-position of ethynyltestosterone to the nitrogen atom of the aromatic ring suggests testosterone and DNA will be in close proximity to each other. Such proximity is likely even closer in the cis-cationic complexes, whereby the steroidal ligand is cis to any metal-ligand DNA interaction. It should be noted that the cis-cationic complexes induce equal or greater unwinding than their trans-cationic counterparts; this may be interpreted as the complexes being more sterically demanding once bound to the DNA helix and accommodation results in greater helical unwinding. Interestingly TC-ET-4-IQ only unwinds DNA by 4° and compared to TC-ET-3-Py the complexes are identical except for the addition of an extra aromatic ring to form an isoquinoline; when the aromatic amine is a quinoline, in the case of TC-ET-3-Q, the angle is between these values. All complexes are shown in Figure 5.5. It is isoquinoline and its interaction with the DNA helix which, perhaps, precludes or reduces contact between the ethynyltestosterone group and DNA helix.

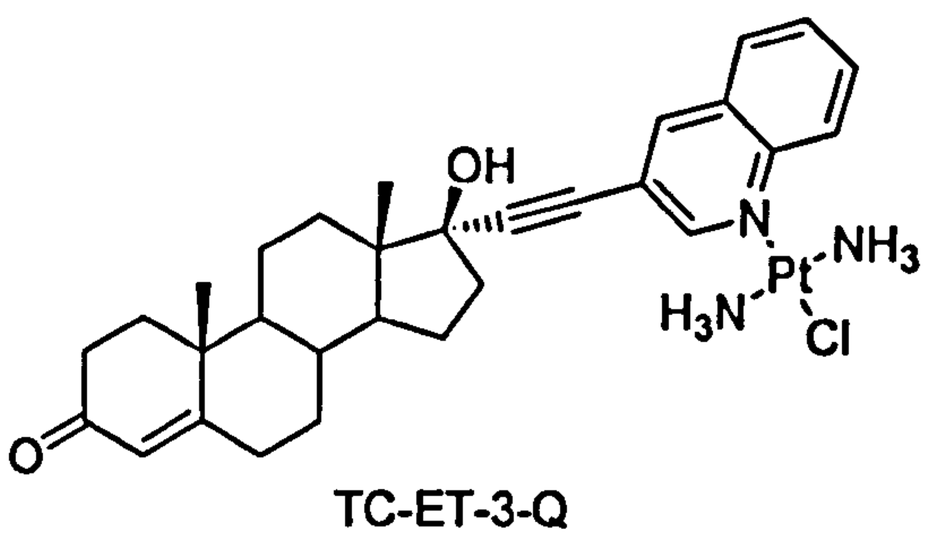

TC-ET-3-Q

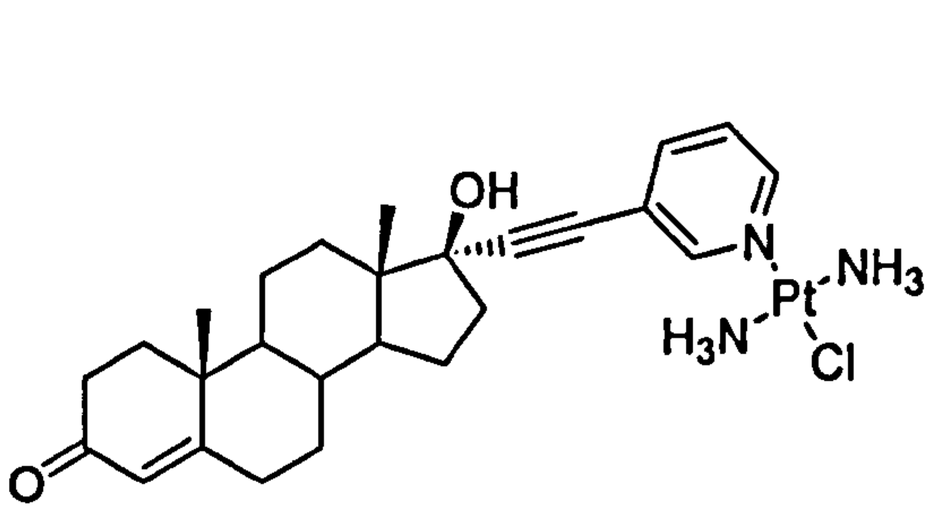

TC-ET-3-Py

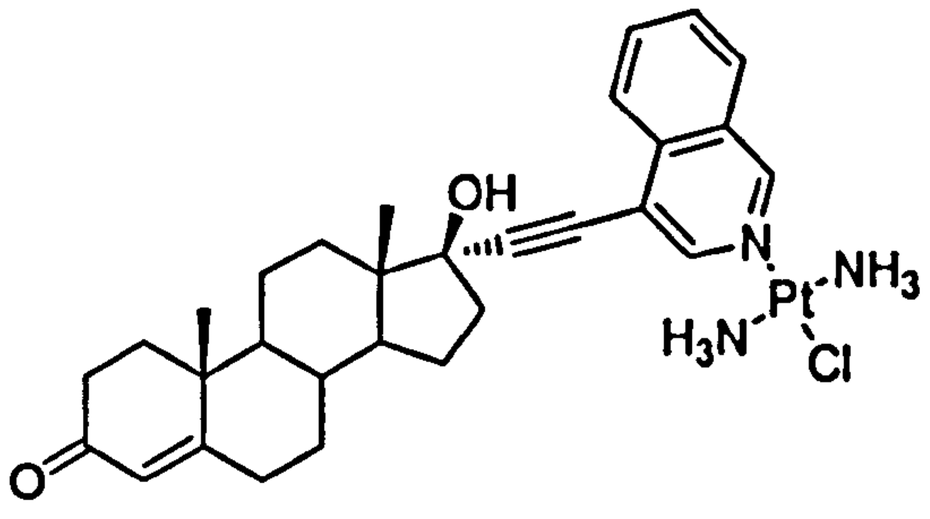

TC-ET-4-IQ

Figure 5.5. The molecular structures of TC-ET-3-Py, TC-ET-3-Q and TC-ET-4-IQ.

5.2.4. UV / visible spectroscopy

5.2.4.1. UV / visible absorption of steroidal platinum complexes

Steroidal platinum complexes have many distinct chromophores; an understanding of these is crucial to have deeper understanding of *LD* spectroscopic data. Formation of the six organic ligands via the joining of ethisterone to a planar aromatic molecule creates a UV / visible spectrum which may be described, to a good first approximation, as an addition of the two spectra, with very little change occurring to band shape, position or relative intensity. Upon binding to platinum(II), the spectra of the newly bonded ligand changes

(representative spectra may be found in Appendix Ten) with the longer wavelength band(s) of pyridine (260 nm), quinoline (275 nm) and isoquinoline (275 nm) found at higher wavelengths in the complexes, *i.e.* a bathochromic shift of approximately 25 nm. In complexes containing quinoline and isoquinoline, the long wavelength transitions lie outside all other transitions of the molecule chromophores. The new wavelengths of the quinoline and isoquinoline transitions lie > 300 nm and as such when complexes containing quinoline or isoquinoline are mixed with DNA (in *LD* experiments) absorption above 300 nm is *primarily* due to the quinoline and isoquinoline longer wavelength transitions. Any LD in this area is therefore due to the transitions of the quinoline or isoquinoline chromophores of the steroidal metal complex. The same cannot be said for pyridine containing complexes whose longer wavelength transitions (275 nm) will overlap with the main transition of DNA in the region (260 nm).

Regarding the complexes in general, there is an important feature to note: CC and TC complexes possessing the same ligand have very similar spectra; hence, the spectrum of TC-ET-3-Py is very similar to that of CC-ET-3-Py; the same may be said of TC-ET-4-IQ / CC-ET-4-IQ, TC-ET-6-Q / CC-ET-6-Q and TC-Py / CC-Py. The different geometries do not result in observable differences in absorption; from this it is reasonable to assume any absorption due to the platinum(II) chromophore, such as $d \rightarrow d$ transitions, are a constant feature when using the same ligands.

5.2.4.2. Film linear dichroism of quinoline and isoquinoline

A more detailed molecular picture of the binding of steroidal metal complexes to the DNA helix may be elucidated by determining the transition moments of quinoline. Using film LD the angle of each $\pi \rightarrow \pi^*$ of quinoline and isoquinoline may be determined. If the relative orientation of quinoline (from, say, TC-ET-3-Q) and DNA is known, the steroidal skeleton position is known (from the crystal structure data of Chapter Three) and this give insight into DNA binding at the molecular level. Calculation of the transition moments of quinoline and isoquinoline according to the method of Rodger and Norden are contained in Appendix Eleven and only the main results will be discussed here. Calculations show quinoline and isoquinoline display 10 individual transitions between 190 and 400 nm (from Appendix Eleven) and the most important are shown in Figure 5.6. Two solutions exist for the angle of each transition moment (clockwise and counter-clockwise from the *z*-axis). The solutions near 0 or 90° therefore have a very small range of angles the transition may occupy and thus may be described as *primarily* *z*-axis or *primarily* *y*-axis polarised transitions.

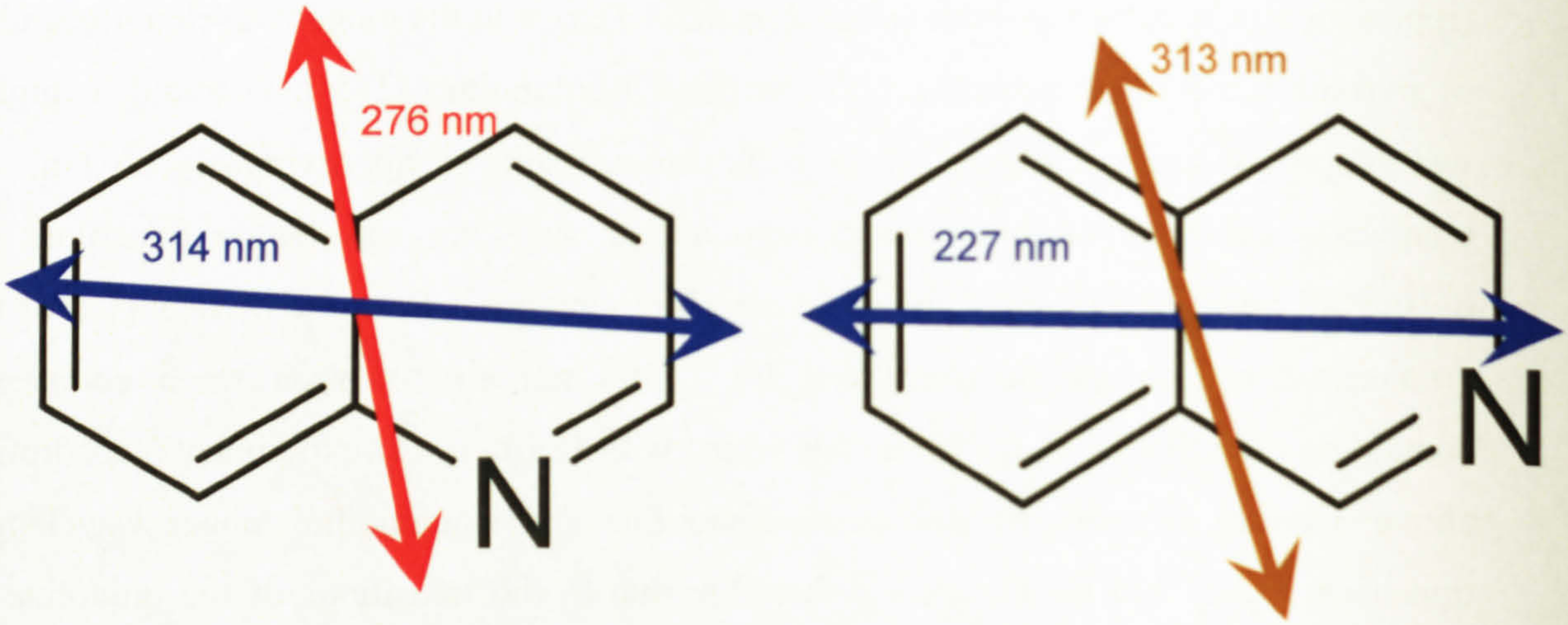

Quinoline Isoquinoline

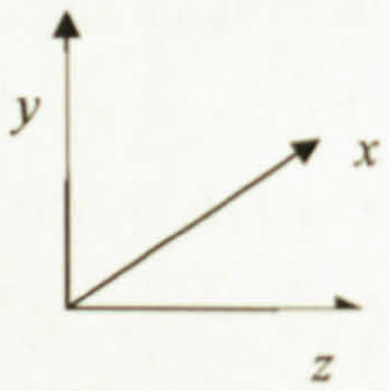

Figure 5.6. The most important transition moments present in quinoline and isoquinoline as suggested using film linear dichroism.

The most important transitions from a point of view of elucidating DNA binding – the ultimate aim of using *LD* – are those *outside* the absorption envelopes due to chromophores present in ethisterone, Pt(II) and DNA. In this respect, the 314 nm transition of quinoline (*z*-polarised) and 313 nm transition of isoquinoline (*y*-polarised) may allow determination of the angles of quinoline / isoquinoline relative to the long axis of the DNA helix. The two transition moments are very close to the *z*- and *y*-axes; therefore the two possible solutions for each are relatively close to each-other in terms of direction, particularly the 314 nm band of quinoline. It should at this point be stressed that these results should be viewed as 'remaining to be confirmed'. Other data, for example IR linear dichroism, fluorescence anisotropy and molecular orbital calculations are required before the angle of each transition is confirmed and also to confirm the presence of a transition at all, some changes to the reduced *LD* were subtle; despite this, the calculations above can be relied upon to give a good description of the approximate angles between DNA and any quinoline or isoquinoline molecules contained within a bound complex.

5.2.4.3. Flow linear dichroism of simple platinum(II) complexes and ct-DNA

All flow *LD* experiments were carried out according to procedures outlined in § 5.5. All the results presented were duplicated in follow up experiments, which are presented in Appendix Twelve. All experiments used a constant DNA concentration (200 μM) in the same couette cell and 1 X TAE buffer. The results of the flow *LD* DNA binding experiments falls into three categories: those of the control complexes TC-Py, CC-Py and TC-Q; those relating to trans-cationic complexes, TC-ET-3-Py, TC-ET-4-Py, TC-ET-3-Q, TC-ET-4-IQ and TC-ET-6-Q; and those relating to cis-cationic complexes, CC-ET-3-Py, CC-ET-4-IQ and CC-ET-6-Q. The *LD* of ct-DNA consists of a single band, at ~260 nm, due to $\pi \rightarrow \pi^*$ transitions of the nucleobases; this signal is negative, as expected; using couette flow alignment the transition moments are ~ 90° to incident radiation.

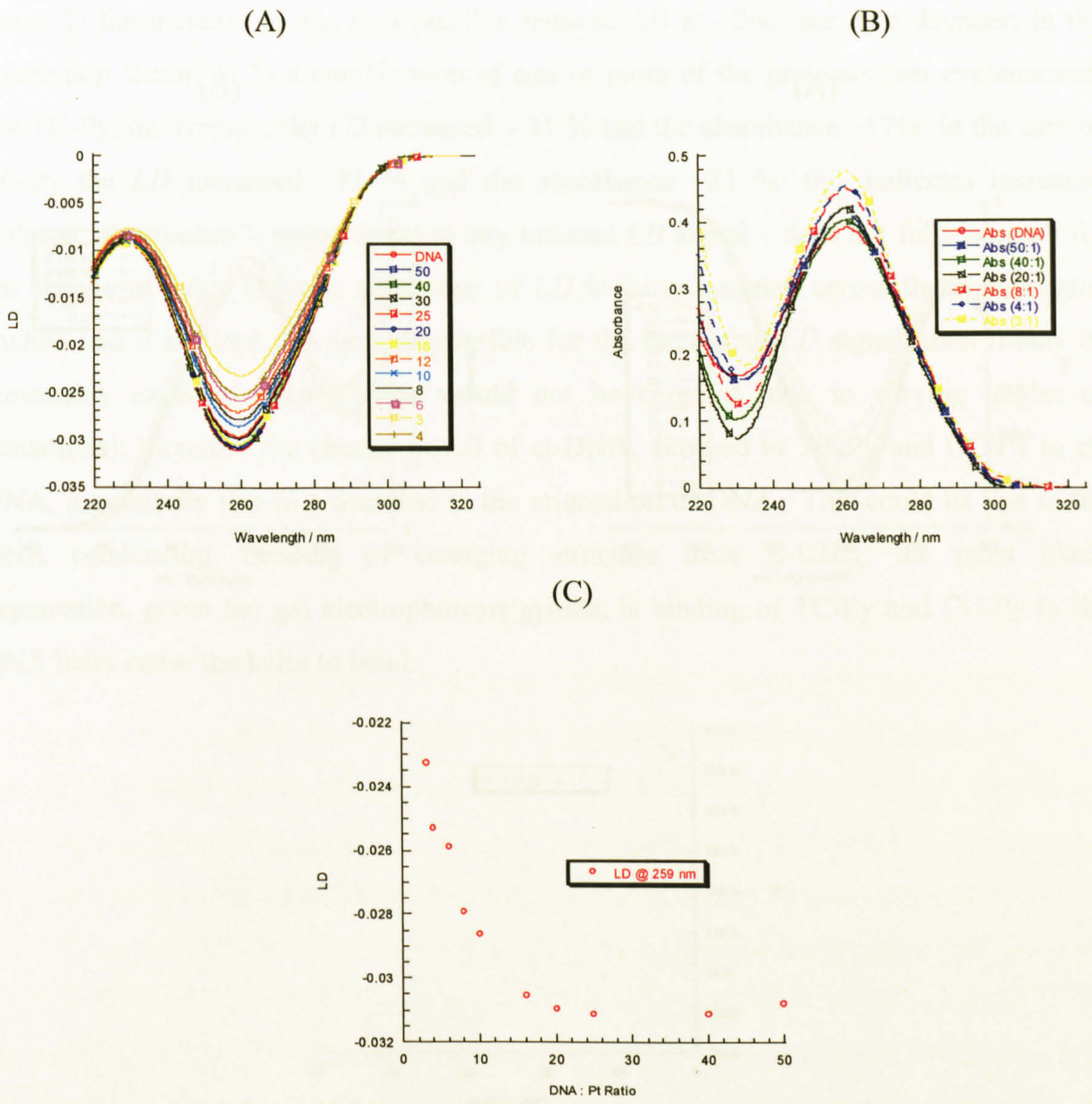

Figure 5.7. The *LD* (A), absorbance spectra (B) and change in *LD* versus loading of TC-Py and ct-DNA (C).

The *LD* spectrum of TC-Py and ct-DNA in Figure 5.7 (also A.12.1) shows a single, negative *LD* signal around 260 nm. The addition of TC-Py causes this peak to become more positive from ~0.031 to ~0.027 at the highest ratio of complex:DNA and, the change in sample absorbance is <0.1. The change in absorbance is due to TC-Py, whose absorption spectrum overlaps with that of DNA. The complex causes a measurable effect on the *LD* spectrum of DNA at loadings >16:1; below this the *LD* is effectively constant at ratios >16:1 the linear nature of the increase of *LD* versus complex : DNA ratio indicates TC-Py is bound in a single binding mode. There is evidence of an induced LD around 295 nm; however this signal is small, although representative of the interaction between DNA and complex. Similar changes are observed when ct-DNA is mixed with CC-Py (Figure 5.8 and A.12.2) indicating both complexes have a very similar effect on the structure of DNA.

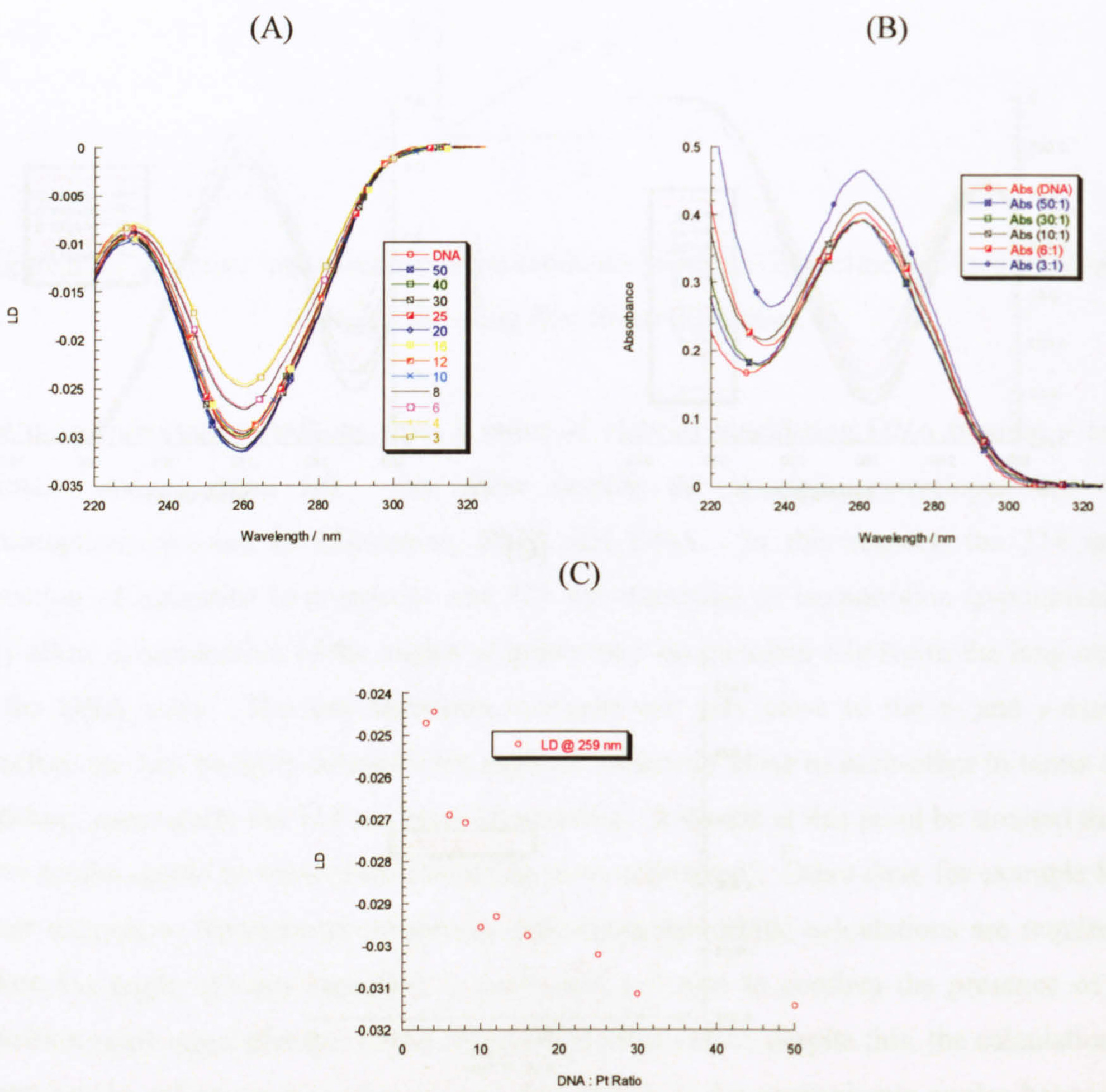

Figure 5.8. The *LD* (A), absorbance spectra (B) and change in *LD* versus loading of CC-Py and ct-DNA (C).

The *LD* spectrum of ct-DNA mixed with TC-Q is shown in Figure 5.9. An induced *LD* signal is observed at longer wavelengths, its magnitude is negative and outside the absorption envelope of DNA. The absorption spectrum (Figure 5.9) shows increases in the regions around 235 nm and > 300 nm; a small increase is observed between 240 and 300 nm. Such increases may be attributed, primarily, to the quinoline chromophore of TC-Q; this is confirmed by comparison with the UV / visible spectrum of TC-Q (Figure A.10.1) whose main absorbance lies at ~235 nm and >275 nm.

In the case of the three control complexes, TC-Py, CC-Py and TC-Q the magnitude of the *LD* signal ~260 nm become more positive but by no means dramatic. Considering $LD^r = \frac{LD}{A}$ and $LD = \frac{3}{2}S(\cos^2\alpha - 1)$, this may be explained in 3 possible ways: 1) the increase is due to a positive induced *LD* at ~260 nm; 2) a decrease in the orientation factor, *S*; 3) a combination of one or more of the previous two explanations. For TC-Py, on average, the *LD* increased ~ 31 % and the absorbance ~17%; in the case of CC-Py the *LD* increased ~31 % and the absorbance ~21 %: this indicates increased isotropic absorbance – proportional to any induced *LD* signal – does not fully account for the change in *LD*. The rate of change of *LD* is fairly constant across the wavelengths studied and if induced *LD* were responsible for the increasing *LD* signal, then it may be reasonably expected such change would not be constant (due to varying angles of transitions); therefore the change in *LD* of ct-DNA, exposed to TC-Py and CC-Py to ct-DNA, is primarily due to a decrease in the orientation of DNA. This could be due to the DNA condensing, bending or changing structure from B-DNA; the most likely explanation, given the gel electrophoresis results, is binding of TC-Py and CC-Py to the DNA helix cause the helix to bend.

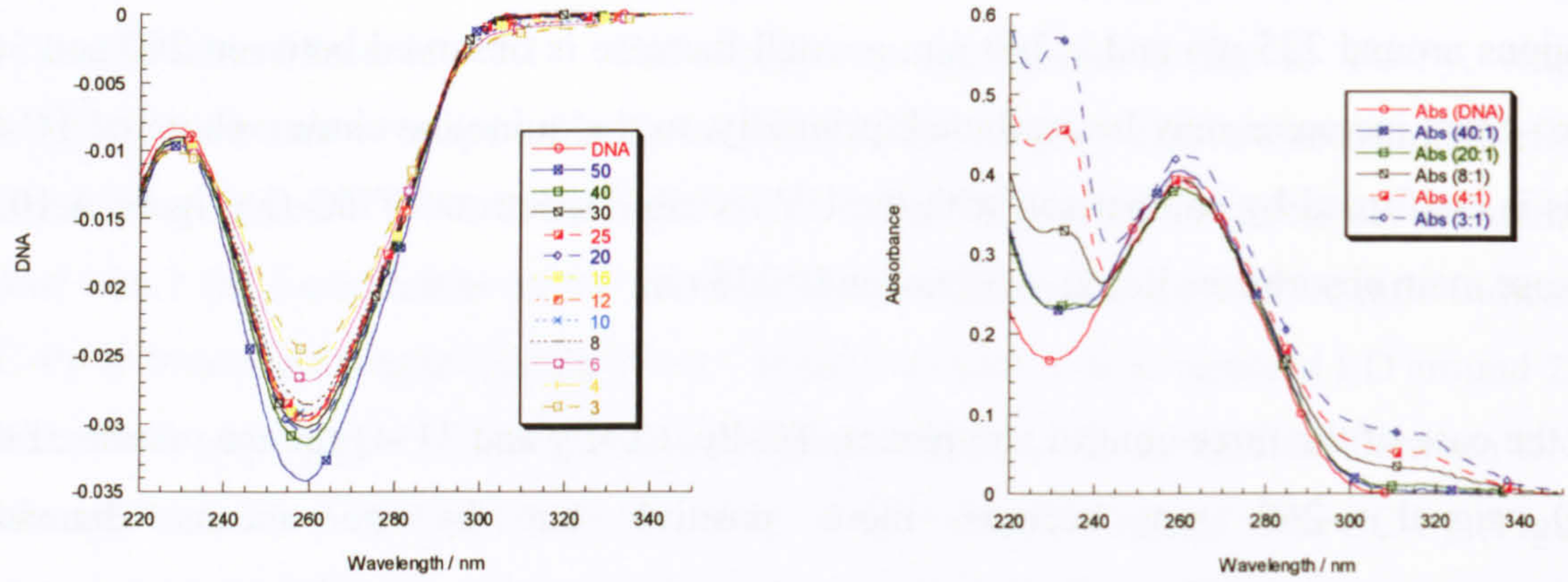

Figure 5.9. The *LD* (A), absorbance spectra (B) and change in *LD* versus loading of TC-Q and ct-DNA (C).

The evidence for TC-Q bending the DNA helix is more pronounced than TC-Py or CC-Py; a decrease in the magnitude of *LD* at 260 nm of ~26 % is accompanied by an increase of absorbance of ~ 10%, thereby indicating TC-Q causes greater DNA bending that TC-Py and CC-Py. Unlike TC-Py and CC-Py, an induced *LD* signal is found above 300 nm, which may be attributed to quinoline and the angle of the transition moment in the region (314 nm), to first approximation, runs along the *z*-axis.

The induced LD can be used to calculate the angle that exists between the z-polarised transition at 314 nm and the helical axis. In determining the angle, three reasonable assumptions have been made: 1) the orientation factor, *S*, is unaffected by complex binding at low loadings; 2) the origin of the absorbance around 314 nm is from bound complex; 3) the complex binding to DNA does not affect the 314 transition. Using the area of

constant LD^r around 260 nm at low loadings (Figure A.12.4) and an angle between nucleobases of 86° allows the orientation factor, *S*, to be calculated from $LD^r = \frac{3}{2}S\left(3\cos^2\alpha - 1\right)$, yielding a result of $S = 0.0514$. Using the same equation, the value of *S* just determined and $LD^r_{314nm} \sim -0.028$ (from A.10.4), the angle of the 314 nm transition of quinoline is calculated to be ~ 63°, relative to the DNA helical axis. The sign of the *LD* signal at 314 nm is negative and the transition angle should be < 54.7°; the disparity between ~63° and < 54.7° may explained by two factors: 1) the DNA helix is bent by the complex, reducing *S*; 2) the reduced *LD* assumes all the absorbance is from bound complex. However a reduction in S (due to DNA bending) and a reduction in reduced LD cause the angle, in calculations, to increase from ~63°. The disparity may be attributed to experimental error, which considering both induced *LD* and absorbance in the region are small with a low signal to noise ratio, is likely to account for the difference.

5.2.4.4. Flow linear dichroism of pyridine-containing steroidal platinum complexes and ct-DNA

The effect of three trans-cationic complexes contain pyridine, TC-ET-3-Py, CC-ET-3-Py, and TC-ET-4-Py on the structure of ct-DNA were studied by flow linear dichroism. The spectra of all three complexes and ct-DNA are very similar; therefore, TC-ET-3-Py is chosen to be representative (the others are contained in Figures A.12.5 - A.12.9). The *LD* spectrum exhibits a negative *LD* signal at ~ 260 nm, assigned to the presence of DNA. Increasing the concentration of complex leads to the negative peak becoming more positive; this is noticeable at very low levels of binding – 100:1 for all three complexes. At such low concentrations of complex the influence of induced linear dichroism can be discounted and the change in the *LD* may be ascribed to a change in the orientation factor, *S*, of DNA, *i.e.* the DNA helix is being bent, a suggestion supported by gel electrophoresis data. The rate of change of *LD* versus complex loading of the ~ 260 nm peak is linear at low loading of complexes up to 30 bp:1, although the overall spectra could be described in terms of a curve or two regions of linearity joined by a curve. The plots (Figure 5.10; Figures A.12.5 - A.12.9) suggest a single binding mode at low loading of complex up to ~ 30:1 where the reduction in the magnitude of the LD signal is linear. Above 30:1 a curve is observed before at higher loading the reduction in the magnitude of the LD signal at 260 nm become linear. The two regions of linearity suggest the complexes have two different modes of binding to DNA with the curved section where the complex begins to attach to DNA in its second binding mode. However, evidence to changes in the shape of the LD signal at 260 nm suggest the influence of a positive induced LD originating from the complex bound to the helix. The rate of change of complex concentration versus ratio of

DNA : complex is not linear – in fact it is described by $y = 200x^{-1}$ – where y is the complex concentration and x the ratio of DNA : complex. The growth of a positive LD arising from the absorbance of the complex in the region of 260 nm would also follow this power rule and may explain curved shape of the LD versus DNA : complex, if a single binding mode was in operation. It is difficult to ascertain which explanation may be applied to the complexes discussed.

(A)

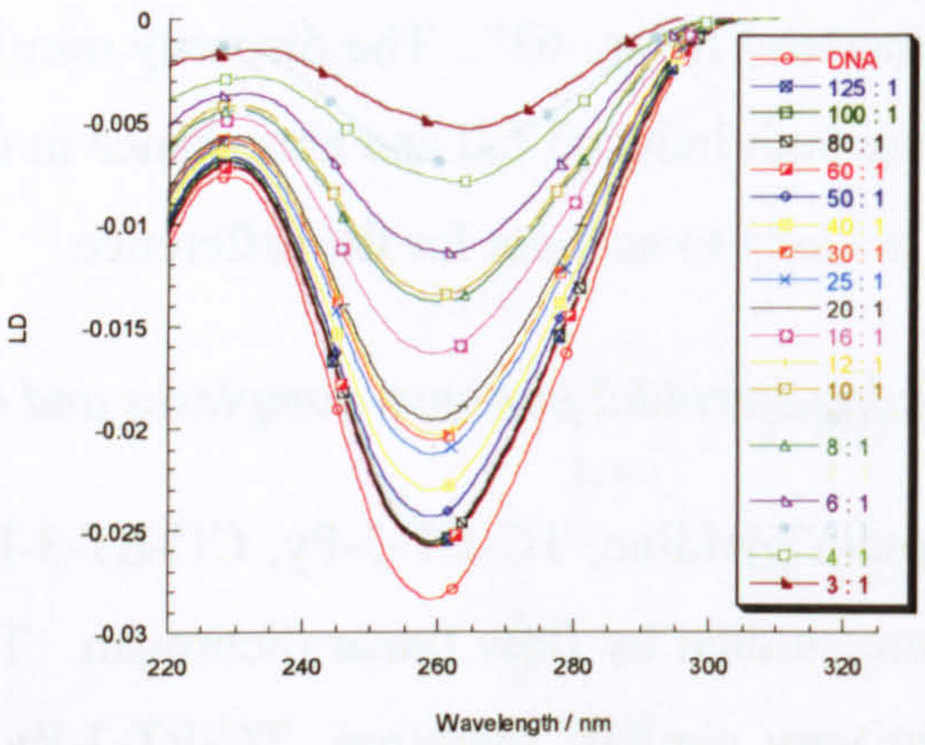

(B)

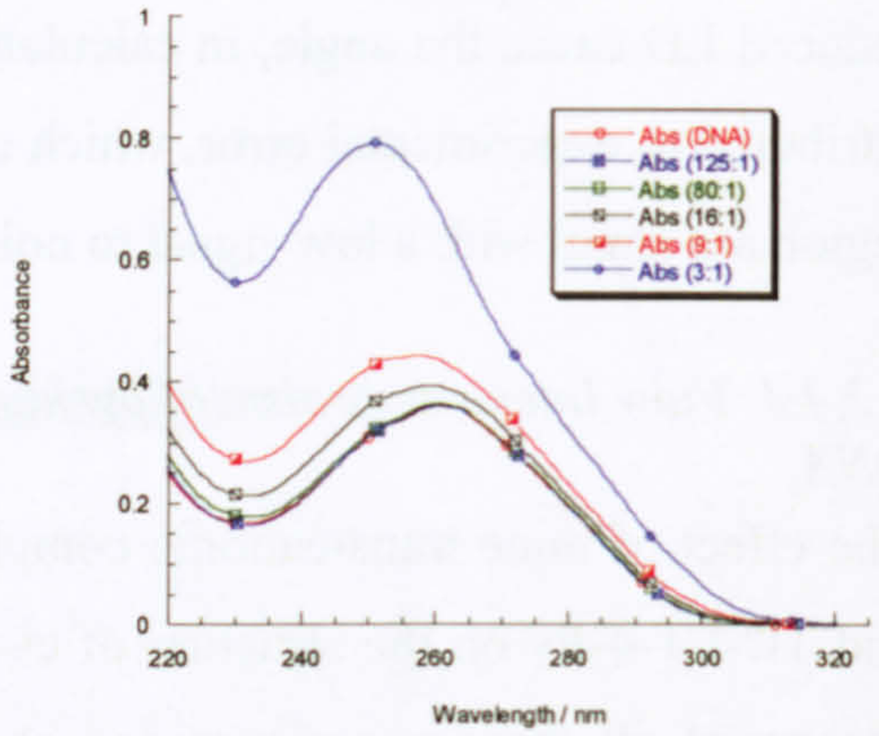

(C)

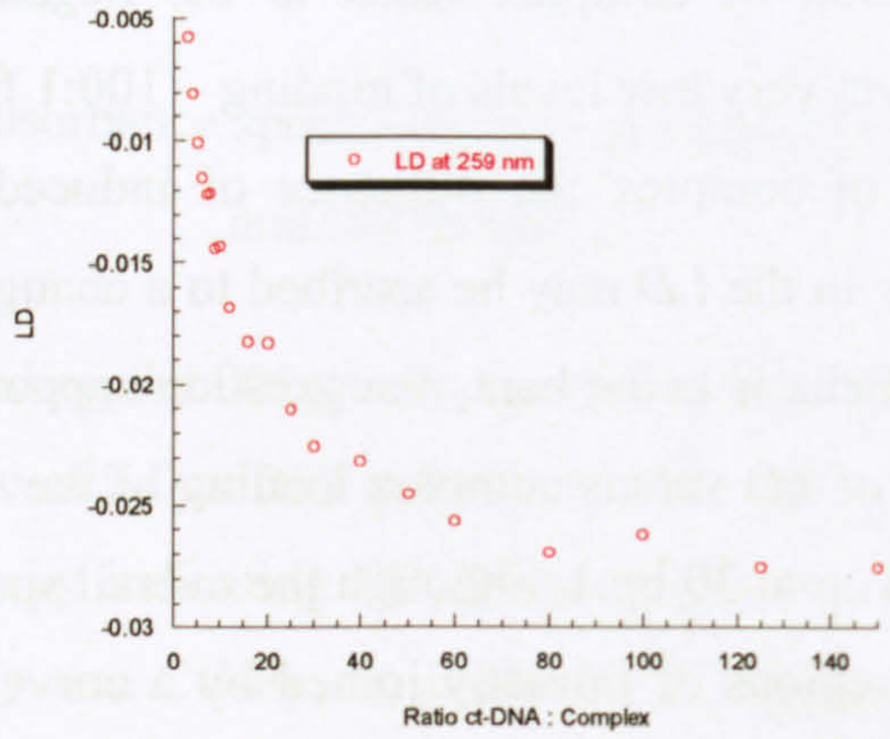

Figure 5.10. The *LD* (A), absorbance spectra (B) and change in *LD* versus loading of TC-ET-3-Py and ct-DNA (C).

The complexes cause a large change to the *LD* of DNA; the % change in absorbance (discounting the very highest loadings) is similar to that of the control complexes whereas the increases to the *LD* signal are very much greater. Table 5.4 is a summary of the data for pyridine-containing steroidal platinum complexes.

Table 5.4. Summary of *LD* data for pyridine-containing steroidal platinum(II) complexes.

	Pyridine-containing steroidal platinum complexes (up to 9:1 DNA:complex)			Control complexes (up to 3:1 DNA:complex)	
Complex	TC-ET-3-Py	CC-ET-3-Py	TC-ET-4-Py	TC-Py	CC-Py
Change in absorbance	23 %	23 %	33 %	17 %	21 %
Change in *LD*	53 %	61 %	36 %	31 %	31 %

The steroidal complexes in Table 5.4 possess a greater ability to affect the *LD* of ct-DNA than non-steroidal complexes at 3 times less the loading; this strongly suggests the steroid-containing complexes bend DNA to a greater extent that either TC-Py or CC-Py; this suggestion is backed up by gel electrophoresis data, whereby steroidal-containing complexes unwound and bent DNA to a greater extent than those not containing steroids. The complex possessing the greatest ability to bend DNA is CC-ET-3-Py, followed by TC-ET-3-Py and TC-ET-4-Py. Interestingly, the order reflects the likely proximity of the steroidal skeleton to the DNA helix; for TC-ET-4-Py the steroid is pointing away from the DNA skeleton, whereas in TC-ET-3-Py the steroid is likely to be in closer proximity due to the 3-substitution of the pyridine ring and even closer in CC-ET-3-Py.

5.2.4.5. Flow linear dichroism of quinoline-containing steroidal platinum(II) complexes and ct-DNA

Solutions of TC-ET-3-Q, TC-ET-6-Q and CC-ET-6-Q were mixed with ct-DNA at various ratios and an LD spectrum taken of each. The linear dichroism spectra of all three complexes are very similar and that of TC-ET-3-Q will be used as an example (other spectra, including repeat experiments can be found in Figure A.12.10 - A.12.14.). The *LD* spectrum of ct-DNA and TC-ET-3-Q shows a single negative peak at 260 nm, originating from ct-DNA. As the amount of complex bound to DNA increases, the *LD* signal magnitude decreases towards zero; the *LD* is significantly affected at ~ 60:1 and above for all three complexes. A summary of the change to the *LD* spectra due to complex binding may be found in Table 5.5.

Table 5.5. The effect of quinoline-containing complexes on the *LD* of ct-DNA.

	Quinoline-containing steroidal platinum complexes (up to 9:1 DNA:complex)			Control complex (up to 3:1 DNA:complex)
Complex	TC-ET-3-Q	TC-ET-6-Q	CC-ET-6-Q	TC-Q
Change in absorbance	34 %	45 %	24 %	10 %
Change in *LD*	51 %	54 %	58 %	26 %

The reduction in the *LD* signal may be attributed to two factors: 1) a reduction in the DNA orientation; 2) positive contributions due to induced *LD* originating from the complexes. Compared to the control complex, all three steroidal complexes cause greater unwinding and bending of the helix; the complexes, in order of ability to bend DNA are CC-ET-6-Q, TC-ET-3-Q and TC-ET-6-Q as indicated by the change in the LD signal, relative to the change in absorbance at 260 nm. At low and high DNA:complex ratios, the rate of change in the *LD* signal is linear but overall the change resembles a curve, reflecting the fact that at higher concentrations of complex, contributions from induced *LD* may begin to affect the signal ~ 260 nm as discussed in § 5.2.4.4.

There is evidence of a positive induced *LD* in the spectra of each complex and DNA; at 270 nm (TC-ET-3-Q); 260 nm (TC-ET-6-Q); 255 and 310 - 320 nm (CC-ET-6-Q); each of these matches a strongly absorbing transition in the absorption spectrum of each complex. The induced *LD* appears as clearly observable bands overlapping the *LD* of ct-DNA, except in the case of the 310 - 320 nm induced *LD* of CC-ET-6-Q and ct-DNA, where it is outside the ct-DNA absorption envelope. The band is weak and calculation of the relative angle of this transition to the DNA helix is not possible. The positive sign of the induced *LD* of CC-ET-6-Q shows the angle of the transition relative to the DNA helix is > 54.7° but little more information may be obtained from the data.

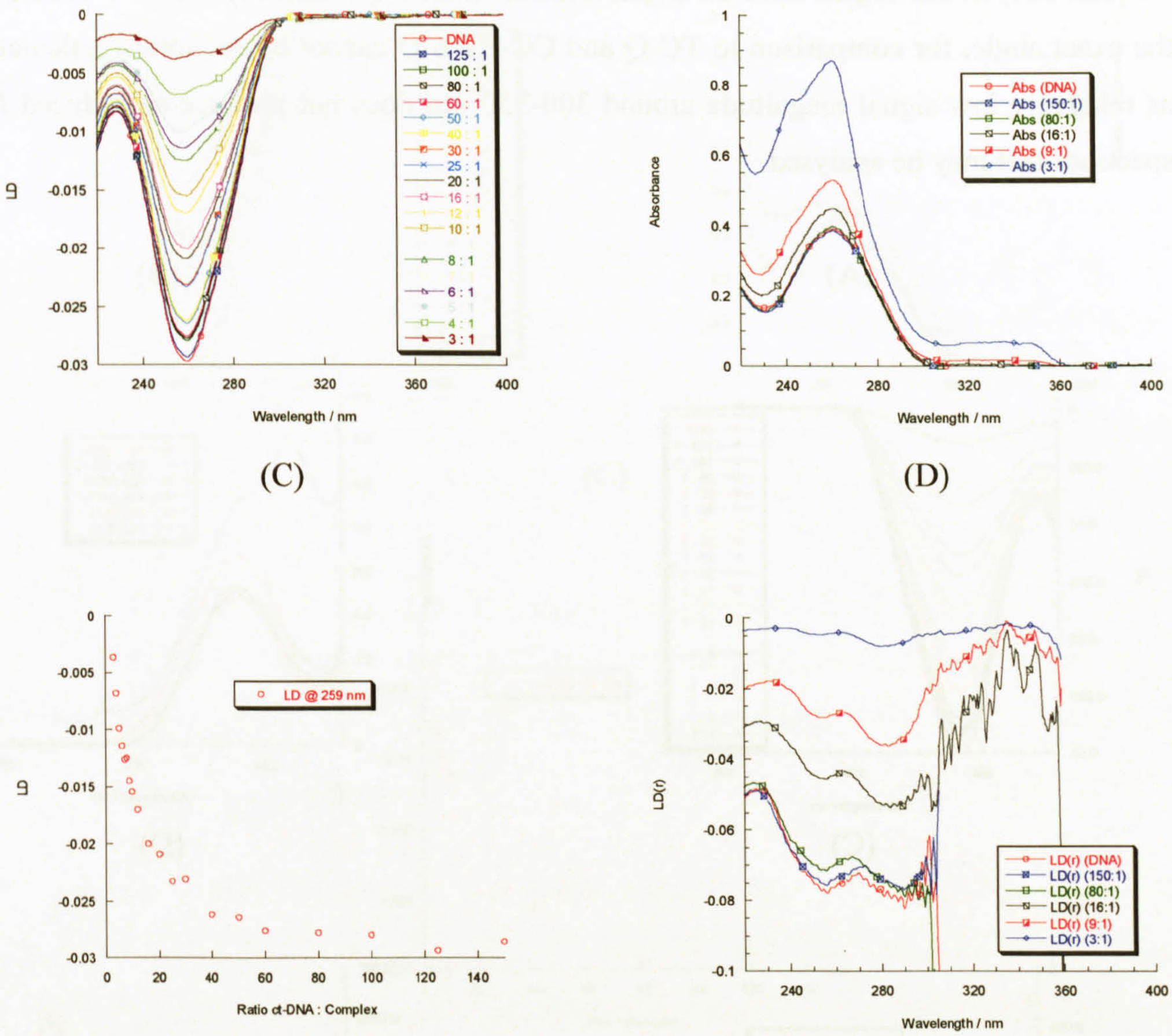

Figure 5.11. The *LD* (A), absorbance spectra (B), change in *LD* versus DNA:complex ratio (C) and LD^r (D) of the complex TC-ET-3-Q with ct-DNA.

5.2.4.6. Flow linear dichroism of isoquinoline-containing steroidal platinum(II) complexes and ct-DNA

Two isoquinoline-containing complexes, TC-ET-4-IQ and CC-ET-4-IQ were assessed for their ability to affect the linear dichroism spectrum of ct-DNA. The spectra of DNA exposed to different concentrations of complex are shown in Figure 5.12 and 5.13; each shows the expected negative signal originating from orientation ct-DNA. Increasing the concentration of complex relative to that of ct-DNA causes the *LD* signal to become less negative for both complexes. Table 5.6 presents a summary of the changes caused by the two complexes to the *LD* spectrum of ct-DNA: it is clear both complexes have a significant effect on DNA as the *LD* approaches very close to zero. The relative changes in absorbance and *LD* signify that an positive induced *LD* cannot account for the change to the *LD* signal; therefore, a change in the orientation factor, *S*, may explain the observed data. This indicates the complexes are causing the complexes to bend the DNA helix. The

positive *LD* observed between 300 - 350 nm in the *LD* spectrum of TC-ET-4-IQ and ct-DNA (Figure 5.12 and A.12.15.) shows the transition moments (almost exclusively from isoquinoline) in this region have an angle, relative to the DNA helix of > 54.7°. However the exact angle, for comparison to TC-Q and CC-ET-6-Q cannot be accurately calculated as relatively low signal magnitude around 300-350 nm does not produce an induced *LD* spectrum that may be analysed.

(A)

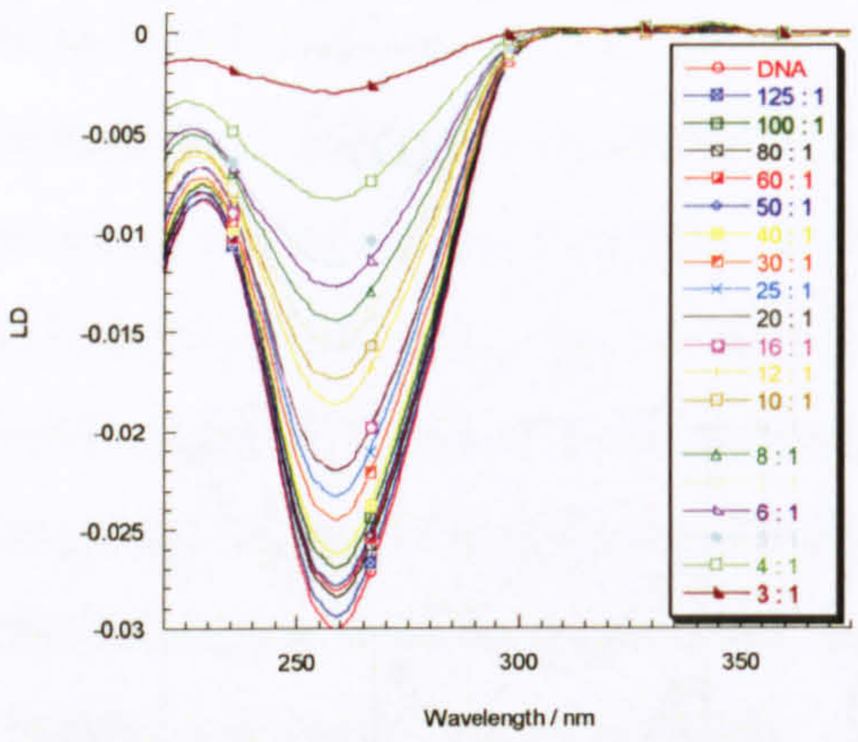

(C)

(B)

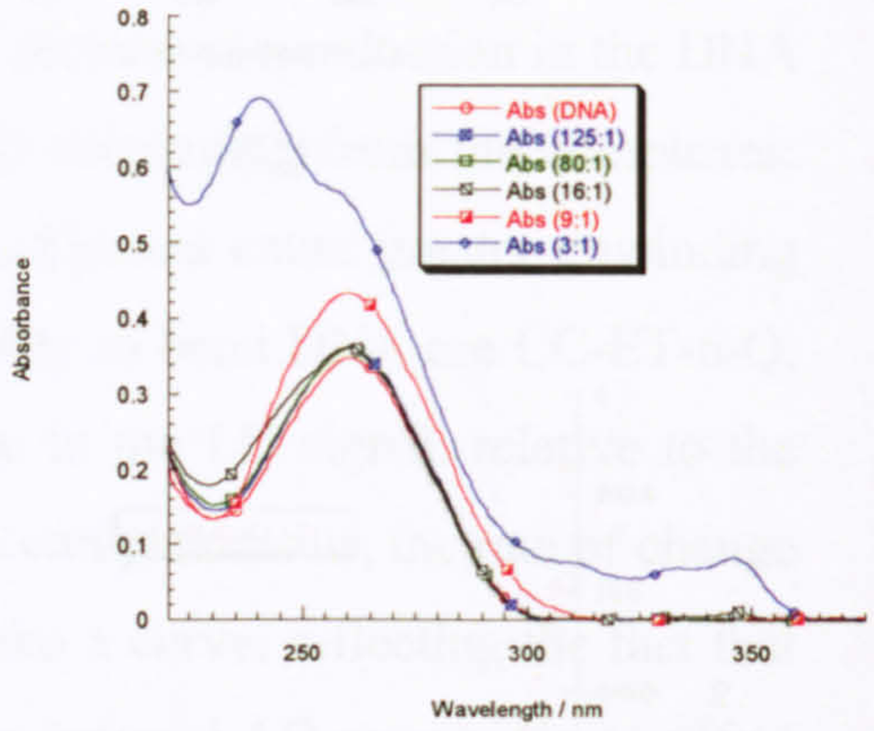

(D)

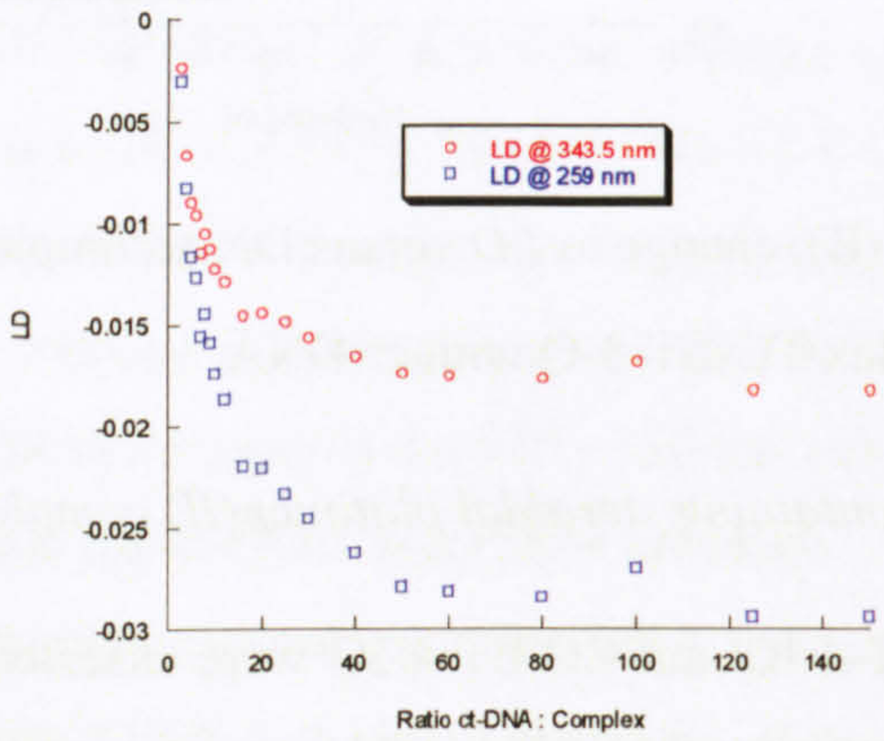

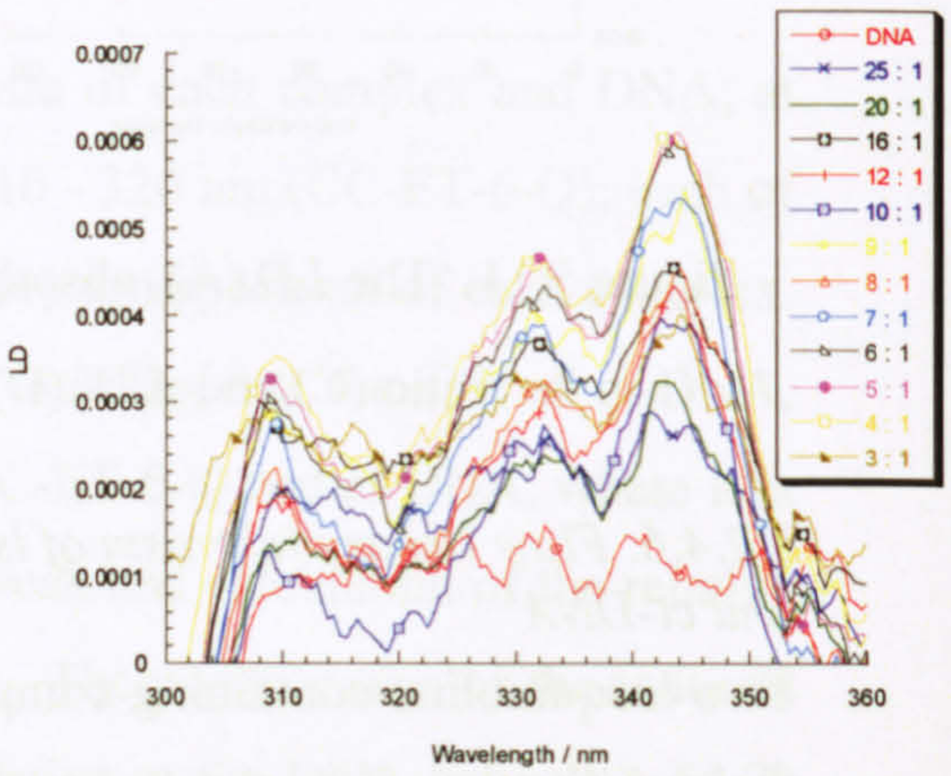

Figure 5.12. The *LD* (A), absorbance spectra (B), change in *LD* versus DNA:complex ratio (C) and expansion of the *LD* spectrum (D) of TC-ET-4-IQ with ct-DNA.

(A)

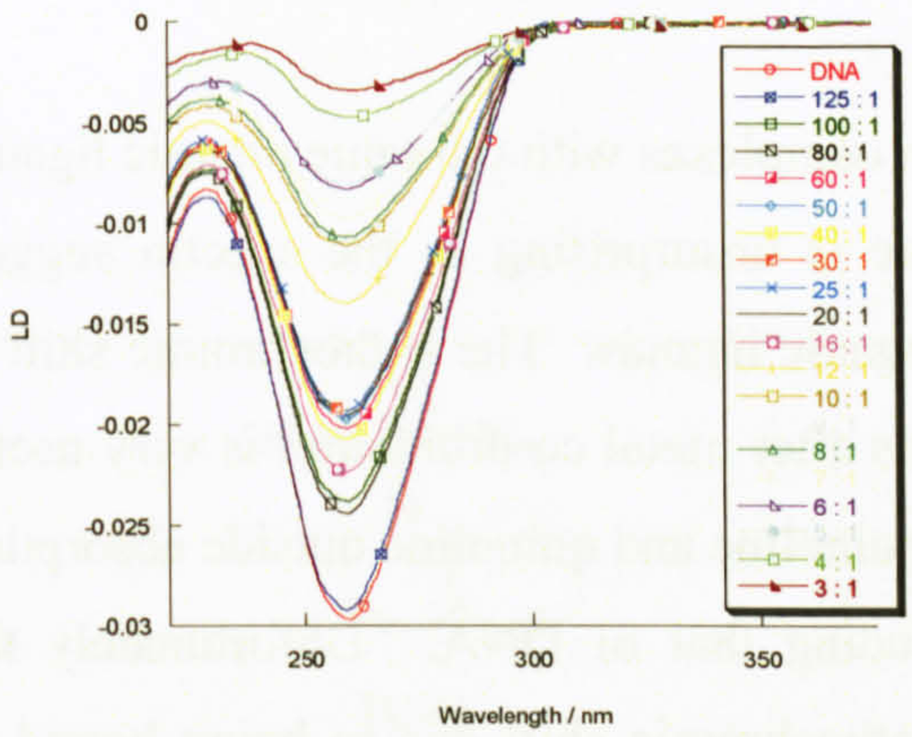

(B)

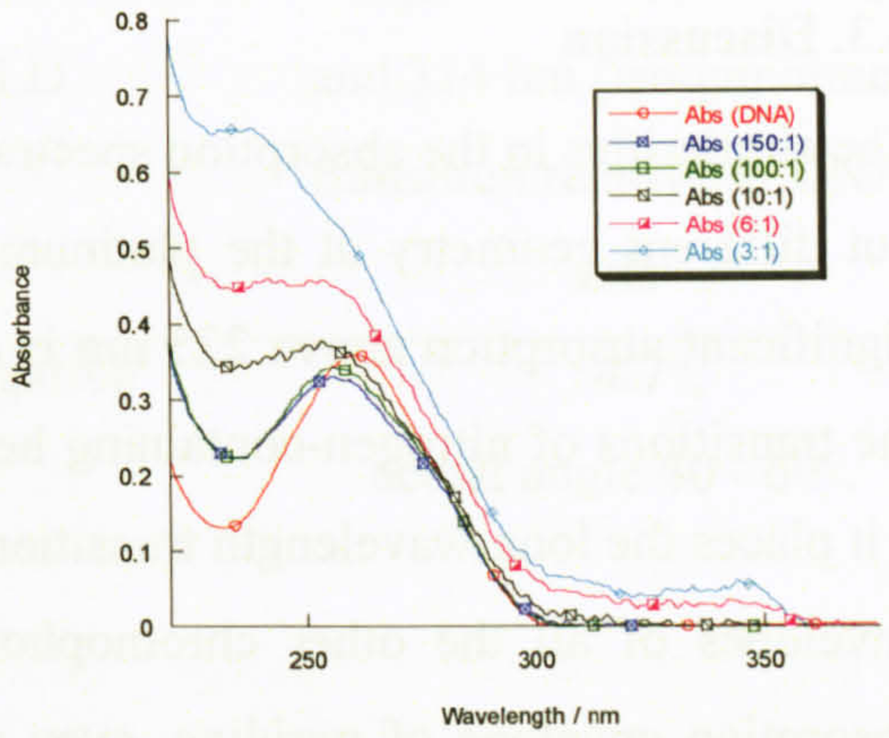

(C)

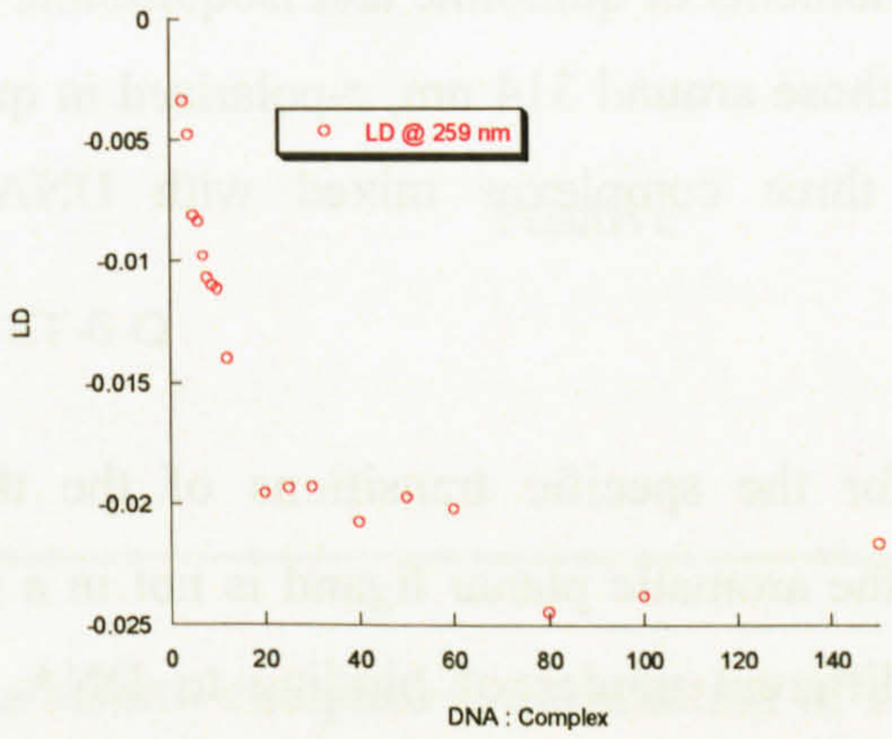

Figure 5.13. The *LD* (A), absorbance spectrum (B) and change in *LD* versus DNA:complex ratio (C) of the complex CC-ET-4-IQ with ct-DNA.

Table 5.6. The effect on the *LD* of ct-DNA by the complexes TC-ET-4-IQ and CC-ET-4-IQ

	Isoquinoline-containing steroidal platinum complex (up to 9:1 DNA:complex)	
Complex	TC-ET-4-IQ	CC-ET-4-IQ
% change in absorbance	18 %	13 %
% change in *LD*	42 %	64 %

The relatively small and large changes in the absorbance and *LD*, respectively due to CC-ET-4-IQ indicate that this complex is potent, with reference to changing the *S* factor of ct-

DNA; in short it is the best complex, as measure by *LD*, in unwinding and bending the DNA helix or possibly causing the DNA to condense.

5.3. Discussion

The similarities in the absorption spectra between complexes with the same organic ligands but different geometry at the platinum(II) centre is unsurprising as the spectra suggest significant absorption above 225 nm is due to organic ligands. The bathochromic shift to the transitions of nitrogen-containing heterocycles after metal co-ordination is very useful – it places the long wavelength transitions of isoquinoline and quinoline outside absorption envelopes of all the other chromophores, including that of DNA. Unfortunately the absorption envelope of pyridine, even with a bathochromic shift due to being bound to platinum still overlaps with absorption arising from DNA.

Whilst all the transition moments of quinoline and isoquinoline have been solved the most important transitions are those around 314 nm, *z*-polarised in quinoline and *y*-polarised in isoquinoline. In total three complexes mixed with DNA exhibited induced LD, summerised in Table 5.7.

The calculated angles for the specific transitions of the three complexes are very interesting; in each case the aromatic planar ligand is not in a similar location indicating the complexes possess different modes of binding to DNA. The negative signal of quinoline in TC-Q and the calculated angle do not match but the disparity may be explained by experimental error – the induced LD signal is small, as is the absorbance in the region. The calculated value does suggest the long axis polarized transition has a magnitude closer to 54.7° as angles of < 20° are unlikely due to steric crowding between the planar ligand and DNA helix. Hence an angle may be suggested of 20 – 55°. This angle is different to that suggested for TC-ET-6-Q, indicating the quinoline moiety in the two complexes occupy different positions, relative to the DNA helix. Following on from this, the two complexes have different binding modes to DNA and this may be ascribed to the presence of the steroidal skeleton. This is true for CC-ET-6-Q, whose angle of the 313 nm transition is > 54.7° to DNA, indicating this transition lies more parallel to the DNA helix that perpendicular. However the transition is ~ 90° to that in quinoline indicating that the isoquinoline rings in CC-ET-6-Q are in a different location, relative to the DNA helix, showing that this complex occupies a different position compared to TC-Q and TC-ET-4-IQ.

Table 5.7. A summary of induced LD signals observed in mixtures of complex and ct-DNA

Complex	Sign of induced LD	Angle of 313 (quinoline) and 314 nm (isoquinoline) transition relative to DNA axis
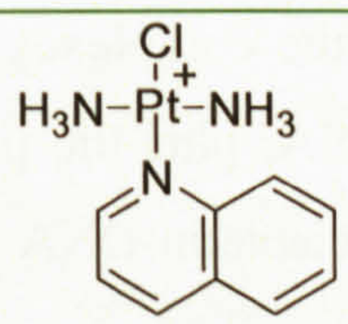 TC-Q	Negative	< 54.7°; actual angle 40 - 60°.
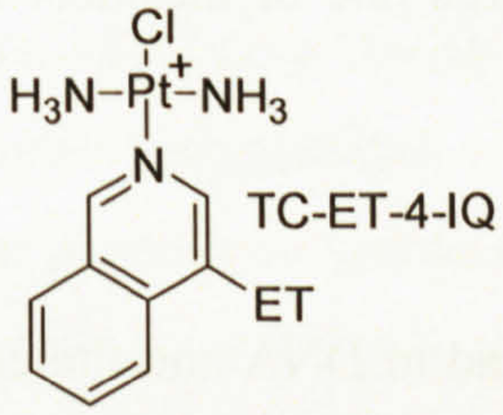 TC-ET-4-IQ	Positive	> 54.7°; actual angle 55 - 75°
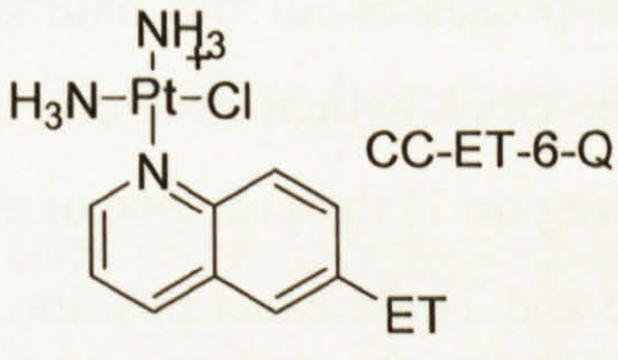 CC-ET-6-Q	Positive	> 54.7°; Actual angle 55 – 75°

In dramatic contrast to the control complexes, the addition of a steroid causes very much greater perturbation to the DNA helix with the *LD* reduced to almost zero as a result of a reduction in the orientation of DNA and the contribution from positive induced *LD* bands hidden by the 260 nm band of DNA. It is difficult to compare the potency of individual complexes as the change in *LD* is due, not only to the helix being bent, but unquantifiable contributions from induced *LD*; however the change in *LD* compared to that of absorbance suggests the most potent complexes are TC-ET-3-Py, CC-ET-3-Py, CC-ET-6-Q and CC-ET-4-IQ, the latter having the largest effect. The large effect to the DNA helix caused by the presence of a steroid is very likely due to an interaction between the DNA helix and the steroidal skeleton. Such large changes are difficult to rationalise without a direct interaction occurring; moreover, cis complexes would force the steroidal skeleton closer to the DNA, and perhaps not surprisingly, trans complexes, whilst potent, are not so efficient at affecting DNA.

The unwinding of the DNA helix, as shown by gel electrophoresis, is an effect common when platinum(II) complexes bind to DNA.[554] In the case of TC and CC complexes the

results are similar and a range of unwinding angles are observed with the CC complexes being more effective at unwinding the helix. When a supercoiled plasmid DNA helix is unwound, it must also bend to accommodate such unwinding; this has been shown by the reduction in the magnitude of the *LD* signal in the spectrum of ct-DNA and complex. When comparing results from gel electrophoresis and *LD*, the most potent complexes at unwinding are also the most potent at bending (measured approximately by reduction in the *LD* signal); the two individual sets of results suggesting the complexes unwind and bend the DNA helix. The unwinding and bending of the DNA, plus the presence of a steroid is likely to produce adducts on DNA that are unlike cisplatin-DNA adducts; the helix is unwound to a greater extent in nearly all cases and the presence of a steroid means a different surface results from the new adduct. This fulfils one of the most important design briefs for new platinum(II) complexes.

5.4. Conclusion

The platinum(II) complexes discussed in this chapter all bind to DNA and the effect they have on the mobility of plasmid DNA in agarose gels possesses all the hallmarks of covalent binding. Once bound, all the complexes affect the DNA helical structure, causing unwinding and bending – but to differing degrees, depending on 1) the presence or absence of a steroidal group attached to an bound aromatic amine and 2) the exact position on the aromatic amine to which the steroidal group is bound. The details of the interactions between the platinum(II) complexes and DNA are not known, nor fully understood. The immediate conclusion is that there is a direct interaction between the DNA helix and the steroidal skeleton. The key conclusion is this: the presence of a steroid transforms an otherwise mediocre complex, in terms of altering DNA structure, to a one causing high levels of unwinding and bending of the helix of DNA.

5.5. Experimental Details

5.5.1. Gel electrophoresis

Plasmid pBR322 (New England Biolabs, UK) and varying amount of complex mixed and incubated for 72 hours. The total solution of 20 μl consists of 1 μl (stock = 1 μg / μl) pBR322, between 1.7 and 17 μl of complex (stock = 600 μM) and the rest with ultra-pure water. After an incubation period of 3 days at 37 °C, 10 μl was removed and added to 3 μl of loading buffer and 10 μl loaded onto an agarose gel. The loading buffer consisted of 30 % glycerol, 0.05% bromophenol blue and 0.025 % cyanol xylene in ultra-pure water. The agarose (Fisher, UK) gel was prepared from 100 ml of 1x TAE buffer and 0.20 g of agarose the gel cast and run using a HE99X Maxi (Amersham Biosciences, UK) submarine

gel kit. The gel was loaded with 8 μl of DNA / loading buffer solution and ran using 1x TAE for 250 minutes at 5 V cm $^{-1}$. The gel was stained after electrophoresis in TAE buffer containing ethidium bromide (0.5 mg ml^{-1} for 40 minutes. The gel was visualized using a UVIdoc Platinum system (UViDoc, Cambridge, UK) at 312 nm.

5.5.2. Machine settings

All UV/vis. spectra were recorded on a Jasco V-570 spectrophotometer operating with the following parameters: dual beam mode; start wavelength, 400 nm; end wavelength, 200 nm; data pitch, 0.5 nm; scanning mode, continuous; scanning speed, 200 nm per min; response, 0.25 seconds; bandwidth, 2.0.

All *LD* spectra were recorded on a Jasco J-715 spectropolarimeter modified for *LD* spectroscopic measurement. The spectropolarimeter was operated in *LD* mode with the following parameters: sensitivity, 100 mdeg; start wavelength, 400 nm; end wavelength, 200 nm; data pitch, 0.5 nm; scanning mode, continuous; scanning speed, 200 nm per min; response, 0.25 seconds; bandwidth, 2.0; accumulation, 4. The *LD* experiments were conducted in duplicate and consistent results were obtained.

5.5.3. Film linear dichroism spectroscopy

A 20 % w/v solution of quinoline in chloroform was added dropwise to a 5 cm x 3 cm strip of PE until the PE was covered in the solution. Once the chloroform had evaporated, further chloroform was added, covering the PE to aid absorption of quinoline into the PE, before more quinoline solution was added, dropwise to begin the process again. Once enough quinoline – as defined by good spectral quality was added – the PE was briefly washed in chloroform and excess chloroform removed using a hair dryer briefly. The PE was immediately stretched to 2.5 times its previous length and a *LD* spectrum obtained.

5.5.4. Flow linear dichroism spectroscopy

Stock solutions of ct-DNA (500 μM) and complex (500 μM) were mixed in varying proportions and made up to 50 μl with 1X TAE to achieved DNA:complex ratios of 150:1, 100:1, 80:1, 70:1, 60:1, 50:1, 40:1, 30:1, 25:1, 20:1, 16:1, 12:1, 10:1, 9:1, 8:1, 7:1, 6:1, 5:1, 4:1 and 3:1. The solutions were incubated at 37 °C for 3 days. The spectrum was measured in a couette flow cell containing 20 μl of solution, rotating at ~ 1000 rpm, ensuring no bubbles were present in the cell. Each experiment was repeated twice and found to duplicate.

BLANK IN ORIGINAL

Chapter Six – The biological effects – *in vitro* – of steroidal platinum(II) complexes

6.1. Introduction

Biological evaluation – evaluating the effect of substances *in vitro* – is the first step in determining whether the complexes synthesised possess any potential in becoming clinically useful drugs. The primary question – are these complexes cytotoxic? – may be answered using a growth inhibition assay commonly used to assess platinum(II) complexes;[557] the second question – is cytotoxicity independent of steroid concentration – may yield information regarding if the steroid component is having any effects. This chapter will detail the biological evaluation of TC and CC steroidal platinum(II) complexes against the non-steroidal complexes: TC-Py, CC-Py and TC-Q.

6.2. Results

The inhibitor effects were ascertained using three cell lines: an ER+ and AR+ ovarian cancer cell line, SKOV-3; an ER+ and AR+ breast cancer cell line, T47D; and an ER- and AR- immortalised breast cell line HBL-100; the results may be found in Figure 6.1. The IC_{50} of a complex is the concentration of substance required to inhibit 50 % of growth, relative to a positive control; the higher the IC_{50}, the less cytoxic a complex is, IC_{50} values under 50 μM are considered as hits. It should be noted that the cytotoxicity of cisplatin, very generally, is often < 15 μM in many cell lines.

In the three cell lines studied the IC_{50} of cisplatin is around that expected and in SK-OV3[558] and HBL-100, although higher than some reports for T47D.[559, 560] It is immediately apparent that the control complexes possess poor cytotoxicity towards the three cells lines with IC_{50} values between ~ 75 – 240 μM, greatly more than that of cisplatin (6 – 32 μM) and steroidal platinum(II) complexes (12.4 – 70 μM). The order of resistance of the three cell lines towards steroidal platinum complexes is, generally, SK-OV-3 > T47D > HBL-100 and reflects the intrinsic sensitivity of the three cell lines to platinum(II) complexes. The fact that HBL-100 is more sensitive to the complexes is unsurprising; being a non-tumourigenic cell line it is unlikely to possess the resistance mechanisms so often associated with tumourigenic cell lines.[248] Another important observation is that the cytoxicity of *cis*-cationic complexes is great than that of trans-cationic complexes, indicating adoption of a cis-geometry rather than trans imparts greater activity; an important exception being TC-Py and CC-Py, where no significant difference is observed. The fact that TC-Py and CC-Py possess very much the same levels of

cytotoxicity, whereas TC-ET-3-Py and CC-ET-3-Py do not, suggests the presence of the *cis* geometry *and* steroidal ligand impart cytotoxicity; although this cannot be confirmed for the remaining complexes. For the other complexes the presence of the steroid skeleton imparts several fold greater activity compared to the controls; comparisons with the steroidal ligand itself are superfluous: a potentially androgenic steroidal ligand would not be considered as a treatment for breast cancer, although the IC_{50} of the ligand ET-3-Py is very much greater (200 μM).[561]

The most interesting complexes are CC-ET-3-Py and CC-ET-6-Q; they are the most active of all the steroidal platinum(II) complexes, in some cell lines they are more cytotoxic than cisplatin; however nearly all of the complexes may be considered to possess good cytotoxicity towards the cell lines studied.

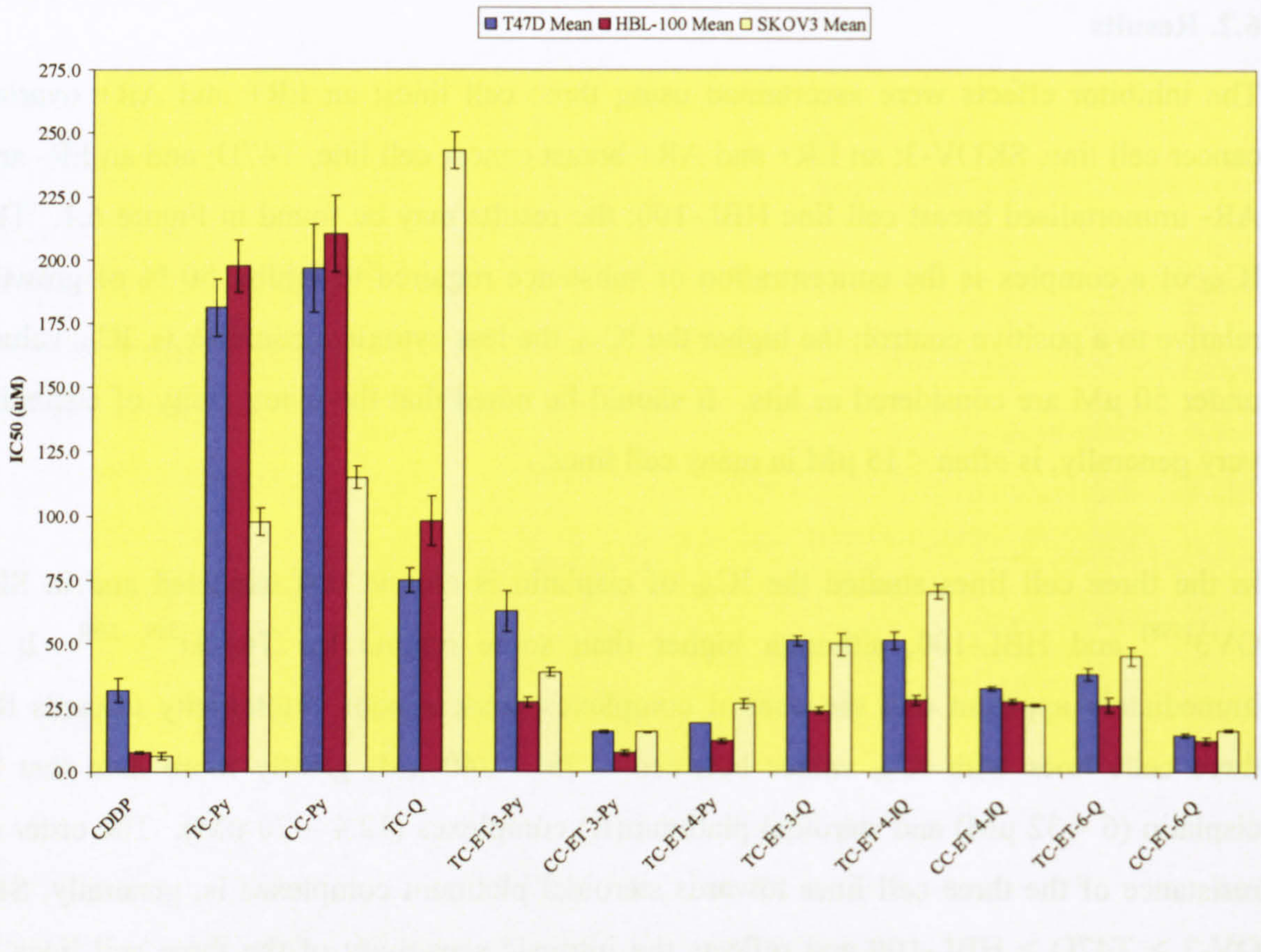

Figure 6.1. The IC_{50} values for a range of platinum(II) complexes.

Table 6.1. The cytoxicity of a range of platinum(II) complexes

Complex	SK-OV-3 IC_{50} (μM)	T47D IC_{50} (μM)	HBL-100 IC_{50} (μM)
CDDP	6 ± 1	32 ± 5	8 ± 0.5
TC-Py	98 ± 6	181 ± 11	198 ± 10
CC-Py	115 ± 5	197 ± 17	210 ± 15
TC-Q	243 ± 7	75 ± 5	98 ± 10
TC-ET-3-Py	39 ± 2	63 ± 8	27 ± 2
CC-ET-3-Py	16 ± 0.5	16 ± 0.5	7 ± 1
TC-ET-4-Py	27 ± 2	19 ± 0.1	12 ± 1
TC-ET-3-Q	50 ± 5	51 ± 2	24 ± 1
TC-ET-4-IQ	71 ± 3	51 ± 4	28 ± 2
CC-ET-4-IQ	26 ± 0.5	33 ± 1	28 ± 1
TC-ET-6-Q	45 ± 4	39 ± 2	26 ± 3
CC-ET-6-Q	16 ± 1	14 ± 1	12 ± 1

One of the hypotheses of this thesis – the addition of a testosterone skeleton to a platinum(II) complex can aid uptake via transportation by steroid receptors – can be tested by removing a significant proportion of androgens from the medium in which the cells are cultured; in this case the cytotoxicity should not be modulated if steroids are removed. A stripping technique (to remove lipids, *e.g.* steroids) using charcoal / dextran, removes significant amounts of steroids from the media,[562] although phenol red - which has weak estrogenic properties[563] – remains. Removing too many growth factors may cause poor cellular growth and is to be avoided. Figure 6.2 shows the ratio of the IC_{50} values in normal media (IC_{50}(+)) compared to reduced steroid media (IC_{50}(-)) and displays some very interesting results. Given the errors present in cell tests, ratios of between 0.5 and 2 are considered normal and values outside this range indicate the cytotoxicity of the complex is modulated, in part at least, by steroid concentration.

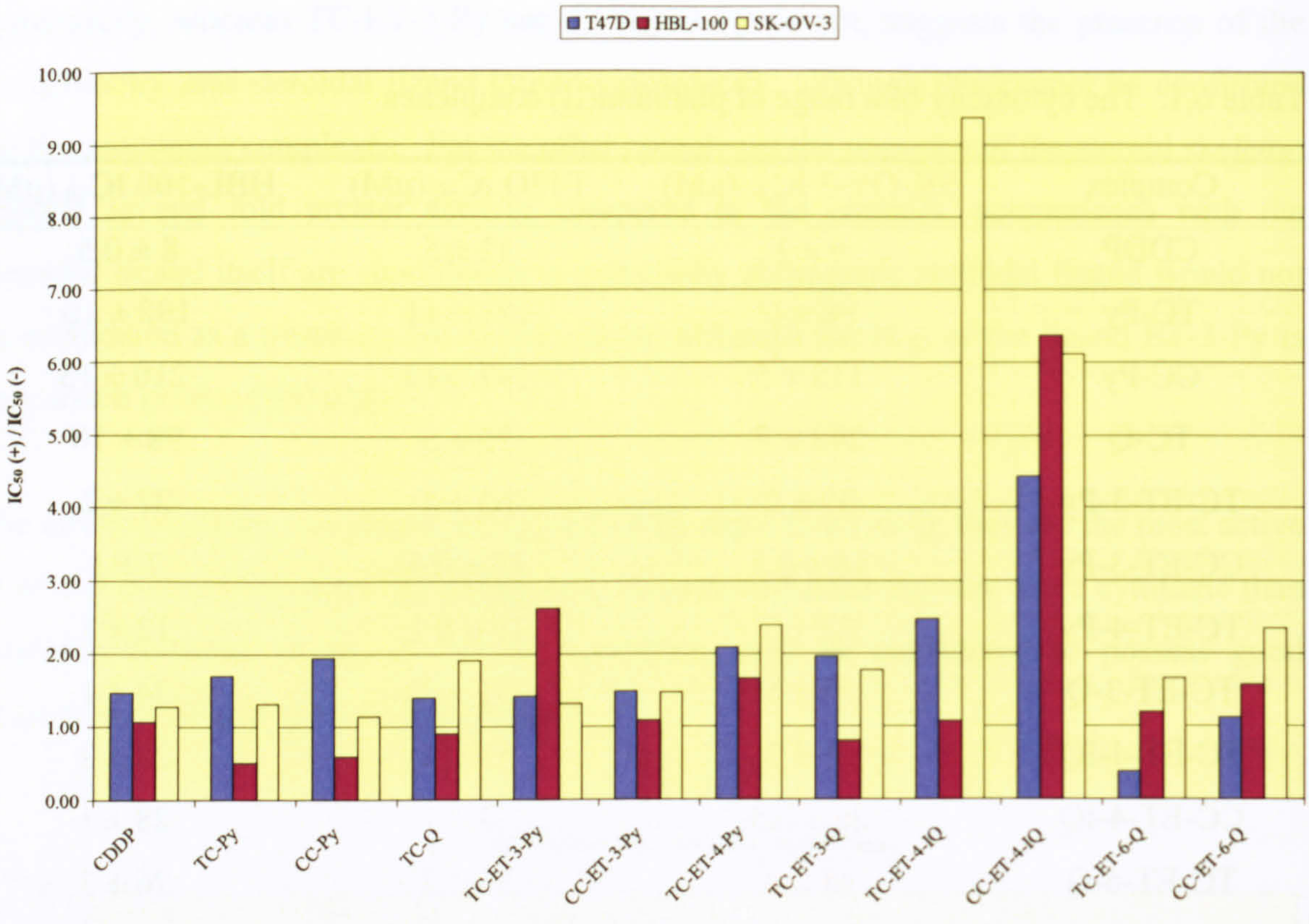

Figure 6.2. The ratio of IC_{50} values in steroid-contaning (+) and steroid-reduced (-) cell media

The most striking feature is the significant enhancement of cytotoxicity of CC-ET-4-IQ between ~ 4.4 – 6.4 fold, observed in all cell lines at reduced steroid concentration; the isomer TC-ET-4-IQ has striking enhancement in SK-OV-3 of ~ 9.4 fold and also ~ 2.4 in T47D; as does TC-ET-4-Py (in T47D and SK-OV-3); in addition to CC-ET-6-Q in SK-OV-3. This indicates perhaps other factors are determining the cytotoxicity of the complexes in steroid-reduced media.

Table 6.2. The cytotoxicity of platinum(II) complexes using media with (+) and without (-) steroids.

Complex	SK-OV-3 IC_{50} (μM)		T47D IC_{50} (μM)		HBL-100 IC_{50} (μM)	
	+ steroids	- steroids	+ steroids	- steroids	+ steroids	- steroids
CDDP	6 ± 1	11 ± 4	32 ± 5	22 ± 2	8 ± 0.5	7 ± 0.5
TC-Py	98 ± 6	75 ± 2	181 ± 11	106 ± 24	198 ± 10	385 ± 33
CC-Py	115 ± 5	101 ± 21	197 ± 17	102 ± 14	210 ± 15	351 ± 3
TC-Q	243 ± 7	127 ± 3	75 ± 5	54 ± 4	98 ± 10	108 ± 3
TC-ET-3-Py	39 ± 2	30 ± 1	63 ± 8	44 ± 2	27 ± 2	10 ± 4
CC-ET-3-Py	16 ± 0.5	11 ± 1	16 ± 0.5	11 ± 0.5	7 ± 1	7 ± 1
TC-ET-4-Py	27 ± 2	11 ± 0.5	19 ± 0.1	9 ± 1	12 ± 1	7 ± 0.5
TC-ET-3-Q	50 ± 5	28 ± 1	51 ± 2	26 ± 2	24 ± 1	30 ± 1
TC-ET-4-IQ	71 ± 3	7 ± 1	51 ± 4	21 ± 1	28 ± 2	26 ± 0.5
CC-ET-4-IQ	26 ± 0.5	4 ± 0.1	33 ± 1	7 ± 0.5	28 ± 1	4 ± 1
TC-ET-6-Q	45 ± 4	27 ± 2	39 ± 2	105 ± 11	26 ± 3	22 ± 0.5
CC-ET-6-Q	16 ± 1	7 ± 0.5	14 ± 1	13 ± 0.5	12 ± 1	7 ± 0.5

Perhaps the most significant result is that of TC-ET-6-Q in T47D; reducing the steroid concentration causes proliferation of the cell line and TC-ET-6-Q is androgenic at low steroid concentrations. This suggests that the effects of the complexes may be two fold: the IC_{50} is a balance between growth inhibition and proliferation, due to the steroidal ligand and platinum(II) centre, respectively; this has been found previously by Jaouen *et al.*[428] linking tamoxifen to platinum(II). Almost all the increases in cytotoxicity are observed for SK-OV-3 and T47D and as these contain the greatest concentration of androgen receptors, this gives validity to the results observed, although the increased activity of TC-ET-3-Py and CC-ET-4-IQ in HBL-100 may indicate other factors in addition to steroid concentrations may modulate the IC_{50}. Cisplatin, TC-Py, CC-Py, TC-Q, CC-ET-3-Py, TC-ET-3-Q are complexes whose IC_{50} is not significantly different in the presence or absence of steroids; the IC_{50} of other complexes is modulated.

6.3. Discussion

In relation to treating cancerous cells with cytotoxic drugs, IC_{50} values are important; they give the first insight into the biological activity of a complex and any structure activity rules that may, or may not exist. When normal levels of steroids are present in the media

the cytotoxicity of the steroidal complexes is very good, in some cases excellent (*i.e.* better than cisplatin) and they represent potential cytotoxic anti-tumour drugs. The presence of an ethynyltestosterone results in substantially increased cytoxicity of the complex relative to the control and in the case of TC- and CC-ET-3-Py, the steroidal ligand itself;[561] this is something that did not occur in previous attempts to link bio-active ligands to platinum complexes.[339, 340, 347, 348] It should be stated at this point that *in vitro* activity might not directly relate to *in vivo* activity; there exists a very large difference between the two environments and cytotoxicity, *in vivo*, depends on many more factors than *in vitro*.

The change in the IC_{50} values for some complexes when low levels of steroids are present in the media indicates steroids modulate cytotoxicity – as would be expected to happen – of steroidal platinum(II) complexes; however, increased cytotoxicity in the cell line HBL-100 of TC-ET-3-Py and CC-ET-4-IQ indicates that other factors are involved that may, or may not relate to any androgenic effects. Lower levels of androgens may promote increased levels of complex binding to the androgen receptor and it is very difficult to envisage the changes this may, or may not induce. Despite this, it is reasonable to suggest that androgens do, in part, regulate the cytotoxicity of steroidal platinum(II) drugs in the cell lines studied. Reports whereby oestrogens regulate cytotoxicity of cisplatin, by overexpression of the HMGB-1 protein, possibly shielding *cis*-GG and *cis*-AG adducts from repair[564] and platinum(II) complexes interfering with oestrogen levels,[565] show that simply increasing the level of a steroid can have effects using other bio-molecules or pathways. There are more reports of hormonal moieties, which may be platinum complexes themselves, sensitising cells to platinum(II) drugs[47, 564-566] and, it cannot be said that simply removing androgens from the media could result in greater amounts of complex being bound to the androgen and, possibly transported to the nucleus causing cell death – the effects are more complicated.

6.4. Conclusion

The cytotoxic assays have determined that the addition of ethynyltestosterone to an aromatic amine bound to a platinum complex of the formula $[Pt(NH_3)_2(L)Cl][NO_3]$ imparts cytotoxicity compared to the complex alone, or in the case of complexes containing ET-3-Py, to the steroidal ligand. Several of the complexes were more cytotoxic in T47D than cisplatin. The cytotoxicity of many of the steroidal complexes is modulated by steroid concentration and the removal of other androgens for the AR leads to more active complexes.

6.5. Materials and Methods

Tissue culture flasks, 96 well plates, RPMI 1640, DMEM, L-glutamine, trypsin-EDTA, HEPES, sodium pyruvate and FCS were obtained from Sigma, UK. Thiazolyl blue tetrazolium bromide (MTT) and DMSO were from Avocado, UK.

Cells were grown in RPMI 1640 or DMEM in 10 % FCS supplemented with 1% L-glutamine, 1% HEPES buffer and 1% sodium pyruvate. Cells were routinely cultured in the absence of antibiotic and antimycotic. FCS was stripped of steroid using a standard protocol and added to the media as normal.[562]

The MTT assay[557] was carried out using 96 well plates. Cells were harvested in logarithmic growth, 15,000 cells were seeded per well and left overnight to attach. The cells were treated, in quadruplicate with 6 difference concentrations of complex dissolved in fresh media; the range of concentrations used is dependent on the complex. The cells were incubated for 72 hours and 20 µl of thaizolyl blue tetrazolium bromide (1mg / ml, 0.2 µm filtered) added. The cell were further incubated for 2 hours for HBL-100 and SK-OV-3 and 3 hours for HBL-100. The media was carefully removed by aspiration and the cells lysed using lysis buffer (20 µl) and 200 µl of DMSO added to dissolve the cells. Absorbance was measured using a 96-well plate reader (Fisher, UK) set at 570 nm. Each cell line was investigated beforehand to determine the correct cell numbers to initially seed and the required amount of time exposed to thiazolyl blue tetrazolium bromide to ensure sensitivity and accuracy.

BLANK IN ORIGINAL

Chapter Seven – The efficacy of steroidal platinum(II) complexes

Judging the efficacy of platinum(II) complexes as potential targeted cytotoxic drugs requires assessing and determining the significance of the information relating to each complex. To this end Tables 7.1 – 7.5 contain a summary of all the information, including – hydrolysis, binding to model nucleobases, unwinding and bending of DNA, and IC_{50} value and factor this reduces with reduced steroids in the cell media.

The efficacy of the complexes refers to the ability of complexes to affect DNA and cause cytotoxicity, both are very important aspects of potential platinum(II) drugs for cancer treatment. The non-steroidal complexes in Table 7.2 possess poor efficacy; they exert few structural changes and the IC_{50} values signify the complexes cannot be considered to possess cytotoxicity near to that required for an anti-metastatic drug. The binding of non-steroidal complexes to DNA likely results in a relatively small mono-functional adduct that causing few structural changes to the DNA helix. Previous reports have shown *some* mono-functional adducts can cause relatively large DNA distortions,[567] including – $[Pt(NH_3)_2(L)Cl]^+$ - type complexes with large heterocyclic ligands,[568-570] particularly with a cis-geometry;[571] also a *few* mono-functional platinum(II) complexes possess impressive cytotoxicity.[332] The complex [Pt(dien)Cl][Cl] can promote a transition from B-DNA to another called Z-DNA – a dramatic change -, which is not seen for the non-steroidal complexes[543] nor steroidal complexes[572] and in the case of the former, these have very little effect on the DNA structure in terms of unwinding and bending. Hollis *et al.*[332] report similar complexes possessing poor or no cytotoxicity – non-steroidal TC-Py, CC-Py and TC-Q fall into this category with two very active complexes. Interestingly, TC-Q is more active than the pyridine-containing complexes and this may be a function of the larger size of the aromatic ligand forcing slightly greater distortion to the DNA helical structure – this has previously been suggested for triamine-type complexes.[571] The fact that the complexes are no more active in media stripped of steroids indicates cytotoxicity is not modulated by steroid concentration and that the cells are not sensitised to platinum(II) drugs due to substantially reduced levels of steroids. In short, the three non-steroidal complexes are not candidates for cytotoxic drugs.

Table 7.1. Summary for TC-Py, CC-Py and TC-Q

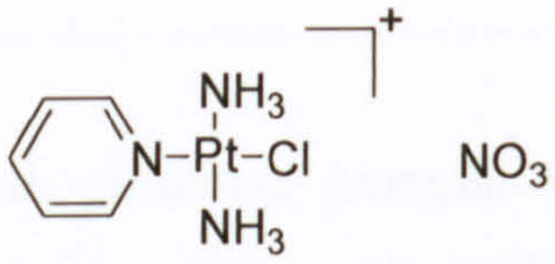 **TC-Py**	**Hydrolysis**	Some detected
	Binding to 5'-GMP / 5'-AMP	Reacts with buffer
	Gel Electrophoresis	Unwinds DNA < 5°
	Linear Dichroism	ΔLD_{260nm} – 31 %
		ΔAbs_{260nm} – 17 %
		Small amount of bending
	IC_{50} (HBL-100 / T47D / SK-OV-3	198 μM / 181 μM / 98 μM (Little change without steroids)
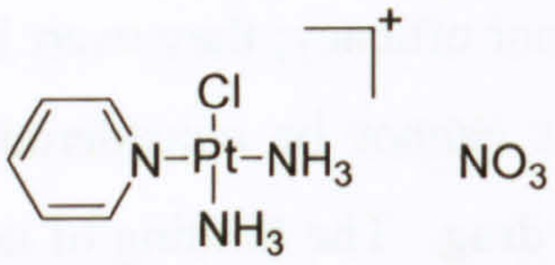 **CC-Py**	**Hydrolysis**	Some detected
	Binding to 5'-GMP / 5'-AMP	Reacts with buffer
	Gel Electrophoresis	Unwinds DNA < 5°
	Linear Dichroism	ΔLD_{260nm} – 31 %
		ΔAbs_{260nm} – 21%
		Small amount of bending
	IC_{50} (HBL-100 / T47D / SK-OV-3	210 μM / 197 μM / 115 μM (Little change without steroids)
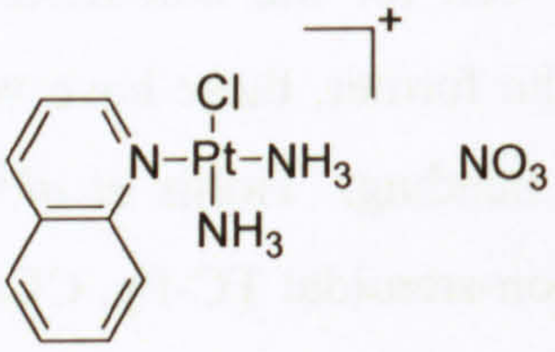 **TC-Q**	**Hydrolysis**	None detected
	Binding to 5'-GMP / 5'-AMP	Reacts with buffer
	Gel Electrophoresis	Unwinds DNA < 5°
	Linear Dichroism	ΔLD_{260nm} – 26 %
		ΔAbs_{260nm} – 10%
		Small amount of bending
	IC_{50} (HBL-100 / T47D / SK-OV-3	98 μM / 75 μM / 243 μM (Little change without steroids)

The results of the various experiments show the presence of an ethnynyl-testosterone moiety on a bound aromatic ligand results in complexes substantially altering the structure of DNA and possessing cytotoxicity; what were complexes resulting in low levels of unwinding and bending of DNA and poor cytotoxicity, have now become very much more active because of the addition of an ethynyl-testosterone component. It should be noted

that steroidal platinum(II) complexes are, in certain aspects, similar to those without steroids; all hydrolyse and appear to the react with nucleobases via direct nucleophilic substitution, as opposed to via solvent species (which are also produced). Drawing parallels between the interaction of nucleobases and DNA, the results suggest the complexes may bind to DNA without the need to hydrolyse; there is support for this from the literature regarding triamine complexes,[547, 548] however hydrolysis is the rate limiting step between ct-DNA and cis-$[Pt(NH_3)_2(4\text{-methylpyridine})Cl][NO_3]$.[573] Regarding the complexes under study, the striking absence and presence of, respectively, parent compound and hydrolysed version in the mixture of steroidal metal complex and base is very persuasive: it is the parent compound that primarily reacts. Once hydrolysed the agarose gels and linear dichroism results show an interaction occurs between DNA and bases, with the steroid crucially influencing the degree to which the complex changes the DNA structure. The gel and LD results complement each other: gels illustrate DNA unwinding, whilst LD shows the helix bends. The nature of a helix is such that to accommodate a bend, the helix is required to unwind/wind-up and the presence of the steroid increases the ability of the complex to do both, in many cases greater than that of cisplatin and other platinum(II) complexes. The steric bulk of the steroid may require greater unwinding / bending of the helix to accommodate the complex and in the case of CC complexes, this is a very persuasive argument, given the similarly large unwinding angles observed ($\geq 19°$) of those complexes. The LD data certainly suggests the presence of the ethnynyltestosterone component causes bending of the helix, complementary to the gel studies showing unwinding that may be explained by a steroid – helix interaction. The nature of the likely interaction between steroidal skeleton and DNA is important and it has been known since at least the 1970's that steroid-like molecules can interact with DNA[574-579] using hydrophobic interactions to stabilise kinks[577] and 3-way DNA junctions[580] – interactions that directly relate to the steroidal complexes under discussions. Whilst the exact interaction between DNA and steroidal skeletons remains elusive and not enough data is available to form structure-activity relationships some conclusions can be drawn. The steroidal skeleton, in many studies bile acid residues, stabilise terminal A:T pairs (via van der Waals interactions) on synthetic oligomers.[575] – a situation not so relevant in the case of steroidal platinum(II) complexes. Of more relevance, perhaps, is those using steroidal skeletons substituted with charged polyamines in the 3 and 17 positions.[577] Whilst the charged moieties, perhaps unsurprisingly, interact with the negative phosphodiester backbone, there is evidence for a roles for the large hydrophobic surface area comprising of most of the steroidal skeleton. Such a situation is not so difficult to envisage in the case of steroidal platinum(II) complexes. The steroidal complexes cause

large structural changes to the structure of DNA and a hydrophobic interactions between the surface of the major groove and steroid may be envisaged and aid stabilising bent DNA, similar to HMGB1 binding to DNA.[266] Although no direct data exists to support this theory – it is however one that would be ideally suited to NMR techniques.

Table 7.2. Summary for steroidal platinum(II) complexes containing ET-3-Py

	Hydrolysis	Hydrolyses
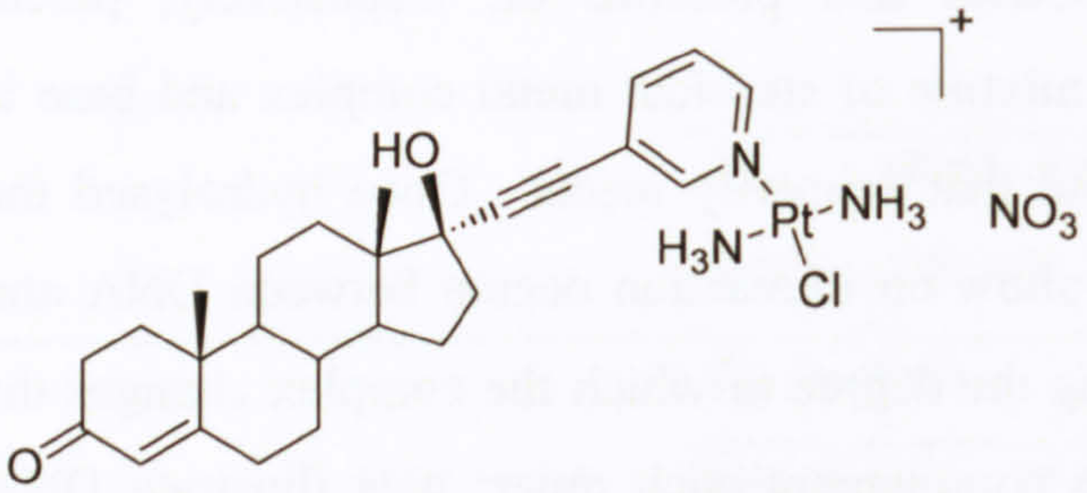 **TC-ET-3-Py**	**Binding to 5'-GMP / 5'-AMP**	Binds to 5'-GMP / 5'-AMP
	Gel Electrophoresis	Unwinds DNA - 19° (condenses at high loading)
	Linear Dichroism	ΔLD_{260nm} – 53 %
		ΔAbs_{260nm} – 23 %
		Significant bending of the helix
	IC_{50} (HBL-100 / T47D / SK-OV-3	27 μM / 63 μM / 39 μM. (Little change without steroids, except in T47D (2.63x)
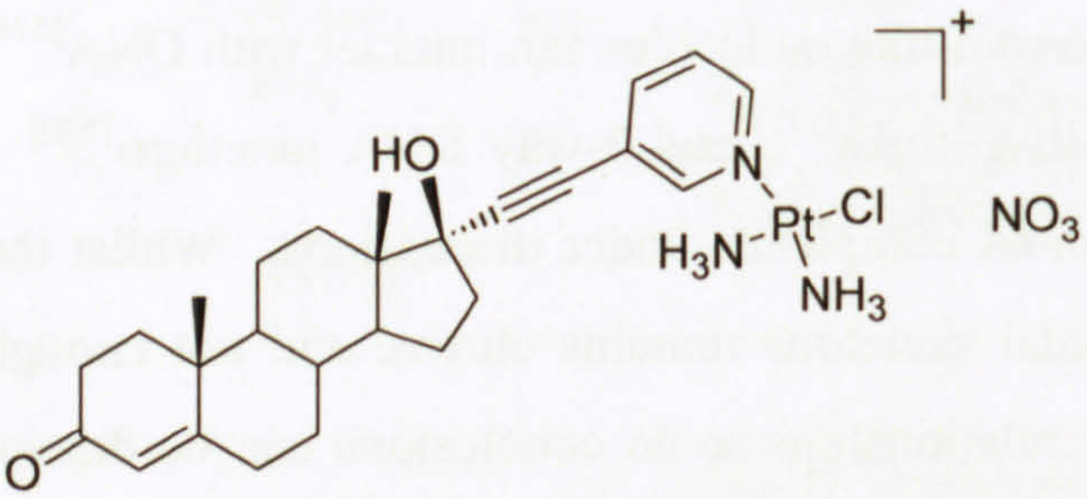 **CC-ET-3-Py**	**Hydrolysis**	Hydrolyses + unidentified signal
	Binding to 5'-GMP / 5'-AMP	Binds to 5'-GMP / 5'-AMP
	Gel Electrophoresis	Unwinds DNA - 21°
	Linear Dichroism	ΔLD_{260nm} – 61 %
		ΔAbs_{260nm} – 23 %
		Very significant bending of the helix
	IC_{50} (HBL-100 / T47D / SK-OV-3	7 μM / 16 μM / 16 μM. (Little change without steroids)

Table 7.3. Summary for steroidal platinum(II) complexes containing ET-4-Py and ET-3-Q

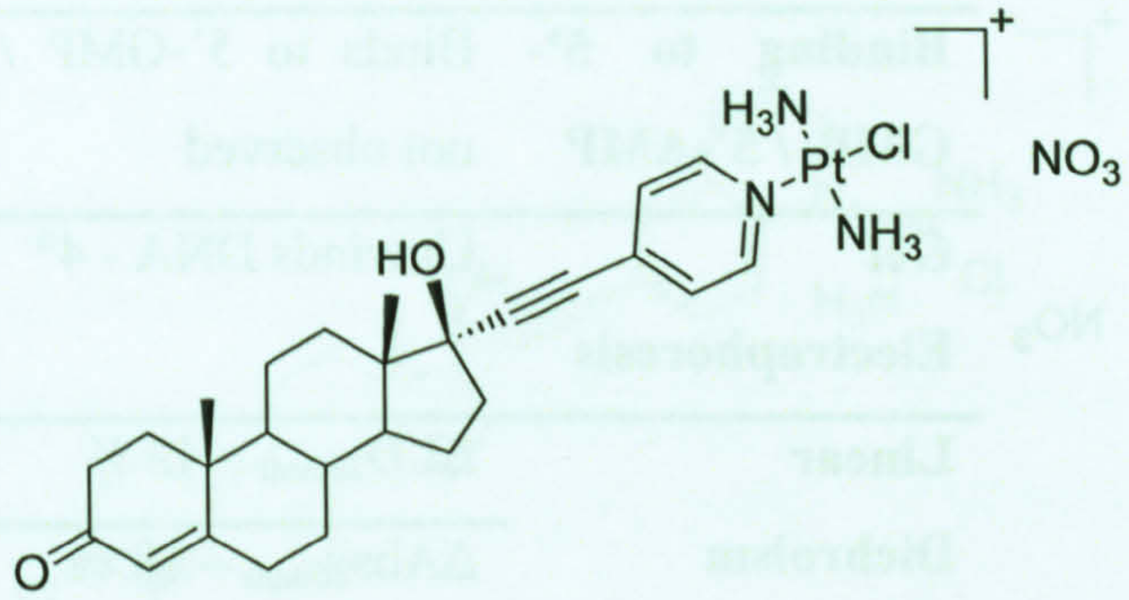

TC-ET-4-Py

Hydrolysis	Hydrolyses
Binding to 5'-GMP / 5'-AMP	Binds to 5'-GMP / not observed
Gel Electrophoresis	Unwinds DNA - 11°
Linear Dichroism	ΔLD_{260nm} – 36 %
	ΔAbs_{260nm} – 33 %
	Medium bending of the helix
IC_{50} (HBL-100 / T47D / SK-OV-3	12 μM / 19 μM / 27 μM. (Little change except in T47D (2.07x) and SK-OV-3 (2.39x)

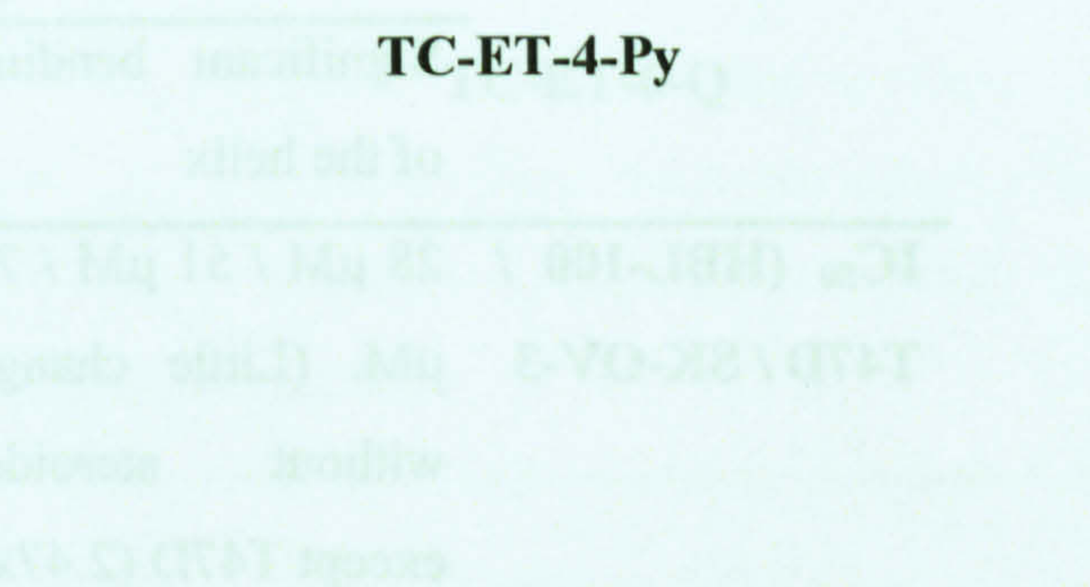

TC-ET-3-Q

Hydrolysis	Hydrolyses
Binding to 5'-GMP / 5'-AMP	Binds to 5'-GMP / 5'-AMP
Gel Electrophoresis	Unwinds DNA - 15° (condenses at high loadings)
Linear Dichroism	ΔLD_{260nm} – 51 %
	ΔAbs_{260nm} – 34 %
	Significant bending of the helix
IC_{50} (HBL-100 / T47D / SK-OV-3	24 μM / 51 μM / 50 μM. (Little change without steroids)

Table 7.4. Summary for steroidal platinum(II) complexes containing ET-4-IQ

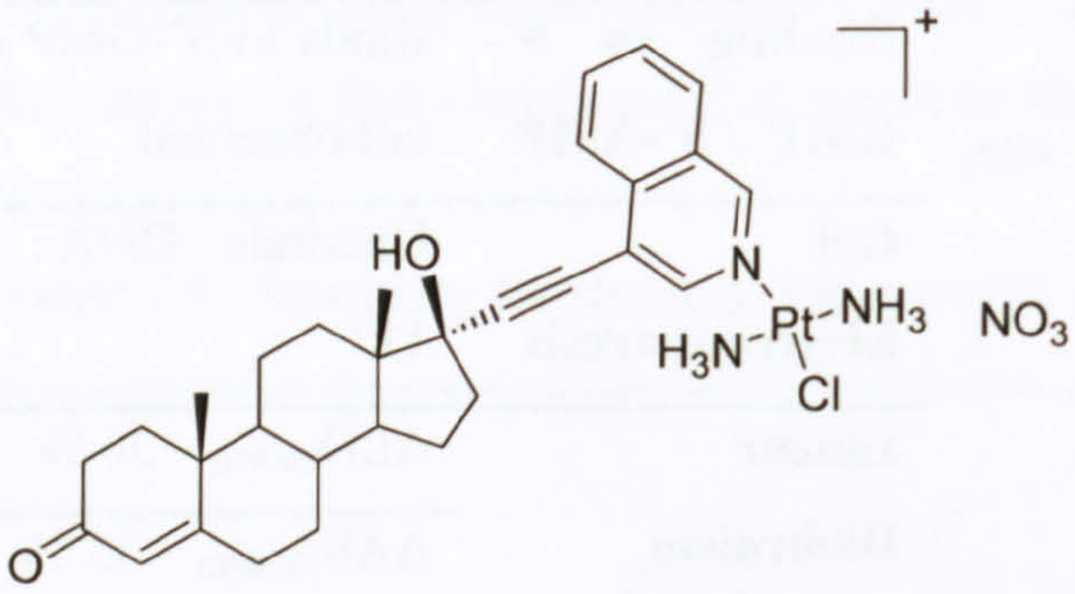

TC-ET-4-IQ

Hydrolysis	Hydrolyses
Binding to 5'-GMP / 5'-AMP	Binds to 5'-GMP / not observed
Gel Electrophoresis	Unwinds DNA - 4°
Linear Dichroism	ΔLD_{260nm} – 42 %
	ΔAbs_{260nm} – 18 %
	Significant bending of the helix
IC_{50} (HBL-100 / T47D / SK-OV-3	28 μM / 51 μM / 70 μM. (Little change without steroids, except T47D (2.47x) and SK-OV-3 (9.37x)

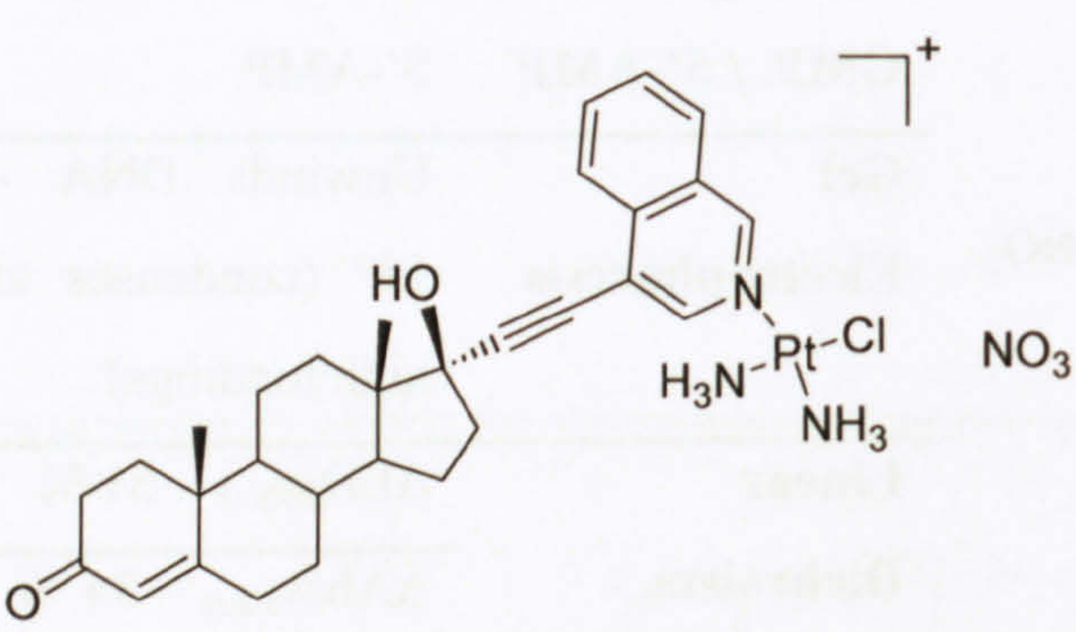

CC-ET-4-IQ

Hydrolysis	Hydrolyses + unidentified signal
Binding to 5'-GMP / 5'-AMP	Binds to 5'-GMP / not observed
Gel Electrophoresis	Unwinds DNA - > 21°
Linear Dichroism	ΔLD_{260nm} – 64 %
	ΔAbs_{260nm} -13 %
	Very significant bending of the helix
IC_{50} (HBL-100 / T47D / SK-OV-3	28 μM / 33 μM / 26 μM. Large changes in HBL-100 (6.37x), T47D (4.43x) and SK-OV-3 (6.11x)

Table 7.5. Summary for steroidal platinum(II) complexes containing ET-6-Q.

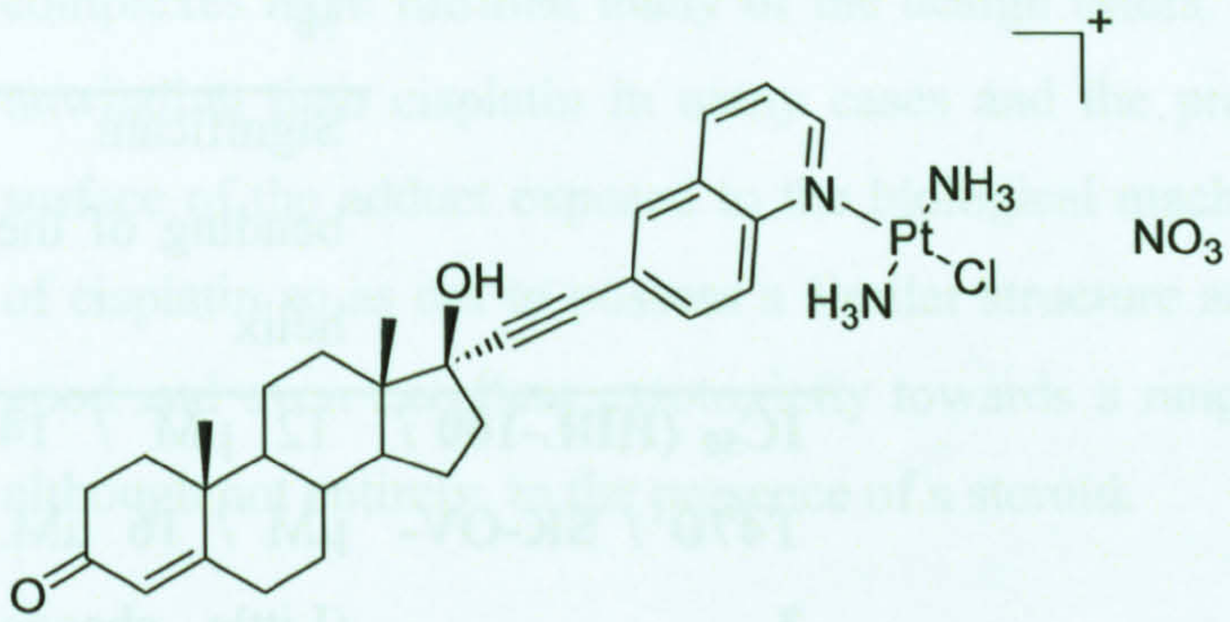

TC-ET-6-Q

Hydrolysis	Hydrolyses
Binding to 5'-GMP / 5'-AMP	Binds to 5'-GMP / 5'-AMP
Gel Electrophoresis	Unwinds DNA - 19° (condenses at high loadings)
Linear Dichroism	ΔLD_{260nm} – 54 %
	ΔAbs_{260nm} – 45 %
	Medium bending of the helix
IC_{50} (HBL-100 / T47D / SK-OV-3	26 μM / 39 μM / 45 μM. (Little change without steroids, except T47D (0.37x)

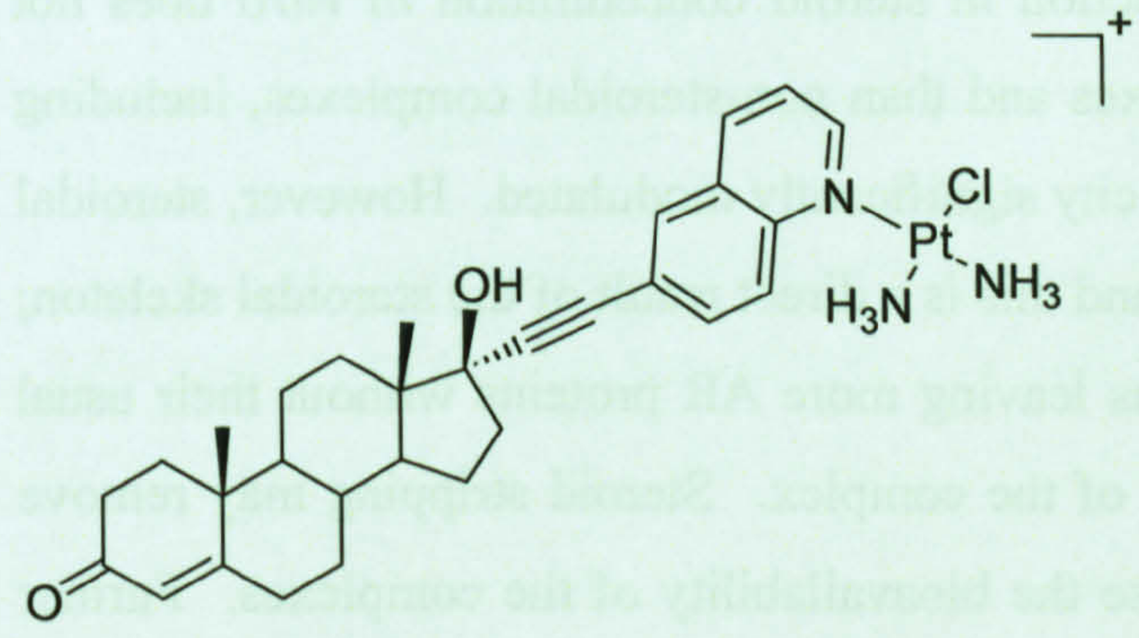

CC-ET-6-Q

Hydrolysis	Hydrolyses + unidentified signal
Binding to 5'-GMP / 5'-AMP	Binds to 5'-GMP / not observed
Gel Electrophoresis	Unwinds DNA - 19° (condenses at higher loadings)
Linear	ΔLD_{260nm} – 58

	Dichroism	%
		ΔAbs_{260nm} – 24 %
		Significant bending of the helix
IC_{50} (HBL-100 / T47D / SK-OV-3		12 μM / 14 μM / 16 μM. (Little change without steroids, except SK-OV-3 (2.34x)

Broadly speaking, from Tables 7.2 – 7.5, the greater the effect a complex has on the DNA structure the lower its IC_{50} value. The most active complexes, the cis-cationic, affect DNA greatly in terms of unwinding (≥19°) and bending whilst, particularly in the case of CC-ET-6-Q, being active in the full range of cell lines studied. At the opposite end of the spectrum the three non-steroidal complexes affect DNA very little, unwinding only a few degrees, causing only small bending whilst possessing high IC_{50} values. This correlation is an interesting one and links the effect the complexes have on DNA in terms of global changes to its structure with cytotoxicity. Given that DNA is thought the target of platinum(II) drugs such a correlation is reasonable and could be a subject of future studies.

An important result is a substantial reduction in steroid concentration *in vitro* does not sensitise the cells to platinum(II) complexes and than non-steroidal complexes, including cisplatin, which do not have their cytotoxicity significantly modulated. However, steroidal platinum(II) complexes (Chapter Six) do and this is a direct result of the steroidal skeleton; this may be due to reduction in androgens leaving more AR proteins without their usual ligands, or it may alter the transportation of the complex. Steroid stripping may remove components that bind steroids and increase the bioavailability of the complexes. Further testing, including ascertaining relative binding affinities of the complexes for the AR is a worthwhile task to undertake.

The design brief for steroidal metal complexes (Chapter Two) stated the complexes must allow good receptor binding, coordination to DNA with a relatively facile synthesis; this is

in addition to those qualities required in a potential cytotoxic drug – altering DNA structure and possessing good cytotoxicity in a range of cell lines. The steroidal metal complexes have fulfilled many of the design briefs. They bind to DNA, causing greater unwinding than cisplatin in many cases and the presence of a steroid should mean the surface of the adduct exposed to the biological machinery is distinctly different from that of cisplatin so as not to possess a similar structure and cross-resistance. They all possess good and even excellent cytotoxicity towards a range of cell lines that may be ascribed, although not entirely, to the presence of a steroid.

In short, the presence of a steroidal skeleton, appended to an aromatic planar ligand of a platinum(II) complex transforms that complex into one causing greater perturbations to the structure of DNA and possessing very much higher cytotoxicity, than complexes without the steroidal skeleton.

A.1.1 ET-2-Py

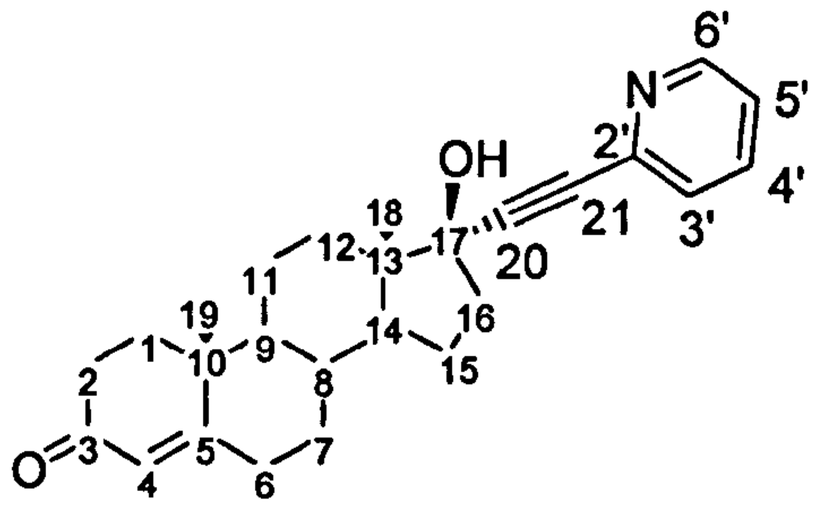

$C_{26}H_{31}NO_2$

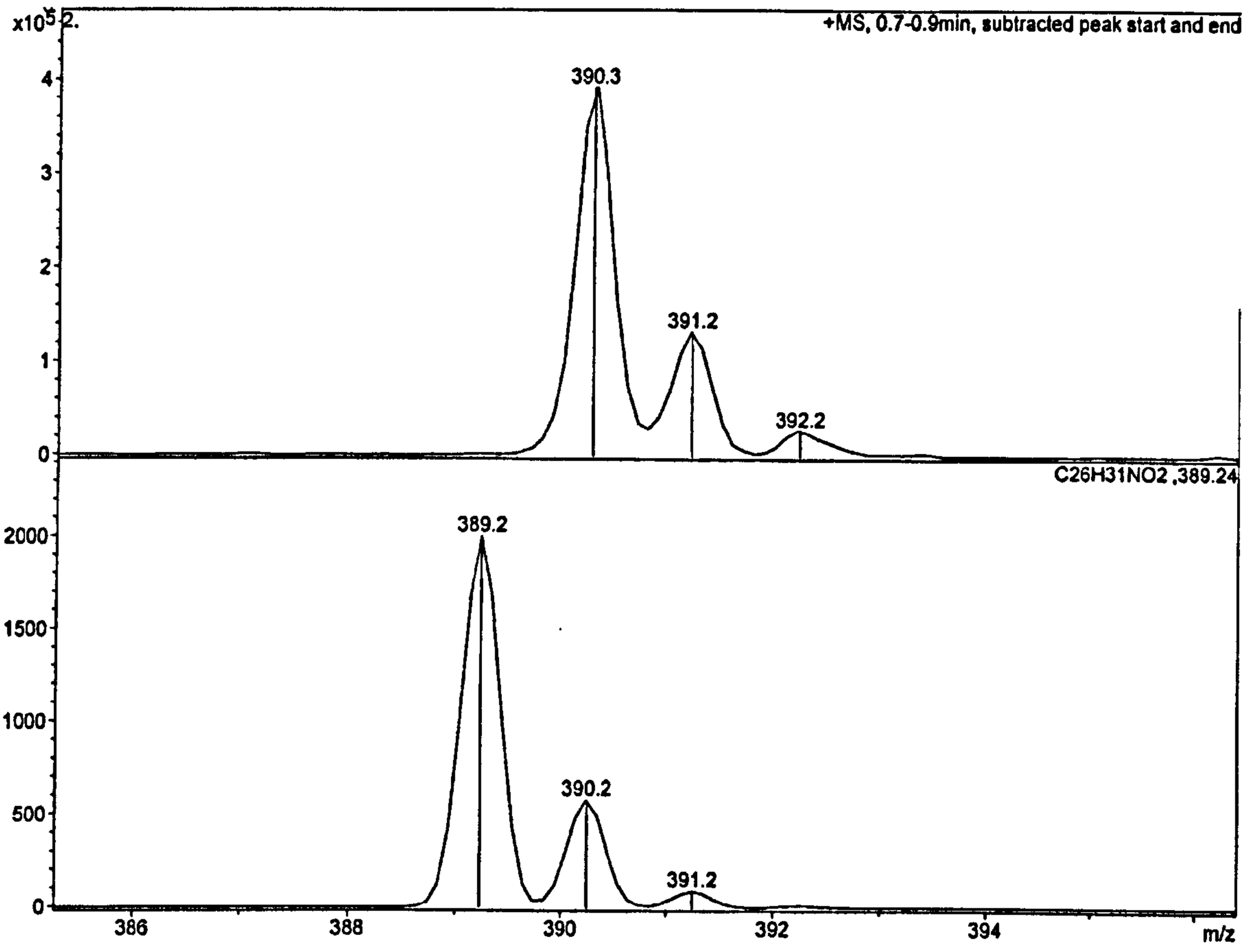

Figure A.1.1. The mass spectrum of ET-2-Py in the region around *m/z* = 391. The experimental (top) and theoretical (bottom) isotope distribution patterns are shown. The theoretical is ET-2-Py, $C_{26}H_{31}NO_2$.

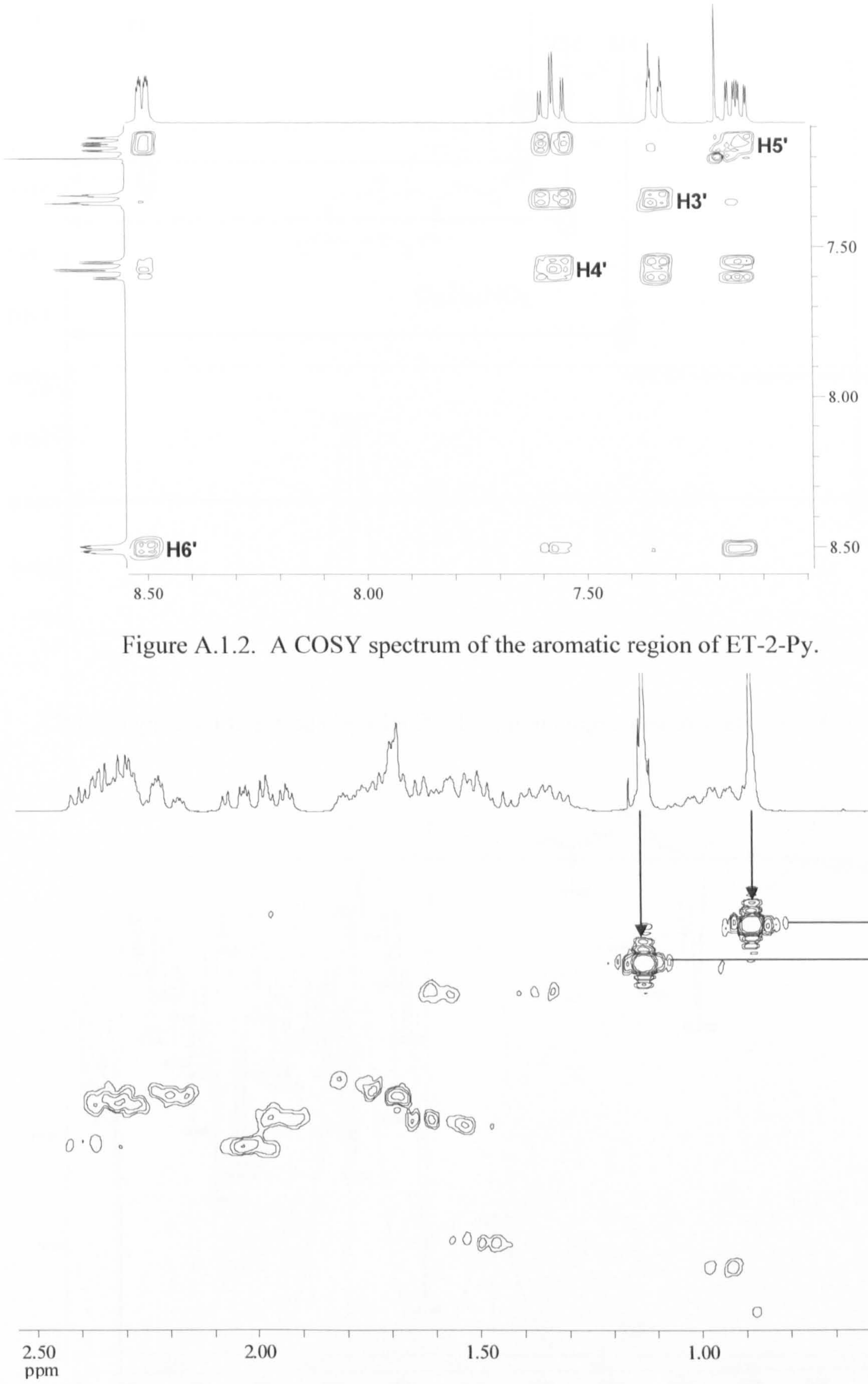

Figure A.1.2. A COSY spectrum of the aromatic region of ET-2-Py.

Figure A.1.3. The aliphatic region in the ^{1}H-^{13}C HMQC spectrum of ET-2-Py.

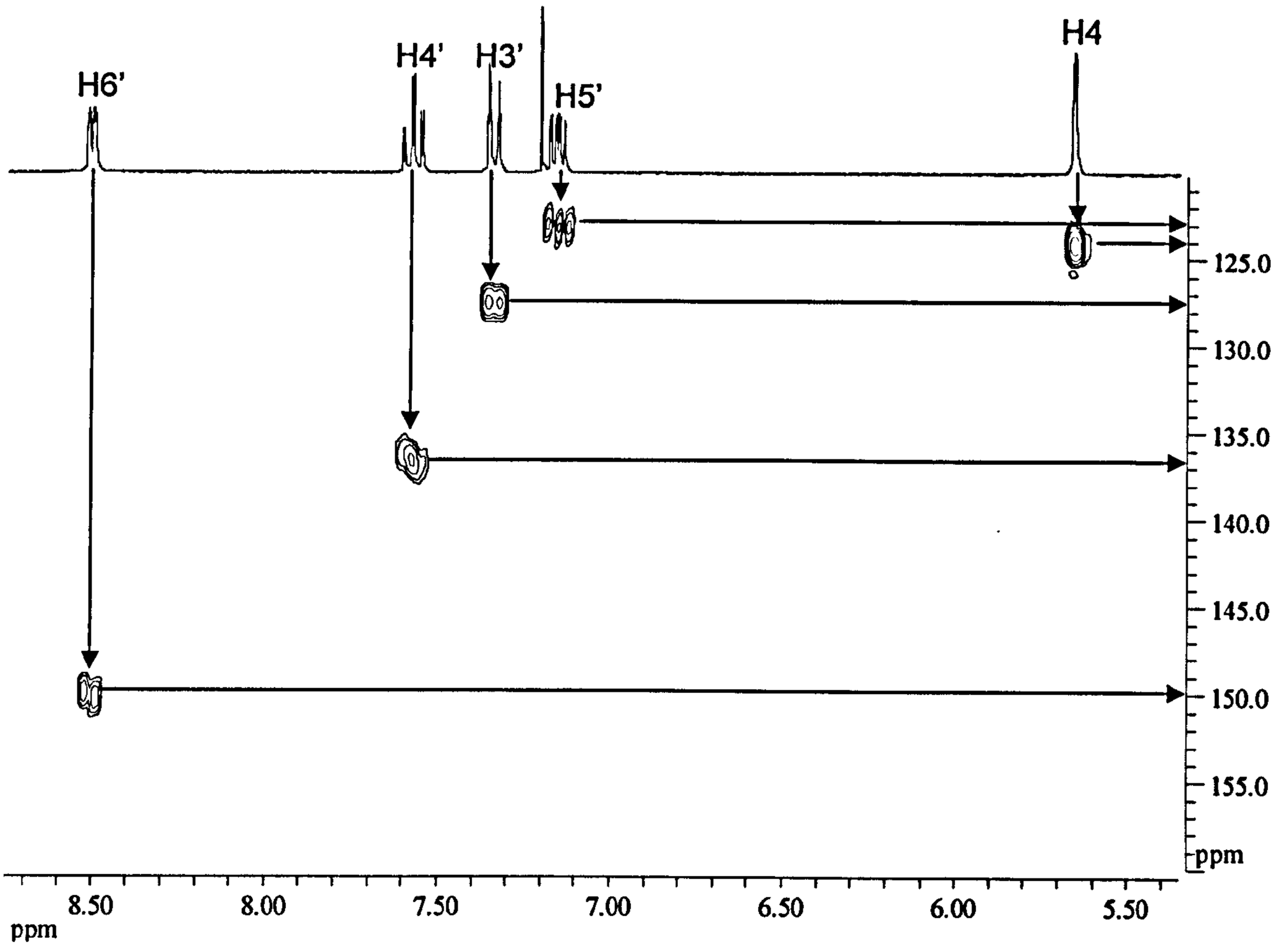

Figure A.1.4. The aromatic region in the ^{1}H-^{13}C HMQC spectra of ET-2-Py in $CDCl_3$.

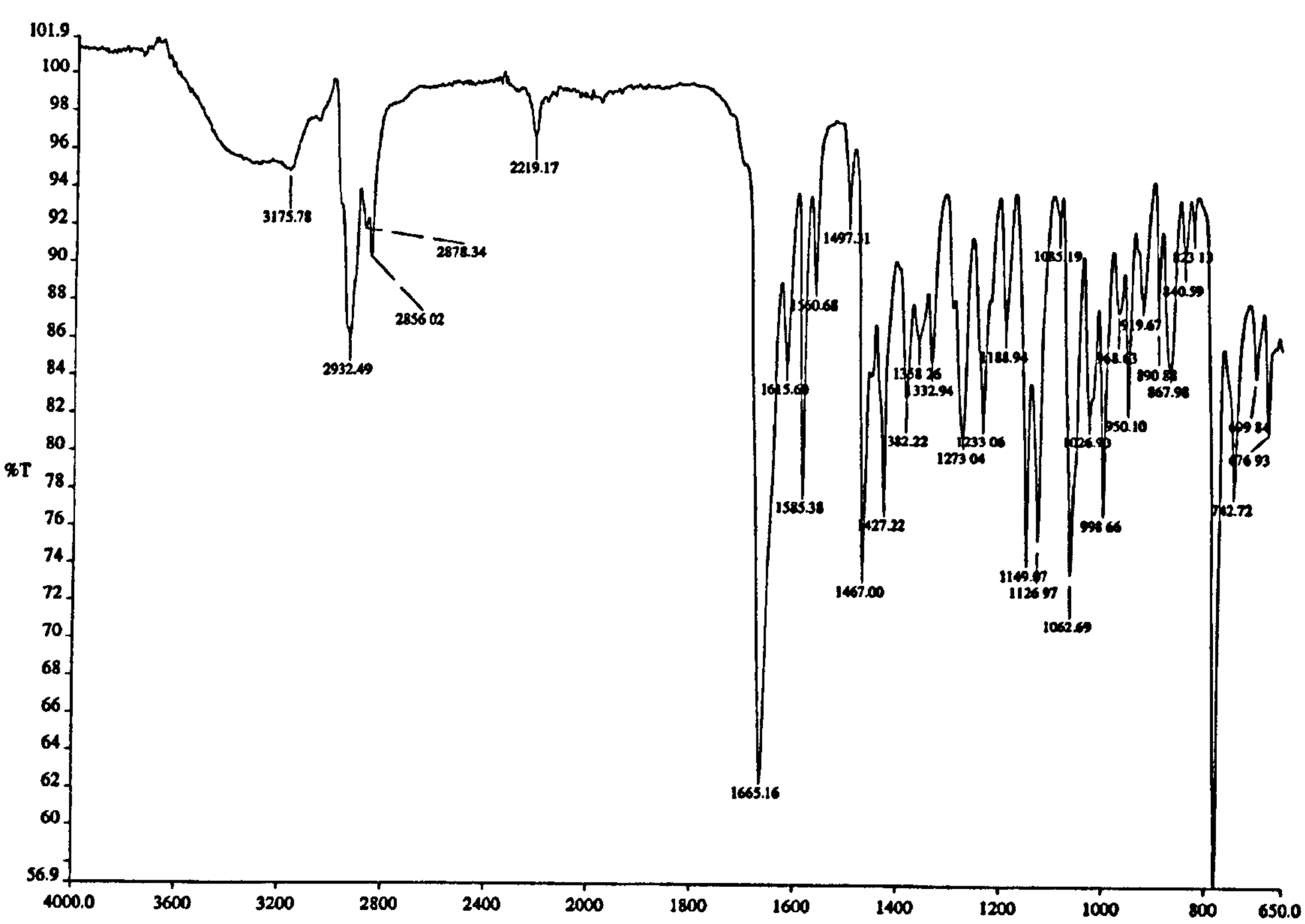

Figure A.1.5. The infrared spectrum of ET-2-Py.

A.1.2. ET-3-Py

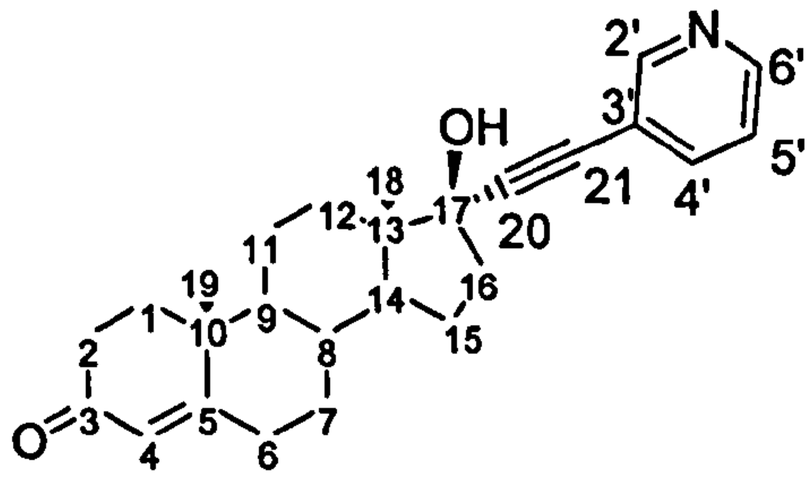

$C_{26}H_{31}NO_2$

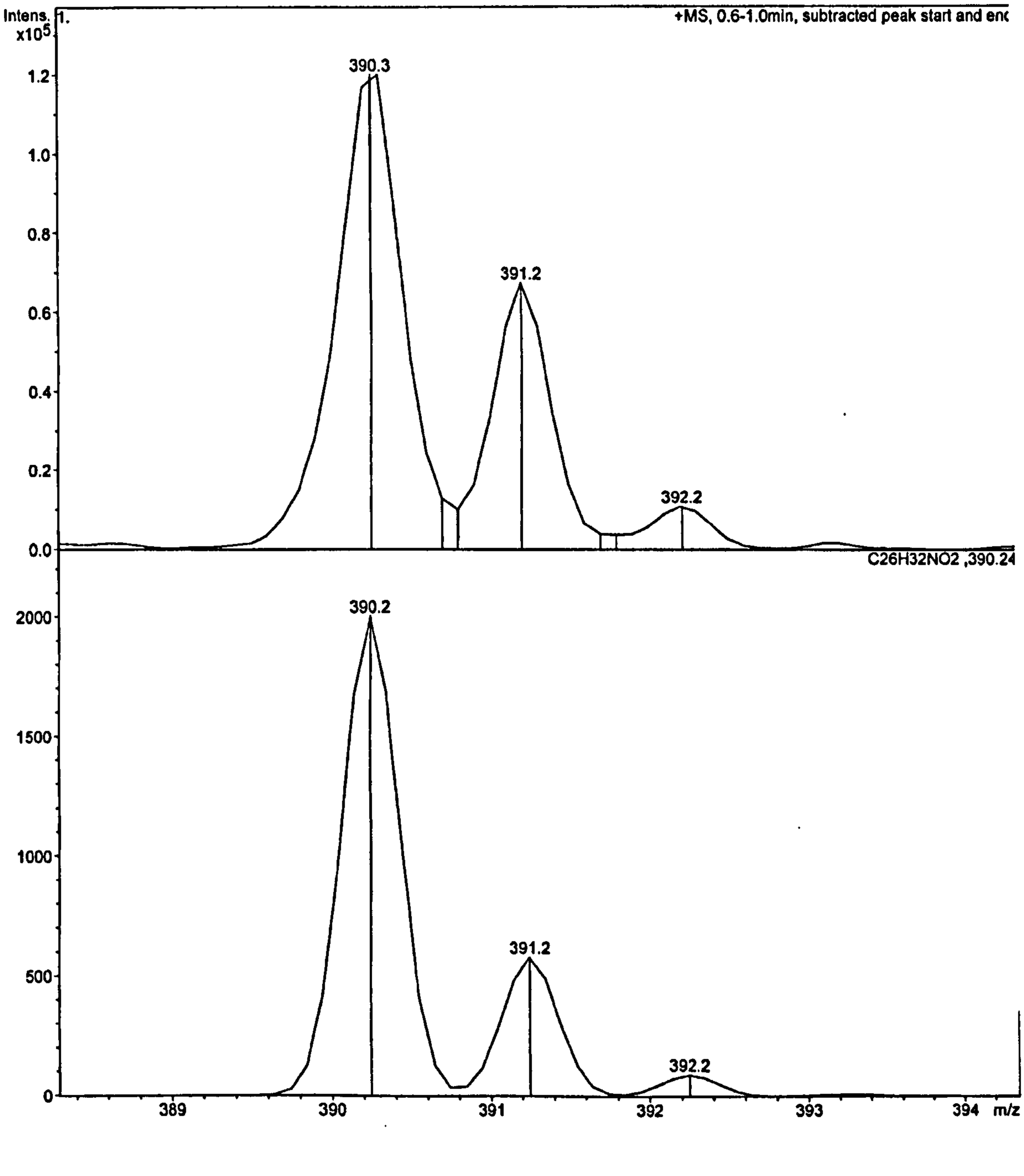

Figure A.1.6. The mass spectrum (ESI, +ve) *m/z* 390.2 peak in ET-3-Py. The experimental peak (upper) and theoretical (lower). The theoretical is $[H(ET\text{-}3\text{-}Py)]^+$.

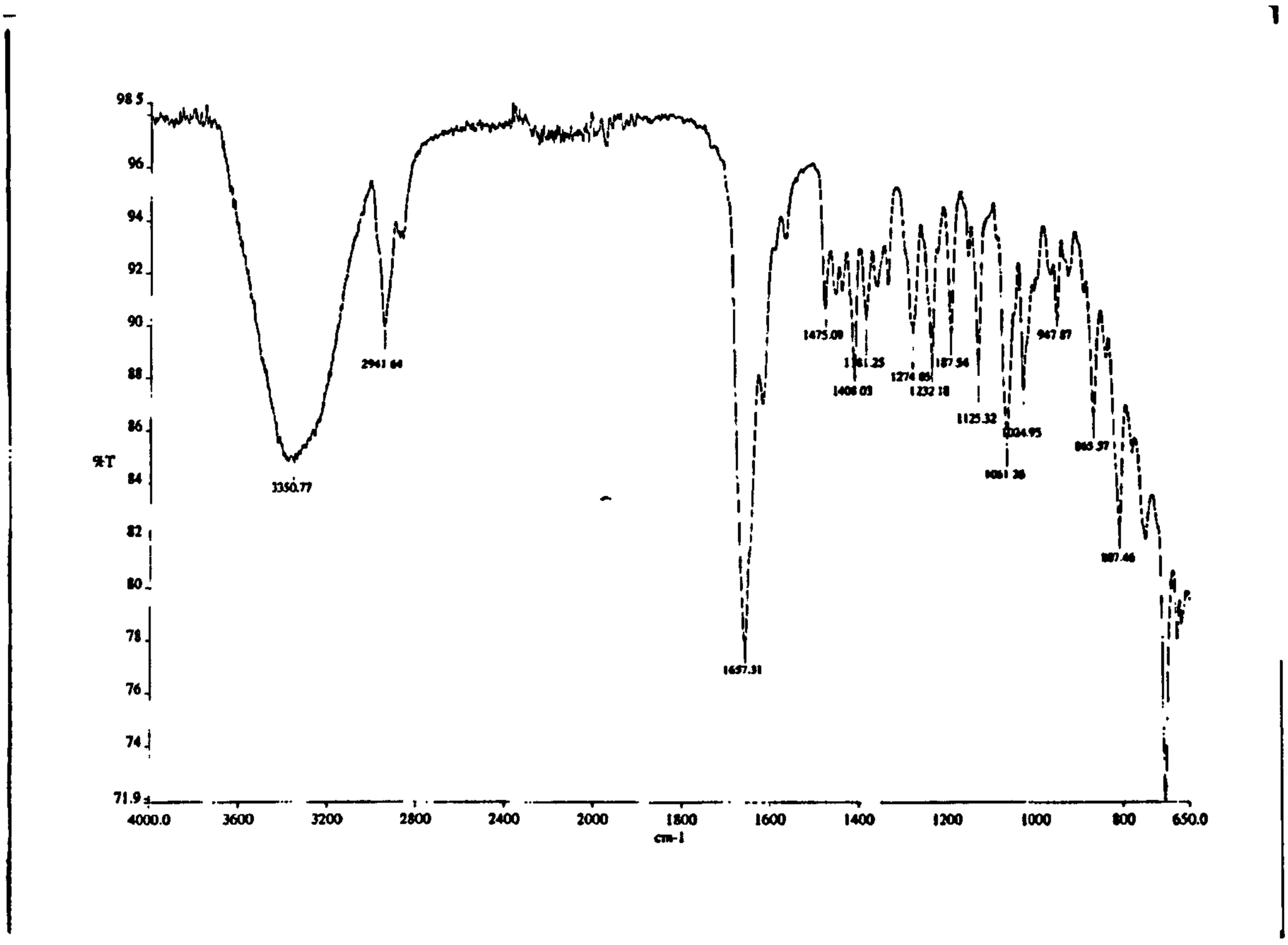

Figure A.1.7. The IR spectrum of ET-3-Py.

A.1.3. ET-4-Py

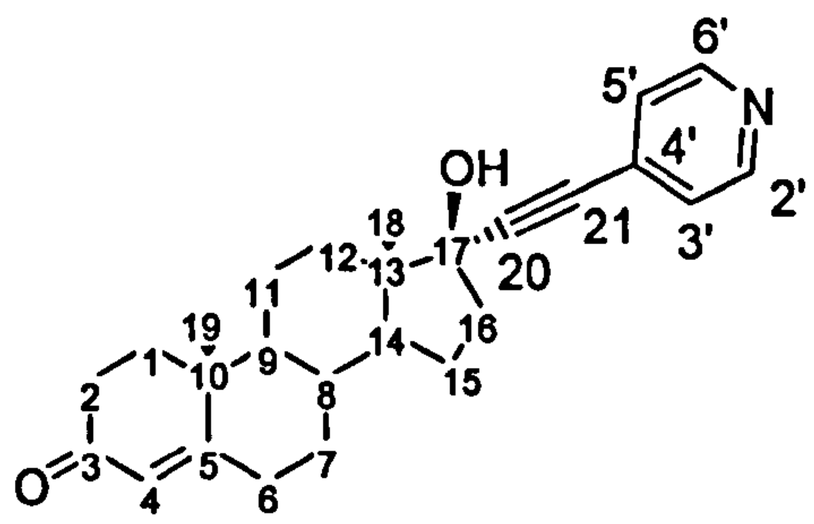

$C_{26}H_{31}NO_2$

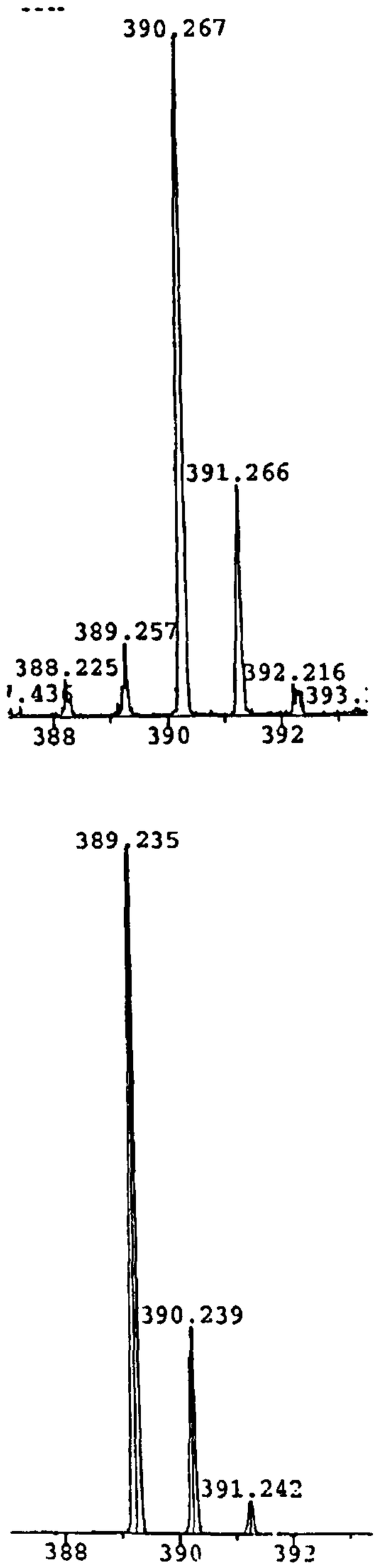

Figure A.1.8. The mass spectrum (ESI, +ve) of ET-4-Py (upper) and theoretical isotope distribution (lower).

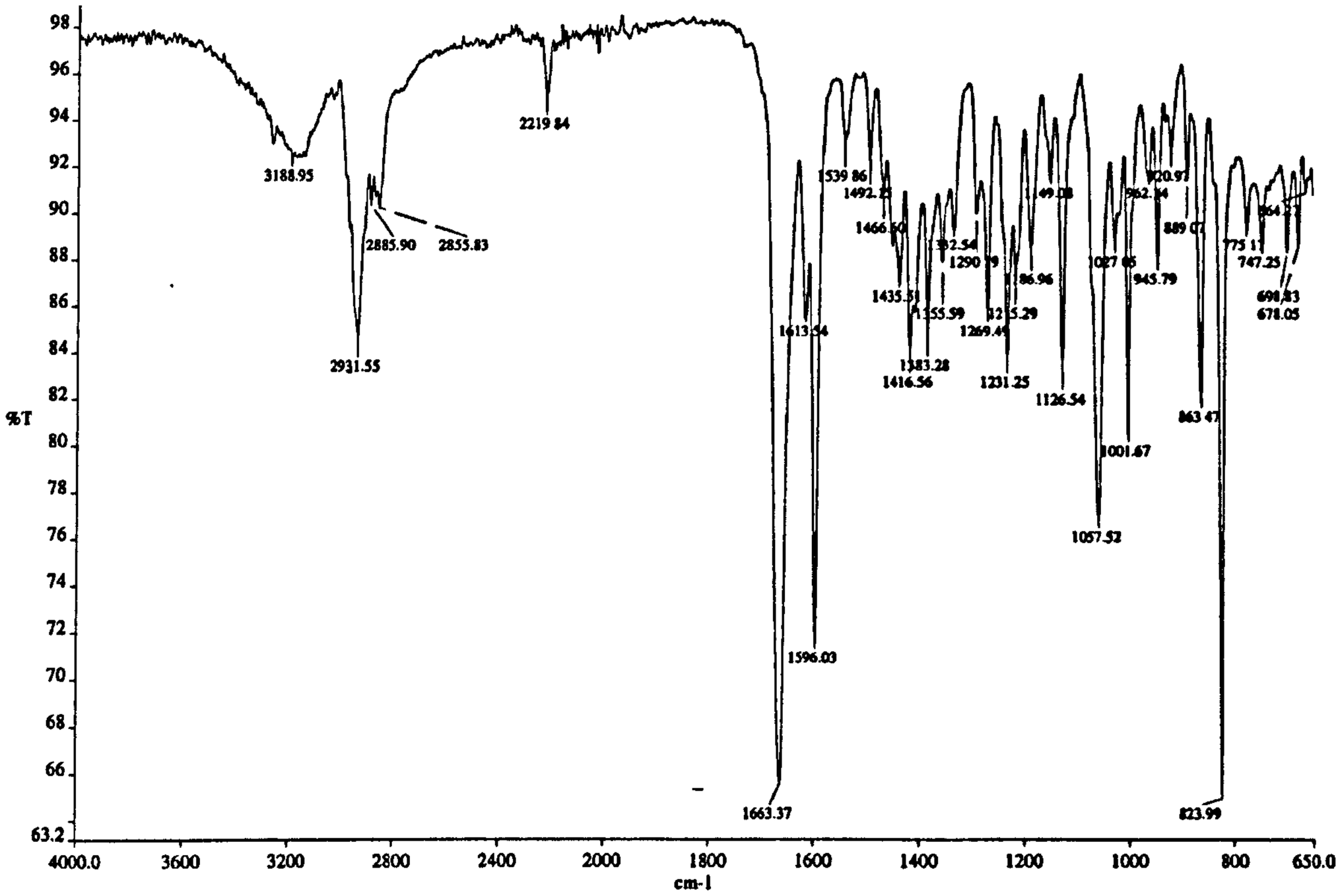

Figure A.1.9. The infrared spectrum of ET-4-Py.

A.1.4. ET-3-Q

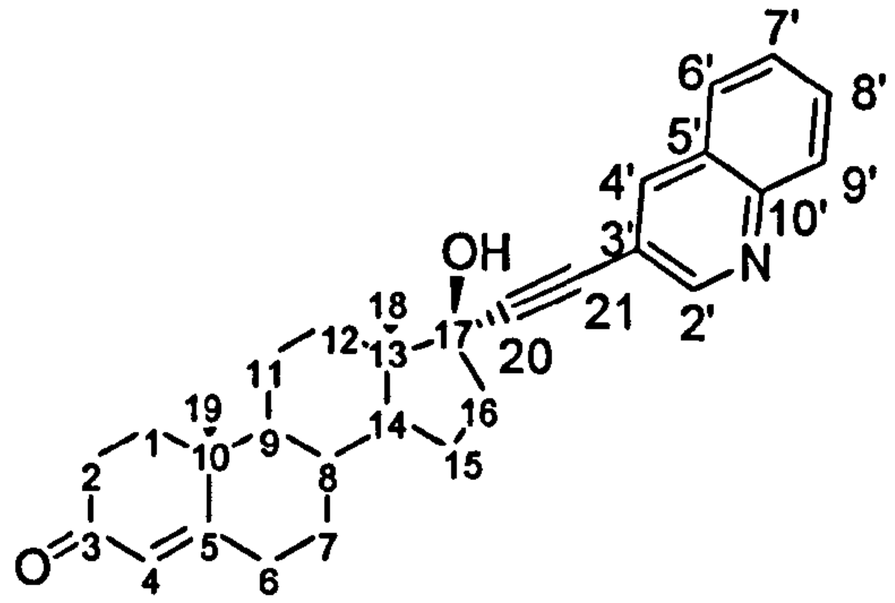

$C_{30}H_{33}NO_2$

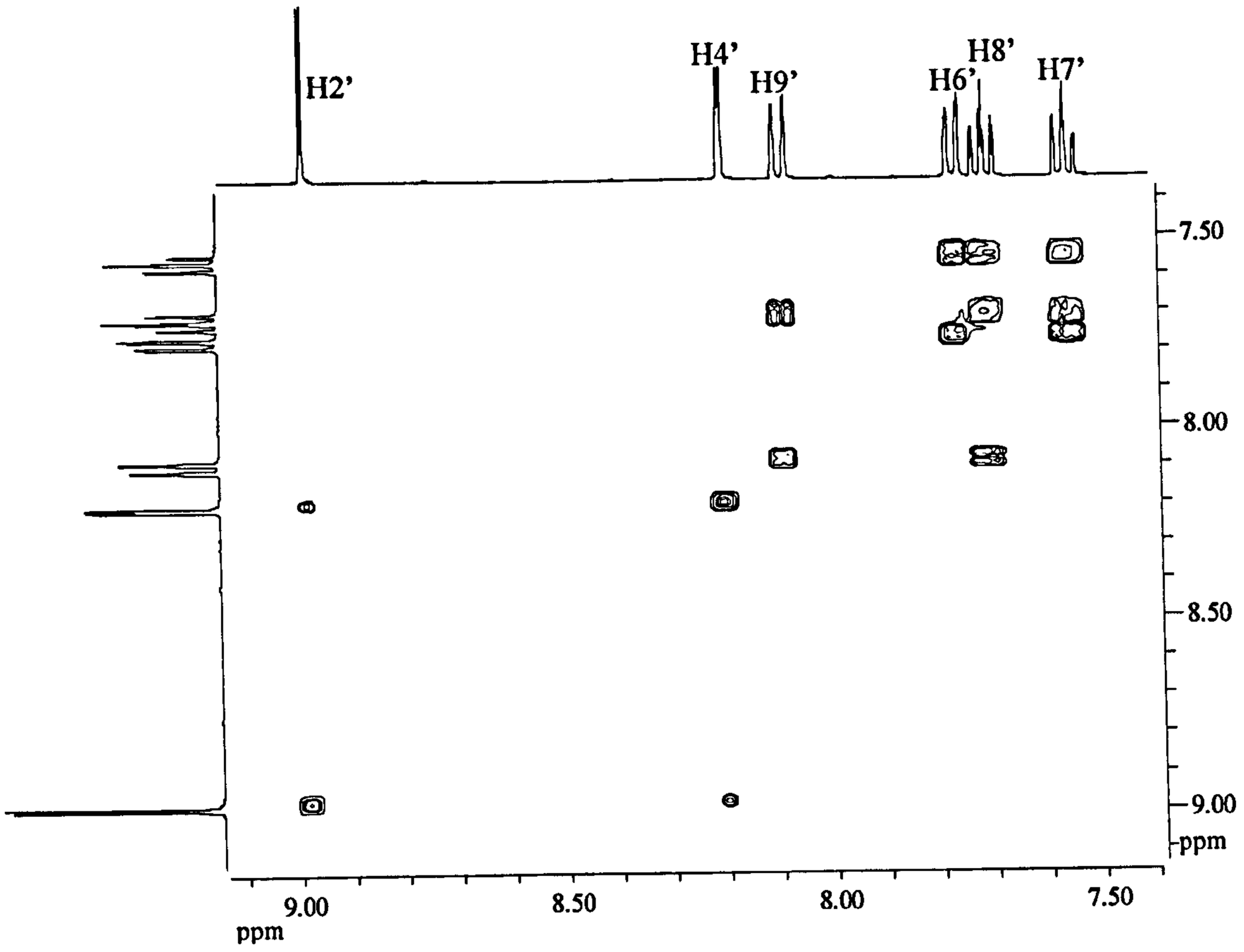

Figure A.1.10. The COSY spectrum of ET-3-Q in $CDCl_3$.

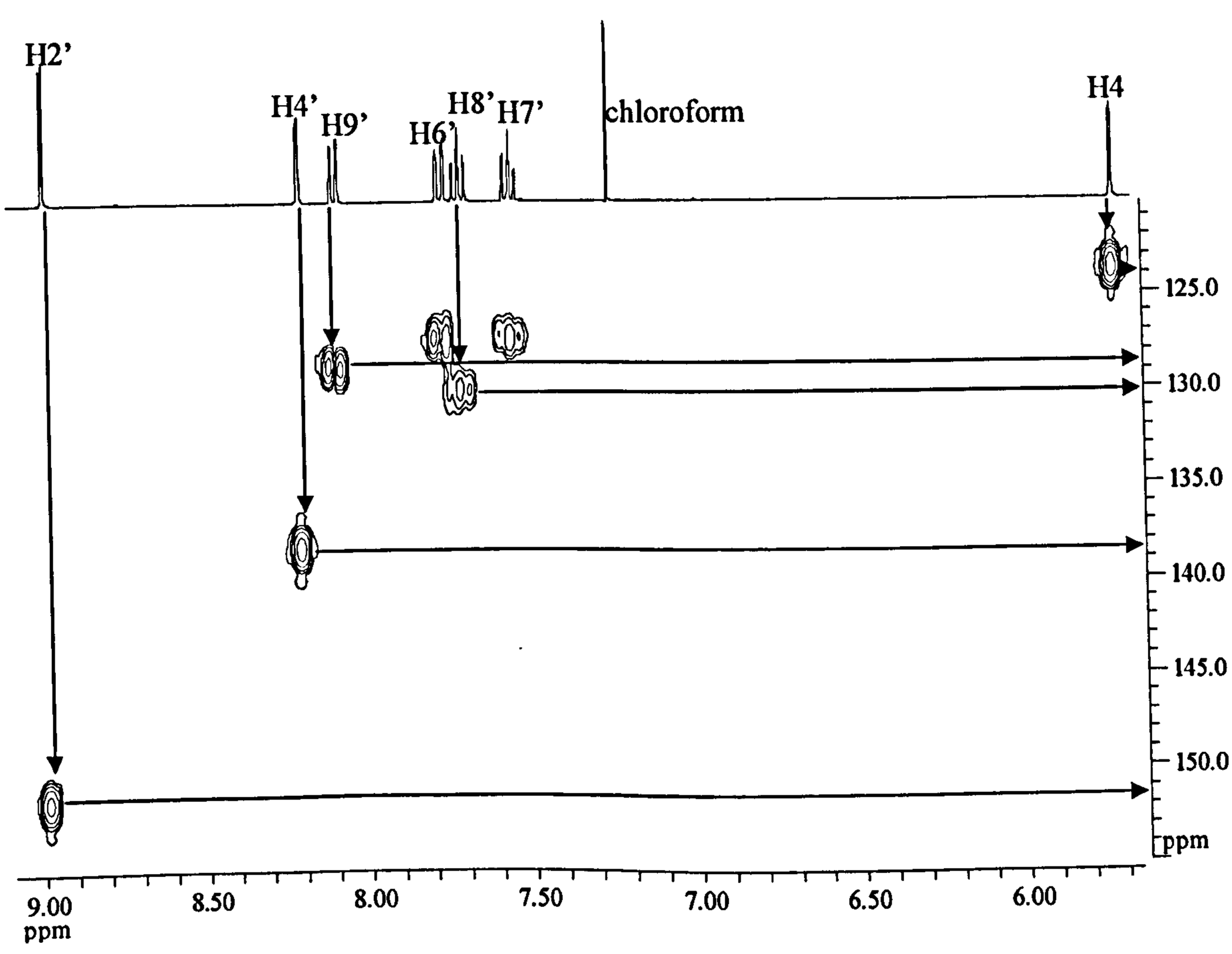

Figure A.1.11. The low field region in the ^{1}H-^{13}C HMQC spectrum of ET-3-Q in $CDCl_3$.

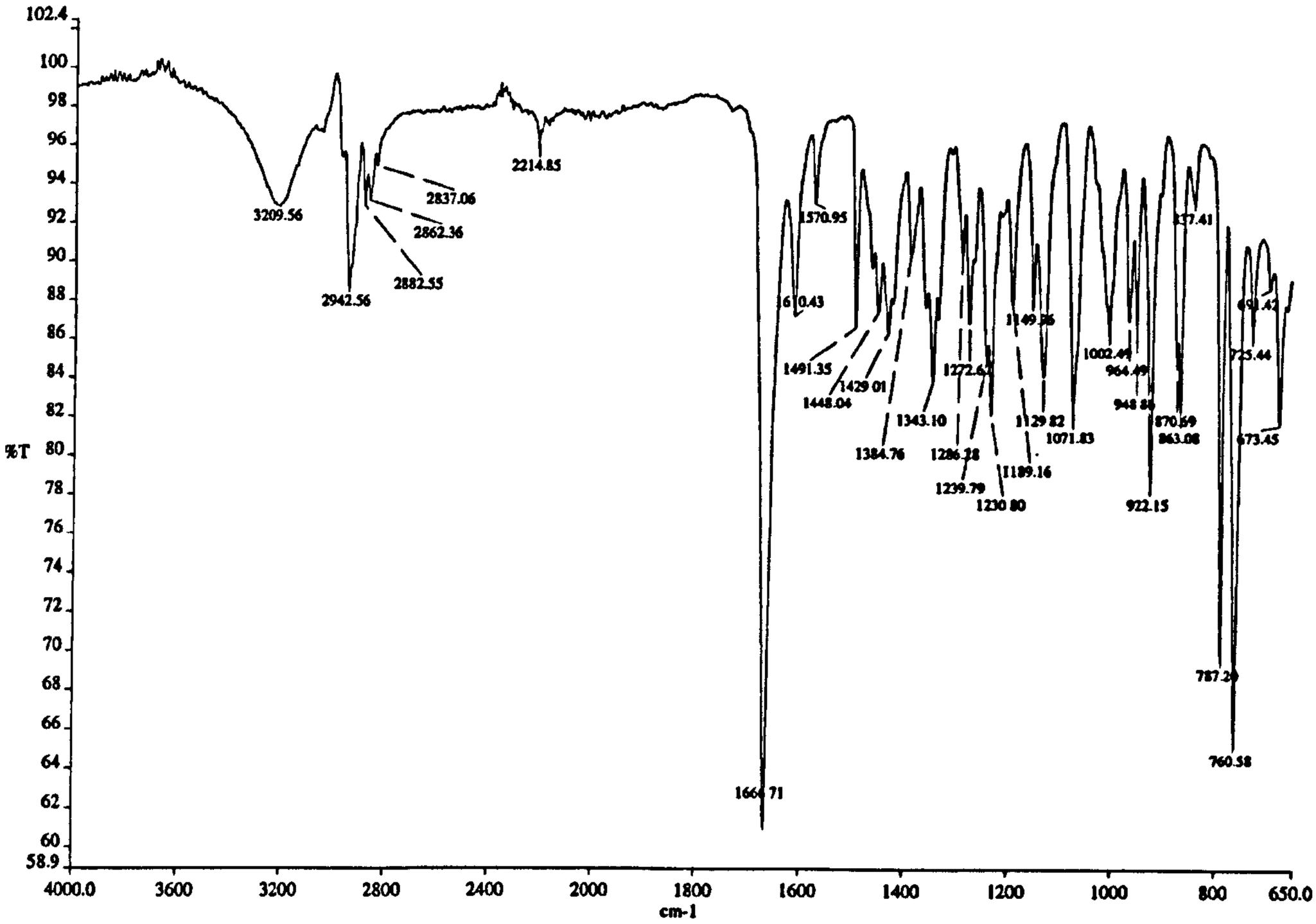

Figure A.1.12. The infrared spectrum of ET-3-Q.

A.1.5. ET-4-IQ

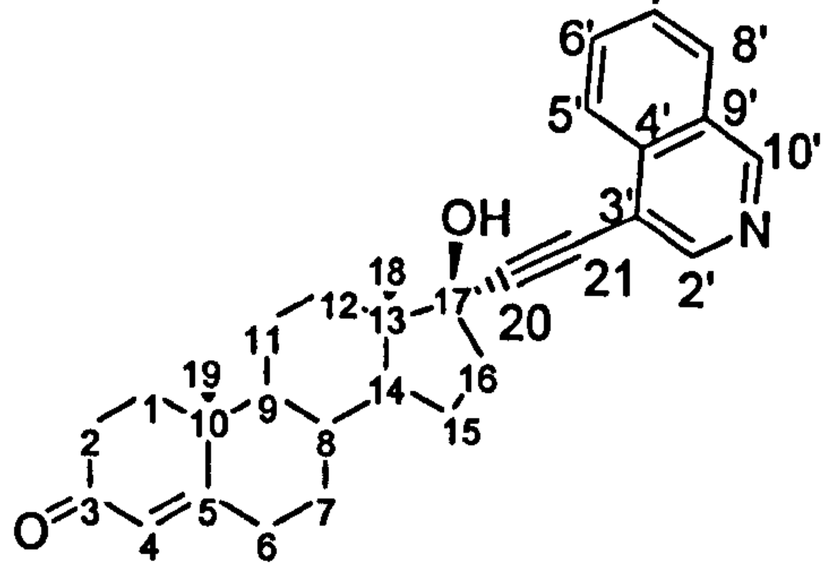

$C_{30}H_{33}NO_2$

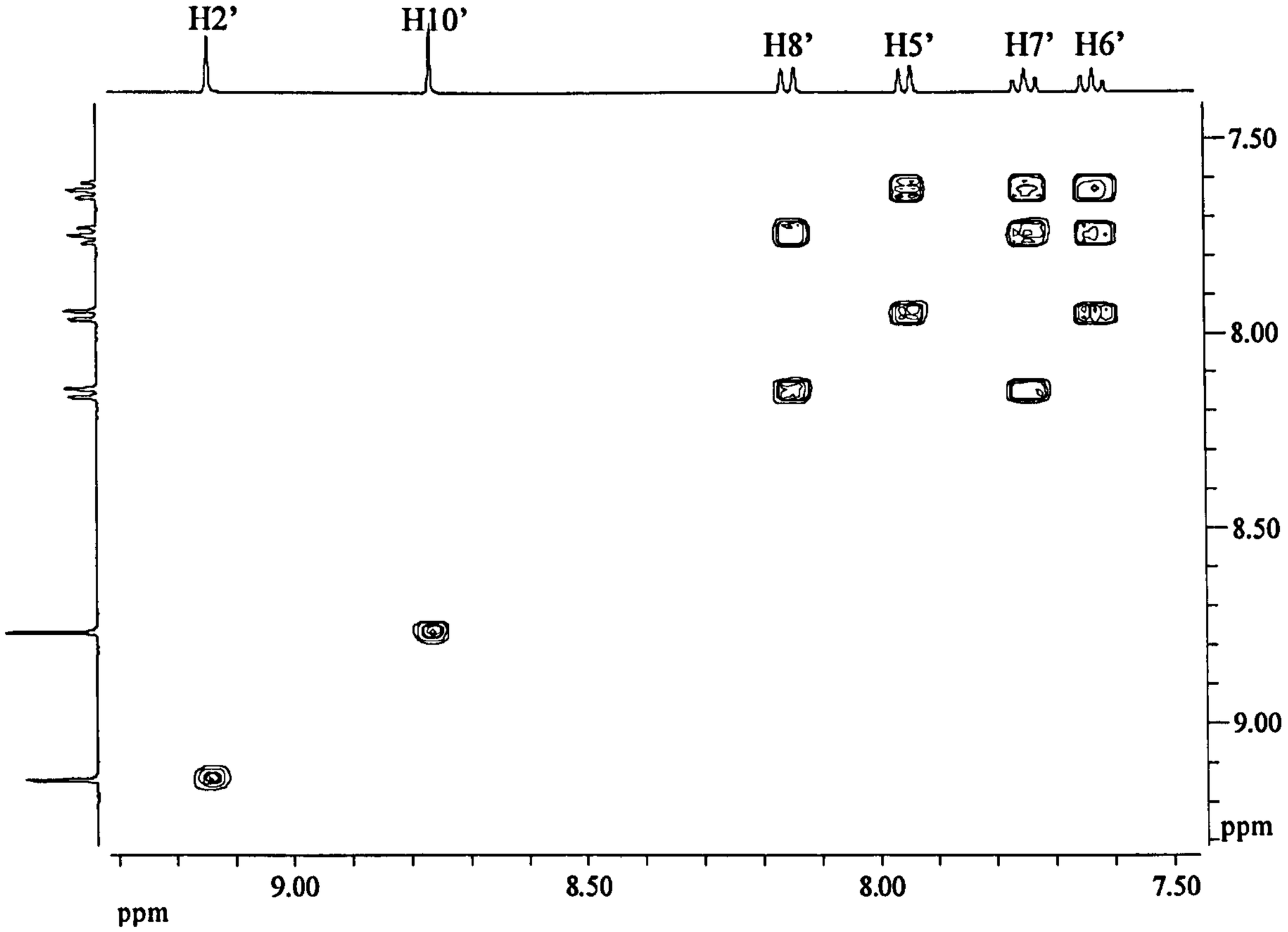

Figure A.1.13. The aromatic region in the COSY spectrum for ET-4-IQ in $CDCl_3$.

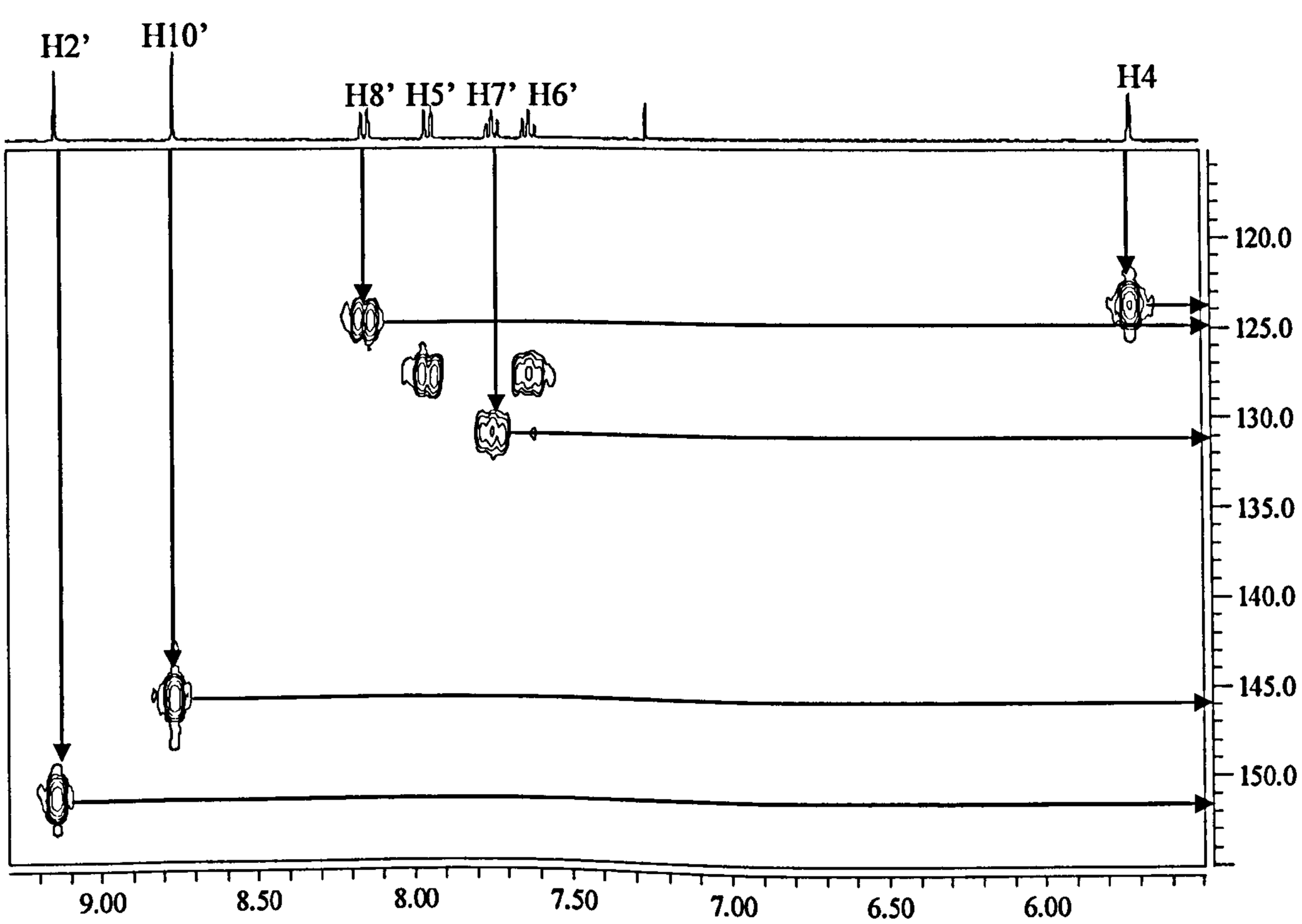

Figure A.1.14. The low field ^{1}H-^{13}C HMQC spectrum of ET-4-IQ in $CDCl_3$

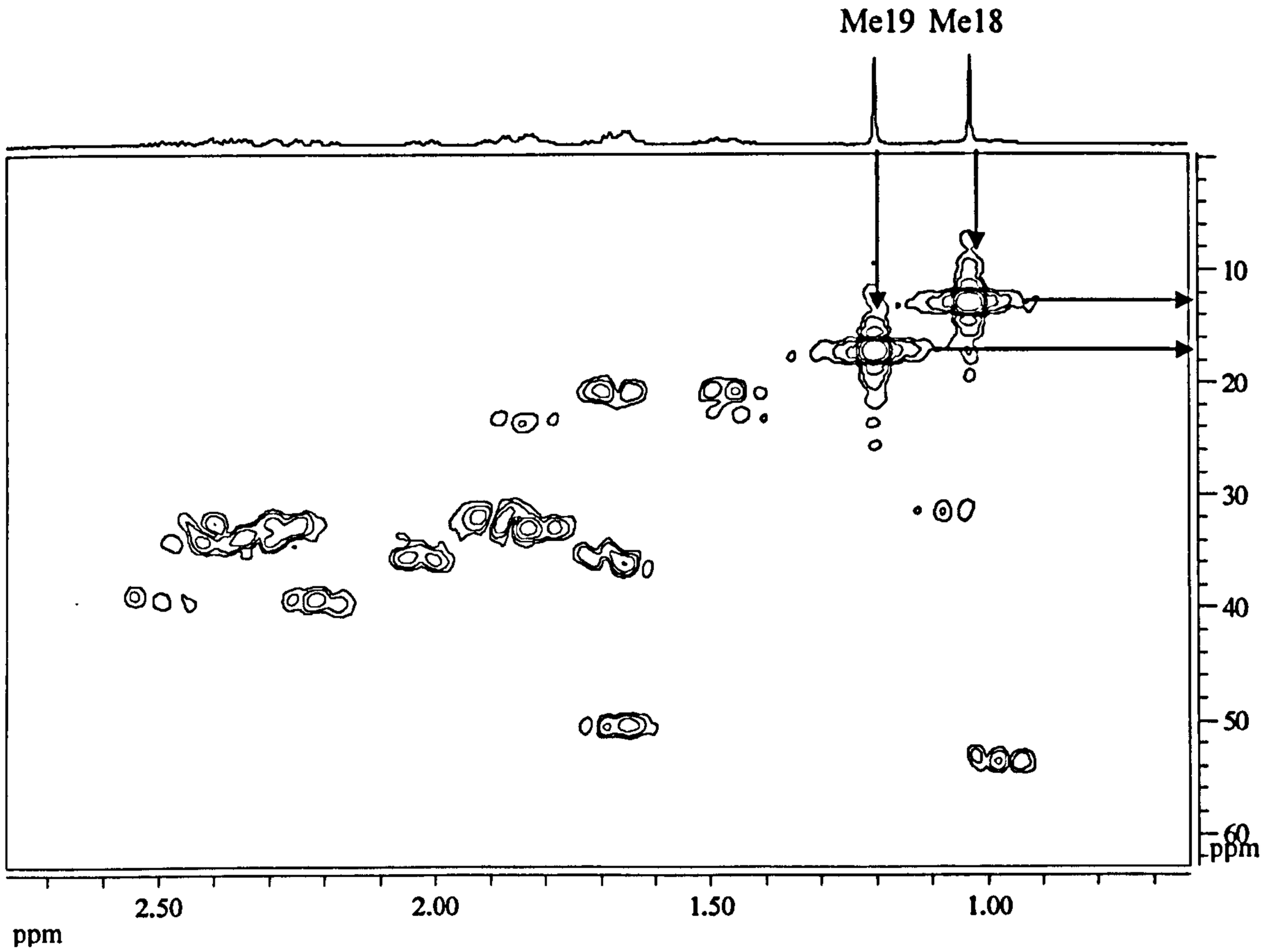

Figure A.1.15. The aliphatic region in the ^{1}H-^{13}C HMQC spectrum of ET-4-IQ in $CDCl_3$.

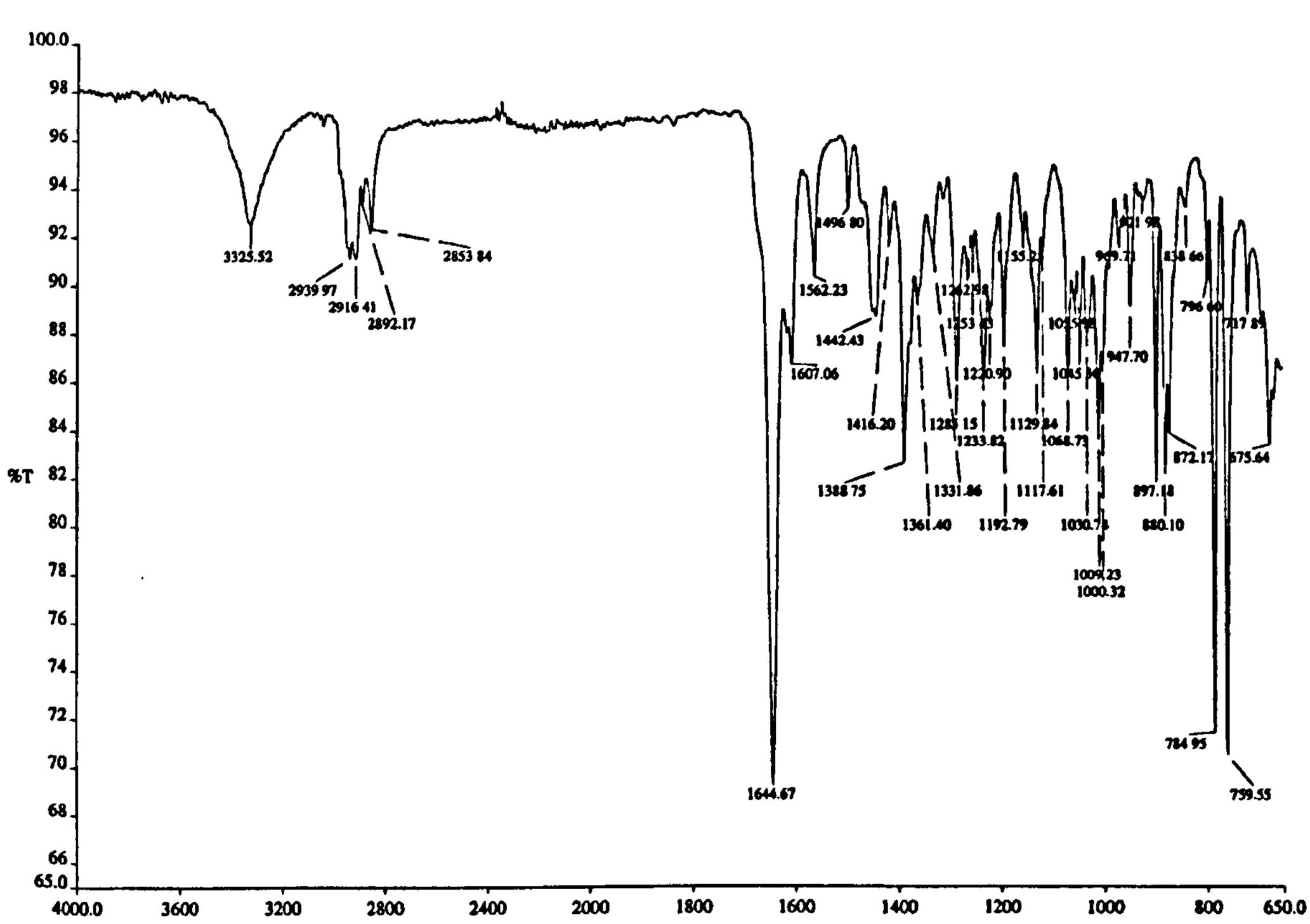

Figure A.1.16. The infrared spectrum of ET-4-IQ.

A.1.6. ET-6-Q

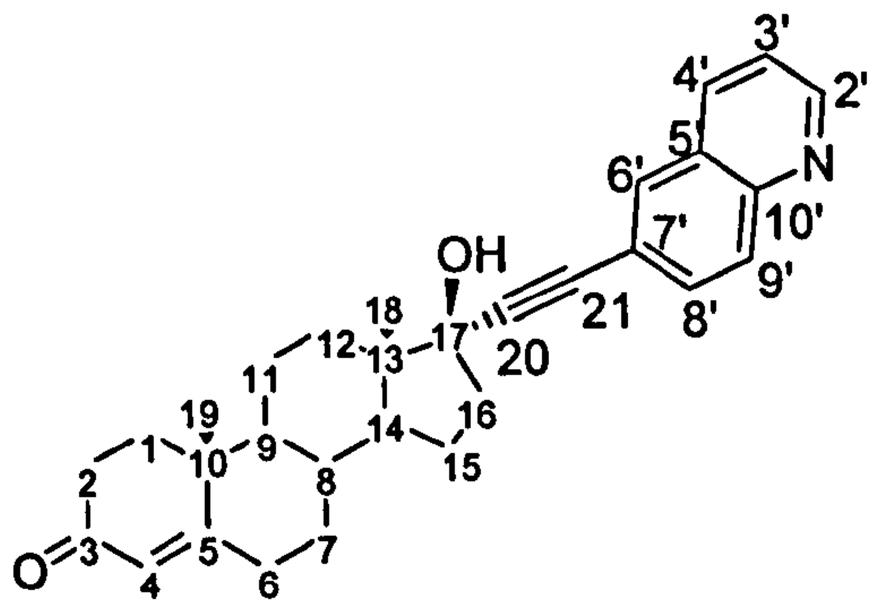

$C_{30}H_{33}NO_2$

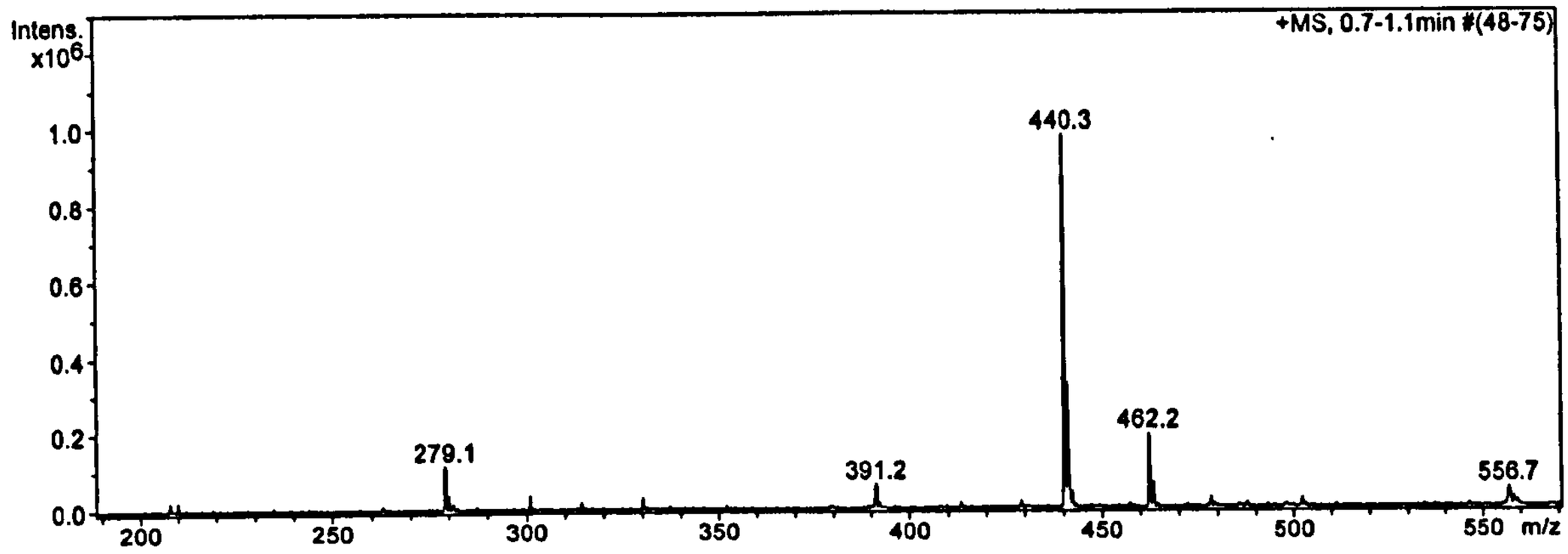

Figure A.1.17. The mass spectrum (ESI, +ve) of ET-6-Q.

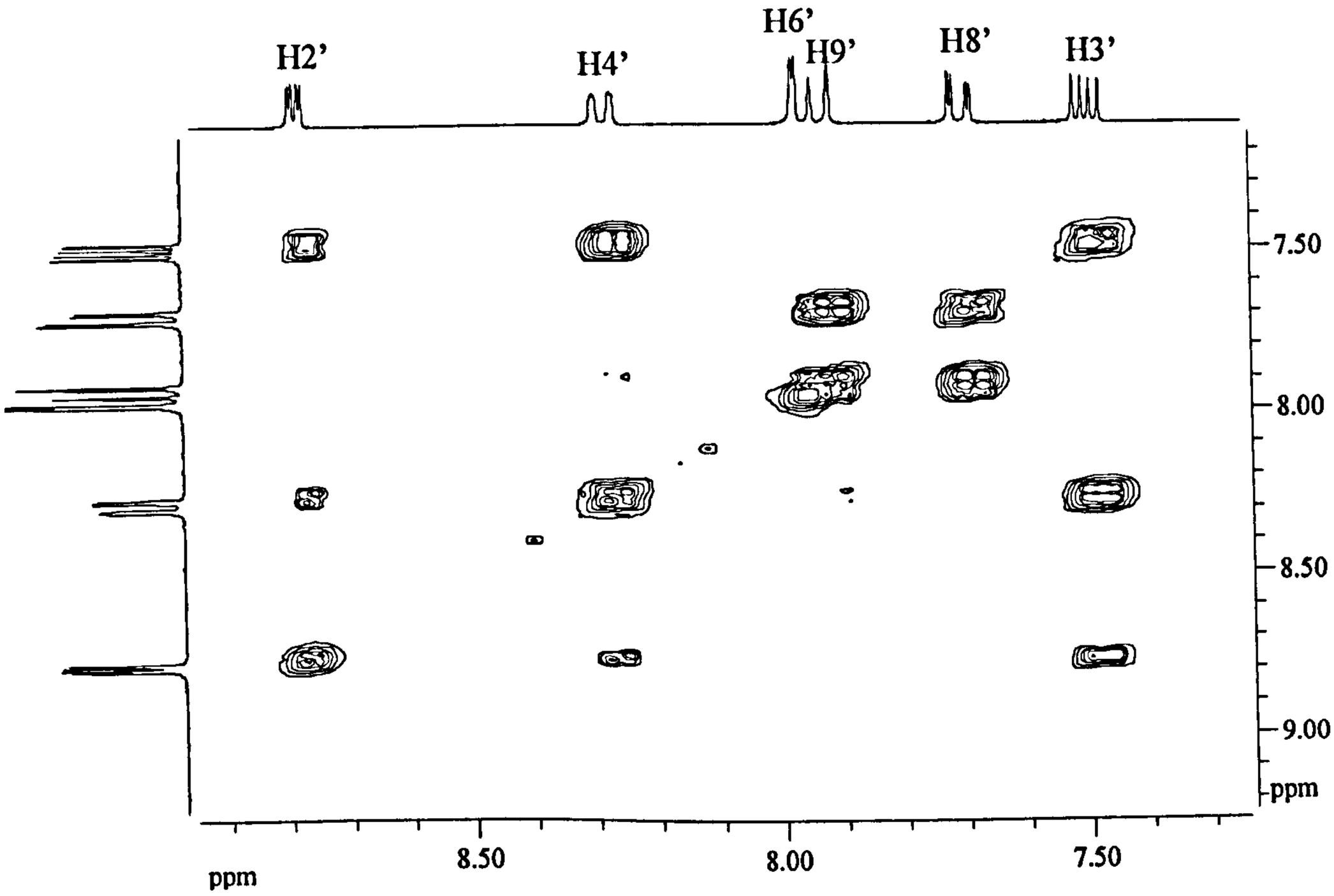

Figure A.1.18. The aromatic region in the COSY spectrum of ET-6-Q.

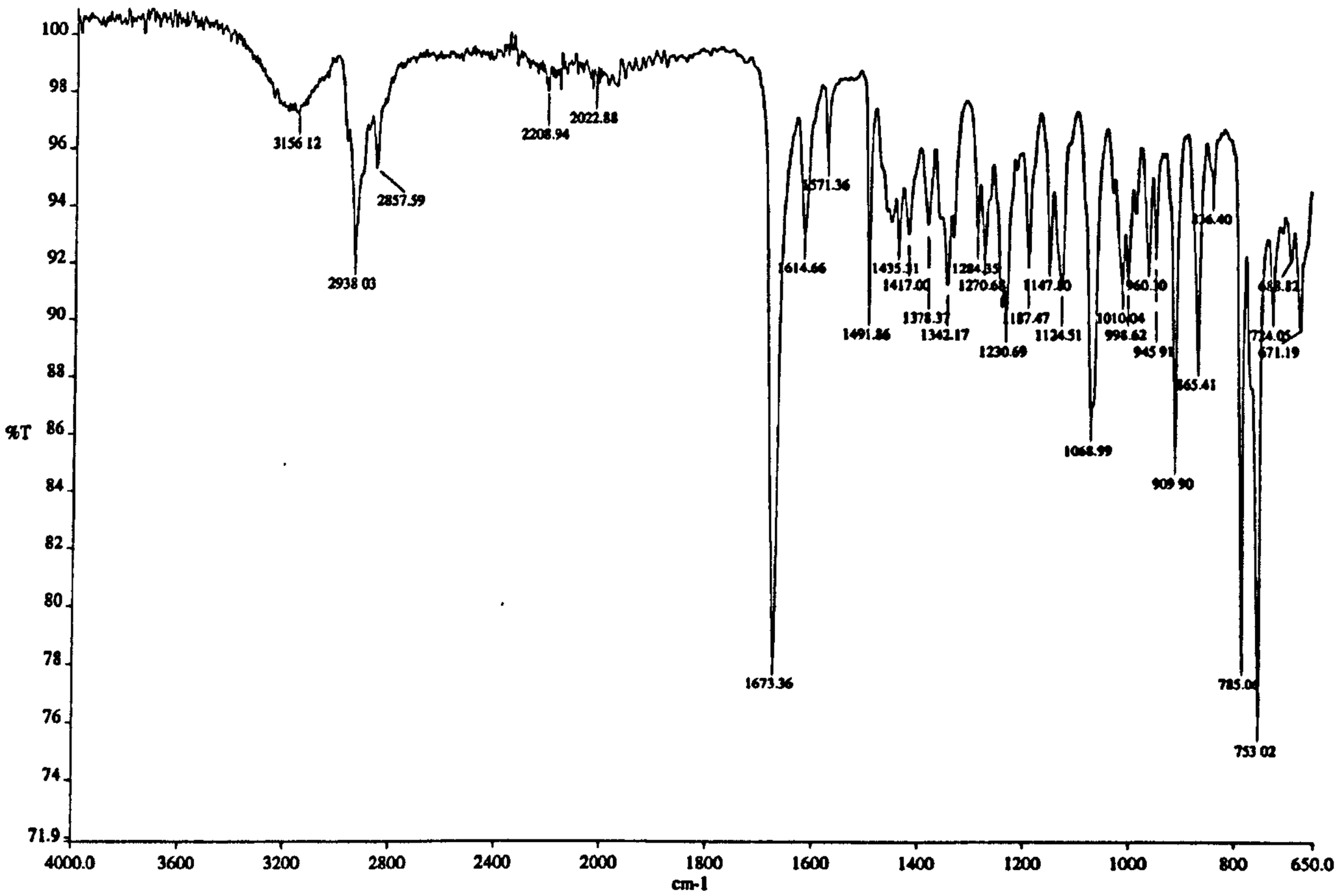

Figure A.1.19. The IR spectrum of ET-6-Q.

Appendix Two - Additional trans-cationic complex spectroscopy

A.2.1. TC-Py

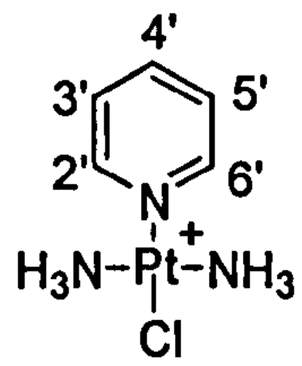

$[C_5H_{11}ClN_3Pt][NO_3]$

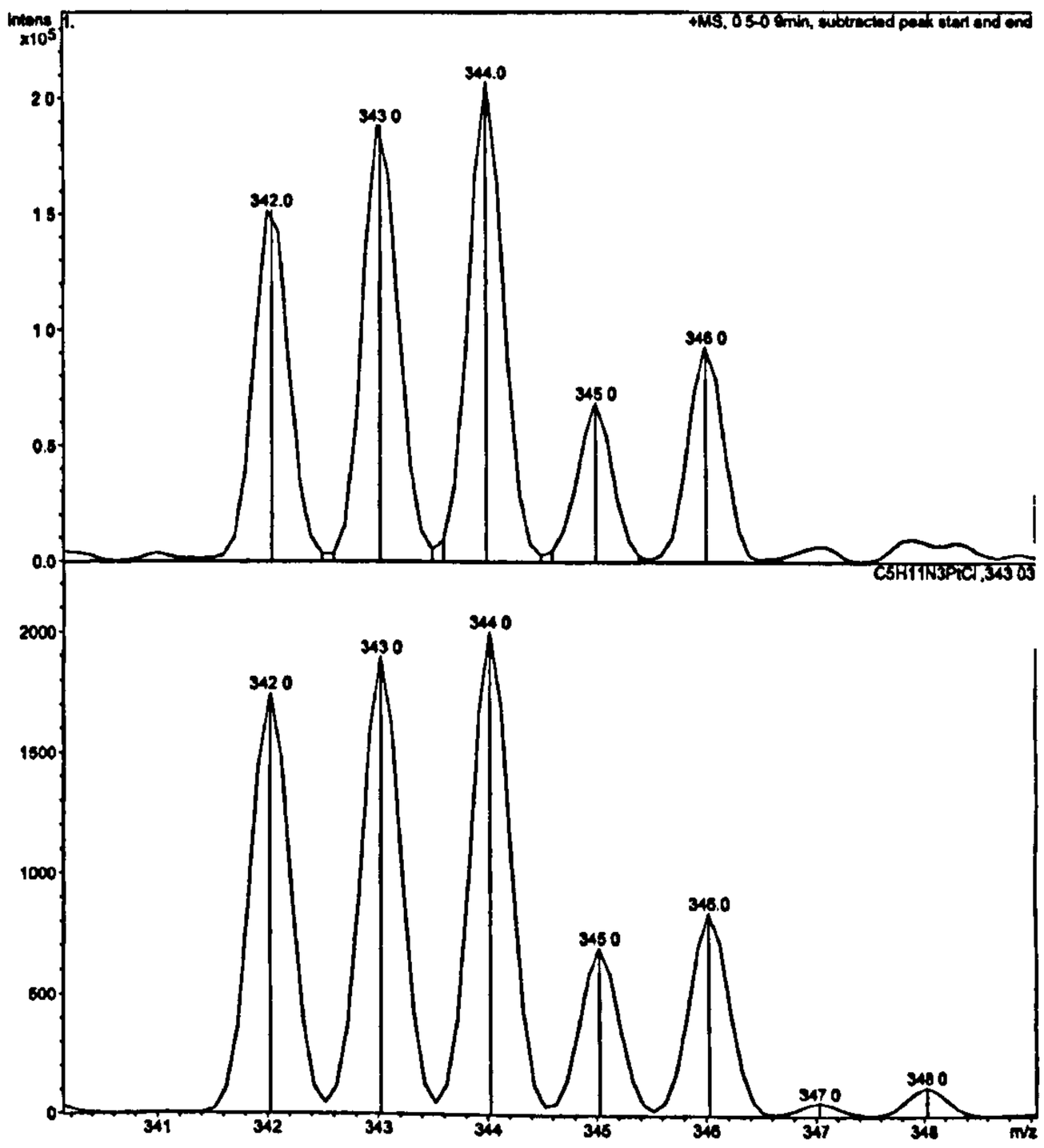

Figure A.2.1. The mass spectrum (ESI, +ve) of TC-Py showing experimental (upper) and theoretical (lower).

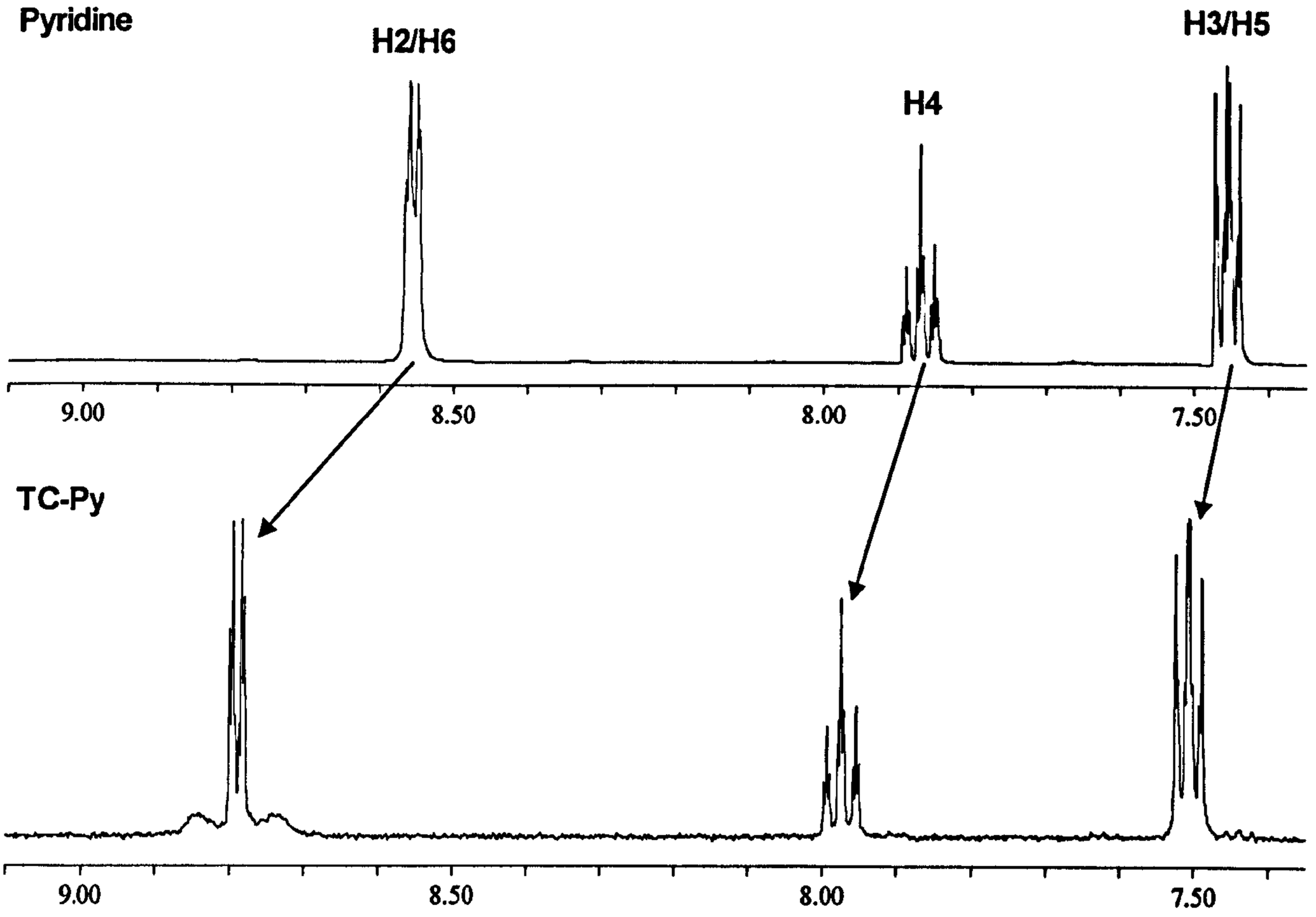

Figure A.2.2. Comparison of the chemical shifts of free pyridine and TC-Py.

A.2.2. TC-Q

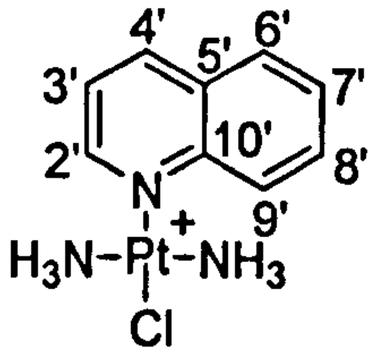

$[C_9H_{13}N_3Pt][NO_3]$

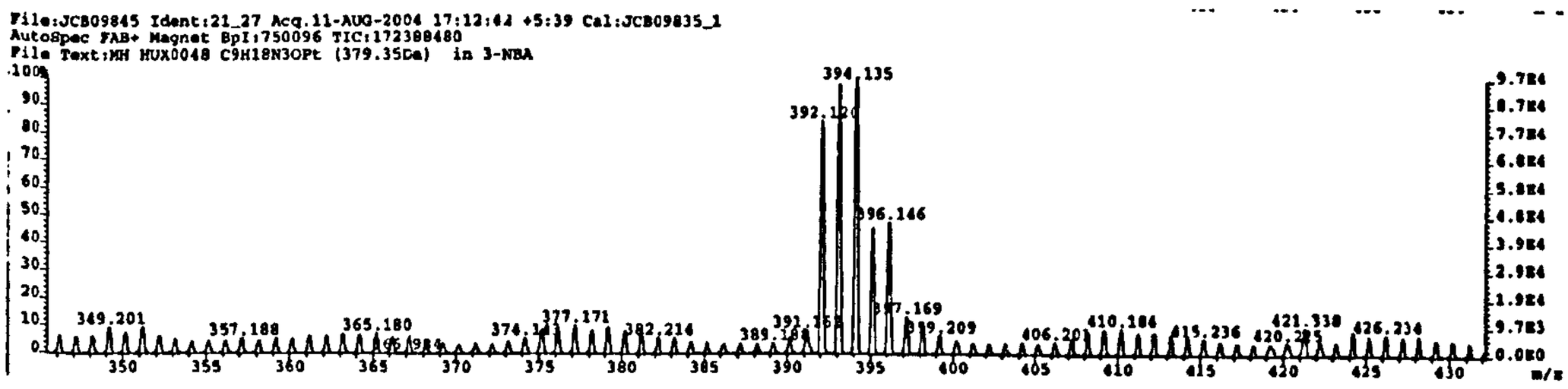

Figure A.2.3. The mass spectrum of TC-Q.

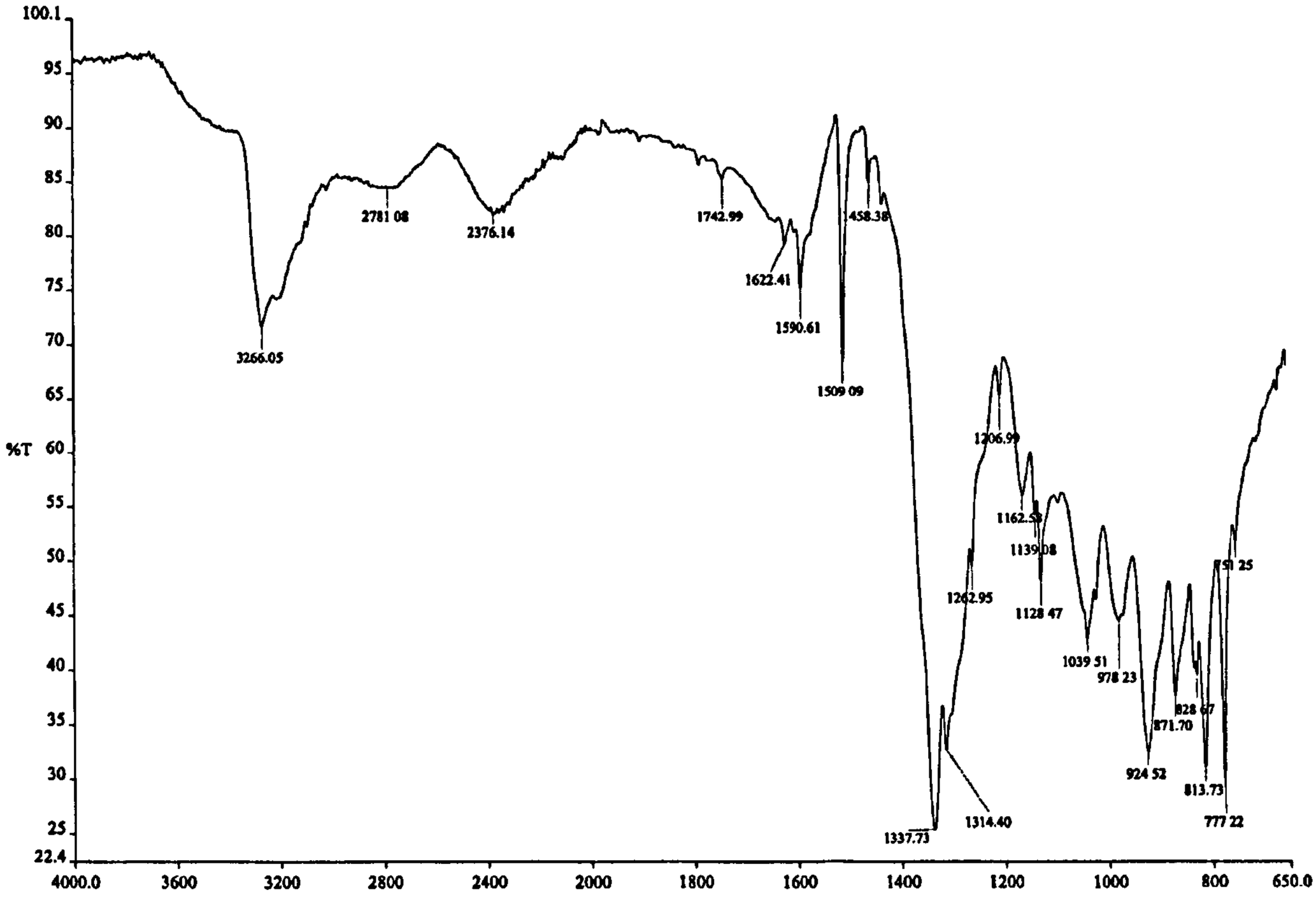

Figure A.2.4. The infrared spectrum of TC-Q.

A.2.3. TC-ET-3-Py

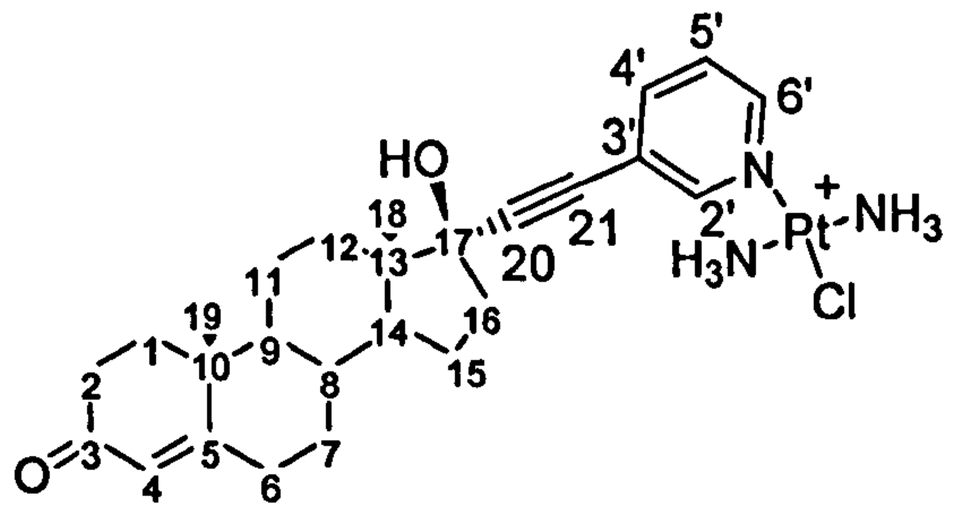

$[C_{26}H_{37}ClN_3O_2Pt][NO_3]$

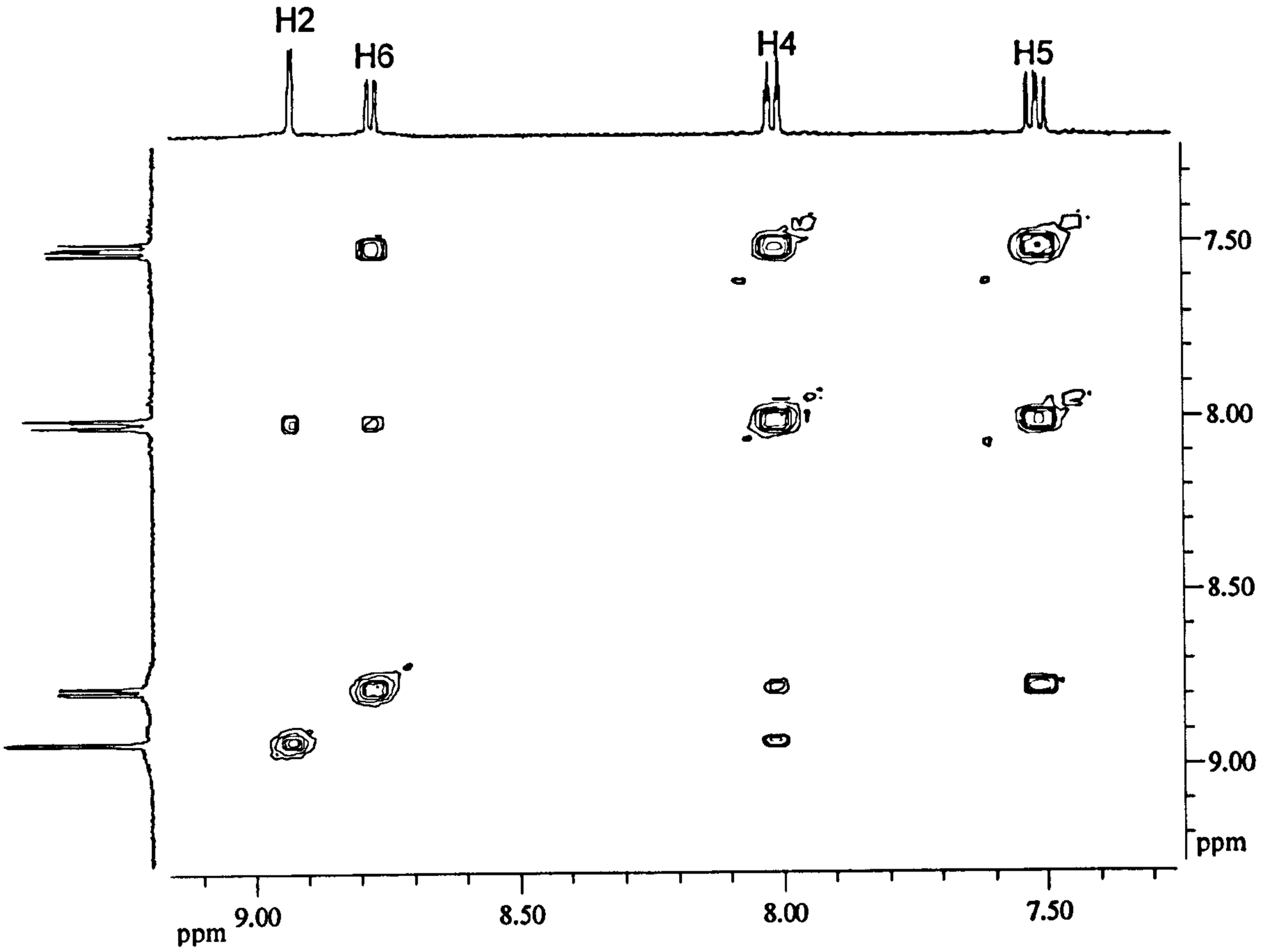

Figure A.2.5. The COSY spectrum for TC-ET-3-Py in CD_3OD.

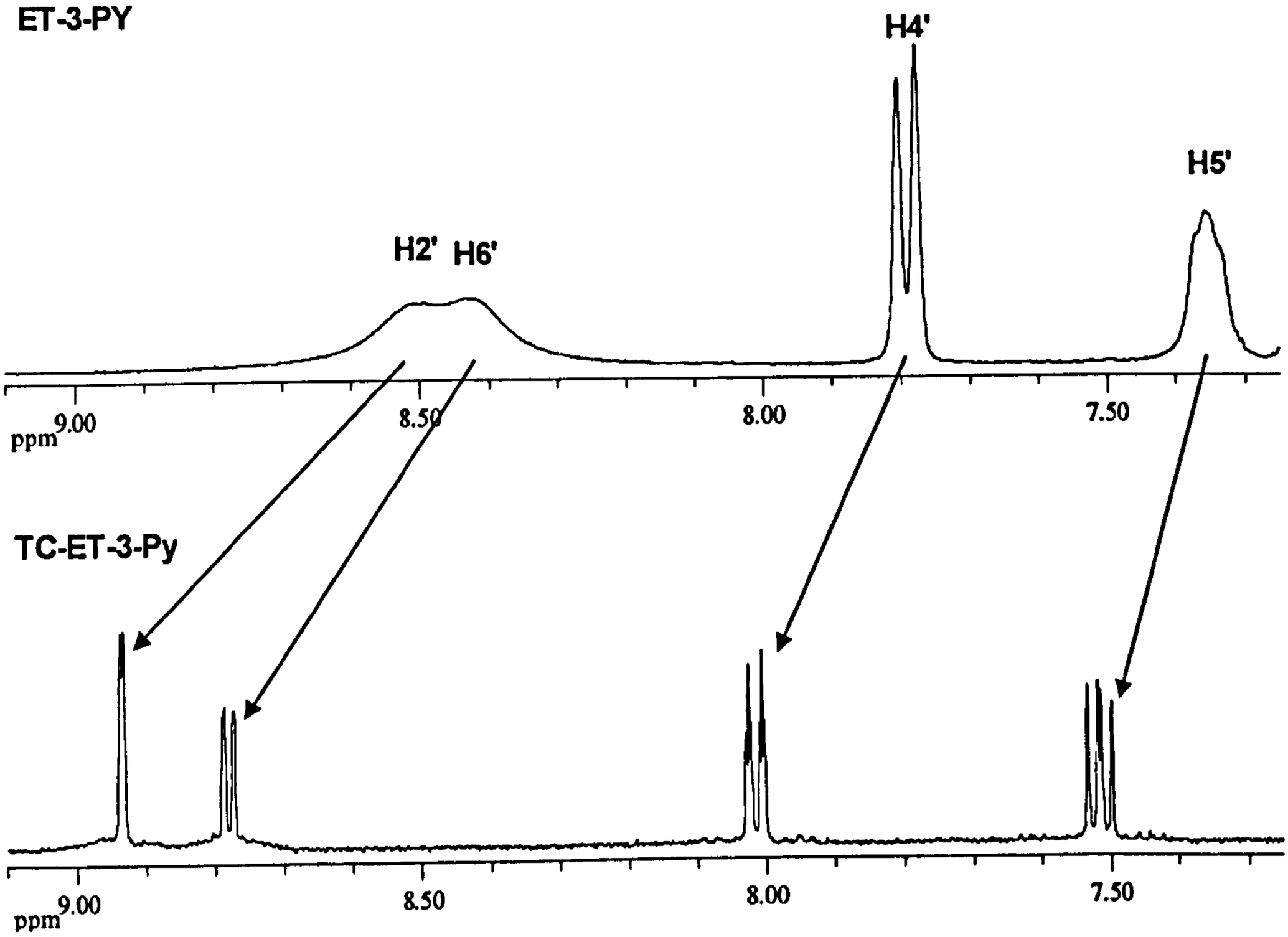

Figure A.2.6. The aromatic region in ^1H NMR spectra of ET-3-Py (upper) and TC-ET-3-Py(lower) in CD_3OD.

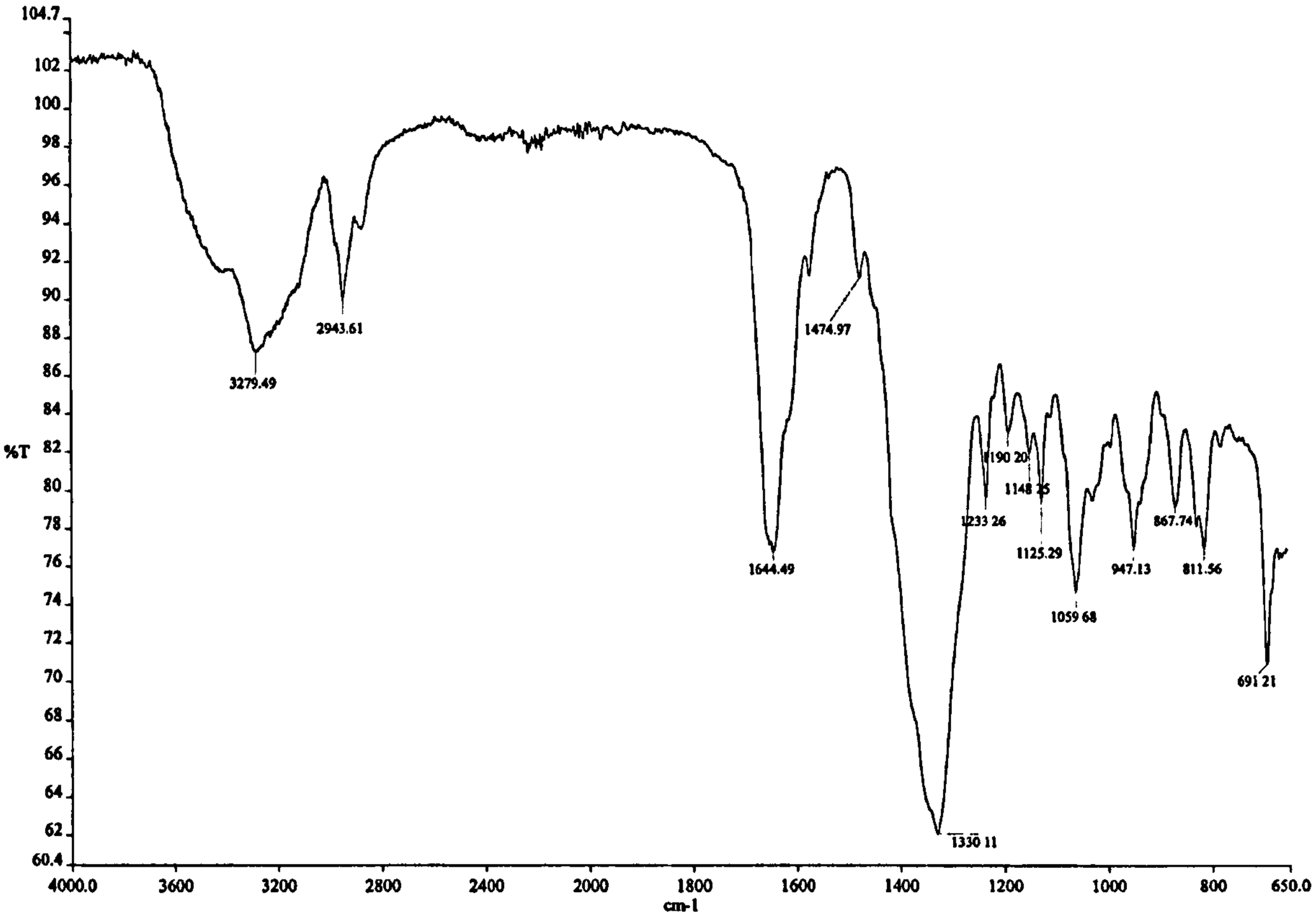

Figure A.2.7. The infrared spectrum of TC-ET-3-Py.

A.2.4. TC-ET-4-Py

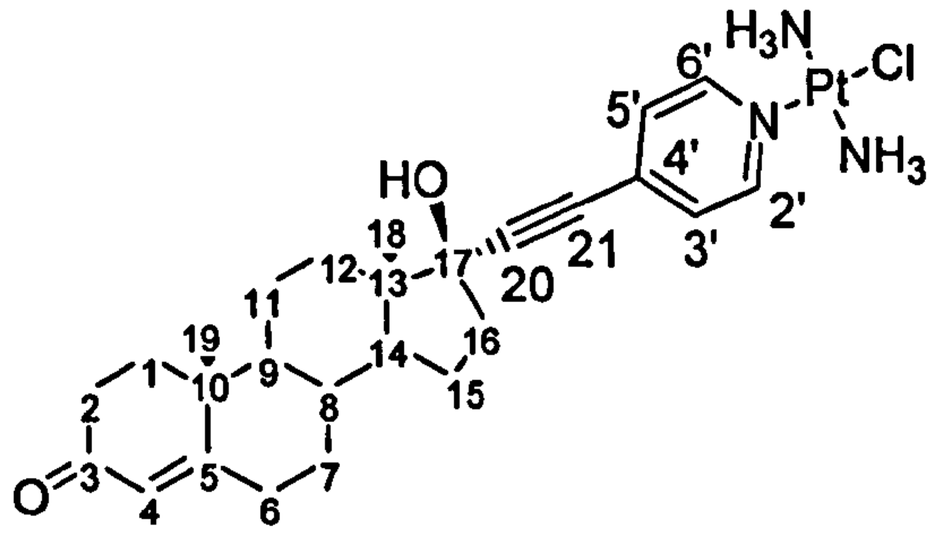

$[C_{26}H_{37}ClN_3O_2Pt][NO_3]$

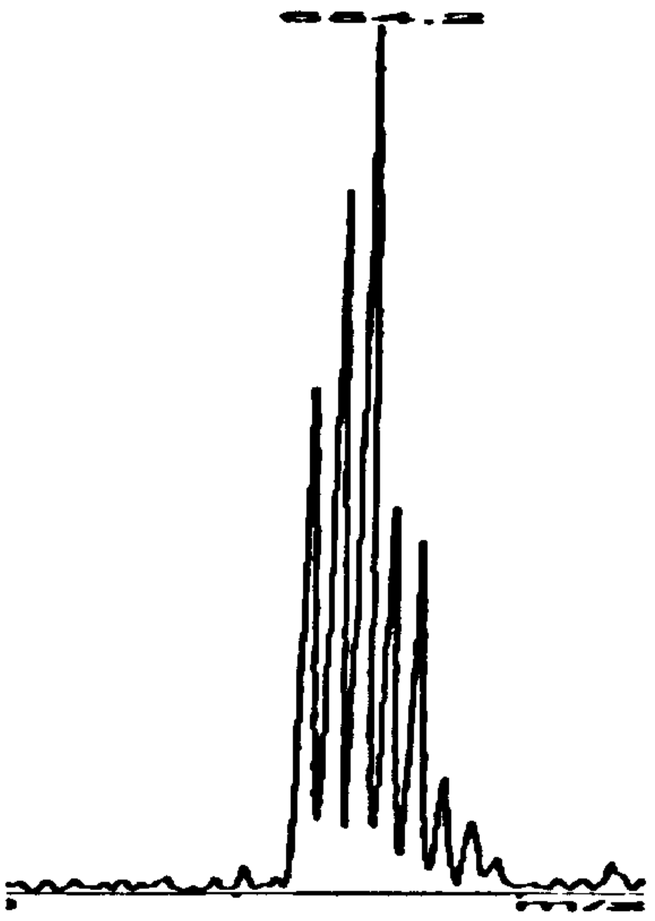

Figure A.2.8. The ESI mass spectra for TC-ET-4-Py showing the parent ion peak.

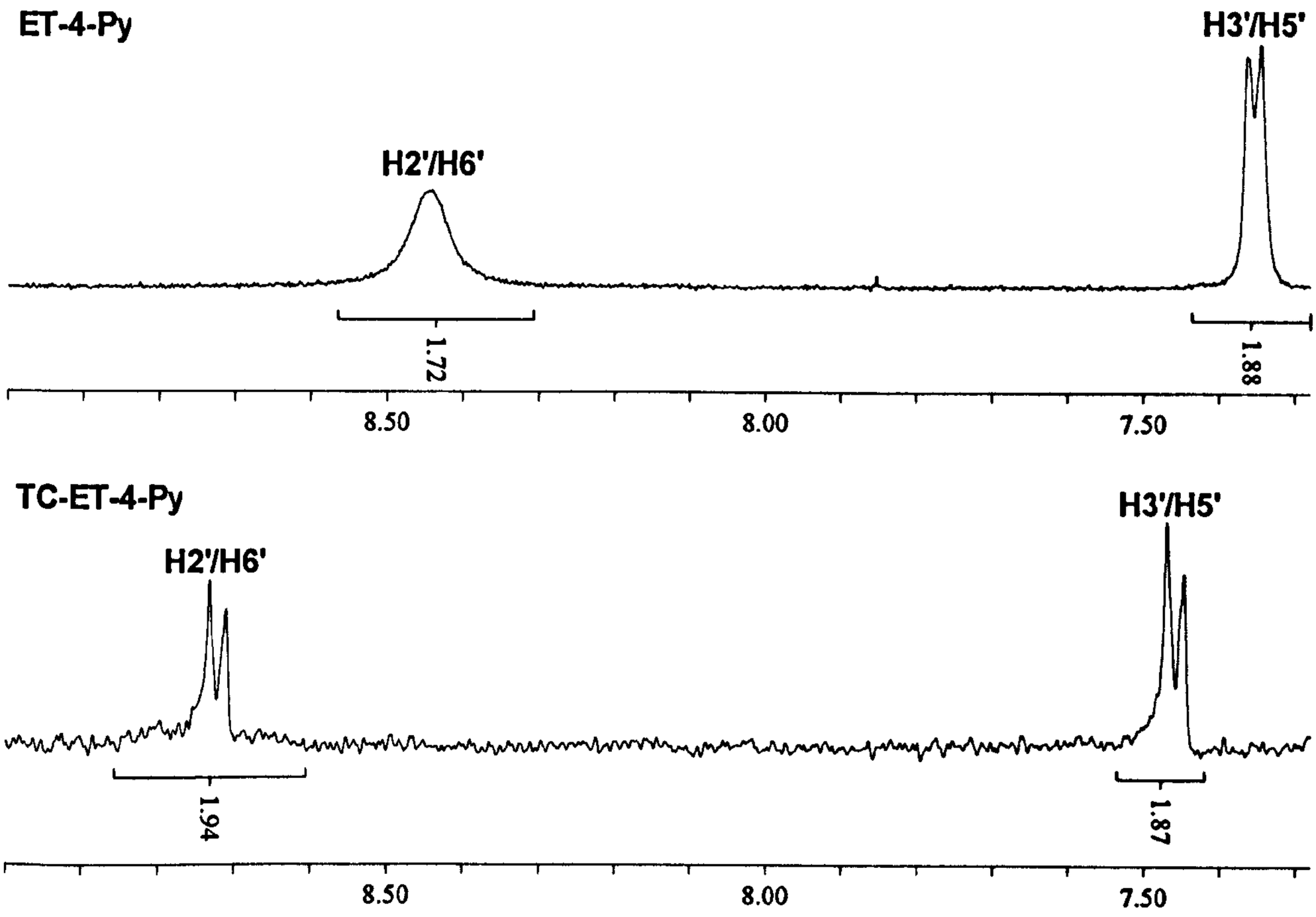

Figure A.2.9. The aromatic region of the ^{1}H NMR spectrum of ET-4-Py and TC-ET-4-Py in CD_3OD.

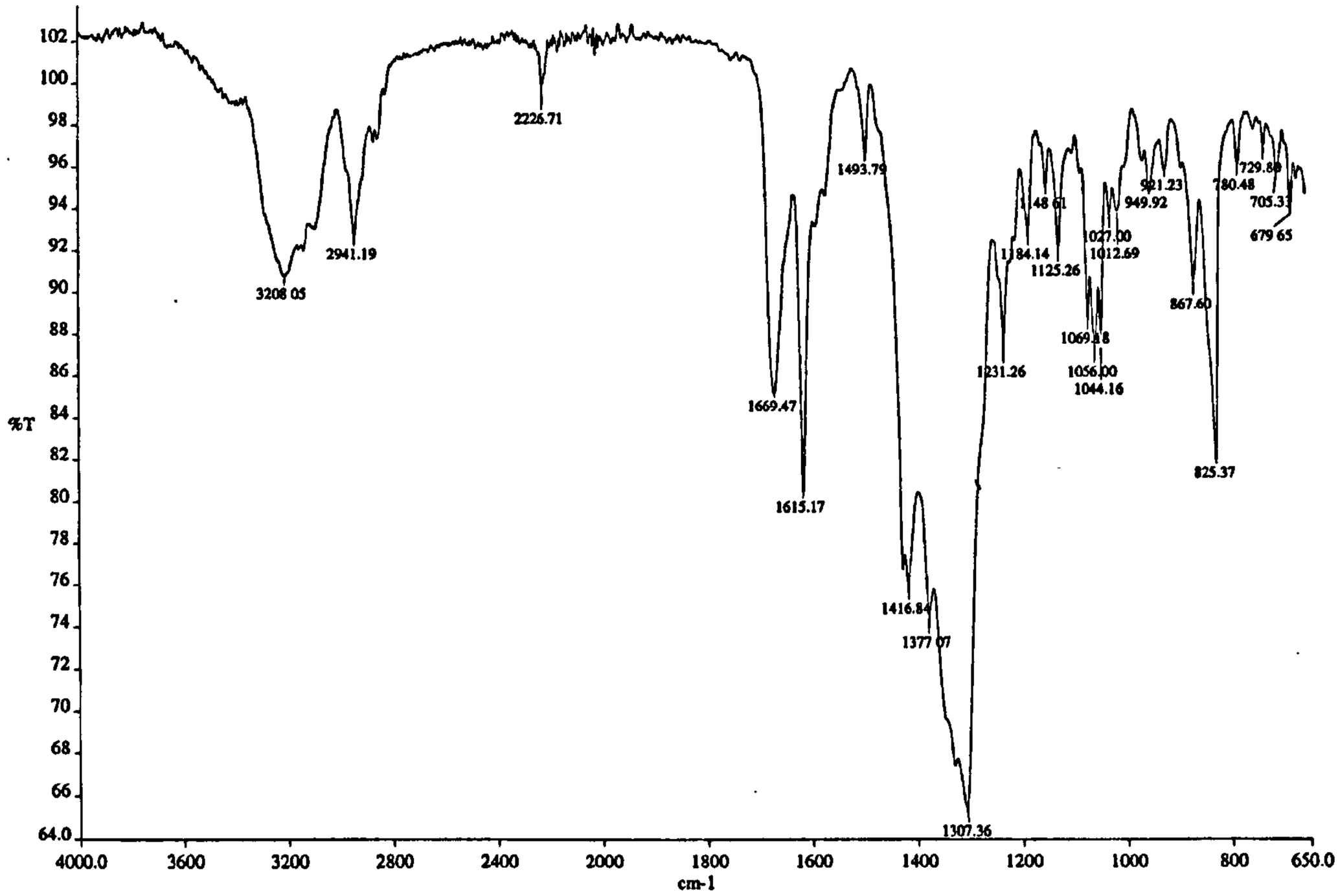

Figure A.2.10. The infrared spectrum of TC-ET-4-Py.

A.2.5. TC-ET-3-Q

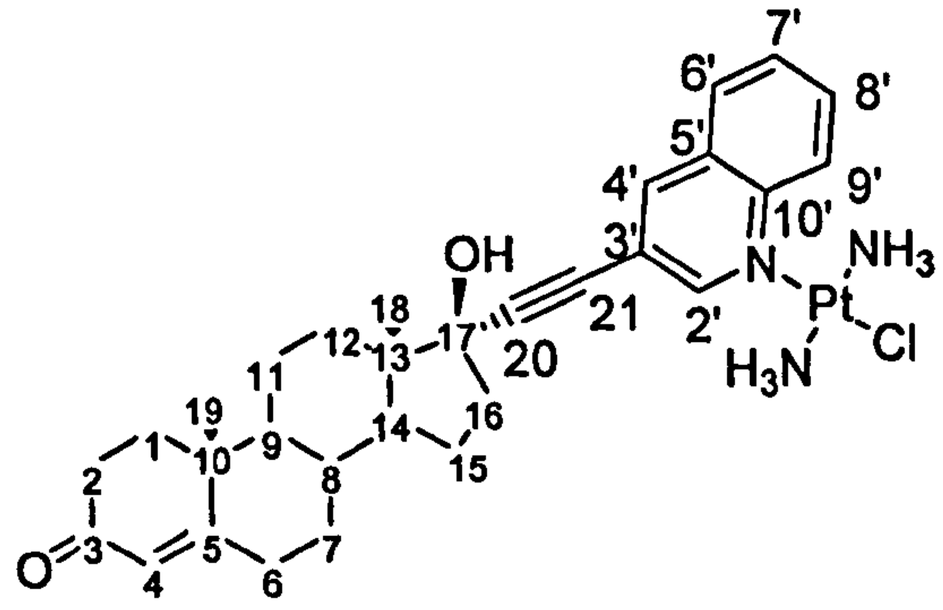

$[C_{30}H_{39}ClN_3O_2Pt][NO_3]$

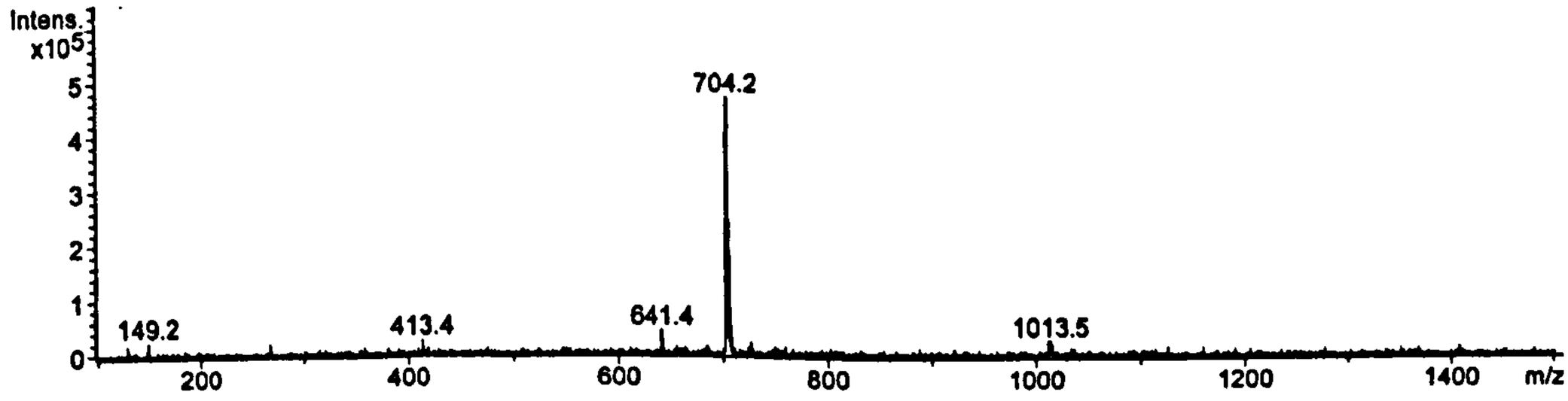

Figure A.2.11. The ESI-MS of TC-ET-3-Q.

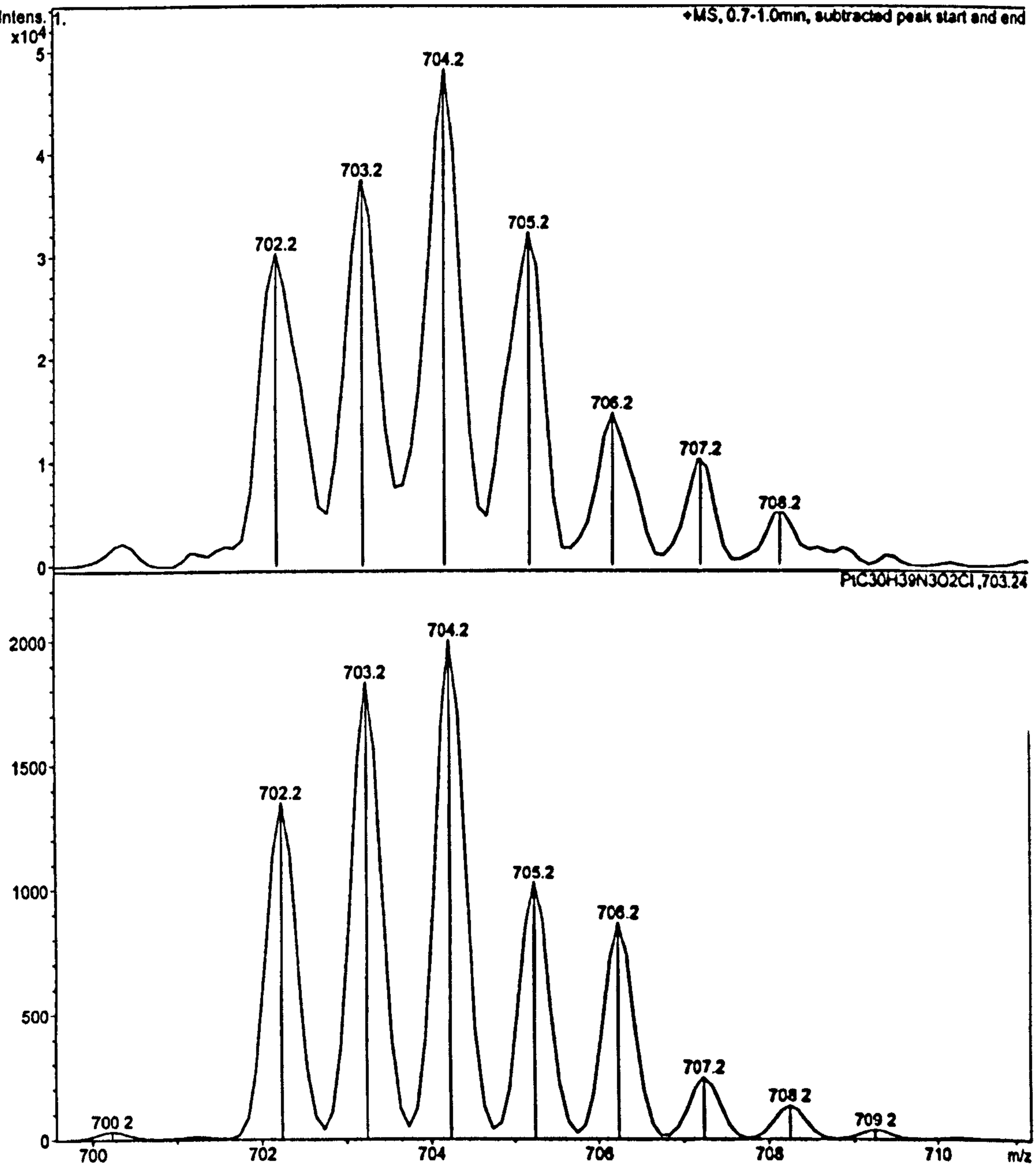

Figure A.2.12. The actual (upper) and theoretical (lower) isotope pattern of the *m/z*= 704.2 peak in the spectrum of TC-ET-3-Q.

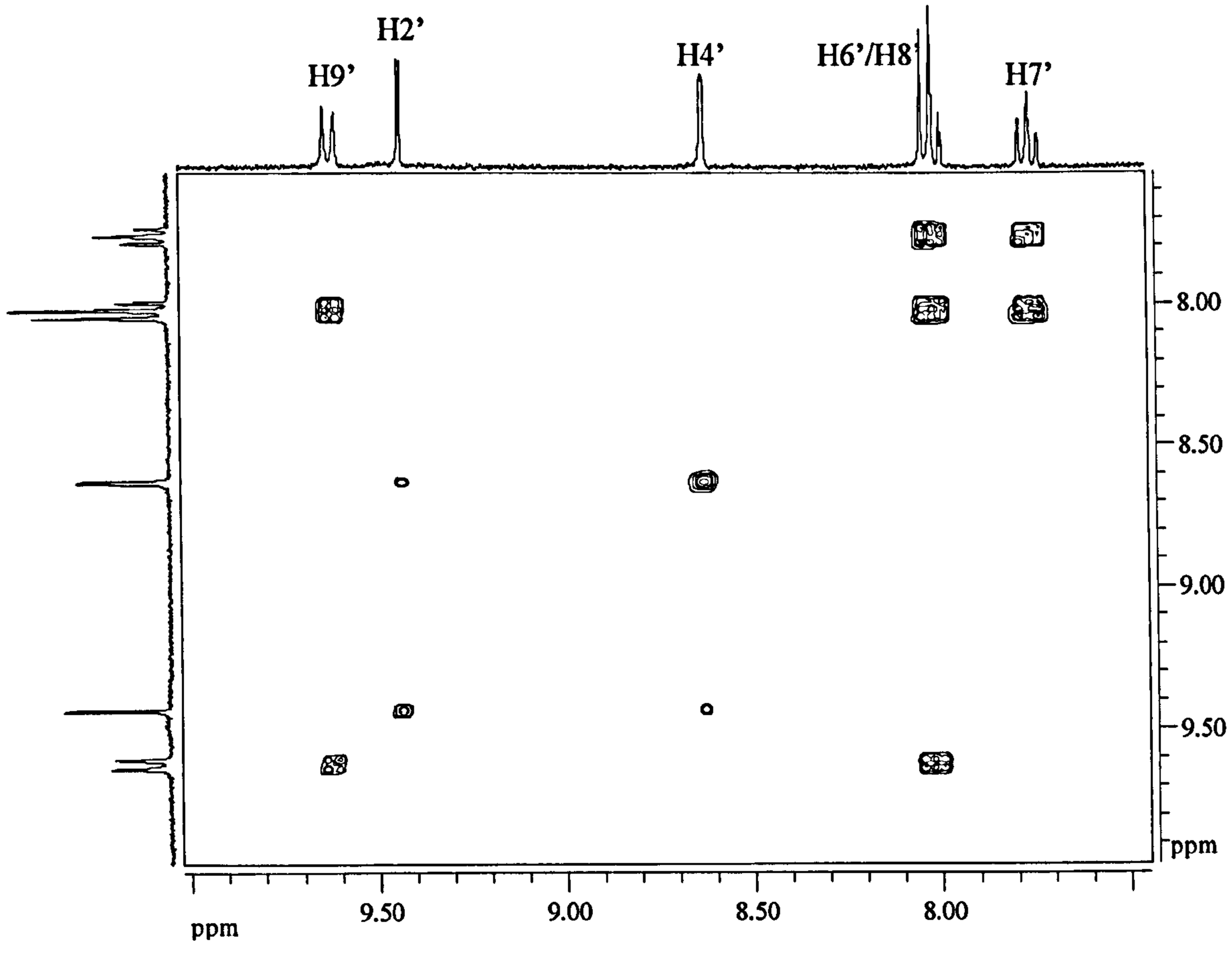

Figure A.2.13. The ^{1}H NMR COSY spectrum of TC-ET-3-Q.

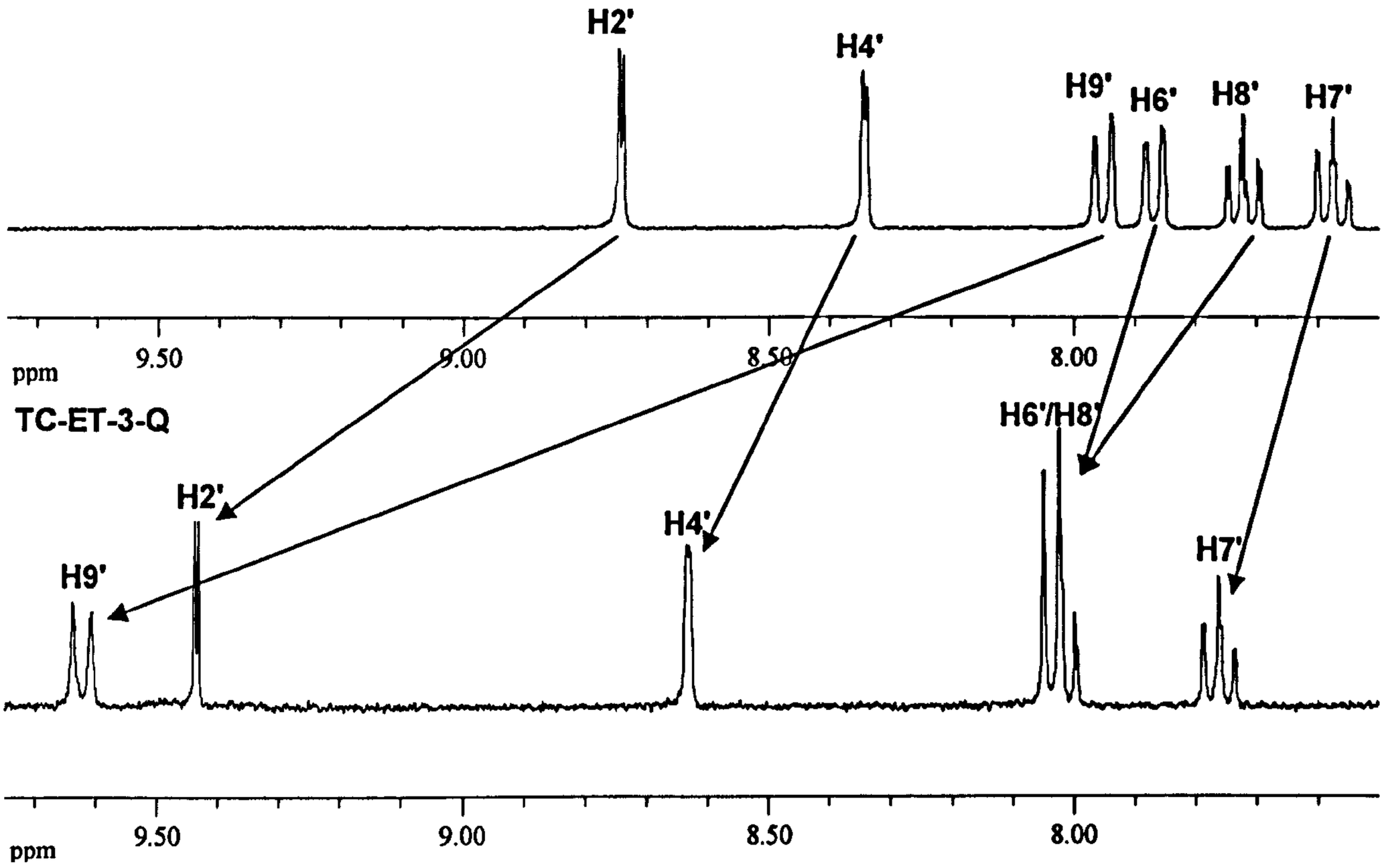

Figure A.2.14. The ^{1}H NMR spectrum of ET-3-Q (upper) and TC-ET-3-Q (lower) in CD_3OD.

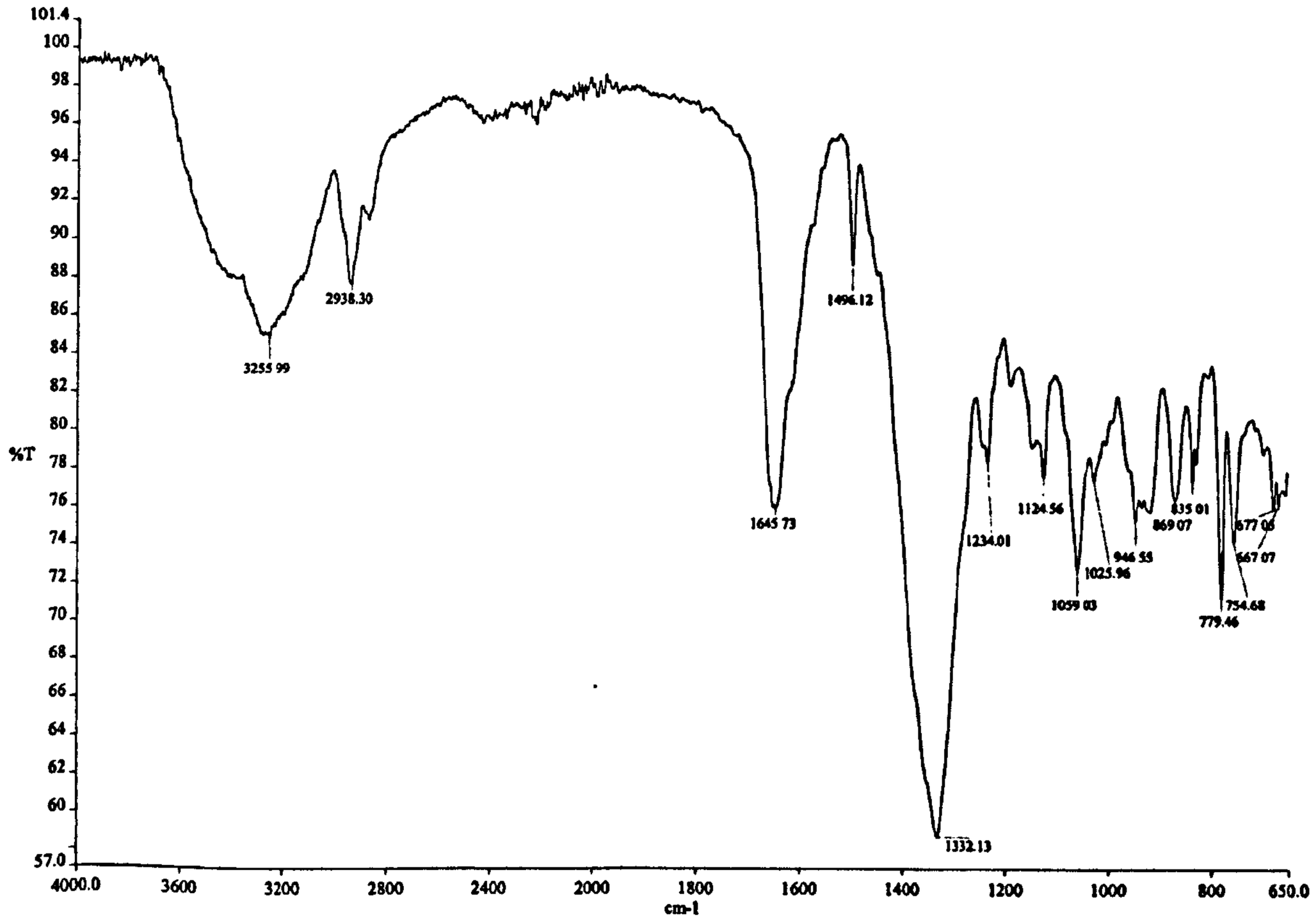

Figure A.2.15. The infrared spectrum of TC-ET-3-Q

A.2.6. TC-ET-4-IQ

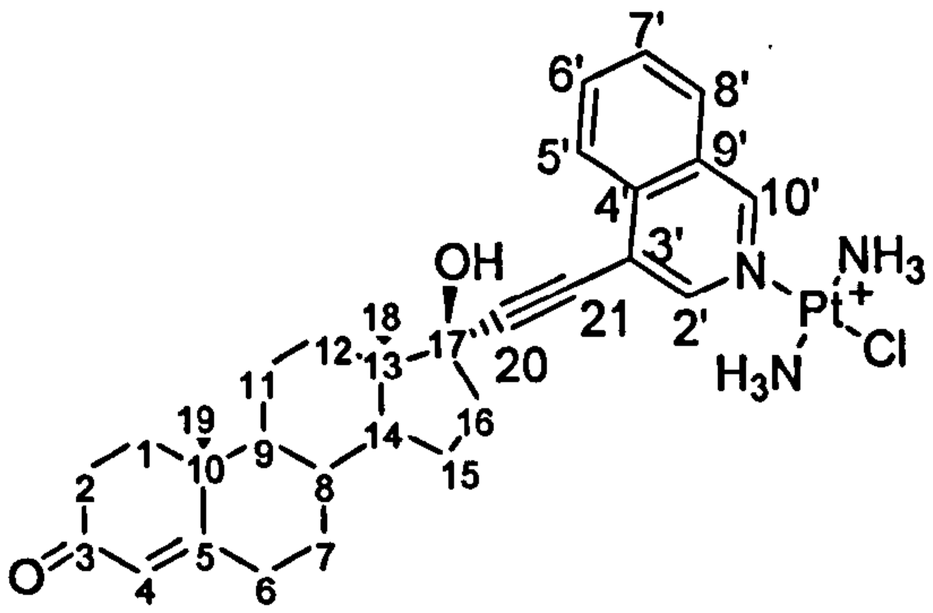

$[C_{30}H_{39}ClN_3O_2Pt][NO_3]$

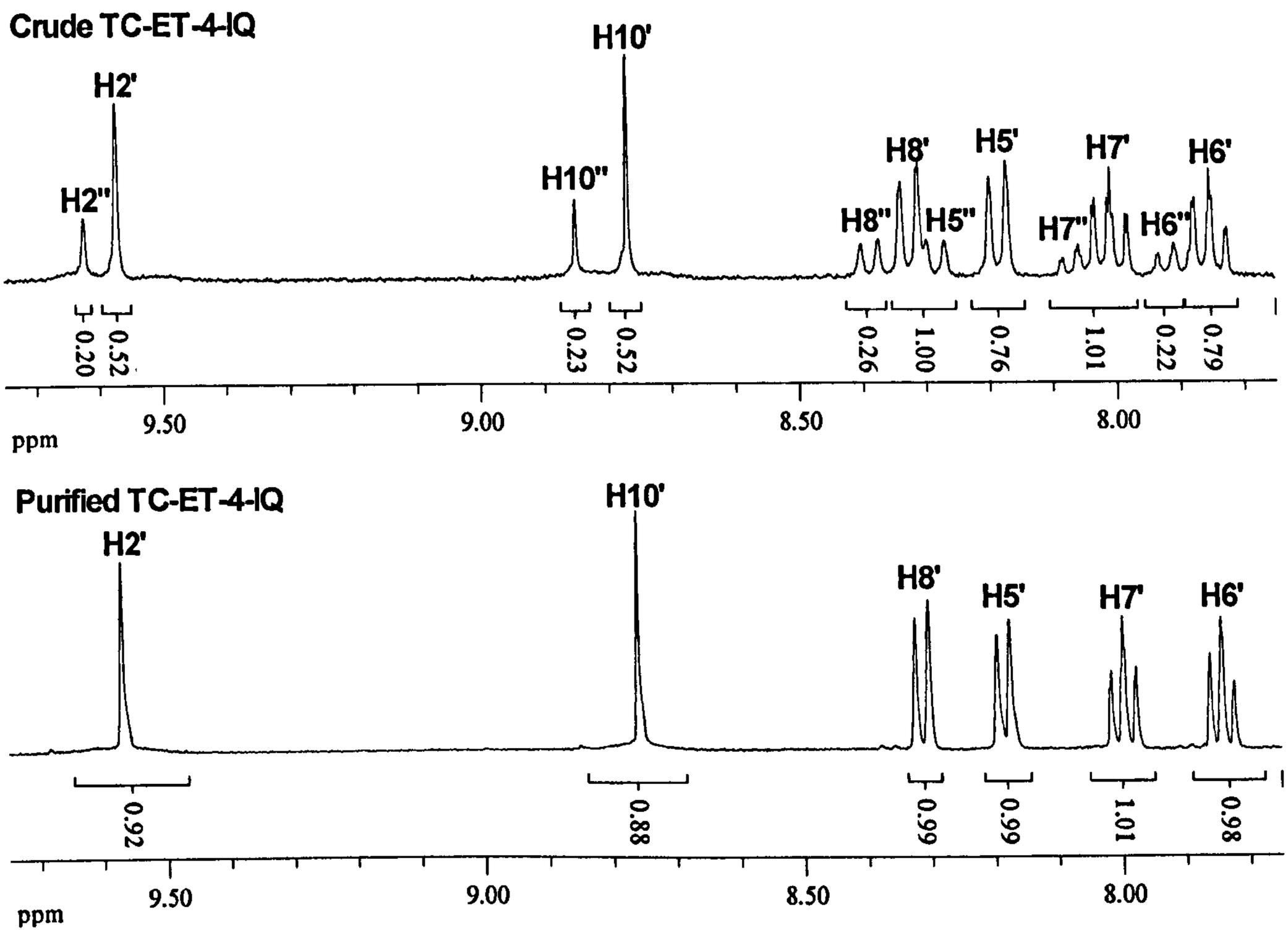

Figure A.2.16. Comparison of the aromatic region of the ^{1}H NMR spectrum of crude (upper) and pure (lower) TC-ET-4-IQ.

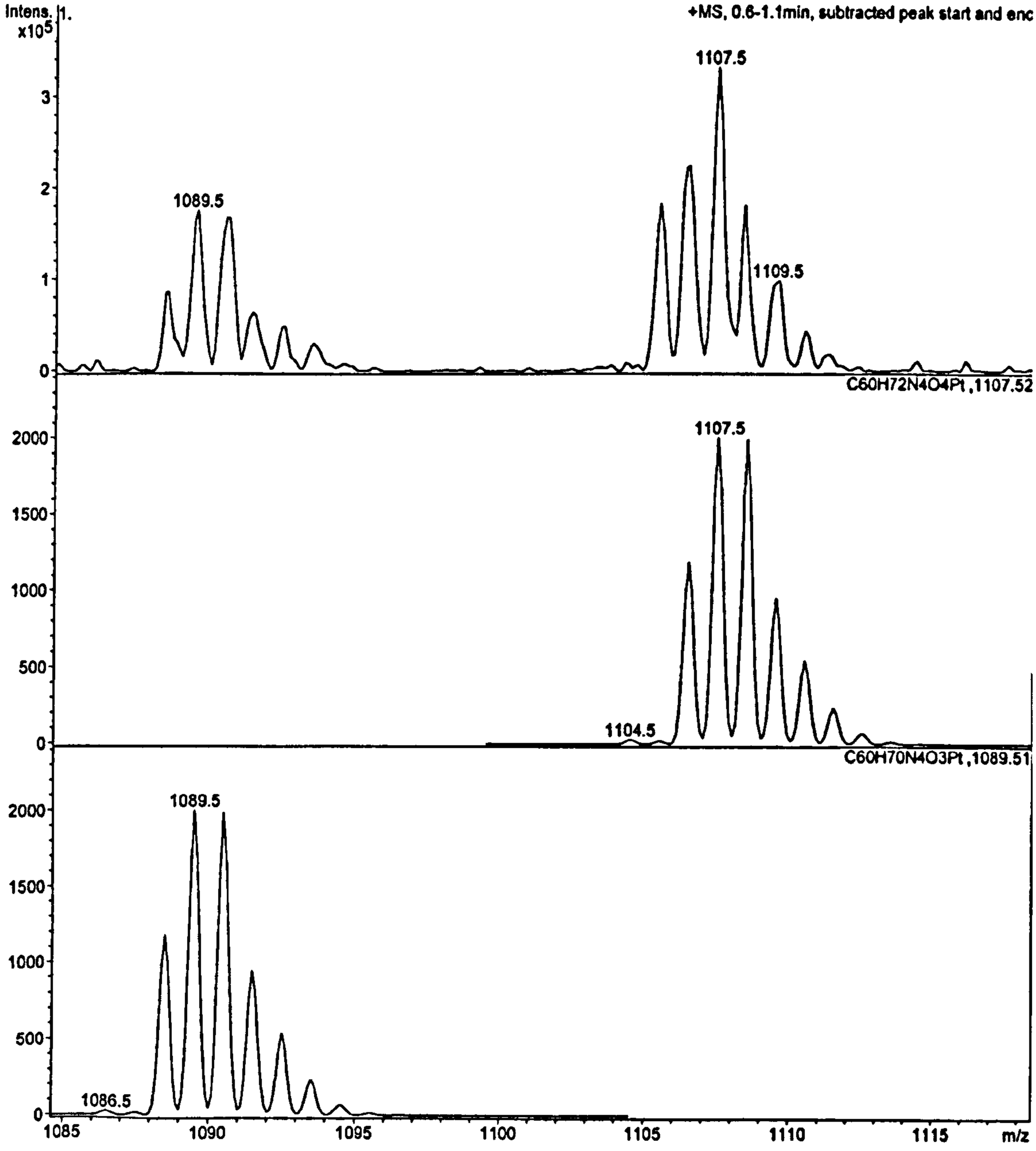

Figure A.2.17. The mass spectrum (ESI, + 83.9V) showing the peaks at *m/z* = 1107.5 and 1089.5 assigned to $[M\text{-}H]^+$ and $[M\text{-}H_2O]^+$, M = $[Pt(NH_3)_2(C_{30}H_{33}NO_2)_2]$.

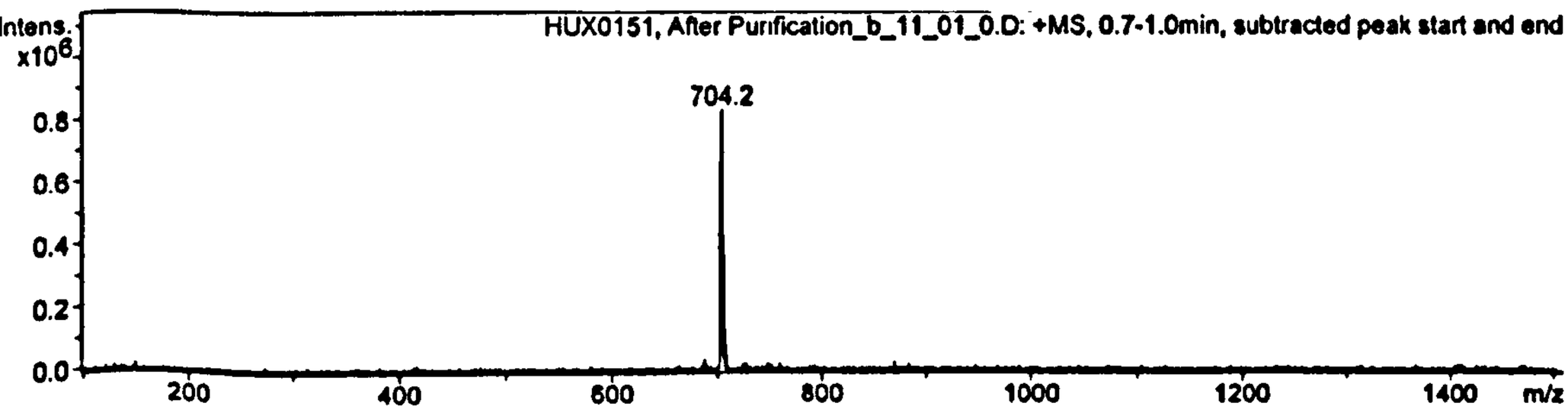

Figure A.2.18. The mass spectrum (ESI, +ve) of purified TC-ET-4-IQ.

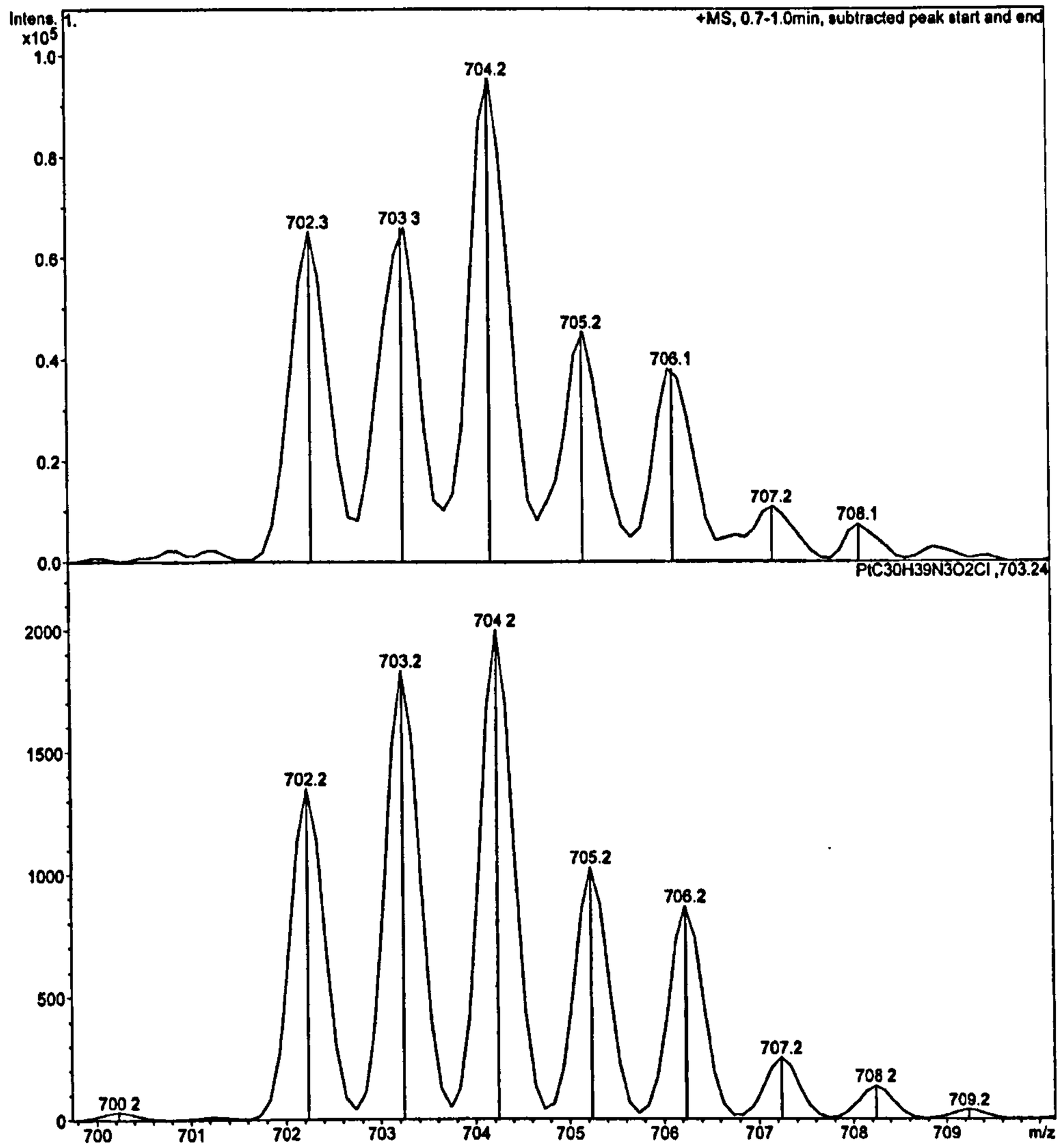

Figure A.2.19. The experimental (upper) and theoretical (lower) isotope distribution patterns for the mass spectrum (ESI, +ve) of TC-ET-4-IQ.

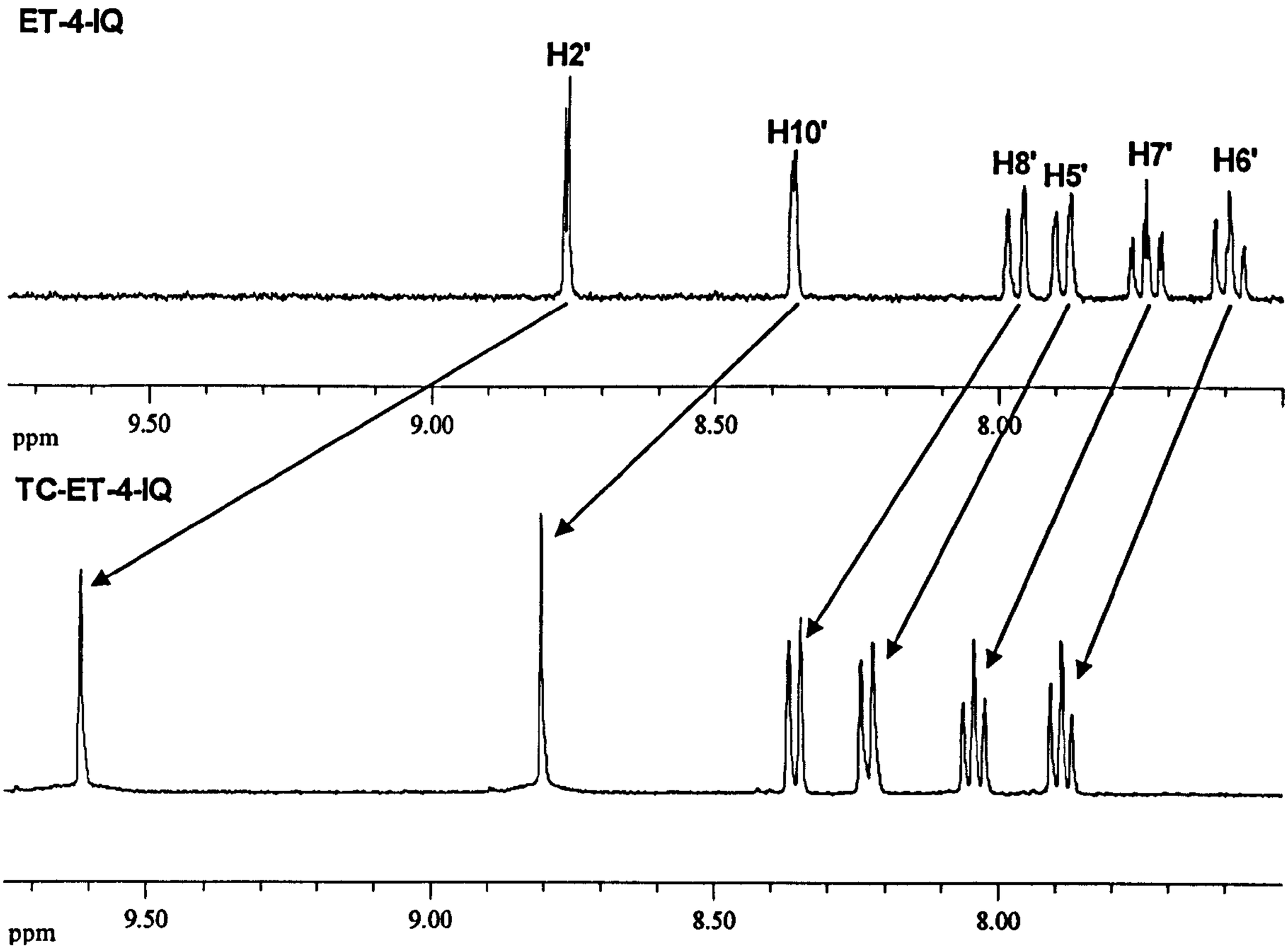

Figure A.2.20. The aromatic region of the ^{1}H NMR spectrum of ET-4-IQ (upper) and TC-ET-4-IQ (lower) in CD_3OD.

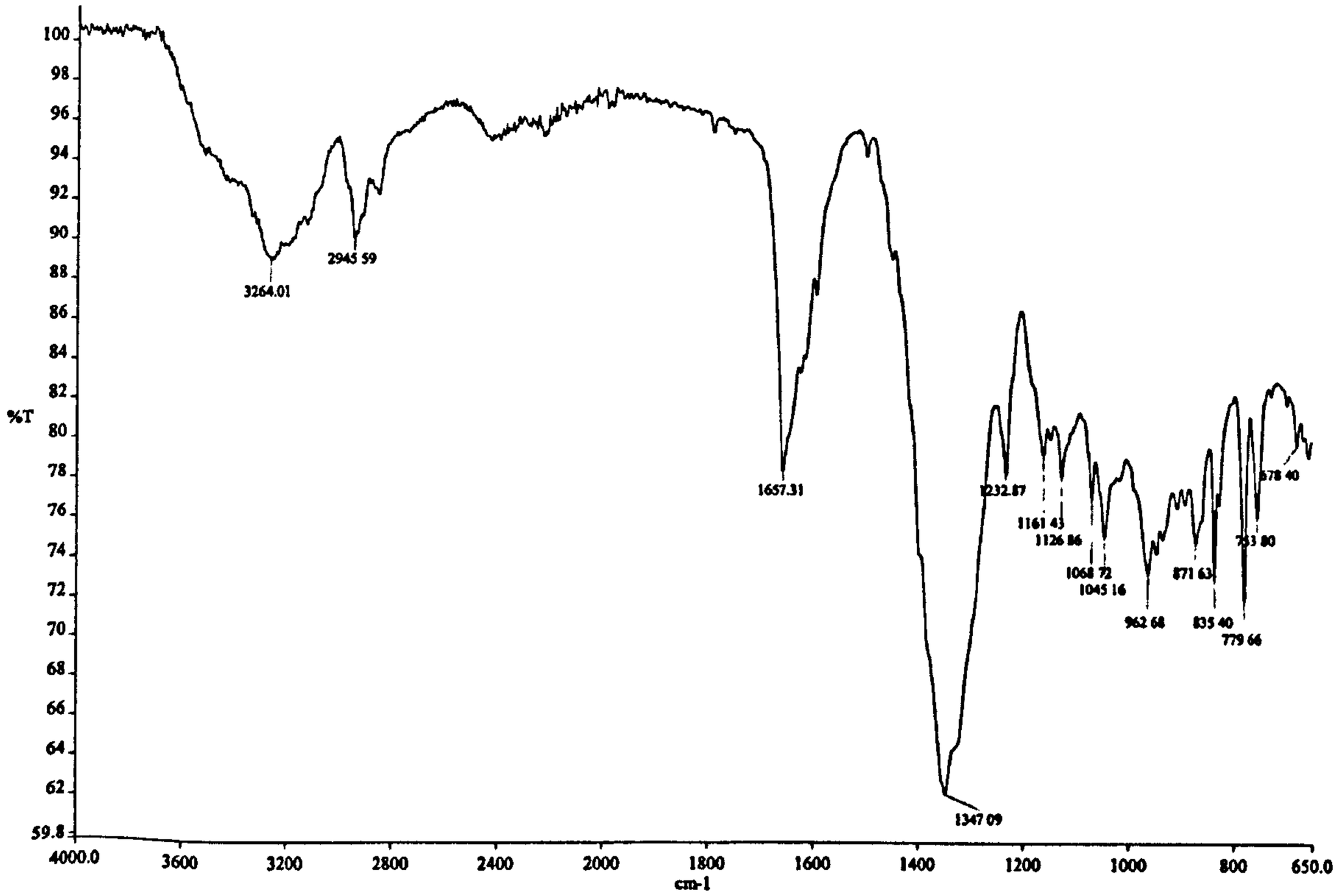

Figure A.2.21. The infrared spectrum of TC-ET-4-IQ.

A.2.7. TC-ET-6-Q

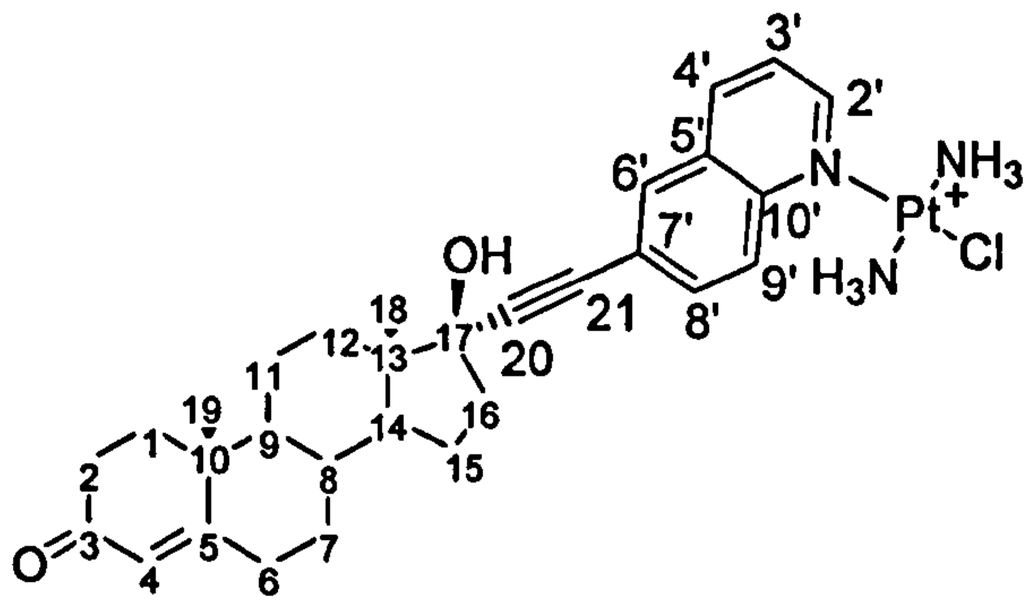

$[C_{30}H_{39}ClN_3O_2Pt][NO_3]$

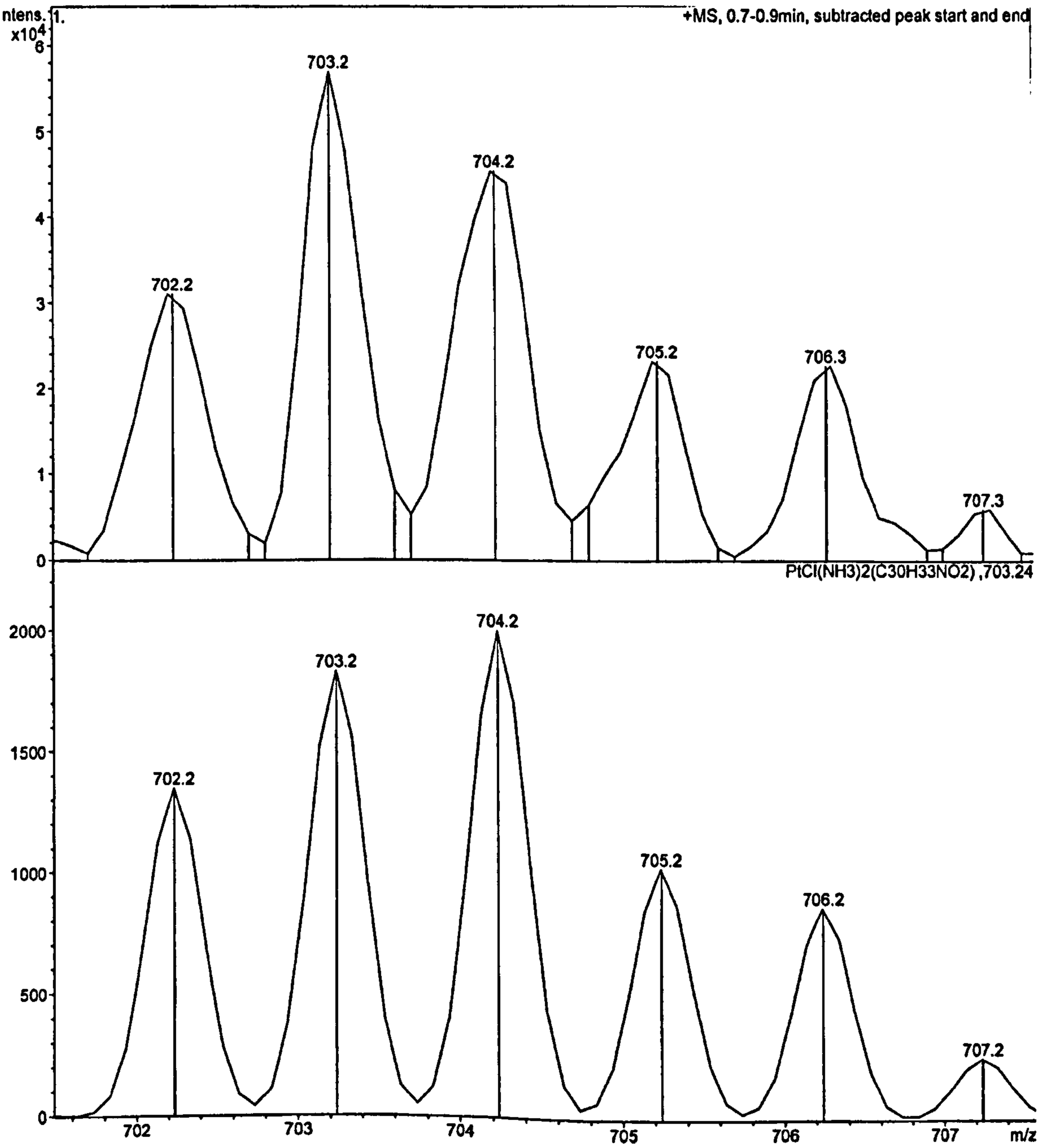

Figure A.2.22. The mass spectrum of TC-ET-6-Q (ESI, +ve).

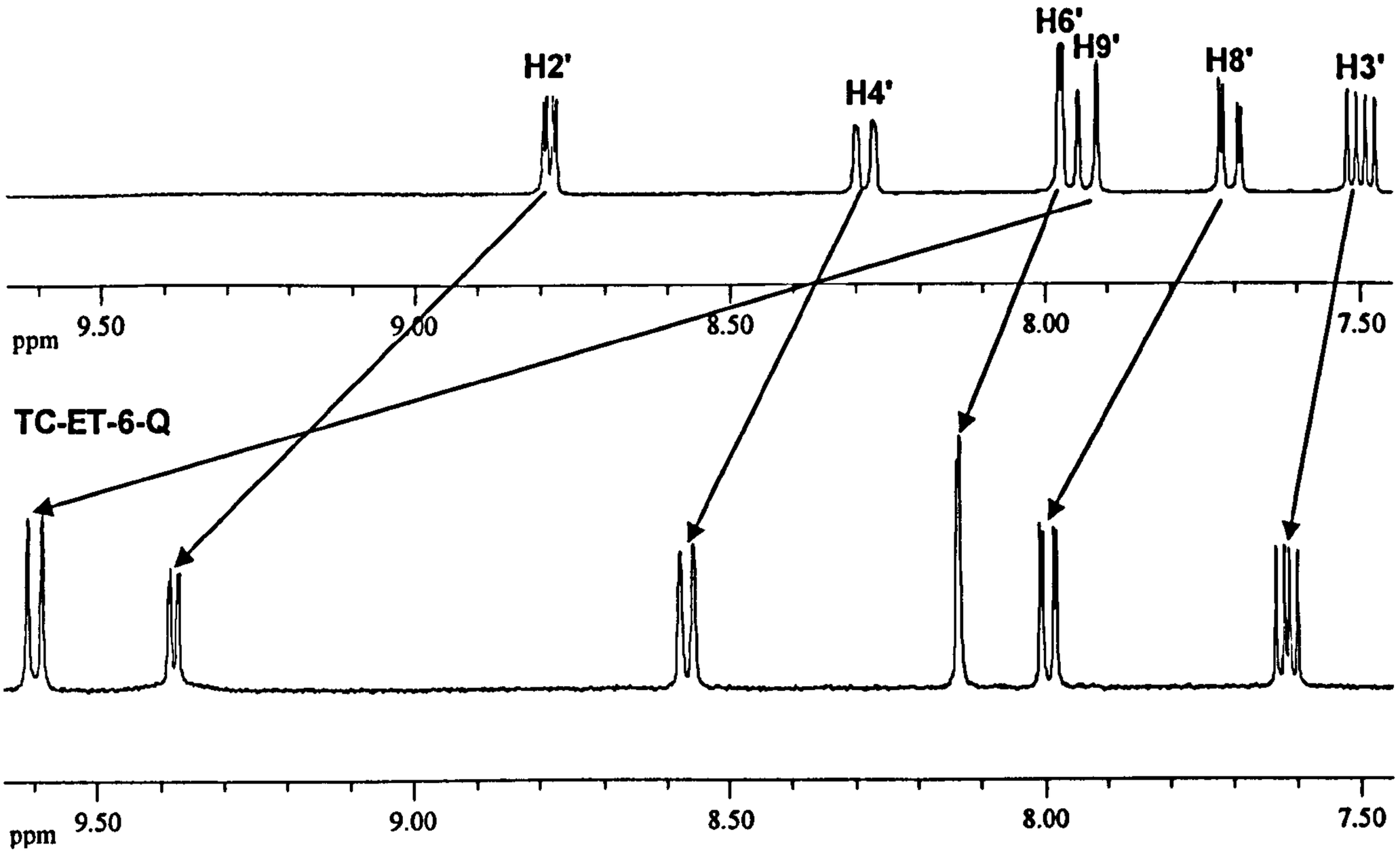

Figure A.2.23. The comparison of the ^{1}H NMR spectra of ET-6-Q and TC-ET-6-Q.

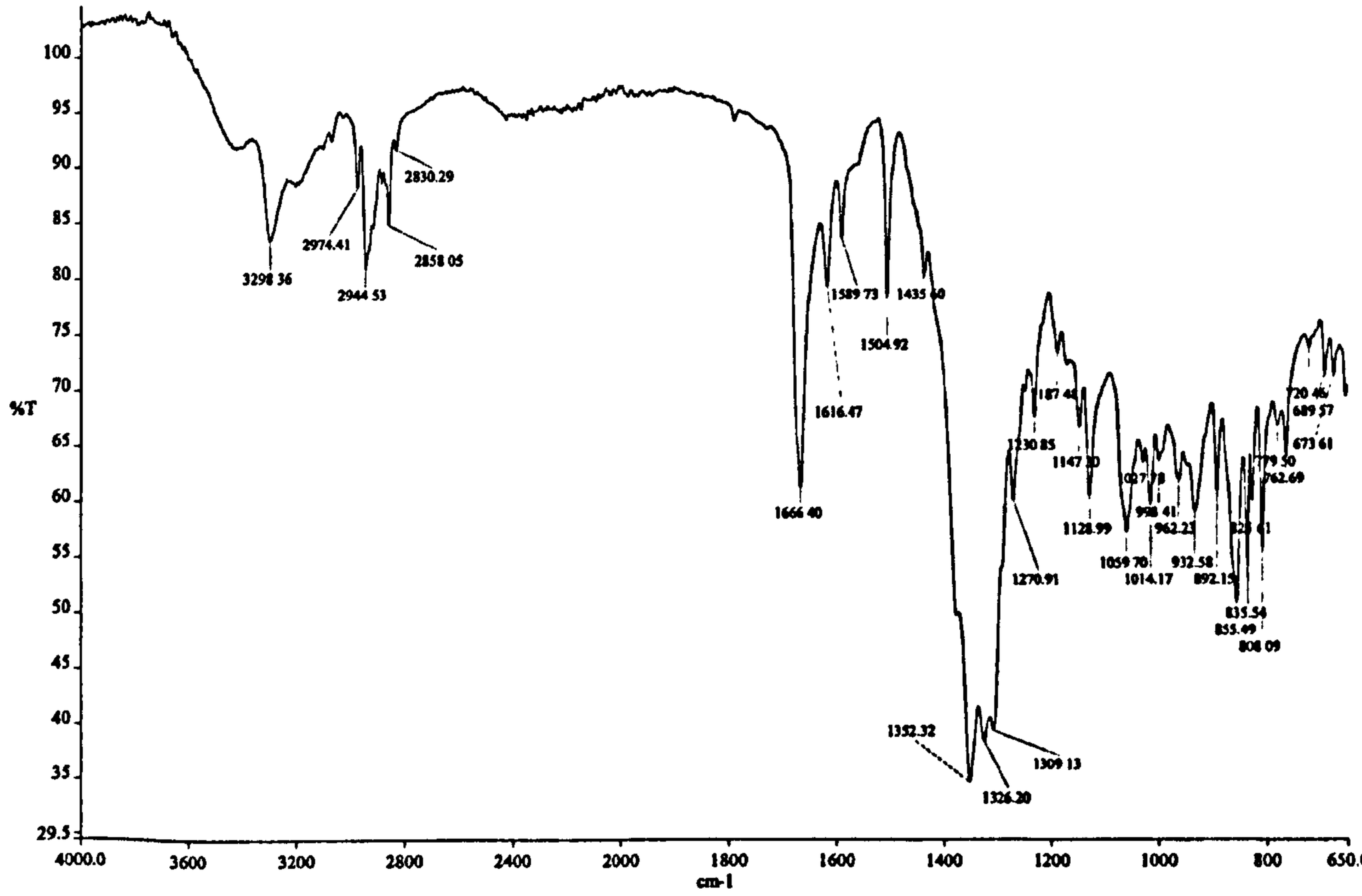

Figure A.2.24. The IR spectrum of TC-ET-6-Q.

Appendix Three - Additional cis-cationic complex Spectroscopy

A.3.1. CC-Py

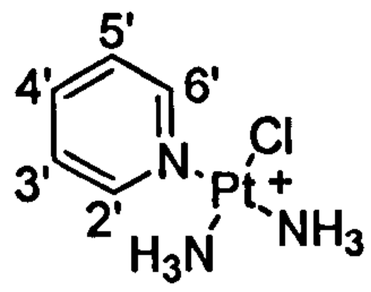

$[C_5H_{11}ClN_3][NO_3]$

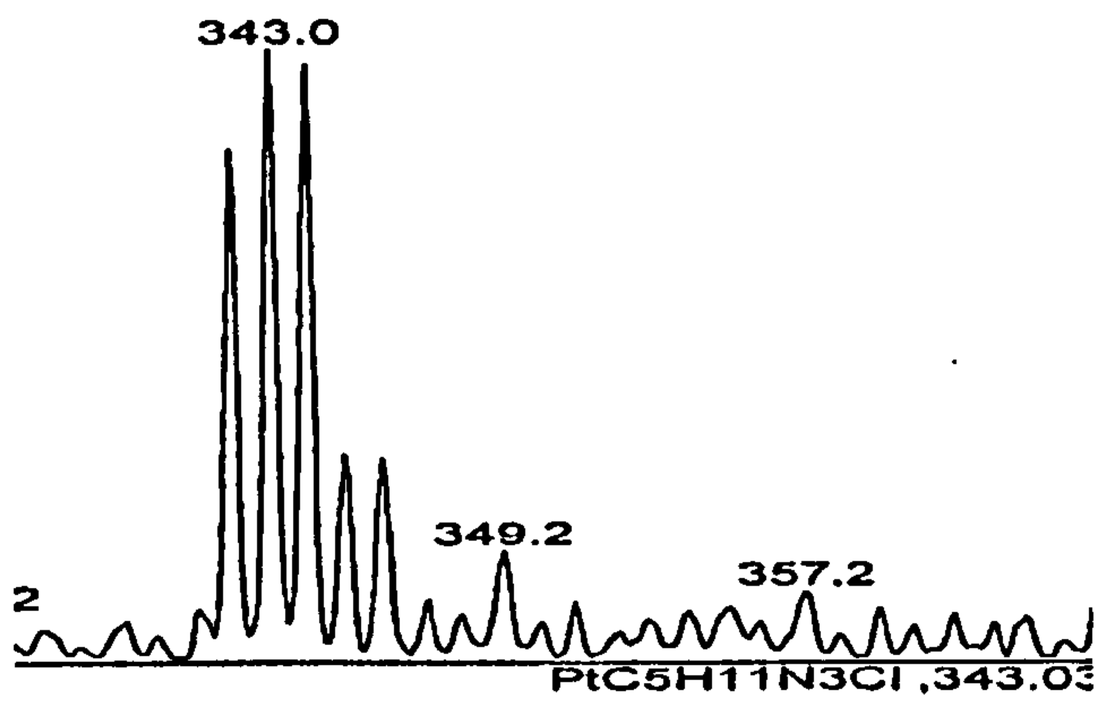

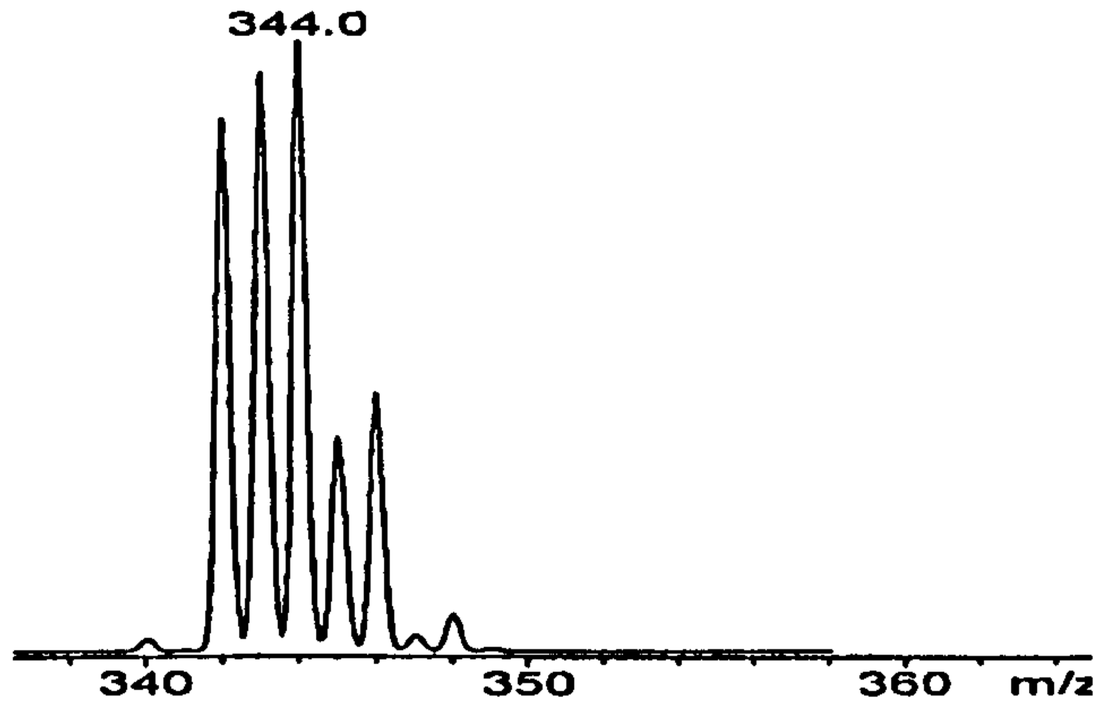

Figure A.3.1. The ESI mass spectrum of CC-Py (upper) and the expected isotope distribution pattern (lower).

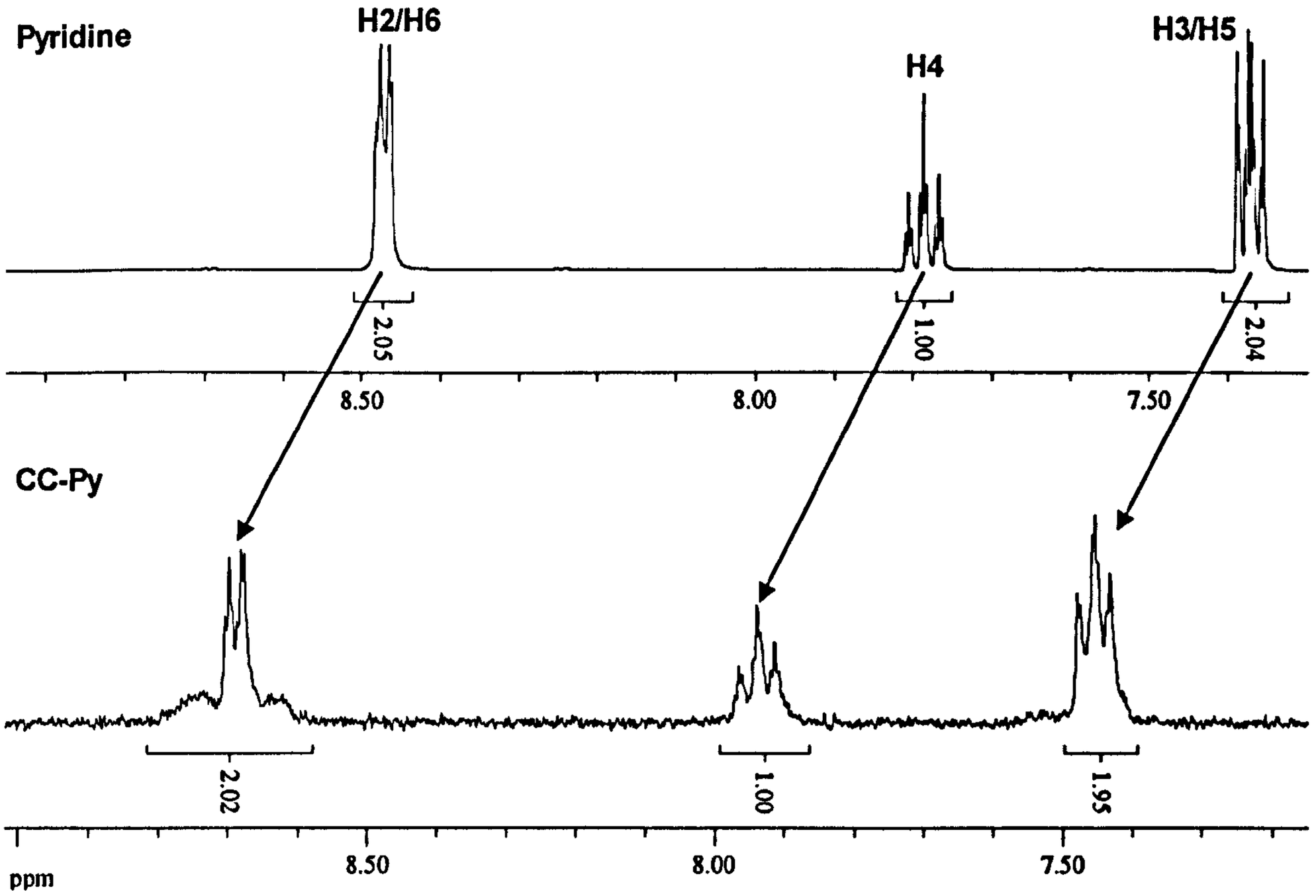

Figure A.3.2. The ^{1}H NMR spectra of pyridine (upper) and CC-Py (lower) in CD_3OD.

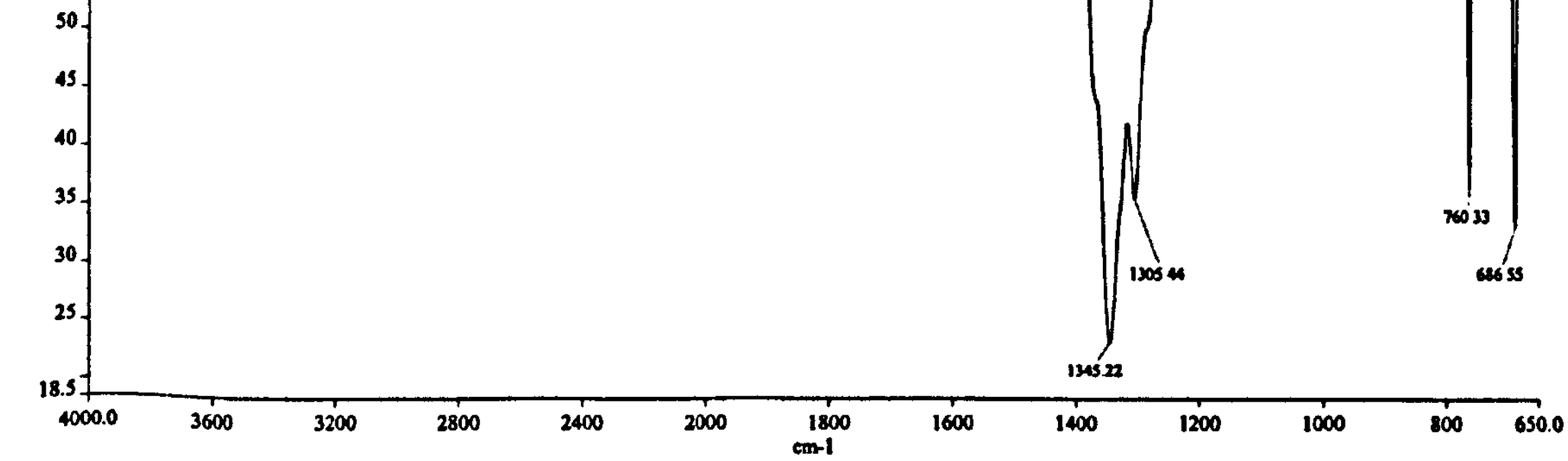

Figure A.3.3. The infrared spectrum of CC-Py.

A.3.2. CC-ET-3-Py

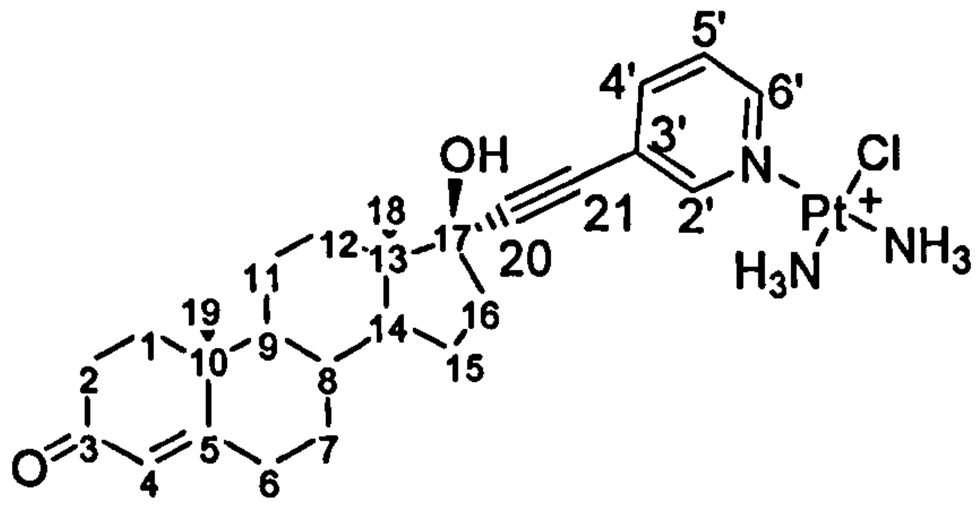

$[C_{26}H_{37}ClN_3O_2Pt][NO_3]$

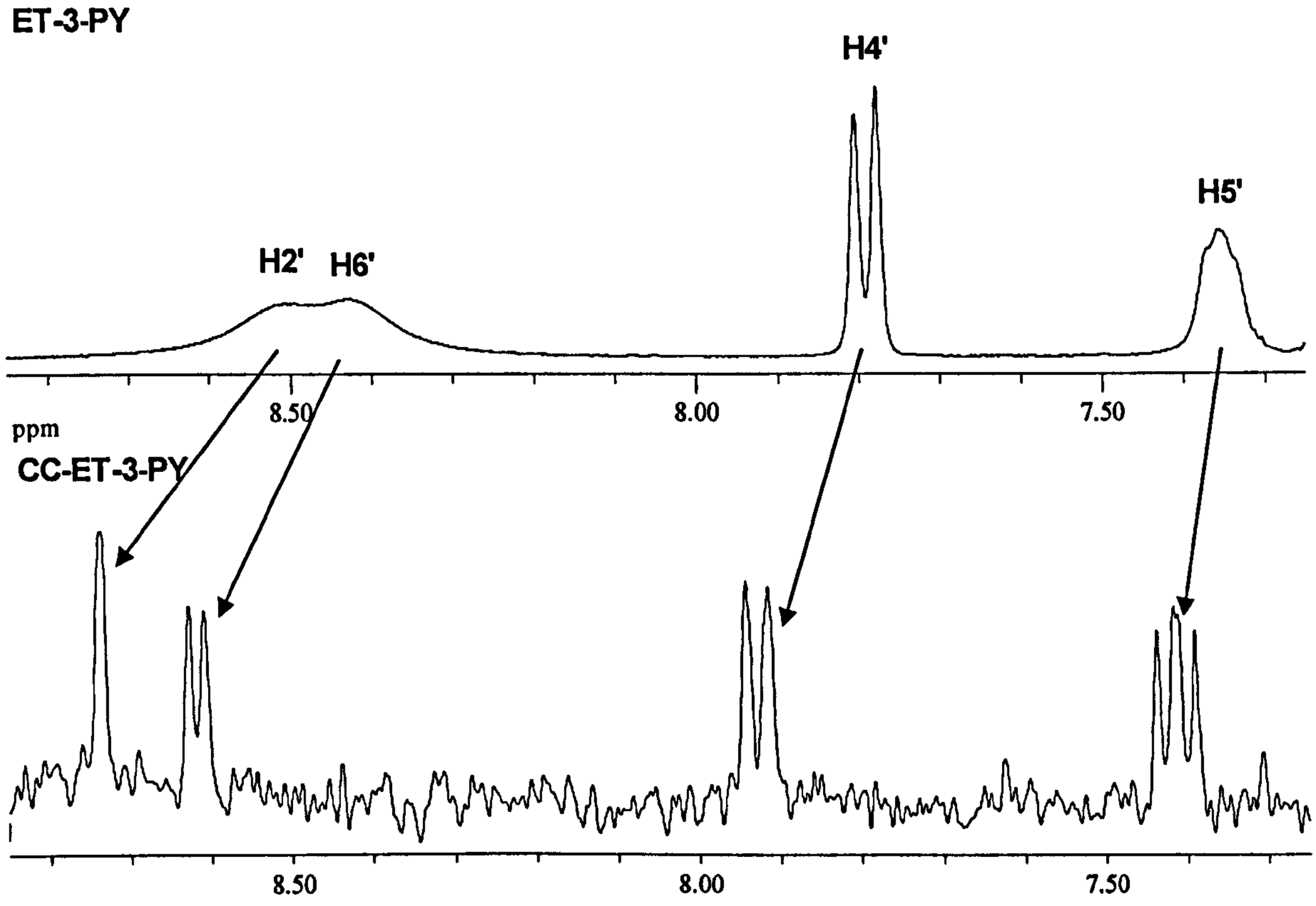

Figure A.3.4. The ^{1}H NMR spectra of ET-3-Py (upper) and CC-ET-3-Py (lower) in CD_3OD.

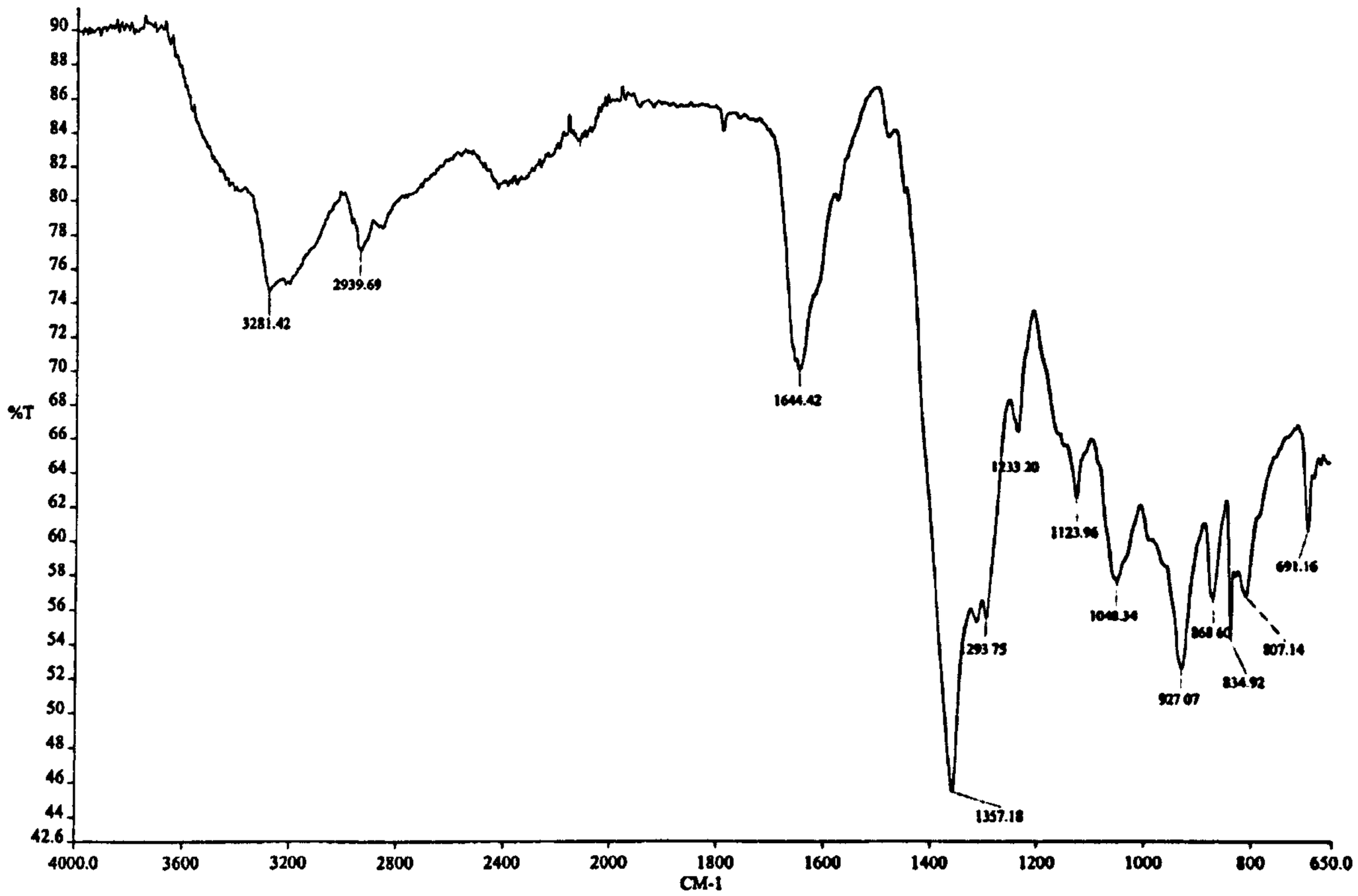

Figure A.3.5. The IR spectrum of CC-ET-3-Py.

A.3.3. CC-ET-4-IQ

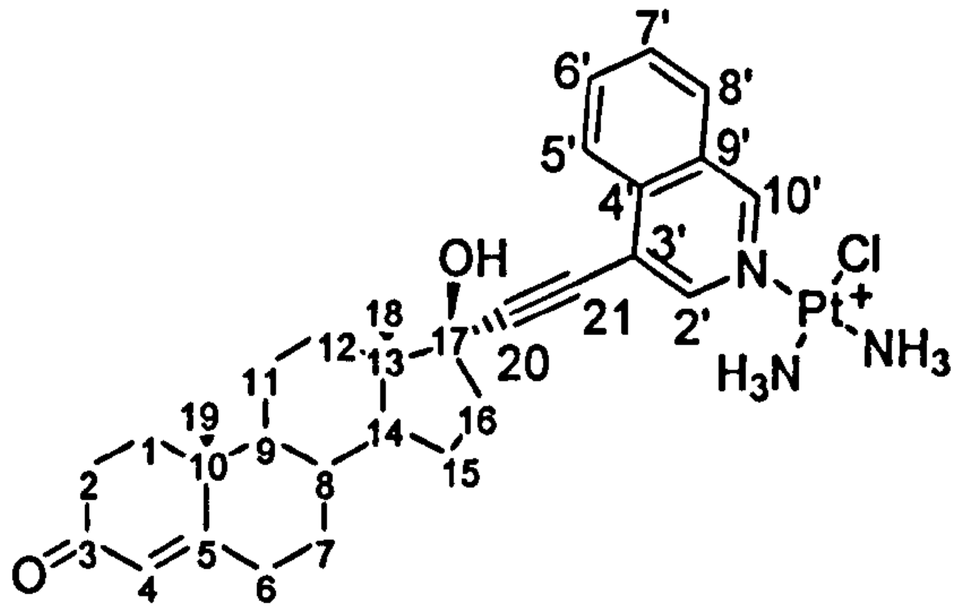

$[C_{30}H_{39}ClN_3O_2Pt][NO_3]$

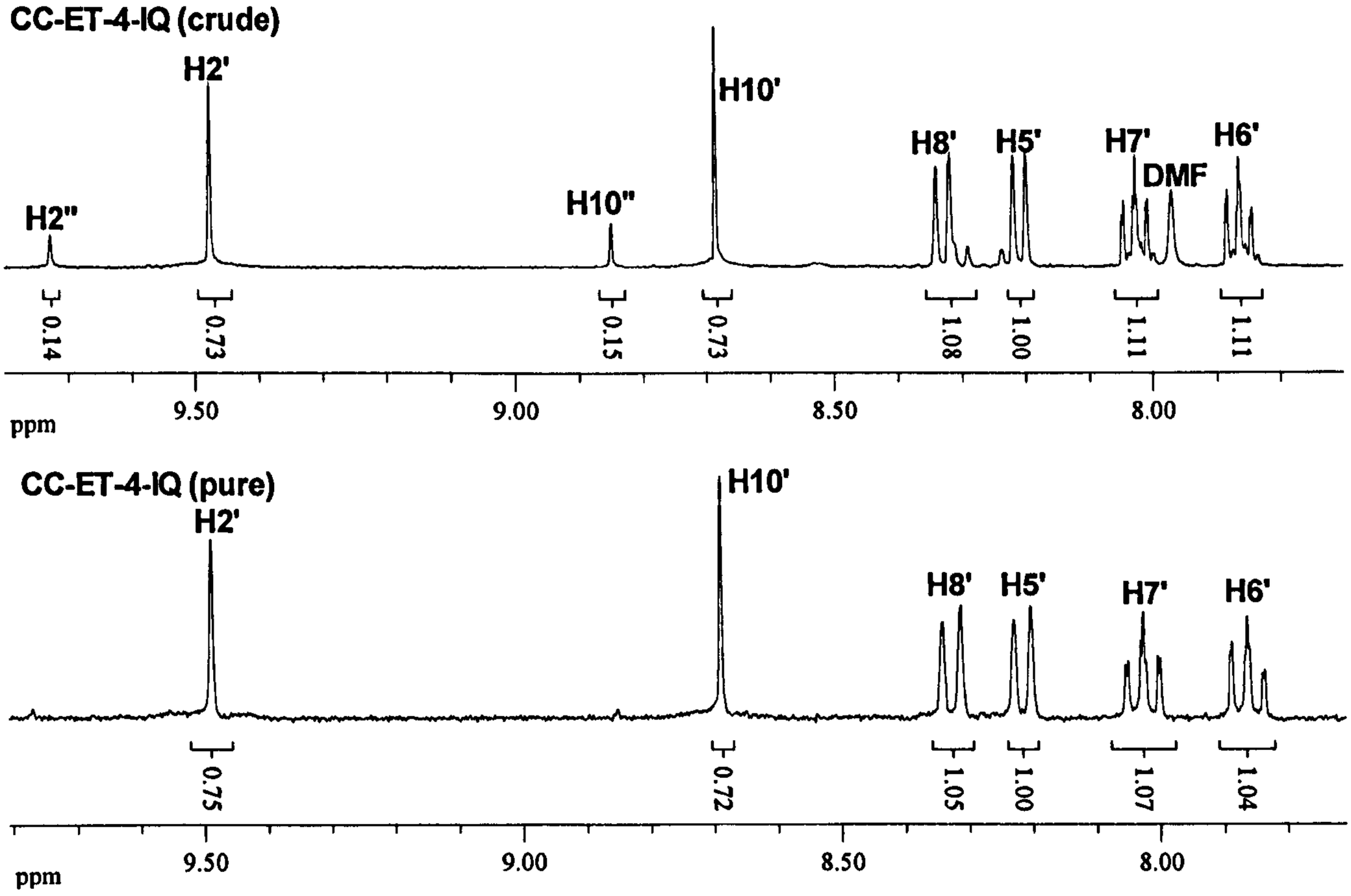

Figure A.3.6. The ^{1}H NMR spectra of CC-ET-4-IQ showing the crude (upper) spectrum and purified (lower) spectrum. Those signals marked double prime represent the disubstituted complex in CD_3OD.

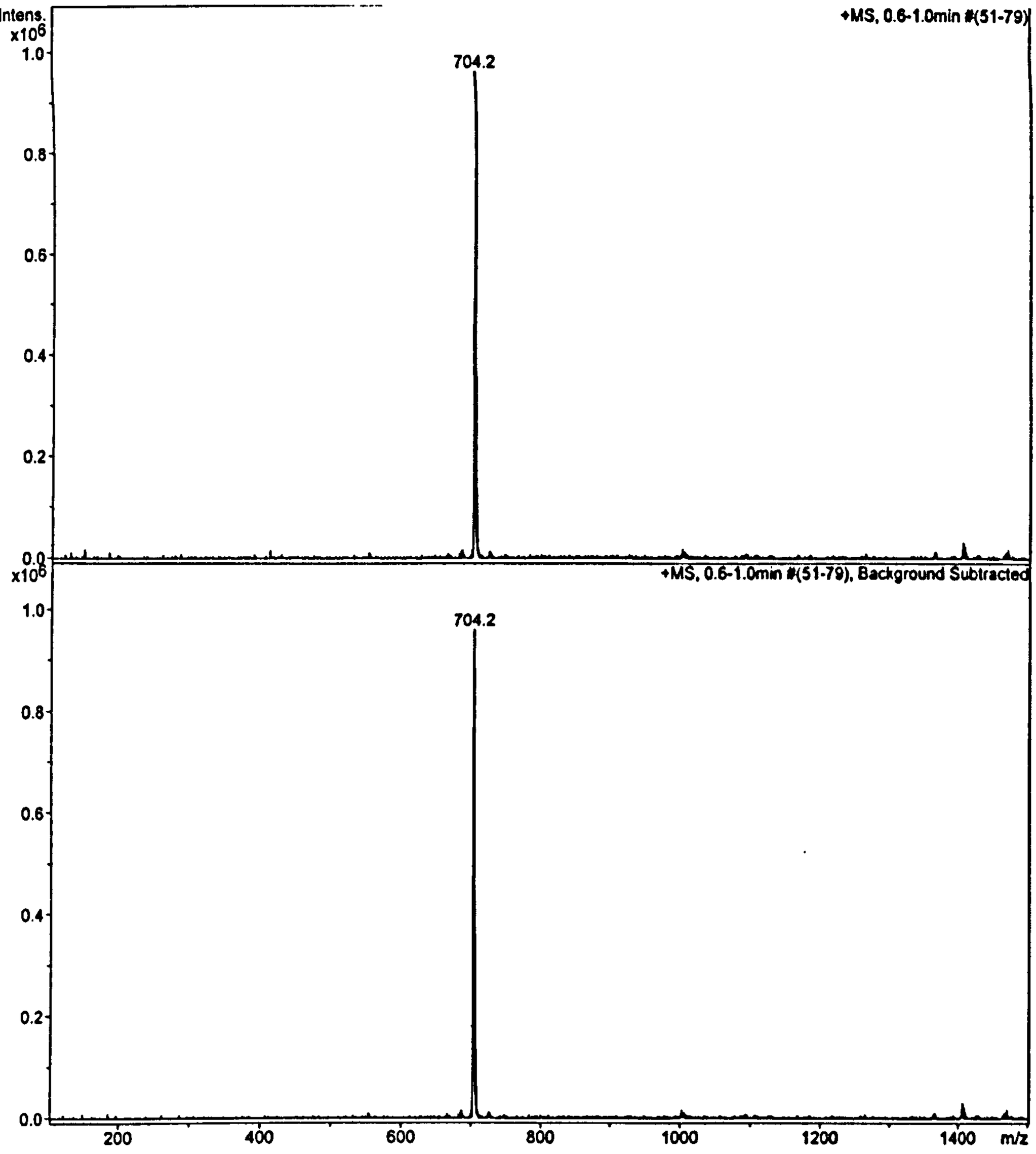

Figure A.3.7. The mass spectrum (ESI, +ve) of CC-ET-4-IQ in the *m/z* = 100 - 1500 region.

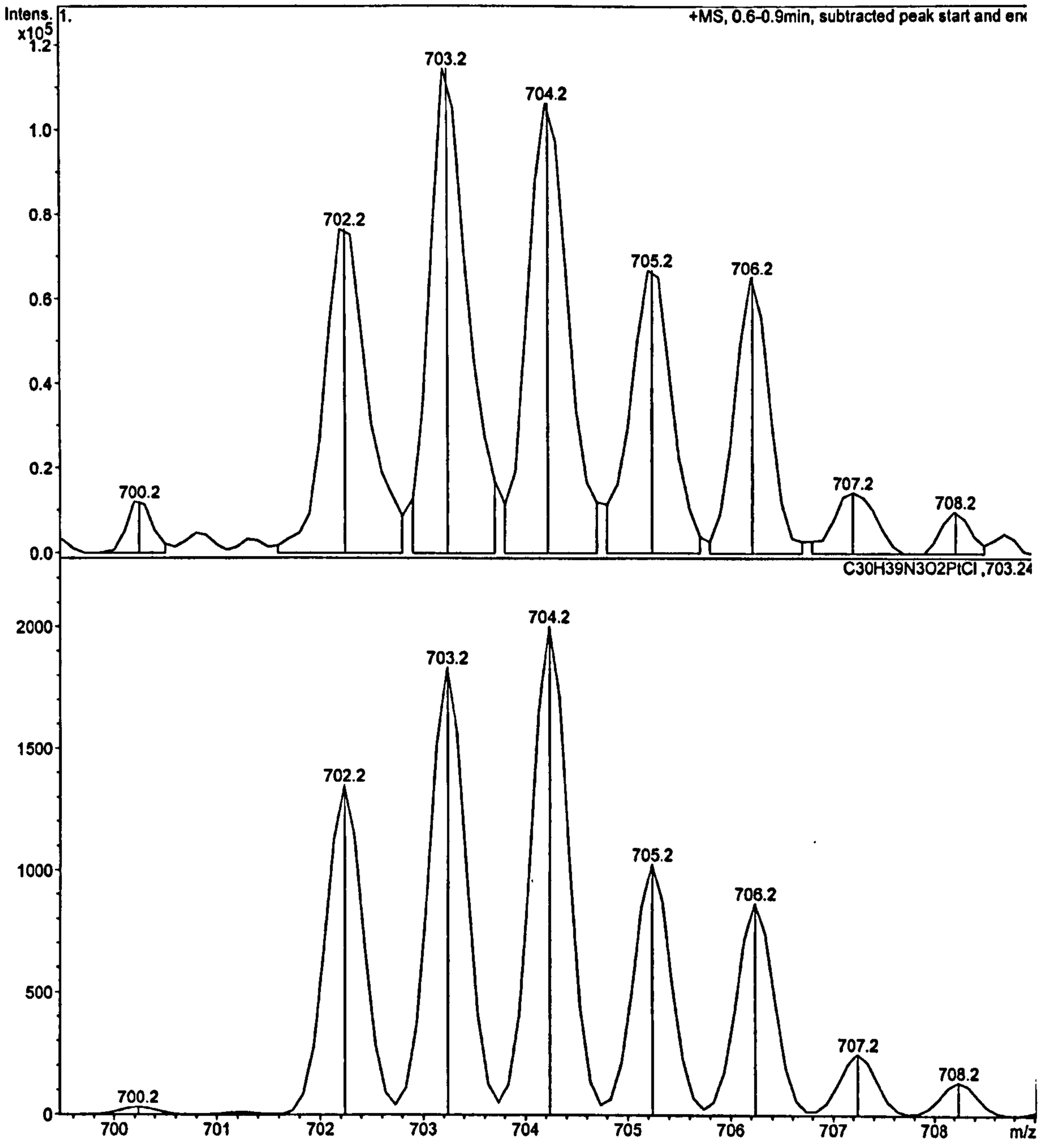

Figure A.3.8. The mass spectrum (ESI, +ve) of CC-ET-4-IQ in the *m/z* = 700 - 710 region.

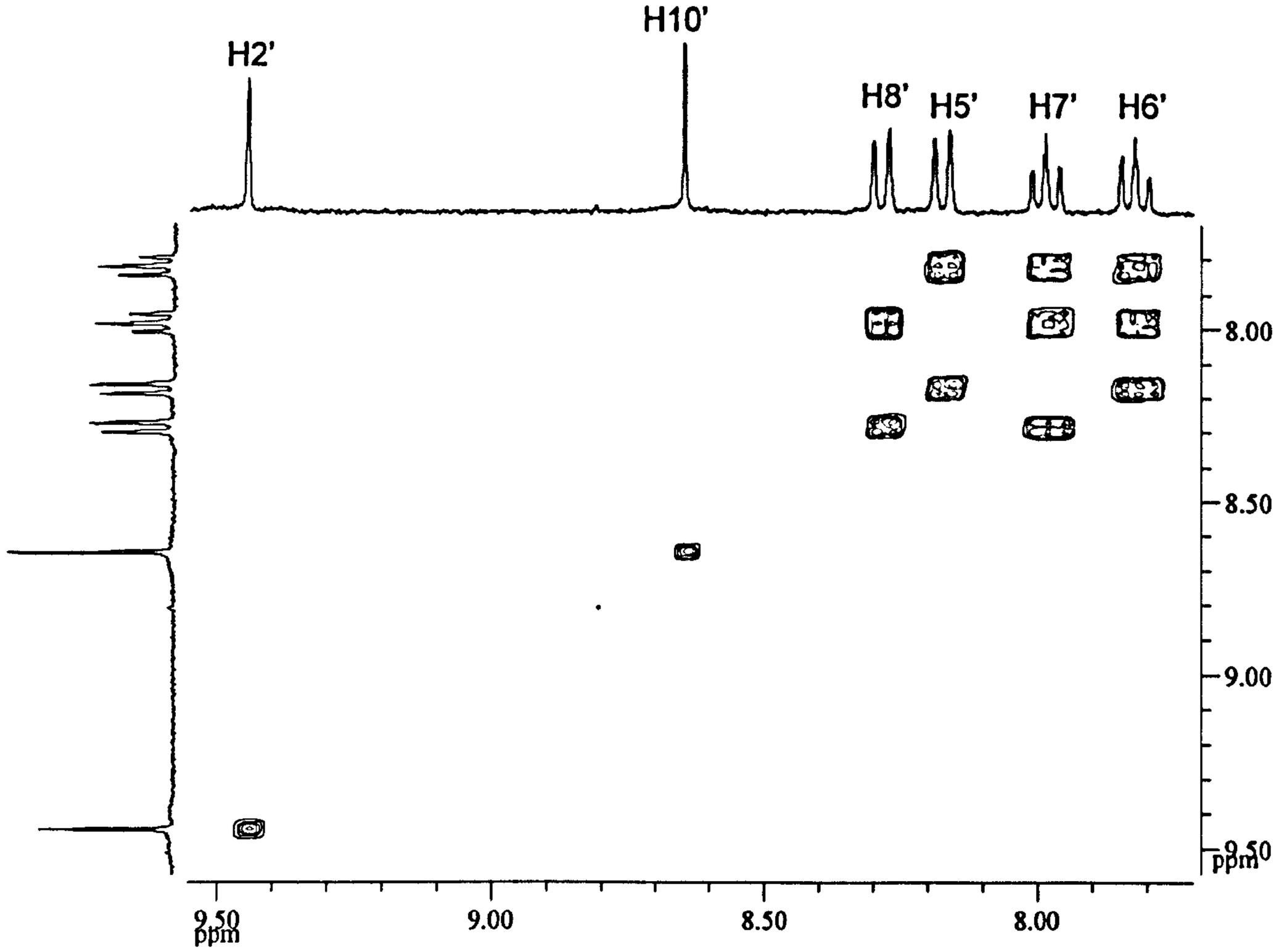

Figure A.3.9. The aromatic region in the COSY spectrum of CC-ET-4-IQ in CD_3OD.

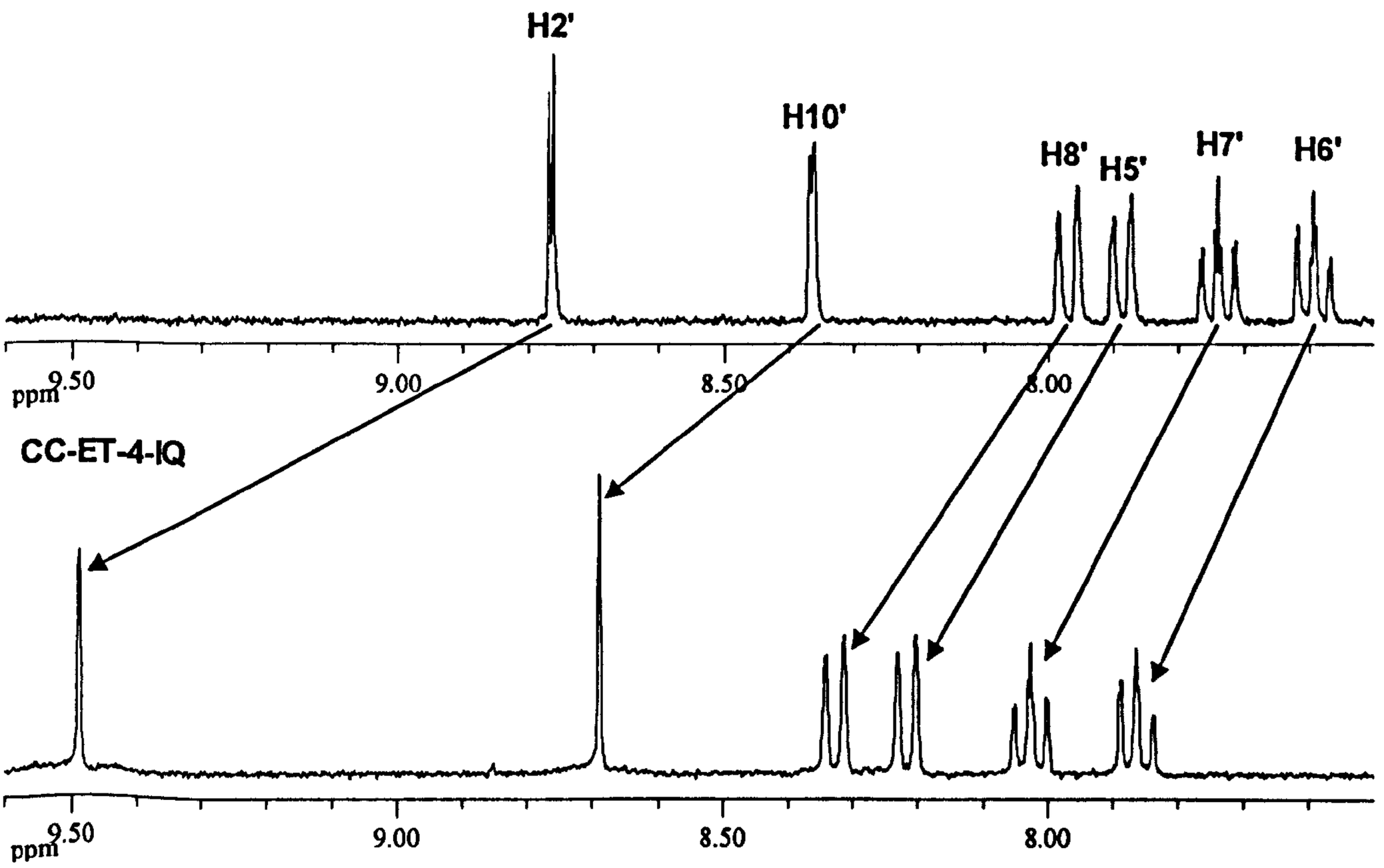

Figure A.3.10. The ^1H NMR spectra of ET-4-IQ and CC-ET-4-IQ in CD_3OD.

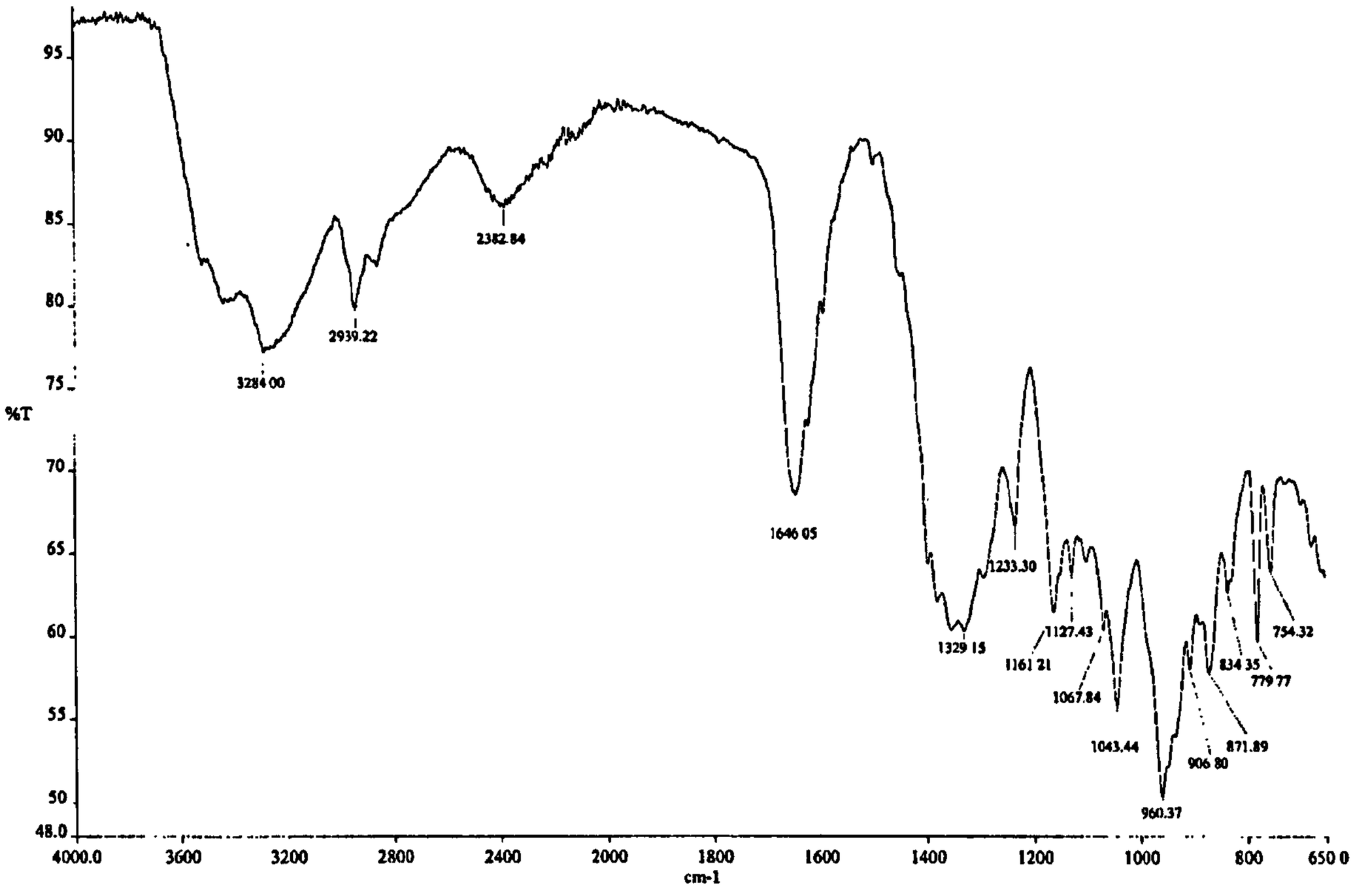

Figure A.3.11. The infrared spectrum of CC-ET-4-IQ.

A.3.4. CC-ET-6-Q

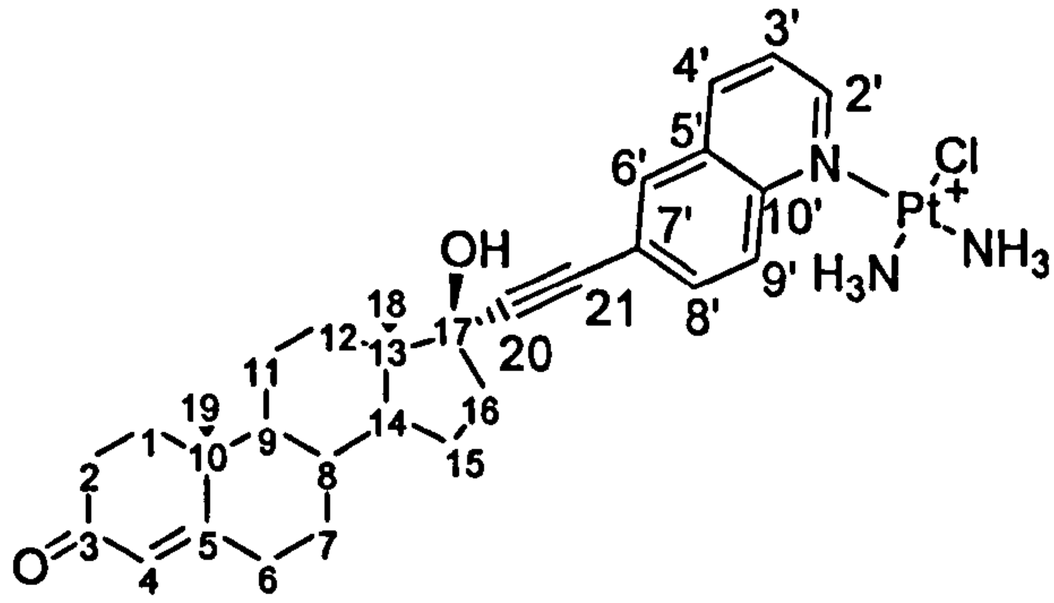

$[C_{30}H_{39}ClN_3O_2Pt][NO_3]$

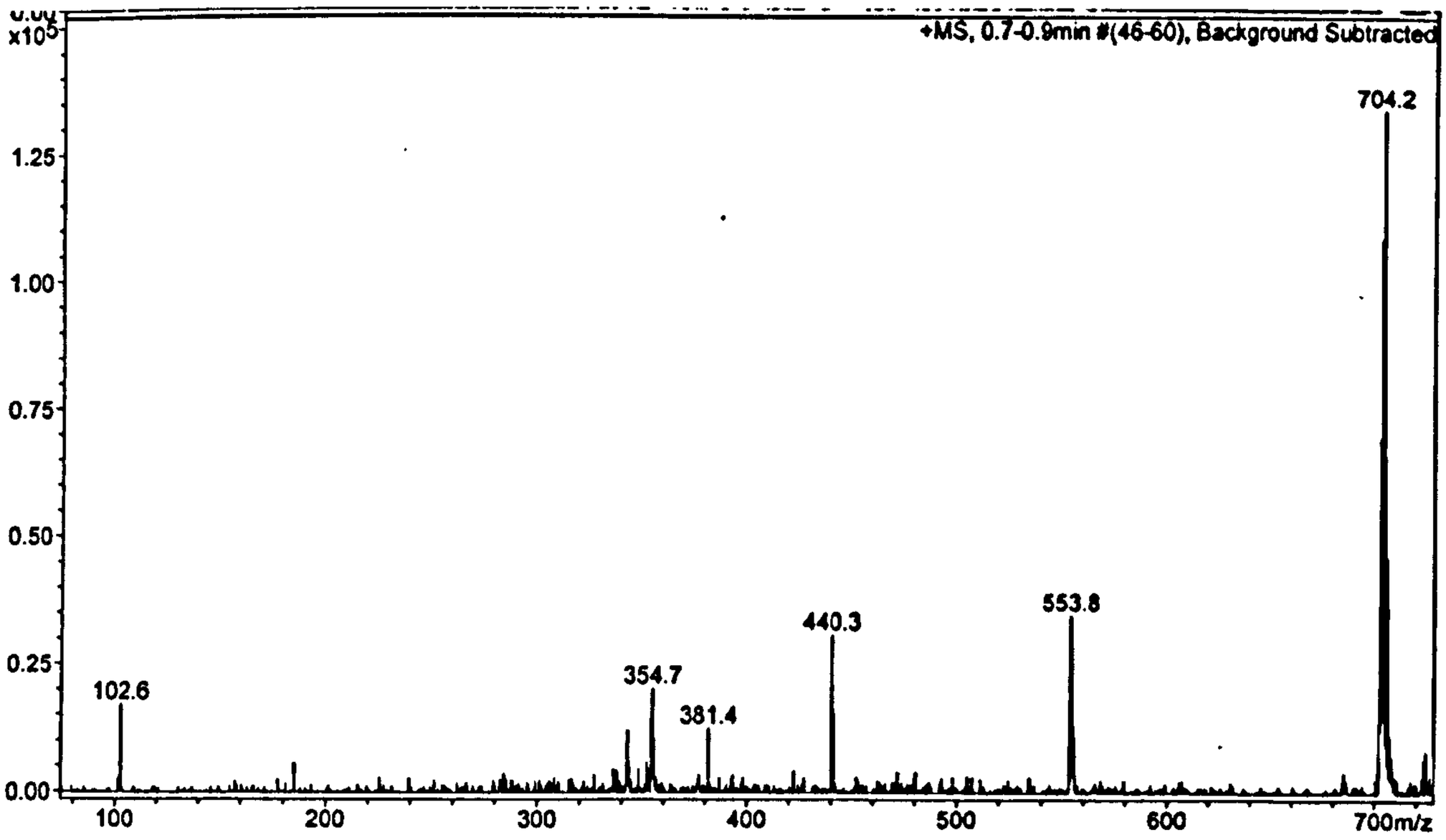

Figure A.3.12. The mass spectrum (ESI, +ve) of crude CC-ET-6-Q. The peaks at *m/z* = 440 and 554 correspond to $[H(ET\text{-}6\text{-}Q)]^+$ and $[Pt(NH_3)_2(ET\text{-}6\text{-}Q)_2]^{2+}$.

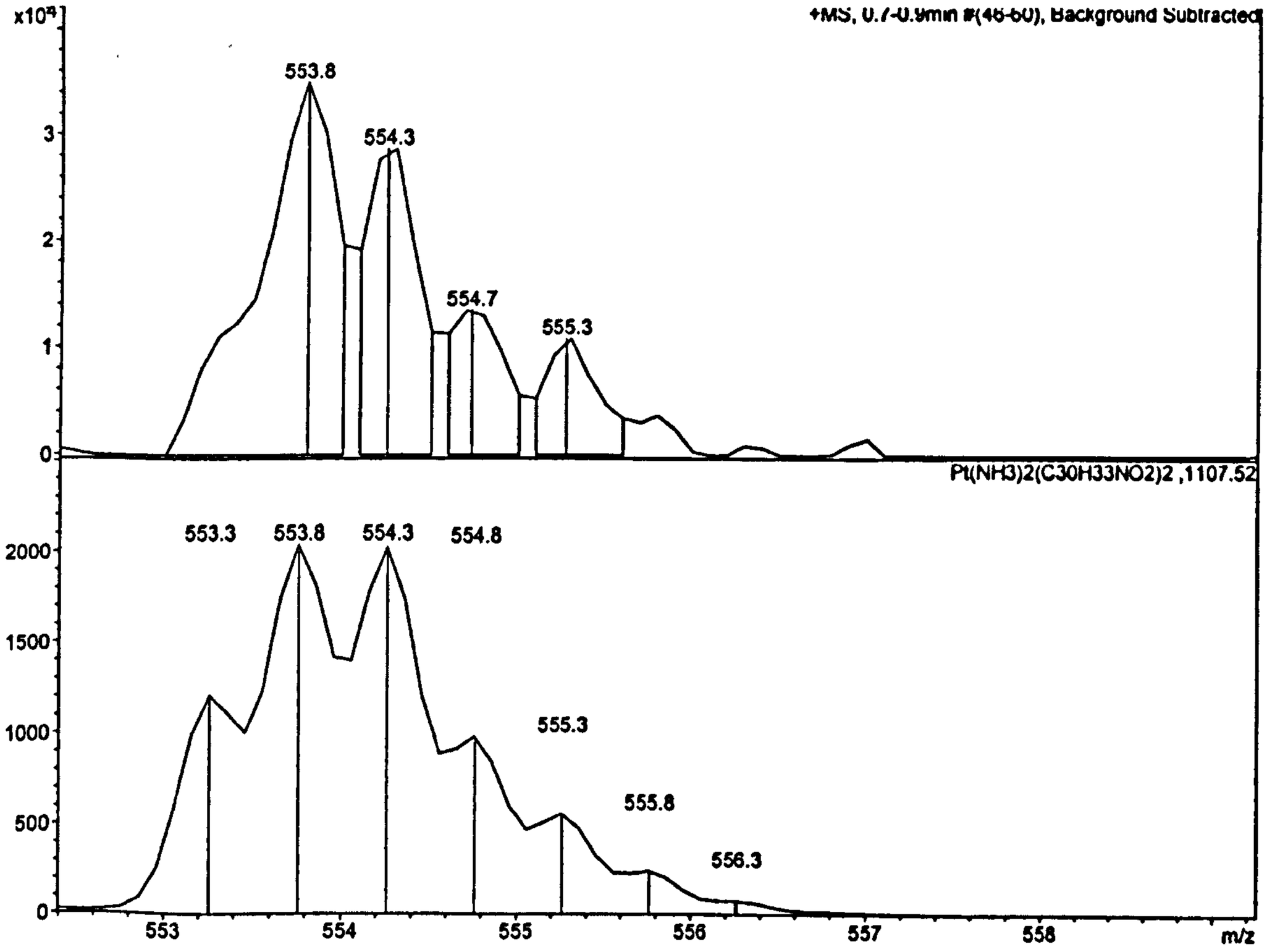

Figure A.3.13. The mass spectrum of CC-ET-6-Q (ESI, +ve) of CC-ET-6-Q with experimental (upper) and theoretical (lower) isotope distributions of $[Pt(NH_3)_2(ET\text{-}6\text{-}Q)_2]$.

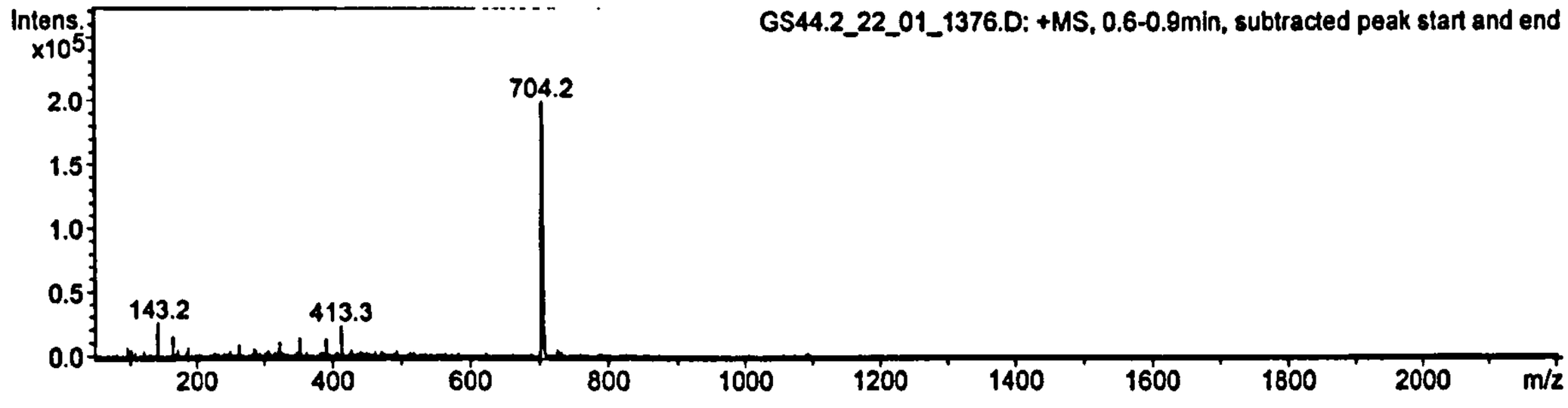

Figure A.3.14. The mass spectrum of CC-ET-6-Q (ESI, +ve).

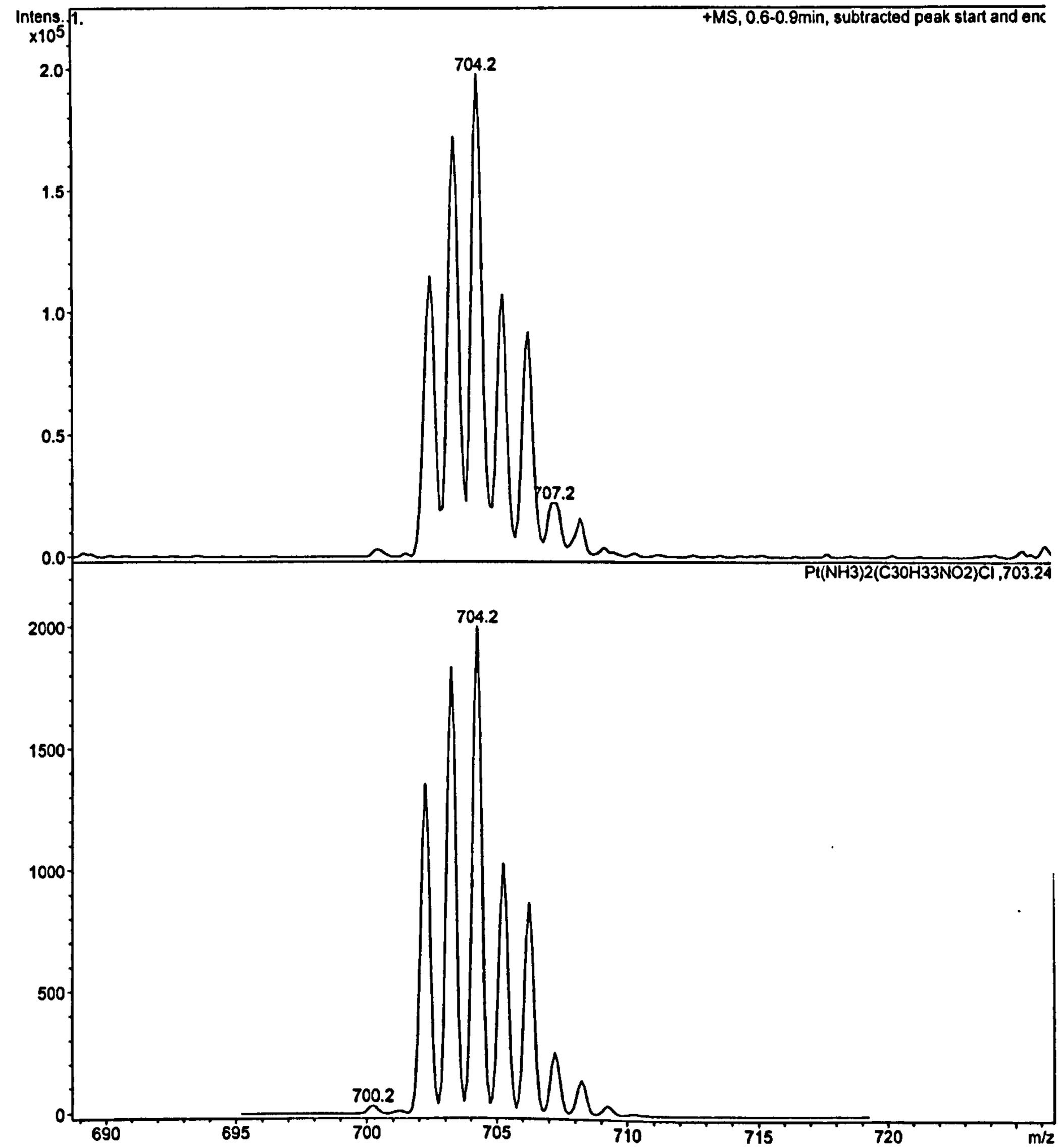

Figure A.3.15. The mass spectrum of CC-ET-6-Q (upper) and theoretical isotope distribution (lower).

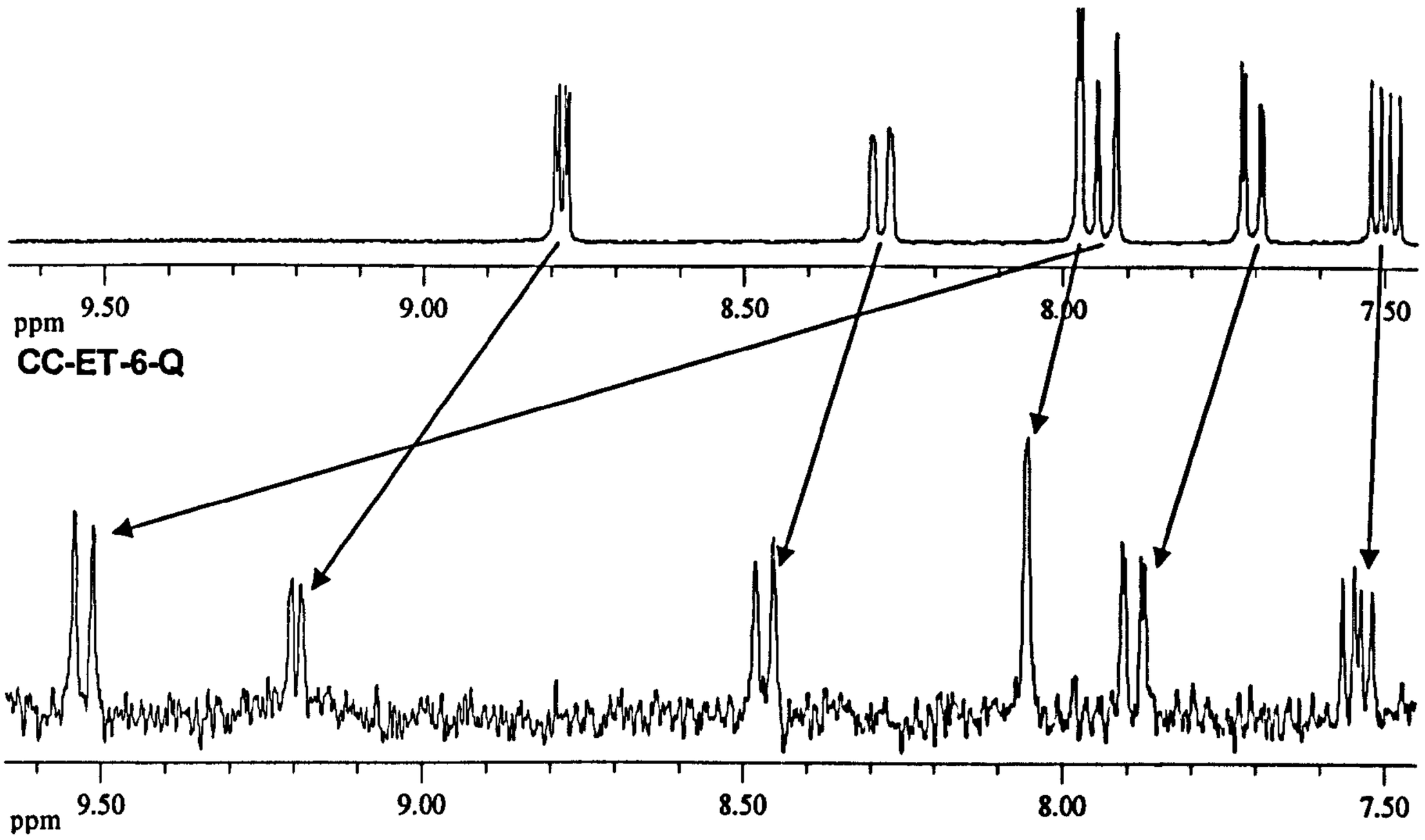

Figure A.3.16. The ^{1}H NMR spectra of CC-ET-6-Q and ET-6-Q in CD_3OD.

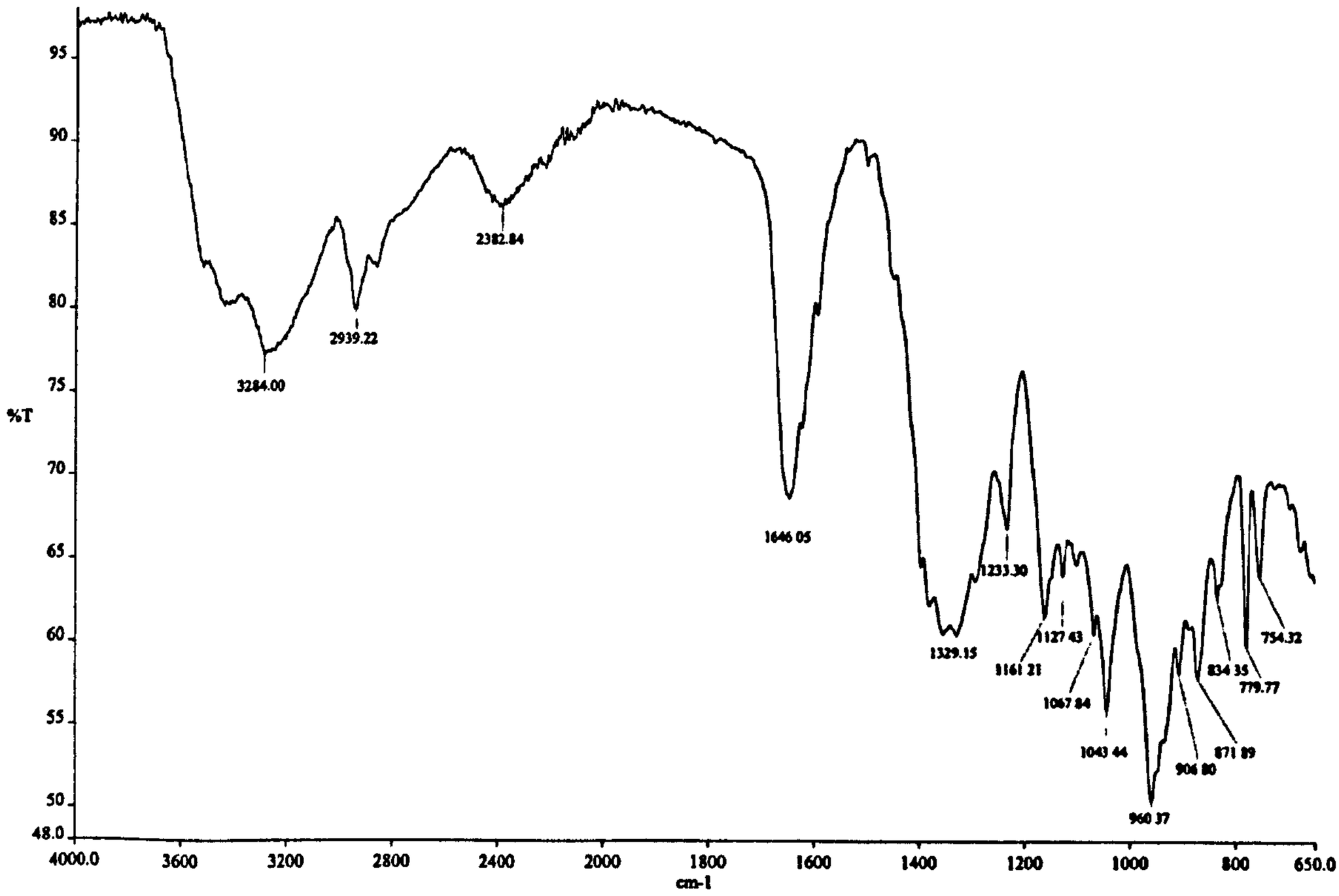

Figure A.3.17. The IR spectrum of CC-ET-6-Q.

Appendix Four – Geometry of TC and CC complexes

A.4.1. TC and CC-Py

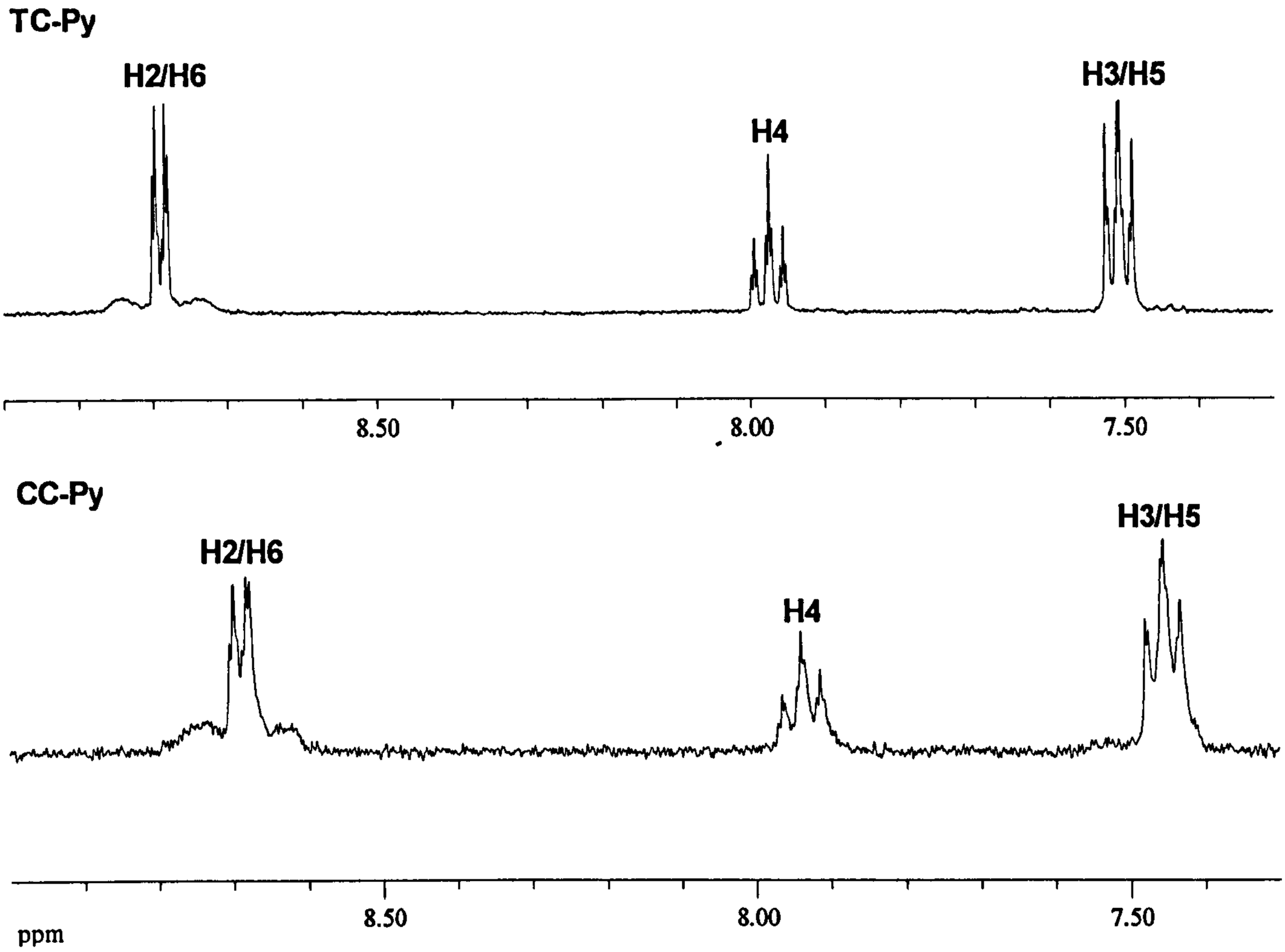

Figure A.4.1. A comparison of the ^{1}H NMR spectra of TC-Py and CC-Py in CD_3OD.

A.4.2. TC and CC-ET-3-Py

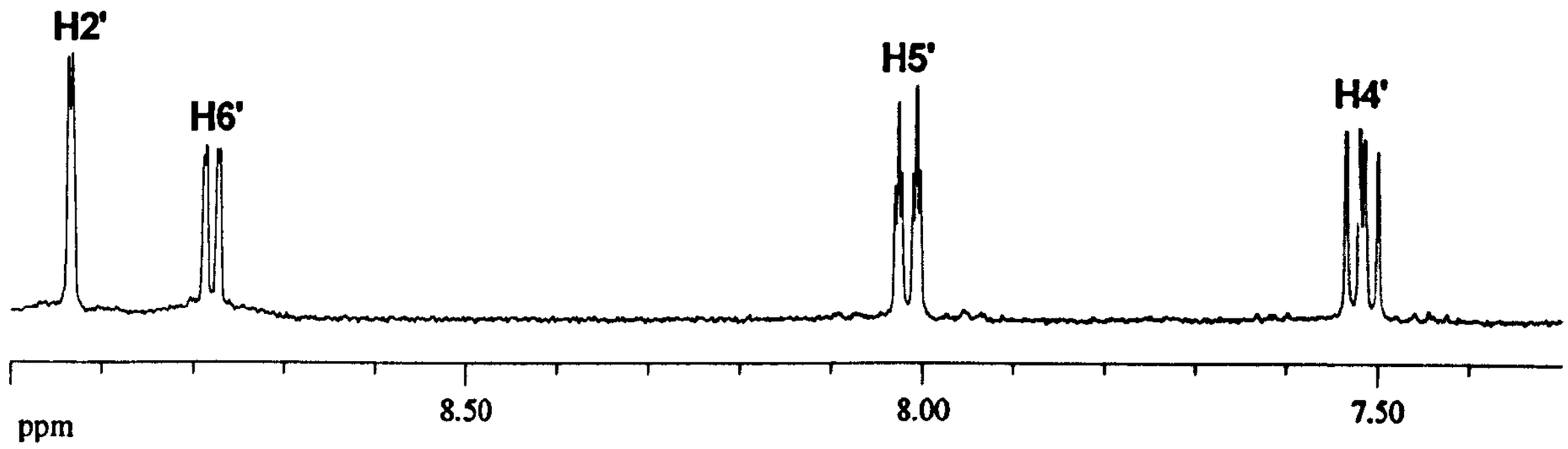

Figure A.4.2. A comparison of the ^{1}H NMR spectra of TC-ET-3-Py and CC-ET-3-Py in CD_3OD.

A.4.3. TC and CC-ET-4-IQ

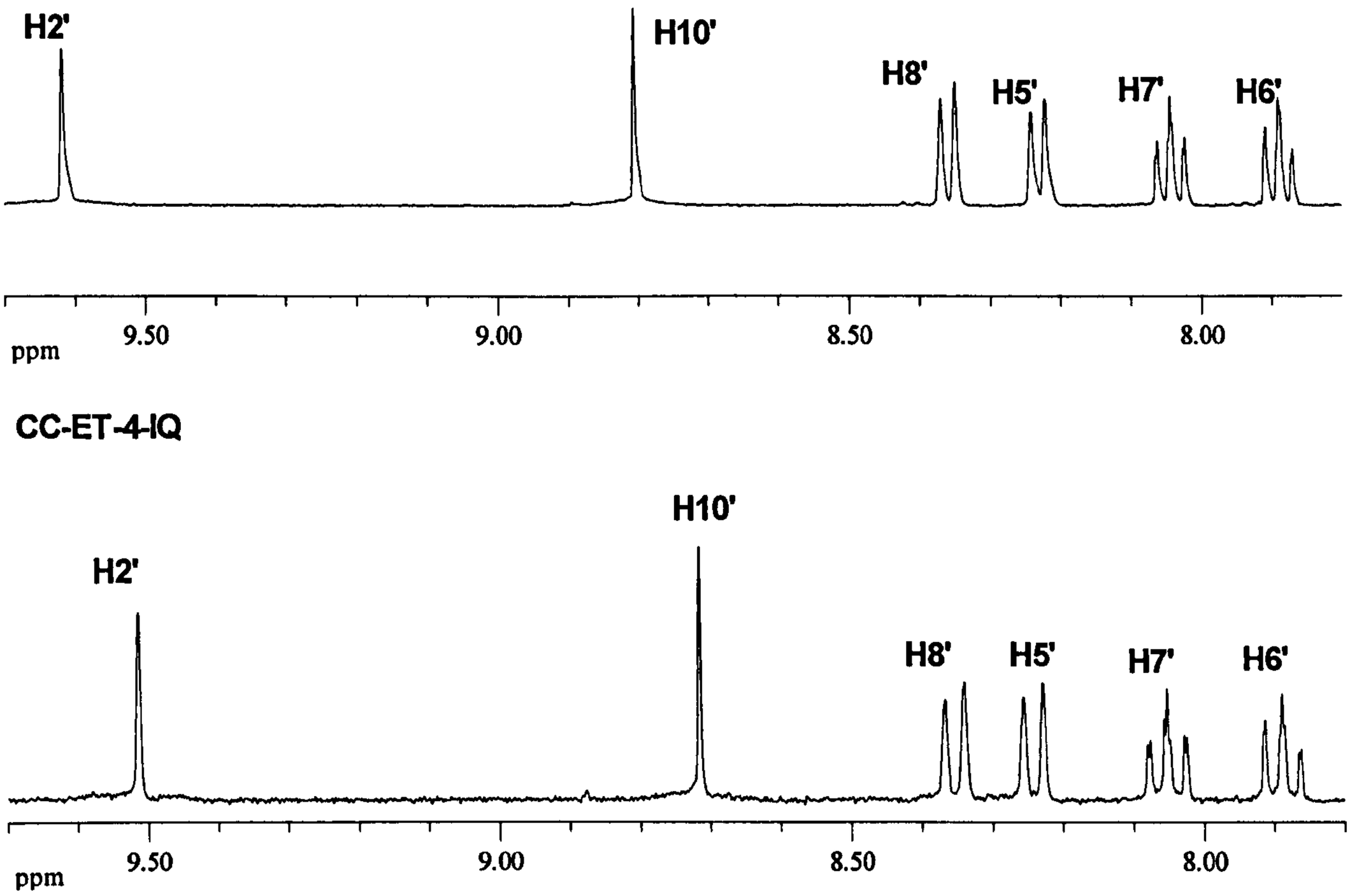

Figure A.4.3. A comparison of the ^{1}H NMR spectra of TC-ET-4-IQ and CC-ET-4-IQ in CD_3OD.

A.4.4. TC and CC-ET-6-Q

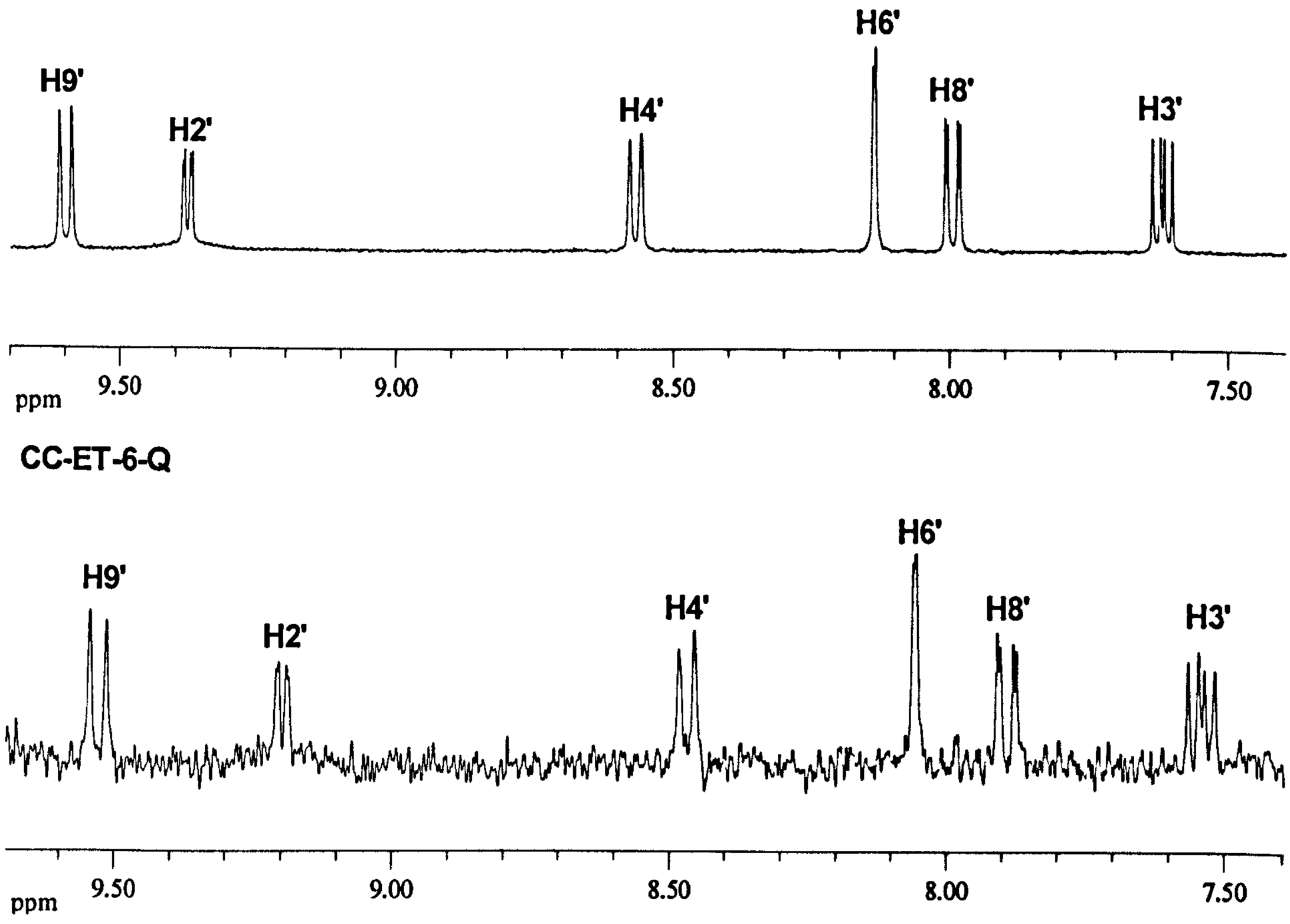

Figure A.4.4. A comparison of the ^{1}H NMR spectra of TC-ET-6-Q and CC-ET-6-Q in CD_3OD.

Appendix Five - Additional complexes with DMSO as a ligand: spectroscopic data

A.5.1. Trans-Pt(Py)(DMSO)Cl_2

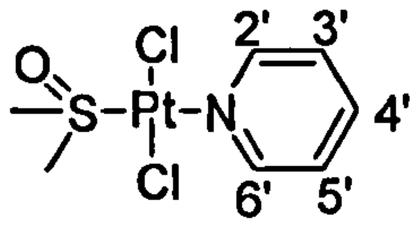

$C_7H_{11}Cl_2NOPtS$

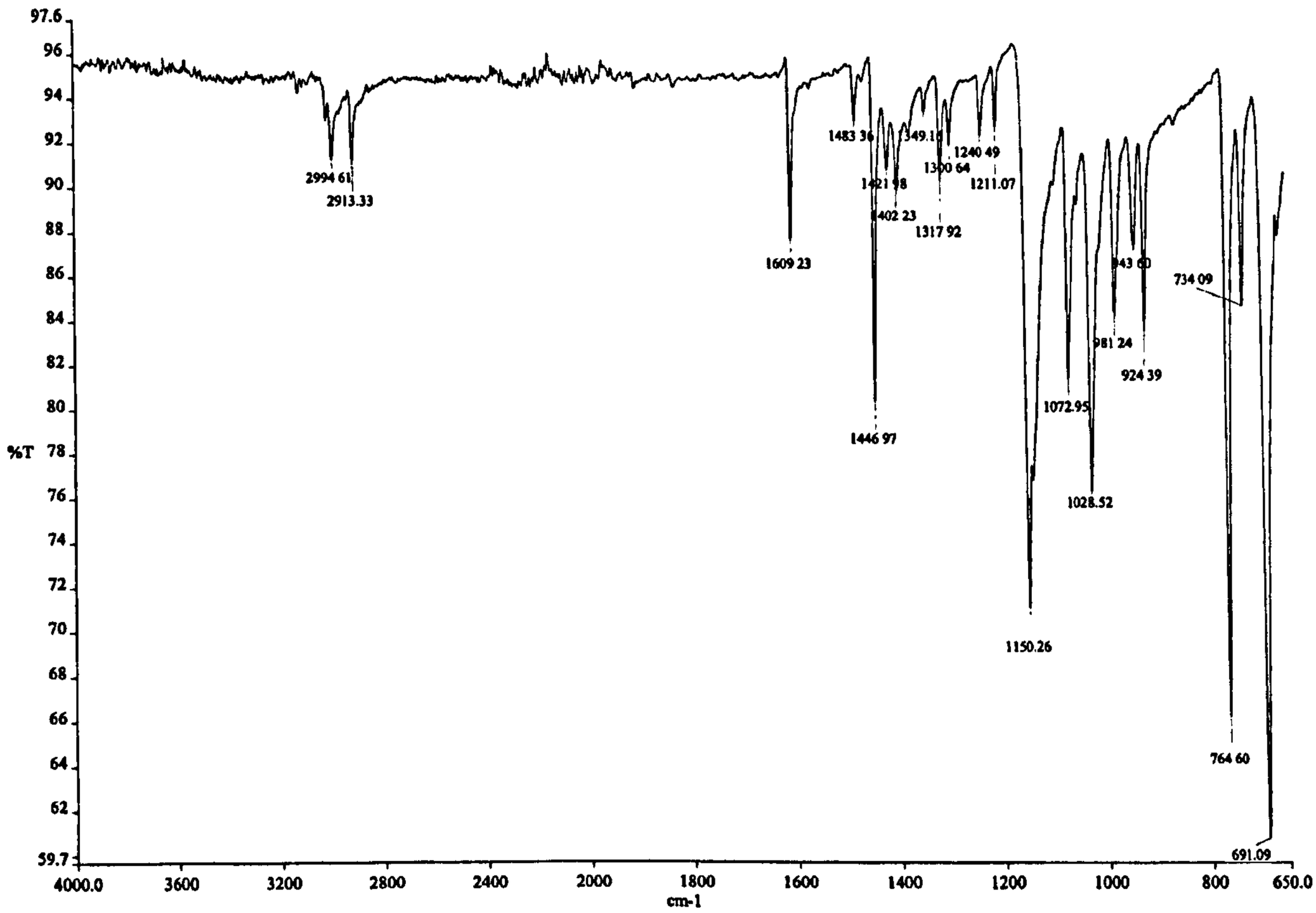

Figure A.5.1. The infrared spectrum of trans-Pt(Py)(DMSO)Cl_2.

A.5.2. Trans-Pt(Quinoline)(DMSO)Cl_2

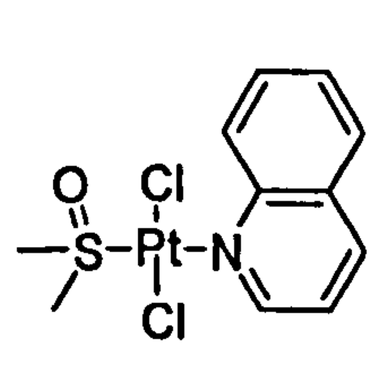

$C_{11}H_{13}Cl_2NOPtS$

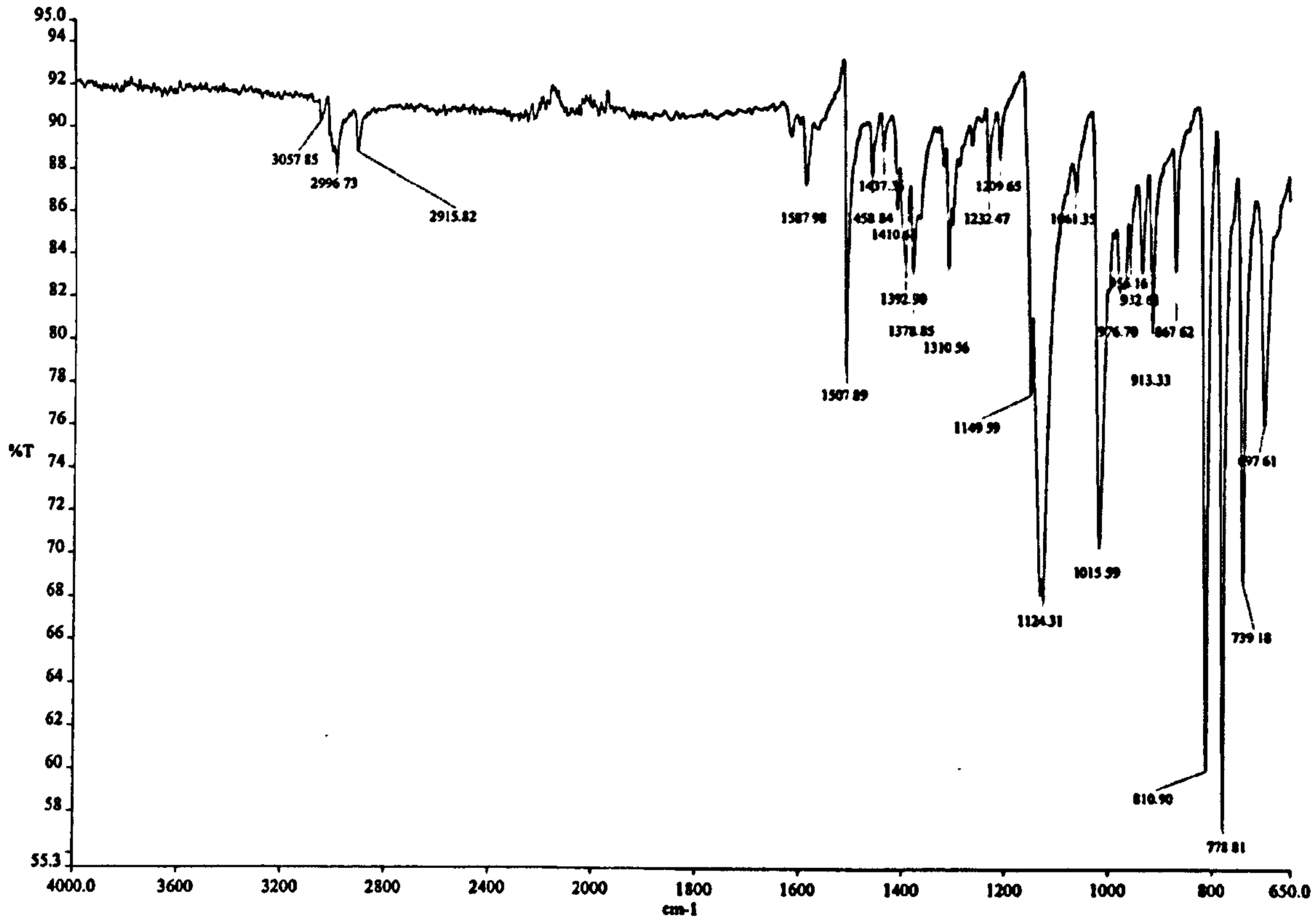

Figure A.5.2. The infrared spectrum of trans-Pt(Quinoline)(DMSO)Cl_2.

A.5.3. Trans-Pt(ET-2-Py)(DMSO)Cl_2

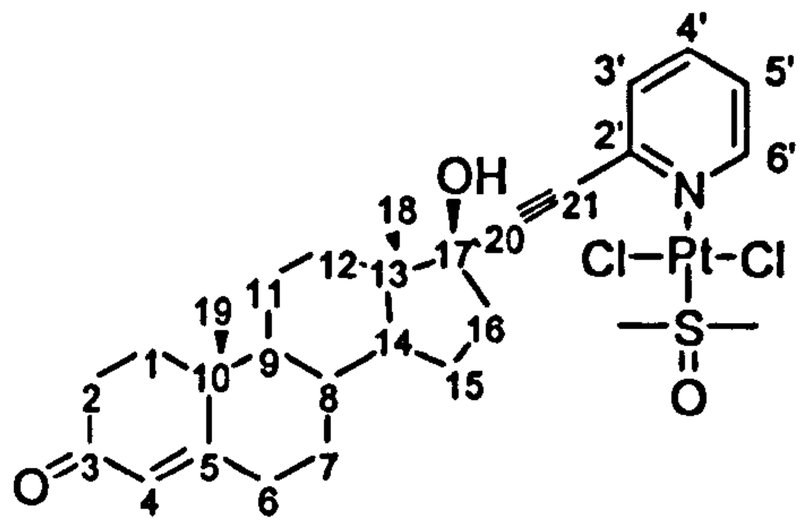

$C_{28}H_{37}Cl_2NO_3PtS$

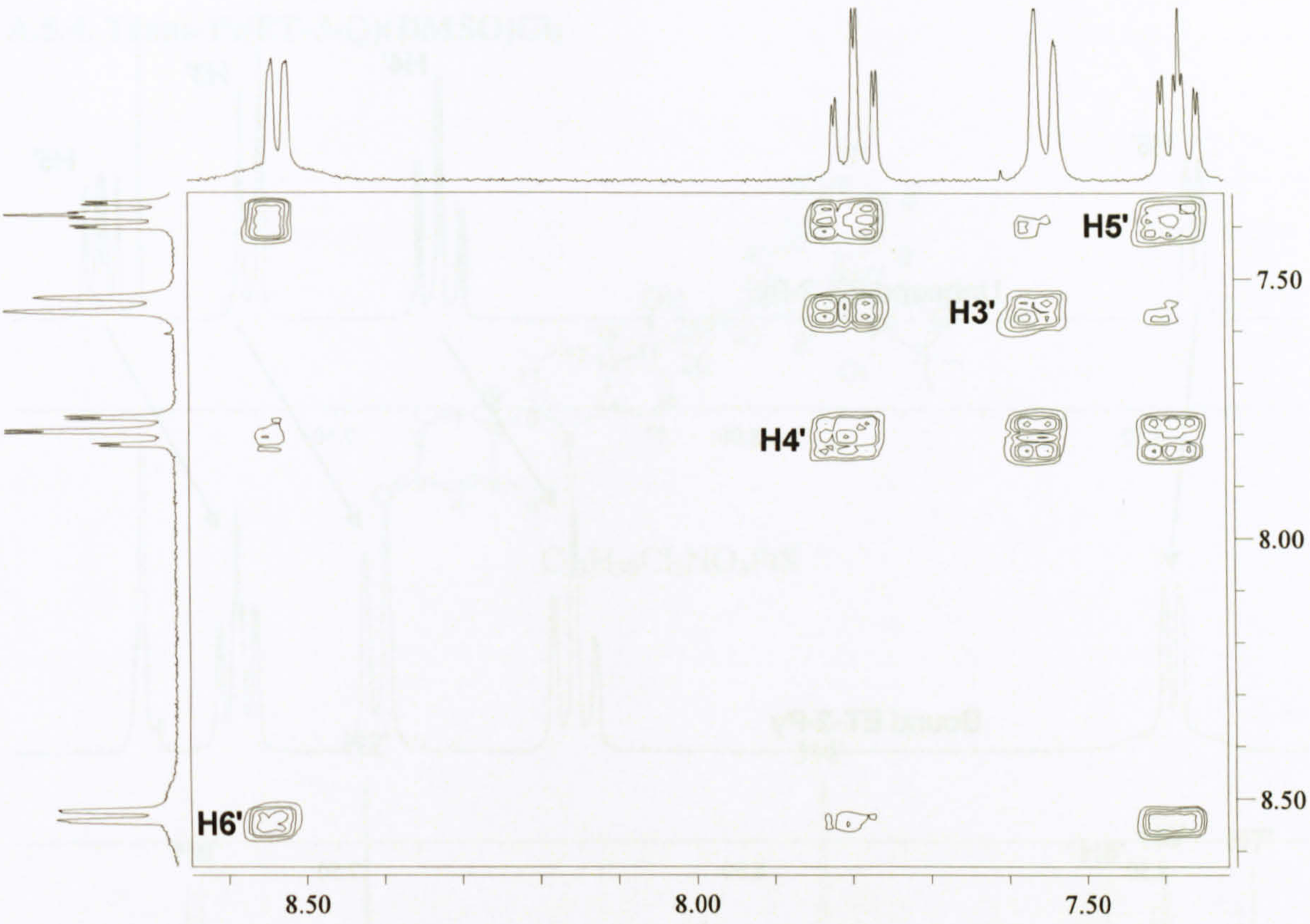

Figure A.5.3. The COSY aromatic region of trans-Pt(ET-2-Py)(DMSO)Cl_2.

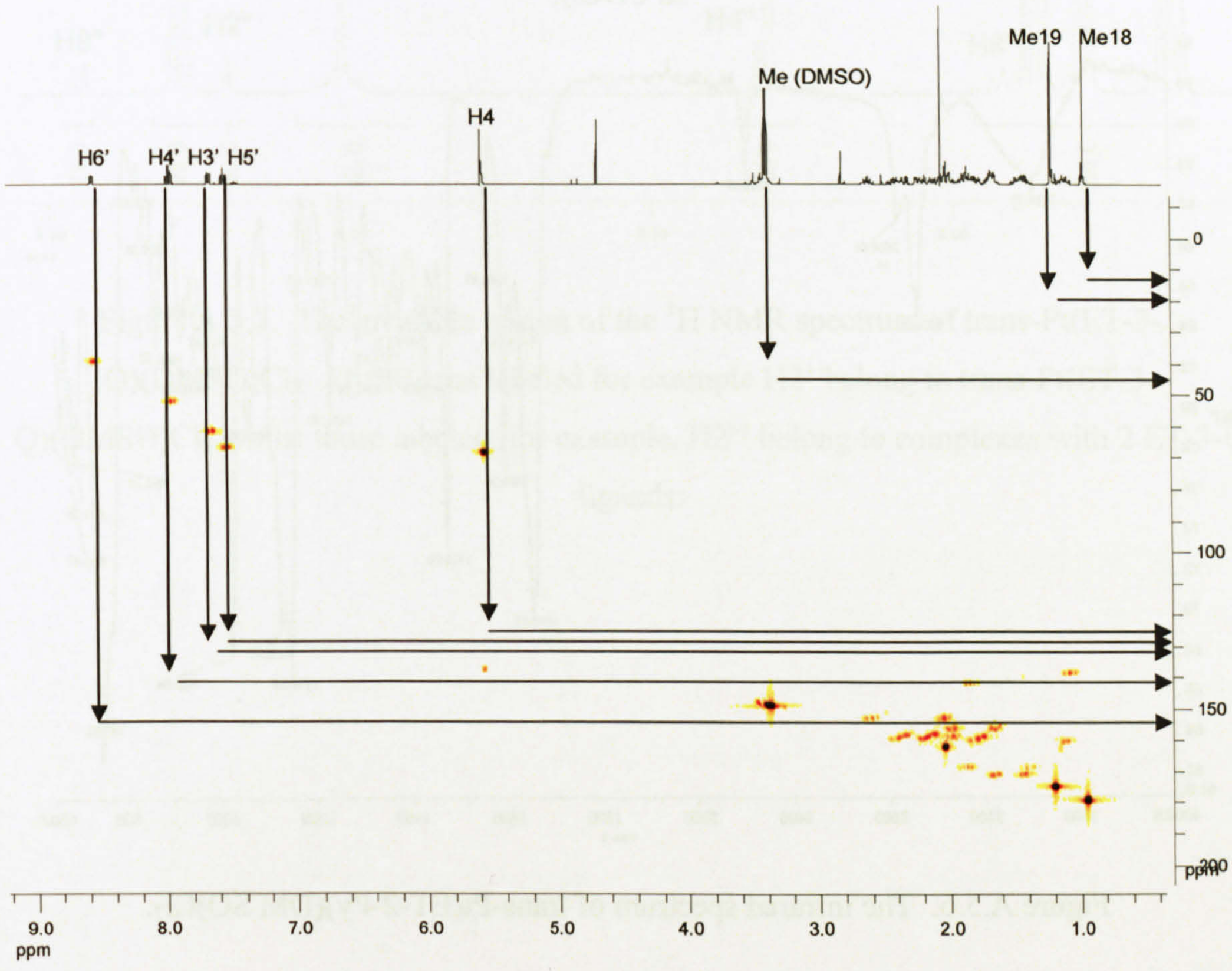

Figure A.5.4. The HMQC ^{1}H-^{13}C correlation spectrum of trans-Pt(ET-2-Py)(DMSO)Cl_2 $(CD_3)_2CO$.

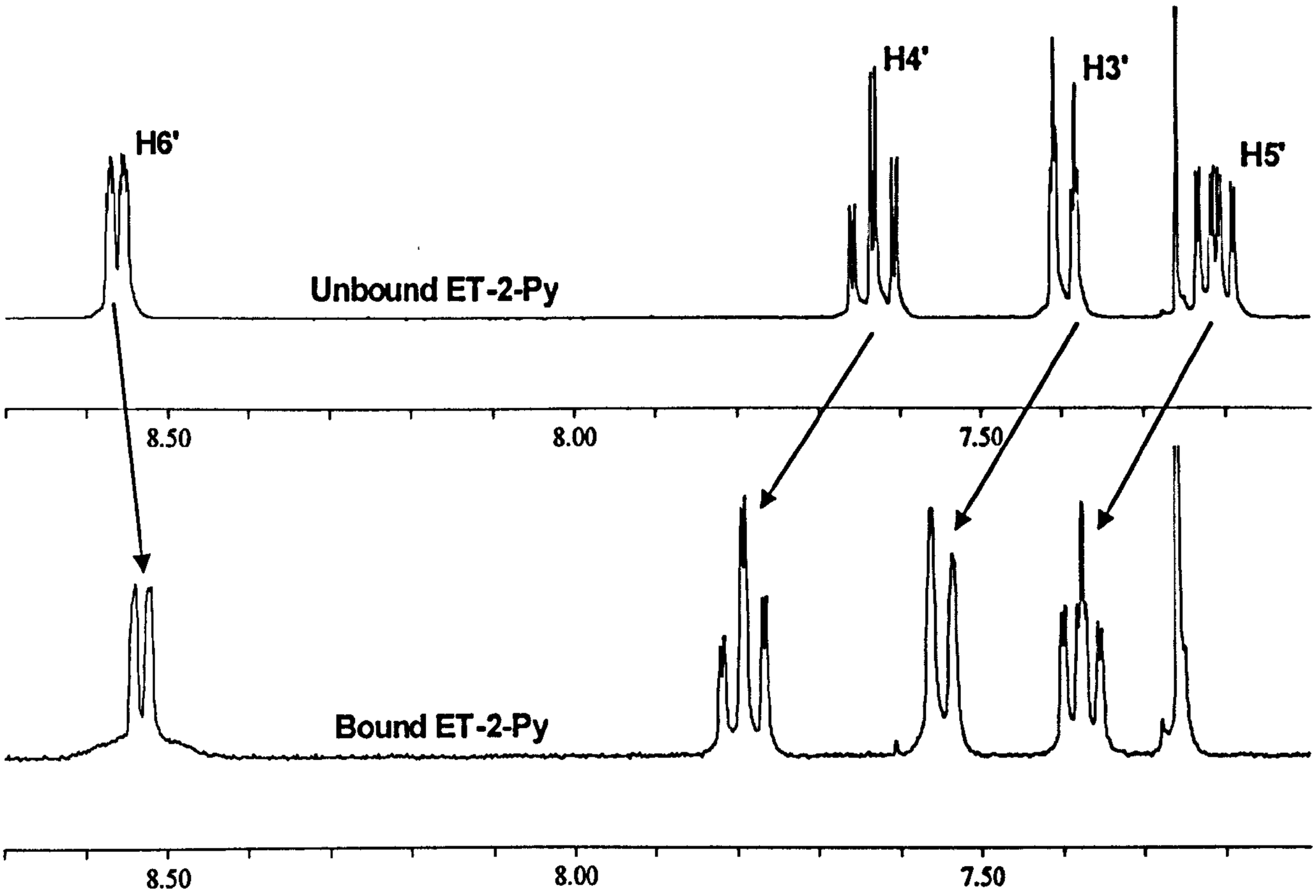

Figure A.5.5. The aromatic region in the ^{1}H NMR spectrum bound and unbound ET-2-Py in $CDCl_3$.

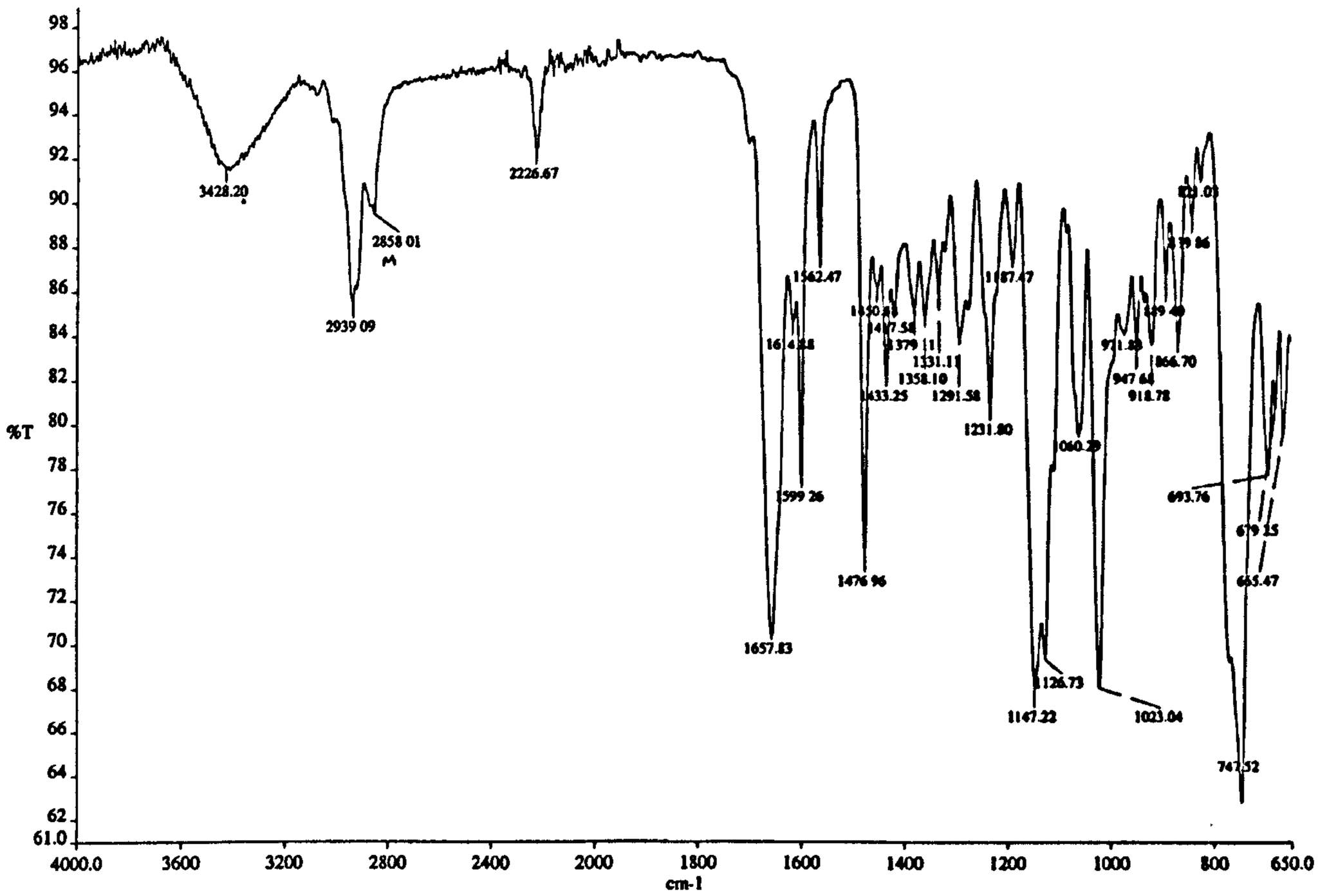

Figure A.5.6. The infrared spectrum of trans-Pt(ET-2-Py)(DM SO)Cl_2.

A.5.4. Trans-Pt(ET-3-Q)(DMSO)Cl_2

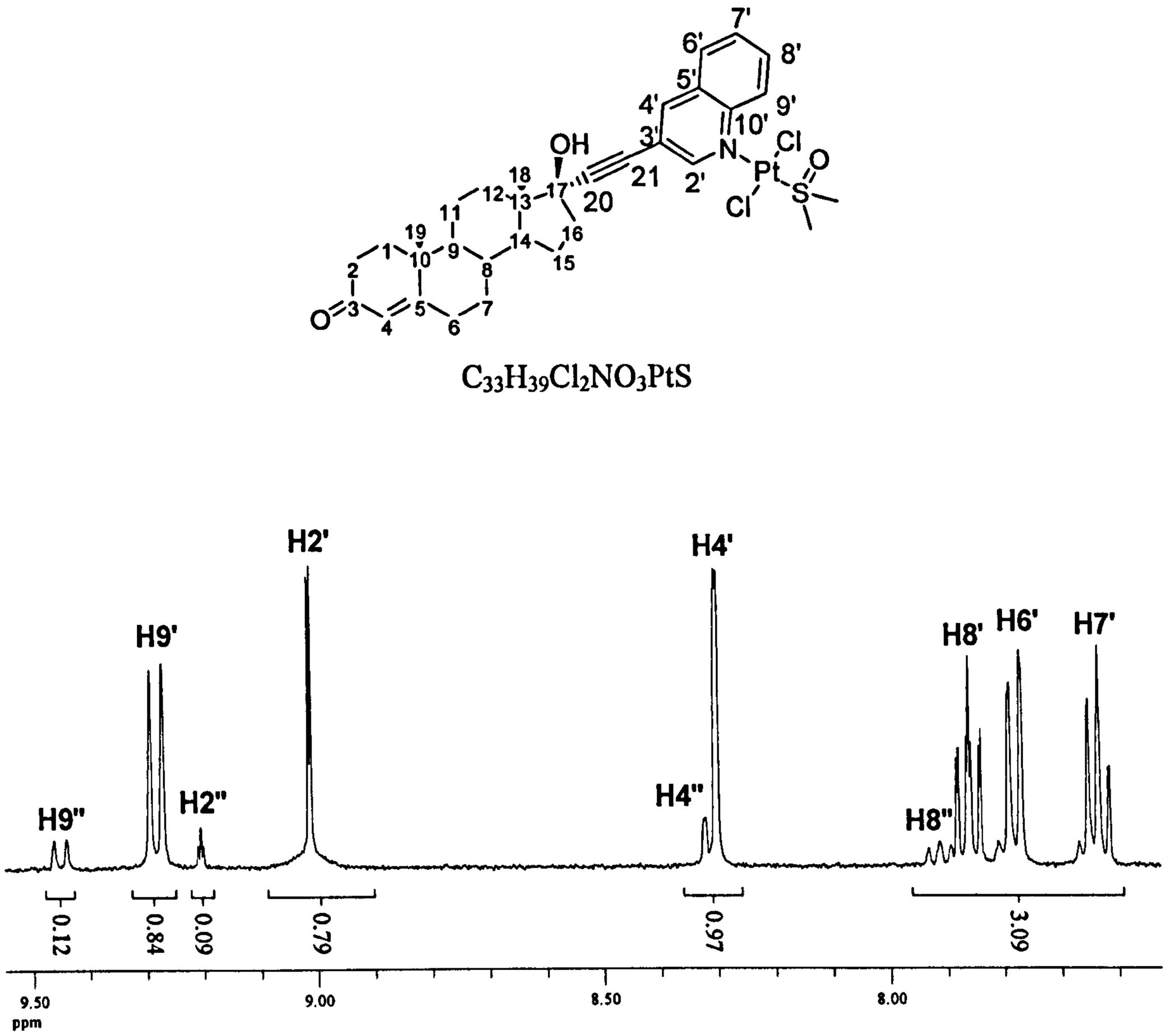

$C_{33}H_{39}Cl_2NO_3PtS$

Figure A.5.7. The aromatic region of the ^1H NMR spectrum of trans-Pt(ET-3-Q)(DMSO)Cl_2. Hydrogens labeled for example H2' belong to trans-Pt(ET-3-Q)(DMSO)Cl_2 whilst those labeled, for example, H2'' belong to complexes with 2 ET-3-Q ligands.

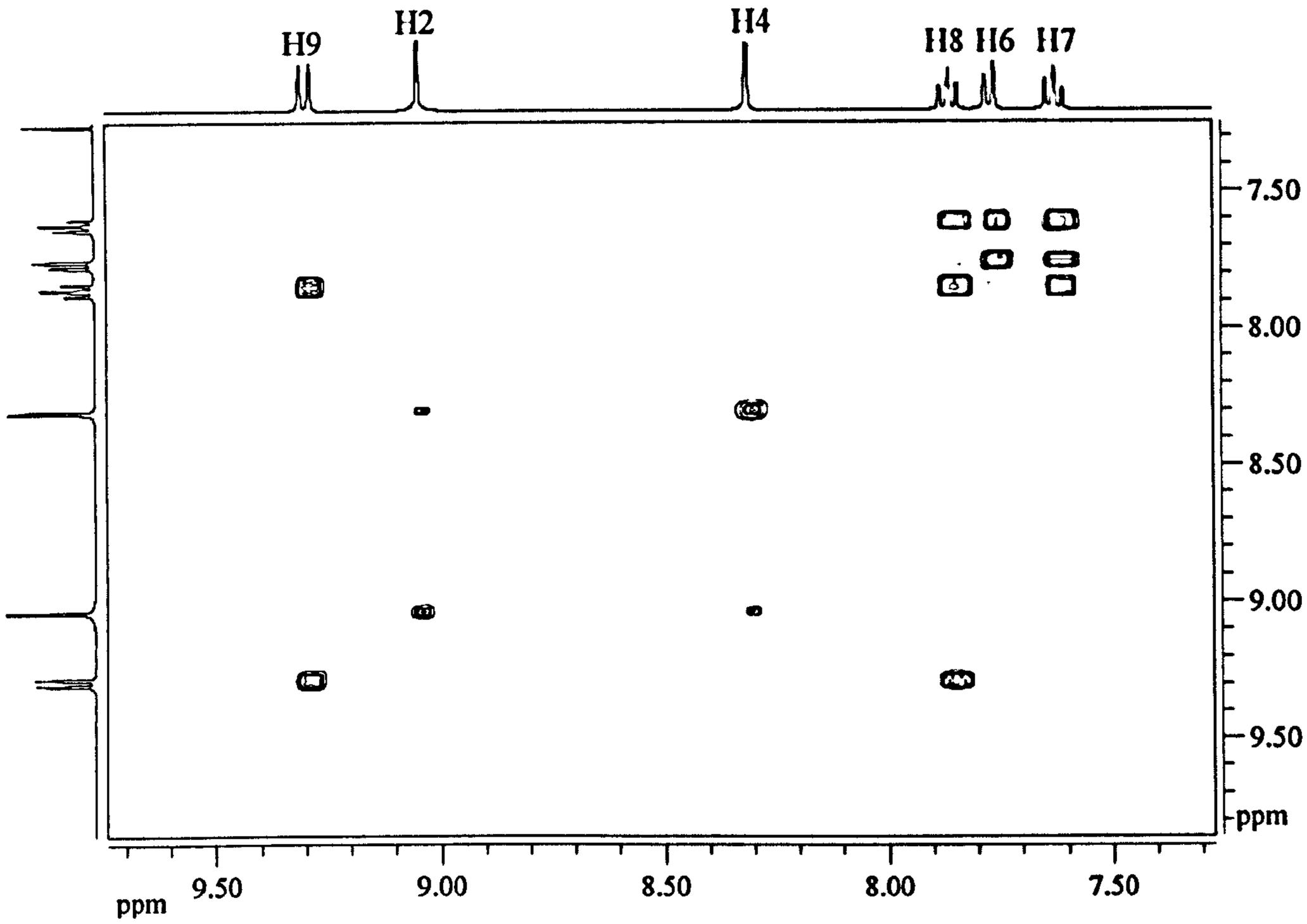

Figure A.5.8. The aromatic region of the COSY spectrum of trans-Pt(ET-3-Q)(DMSO)Cl_2.

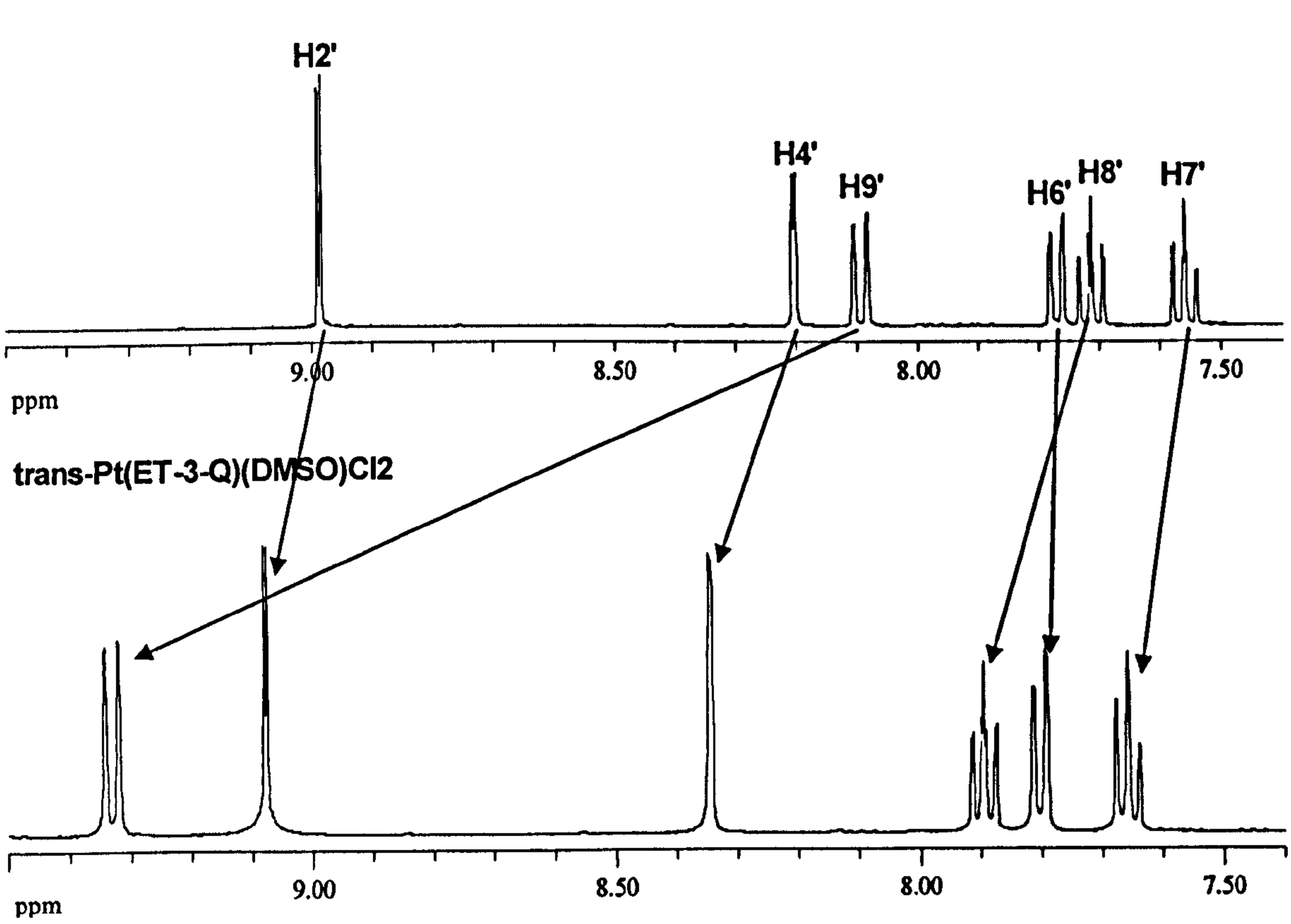

Figure A.5.9. A comparison of the aromatic region in the ^{1}H NMR spectra of ET-3-Q and trans-Pt(ET-3-Q)(DMSO)Cl_2.

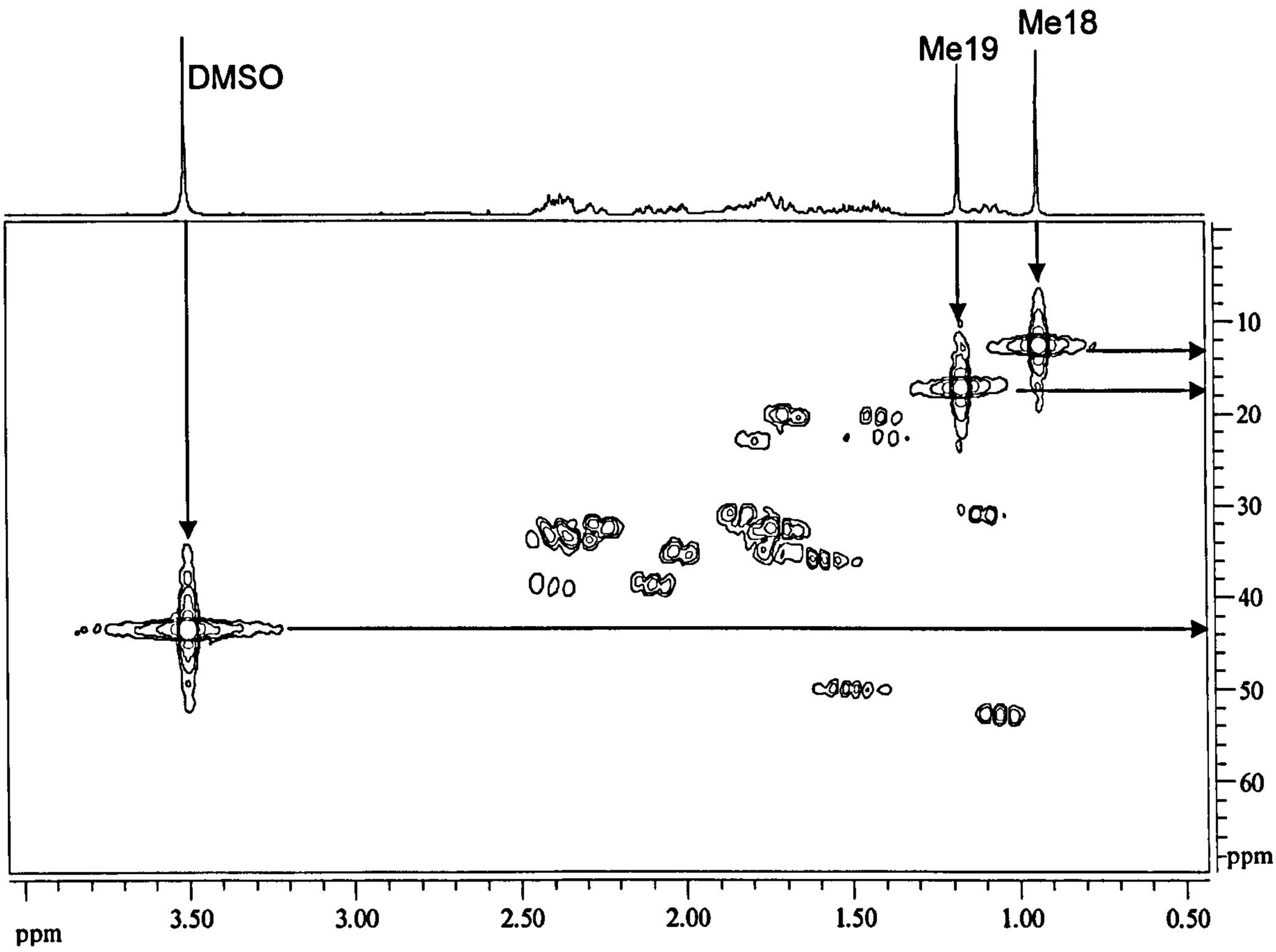

Figure A.5.10. The low chemical shift range in the HMQC spectrum of trans-Pt(ET-3-Q)(DMSO)Cl_2.

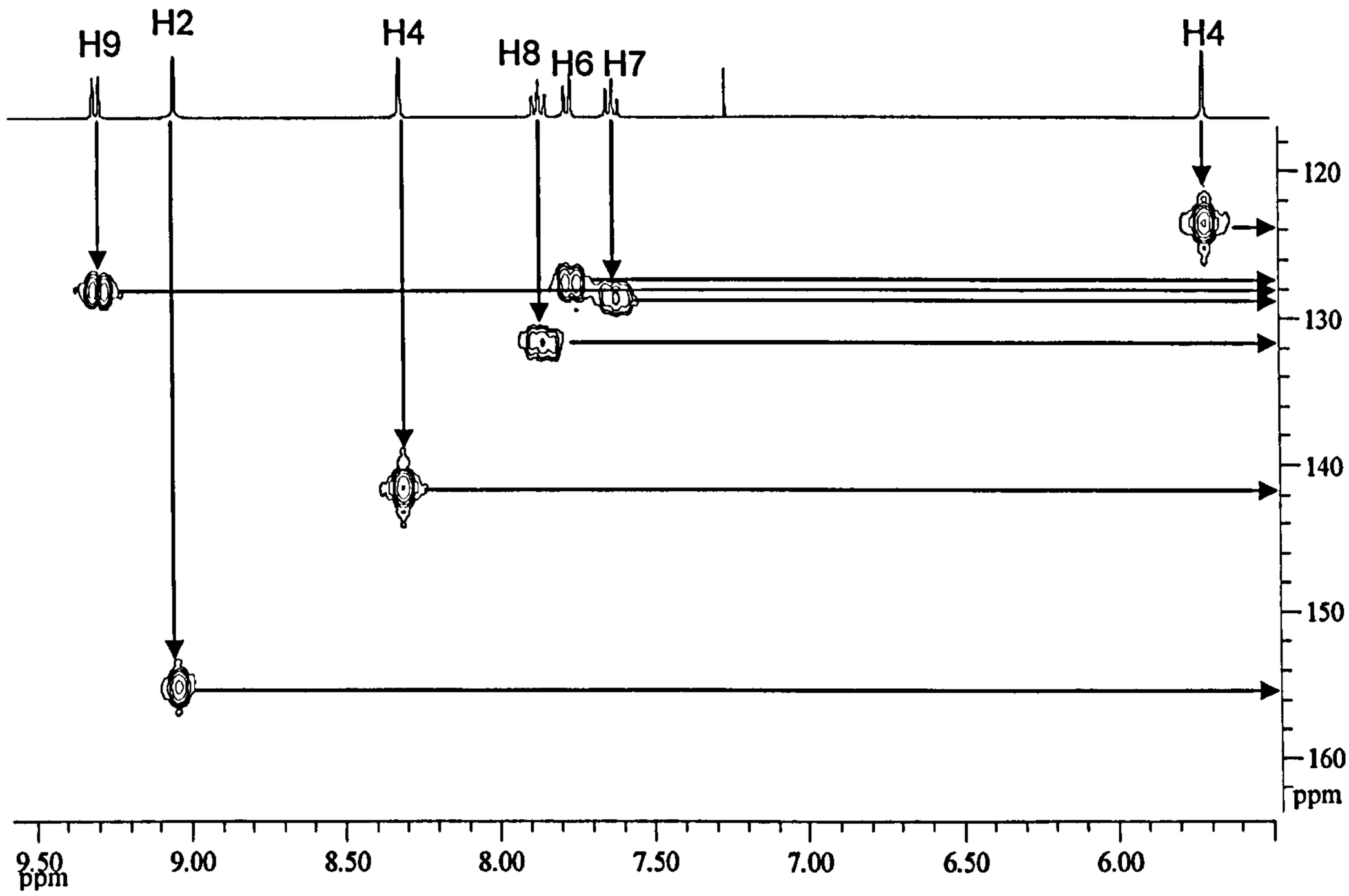

Figure A.5.11. The low field chemical shift range in the HMQC spectrum of trans-Pt(ET-3-Q)(DMSO)Cl_2.

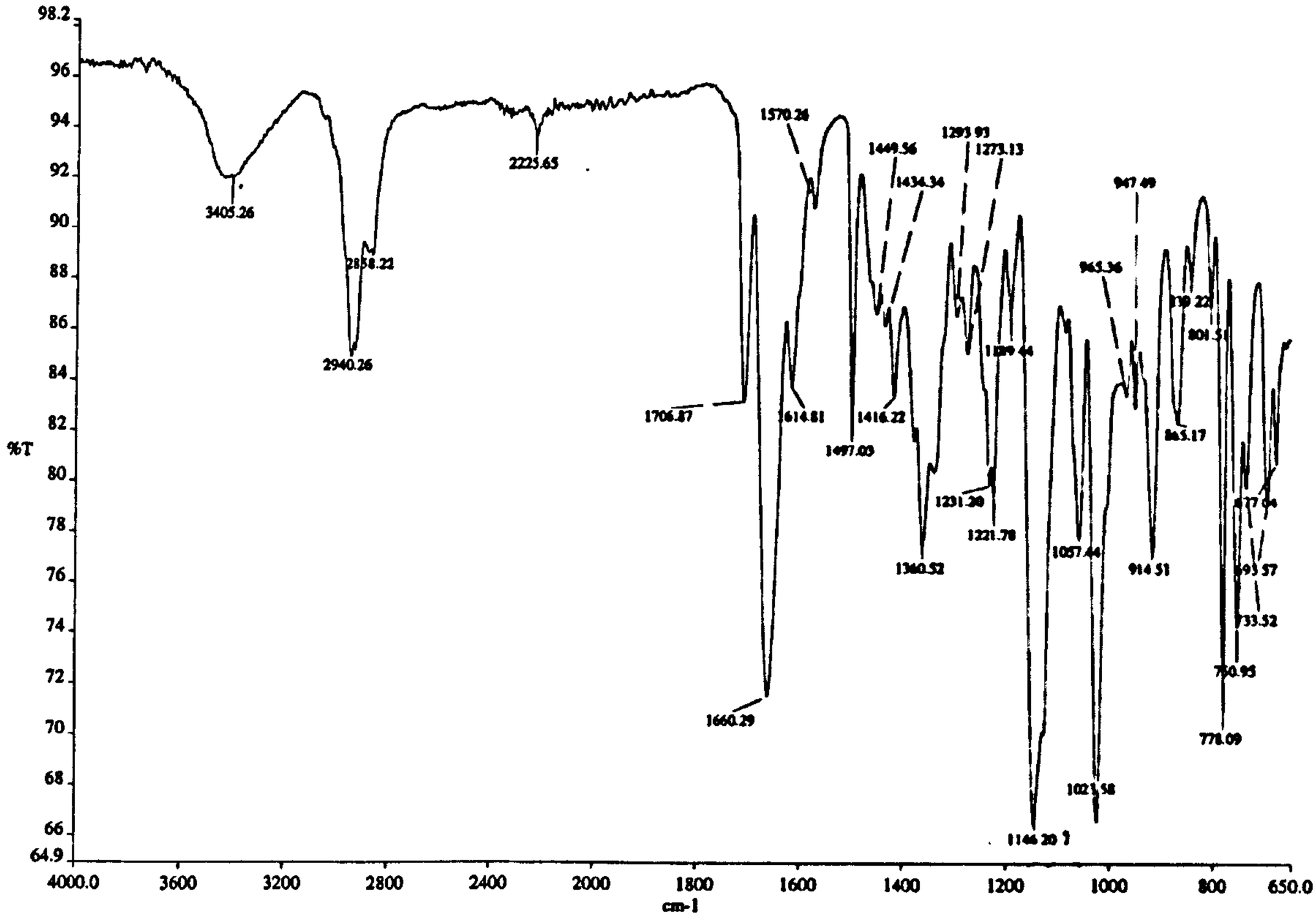

Figure A.5.12. The infrared spectrum of trans-Pt(ET-3-Q)(DMSO)Cl_2.

Appendix Six - Additional platinum starting complexes spectroscopy

A.6.1. Cis-diamminediiodoplatinum(II)

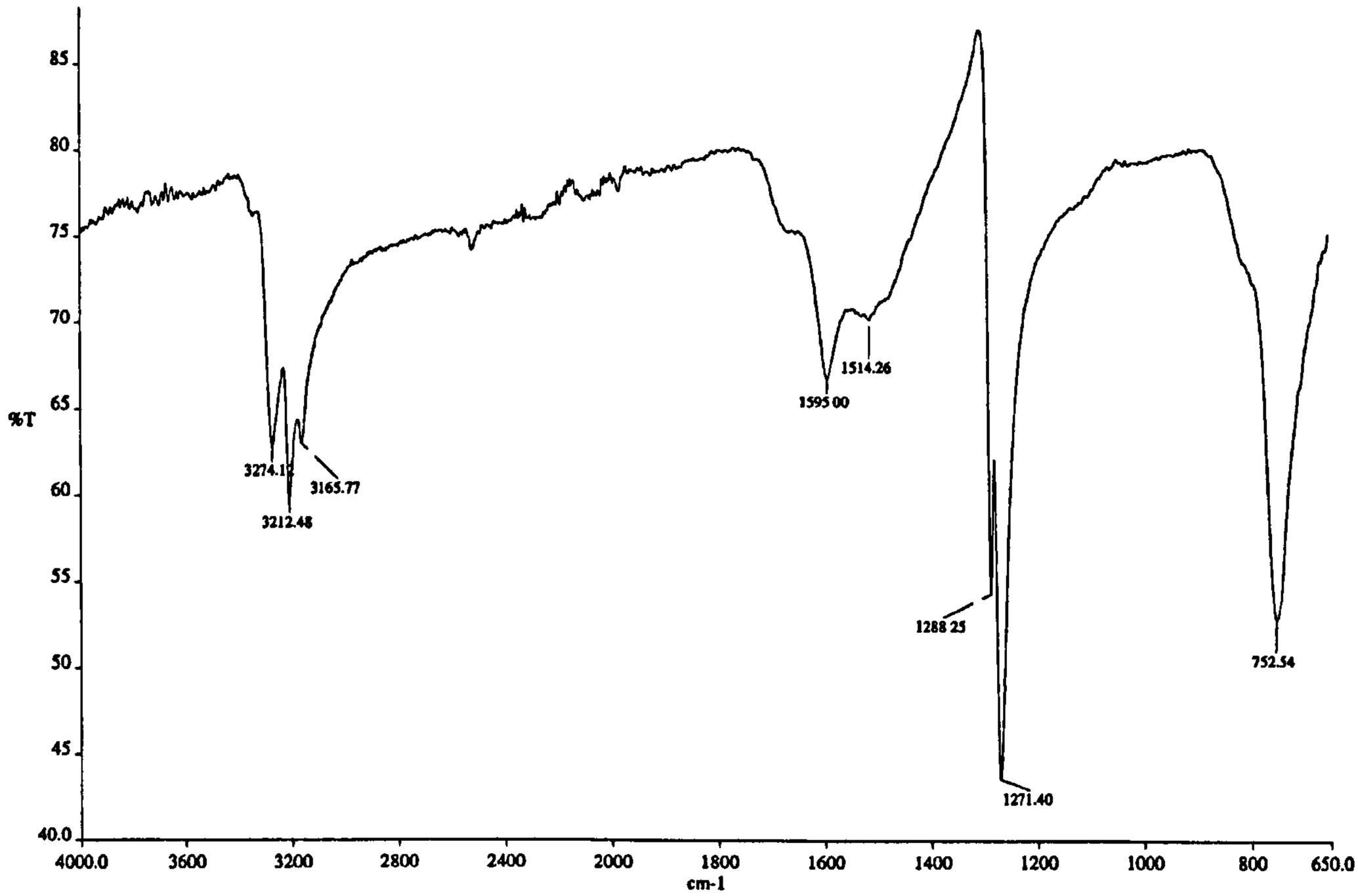

Figure A.6.1. The infrared spectrum of cis-diamminediiodoplatinum(II).

A.6.2. Cis-diamminedichloroplatinum(II)

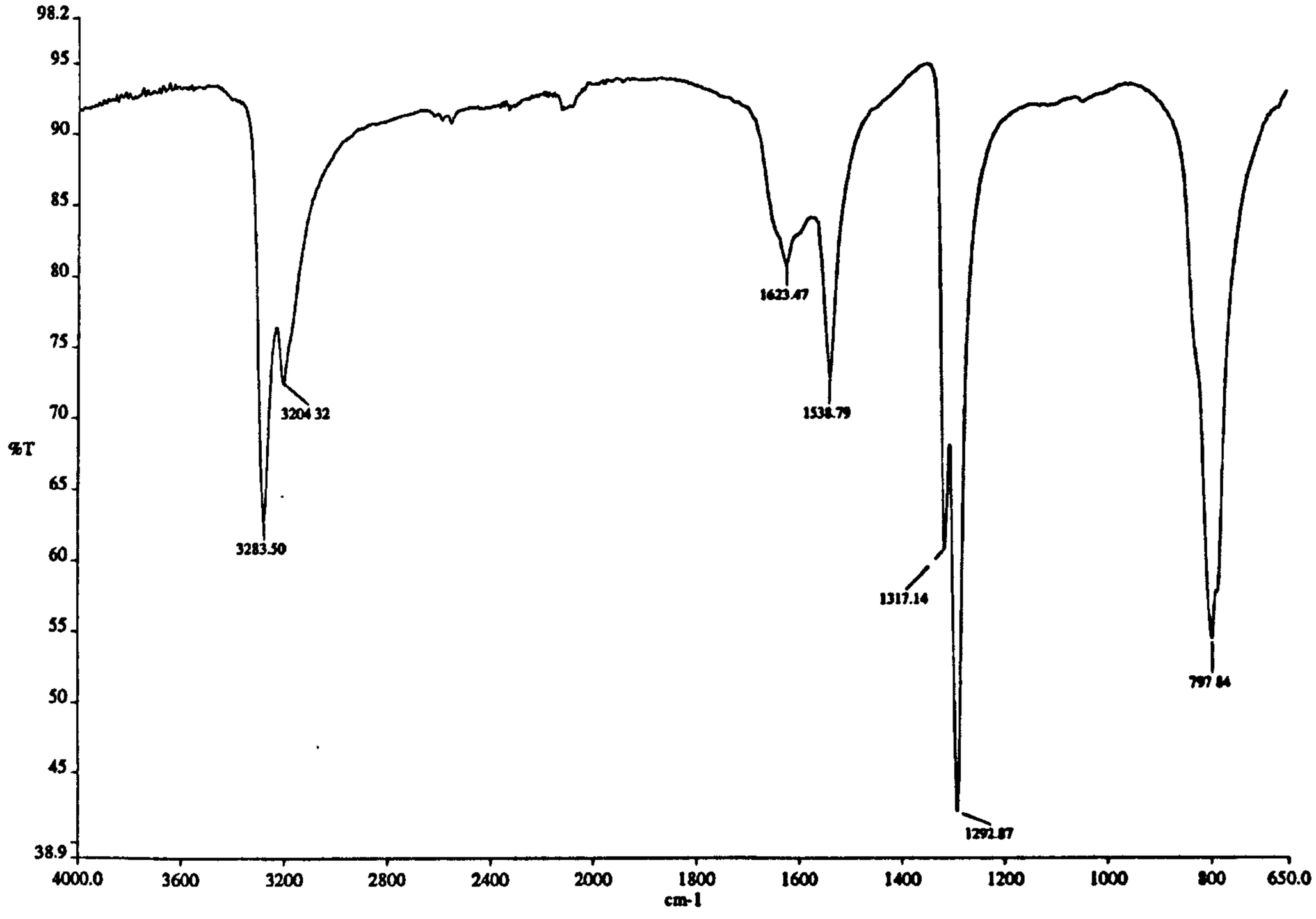

Figure A.6.2. The infrared spectrum of cis-diamminedichloroplatinum(II).

A.6.3. Trans-diamminedichloroplatinum(II)

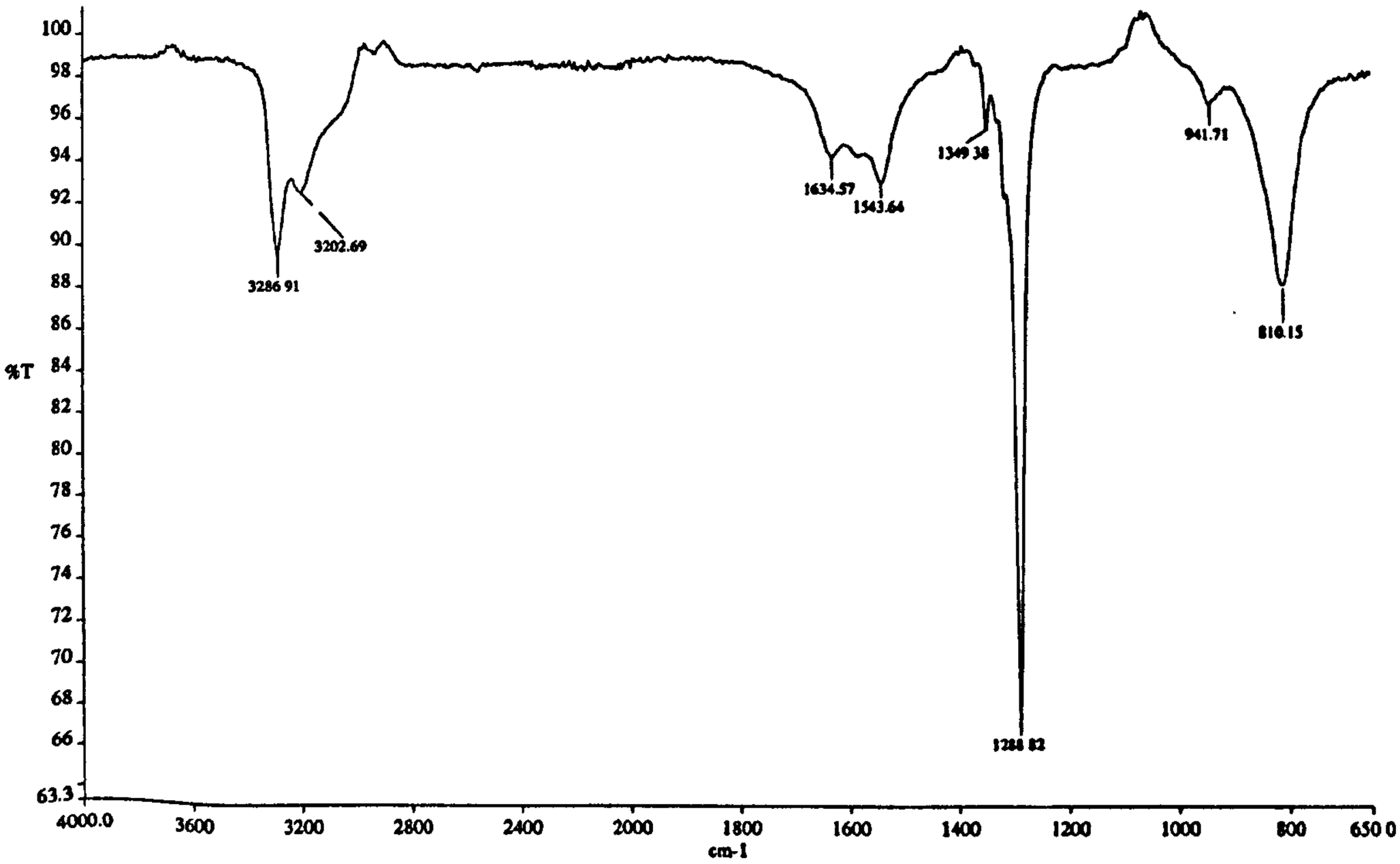

Figure A.6.3. The infrared spectrum of trans-diamminedichloroplatinum(II).

A.6.4. Cis-bis(dimethylsulphoxide)dichloroplatinum(II)

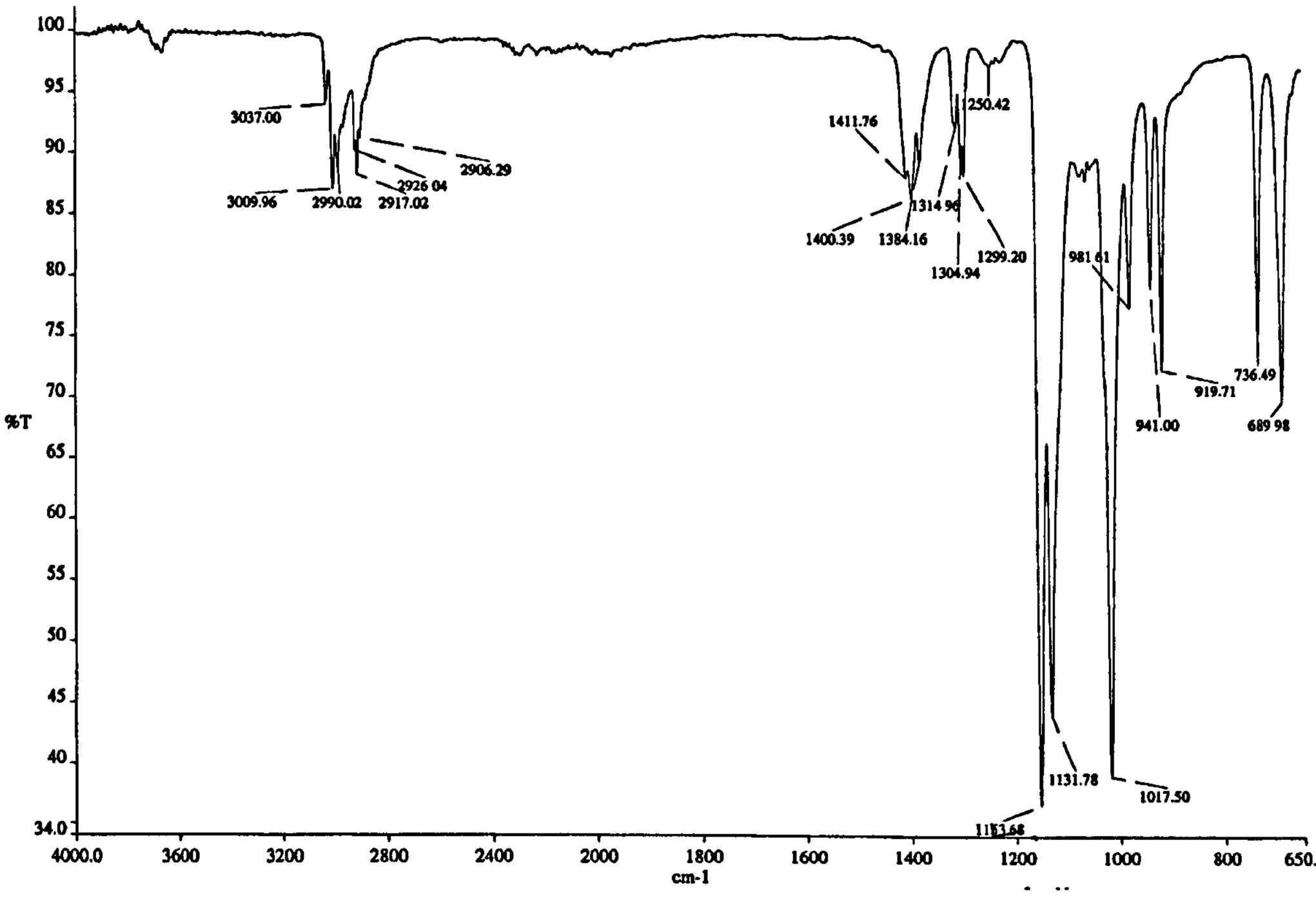

Figure A.6.4. The infrared spectrum of cis-bis(dimethylsulphoxide)dichloroplatinum(II).

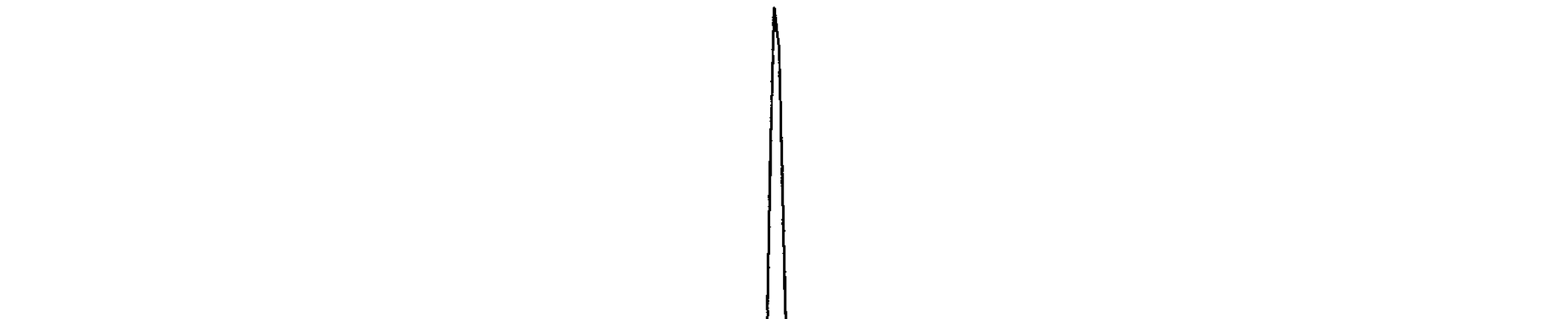

Figure A.6.5. The ^{1}H NMR spectrum of cis-bis(dimethylsulphoxide)dichloroplatinum(II).

Appendix Seven – ESI Mass Spectroscopy of Complexes illustrating hydrolysis

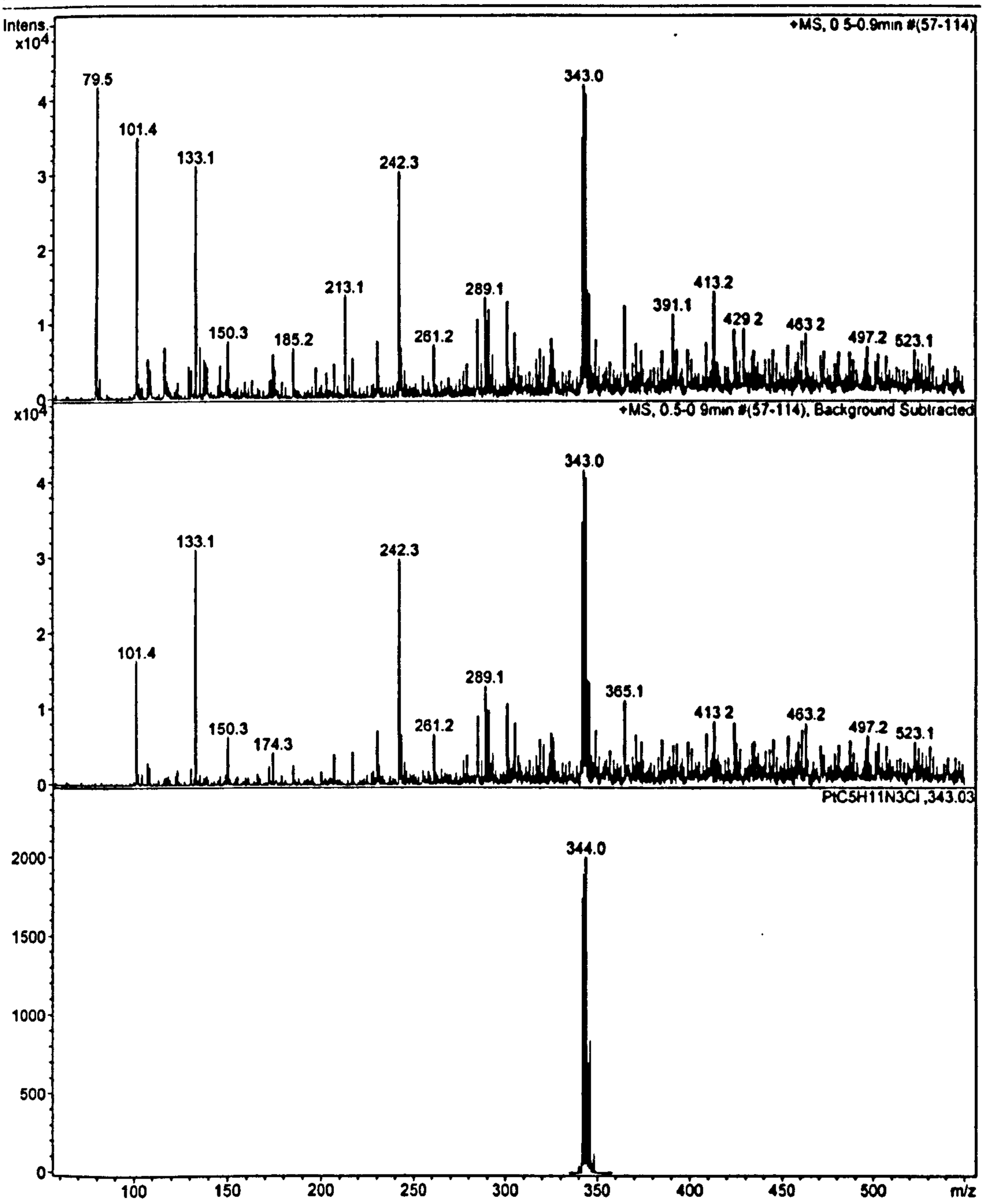

Figure A.7.1. ESI-MS (+ve) spectra of TC-Py; upper and middle, up to *m/z* = 500; lower, expansion and calculated isotope distribution patterns.

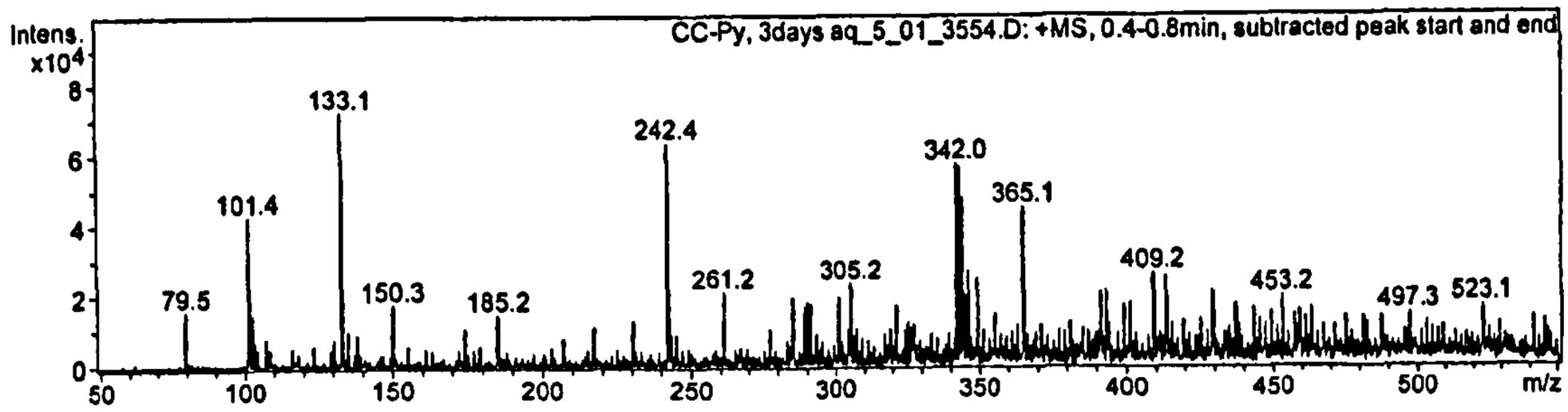

Figure A.7.2. ESI-MS (+ve) spectra of CC-Py up to *m/z* = 500.

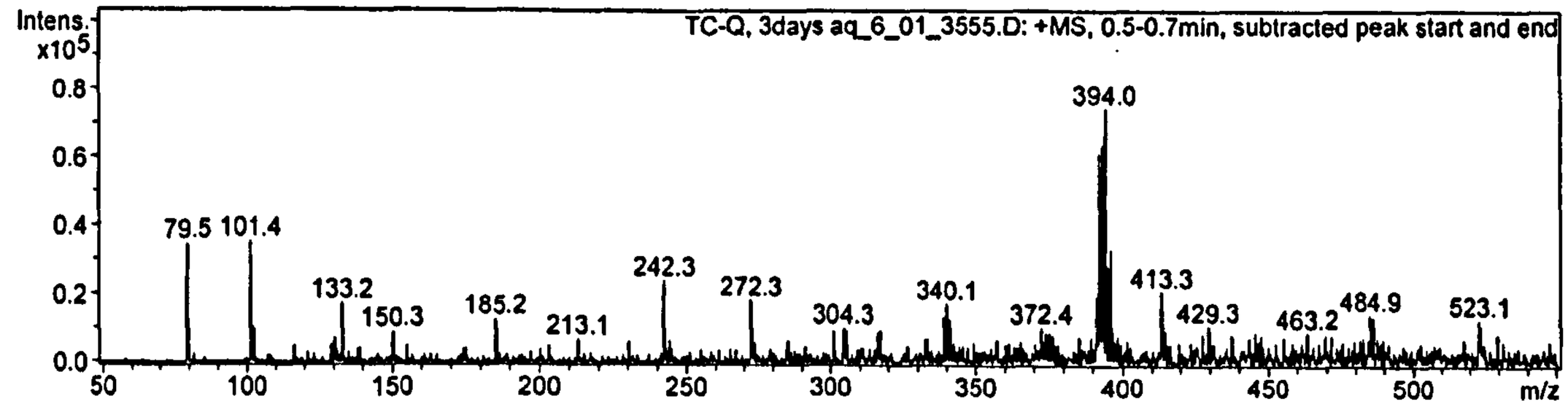

Figure A.7.3. ESI-MS (+ve) spectra of TC-Q up to *m/z* = 500.

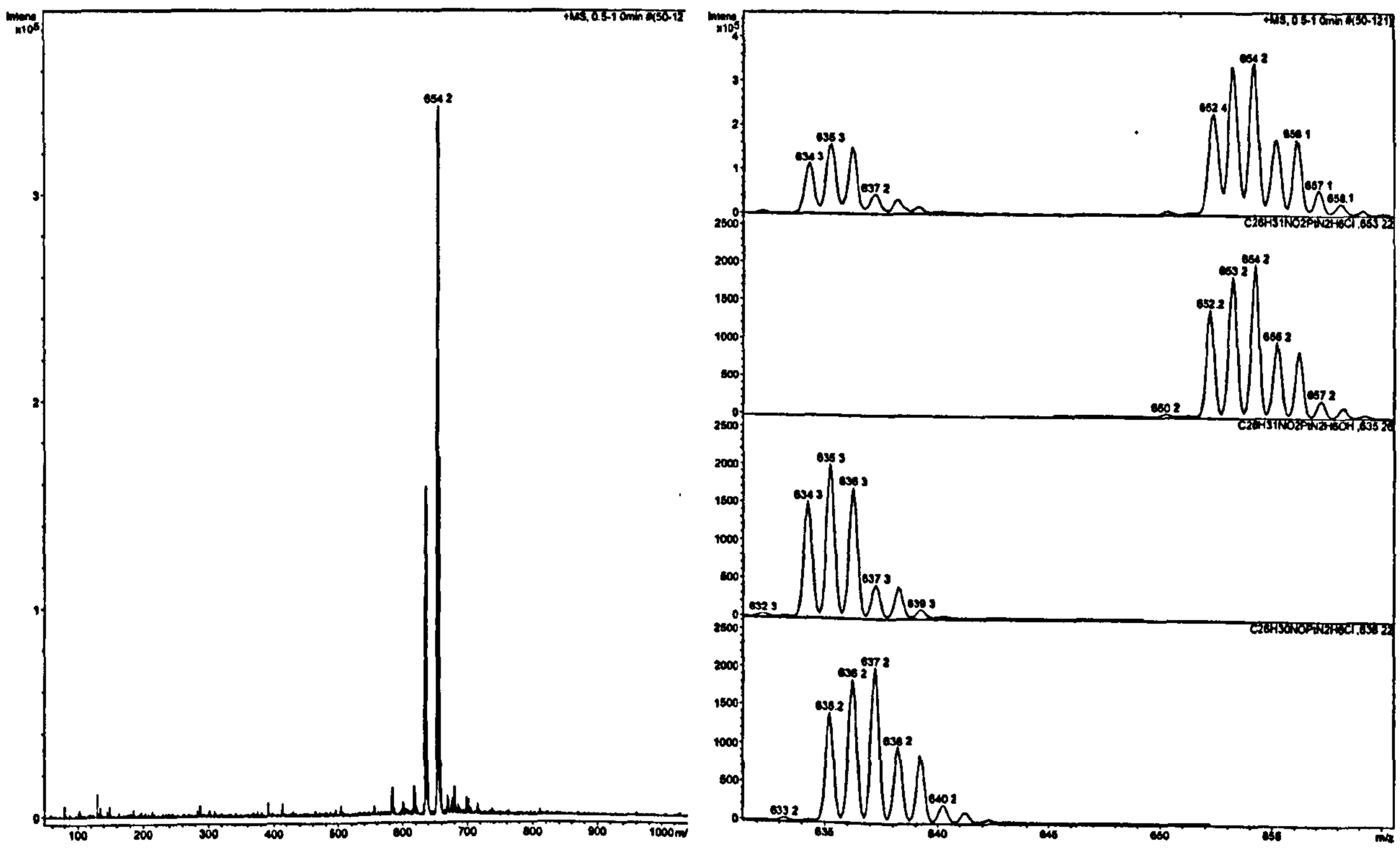

Figure A.7.4. ESI-MS (+ve) spectra of TC-ET-3-Py; left, up to *m/z* = 1000; right, expansion and calculated isotope distribution patterns.

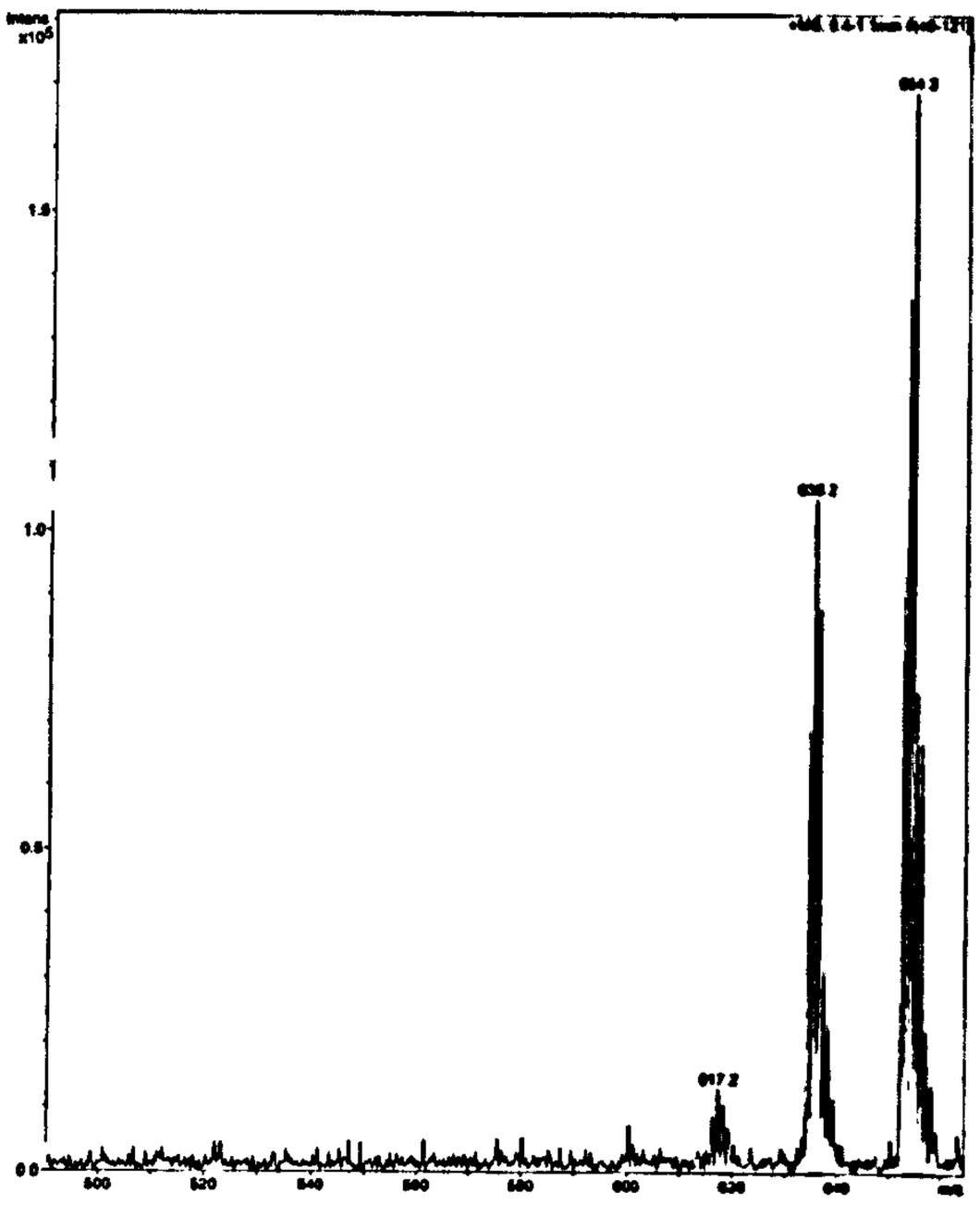

Figure A.7.5. ESI-MS (+ve) spectra of TC-ET-4-Py.

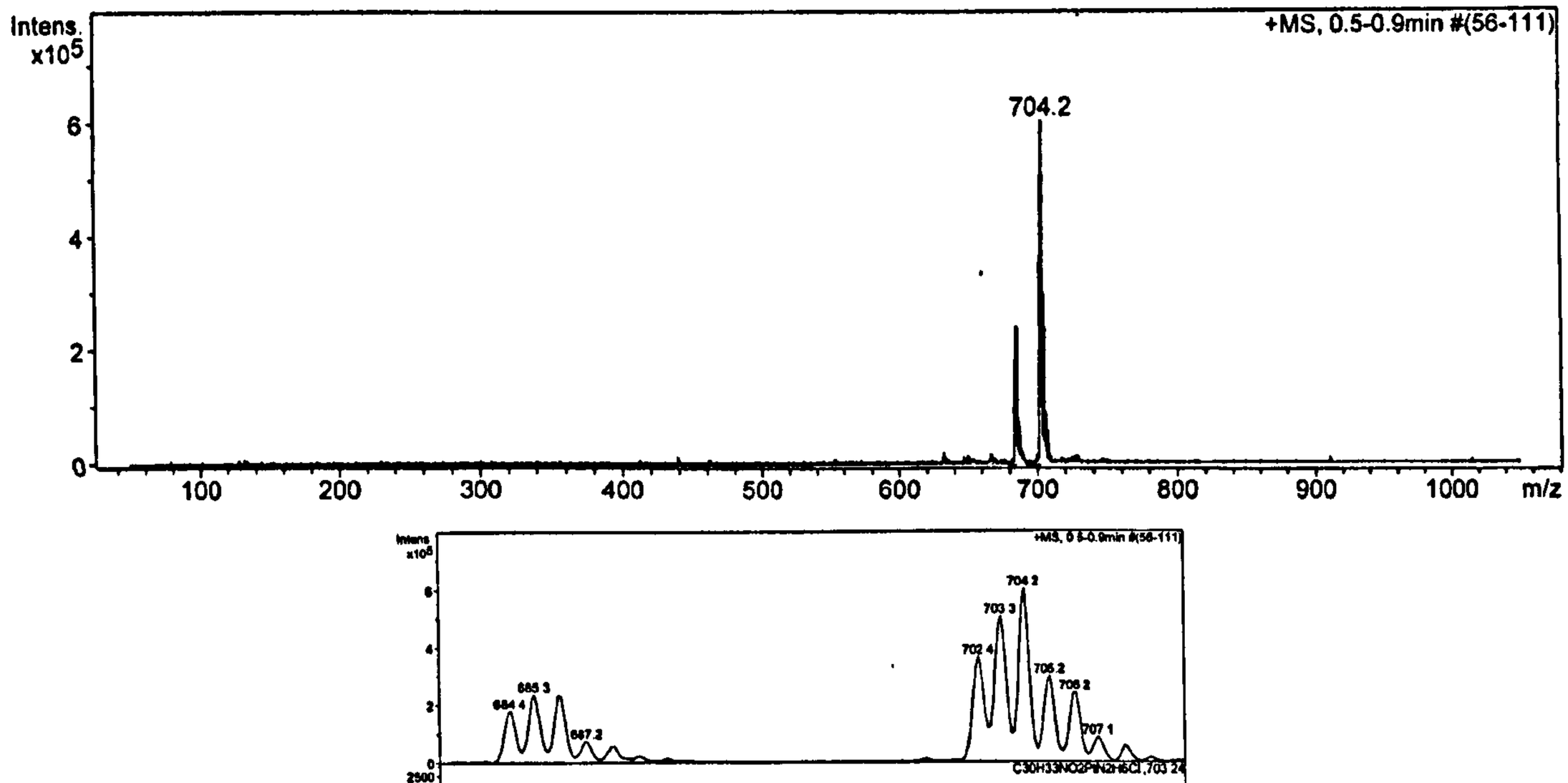

Figure A.7.6. ESI-MS (+ve) spectra of TC-ET-3-Q; upper, up to *m/z* = 1000; lower, expansion and calculated isotope patterns.

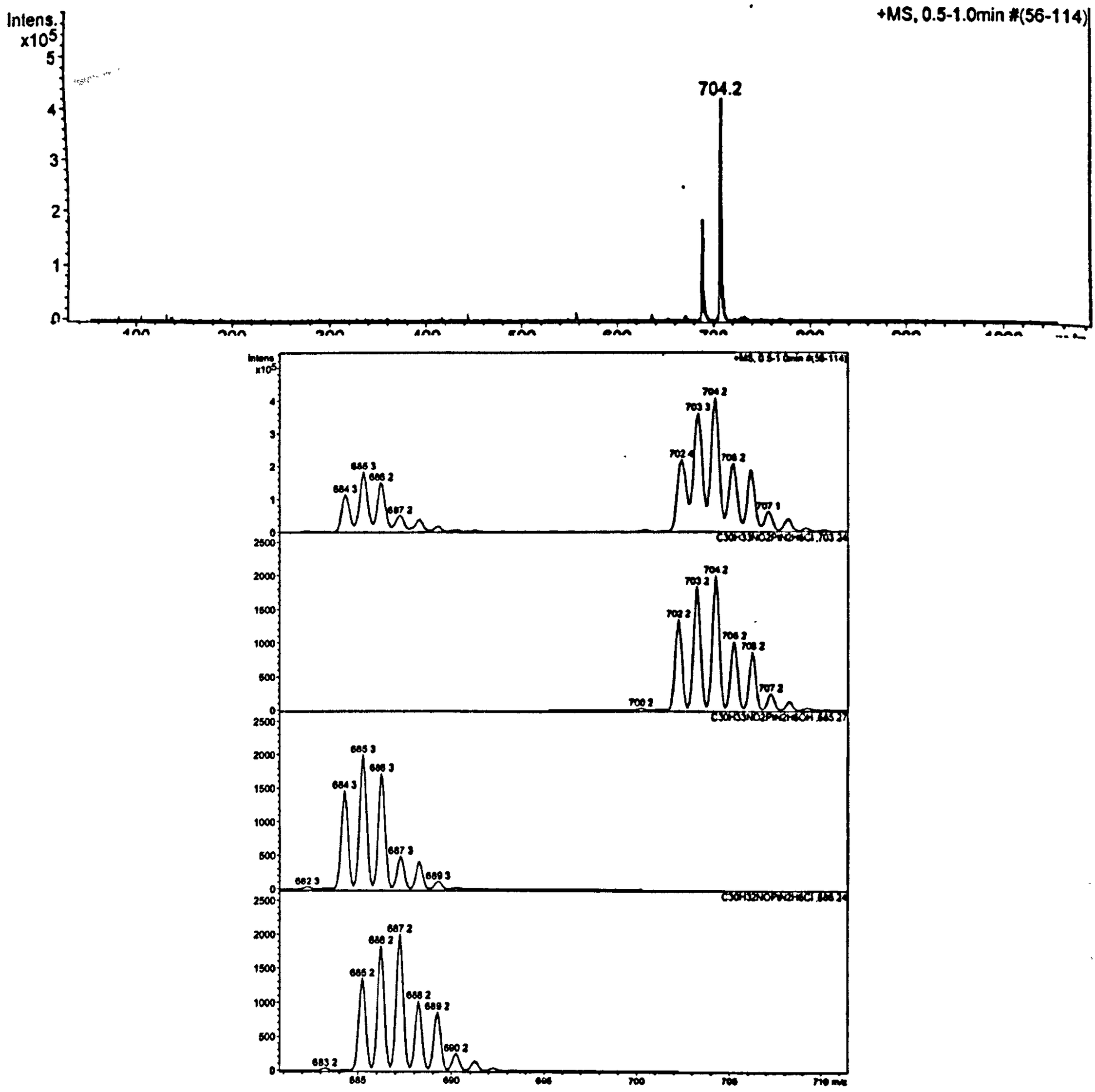

Figure A.7.7. ESI-MS (+ve) spectra of TC-ET-4-IQ; a) upper, up to *m/z* = 1000; lower, expansion and calculated isotope patterns.

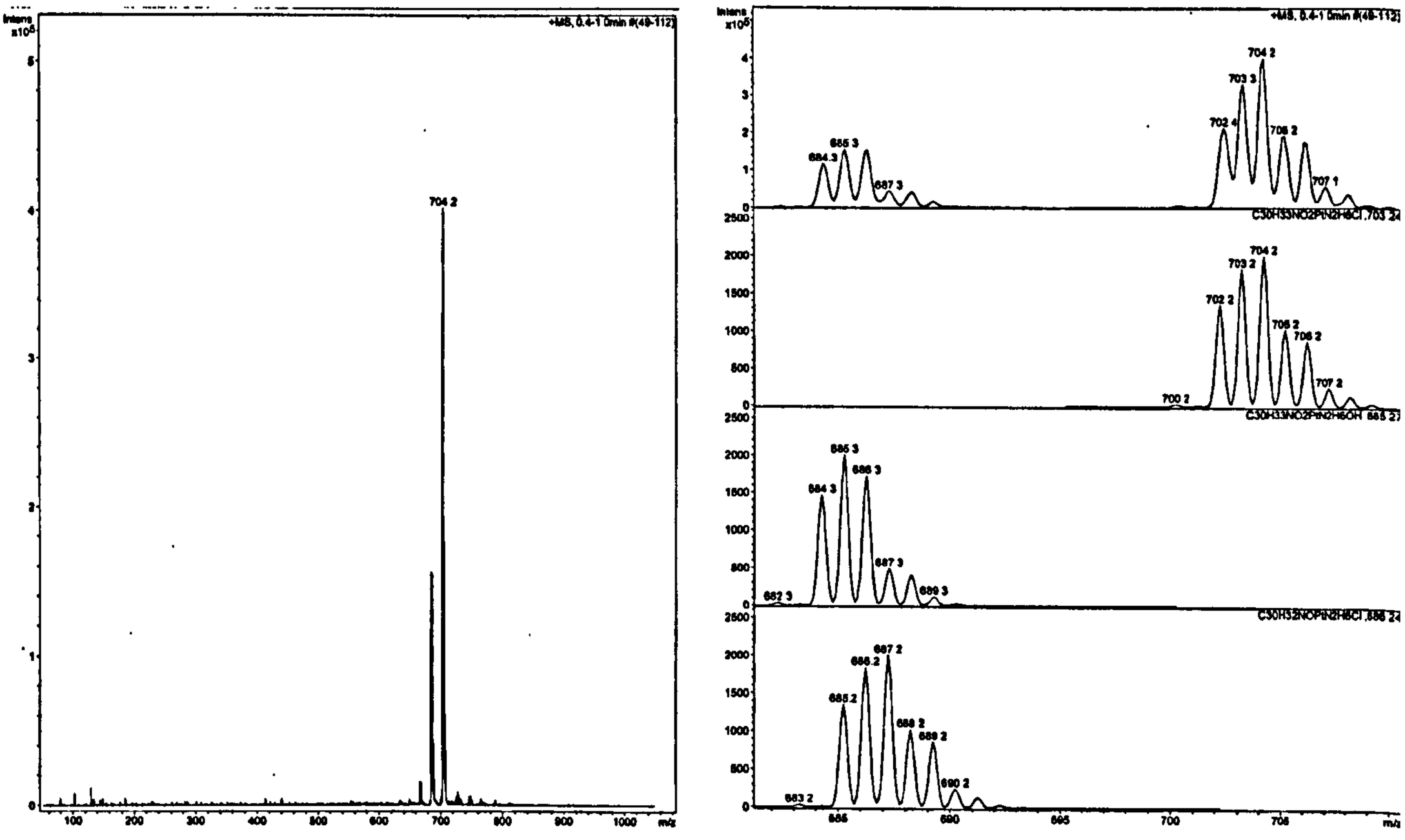

Figure A.7.8. ESI-MS (+ve) spectra of TC-ET-6-Q; left, up to *m/z* = 1000; right, expansion and calculated isotope patterns.

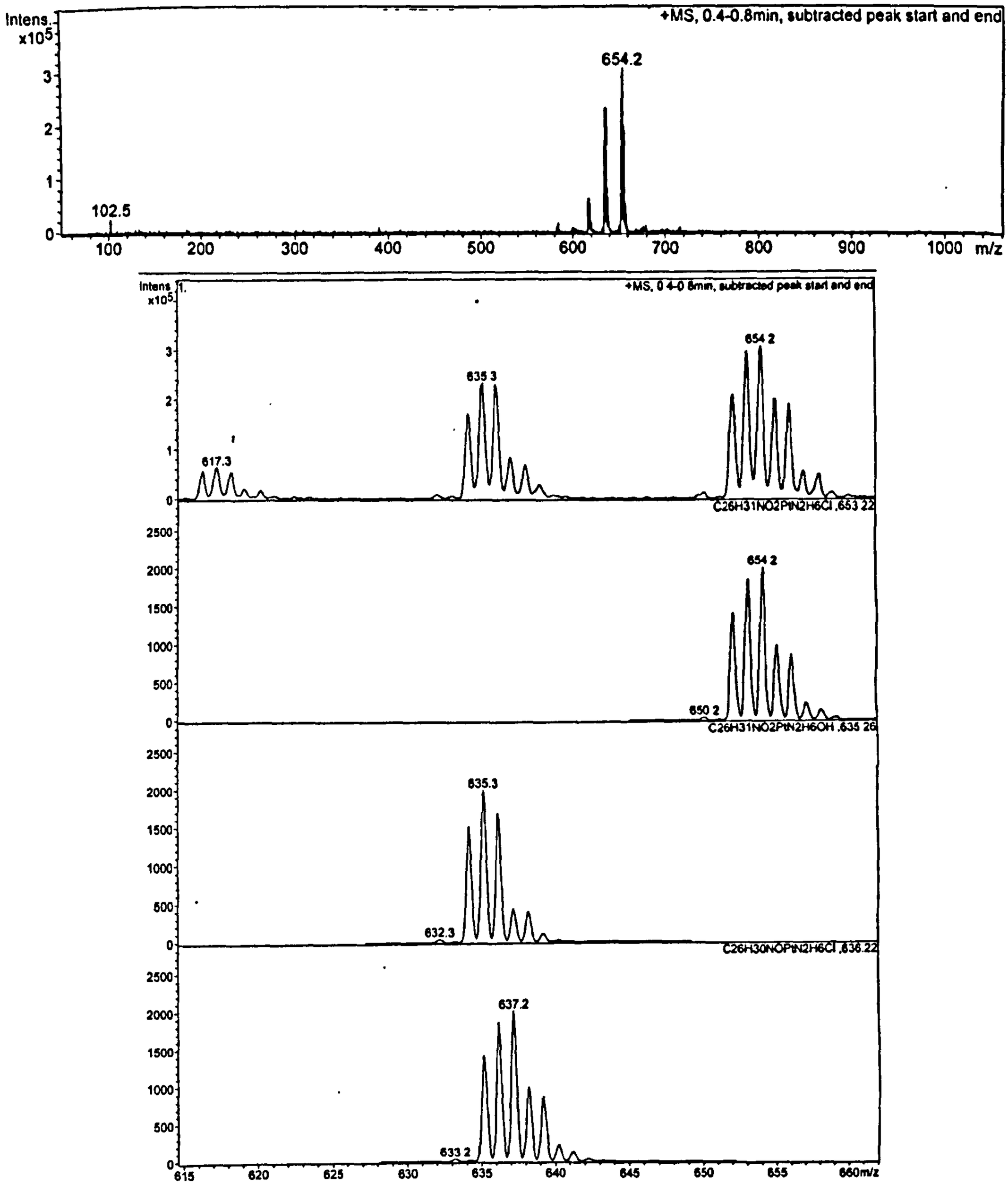

Figure A.7.9. ESI-MS (+ve) spectra of CC-ET-3-Py; a) upper, up to *m/z* = 1000; lower, expansion and calculated isotope patterns.

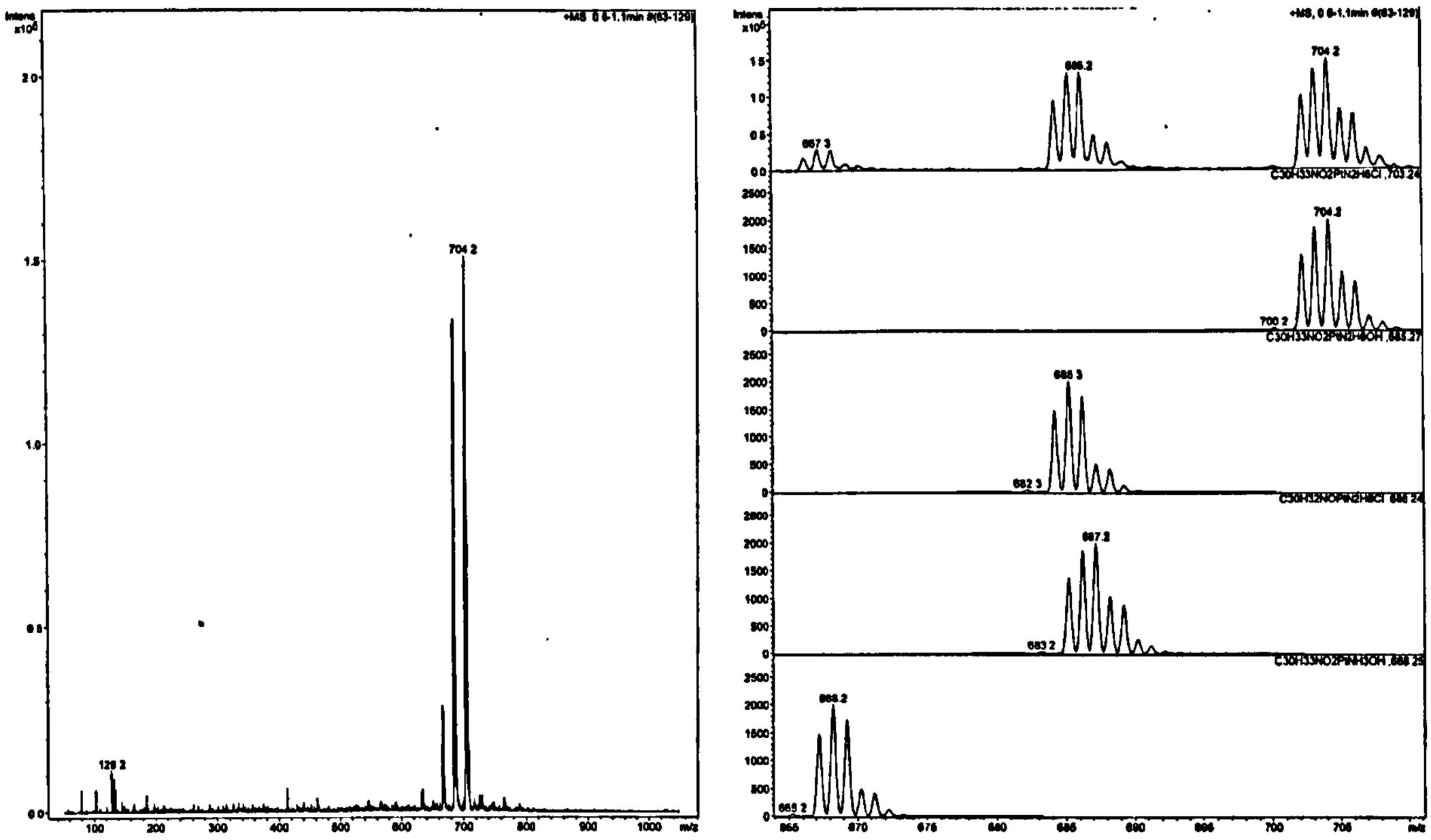

Figure A.7.10. ESI-MS (+ve) spectra of CC-ET-4-IQ; a) left, up to *m/z* = 1000, b) right, expansion and calculated isotope patterns.

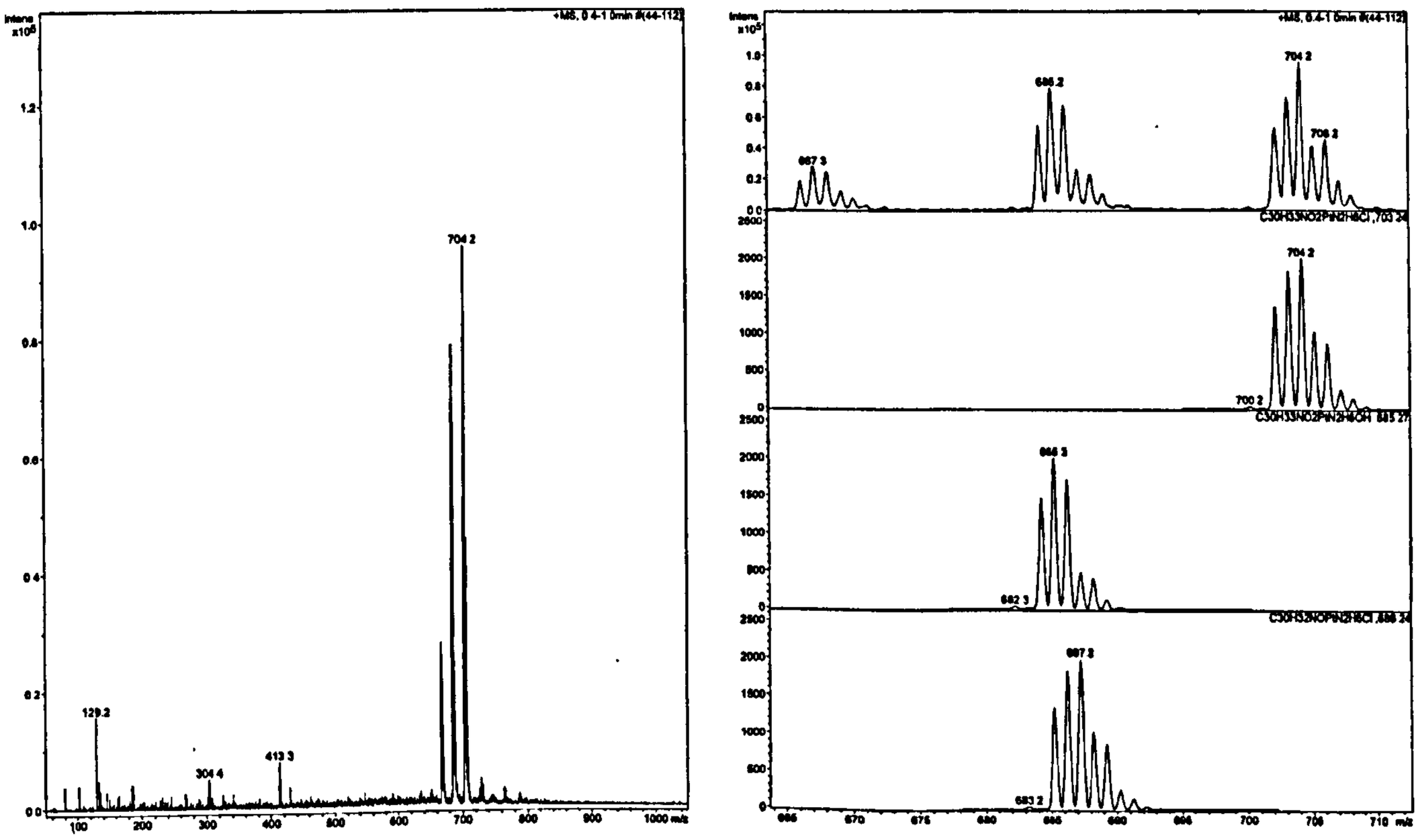

Figure A.7.11. ESI-MS (+ve) spectra of CC-ET-6-Q; left up to *m/z* = 1000; right, expansion and calculated isotope patterns.

Appendix Eight – ESI mass spectroscopy of complexes illustrating nucleophilic substitution

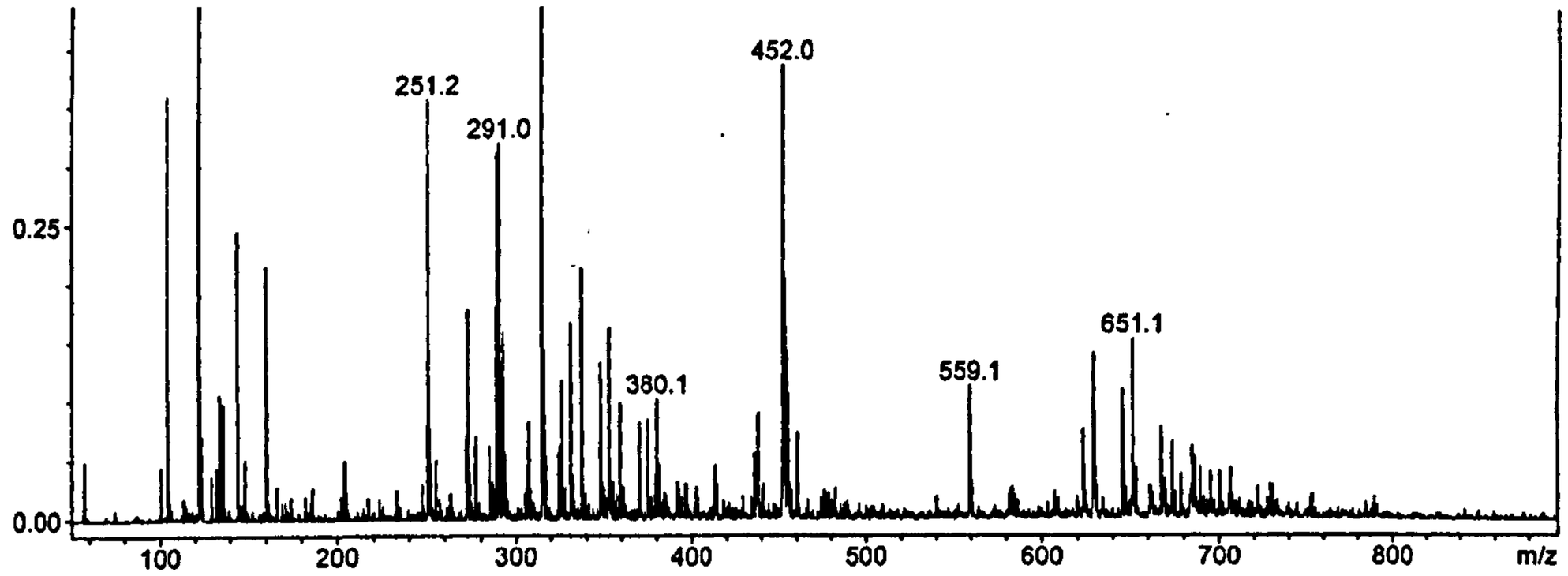

Figure A.8.1. ESI-MS (+ve) spectra of TC-Py + 5'-GMP in the range *m/z* = 0 – 1000.

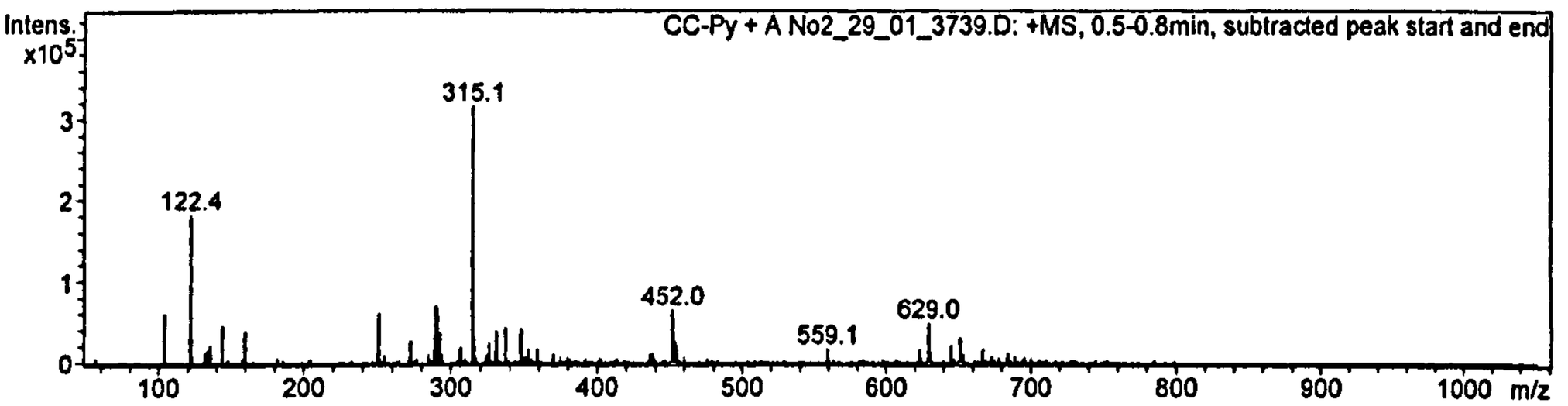

Figure A.8.2. ESI-MS (+ve) spectra of CC-Py + 5'-GMP in the range *m/z* 0 – 500.

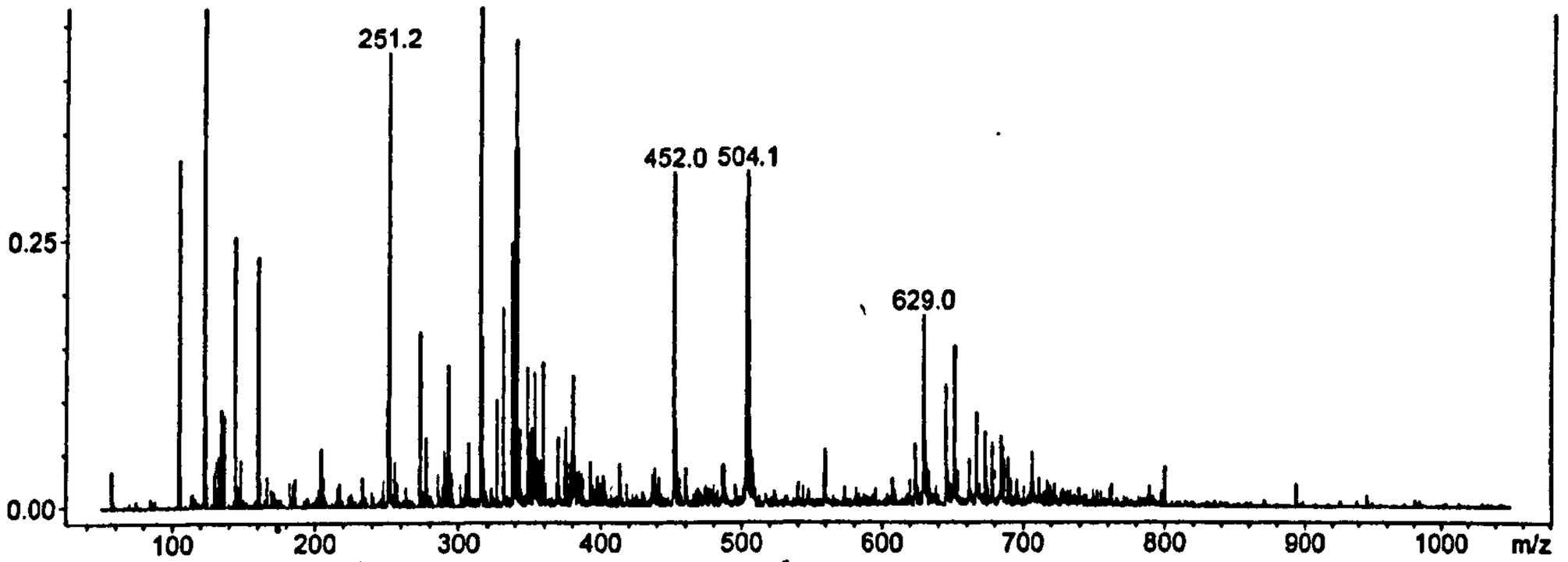

Figure A.8.3. ESI-MS (+ve) spectra of TC-Py + 5'-GMP in the range *m/z* = 0 – 500.

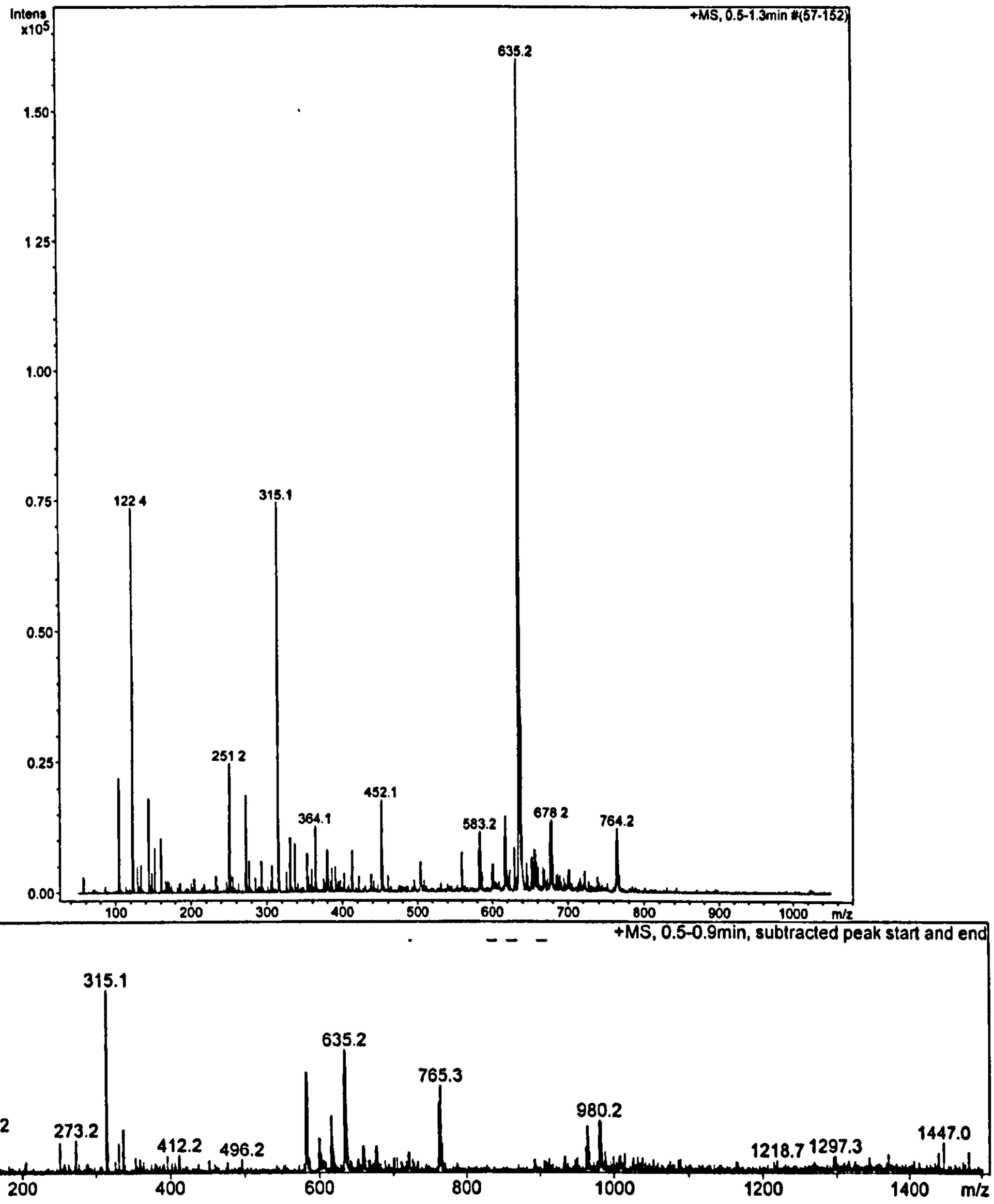

Figure A.8.4. ESI-MS (+ve) spectra of TC-ET-3-Py + 5'-GMP; top, range from *m/z* = 0 - 1000; bottom, range from *m/z* 1000 – 1500.

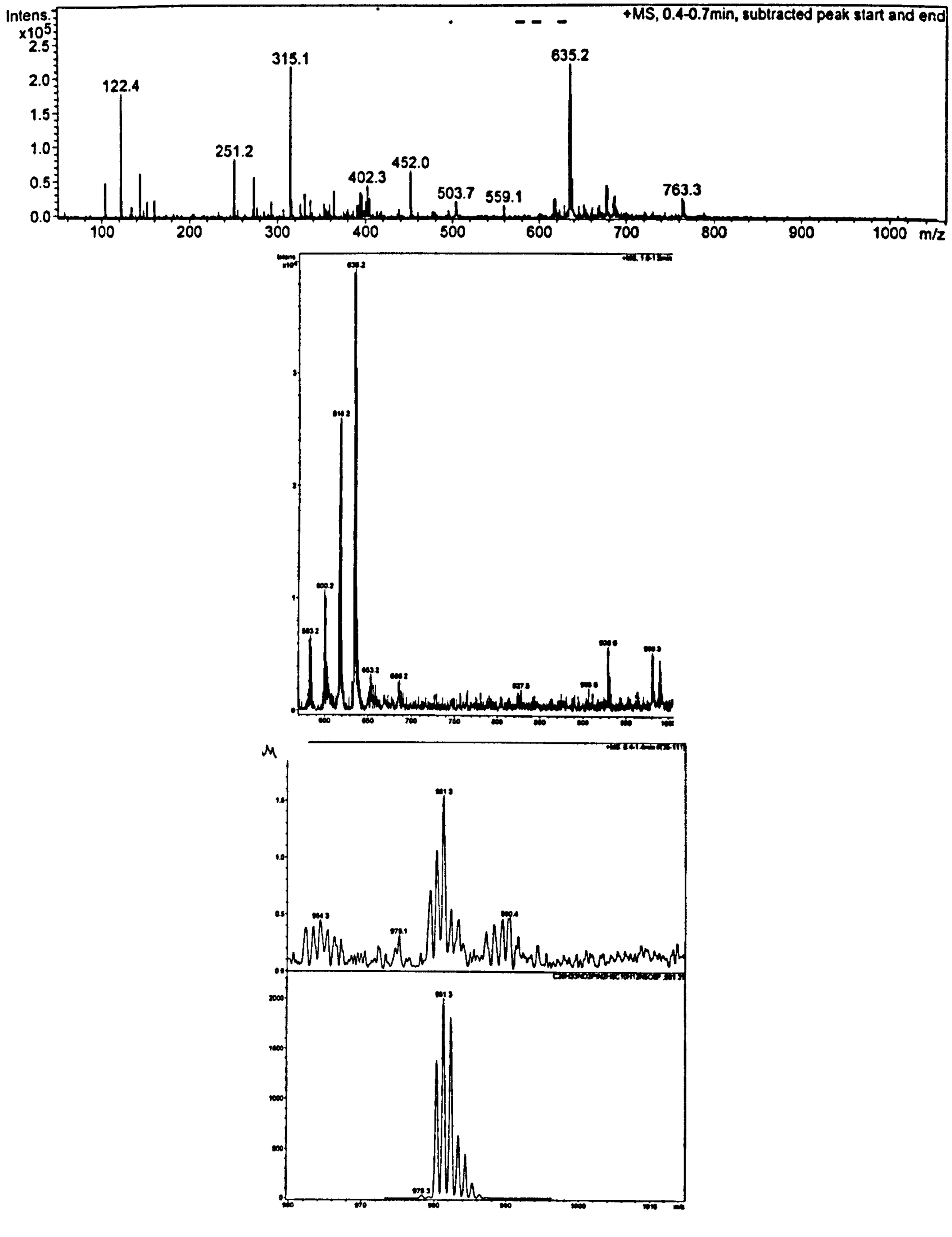

Figure A.8.5. ESI-MS (+ve) spectra of TC-ET-4-Py + 5'-GMP; upper, range from *m/z* = 500 – 1000; middle, range from *m/z* = 1000 – 1500; lower, expansion and calculated isotope distribution pattern for adduct, around *m/z* = 980.

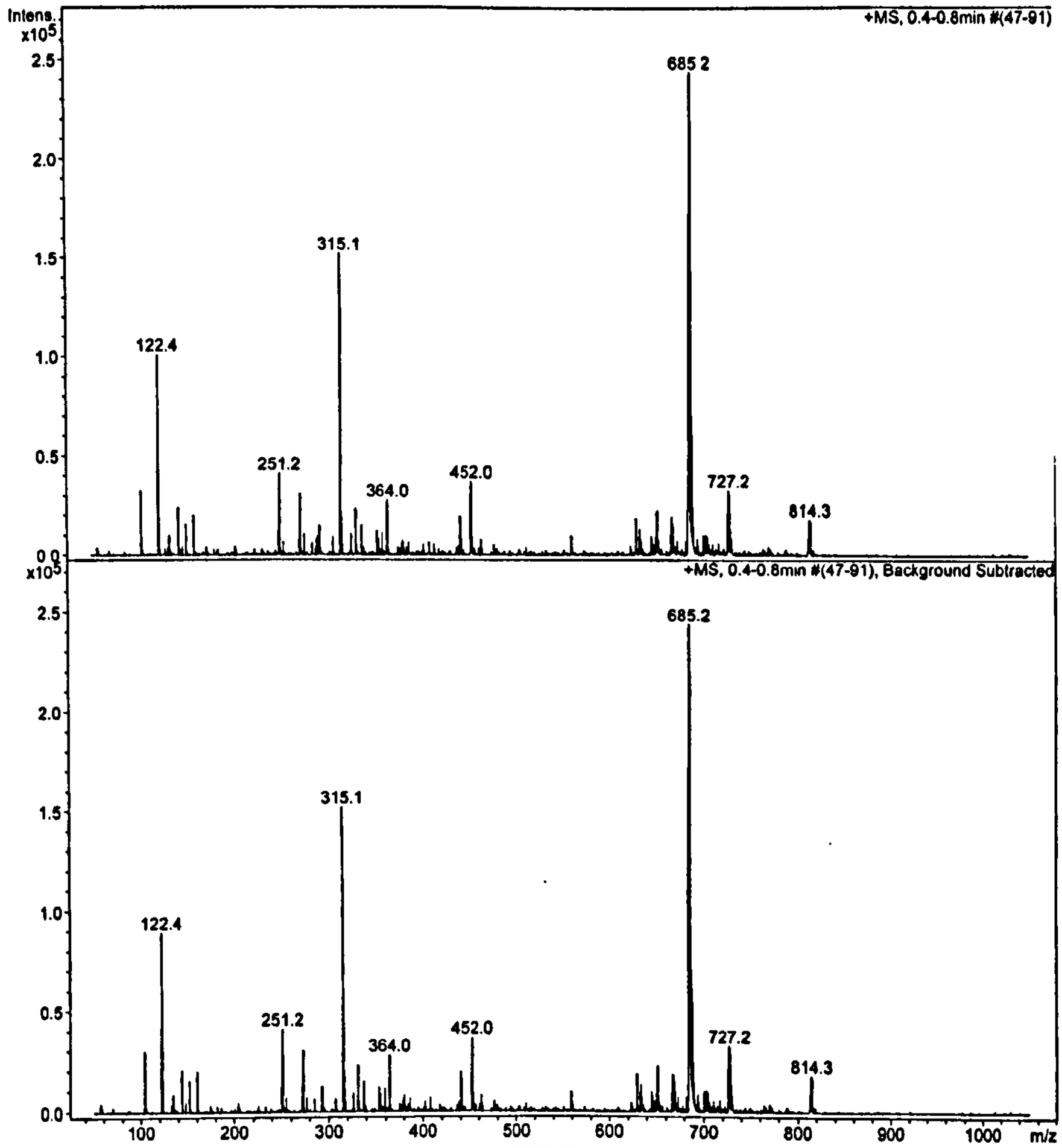
Intens.
x10^5
2.5
2.0
1.5
1.0
0.5
0.0
+MS, 0.4-0.8min #(47-91)
685.2
315.1
122.4
251.2
364.0
452.0
727.2
814.3
+MS, 0.4-0.8min #(47-91), Background Subtracted
685.2
315.1
122.4
251.2
364.0
452.0
727.2
814.3
100
200
300
400
500
600
700
800
900
1000
m/z

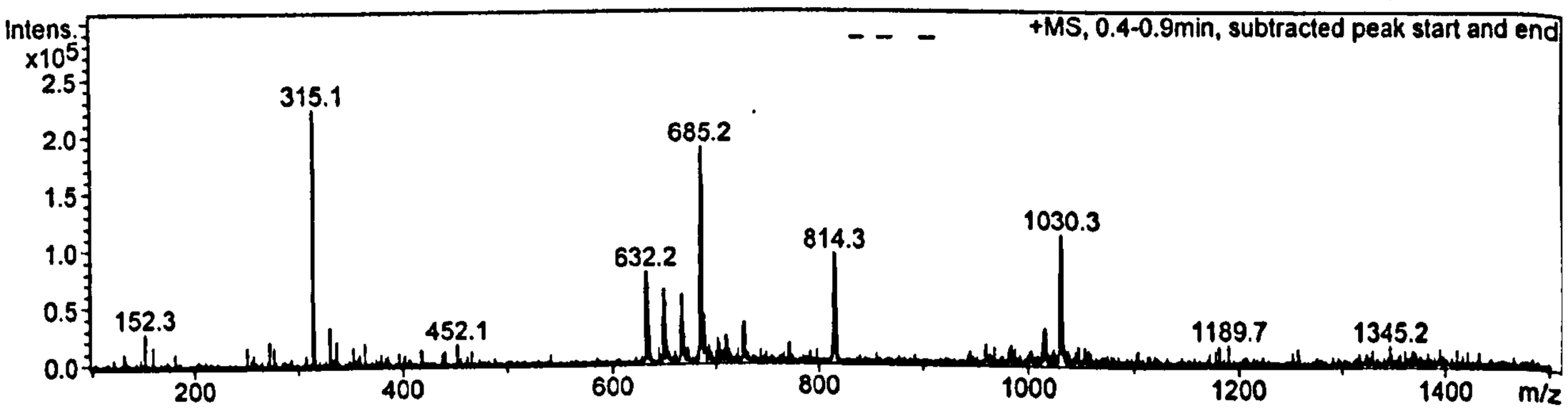
Intens.
x10^5
2.5
2.0
1.5
1.0
0.5
0.0
+MS, 0.4-0.9min, subtracted peak start and end
315.1
685.2
632.2
814.3
1030.3
152.3
452.1
1189.7
1345.2
200
400
600
800
1000
1200
1400
m/z

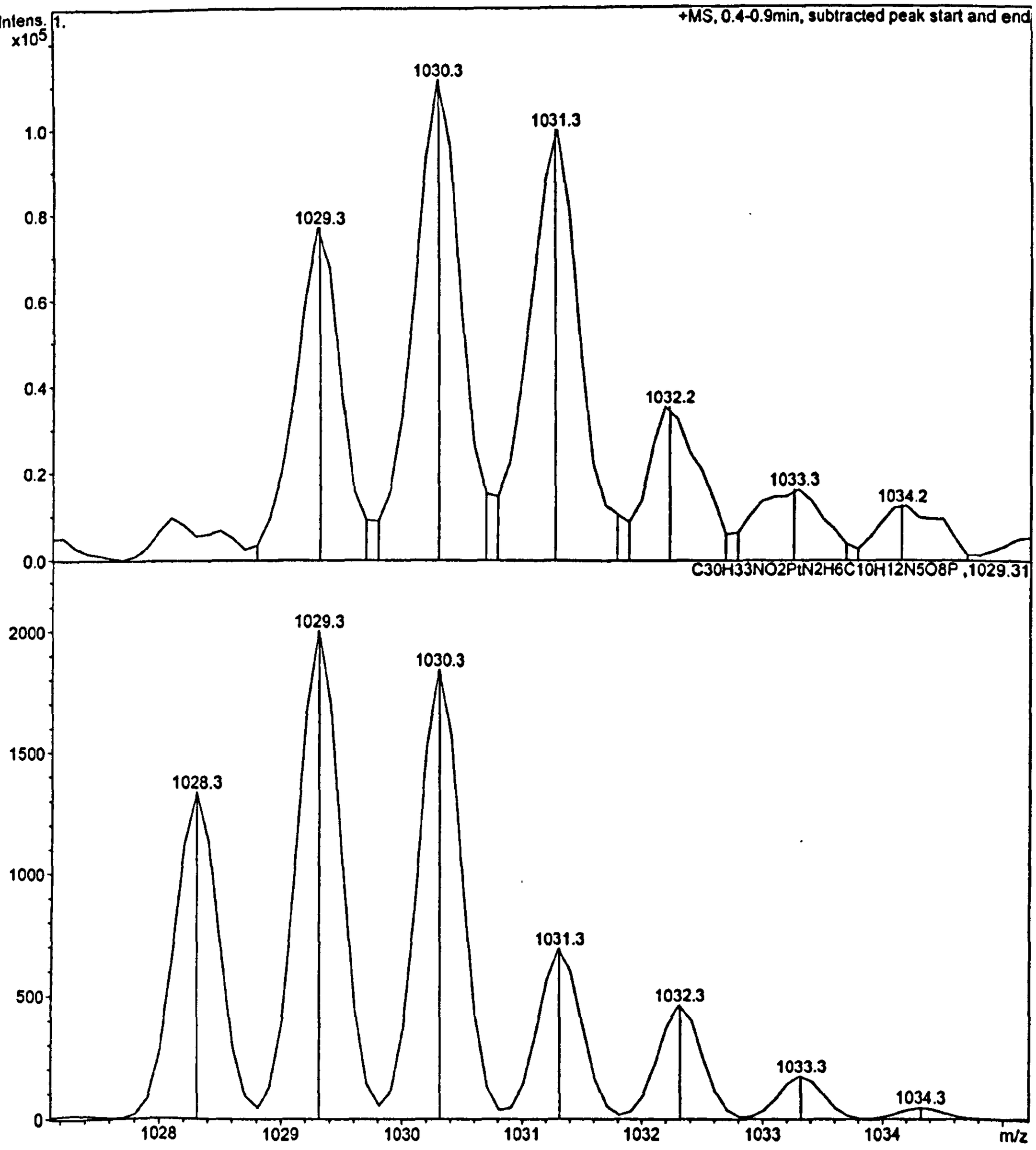

Figure A.8.6. ESI-MS (+ve) spectra of TC-ET-3-Q + 5'-GMP; upper, range from 500-1000 *m/z* = 500 – 1000; middle, range from *m/z* = 1000 – 1500; lower, expansion and calculated isotope distribution pattern for adduct, around *m/z* = 1030.

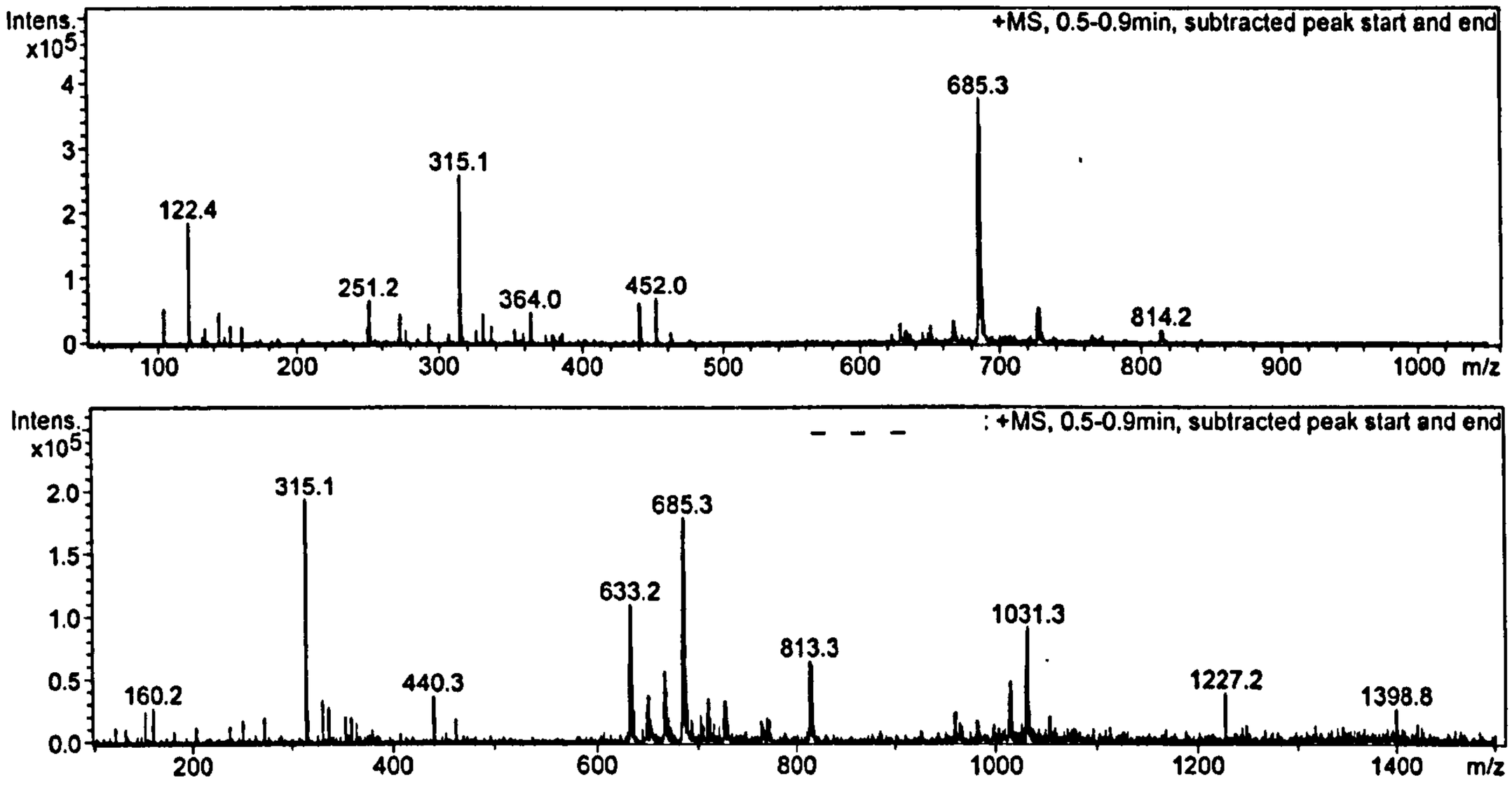

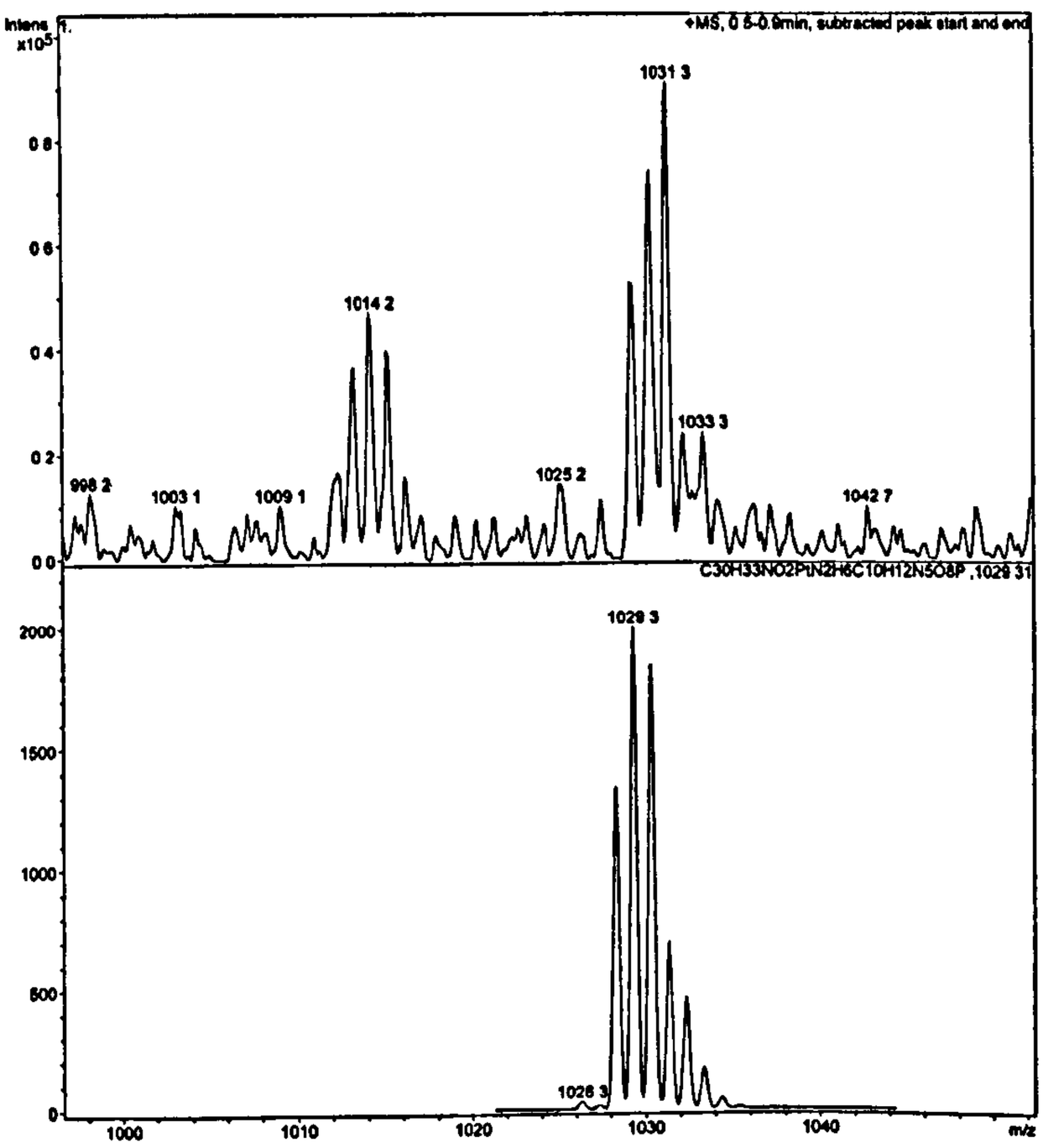

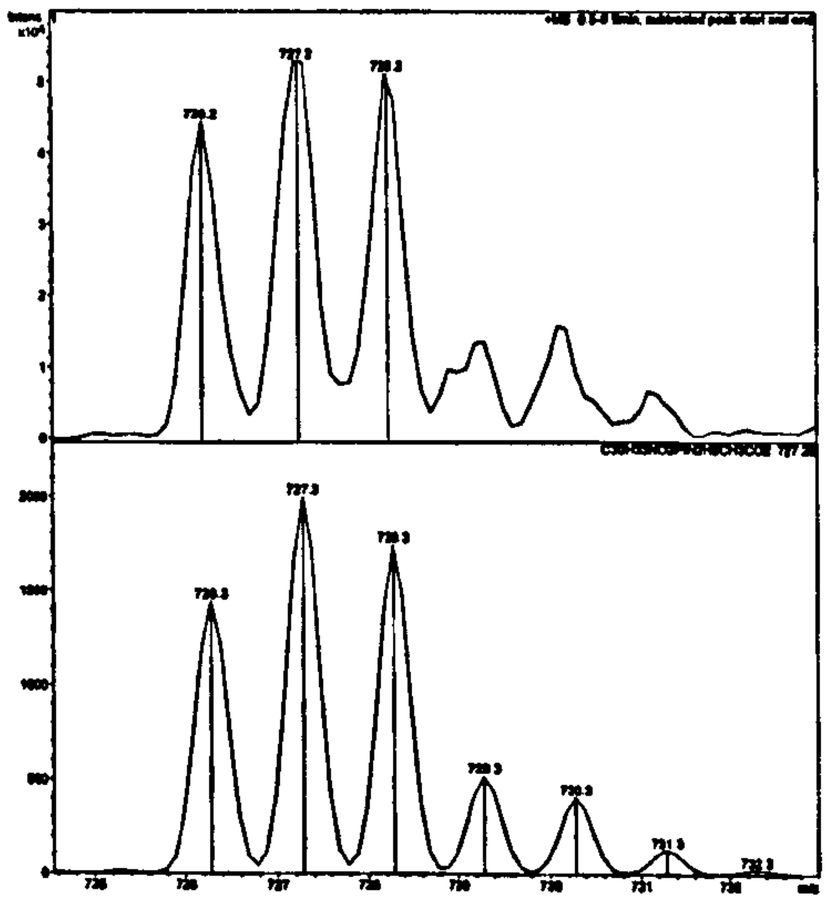

Figure A.8.7. ESI-MS (+ve) spectra of TC-ET-4-IQ + 5'-GMP; upper, range from *m/z* = 500 - 1000; middle, range from 1000-1500 *m/z* = 1000 – 1500; lower left, expansion and calculated isotope distribution pattern for adduct, around *m/z* = 1030; lower right, expansion and calculated distribution pattern for $[Pt(NH_3)_2(ET\text{-}4\text{-}IQ)(OAc)$.

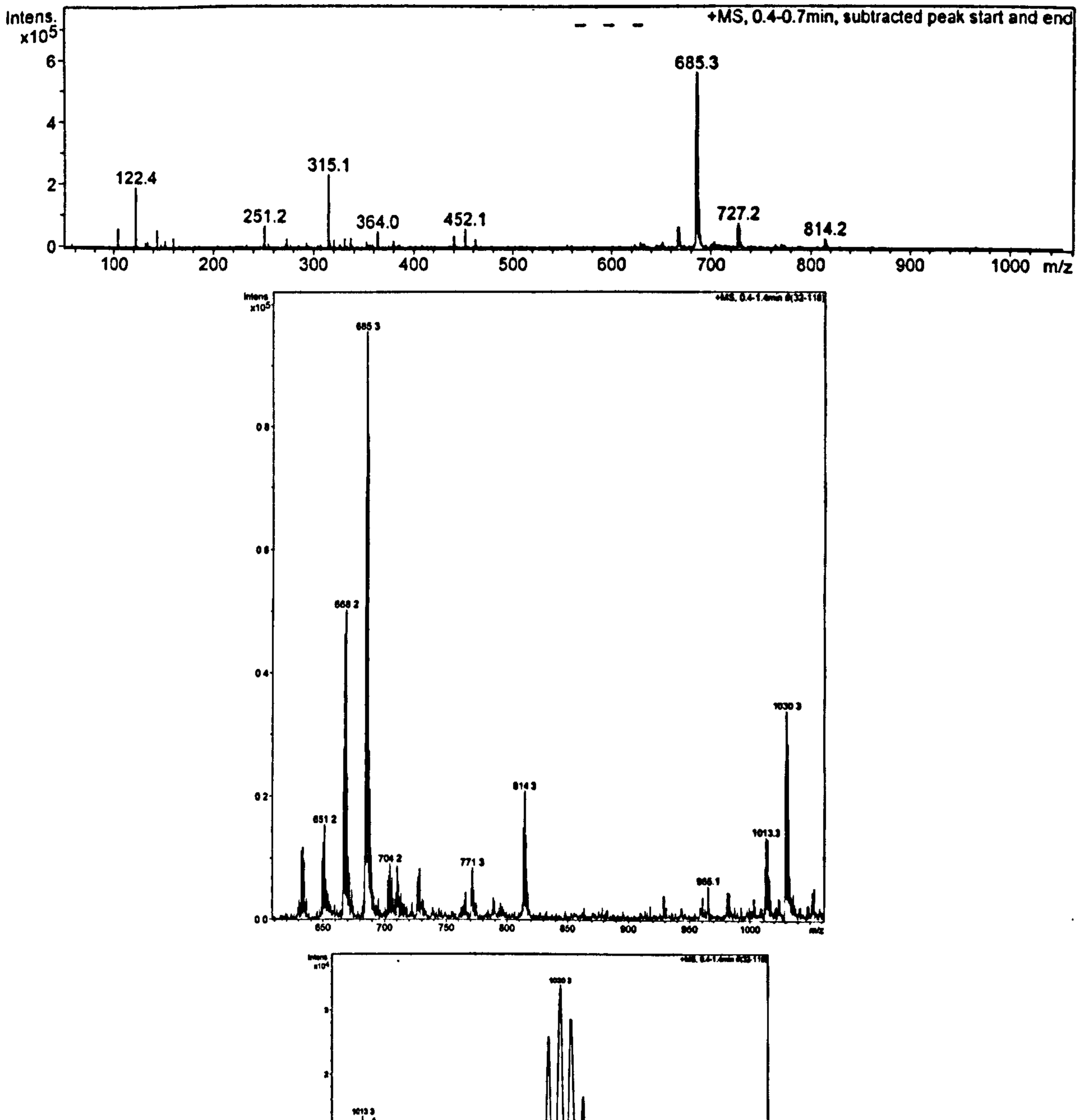

Figure A.8.8. ESI-MS (+ve) spectra of TC-ET-6-Q + 5'-GMP; upper, range from 500-1000 *m/z*; b) middl, range from 1000-1500 *m/z*; c) lower, expansion and calculated isotope distribution pattern for adduct around 1030 *m/z*.

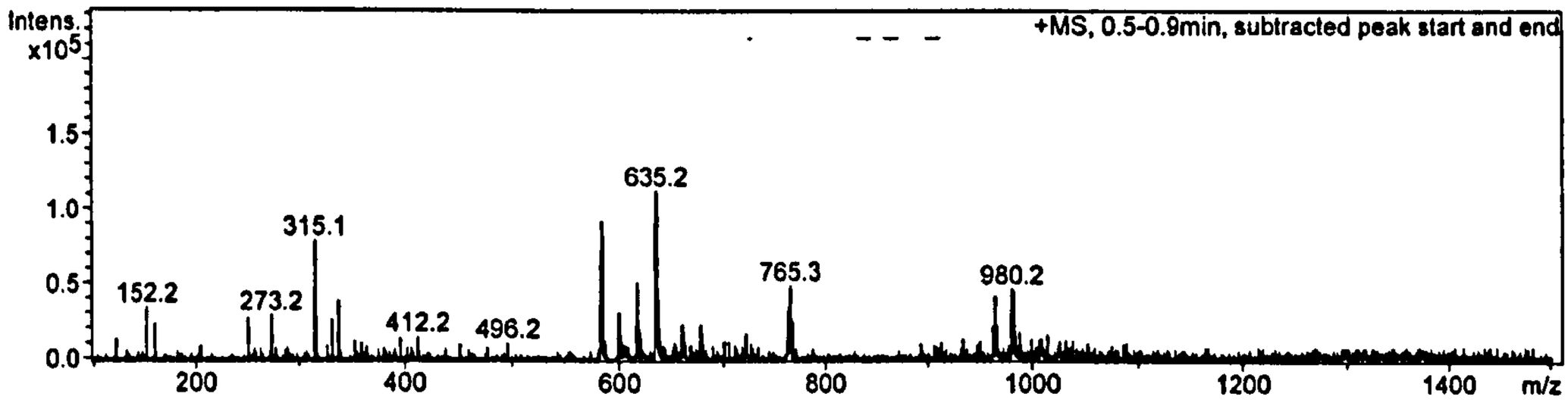

Figure A.8.9. ESI-MS (+ve) spectra of CC-ET-3-Py + 5'-GMP from *m/z* = 500 – 1000.

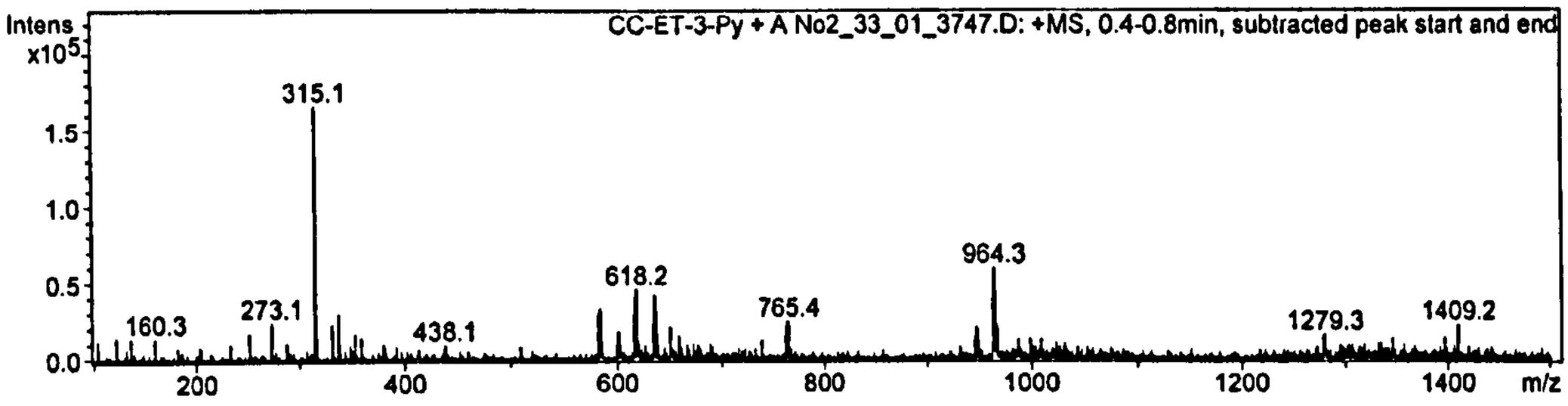

Figure A.8.10. ESI-MS (+ve) spectra of CC-ET-3-Py + 5'-AMP, range from *m/z* = 500 – 1000.

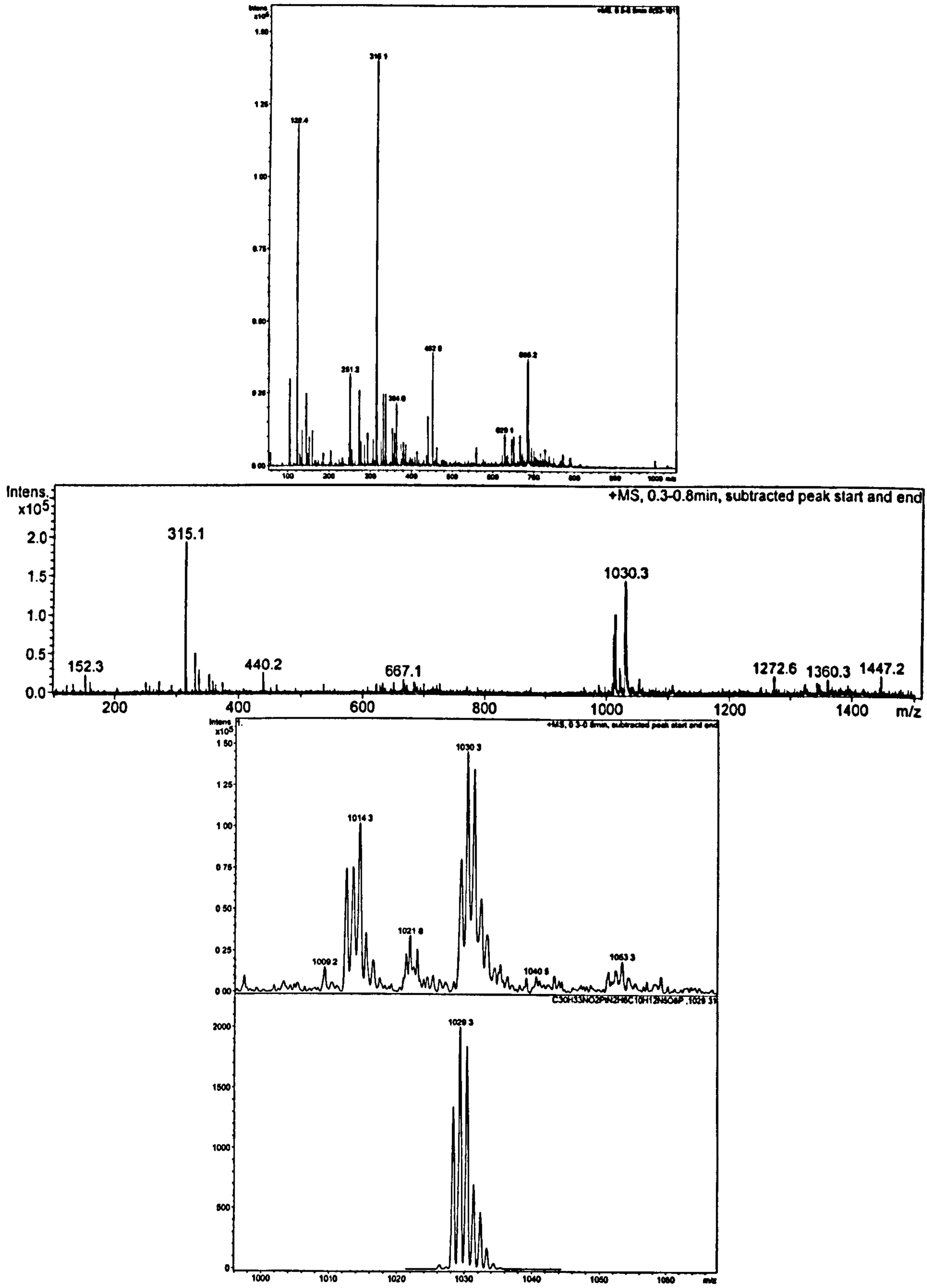

Figure A.8.11. ESI-MS (+ve) spectra of CC-ET-4-IQ + 5'-GMP; upper, range from *m/z* = 500 – 1000; middle, range from *m/z* = 1000 – 15000; lower, expansion and calculated isotope distribution pattern for adduct around *m/z* = 1030.

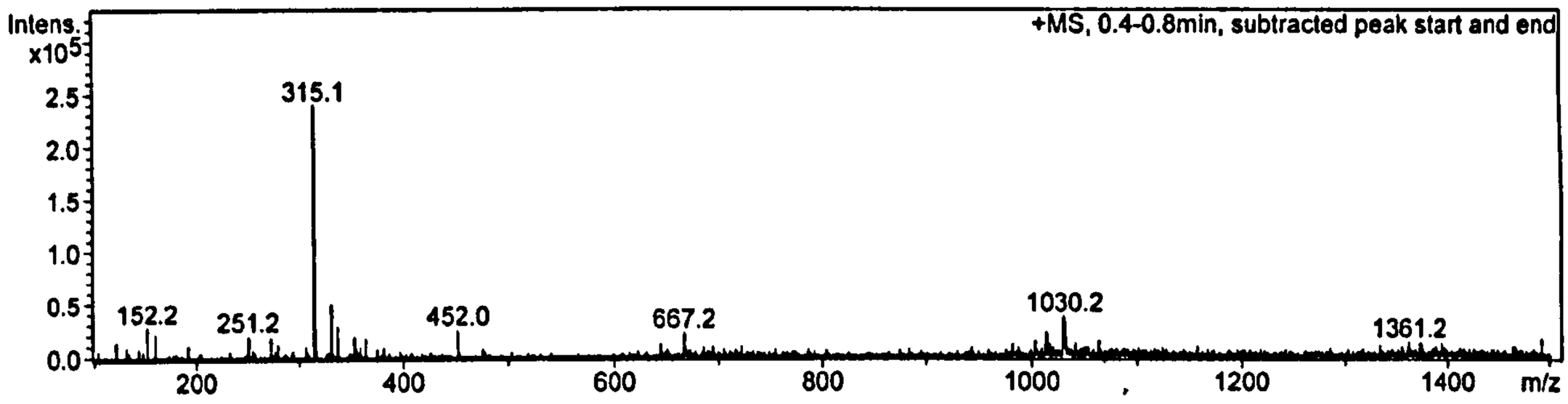

Figure A.8.12. ESI-MS (+ve) spectra of CC-ET-6-Q + 5'-GMP. Ranging from 1000-1500 *m/z*.

Appendix Nine – Absorbance spectroscopy, linear dichroism and gel electrophoresis

A.9.1. Electromagnetic radiation

Electromagnetic radiation, of which the visible light around us forms a small part, is an important technique for biophysical investiga; it consists of electric and magnetic components, oscillating ~ 90° to each other and, to the direction of propogation. Electromagnetic radiation may also be characterised in terms of polarisation: *e.g.* linear and circular. The electric field of circularly polarised light remains equal in magnitude but rotates around the axis of the propagation direction; the combination of rotation and propagation traces out a helix, which may be right handed or left handed depending on the direction of rotation of E, the electric field. Linearly polarised light has the electric field, E, oscillating in a single plane, at 90° to the direction of propogration.

A.9.1.1. Absorption spectroscopy

Spectroscopy is the investigation into the interactions between electromagnetic radiation and matter. The interaction of electromagnetic radiation with matter often results in the transfer of energy from the photons of incoming radiation to the molecules the matter is composed off; the molecules may scatter the photons, absorb the photons or emit photons, or combination of the three in varying proportions.

There exists a difference of several orders of magnitude between the highest and lowest electromagnetic energies; the effect of high energy radiation on matter is vastly different from that of low energy, for example molecules may be rotated by microwave radiation (wavelengths of $10^6 - 10^9$ nm); chemical bonds vibrated by far-infrared radiation ($2 \times 10^3 - 2 \times 10^4$ nm); electrons are promoted to higher energy levels when irradiated with UV / visible light (800 – 170 nm); using radiation – very high energy – in the forms of extreme UV (10 nm) breaks chemical bonds and, X-rays ($10^{-2} - 10^{-4}$ nm) completely remove electrons from atoms.

In the UV (λ = 170 – 400 nm) and visible (λ = 400 – 700 nm) regions of the electromagnetic spectrum the energy of the photons is similar to the difference between energy levels in the electron containing atomic and molecular orbitals; this can promote rearrangement of electron distribution within a molecule. This phenomenon results in an absorbance spectrum characteristic of the energy levels and transitions of the molecule being studied. The rearrangement of electron density during an electronic transition may

be described in terms of a net linear displacement of charge; displacement is described by a vector, the *transition moment*, μ, with a defined magnitude (length) and direction (polarisation). The direction of this displacement is the *polarisation of the transition* where $\mu^2 \propto A$, where A is the absorbance of the transition.

The intensity of the transition is related to absorbance by $A = \log_{10}\left(\frac{I}{I_0}\right)$, where A is the sample absorbance at a defined wavelength, I_0 is the intensity of light incident on the sample and I the intensity of light emerging from the sample. Absorbance may be directly related to the concentration of the sample by the Beer-Lambert law which states, $A = \varepsilon cl$, where c is the concentration of the molecule in question in unit of mol dm^{-3} and l is the length of sample the light travels though in units of centimetres; the molar absorption co-efficient, ε, is constant for a given substance at a given wavelength in defined conditions; the magnitude of ε is related to the probability of the transition (P) and the chromophore area (a), where $\varepsilon = 0.87\left(10^{20}\, Pa\right)$. Deviations from the linear relationship summarised by the Beer-Lambert law occur: too concentrated a solution may often lead too few photos emerging from the sample with resulting poor signal to noise ratio; too high a concentration may also lead to deviations due to intermolecular interactions and changes in refractive index are not accounted for in the law; scattering is prevented by ensuring no particles are present in the sample.

Experimentally an electronic transition is not a sharp peak but is broadened as the absorbed photons are of slight different energies. Such broadening is due to several factors including intermolecular interactions with the solvent, rotational and vibrational transitions and the uncertainty principle where the energy of the transition and the lifetime of the excited state cannot be known simultaneously.

A.9.1.2. Spectroscopic transitions

The movement of electrons during an electronic transition may originate from several types of orbital as shown in Figure A.9.1.

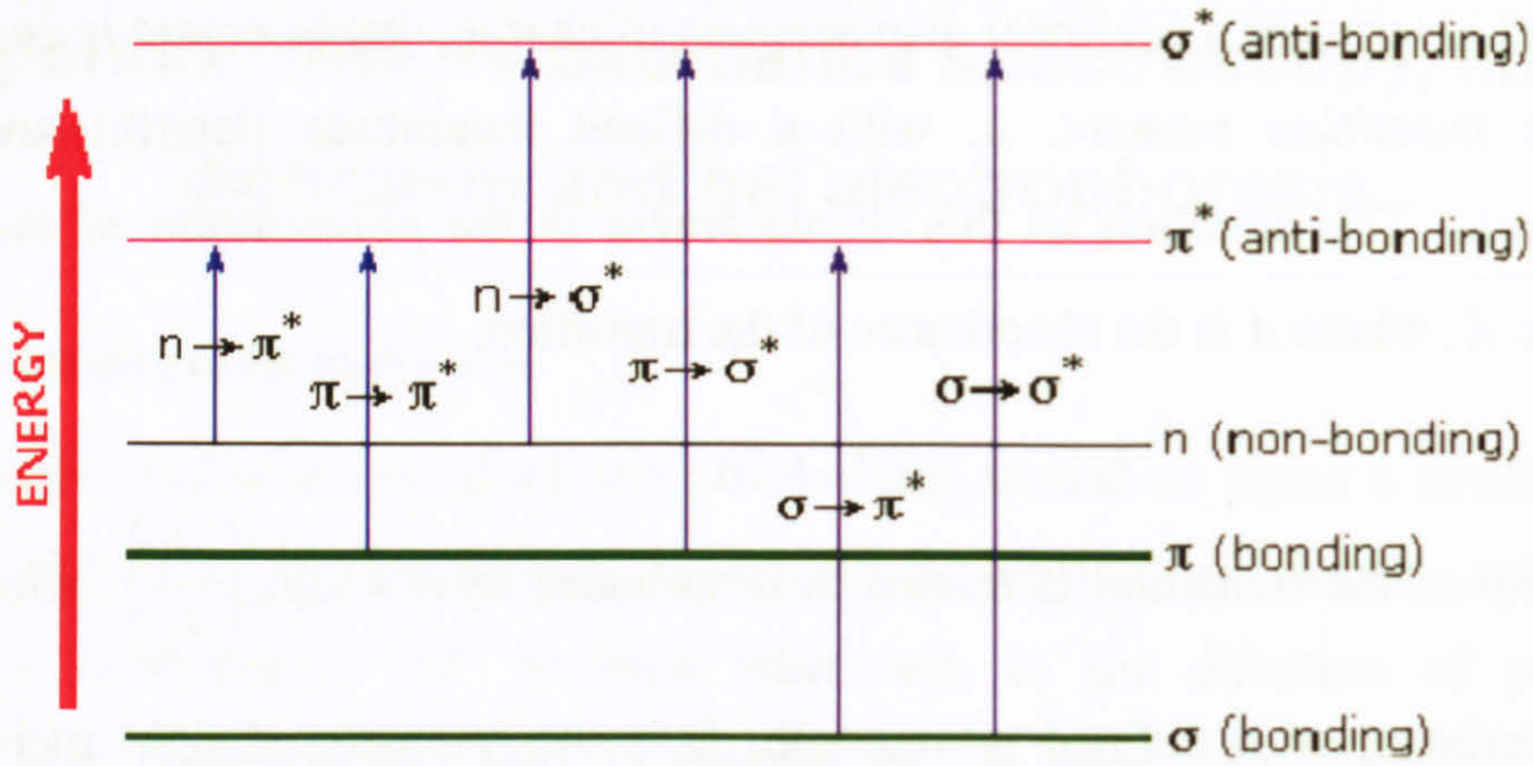

Figure A.9.1. Types of UV-vis. spectroscopic transitions seen in organic molecules.

Absorption originating from $\pi - \pi^*$ and $\sigma - \sigma^*$ transitions typically exhibits intense bands ($\varepsilon_{max} > 10^4$ mol $^{-1}$ dm ^{3} cm $^{-1}$) whilst weak bands ($\varepsilon_{max} < 10^2$ mol $^{-1}$ dm ^{3} cm $^{-1}$) may be assigned to $n - \pi^*$ and $n - \sigma^*$ transitions. Many bands from $\sigma - \sigma^*$ transitions are predominately found at wavelengths below 200 nm in the vacuum-UV whilst $\pi - \pi^*$ and $n - \pi^*$ transitions are found above 200 nm.

Metallo-organic entities have additional transitions as a consequence of the presence of metals and their bonding to the organic component. Transition metal metallo-organic complexes here exhibit $d \rightarrow d$ transitions due to partially filled d-orbitals; metal centred transitions from π to σ orbitals ($\pi_M - \sigma_M^*$ for example) and metal-to-ligand (MLCT) and / or ligand-to-metal (LMCT) charge transfer transitions, for example from the π orbitals of the metal to those of the ligand; the movement of charge between ligands and / or between the ligand and metal centre lead to charge transfer (CT) transitions.

A.9.1.3. DNA transitions

DNA solutions are colourless, exhibit absorbance below 300 nm ($\lambda_{max} \sim 260$ nm) arising from the nucleobases; specifically the $\pi - \pi^*$ electronic transitions of the purine and pyrimidine bases give rise to a characteristic absorbance centred on 260 nm. The concentration of duplex DNA solutions may be calculated using the Beer-Lambert law as ε is known for several duplex DNA's; for example, duplex calf thymus DNA $\varepsilon_{258nm} = 6600$ mol $^{-1}$ dm ^{3} cm $^{-1}$.

A.9.2. Linear dichroism spectroscopy

Linear dichrosim (*LD*) is the difference in absorption between light, linearly polarised parallel and perpendicular to a defined orientation axis at a giben wavelength; it may be used to investigate DNA-molecule interactions as the DNA helix may be aligned in

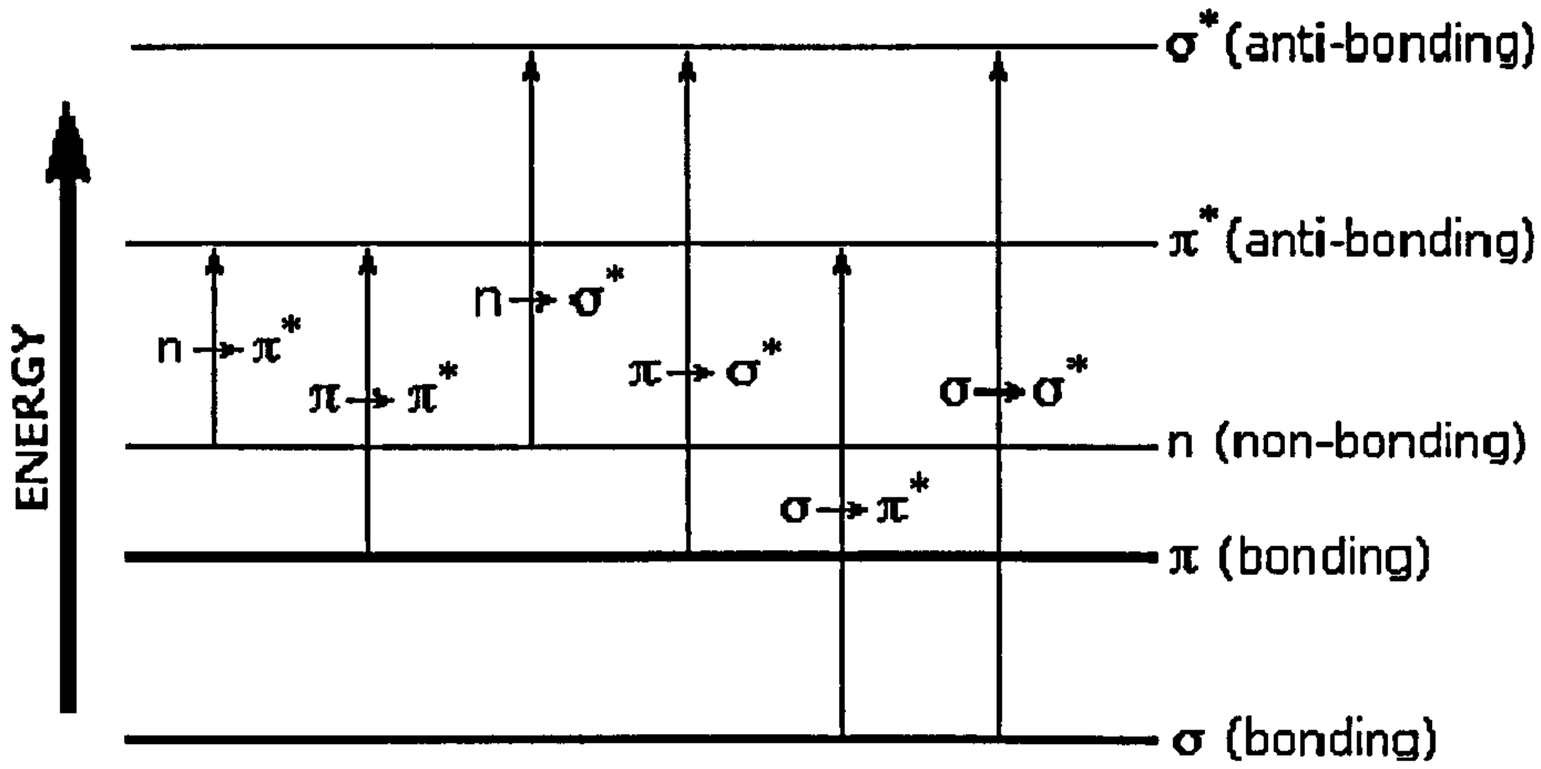

Figure A.9.1. Types of UV-vis. spectroscopic transitions seen in organic molecules.

Absorption originating from $\pi - \pi^*$ and $\sigma - \sigma^*$ transitions typically exhibits intense bands ($\varepsilon_{max} > 10^4$ mol $^{-1}$ dm ^{3} cm $^{-1}$) whilst weak bands ($\varepsilon_{max} < 10^2$ mol $^{-1}$ dm ^{3} cm $^{-1}$) may be assigned to $n - \pi^*$ and $n - \sigma^*$ transitions. Many bands from $\sigma - \sigma^*$ transitions are predominately found at wavelengths below 200 nm in the vacuum-UV whilst $\pi - \pi^*$ and $n - \pi^*$ transitions are found above 200 nm.

Metallo-organic entities have additional transitions as a consequence of the presence of metals and their bonding to the organic component. Transition metal metallo-organic complexes here exhibit $d \rightarrow d$ transitions due to partially filled d-orbitals; metal centred transitions from π to σ orbitals ($\pi_M - \sigma_M^*$ for example) and metal-to-ligand (MLCT) and / or ligand-to-metal (LMCT) charge transfer transitions, for example from the π orbitals of the metal to those of the ligand; the movement of charge between ligands and / or between the ligand and metal centre lead to charge transfer (CT) transitions.

A.9.1.3. DNA transitions

DNA solutions are colourless, exhibit absorbance below 300 nm ($\lambda_{max} \sim 260$ nm) arising from the nucleobases; specifically the $\pi - \pi^*$ electronic transitions of the purine and pyrimidine bases give rise to a characteristic absorbance centred on 260 nm. The concentration of duplex DNA solutions may be calculated using the Beer-Lambert law as ε is known for several duplex DNA's; for example, duplex calf thymus DNA $\varepsilon_{258nm} = 6600$ mol $^{-1}$ dm ^{3} cm $^{-1}$.

A.9.2. Linear dichroism spectroscopy

Linear dichrosim (*LD*) is the difference in absorption between light, linearly polarised parallel and perpendicular to a defined orientation axis at a giben wavelength; it may be used to investigate DNA-molecule interactions as the DNA helix may be aligned in

specific orientation using a variety of techniques. Mathematically, *LD* is defined as $LD = A_{//} - A_{\perp}$, where $A_{//}$ is absorption of linearly polarised light parallel to the orientation axis and $A_{\perp}$ is absorption of linearly polarized light perpendicular to the same orientation axis. A consequence of the directional component of the electronic transition of the orientated chromphore is differential absorption of parallel and perpendicular linearly polarised light of oriented samples resulting in an *LD* spectrum. For a transition whose *transition moment* is aligned at exactly 90 degrees to the orientation axis (assuming uniaxial orientation), *LD* at λ_{max} is $\frac{-A_{\perp}}{2}$ i.e. $LD < 0$, a negative signal; the *LD* is exactly zero if the transition moment is at the magic angle, 54.7°, to the orientation axis; whilst it is positive for transitions whose transition moment lies at angles >54.7° to the orientation axis. In the case of DNA, transition moments of the $\pi - \pi^*$ transition of the nucleobases are at the angle of ~90° to the orientation axis of DNA, so that *LD* spectroscopy is able to probe the roll and tilt of the bases relative to the orientation axis.

Furthermore, quantitative information may be gained from the reduced linear dichroism (LD^r): $LD^r = \frac{LD}{A} = \frac{A_{//} - A_{\perp}}{A} = \frac{3}{2}S\left(3\cos^2\alpha - 1\right)$, where A is the average absorption over all possible orientations, i.e. the isotropic absorption; S defines the efficiency of macroscopic orientation, *i.e.* S = 1 for perfect orientation; the angle between the orientation axis and *transition moment* or the transition in question is α. The magnitude of the LD^r is constant across the absorption band of a single transition; therefore, LD^r can identify different electronic transitions that are perhaps not so apparent using absorption spectroscopy. A change in LD^r suggests another electronic transition. In an ideal situation, sections of constant LD^r will be clearly seen; however, for transitions whose absorption envelope overlap, sections of constant LD^r are more difficult to identify; in this situation a change of LD^r is may be interpreted as entering another absorption envelope.

Orientation of chromophores is achieved in many ways: long polymers, such as ct-DNA (>1000 base pairs), are orientated using shear flow; smaller chromophores require different techniques that possess a greater ability to orientate, such as stretching a film loaded with analyte.

A.9.2.1. Stretched polymer film linear dichroism spectroscopy

Polymers, such as polyvinyl alcohol (PVA) or polyethylene (PE) may absorb small molecules onto their surface and into their matrix. The small molecules then align when

the film is stretched; the alignment is along the long axis of the molecule in the direction of the stretch (Figure A.9.2). Small molecules may either be cast within the film (such as with polyvinyl alcohol) or the solution added to the film and the solvent allowed to evaporate (such as polyethylene) before or after the film is stretched to align the molecules.

The orientation power of film *LD* is superior compared to other techniques for small molecules but no method, except perhaps crystallisation, produces a perfectly orientated sample and orientation of samples must be considered to be a distribution around the orientation direction; the distribution results as individual molecules are not all exactly alined with the orientation axis.

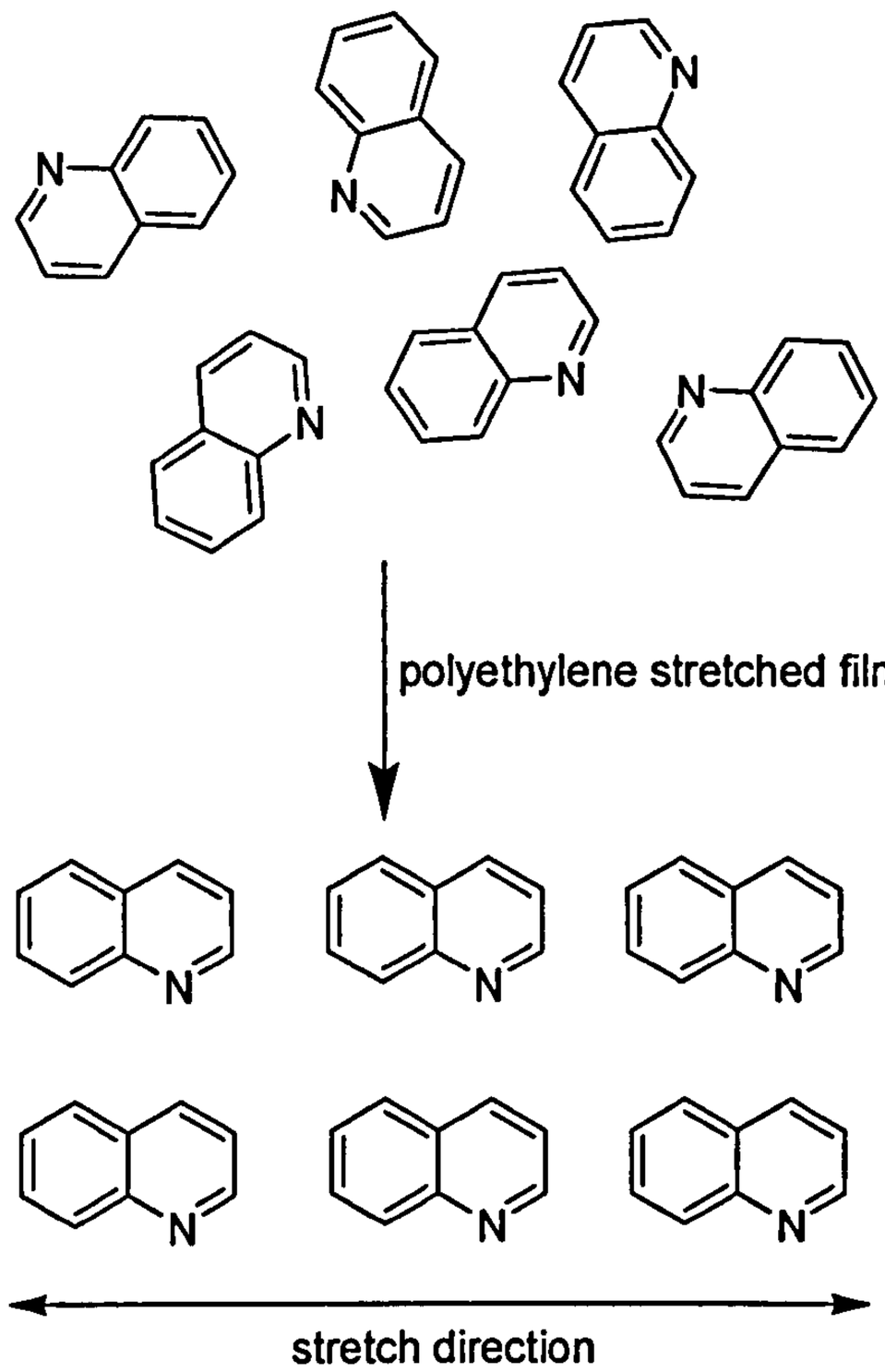

Figure A.9.2. Pictorial representation of the orientation of quinoline using a polyethylene film.

A mathematical description of the degree of orientation of a molecule in a matrix used the three vectors S_{zz}, S_{yy} and S_{xx}. The orientation factor, *S*, defines the efficiency of macroscopic orientation, which may be split into three vectors relating to the efficiency of macroscopic orientation along the *x*, *y*, and *z* axes. They are a measure of the degree to which molecules aligns within a matrix (often polyethylene in film *LD*). The orientation triangle (Figure A.9.3.) defines the possible combinations of the orientation parameters S_{yy}

and S_{zz} and illustrates several different molecules and the degree to which they align; long thin molecules tend to align better and magnitude of S_{yy} and S_{zz} tend to be high.

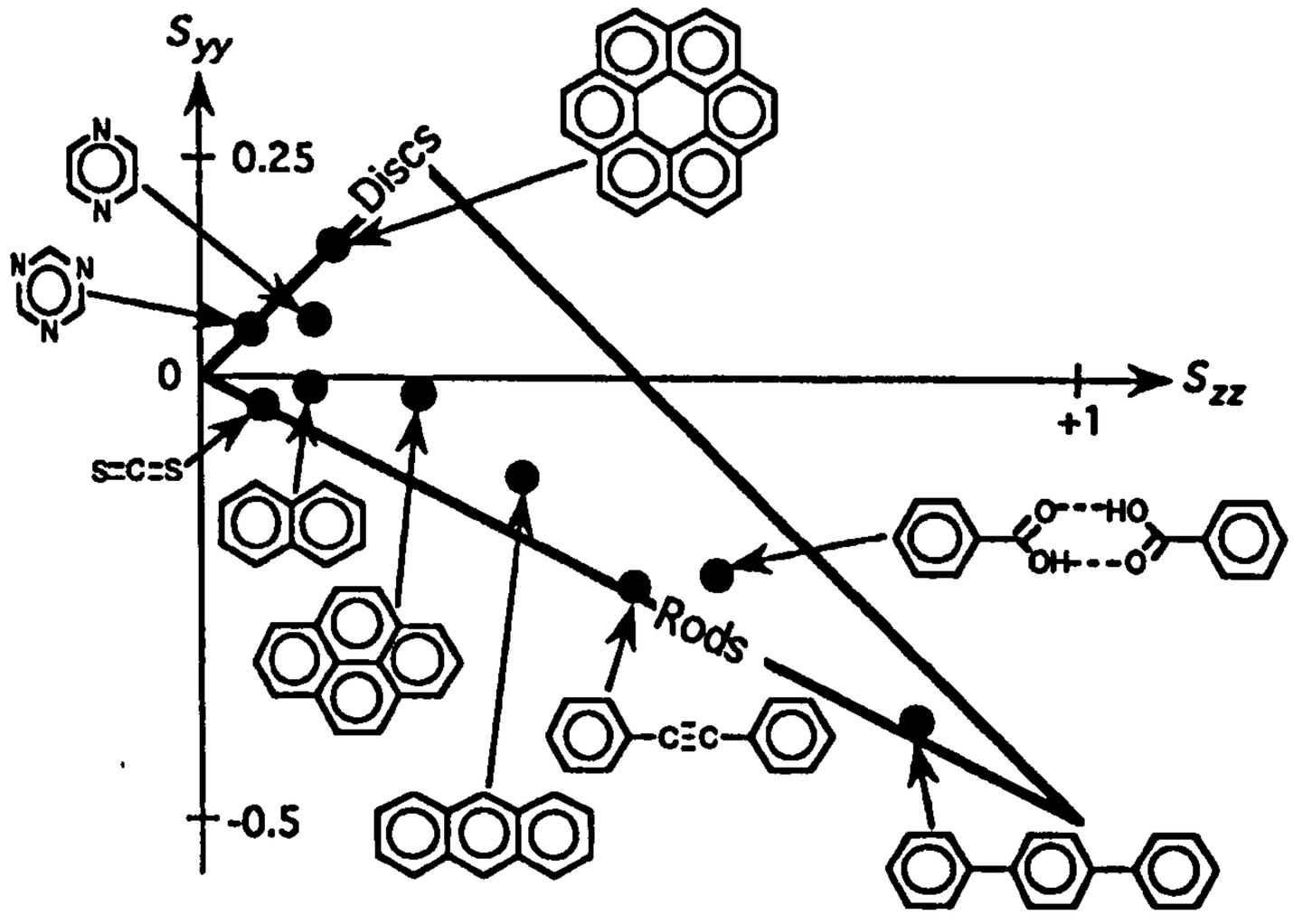

Figure A.9.3. The orientation triangle. The orientation parameters (S_{zz} and S_{yy}) for molecules orientated in stretched PE.[581] The *z*-axes are horizontal.

LD spectra obtained using the stretched film method can yield valuable information; polarised absorbance and transition moments may be derived for example. LD^r may be further defined was as $LD^r(\lambda) = \frac{LD(\lambda)}{A(\lambda)} = 3\left(\frac{S_{zz}\varepsilon_z(\lambda) + S_{yy}\varepsilon_y(\lambda) + S_{xx}\varepsilon_x(\lambda)}{\varepsilon_z(\lambda) + \varepsilon_y(\lambda) + \varepsilon_x(\lambda)}\right)$, where A is the absorbance of an un-orientated sample and $\varepsilon_z(\lambda)$ *etc.* are the extinction coefficients. The subscripts *x*, *y* and *z* indicate the axis to which incident light is parallel too; *S* is the degree to which the molecule is orientated in the direction indicated by its subscript.

For disk shaped molecules used in this thesis, *i.e.* quinoline and isoquinoline, for transitions whose direction lies solely in the *x*, *y* or *z* axis, the reduced linear dichroism is given by: $LD^r(z) = 3S_{zz}$; $LD^r(y) = 3S_{yy}$; $LD^r(x) = 3S_{xx}$. In quinoline *x*, *y*, and *z* are defined by symmetry – the *z* axis follows the long axis of the molecule. Identification of pure *z*-polarised and pure *y*-polarised transitions may be achieved by observing the large positive LD^r (for *z*-polarised transitions) and lower or negative LD^r (for *y*-polarised transitions); from this the orientation parameters, S_{zz} and S_{yy}, are calculated. Once calculated, S_{zz} and S_{yy} are used to determine $A_z(\lambda)$ and $A_y(\lambda)$; these represent the absorbance of the sample if the incident radiation is polarized along, respectively, the *z* and

y axes. Symmetry rules predict planar aromatic molecules *must* have in plane $\pi \rightarrow \pi^*$ transitions: using our coordinate system $\varepsilon_x(\lambda) = 0$ and we may write $LD = S_{zz}A_z(\lambda) + S_{yy}A_y(\lambda)$, which once solved for A_z and A_y, determines the absorbance of z- and y-polarised light, respectively. Towards the goal of establishing the transition moments for each absorbance band in planar aromatic molecules, absorbance of x-polarised light is ignored as the transition are all in plane, hence

$$LD^r(\lambda) = 3\left(\frac{S_{zz}\varepsilon_z(\lambda) + S_{yy}\varepsilon_y(\lambda) + S_{xx}\varepsilon_x(\lambda)}{\varepsilon_z(\lambda) + \varepsilon_y(\lambda) + \varepsilon_x(\lambda)}\right)$$

$$\text{reduces to } LD^r(\lambda) = 3\left(\frac{S_{zz}\varepsilon_z(\lambda) + S_{yy}\varepsilon_y(\lambda)}{\varepsilon_z(\lambda) + \varepsilon_y(\lambda)}\right) = 3\left(\frac{S_{zz}\dfrac{\varepsilon_z}{\varepsilon_y} + S_{yy}}{\dfrac{\varepsilon_z}{\varepsilon_y} + 1}\right)$$

which, after further rearrangement: $\dfrac{\varepsilon_z}{\varepsilon_y} = \dfrac{LD^r(\lambda) - 3S_{yy}}{LD^r(\lambda) - 3S_{zz}} = \dfrac{\cos^2\alpha}{\sin^2\alpha} = \cot^2\alpha$ where $\alpha =$ angle that defines the transition moment that causes absorption at a given wavelength relative to the orientation axis.[581]

A.9.2.2. Flow LD

Orientation of long polymers such as DNA requires a lesser orientation force compared to small molecules. In flow *LD*, long molecules are orientated by placing a solution between two cylindrical surfaces rotating relative to each other which orientates DNA biaxially, although the helical nature of DNA means that orientation is considered to be uniaxial.

A Couette flow cell (Figure A.9.4) is capable of sufficient orientation of DNA (>1000 bases pairs). In this work, the flow cell used consists of a fixed outer cylinder with a rotating inner cylinder with a small annular gap between the two surfaces causing a viscous drag and alignment of DNA; greater orientation of the DNA strands is achieved by increasing the speed of the cylinders relative to each-other, but not so high to avoid turbulent flow, that gives rise to air bubbles and artefacts in the *LD* spectrum.

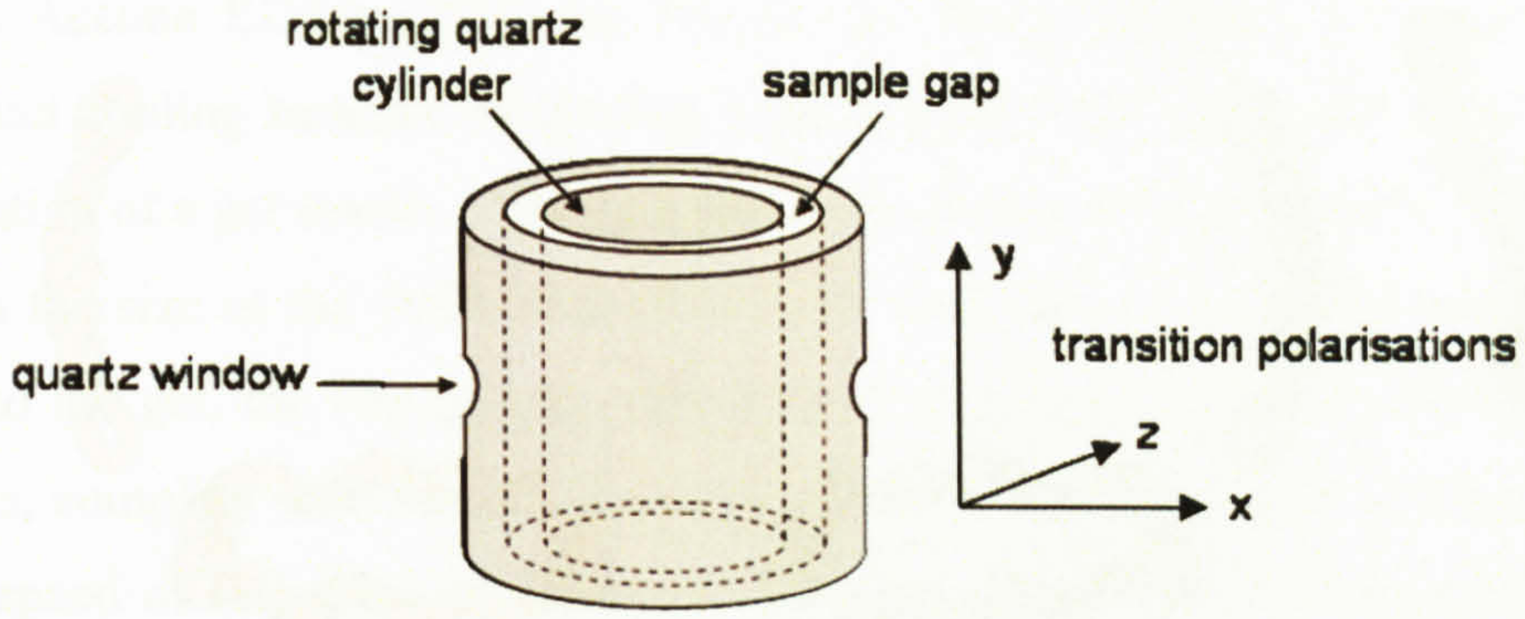

Figure A.9.4. The design of a couette flow cell

Reduction of volumes, important when using biological samples, has lead to the design of micro-volume couette cell and based on the same principle as the larger design. A quartz cylindrical cell (~ 5 mm OD, ~ 3 mm ID) rotates and an inserted stationary rod (~ 2.5 mm OD) causing a 0.25 mm annular gap between the cell and rod resulting in orientation of DNA.[582] Most of the data reported in this work is collected with a micro-volume Couette cell.

A.9.2.3. Linear dichroism of DNA – molecule conjugates

LD is a powerful tool in determining the binding orientation of a molecule to DNA with the provision that the molecule is spectroscopically active, whose transitions are assigned and, preferably do not overlap with the $\pi - \pi^*$ transitions of the nuclear bases. An *LD* signal from a transition assigned to the binding molecule signifies that the molecule is bound to DNA in a specific orientation; coupled with further knowledge regarding the transition moment and the orientation of the molecule may be determined and, although the exact location of binding cannot be assigned, it provides clues to possible sites of binding.

A.9.3. Supercoiled DNA and gel electrophoresis

It is possible for DNA duplexes to exist in other conformations: one of the most important is *supercoiled*, where the duplex twists around itself and, depending on the direction of twisting, DNA may form right-handed (negatively supercoiled) or left-handed (positively supercoiled) topologies; examples of supercoiled DNA are shown in Figure A.9.5.

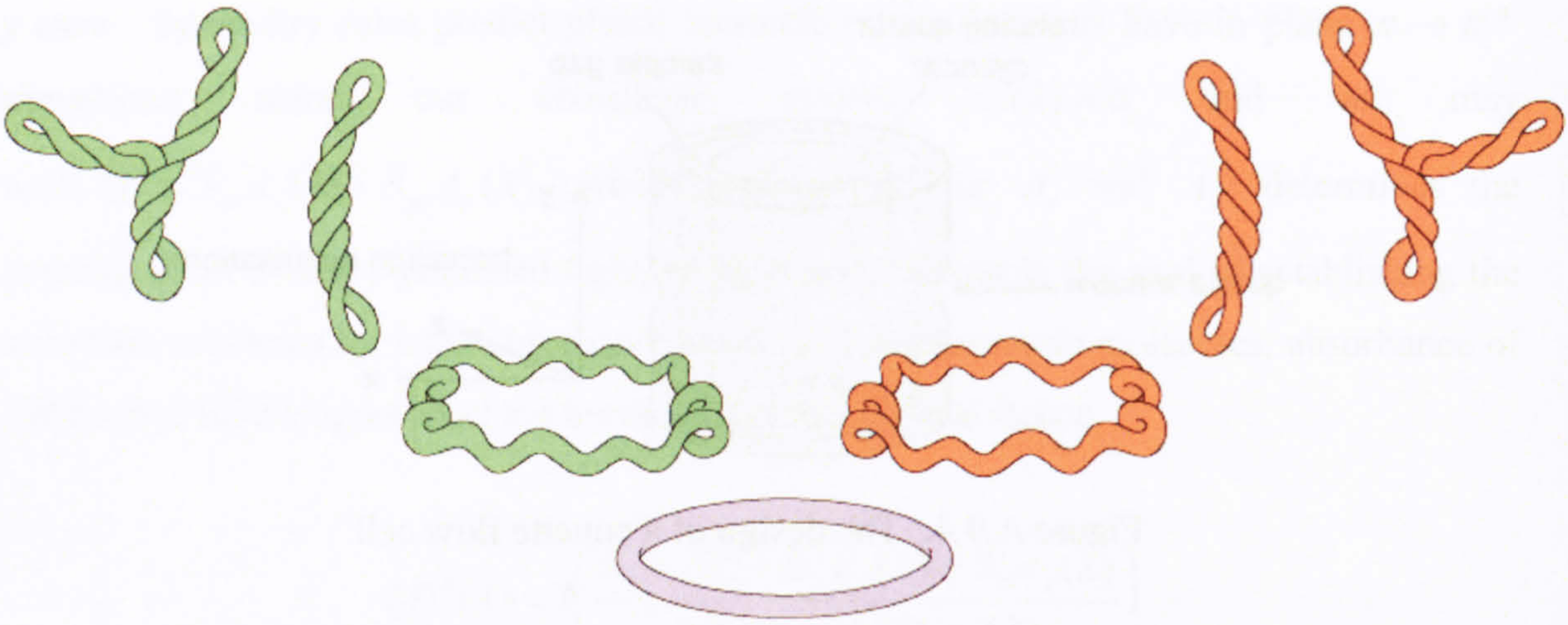

Figure A.9.5. Examples of relaxed (centre) and increasingly supercoiled DNA: increasingly negative supercoiling (far left) and increasingly positive supercoiling (far right).

Negative supercoiling causes a torsional stress to the DNA favouring unwinding of the duplex, whereas positive supercoiling favours winding up of the duplex. Conformational changes to the duplex affects the degree of supercoiling and *visa versa*, which can result from interactions with bound molecules. Many differenct methods of analysis are employed to investigate this interaction; one of the most common uses gel electrophoresis – the movement of charged particles through a porous medium such as a gel – that separates on the basis of size. The DNA's shown in Figure A.9.5 are all different sizes, supercoiled DNA is smaller than relaxed for example and will travel through gels at different speeds. If for some reason the supercoiling is reduced the bands in the gels eventually slows to that of the relaxed form; this fact can be used to characterized the degree to which a platinum(II) complex may unwind the helix. Using the mathematical properties of supercoiling, electrophoresis can quantify unwinding according to the equation: $\phi = \frac{18\sigma}{r_{b(c)}}$, where ϕ = the unwinding angle, σ = superhelicity constant and $r_{b(c)}$ the ratio where supercoiled and relaxed DNA co-migrate.[583] The superhelicity contant is a quantitative measure of supercoiled – it is the average number of superhelical turns per 10 base pairs.

Electrophoresis is derived from the Latin *electrum* and Greek ηλεκτ ρου (meaning amber, the rubbing of). The medium for electrophoretic separation of DNA is agarose, a linear galactan hydrocolloid from agar, and is the standard medium of size-based separation of DNA fragments using electrophoresis. Gels are cast by melting agarose in the present of

buffer – Tris Acetate EDTA (TAE) or Tris Borate EDTA (TBE) – by pouring into a casting tray and cooling beneath the gelling point (approx 32°C) thus allowing hardening and the formation of a gel matrix. The agarose concentration varies from 0.3 % - 2 % w/v, depending on the size of the DNA fragments to be separated. Once DNA is loaded into wells cast into the gel, the casting tray and gel are submerged in buffer solution and the DNA samples, complete with the tracking dyes xylene cyanol and bromophenol blue, are added. The speed of migration of bromophenol blue and the DNA plasmid pBR322 are similar for example, allowing the location of DNA to be pin-pointed. Since the DNA cannot be directly visualised, the gel is finally soaked in a solution of ethidium bromide which contains a planar aromatic group that intercalates between DNA base pairs in the helix; once bound the fluorescence of ethidium bromide increases and irradiation of the gel at 254 nm is absorbed and light is emitted at 590 nm.

Appendix Ten – UV / visible spectroscopy of ligands and complexes

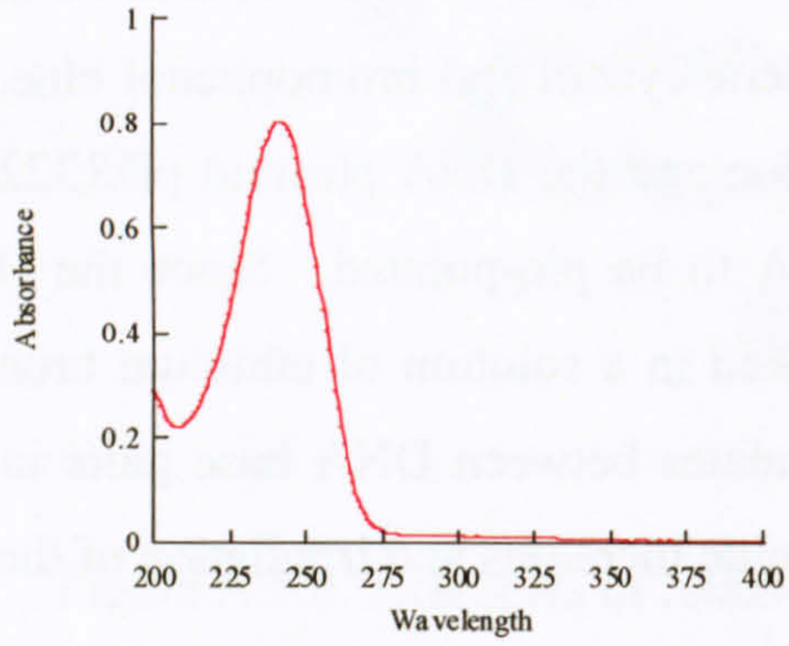

Ethisterone

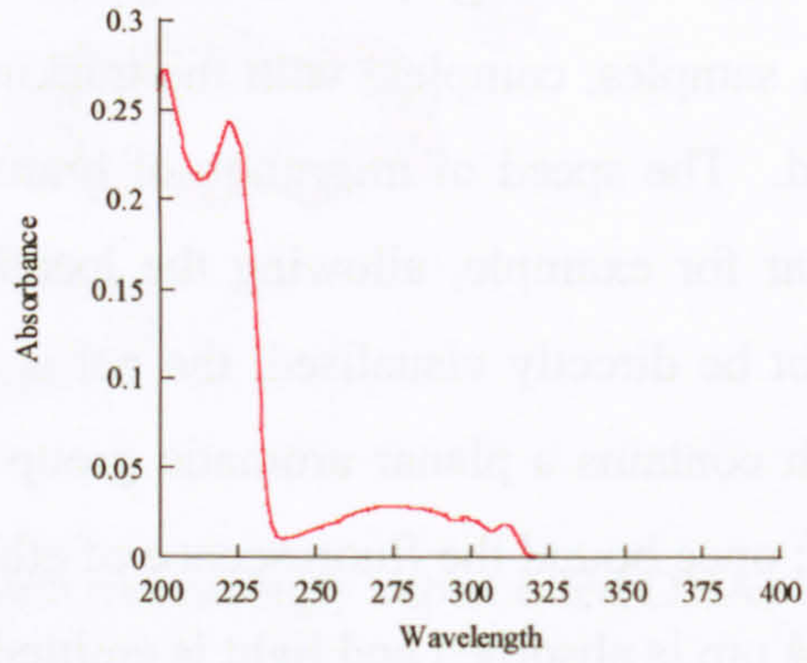

Quinoline

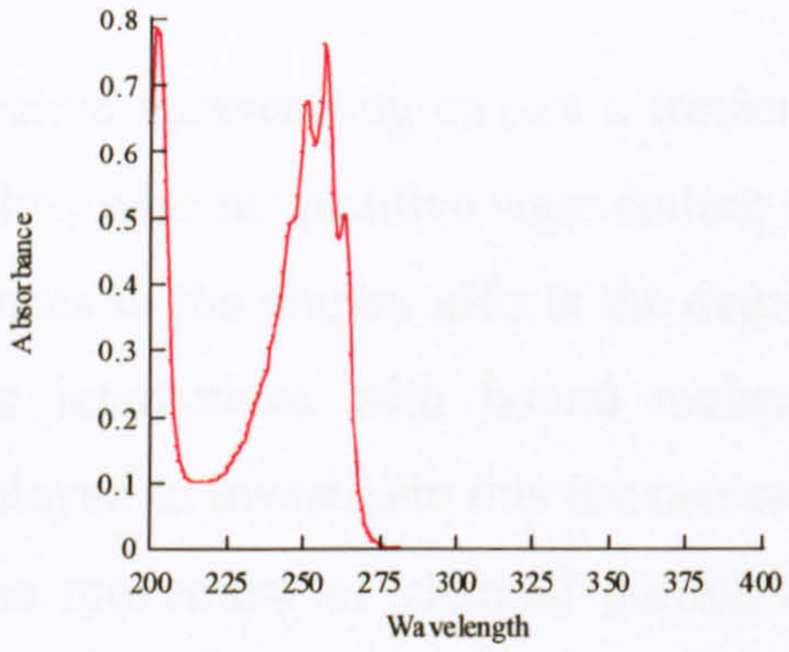

Pyridine

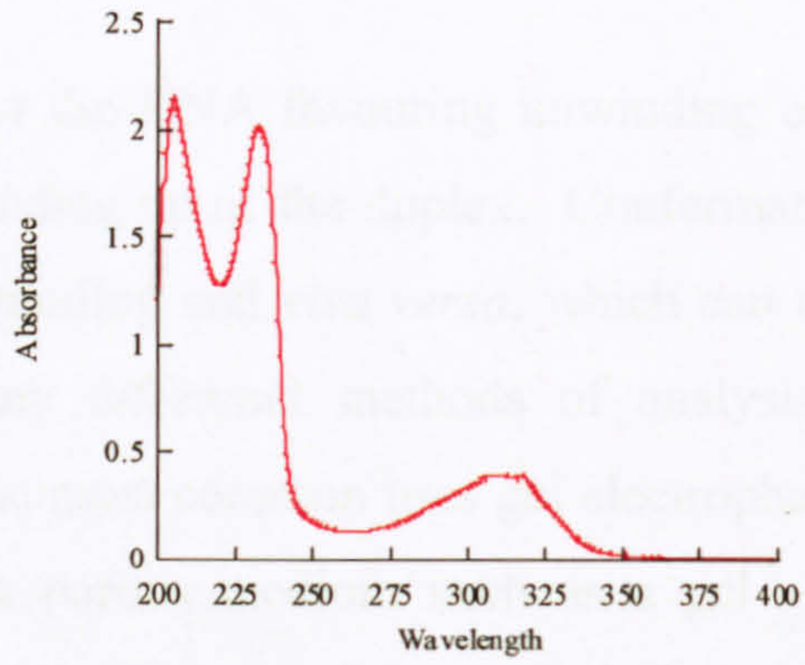

TC-Q

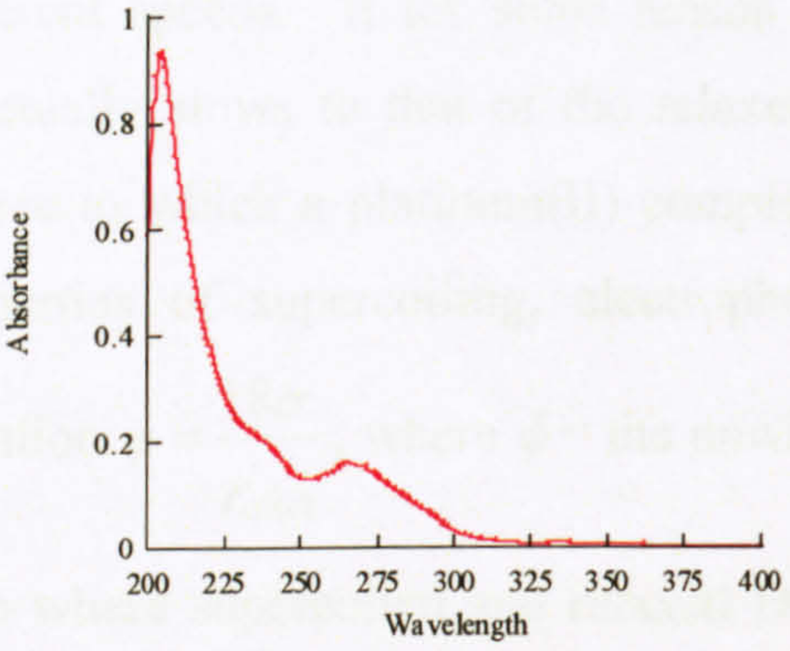

TC-Py

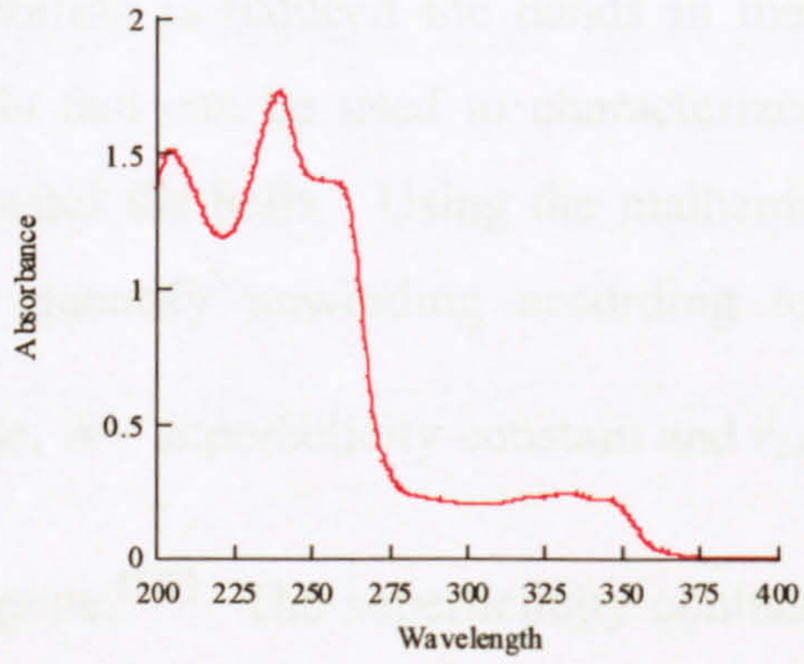

TC-ET-3-Q

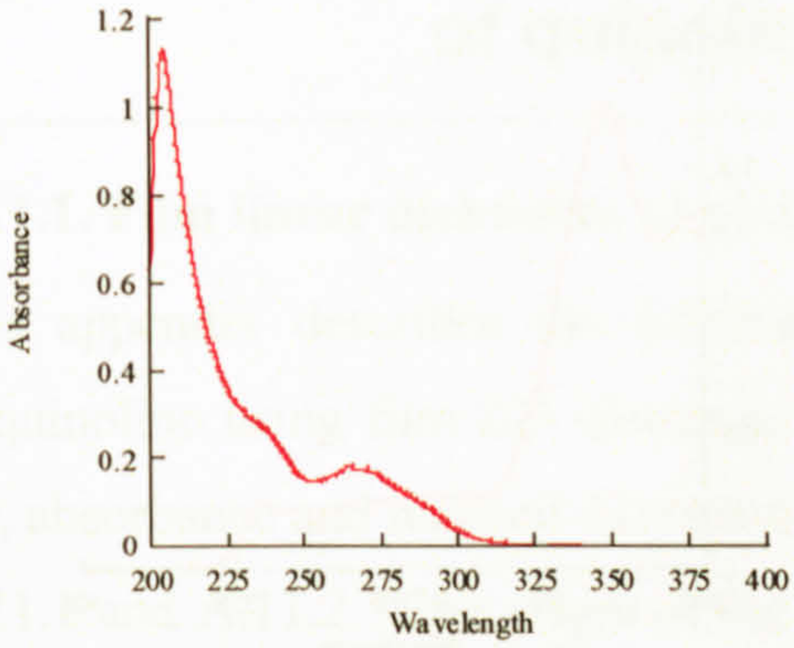

CC-Py

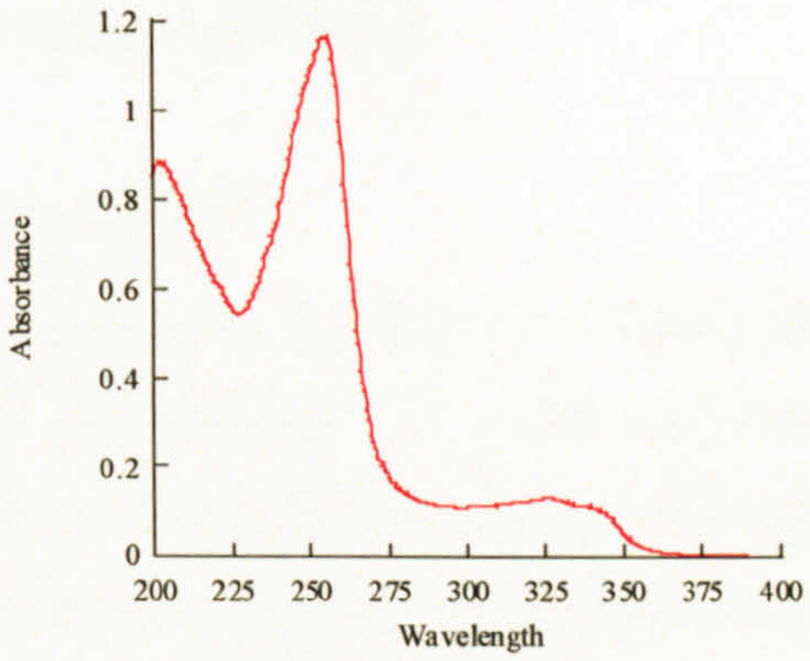

TC-ET-6-Q

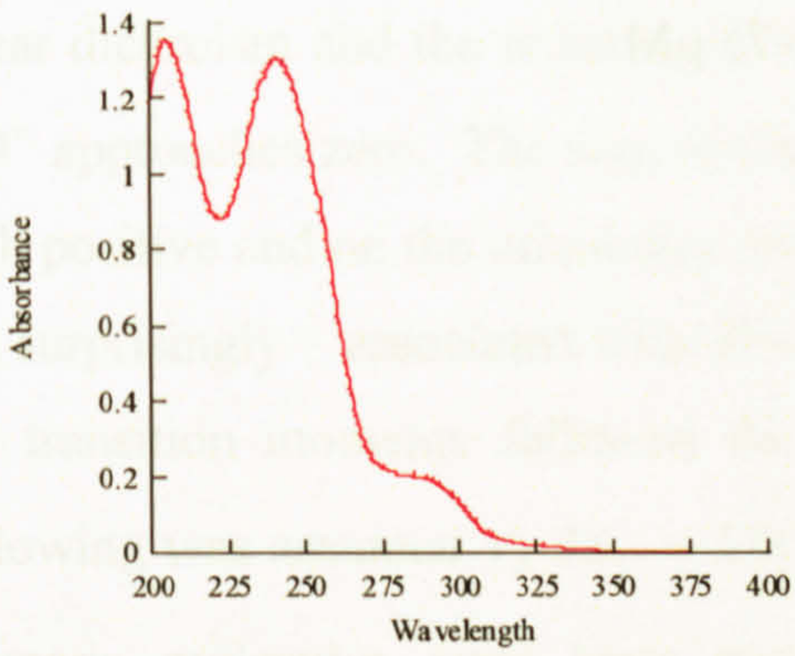

TC-ET-3-Py

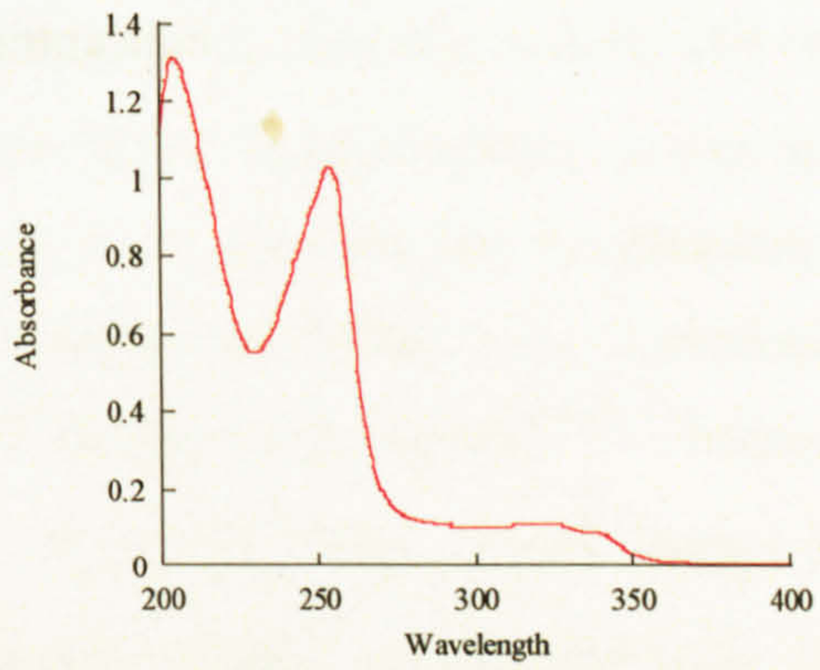

CC-ET-6-Q

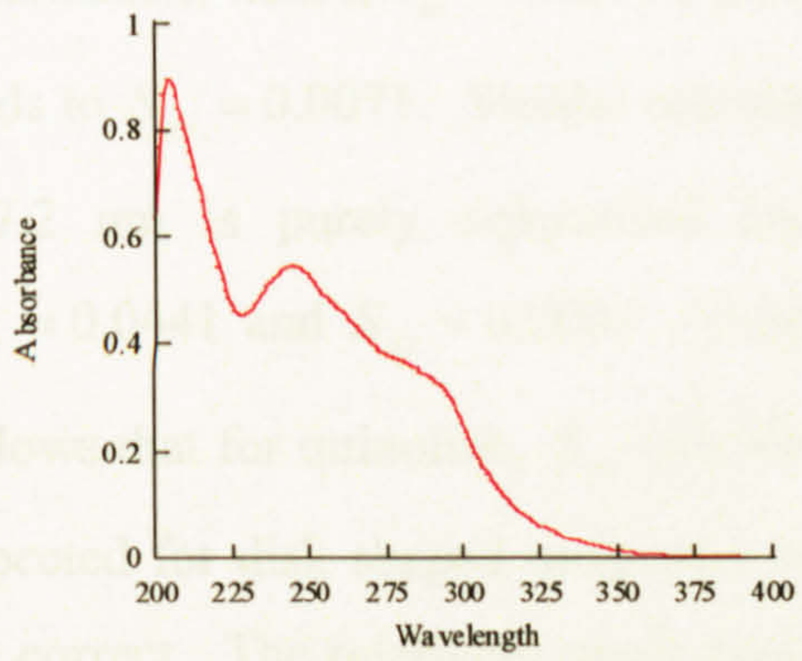

TC-ET-4-Py

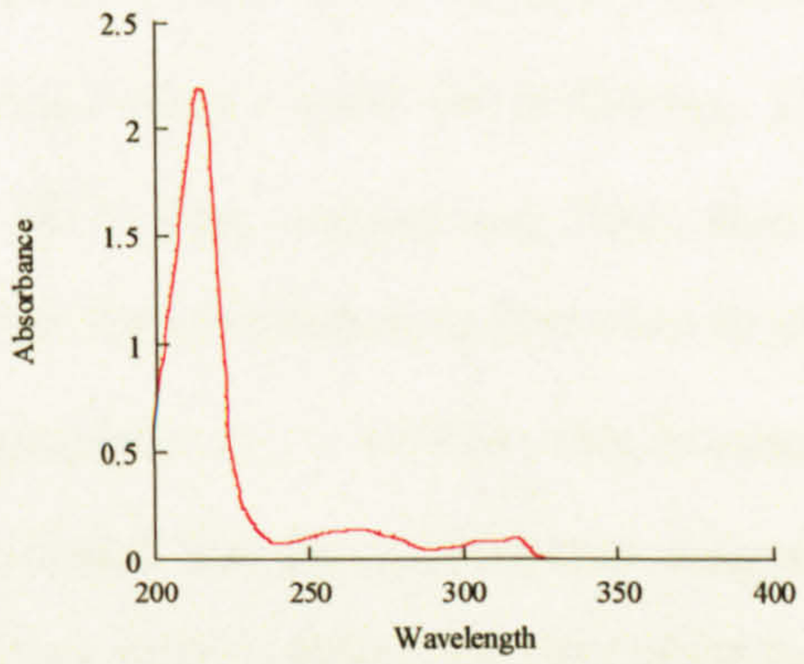

Isoquinoline

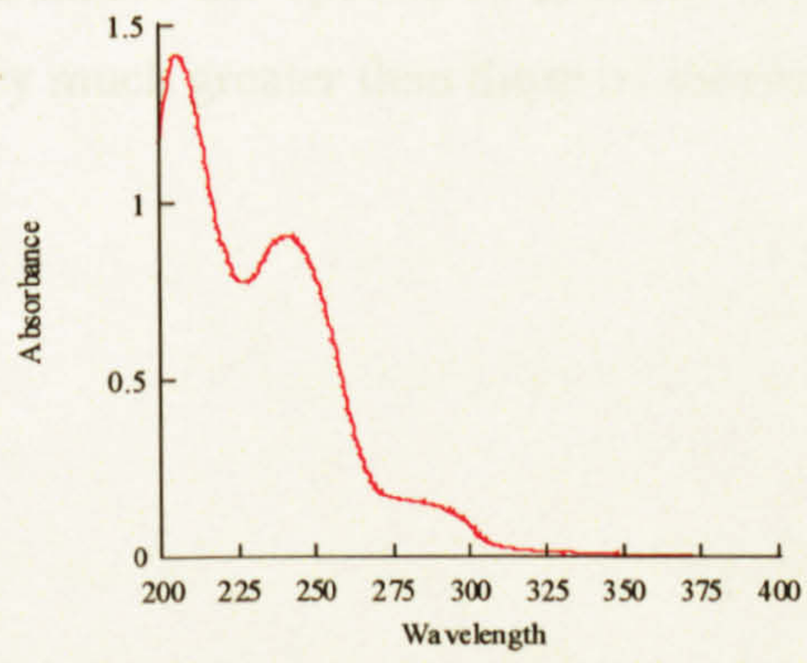

CC-ET-3-Py

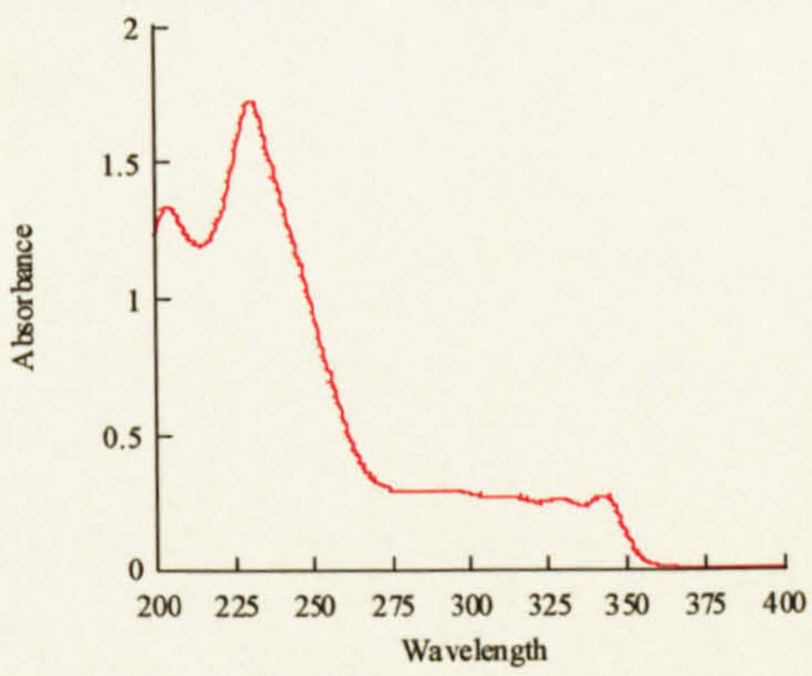

TC-ET-4-IQ

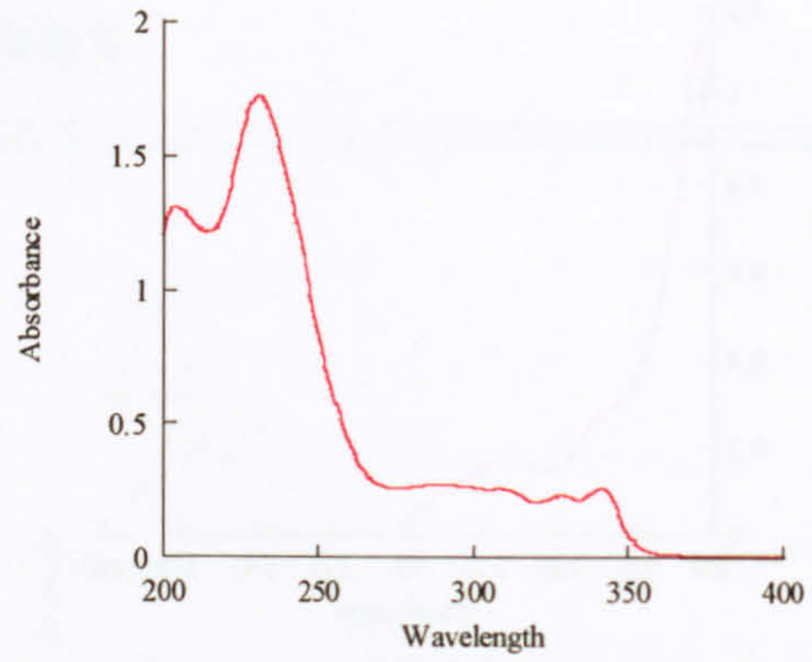

CC-ET-4-IQ

Figure A.10.1. Absorption spectroscopy of various ligands and complexes at concentrations of 25-75 μM

Appendix Eleven – Calculation of the transition moments of quinoline and isoquinoline

A.11.1. Film linear dichroism of quinline and isoquinoline

This appendix describes the calculation of the transition moments of quinoline and isoquinoline using film *LD* spectrum collected as outlined in § 5.7. Representative film *LD*, absorbance and reduced *LD* spectra of quinoline and isoquinoline are shown in Figures A.11.1 and A.11.2. The origin of the absorbance is clear from the molecular structure of quinoline and its isomer: $\pi \rightarrow \pi^*$ and $n \rightarrow \pi^*$ transitions; although $n \rightarrow \pi^*$ transitions are likely to be weak. In the wavelengths studied, quinoline and isoquinoline display only positive linear dichroism and the reduced *LD* signal is also positive; however, around 280 nm the LD^r approaches zero. The sign of the LD^r means the orientation factors, S_{zz} and S_{yy}, are both positive and on the orientation triangle (Figure 5.11) quinoline and isoquinoline are – not surprisingly – associated with disc shaped molecules rather than rods. Calculation of the transition moments followed the method of Rodger and Norden;[581] briefly, the following was assumed 1) $3S_{zz} = LD^r(\text{max})$; 2) $3S_{yy} = LD^r(\text{min})$; 3) disk shaped planar aromatic molecules *must* have transition moments parallel or perpendicular to the molecular plane. For quinoline, the peak at 314.5 nm was assumed to be of pure *z*-polarisation; hence, $S_{zz} = 0.0393$; assuming the trough at 280 nm is of pure *y*-polarisation leads to $S_{yy} = 0.0071$. Similar calculations for isoquinoline assume the following: LD^r at 227.2 nm is purely *z*-polarised and that at 282.6 nm, *y*-polarised; this results in $S_{zz} = 0.0441$ and $S_{yy} = 0.0093$. Using the fact that the orientation factors sum to zero, it follows that for quinoline, $S_{xx} = 0.0464$ and isoquinoline, $S_{xx} = 0.0534$; this is exactly as expected for disk shaped molecules and it is concluded that the polarisation assignments are correct. The relatively small magnitudes of these values reflect the poor alignment of such molecules; this correlates with the large loading of analyte required to obtain a reasonable *LD* spectra in addition to the problem that longer wavelength coefficients are very much greater than those of shorter wavelengths.

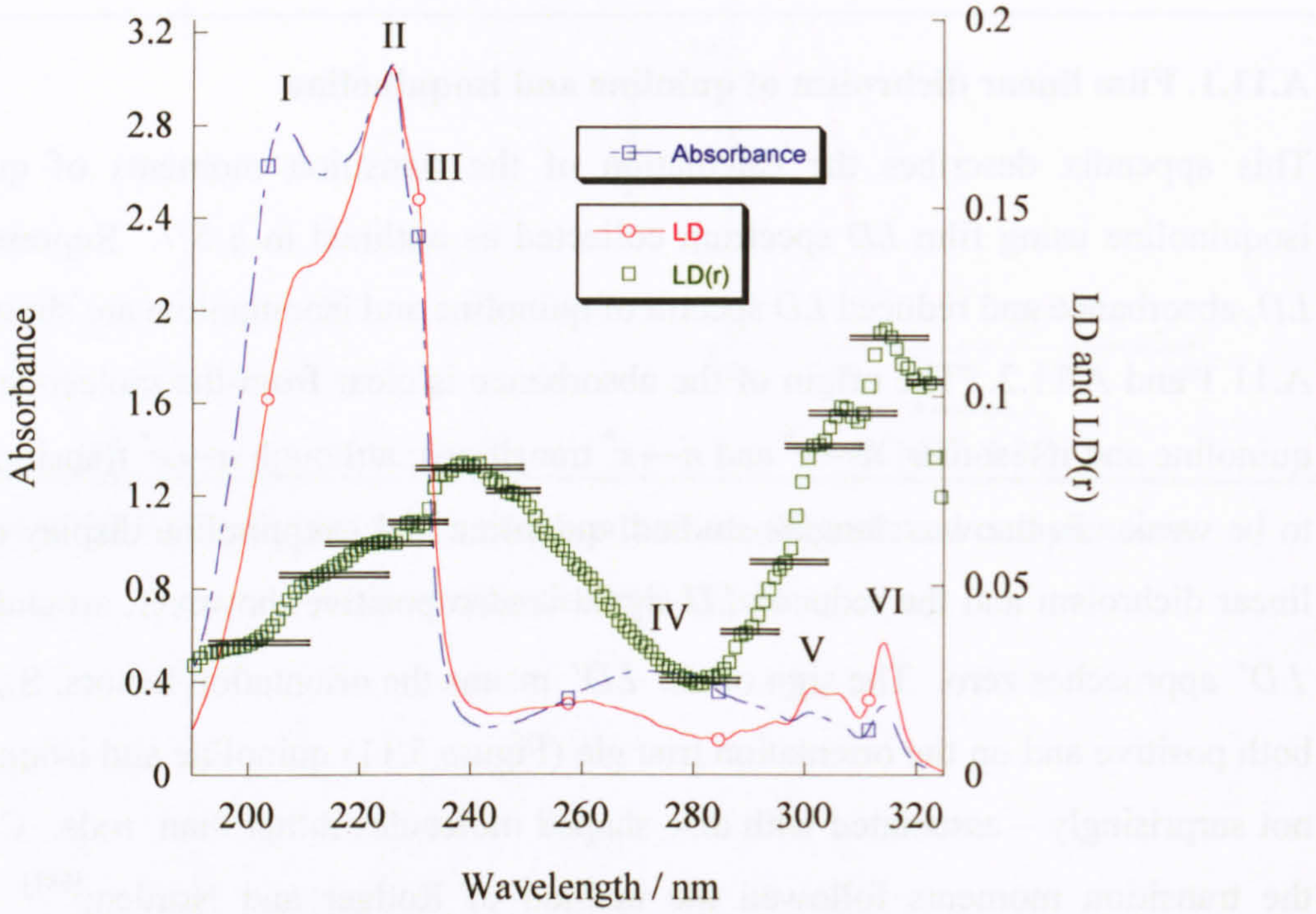

Figure A.11.1. The film *LD*, absorbance and LD^r spectra of quinoline using PE film.

Lines represent minimum, maximum or flat regions of LD^r.

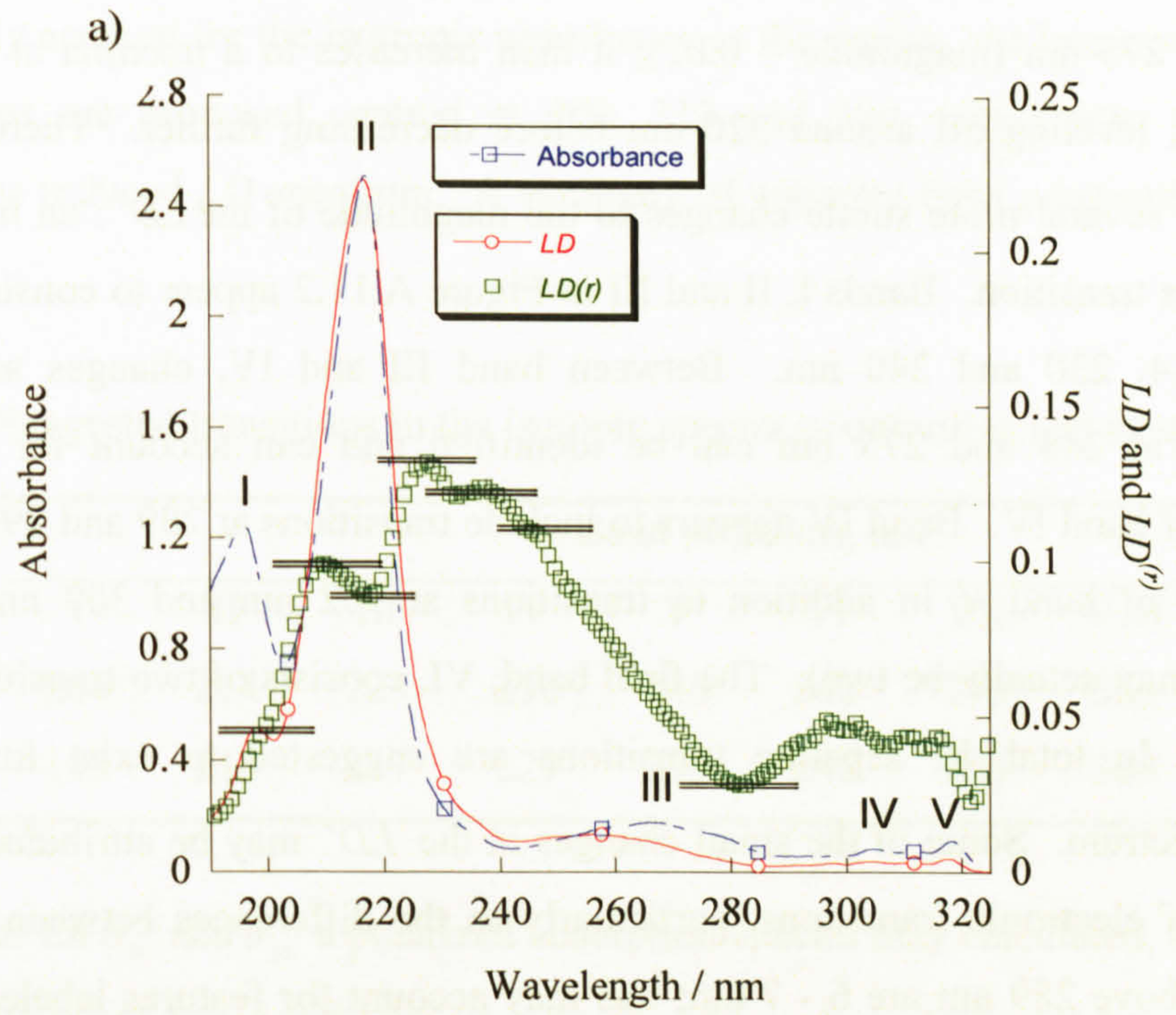

Figure A.11.2. a) The *LD*, absorbance and LD^r of isoquinoline on PE film. b) expansion of the LD^r spectrum; lines represent minimum, maximum or flat regions of LD^r.

The isotropic spectrum of quinoline in Figure A.11.1 displays 6 bands, at 206, 226, 230, 275, 310 and 314 nm and no absorption (likely to arise from $n \rightarrow \pi^*$ transitions) is

present above 325 nm. The LD' of quinoline is complicated; it increases from 195 nm (magnitude ~ 0.03) to a maximium at 240 nm (magnitude ~ 0.075) before decreasing to a minima at 275 nm (magnitude ~ 0.02); it then increases to a maxima at 314 nm before decreasing, leveling off around 320 nm before decreasing further. There exists several abrupt and several more subtle changes to the magnitude of the LD': an indication of the present of a transition. Bands I, II and III in Figure A.11.2 appear to consist of transitions at 206, 214, 230 and 240 nm. Between band III and IV, changes are very subtle; transitions at 248 and 275 nm can be identified and can account for the absorption envelope of band IV. Band IV appears to include transitions at 289 and 296 nm; the latter forms part of band V in addition to transitions at 302 nm and 309 nm (the 309 nm transition may actually be two). The final band, VI, consists of two transitions at 312 and 320 nm. In total 12 separate transitions are suggested to exist for quinoline in the LD' spectrum. Some of the small changes in the LD' may be attributed to vibrational structure of electronic transitions, particularly as the differences between apparent band positions above 289 nm are 6 - 7 nm; this may account for features labeled as individual transitions, it may be suggested that instead of 12 transitions in the UV / visible spectrum of quinoline there are very much fewer, and these occur at 314, 305, 276, 248, 240, 230, 225, 214 and 206 nm. It is proposed that these are true electronic transitions present in the isotropic absorbance spectrum of quinoline and to the author's best knowledge this information does not exist in the literature.

Isoquinoline (Figure A.11.2.) possesses an even more complicated spectrum than quinoline, with particular reference to longer wavelengths. A total of five bands are observed between 195 and 325 nm; no absorption is observed at longer wavelengths. The magnitude of the LD' increases from ~ 0.02 (at 195 nm) to a maximium ~ 0.13 (at 227nm); the LD' then decreases, to minima of ~0.03 (at 256 nm) before increasing again to a maximum magnitude at 308 nm. At longer wavelengths the LD' fluctuates, before decreasing in magnitude to minima at 320 nm. Band I appears to consist of three transitions, <196, 198 and 210 nm; the latter also contributes towards band II, in addition to a transition at 227 nm. At least three transitions appear to contribute to towards band III, at 237, 248 and 265 nm. Towards higher wavelengths the fluctuation of the LD' introduce difficulties, with 11 separate changes in magnitudes suggesting 11 individual transitions; a rather high number. In a similar way to that of quinoline, some of the small changes observed in the reduced LD spectrum may be due to vibrational structure present on electronic transitions; this reduces the number of transitions though present in

isoquinoline to those occurring at 198, 210, 217, 227, 237, 248, 265, 300, 313 and 320 nm. The small change present at 248 nm may be considered as a vibrational component but is required to fully account for the isotropic absorbance in the region. At longer wavelengths three transitions are proposed centred at 300, 313 and 320, taking into account the variations in the reduced *LD* spectrum. A summary of apparent band positions is given in Table A.11.1.

Table A.11.1. Suggested transitions in the isotopic spectra of quinoline and isoquinoline.

	Band positions, nm									
	I	II	III	IV	V	VI	VII	VIII	IX	X
Quinoline	206	214	225	230	240	248	276	305	314	320
Isoquinoline	198	210	217	227	237	248	265	300	313	

From the values for S_{zz} and S_{yy} a polarized absorption spectra may calculated, as described in Appendix Nine, which quantifies the absorbance of *z*- and *y*-polarised light.

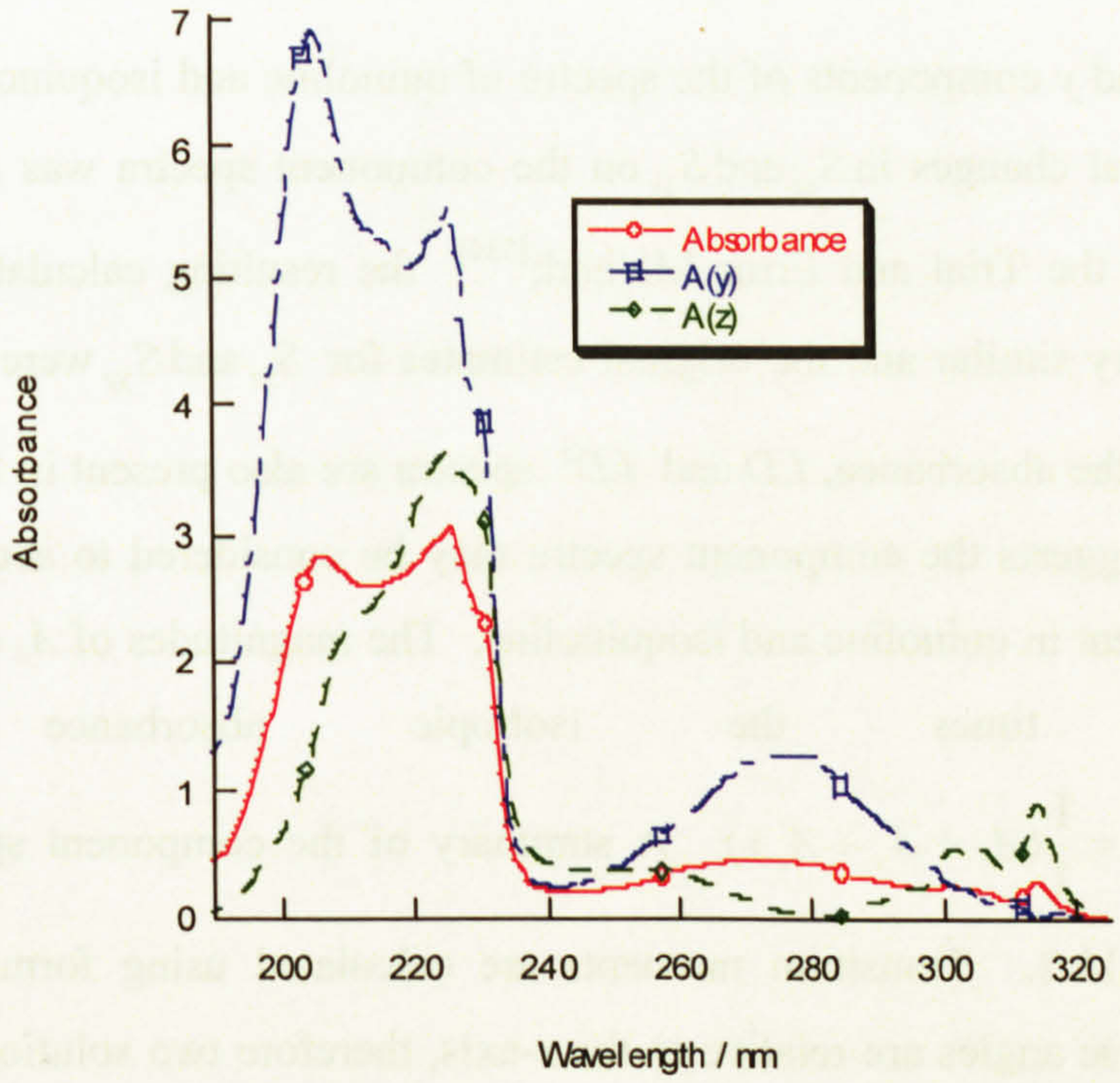

Figure A.11.3. Polarised absorption spectrum of quinoline.

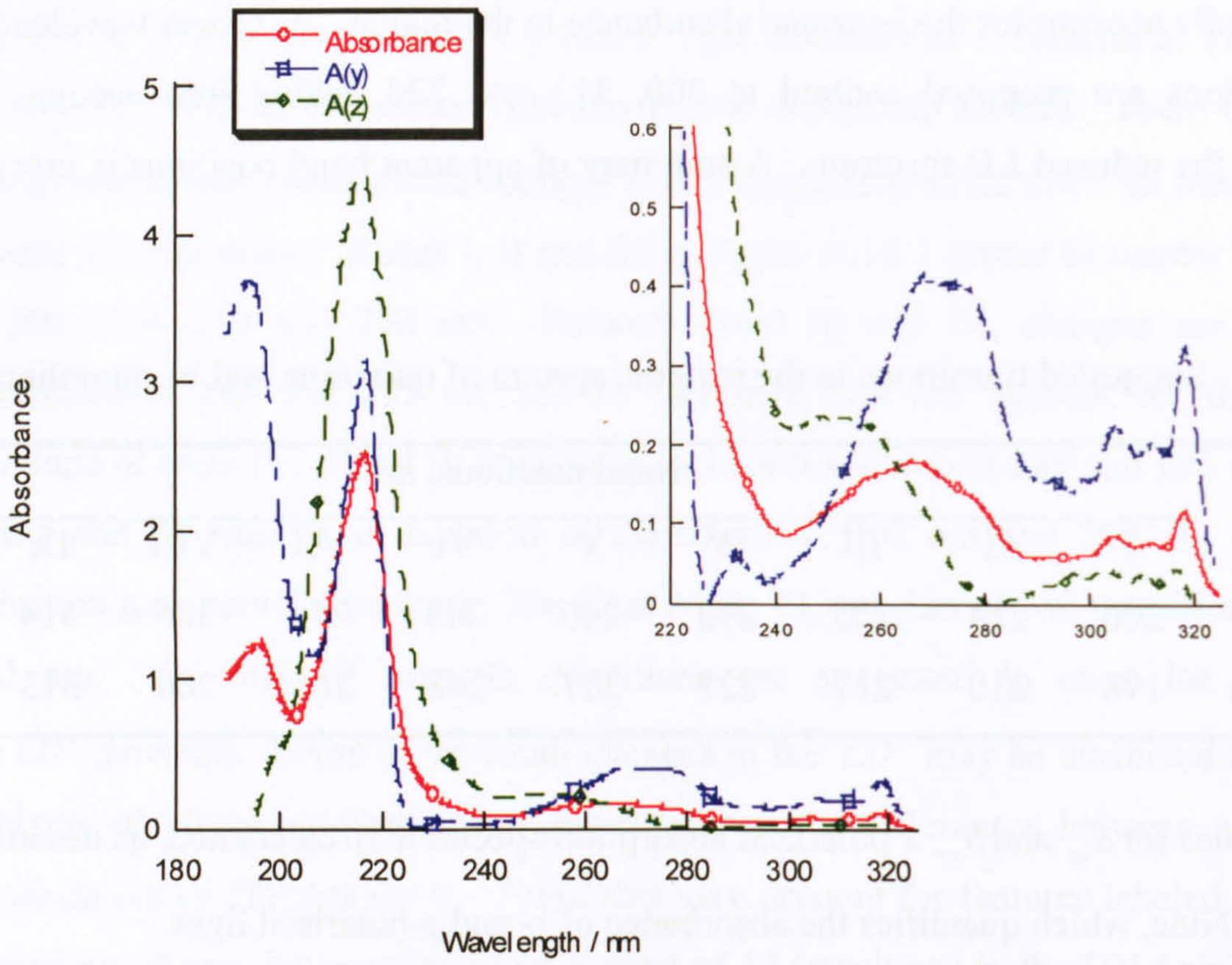

Figure A.11.4. Polarised absorption spectrum of isoquinoline. Insert: expansion in the region 220 - 325 nm.

In determining *z* and *y* components of the spectra of quinoline and isoquinoline, the effect of small incremental changes in S_{zz} and S_{yy} on the component spectra was assessed, three times, in line with the Trial and Error Method;[584] the resulting calculated component spectra were all very similar and the original estimates for S_{zz} and S_{yy} were used. All the features present in the absorbance, *LD* and LD^r spectra are also present in Figures A.11.3 and A.11.4; this suggests the component spectra may be considered to accurately reflect the transitions present in quinoline and isoquinoline. The magnitudes of A_z and A_y are less than three times the isotropic absorbance (isotropic absorbance, $A_{isotropic} = \frac{1}{3}(A_x + A_y + A_z)$). A summary of the component spectra may be found in Table A.11.2. Transition moments are calculated using formulae found in Appendix Nine; these angles are relative to the *z*-axis, therefore two solutions exist: those measured clockwise and counter-clockwise from the *z*-axis; Table A.11.2 gives the solutions clockwise from the *z*-axis.

Table A.11.2. Polarisation in the absorbance spectra of quinoline and isoquinoline (based on 2 independent experiments).

Quinoline		Isoquinoline	
Band position	***TM* angle**	Band position	***TM* angle**
206	***64 or 116 ± 3***	198	***65 or 115 ± 5***
214	***56 or 124 ± 3***	210	***30 or 150 ± 2***
225	***51 or 129 ± 2***	217	***36 or 144 ± 2***
230	***48 or 132 ± 3***	227	***0***
240	***39 or 141 ± 3***	237	***23 or 157 ± 3***
248	***43 or 137 ± 1***	248	***35 or 145 ± 1***
276	***79 or 111 ± 4***	265	***56 or 124 ± 4***
305	***31 or 149 ± 3***	300	***54 or 126 ± 3***
314	***3 or 177 ± 3***	313	***62 or 118 ± 3***
320	***22 or 158 ± 1***	320	***71 or 109 ± 3***

Appendix Twelve – UV / visible flow linear dichroism spectroscopy of steroidal metal complexes

(A)

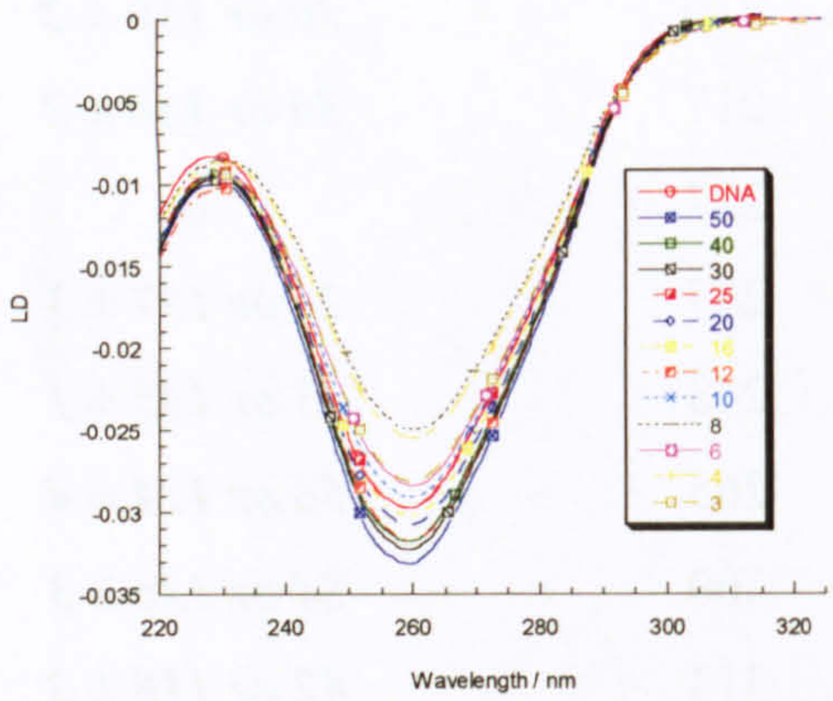

(B)

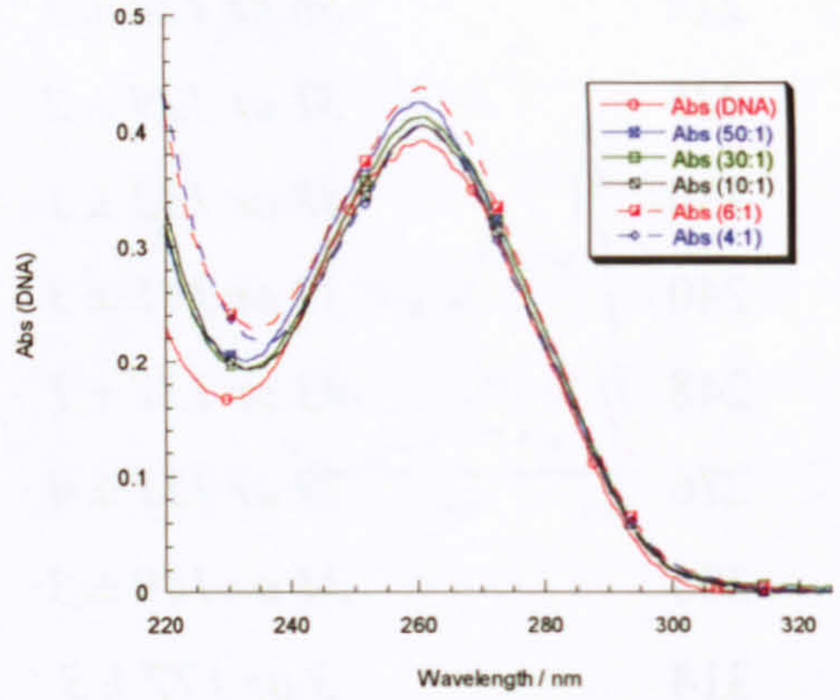

(C)

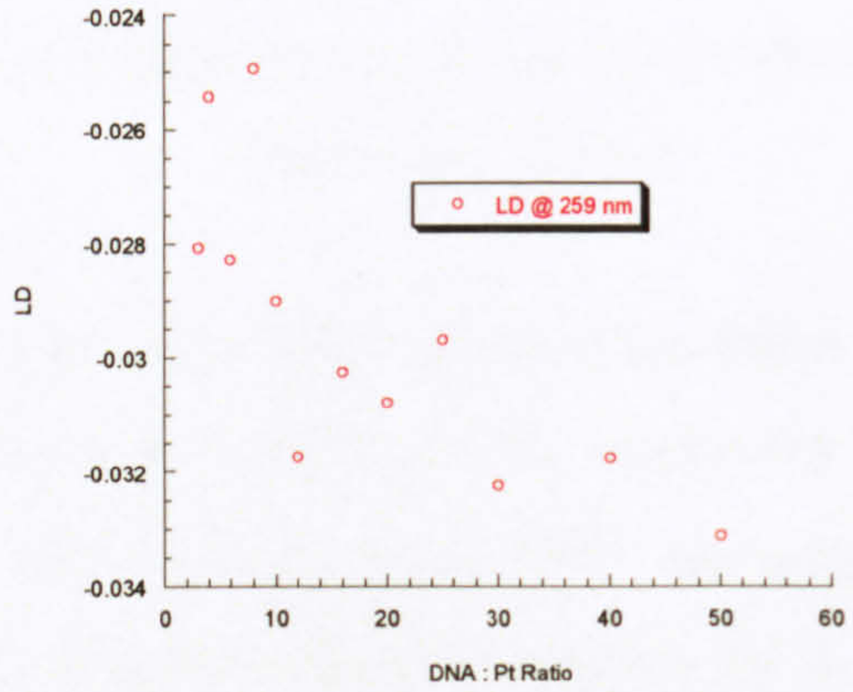

Figure A.12.1. The *LD* (A) and absorbance spectra (B) of TC-Py and ct-DNA; the change of *LD* versus DNA : complex ratio (C). Experimental repeat.

(A)

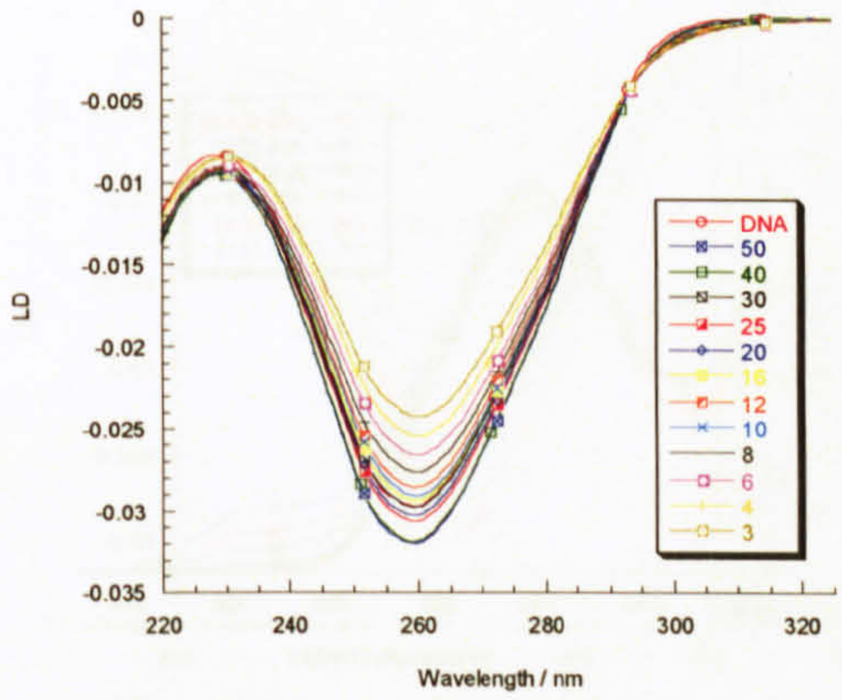

(B)

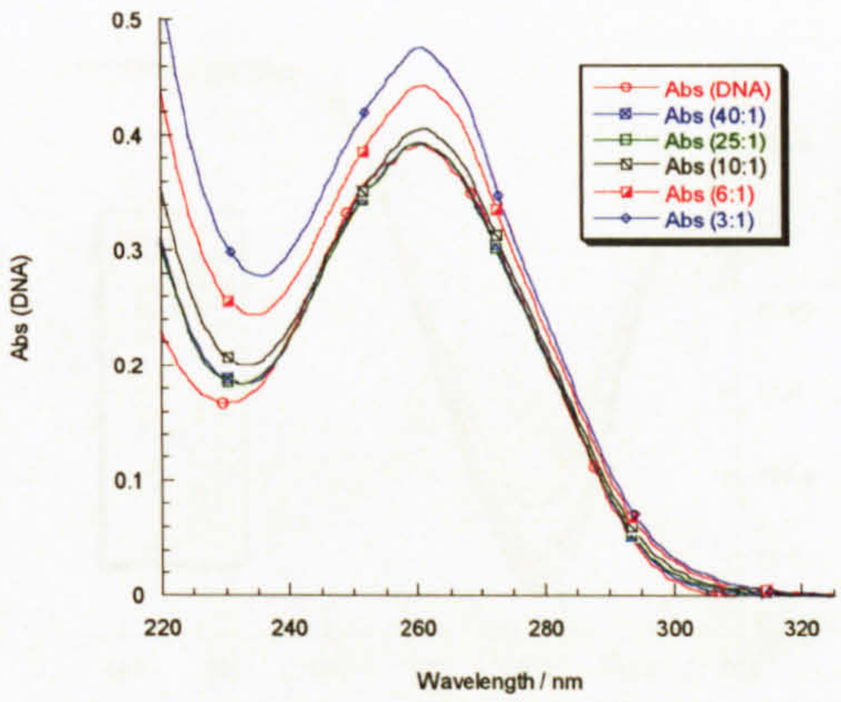

(C)

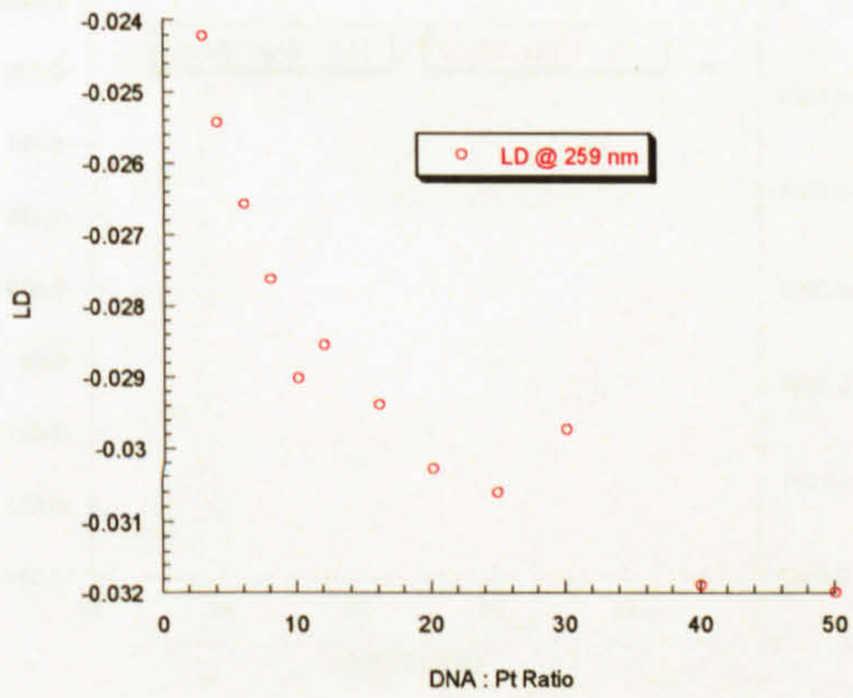

Figure A.12.2. The *LD* (A) and absorbance spectra (B) of CC-Py and ct-DNA; the change of *LD* versus DNA : complex ratio (C). Experimental repeat.

(A)

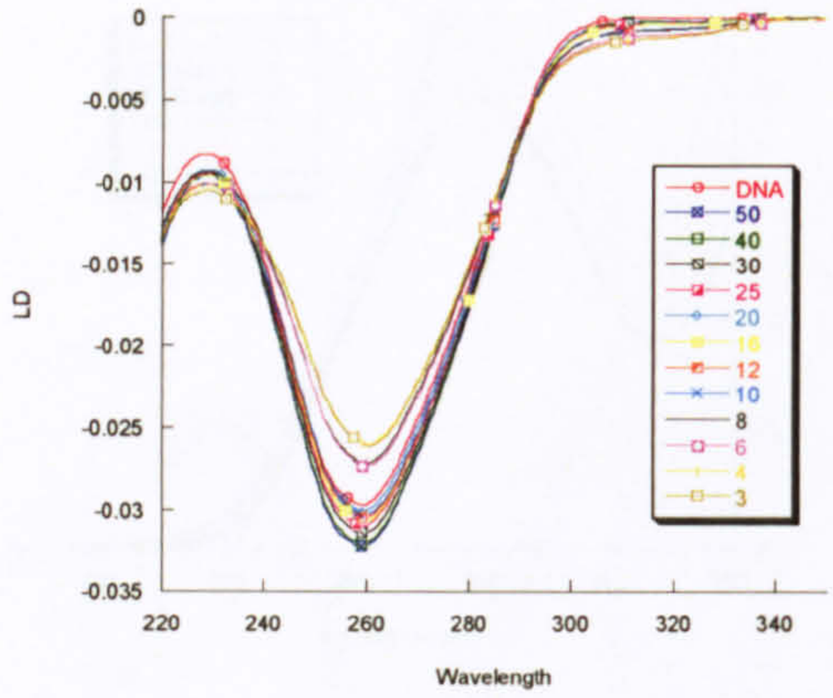

(B)

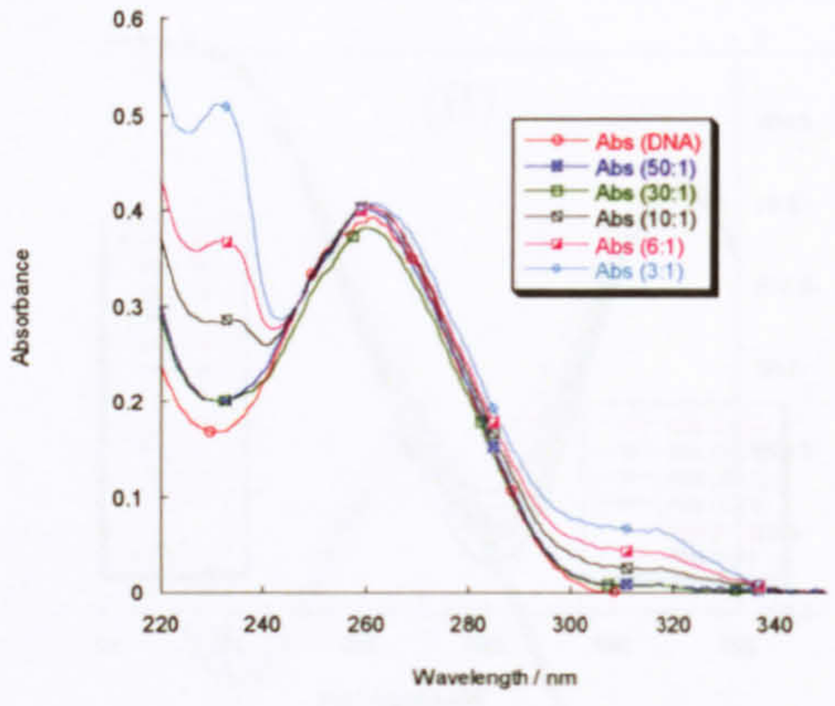

(C)

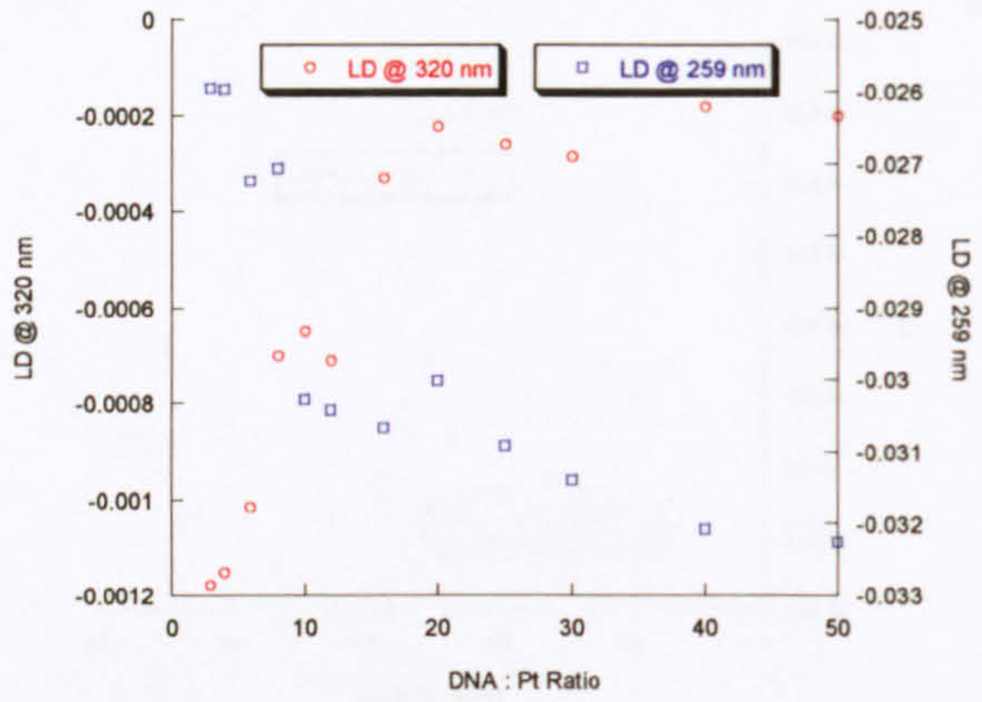

Figure A.12.3. The *LD* (A) and absorbance spectra (B) of TC-Q and ct-DNA; the change of *LD* versus DNA : complex ratio (C). Experimental repeat.

(A)

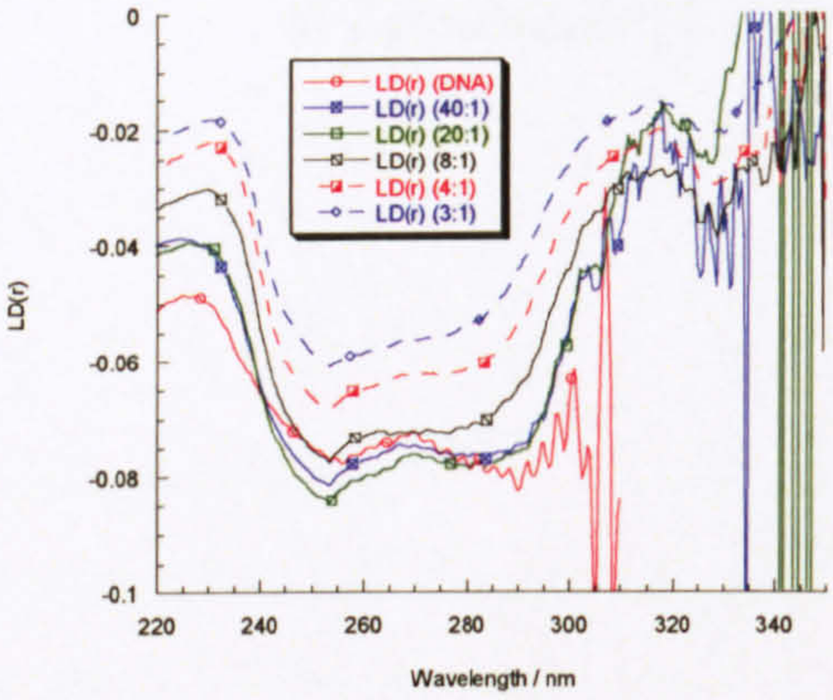

(B)

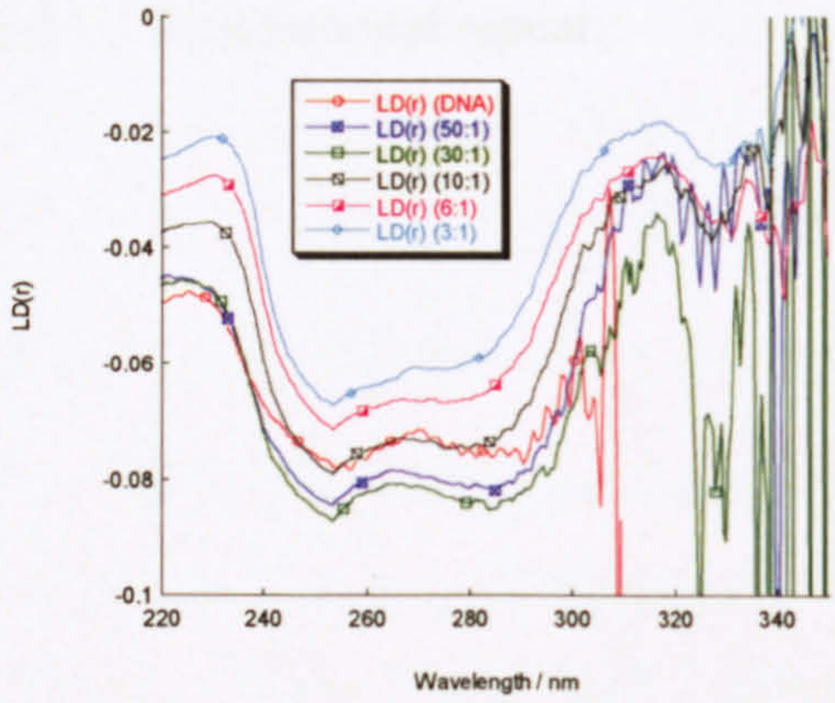

Figure A.12.4. The reduced *LD* spectra (A) of TC-Q treated ct-DNA and repeat (B).

(A)

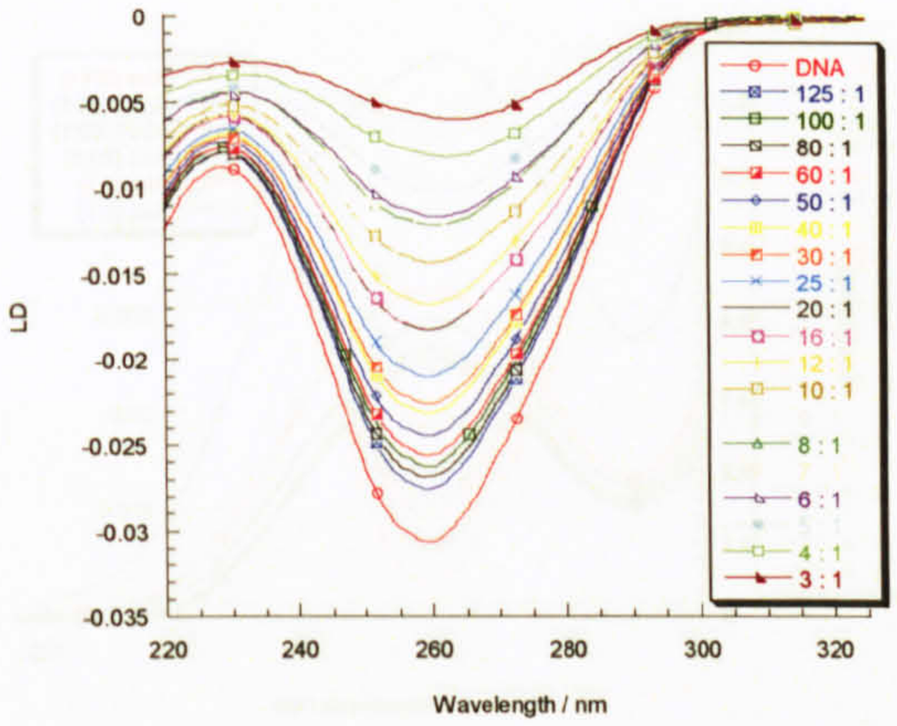

(B)

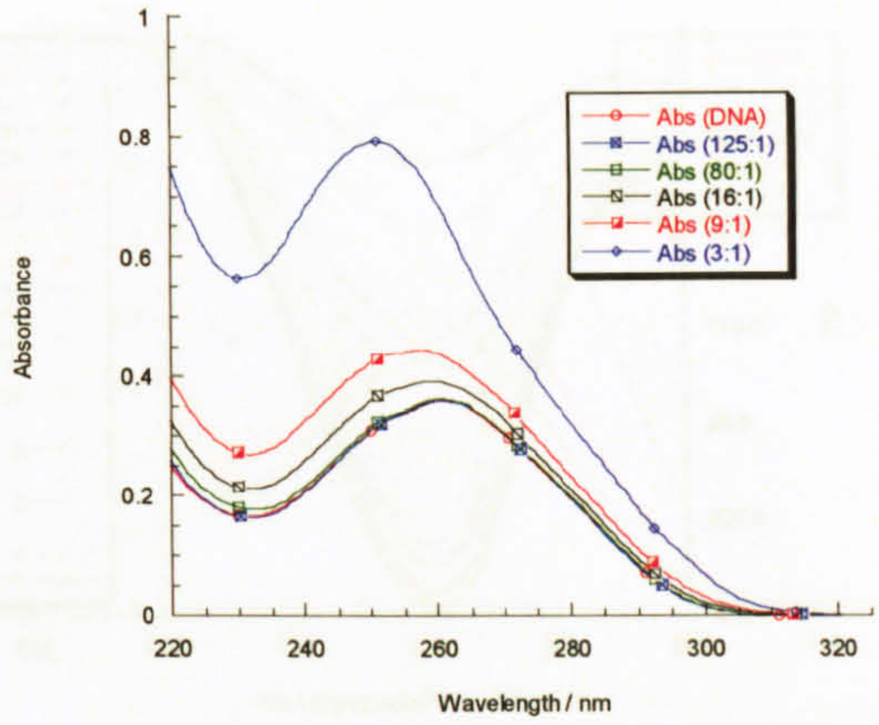

(C)

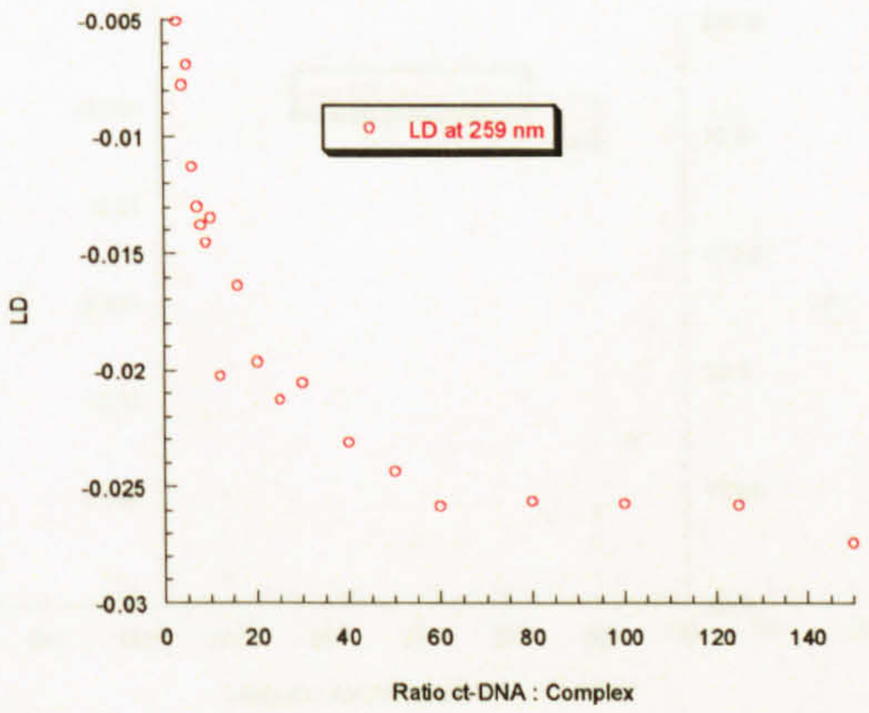

Figure A.12.5. The *LD* (A) and absorbance spectra (B) of TC-ET-3-Py and ct-DNA; the change of *LD* versus DNA : complex ratio (C). Experimental repeat.

(A)

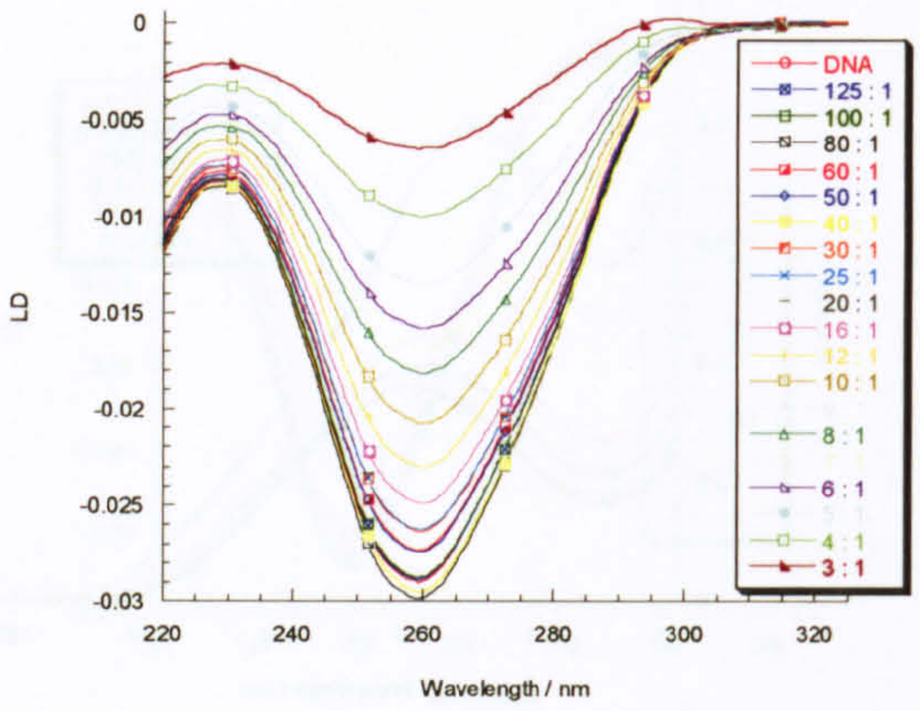

(B)

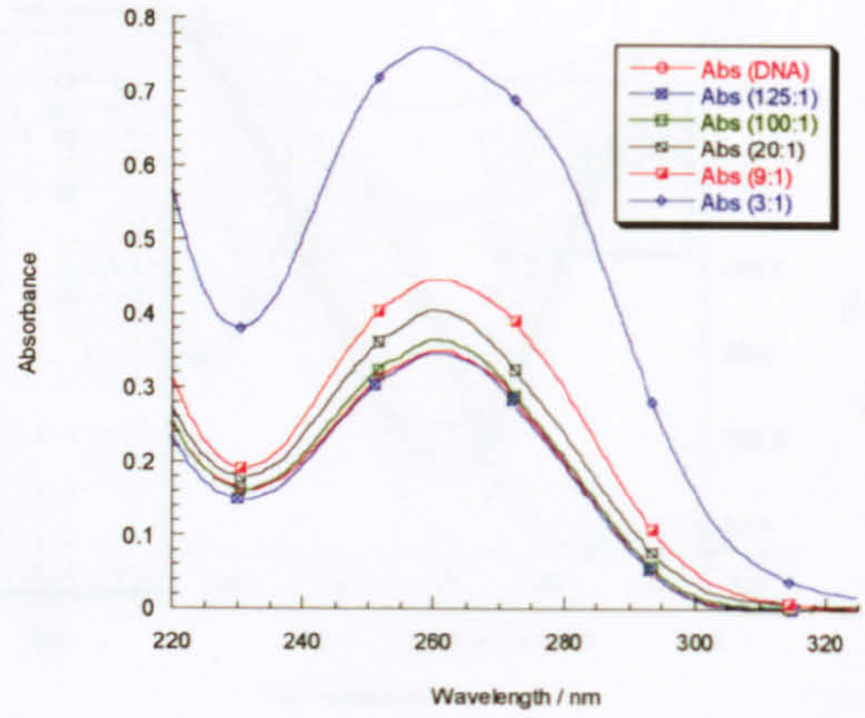

(C)

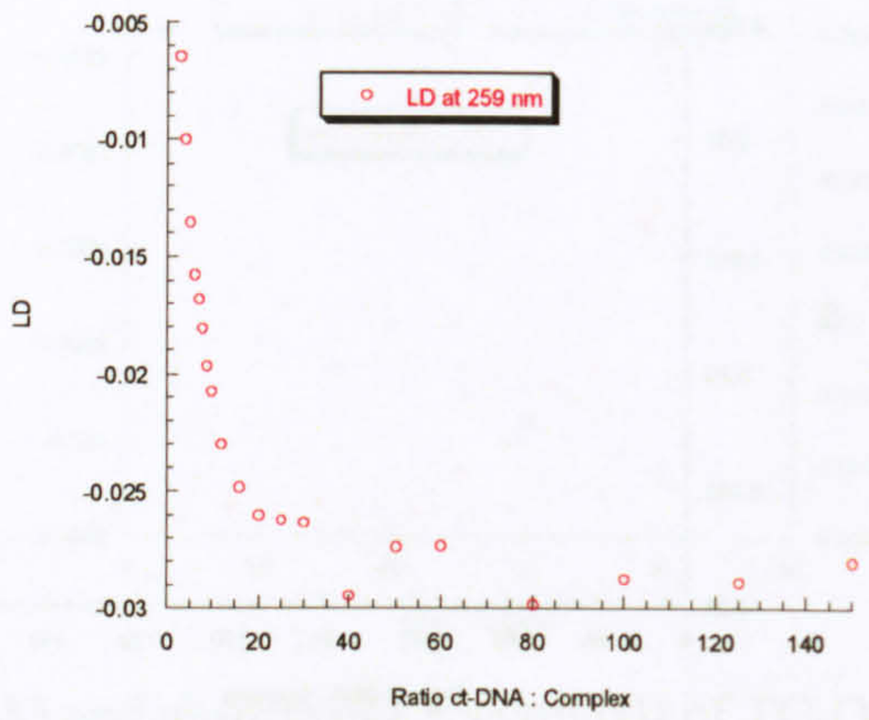

Figure A.12.6. The *LD* (A) and absorbance spectra (B) of TC-ET-4-Py and ct-DNA; the change of *LD* versus DNA : complex ratio (C). Experiment One.

(A)

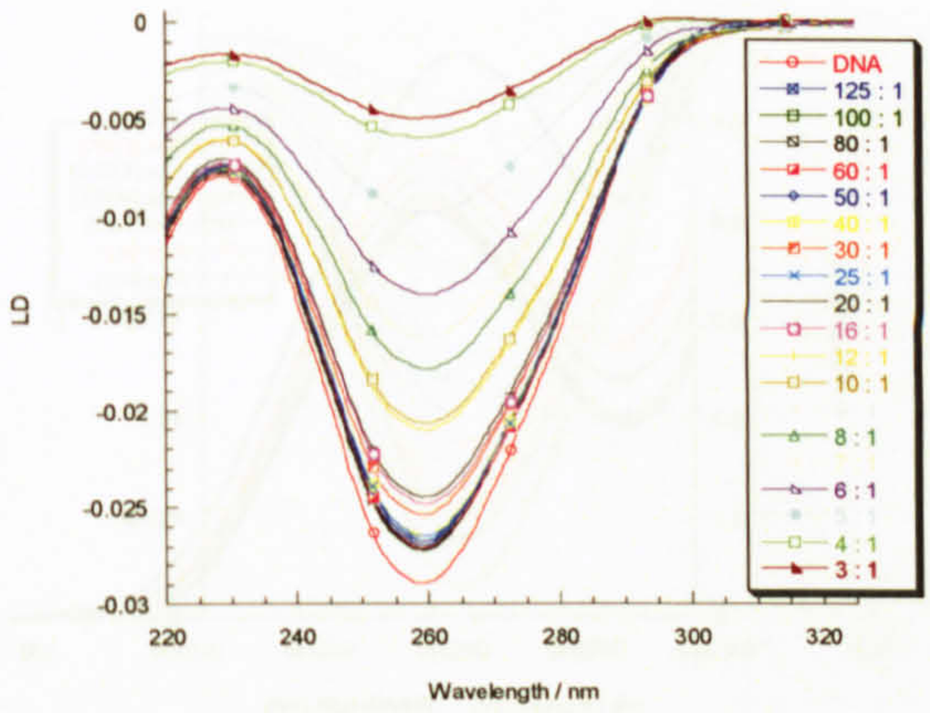

(B)

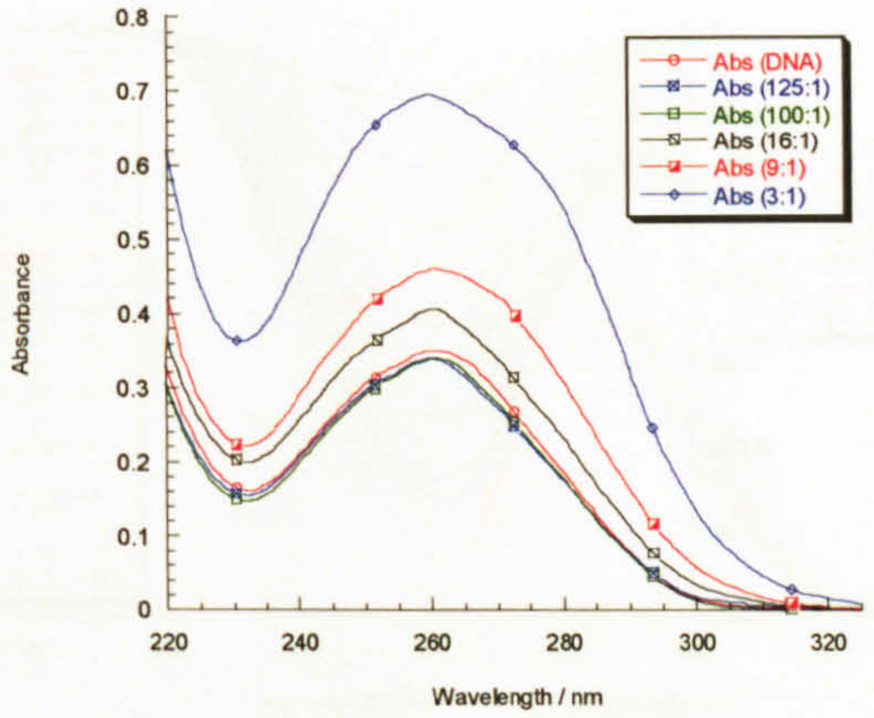

(C)

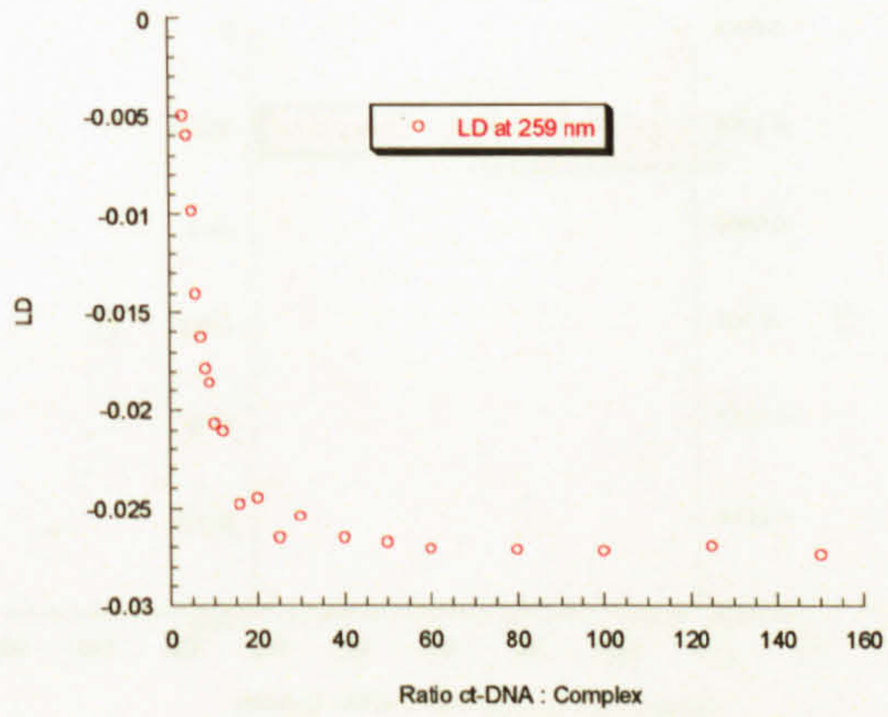

Figure A.12.7. The *LD* (A) and absorbance spectra (B) of TC-ET-4-Py and ct-DNA; the change of *LD* versus DNA : complex ratio (C). Experiment Two.

(A)

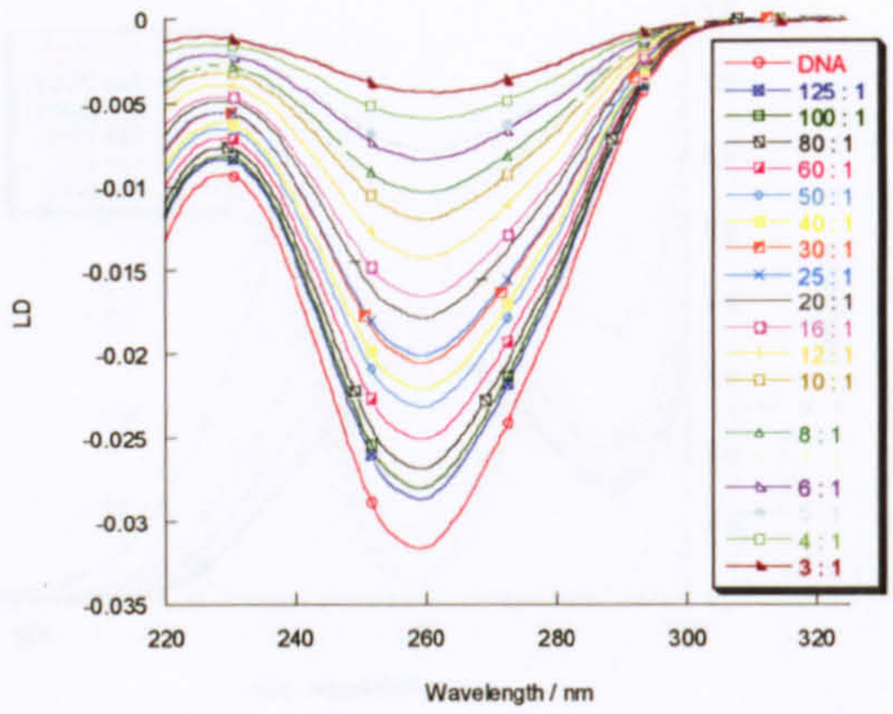

(B)

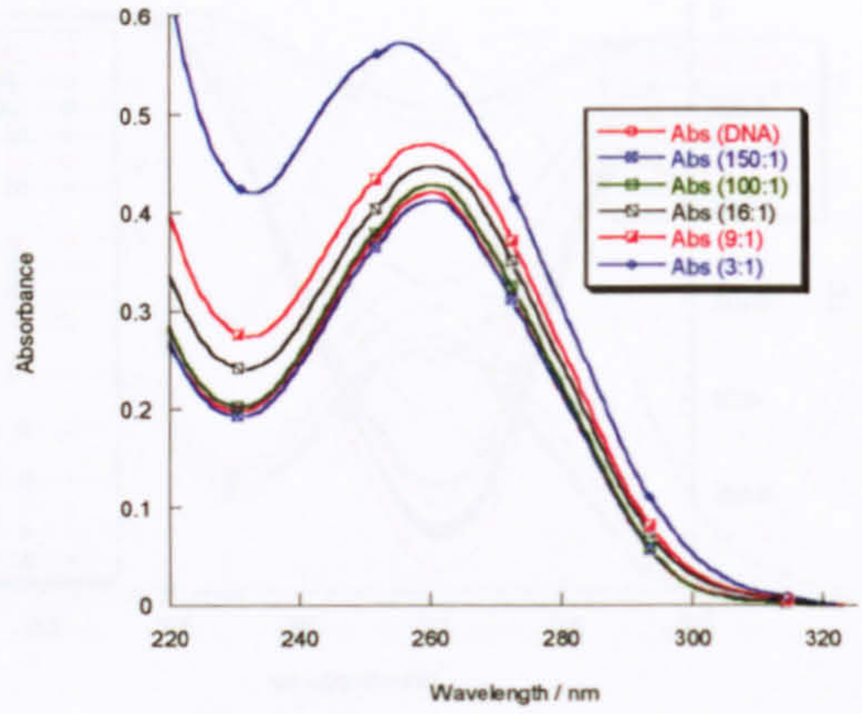

(C)

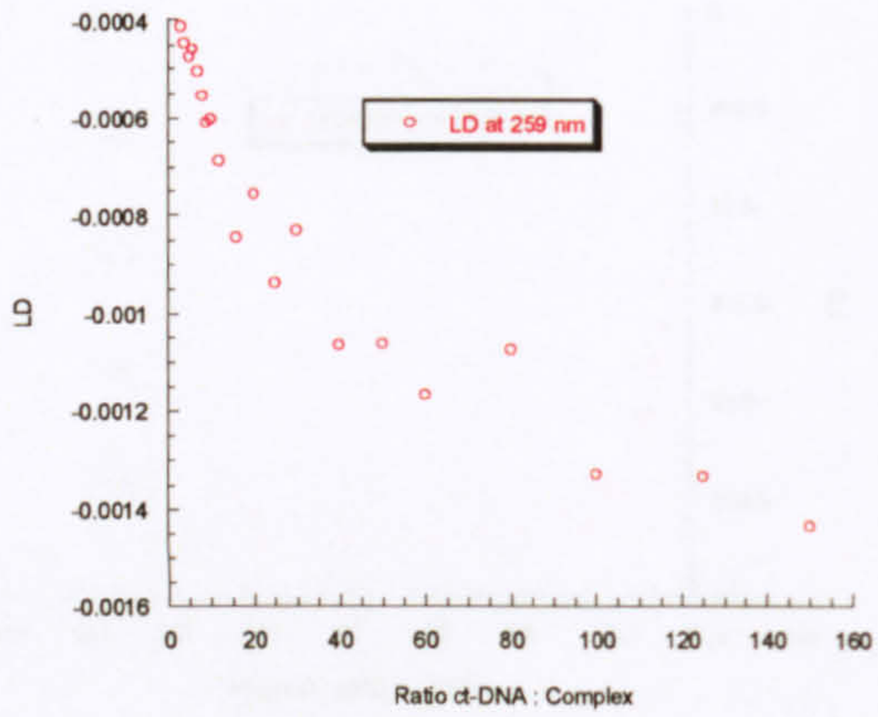

Figure A.12.8. The *LD* (A) and absorbance spectra (B) of CC-ET-3-Py and ct-DNA; the change of *LD* versus DNA : complex ratio (C). Experiment One.

(A)

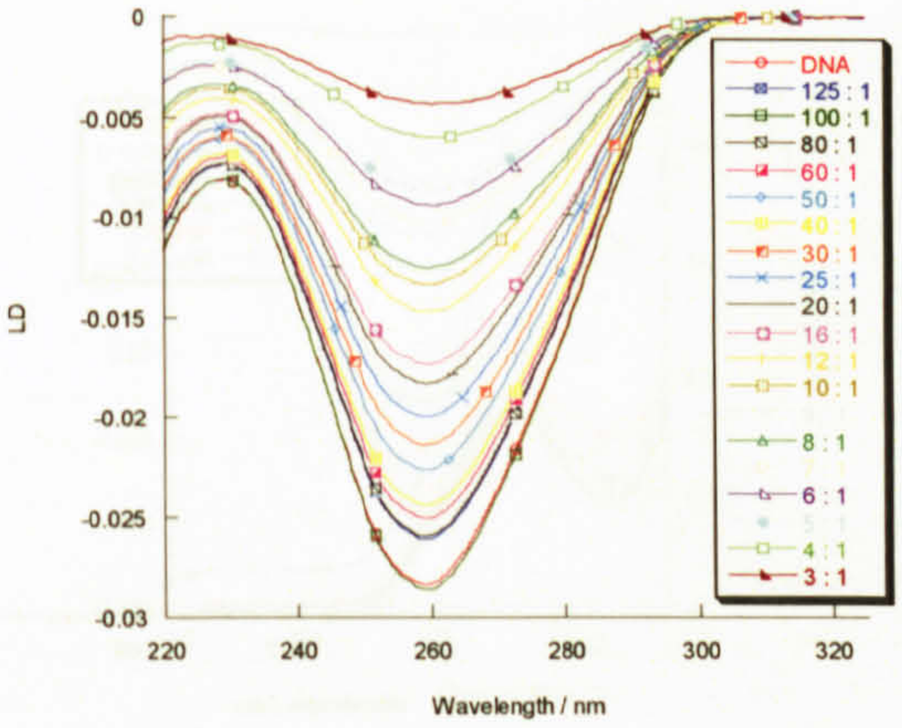

(B)

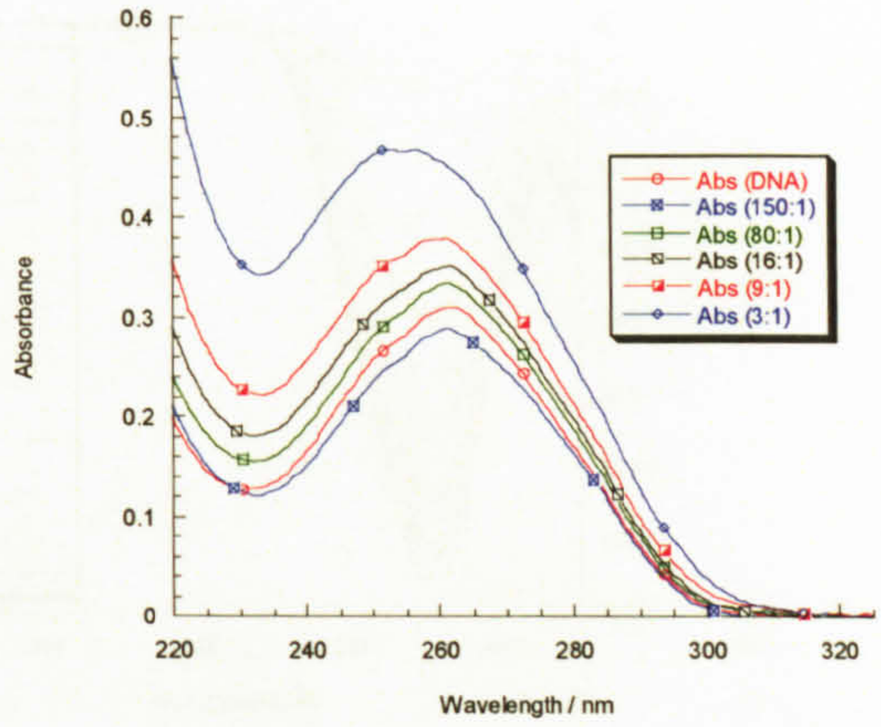

(C)

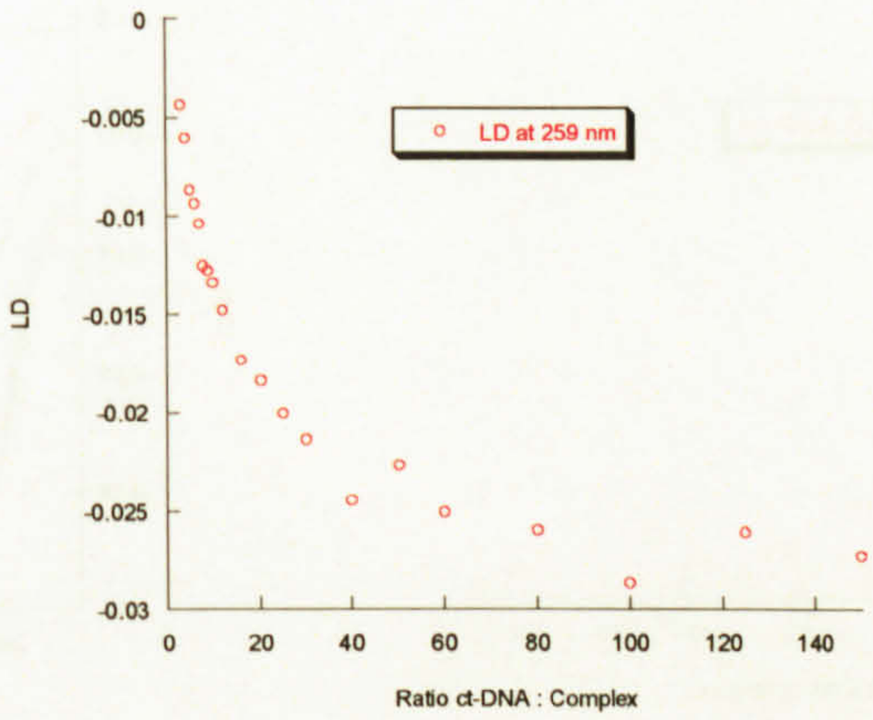

Figure A.12.9. The *LD* (A) and absorbance spectra (B) of CC-ET-3-Py and ct-DNA; the change of *LD* versus DNA : complex ratio (C). Experiment Two.

(A)

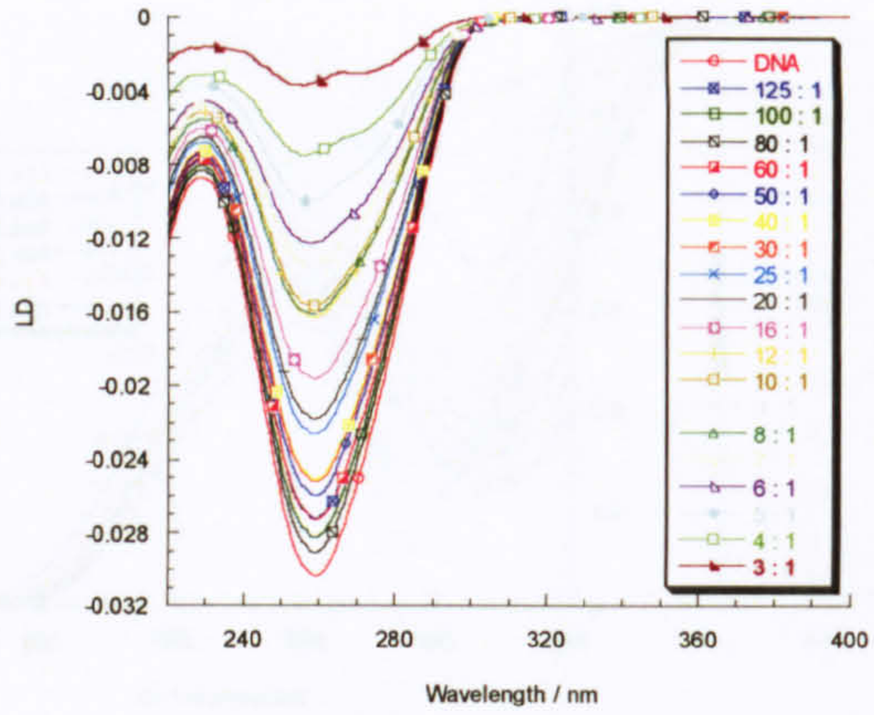

(B)

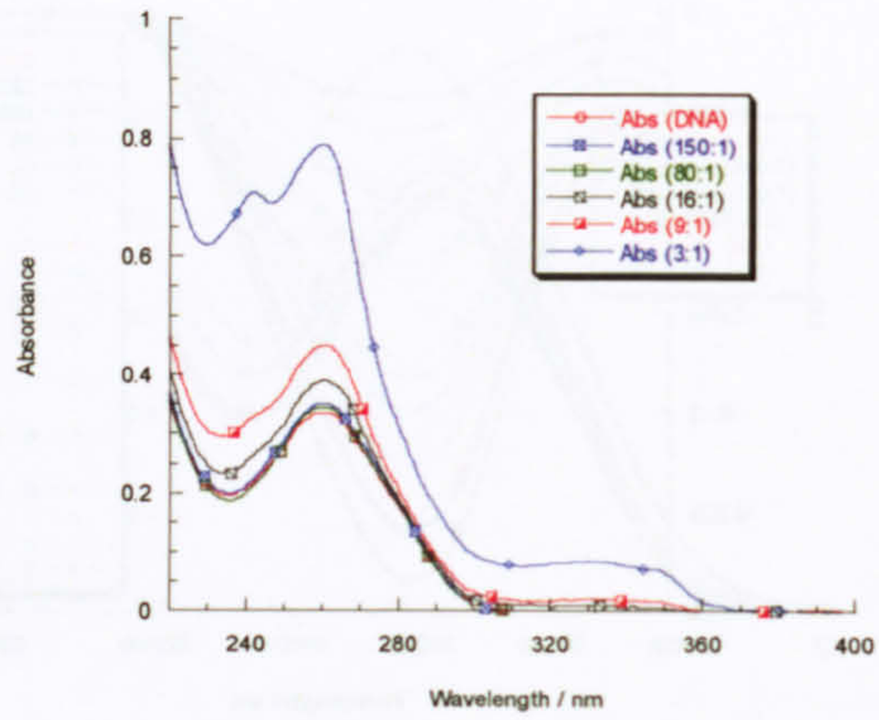

(C)

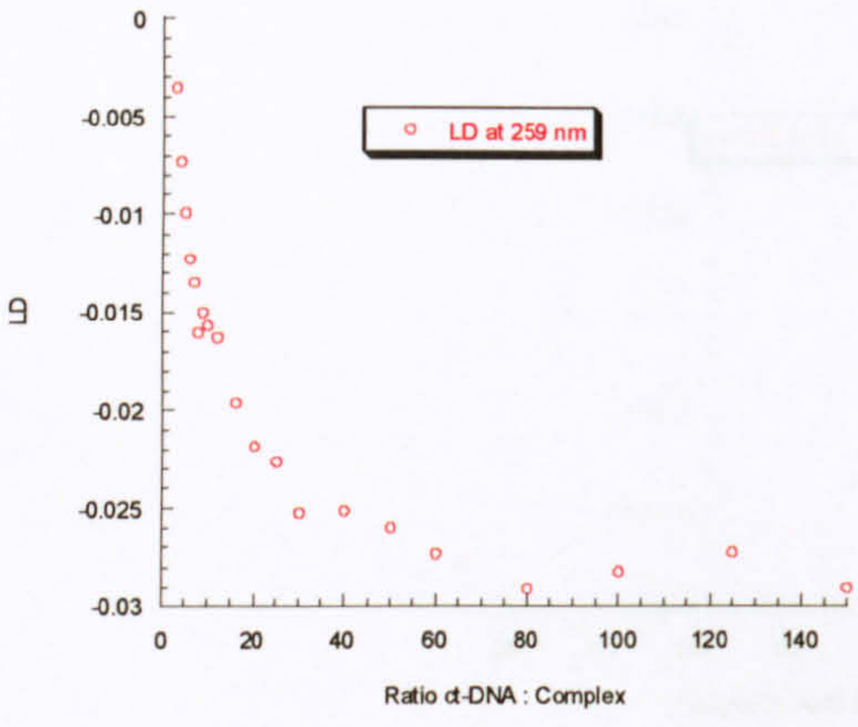

(D)

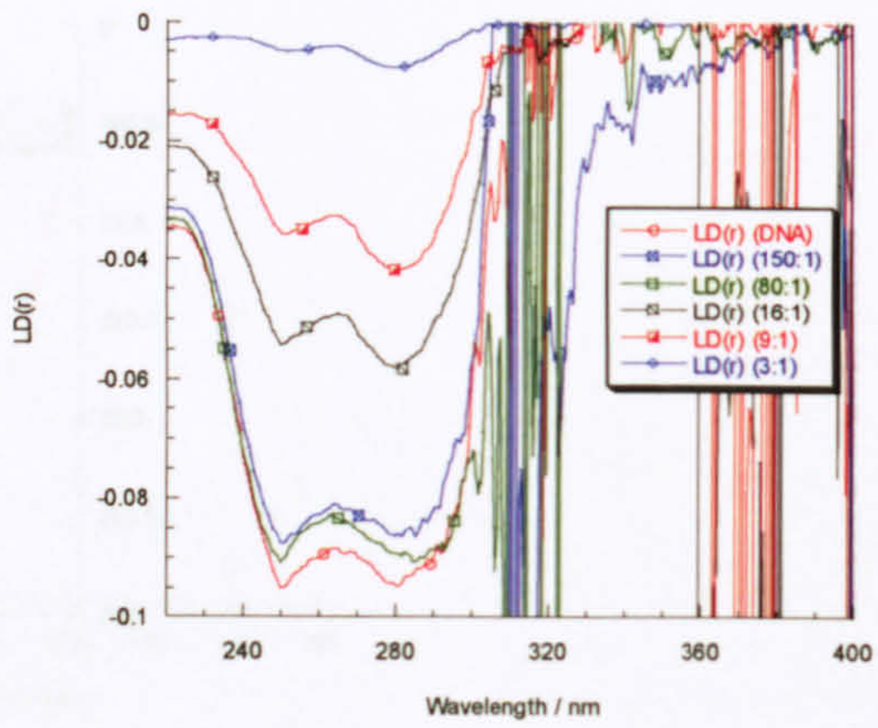

Figure A.12.10. The *LD* (A) and absorbance spectra (B) of TC-ET-3-Q and ct-DNA, the change of *LD* versus DNA : complex ratio (C) and the reduced *LD* (D). Experimental repeat.

(A)

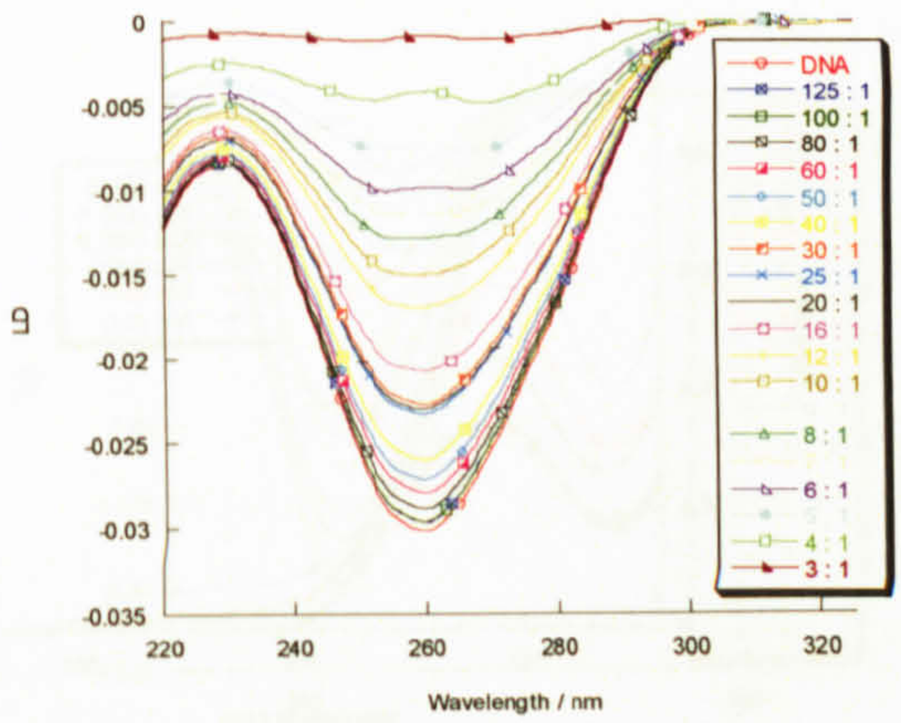

(B)

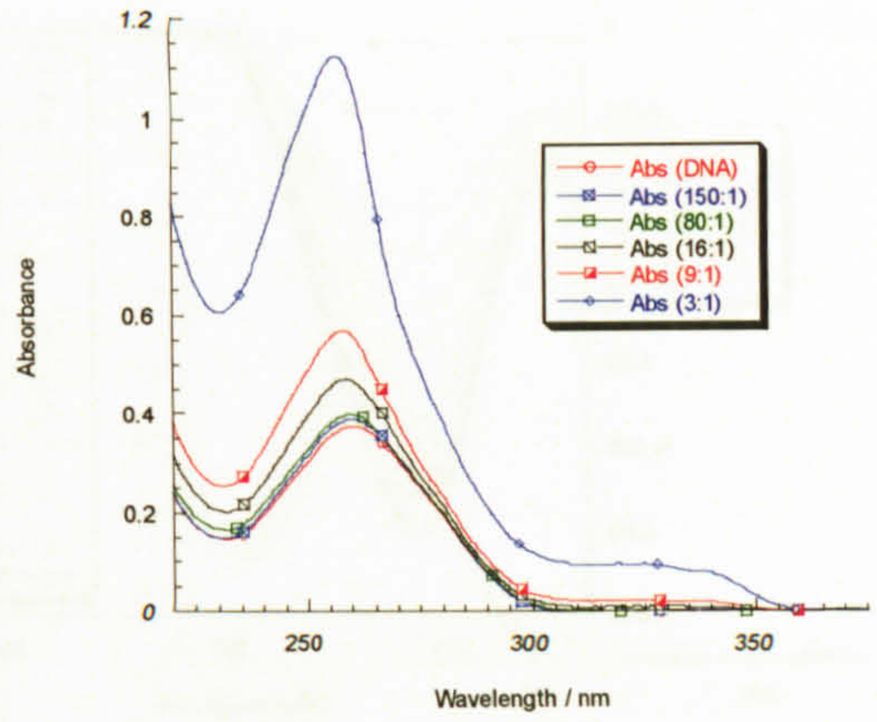

(C)

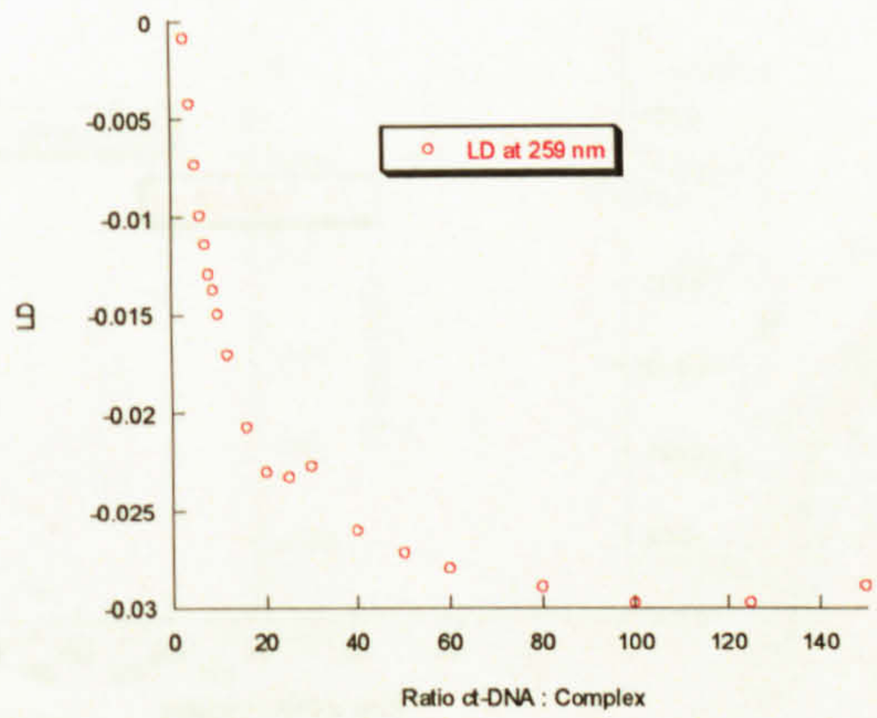

Figure A.12.11. The *LD* (A) and absorbance spectra (B) of TC-Py and ct-DNA; the change of *LD* versus DNA : complex ratio (C). Experiment One.

(A)

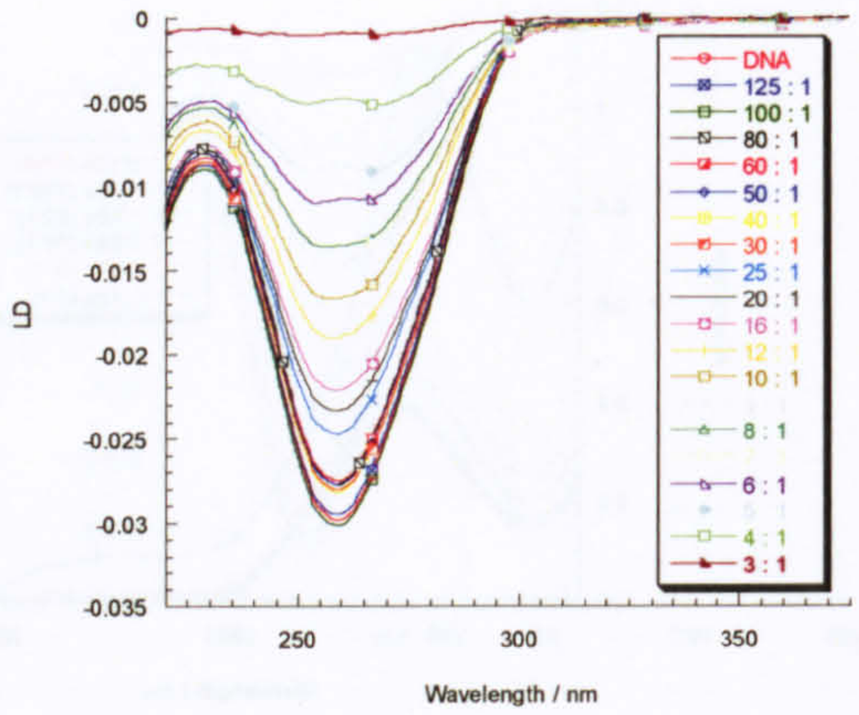

(B)

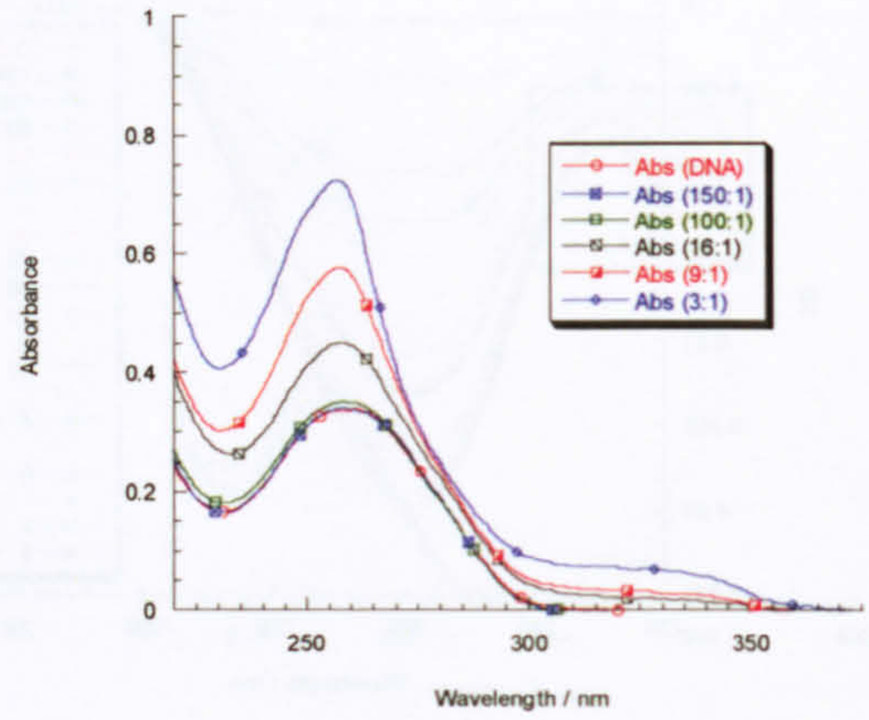

(C)

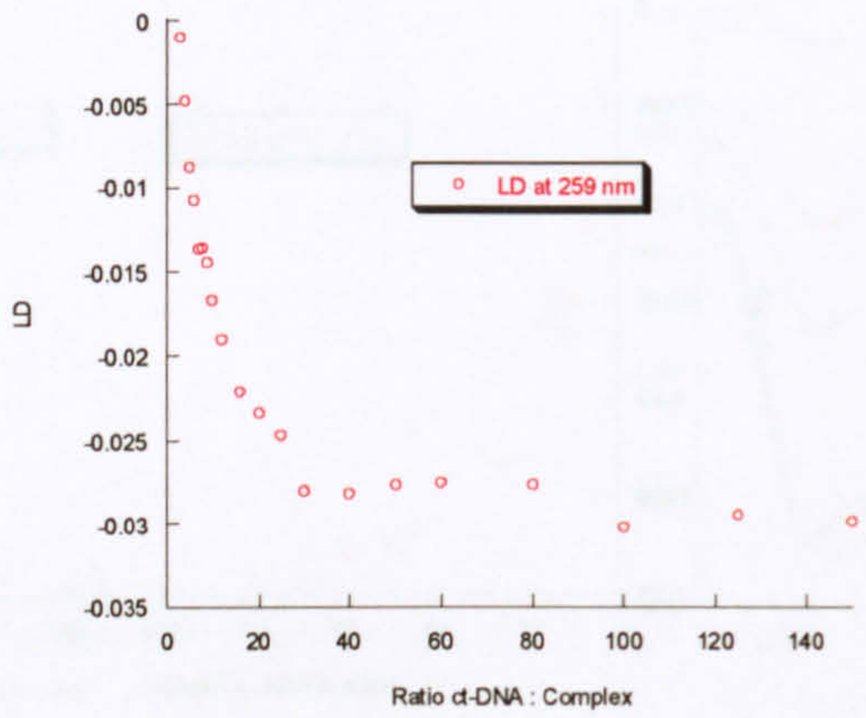

Figure A.12.12. The *LD* (A) and absorbance spectra (B) of TC-ET-6-Q and ct-DNA; the change of *LD* versus DNA : complex ratio (C). Experiment Two.

(A)

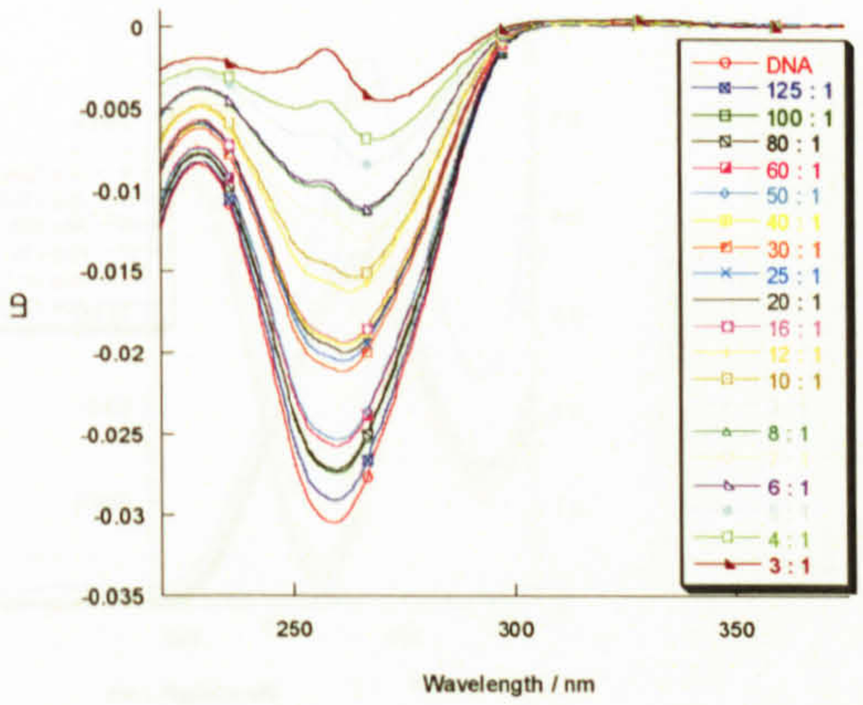

(B)

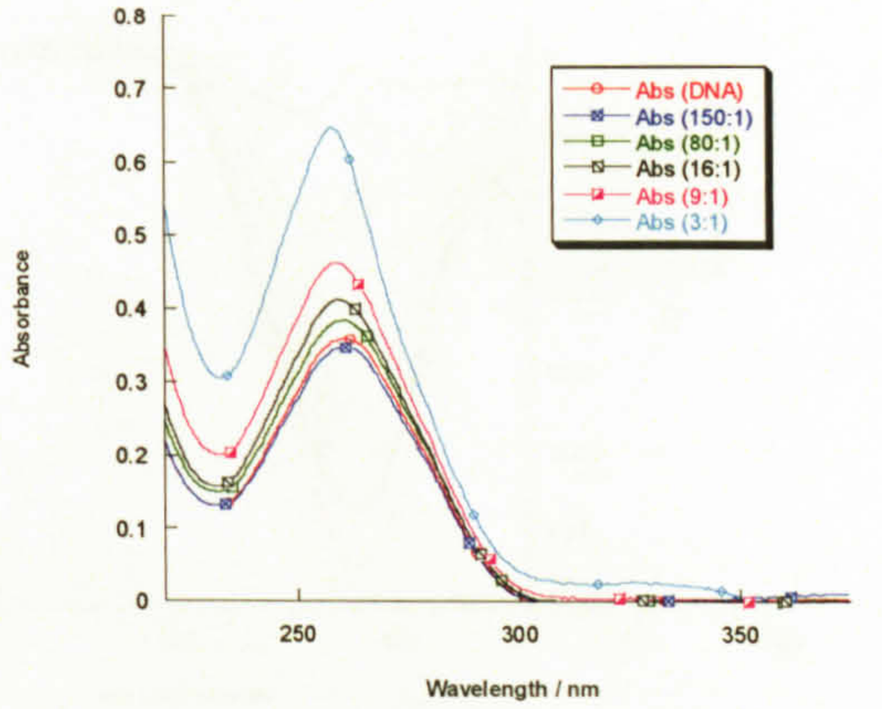

(C)

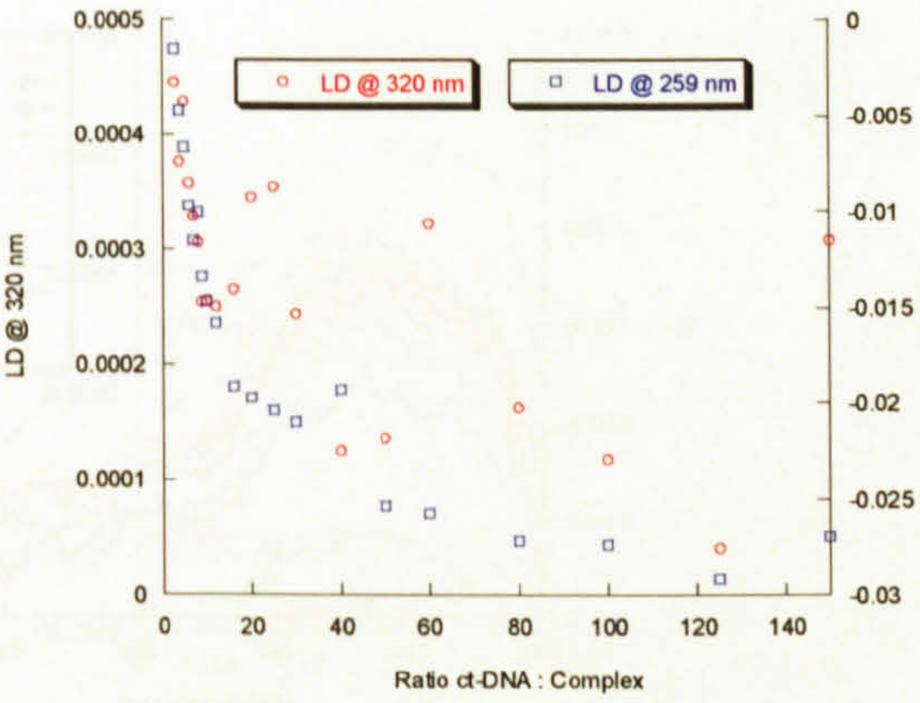

(D)

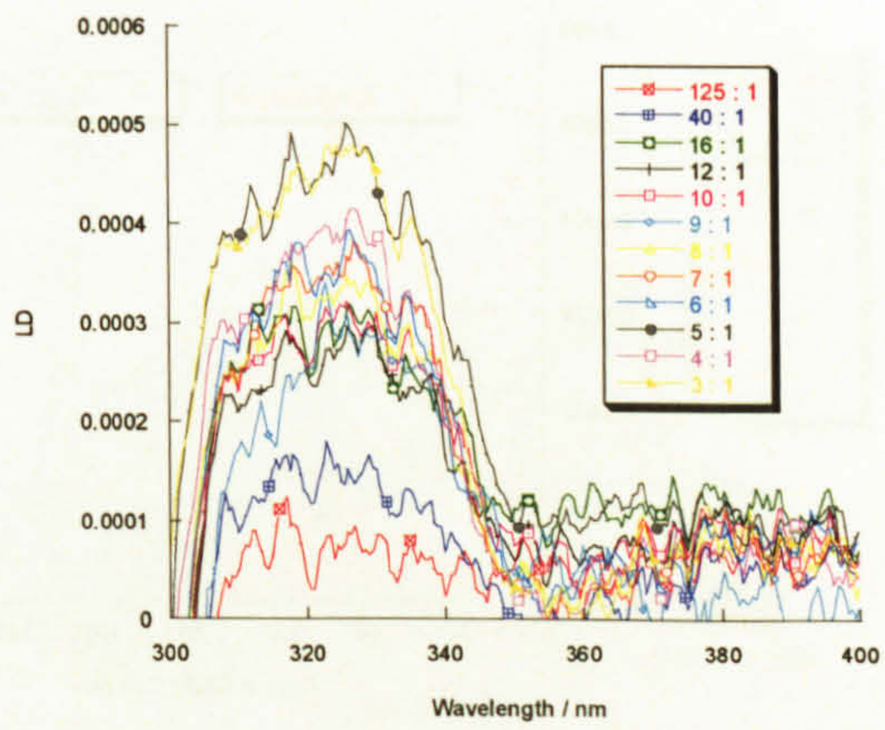

Figure A.12.13. The *LD* (A) and absorbance spectra (B) of CC-ET-6-Q and ct-DNA, the change of *LD* versus DNA : complex ratio (C) and the reduced *LD* (D). Experiment One.

(A)

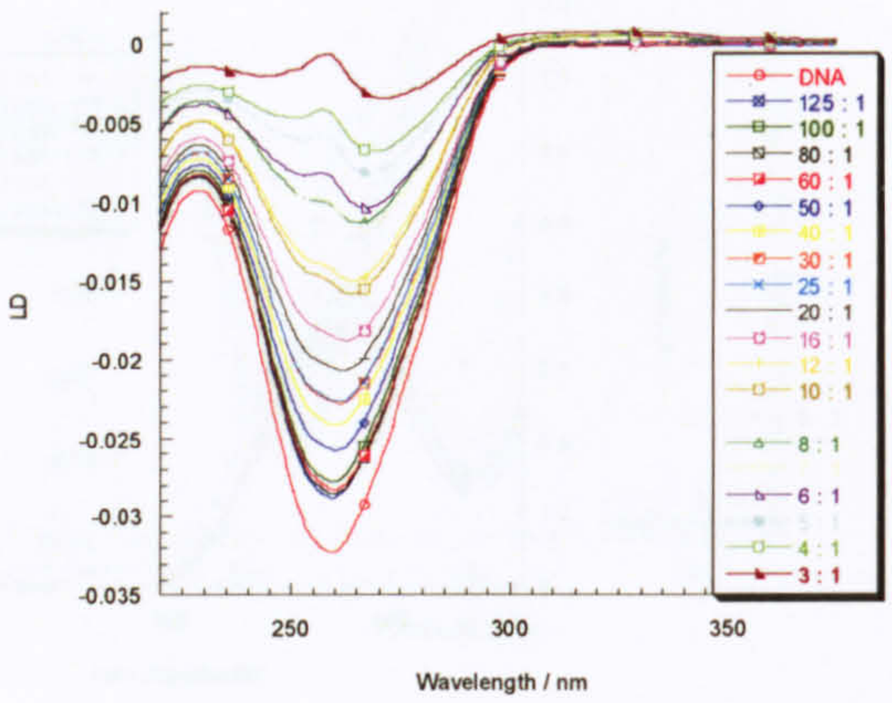

(B)

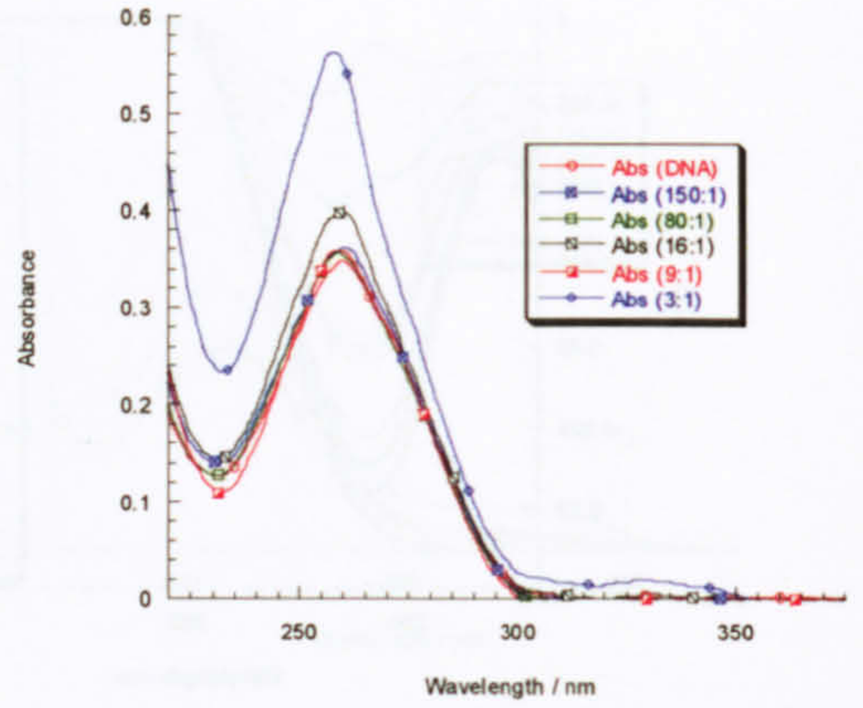

(C)

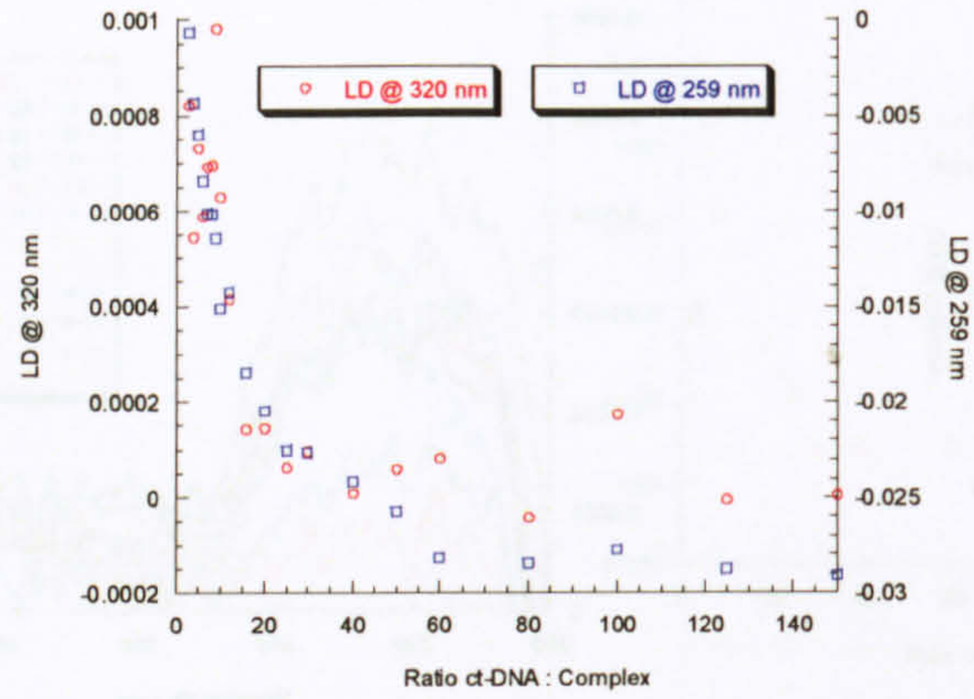

(D)

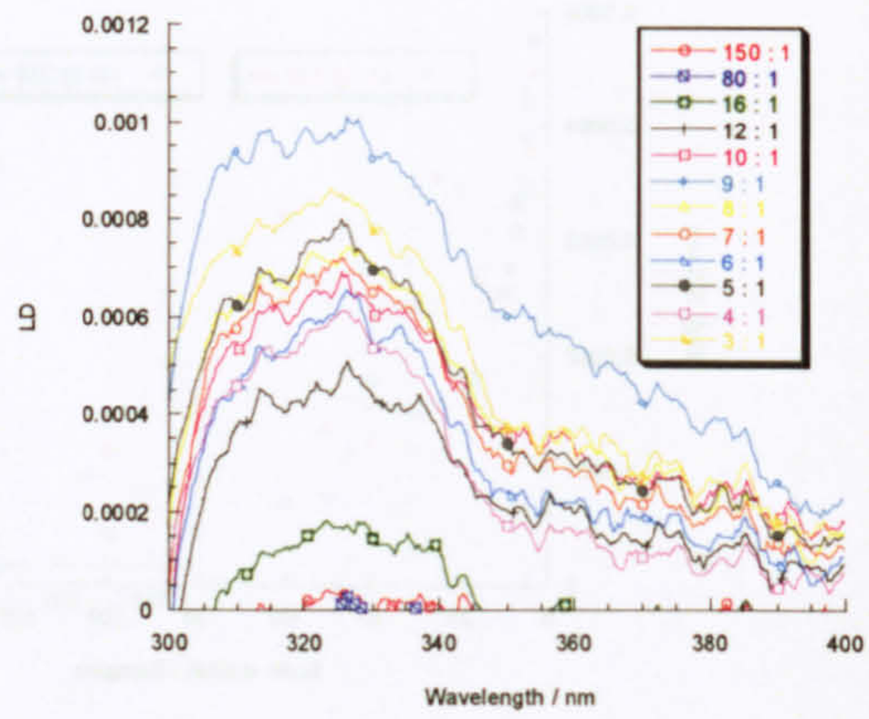

Figure A.12.14. The *LD* (A) and absorbance spectra (B) of CC-ET-6-Q and ct-DNA, the change of *LD* versus DNA : complex ratio (C) and the reduced *LD* (D). Experiment Two.

(A)

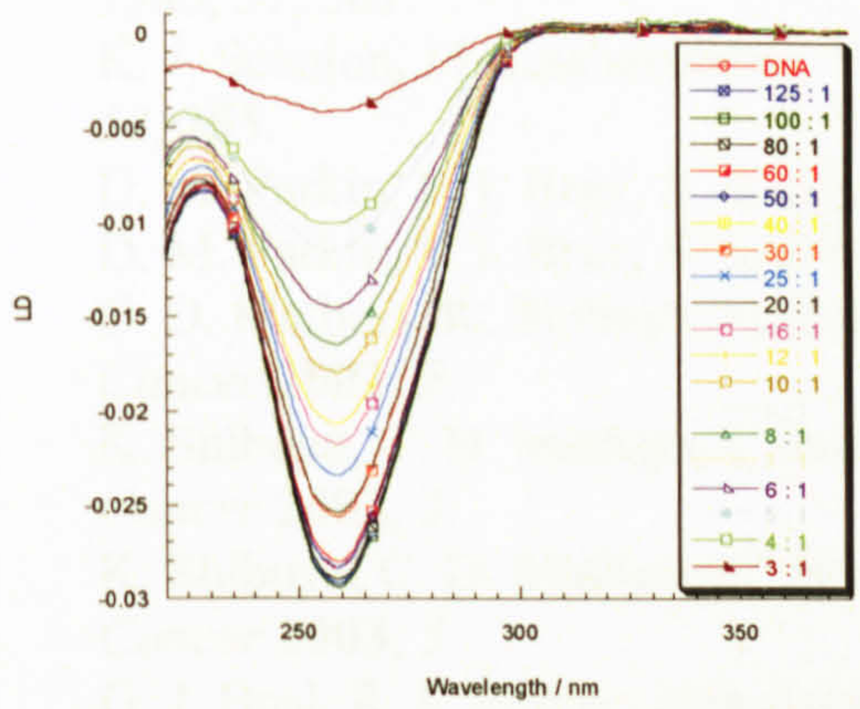

(B)

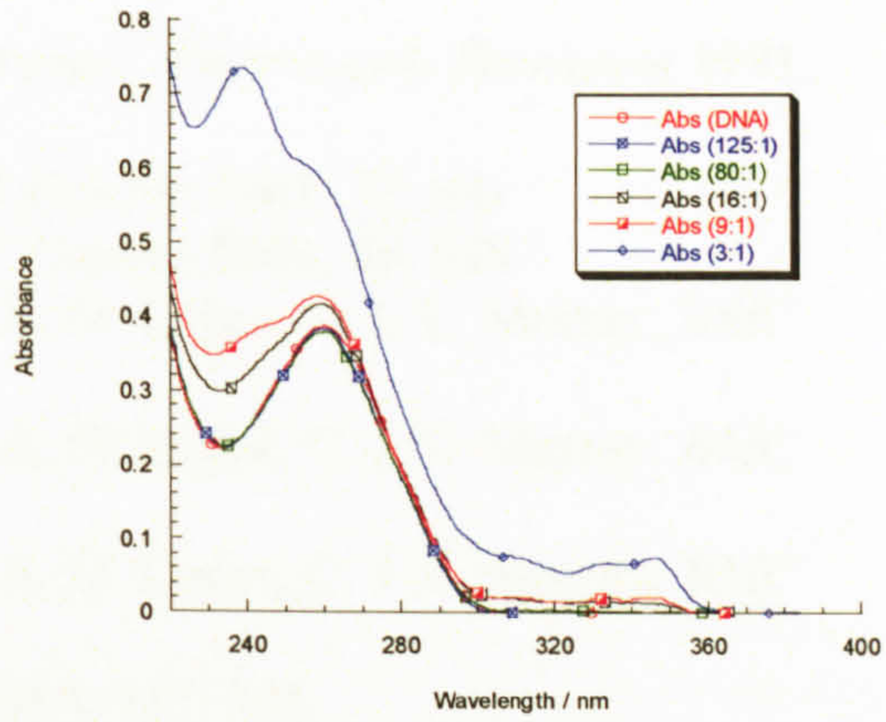

(C)

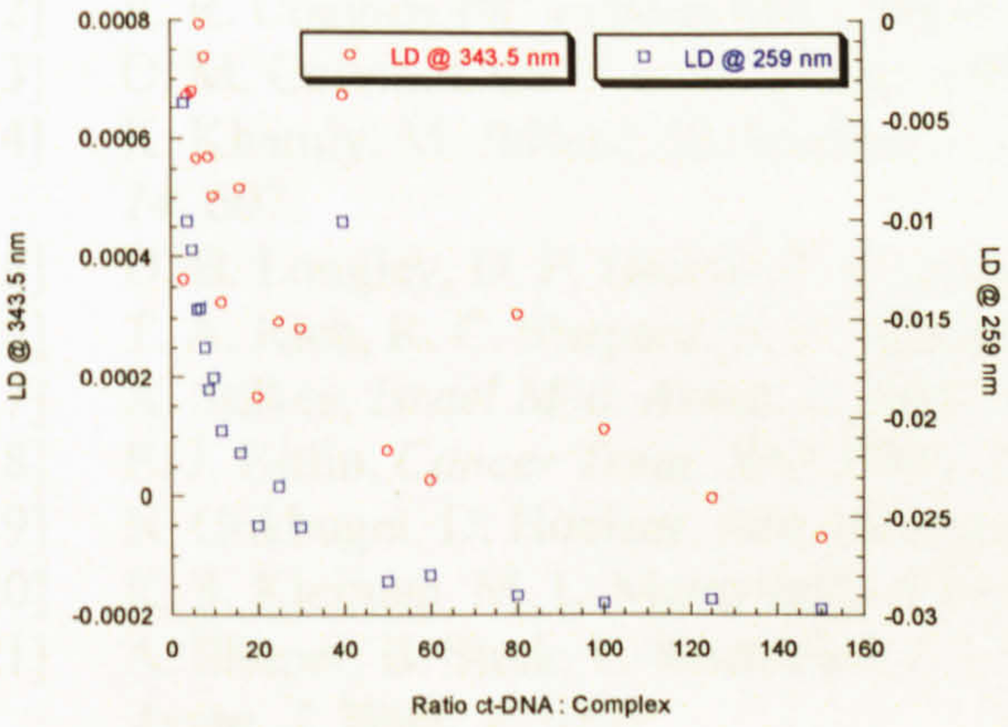

(D)

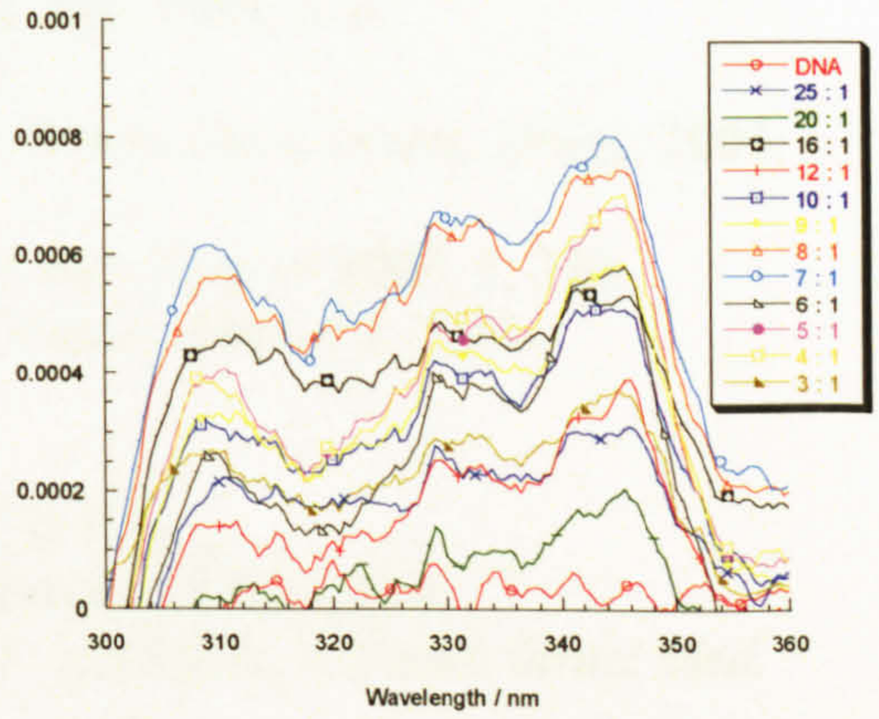

Figure A.12.15. The *LD* (A) and absorbance spectra (B) of TC-ET-4-IQ and ct-DNA, the change of *LD* versus DNA : complex ratio (C) and the reduced *LD* (D). Experiment Two.

BLANK IN ORIGINAL

References

[1] T. Boulikas, M. Vougiouka, *Oncol. Rep.* **2004**, *11*, 559.
[2] R. E. Taylor, W. Duncan, P. Davey, A. J. Munro, M. A. Cornbleet, *Brit. J. Urol.* **1985**, *57*, 567.
[3] K. J. Scanlon, M. Kashanisabet, T. Tone, T. Funato, *Pharmacol. Therapeut* **1991**, *52*, 385.
[4] D. M. Parkin, F. I. Bray, S. S. Devesa, *Eur. J. Cancer* **2001**, *37*, S4.
[5] D. M. Parkin, F. I. Bray, S. S. Devesa, *Eur. J. Cancer* **2003**, *39*, 848.
[6] C. D. Mathers, K. Shibuya, C. Boschi-Pinto, A. D. Lopez, C. J. L. Murray, *BMC Cancer* **2002**, *2*.
[7] K. Shibuya, C. D. Mathers, C. Boschi-Pinto, A. D. Lopez, C. J. L. Murray, *BMC Cancer* **2002**, *2*.
[8] K. Shibuya, C. D. Mathers, C. Boschi-Pinto, A. D. Lopez, C. J. L. Murray, *BMC Cancer* **2003**, *3*.
[9] G. J. Bosl, R. J. Motzer, *New Engl. J. Med.* **1997**, *337*, 242.
[10] M. J. Peckham, A. Barrett, K. H. Liew, A. Horwich, B. Robinson, H. J. Dobbs, T. J. McElwain, W. F. Hendry, *Brit. J. Cancer* **1983**, *47*, 613.
[11] P. C, *Melphalan, Therapeutic Drugs, Vol. 2*, Churchill Livingstone, London, UK, **1991**.
[12] R. R. Coggins PR, Eisman SH, *Cancer Chemoth. Rep.* **1959**, *3*, 9.
[13] O. M. Colvin, *Curr. Pharm. Design* **1999**, *5*, 555.
[14] K. Khamly, M. Jefford, M. Michael, J. Zalcberg, *Invest. Opin. Invest. Drugs.* **2005**, *14*, 607.
[15] D. B. Longley, D. P. Harkin, P. G. Johnston, *Nat. Rev. Cancer* **2003**, *3*, 330.
[16] T. A. Rich, R. C. Shepard, S. T. Mosley, *J. Clin. Oncol.* **2004**, *22*, 2214.
[17] A. Sulkes, *Israel Med. Assoc. J.* **2001**, *3*, 278.
[18] E. J. Estlin, *Cancer Treat. Rev.* **2001**, *27*, 351.
[19] N. Gokbuget, D. Hoelzer, *Ann. Hematol.* **1996**, *72*, 194.
[20] K. S. Kleiman, M. L. Mahowald, *JCR-J. Clin. Rheum.* **1998**, *4*, 254.
[21] A. Shuper, B. Stark, L. Kornreich, I. J. Cohen, G. Avrahami, I. Yaniv, *Israel Med. Assoc. J.* **2002**, *4*, 1050.
[22] G. H. Elgemeie, *Curr. Pharm. Design* **2003**, *9*, 2627.
[23] M. Schwab, K. Herrlinger, E. Schaeffeler, E. F. Stange, *Deutsche Med.* **2003**, *128*, 378.
[24] D. W. Sherer, M. G. Lebwohl, *J. Cutan. Med. Sur.* **2002**, *6*, 546.
[25] O. H. Nielsen, B. Vainer, J. Rask-Madsen, *Aliment. Pharm. Therap.* **2001**, *15*, 1699.
[26] C. Y. Su, G. R. Lichtenstein, *Gastro. Clin. N. Amer.* **2004**, *33*, 209.
[27] L. R. Huang, Y. Xie, J. W. Lown, *Exp. Opin. Therap. Pat.* **1996**, *6*, 893.
[28] U. Galm, M. H. Hager, S. G. Van Lanen, J. H. Ju, J. S. Thorson, B. Shen, *Chem. Rev.* **2005**, *105*, 739.
[29] S. M. Hecht, *J. Nat. Products* **2000**, *63*, 158.
[30] L. M. Mir, O. Tounekti, S. Orlowski, *Gen. Pharmcol.* **1996**, *27*, 745.
[31] J. Stubbe, J. W. Kozarich, *Chem. Rev.* **1987**, *87*, 1107.
[32] N. Sugiyama, T. Kumagai, *J. Biosci. Bioeng.* **2002**, *93*, 105.
[33] U. Hollstei, *Chem. Rev.* **1974**, *74*, 625.
[34] L. Gianni, B. J. Corden, C. E. Myers, *Rev. Biochem. Toxico.* **1983**, 1.
[35] R. C. Young, R. F. Ozols, C. E. Myers, *New. Engl. J. Med.* **1981**, *305*, 139.
[36] G. Fournier, A. Valeri, P. Mangin, O. Cussenot, *Ann. Urol.* **2004**, *38*, 225.
[37] S. Florio, U. Pagnini, A. Crispino, C. Pacilio, L. Crispino, A. Giordano, *Front. Biosci.* **2002**, *7*, D1590.

[38] H. J. Smith, P. J. Nicholls, C. Simons, R. Le Lain, *Exp. Opin. Therap. Pat.* **2001**, *11*, 789.
[39] C. Mahler, J. Verhelst, L. Denis, *Clin. Pharmacokinet.* **1998**, *34*, 405.
[40] F. M. J. Debruyne, G. A. Dijkman, *Euro. Urol.* **1995**, *28*, 177.
[41] M. Clemons, S. Danson, A. Howell, *Cancer Treat. Rev.* **2002**, *28*, 165.
[42] K. Dhingra, *Invest. New Drugs* **1999**, *17*, 285.
[43] V. C. Jordan, *Nat. Rev. Drug Discov.* **2003**, *2*, 205.
[44] R. M. O'Regan, V. C. Jordan, *Lancet Oncol.* **2002**, *3*, 207.
[45] M. J. McKeage, *Invest. Opin. Invest. Drugs.* **2005**, *14*, 1033.
[46] H. Zorbas, B. K. Keppler, *Chembiochem* **2005**, *6*, 1157.
[47] K. R. Barnes, S. J. Lippard, in *Metal Ions In Biolgical Systems, Vol 42: Metal Complexes In Tumor Diagnosis And As Anticancer Agents, Vol. 42*, **2004**, pp. 143.
[48] S. G. Chaney, S. L. Campbell, E. Bassett, Y. B. Wu, *Crit. Rev. Oncol. Hematol.* **2005**, *53*, 3.
[49] T. Boulikas, M. Vougiouka, *Oncol. Rep.* **2003**, *10*, 1663.
[50] M. Crul, R. van Waardenburg, J. H. Beijnen, J. H. M. Schellens, *Cancer Treat. Rev.* **2002**, *28*, 291.
[51] S. M. Cohen, S. J. Lippard, in *Prog. Nucleic. Acid. Re., Vol 67, Vol. 67*, **2001**, pp. 93.
[52] M. Peyrone, *Ann. Chem. Pharm.* **1844**, *51*, 1.
[53] B. Rosenberg, L. Van Camp, T. Krigas, *Nature* **1965**, *205*, 698.
[54] B. Rosenberg, L. Van Camp, E. B. Grimley, A. J. Thomson, *J. Biol. Chem.* **1967**, *40*, 1347.
[55] B. Rosenberg, L. Van Camp, J. E. Trosko, V. H. Mansour, *Nature* **1969**, *222*, 385.
[56] M. Dentino, F. C. Luft, M. N. Yum, S. D. Williams, L. H. Einhorn, *Cancer* **1978**, *41*, 1274.
[57] A. J. Lippman, C. Helson, L. Helson, I. H. Krakoff, *Cancer. Chemo. Rep. Part 1* **1973**, *57*, 191.
[58] A. H. Rossof, R. E. Slayton, C. P. Perlia, *Cancer* **1972**, *30*, 1451.
[59] I. J. Piel, C. P. Perlia, *Cancer. Chemo. Rep. Part 1* **1975**, *59*, 995.
[60] E. Cvitkovic, J. Spaulding, V. Bethune, J. Martin, W. F. Whitmore, *Cancer* **1977**, *39*, 1357.
[61] I. J. Piel, D. Meyer, C. P. Perlia, V. I. Wolfe, *Cancer. Chemo. Rep. Part 1* **1974**, *58*, 871.
[62] P. Richardson, B. M. J. Cantwell, *Brit. Med. J.* **1990**, *300*, 1466.
[63] A. Greenspan, J. Treat, *American J. Clin. Oncol.-Cancer Clin. Trials* **1988**, *11*, 660.
[64] Y. Ostchega, M. Donohue, N. Fox, *Cancer Nurs.* **1988**, *11*, 23.
[65] M. Pages, A. M. Pages, L. Boriesazeau, *J. Neurol. Neuros. Ps.* **1986**, *49*, 333.
[66] S. W. Thompson, L. E. Davis, M. Kornfeld, R. D. Hilgers, J. C. Standefer, *Cancer* **1984**, *54*, 1269.
[67] R. I. Roelofs, W. Hrushesky, J. Rogin, L. Rosenberg, *Neurology* **1984**, *34*, 934.
[68] C. S. Rosenfeld, L. E. Broder, *Cancer Treat. Rep.* **1984**, *68*, 659.
[69] H. Lajer, G. Daugaard, *Cancer Treat. Rev.* **1999**, *25*, 47.
[70] C. Gonzalez, U. Villasanta, *Obs. Gynecol.* **1982**, *59*, 732.
[71] D. L. Bodenner, P. C. Dedon, P. C. Keng, R. F. Borch, *Cancer Res.* **1986**, *46*, 2745.
[72] R. C. Manaka, W. Wolf, *Chem-Biol. Interact.* **1978**, *22*, 353.
[73] J. J. Gullo, C. L. Litterst, P. J. Maguire, B. I. Sikic, D. F. Hoth, P. V. Woolley, *Cancer Chemoth. Pharm.* **1980**, *5*, 21.
[74] S. J. Bannister, L. A. Sternson, A. J. Repta, G. W. James, *Clin. Chem.* **1977**, *23*, 2258.
[75] W. C. Cole, W. Wolf, *Chem-Biol. Interact.* **1980**, *30*, 223.
[76] L. Hegedus, W. J. F. Vandervijgh, I. Klein, S. Kerpelfronius, H. M. Pinedo, *Cancer Chemoth. Pharm.* **1987**, *20*, 211.

[77] J. L. Aull, R. L. Allen, A. R. Bapat, H. H. Daron, M. E. Friedman, J. F. Wilson, *Biochim. Biophys. Acta* **1979**, *571*, 352.
[78] H. H. Zeng, Z. H. Xu, K. Wang, *Inter. J. Biol. Macromol.* **1997**, *20*, 107.
[79] S. V. Pizzo, M. W. Swaim, P. A. Roche, S. L. Gonias, *J. Inorg. Biochem.* **1988**, *33*, 67.
[80] A. I. Ivanov, J. Christodoulou, J. A. Parkinson, K. J. Barnham, A. Tucker, J. Woodrow, P. J. Sadler, *J. Biol. Chem.* **1998**, *273*, 14721.
[81] A. Eastman, *Chem-Biol. Interact.* **1987**, *61*, 241.
[82] S. Vanboom, J. Reedijk, *J. Chem. Soc. Chem. Comm.* **1993**, 1397.
[83] Y. Chen, Z. J. Guo, P. D. Murdoch, E. L. Zang, P. J. Sadler, *J. Chem. Soc. Dalton. Trans.* **1998**, 1503.
[84] J. M. Teuben, S. vanBoom, J. Reedijk, *J. Chem. Soc. Dalton. Trans.* **1997**, 3979.
[85] K. J. Barnham, Z. J. Guo, P. J. Sadler, *J. Chem. Soc. Dalton. Trans.* **1996**, 2867.
[86] G. Speelmans, W. Sips, R. J. H. Grisel, R. Staffhorst, A. M. J. FichtingerSchepman, J. Reedijk, B. deKruijff, *Biochim. Biophys. Acta-Biomembranes* **1996**, *1283*, 60.
[87] G. Speelmans, R. Staffhorst, K. Versluis, J. Reedijk, B. deKruijff, *Biochemistry* **1997**, *36*, 10545.
[88] R. A. Hromas, J. A. North, C. P. Burns, *Cancer Lett.* **1987**, *36*, 197.
[89] G. R. Gale, C. R. Morris, L. M. Atkins, A. B. Smith, *Cancer Res.* **1973**, *33*, 813.
[90] S. P. Binks, M. Dobrota, *Biochem. Pharmacol.* **1990**, *40*, 1329.
[91] L. R. Kelland, P. Mistry, G. Abel, S. Y. Loh, C. F. Oneill, B. A. Murrer, K. R. Harrap, *Cancer Res.* **1992**, *52*, 3857.
[92] S. C. Mann, P. A. Andrews, S. B. Howell, *Cancer Chemoth. Pharm.* **1990**, *25*, 236.
[93] S. Ishida, J. Lee, D. J. Thiele, I. Herskowitz, *Proc. Natl. Acac. Sci. U.S.A.* **2002**, *99*, 14298.
[94] X. J. Lin, T. Okuda, A. Holzer, S. B. Howell, *Mol. Pharmacol.* **2002**, *62*, 1154.
[95] X. Lin, T. Okuda, A. Holzer, S. B. Howell, *Mol. Pharmacol.* **2003**, *63*, 957.
[96] G. L. Beretta, L. Gatti, S. Tinelli, E. Corna, D. Colangelo, F. Zunino, P. Perego, *Biochem. Pharmacol.* **2004**, *68*, 283.
[97] G. Samimi, R. Safaei, K. Katano, A. K. Holzer, M. Rochdi, M. Tomioka, M. Goodman, S. B. Howell, *Clin. Cancer Res.* **2004**, *10*, 4661.
[98] G. Samimi, K. Katano, A. K. Holzer, R. Safaei, S. B. Howell, *Mol. Pharmacol.* **2004**, *66*, 25.
[99] K. Katano, R. Safaei, G. Samimi, A. Holzer, M. Tomioka, M. Goodman, S. B. Howell, *Clin. Cancer Res.* **2004**, *10*, 4578.
[100] H. Miyashita, Y. Nitta, S. Mori, A. Kanzaki, K. Nakayama, K. Terada, T. Sugiyama, H. Kawamura, A. Sato, H. Morikawa, K. Motegi, Y. Takebayashi, *Oral Oncol.* **2003**, *39*, 157.
[101] K. Nakayama, A. Kanzaki, K. Ogawa, K. Miyazaki, N. Neamati, Y. Takebayashi, *Int. J. Cancer* **2002**, *101*, 488.
[102] K. Nakayama, K. Miyazaki, A. Kanzaki, M. Fukumoto, Y. Takebayashi, *Oncol. Rep.* **2001**, *8*, 1285.
[103] M. Komatsu, T. Sumizawa, M. Mutoh, Z. S. Chen, K. Terada, T. Furukawa, X. L. Yang, H. Gao, N. Miura, T. Sugiyama, S. Akiyama, *Cancer Res.* **2000**, *60*, 1312.
[104] E. M. Witkin, *P. Natl. Acad. Sci. U.S.A.*. **1967**, *57*, 1275.
[105] J. M. Pascoe, J. J. Roberts, *Biochem. Pharmacol.* **1974**, *23*, 1345.
[106] J. A. Howle, G. R. Gale, *Biochem. Pharmacol.* **1970**, *19*, 2757.
[107] H. C. Harder, B. Rosenberg, *Int. J. Cancer* **1970**, *6*, 207.
[108] F. J. Dijt, A. M. J. Fichtingerschepman, F. Berends, J. Reedijk, *Cancer Res.* **1988**, *48*, 6058.
[109] H. N. A. Fraval, C. J. Rawlings, J. J. Roberts, *Mutat. Res.* **1978**, *51*, 121.
[110] N. P. Johnson, J. D. Hoeschele, R. O. Rahn, J. P. Oneill, A. W. Hsie, *Cancer Res.* **1980**, *40*, 1463.
[111] R. E. Meyn, S. F. Jenkins, L. H. Thompson, *Cancer Res.* **1982**, *42*, 3106.

[112] D. J. Beck, R. R. Brubaker, *J. Bacteriology* **1973**, *116*, 1247.
[113] S. C. Popoff, D. J. Beck, W. D. Rupp, *Mutat. Res.* **1987**, *183*, 129.
[114] R. Alazard, M. Germanier, N. P. Johnson, *Mutat. Res.* **1982**, *93*, 327.
[115] D. J. Beck, S. Popoff, A. Sancar, W. D. Rupp, *Nucl. Acids Res.* **1985**, *13*, 7395.
[116] J. Brouwer, P. Vandeputte, A. M. J. Fichtingerschepman, J. Reedijk, *P. Natl. Acad. Sci. U.S.A.-Biol. Sci.* **1981**, *78*, 7010.
[117] J. Drobnik, Urbankov.M, Krekulov.A, *Mutat. Res.* **1973**, *17*, 13.
[118] R. J. Fram, P. S. Cusick, J. M. Wilson, M. G. Marinus, *Mol. Pharmacol.* **1985**, *28*, 51.
[119] B. E. Markham, R. R. Brubaker, *J. Bacteriology* **1980**, *143*, 455.
[120] L. J. K. Boerner, J. M. Zaleski, *Curr. Opin. Chem. Biol.* **2005**, *9*, 135.
[121] C. Metcalfe, J. A. Thomas, *Chem. Soc. Rev.* **2003**, *32*, 215.
[122] V. G. Bregadze, in *Metal Ions In Biological Systems, Vol 32, Vol. 32*, **1996**, pp. 419.
[123] P. Horacek, J. Drobnik, *Biochim. Biophys. Acta* **1971**, *254*, 341.
[124] P. J. Stone, A. D. Kelman, F. M. Sinex, *Nature* **1974**, *251*, 736.
[125] J. P. Macquet, T. Theophanides, *Bioinorg. Chem.* **1975**, *5*, 59.
[126] L. L. Munchausen, R. O. Rahn, *Biochim. Biophys. Acta* **1975**, *414*, 242.
[127] H. M. Ushay, T. D. Tullius, S. J. Lippard, *Biochemistry* **1981**, *20*, 3744.
[128] G. L. Cohen, J. A. Ledner, W. R. Bauer, H. M. Ushay, C. Caravana, S. J. Lippard, *J. Am. Chem. Soc.* **1980**, *102*, 2487.
[129] B. Royerpokora, L. K. Gordon, W. A. Haseltine, *Nucl. Acids Res.* **1981**, *9*, 4595.
[130] T. D. Tullius, S. J. Lippard, *J. Am. Chem. Soc.* **1981**, *103*, 4620.
[131] B. Reiner, S. Zamenhof, *J. Biol. Chem.* **1957**, *225*, 475.
[132] A. M. J. Fichtingerschepman, P. H. M. Lohman, J. Reedijk, *Nucl. Acids Res.* **1982**, *10*, 5345.
[133] A. M. J. Fichtingerschepman, J. L. Vanderveer, J. H. J. Denhartog, P. H. M. Lohman, J. Reedijk, *Biochemistry* **1985**, *24*, 707.
[134] A. B. Robins, *Chem-Biol. Interact.* **1973**, *6*, 35.
[135] P. C. Kong, Theophan.T, *Inorg. Chem.* **1974**, *13*, 1981.
[136] A. B. Robins, *Chem-Biol. Interact.* **1973**, *7*, 11.
[137] S. Mansy, G. Y. H. Chu, R. E. Duncan, R. S. Tobias, *J. Am. Chem. Soc.* **1978**, *100*, 607.
[138] P. C. Kong, Theophan.T, *Inorg. Chem.* **1974**, *13*, 1167.
[139] A. Eastman, *Biochemistry* **1982**, *21*, 6732.
[140] U. Warnke, C. Rappel, H. Meier, C. Kloft, M. Galanski, C. G. Hartinger, B. K. Keppler, U. Jaehde, *Chembiochem* **2004**, *5*, 1543.
[141] S. Hann, A. Zenker, M. Galanski, T. L. Bereuter, G. Stingeder, B. K. Keppler, *Fres. J. Anal. Chem.* **2001**, *370*, 581.
[142] K. Inagaki, Y. Kidani, *J. Inorg. Biochem.* **1979**, *11*, 39.
[143] A. Eastman, *Biochemistry* **1983**, *22*, 3927.
[144] A. Eastman, *P. Am. Assoc. Canc. Res.* **1984**, *25*, 367.
[145] A. Eastman, *Biochemistry* **1986**, *25*, 3912.
[146] J. L. Vanderveer, H. Vandenelst, J. H. J. Denhartog, A. M. J. Fichtingerschepman, J. Reedijk, *Inorg. Chem.* **1986**, *25*, 4657.
[147] J. J. Roberts, F. Friedlos, *Biochim. Biophys. Acta* **1981**, *655*, 146.
[148] A. Eastman, *Biochemistry* **1985**, *24*, 5027.
[149] L. A. Zwelling, K. W. Kohn, W. E. Ross, R. A. G. Ewig, T. Anderson, *Cancer Res.* **1978**, *38*, 1762.
[150] A. C. M. Plooy, A. M. J. Fichtingerschepman, H. H. Schutte, M. Vandijk, P. H. M. Lohman, *Carcinogenesis* **1985**, *6*, 561.
[151] M. C. Poirier, S. J. Lippard, L. A. Zwelling, H. M. Ushay, D. Kerrigan, C. C. Thill, R. M. Santella, D. Grunberger, S. H. Yuspa, *P. Natl. Acad. Sci. U.S.A.-Biol.* **1982**, *79*, 6443.

[152] A. M. J. Fichtingerschepman, R. A. Baan, A. Luitenschuite, M. Vandijk, P. H. M. Lohman, *Chem-Biol. Interact.* **1985**, *55*, 275.
[153] A. M. J. Fichtingerschepman, S. D. Vanderveldevisser, H. C. M. Vandijkknijnenburg, A. T. Vanoosterom, R. A. Baan, F. Berends, *Cancer Res.* **1990**, *50*, 7887.
[154] A. M. J. Fichtingerschepman, A. T. Vanoosterom, P. H. M. Lohman, F. Berends, *Cancer Res.* **1987**, *47*, 3000.
[155] E. Reed, Y. Ostchega, S. M. Steinberg, S. H. Yuspa, R. C. Young, R. F. Ozols, M. C. Poirier, *Cancer Res.* **1990**, *50*, 2256.
[156] E. Reed, R. F. Ozols, R. Tarone, S. H. Yuspa, M. C. Poirier, *P. Natl. Acad. Sci. U.S.A.*. **1987**, *84*, 5024.
[157] M. C. Poirier, E. Reed, R. F. Ozols, T. Fasy, S. H. Yuspa, *Prog. Exp. Tumor Res.* **1987**, *31*, 104.
[158] L. A. Zwelling, M. O. Bradley, N. A. Sharkey, T. Anderson, K. W. Kohn, *Mutat. Res.* **1979**, *67*, 271.
[159] L. A. Zwelling, T. Anderson, K. W. Kohn, *Cancer Res.* **1979**, *39*, 365.
[160] S. E. Sherman, D. Gibson, A. H. J. Wang, S. J. Lippard, *Science* **1985**, *230*, 412.
[161] S. E. Sherman, D. Gibson, A. H. J. Wang, S. J. Lippard, *J. Am. Chem. Soc.* **1988**, *110*, 7368.
[162] N. Poklar, D. S. Pilch, S. J. Lippard, E. A. Redding, S. U. Dunham, K. J. Breslauer, *P. Natl. Acad. Sci. U.S.A.*. **1996**, *93*, 7606.
[163] G. Admiraal, J. L. Vanderveer, R. A. G. Degraaff, J. H. J. Denhartog, J. Reedijk, *J. Am. Chem. Soc.* **1987**, *109*, 592.
[164] B. Vanhemelryck, E. Guittet, G. Chottard, J. P. Girault, F. Herman, T. Huynhdinh, J. Y. Lallemand, J. Igolen, J. C. Chottard, *Biochem. Bioph. Res. Co.* **1986**, *138*, 758.
[165] B. Vanhemelryck, J. P. Girault, G. Chottard, P. Valadon, A. Laoui, J. C. Chottard, *Inorg. Chem.* **1987**, *26*, 787.
[166] W. I. Sundquist, S. J. Lippard, B. D. Stollar, *P. Natl. Acad. Sci. U.S.A.*. **1987**, *84*, 8225.
[167] A. Schwartz, L. Marrot, M. Leng, *Biochemistry* **1989**, *28*, 7975.
[168] P. M. Takahara, C. A. Frederick, S. J. Lippard, *J. Am. Chem. Soc.* **1996**, *118*, 12309.
[169] P. M. Takahara, A. C. Rosenzweig, C. A. Frederick, S. J. Lippard, *Nature* **1995**, *377*, 649.
[170] A. Gelasco, S. J. Lippard, *Biochemistry* **1998**, *37*, 9230.
[171] S. U. Dunham, S. U. Dunham, C. J. Turner, S. J. Lippard, *J. Am. Chem. Soc.* **1998**, *120*, 5395.
[172] D. Z. Yang, S. Vanboom, J. Reedijk, J. H. Vanboom, A. H. J. Wang, *Biochemistry* **1995**, *34*, 12912.
[173] D. Tsankov, B. Kalisch, H. V. de Sande, H. Wieser, *J. Phys. Chem. B* **2003**, *107*, 6479.
[174] F. Herman, J. Kozelka, V. Stoven, E. Guittet, J. P. Girault, T. Huynhdinh, J. Igolen, J. Y. Lallemand, J. C. Chottard, *Eur. J. Biochem.* **1990**, *194*, 119.
[175] J. Kozelka, S. Archer, G. A. Petsko, S. J. Lippard, G. J. Quigley, *Biopolymers* **1987**, *26*, 1245.
[176] J. Kozelka, J. C. Chottard, *Biophys. Chem.* **1990**, *35*, 165.
[177] J. Kozelka, G. A. Petsko, S. J. Lippard, G. J. Quigley, *J. Am. Chem. Soc.* **1985**, *107*, 4079.
[178] J. Kozelka, G. A. Petsko, G. J. Quigley, S. J. Lippard, *Inorg. Chem.* **1986**, *25*, 1075.
[179] J. A. Rice, D. M. Crothers, A. L. Pinto, S. J. Lippard, *P. Natl. Acad. Sci. U.S.A.*. **1988**, *85*, 4158.
[180] S. F. Bellon, S. J. Lippard, *Biophys. Chem.* **1990**, *35*, 179.
[181] M. F. Anin, M. Leng, *Nucl. Acids Res.* **1990**, *18*, 4395.

[182] J. M. Teuben, C. Bauer, A. H. J. Wang, J. Reedijk, *Biochemistry* **1999**, *38*, 12305.
[183] C. J. Vangarderen, L. P. A. Vanhoute, *Eur. J. Biochem.* **1994**, *225*, 1169.
[184] F. Coste, J. M. Malinge, L. Serre, W. Shepard, M. Roth, M. Leng, C. Zelwer, *Nucl. Acids Res.* **1999**, *27*, 1837.
[185] F. Paquet, C. Perez, M. Leng, G. Lancelot, J. M. Malinge, *J. Biomol. Struct. Dyn.* **1996**, *14*, 67.
[186] H. F. Huang, L. M. Zhu, B. R. Reid, G. P. Drobny, P. B. Hopkins, *Science* **1995**, *270*, 1842.
[187] M. Sip, A. Schwartz, F. Vovelle, M. Ptak, M. Leng, *Biochemistry* **1992**, *31*, 2508.
[188] J. M. Malinge, C. Perez, M. Leng, *Nucl. Acids Res.* **1994**, *22*, 3834.
[189] A. T. M. Marcelis, J. H. J. Denhartog, G. A. Vandermarel, G. Wille, J. Reedijk, *Eur. J. Biochem.* **1983**, *135*, 343.
[190] J. H. J. Denhartog, C. Altona, H. Vandenelst, G. A. Vandermarel, J. Reedijk, *Inorg. Chem.* **1985**, *24*, 983.
[191] L. Marrot, M. Leng, *Biochemistry* **1989**, *28*, 1454.
[192] A. Eastman, M. M. Jennerwein, D. L. Nagel, *Chem-Biol. Interact.* **1988**, *67*, 71.
[193] P. J. Stone, A. D. Kelman, F. M. Sinex, M. M. Bhargava, H. O. Halvorson, *J. Mol. Biol.* **1976**, *104*, 793.
[194] A. Eastman, M. A. Barry, *Biochemistry* **1987**, *26*, 3303.
[195] K. M. Comess, C. E. Costello, S. J. Lippard, *Biochemistry* **1990**, *29*, 2102.
[196] R. Dalbies, M. Boudvillain, M. Leng, *Nucl. Acids Res.* **1995**, *23*, 949.
[197] R. Dalbies, D. Payet, M. Leng, *P. Natl. Acad. Sci. U.S.A..* **1994**, *91*, 8147.
[198] C. A. Lepre, K. G. Strothkamp, S. J. Lippard, *Biochemistry* **1987**, *26*, 5651.
[199] D. Gibson, S. J. Lippard, *Inorg. Chem.* **1987**, *26*, 2275.
[200] O. Krizanovic, F. J. Pesch, B. Lippert, *Inorg. Chim. Acta* **1989**, *165*, 145.
[201] F. J. Pesch, M. Wienken, H. Preut, A. Tenten, B. Lippert, *Inorg. Chim. Acta* **1992**, *197*, 243.
[202] M. Boudvillain, R. Dalbies, C. Aussourd, M. Leng, *Nucl. Acids Res.* **1995**, *23*, 2381.
[203] C. A. Lepre, L. Chassot, C. E. Costello, S. J. Lippard, *Biochemistry* **1990**, *29*, 811.
[204] V. Brabec, M. Leng, *P. Natl. Acad. Sci. U.S.A..* **1993**, *90*, 5345.
[205] V. Brabec, M. Sip, M. Leng, *Biochemistry* **1993**, *32*, 11676.
[206] F. Paquet, M. Boudvillain, G. Lancelot, M. Leng, *Nucl. Acids Res.* **1999**, *27*, 4261.
[207] C. Hofr, V. Brabec, *Biopolymers* **2005**, *77*, 222.
[208] C. Hofr, V. Brabec, *J. Biol. Chem.* **2001**, *276*, 9655.
[209] J. Drobnik, P. Horacek, *Chem-Biol. Interact.* **1973**, *7*, 223.
[210] J. A. Howle, A. B. Smith, G. R. Gale, *Biochem. Pharmacol.* **1972**, *21*, 1465.
[211] N. P. Johnson, J. D. Hoeschele, R. O. Rahn, *Chem-Biol. Interact.* **1980**, *30*, 151.
[212] D. P. Bancroft, C. A. Lepre, S. J. Lippard, *J. Am. Chem. Soc.* **1990**, *112*, 6860.
[213] J. Kozelka, F. Legendre, F. Reeder, J. C. Chottard, *Coord. Chem. Rev.* **1999**, *192*, 61.
[214] M. Jennerwein, P. A. Andrews, *Drug Metab. Dispol.* **1995**, *23*, 178.
[215] M. Jennerwein, P. A. Andrews, *Cancer Lett.* **1994**, *81*, 215.
[216] M. F. Pera, C. J. Rawlings, J. J. Roberts, *Chem-Biol. Interact.* **1981**, *37*, 245.
[217] F. Oshita, A. Eastman, *Oncol. Res.* **1993**, *5*, 111.
[218] N. P. Johnson, J. D. Hoeschele, N. B. Kuemmerle, W. E. Masker, R. O. Rahn, *Chem-Biol. Interact.* **1978**, *23*, 267.
[219] H. C. Harder, R. G. Smith, A. F. Leroy, *Cancer Res.* **1976**, *36*, 3821.
[220] A. L. Pinto, S. J. Lippard, *P. Natl. Acad. Sci. U.S.A..* **1985**, *82*, 4616.
[221] J. D. Gralla, S. Sassedwight, L. G. Poljak, *Cancer Res.* **1987**, *47*, 5092.
[222] G. Villani, U. Hubscher, J. L. Butour, *Nucl. Acids Res.* **1988**, *16*, 4407.
[223] J. S. Hoffmann, N. P. Johnson, G. Villani, *J. Biol. Chem.* **1989**, *264*, 15130.
[224] K. M. Comess, J. N. Burstyn, J. M. Essigmann, S. J. Lippard, *Biochemistry* **1992**, *31*, 3975.

[225] C. M. Sorenson, A. Eastman, *Cancer Res.* **1988**, *48*, 6703.
[226] C. M. Sorenson, A. Eastman, *Cancer Res.* **1988**, *48*, 4484.
[227] B. Salles, J. L. Butour, C. Lesca, J. P. Macquet, *Biochem. Bioph. Res. Co.* **1983**, *112*, 555.
[228] S. Doublie, S. Tabor, A. M. Long, C. C. Richardson, T. Ellenberger, *Nature* **1998**, *391*, 251.
[229] Y. Corda, C. Job, M. F. Anin, M. Leng, D. Job, *Biochemistry* **1991**, *30*, 222.
[230] Y. Corda, M. F. Anin, M. Leng, D. Job, *Biochemistry* **1992**, *31*, 1904.
[231] C. Cullinane, S. J. Mazur, J. M. Essigmann, D. R. Phillips, V. A. Bohr, *Biochemistry* **1999**, *38*, 6204.
[232] S. Tornaletti, S. M. Patrick, J. J. Turchi, P. C. Hanawalt, *J. Biol. Chem.* **2003**, *278*, 35791.
[233] Y. W. Jung, S. J. Lippard, *J. Biol. Chem.* **2003**, *278*, 52084.
[234] J. A. Mello, S. J. Lippard, J. M. Essigmann, *Biochemistry* **1995**, *34*, 14783.
[235] M. Gniazdowski, W. A. Denny, S. M. Nelson, M. Czyz, *Expert. Opin. Ther. Tar.* **2005**, *9*, 471.
[236] M. Gniazdowski, W. A. Denny, S. M. Nelson, M. Czyz, *Curr. Med. Chem.* **2003**, *10*, 909.
[237] W. Dempke, W. Voigt, A. Grothey, B. T. Hill, H. J. Schmoll, *Anticancer Drugs* **2000**, *11*, 225.
[238] C. G. Ferreira, C. Tolis, G. Giaccone, *Ann. Oncol.* **1999**, *10*, 1011.
[239] K. J. Scanlon, M. Kashanisabet, H. Miyachi, *Cancer Inves.* **1989**, *7*, 581.
[240] D. Hanahan, R. A. Weinberg, *Cell* **2000**, *100*, 57.
[241] J. Searle, J. F. R. Kerr, C. J. Bishop, *Pathol. Annu.* **1982**, *17*, 229.
[242] S. W. Fesik, *Nat. Rev. Cancer* **2005**, *5*, 876.
[243] A. Eastman, in *Cisplatin. Chemistry and Biochemistry of a Leading Anticancer Drug* (Ed.: B. Lippert), Wiley-VCH, Basel, **1999**, pp. 111.
[244] V. M. Gonzalez, M. A. Fuertes, C. Alonso, J. M. Perez, *Mol. Pharmacol.* **2001**, *59*, 657.
[245] K. M. Henkels, J. J. Turchi, *Cancer Res.* **1999**, *59*, 3077.
[246] J. Zlatanova, J. Yaneva, S. H. Leuba, *FASEB J.* **1998**, *12*, 791.
[247] G. Chu, *J. Biol. Chem.* **1994**, *269*, 787.
[248] Z. H. Siddik, *Oncogene* **2003**, *22*, 7265.
[249] M. Kartalou, J. M. Essigmann, *Mut. Res-Fund. Mol. M.* **2001**, *478*, 23.
[250] C. X. Zhang, P. V. Chang, S. J. Lippard, *J. Am. Chem. Soc.* **2004**, *126*, 6536.
[251] D. B. Zamble, S. J. Lippard, *Trends Biochem. Sci.* **1995**, *20*, 435.
[252] E. R. Jamieson, S. J. Lippard, *Chem. Rev.* **1999**, *99*, 2467.
[253] D. Mu, D. S. Hsu, A. Sancar, *J. Biol. Chem.* **1996**, *271*, 8285.
[254] J. T. Reardon, A. Sancar, in *Prog. Nucleic. Acid. Re. Vol. 79*, **2005**, pp. 183.
[255] A. Sancar, L. A. Lindsey-Boltz, K. Unsal-Kacmaz, S. Linn, *Ann. Rev. Biochem.* **2004**, *73*, 39.
[256] R. C. A. van Waardenburg, L. A. de Jong, F. van Delft, M. A. J. van Eijndhoven, M. Bohlander, M. A. Bjornsti, J. Brouwer, J. H. M. Schellens, *Mol. Cancer Ther.* **2004**, *3*, 393.
[257] V. Beljanski, L. G. Marzilli, P. W. Doetsch, *Mol. Pharmacol.* **2004**, *65*, 1496.
[258] J. A. Simon, P. Szankasi, D. K. Nguyen, C. Ludlow, H. M. Dunstan, C. J. Roberts, E. L. Jensen, L. H. Hartwell, S. H. Friend, *Cancer Res.* **2000**, *60*, 328.
[259] L. J. Barber, T. A. Ward, J. A. Hartley, P. J. McHugh, *Mol. Cell Biol.* **2005**, *25*, 2297.
[260] R. Reeves, J. E. Adair, *DNA Repair* **2005**, *4*, 926.
[261] M. E. Bianchi, A. Agresti, *Curr. Opin. Gen. Devel.* **2005**, *15*, 496.
[262] M. Bustin, *Trends Biochem. Sci.* **2001**, *26*, 431.
[263] R. Reeves, L. Beckerbauer, *BBA-Gen. Struct. Expr.* **2001**, *1519*, 13.

[264] P. C. Billings, R. J. Davis, B. N. Engelsberg, K. A. Skov, E. N. Hughes, *Biochem. Bioph. Res. Co.* **1992**, *188*, 1286.
[265] E. N. Hughes, B. N. Engelsberg, P. C. Billings, *J. Biol. Chem.* **1992**, *267*, 13520.
[266] P. M. Pil, S. J. Lippard, *Science* **1992**, *256*, 234.
[267] J. J. Turchi, M. Li, K. M. Henkels, *Biochemistry* **1996**, *35*, 2992.
[268] U. M. Ohndorf, M. A. Rould, Q. He, C. O. Pabo, S. J. Lippard, *Nature* **1999**, *399*, 708.
[269] E. Martz, *Trends Biochem. Sci.* **2002**, *27*, 107.
[270] D. E. Szymkowski, K. Yarema, J. M. Essigmann, S. J. Lippard, R. D. Wood, *P. Natl. Acad. Sci. U.S.A.*. **1992**, *89*, 10772.
[271] J. G. Moggs, D. E. Szymkowski, M. Yamada, P. Karran, R. D. Wood, *Nucl. Acids Res.* **1997**, *25*, 480.
[272] D. B. Zamble, D. Mu, J. T. Reardon, A. Sancar, S. J. Lippard, *Biochemistry* **1996**, *35*, 10004.
[273] S. J. Brown, P. J. Kellett, S. J. Lippard, *Science* **1993**, *261*, 603.
[274] J. C. Huang, D. B. Zamble, J. T. Reardon, S. J. Lippard, A. Sancar, *P. Natl. Acad. Sci. U.S.A.*. **1994**, *91*, 10394.
[275] T. A. Kunkel, D. A. Erie, *Ann. Rev. Biochem.* **2005**, *74*, 681.
[276] D. R. Duckett, J. T. Drummond, A. I. H. Murchie, J. T. Reardon, A. Sancar, D. M. Lilley, P. Modrich, *P. Natl. Acad. Sci. U.S.A.*. **1996**, *93*, 6443.
[277] J. A. Mello, S. Acharya, R. Fishel, J. M. Essigmann, *Chem. Biol.* **1996**, *3*, 579.
[278] D. Fink, H. Zheng, S. Nebel, P. S. Norris, S. Aebi, T. P. Lin, A. Nehme, R. D. Christen, M. Haas, C. L. MacLeod, S. B. Howell, *Cancer Res.* **1997**, *57*, 1841.
[279] J. T. Drummond, A. Anthoney, R. Brown, P. Modrich, *J. Biol. Chem.* **1996**, *271*, 19645.
[280] S. Aebi, B. KurdiHaidar, R. Gordon, B. Cenni, H. Zheng, D. Fink, R. D. Christen, C. R. Boland, M. Koi, R. Fishel, S. B. Howell, *Cancer Res.* **1996**, *56*, 3087.
[281] A. B. Buermeyer, S. M. Deschenes, S. M. Baker, R. M. Liskay, *Annu. Rev. Genet.* **1999**, *33*, 533.
[282] P. Modrich, *J. Biol. Chem.* **1997**, *272*, 24727.
[283] A. Nehme, R. Baskaran, S. Aebi, D. Fink, S. Nebel, B. Cenni, J. Y. J. Wang, S. B. Howell, R. D. Christen, *Cancer Res.* **1997**, *57*, 3253.
[284] A. Nehme, R. Baskaran, S. Nebel, D. Fink, S. B. Howell, J. Y. J. Wang, R. D. Christen, *Brit. J. Cancer* **1999**, *79*, 1104.
[285] A. Vaisman, M. Varchenko, A. Umar, T. A. Kunkel, J. I. Risinger, J. C. Barrett, T. C. Hamilton, S. G. Chaney, *Cancer Res.* **1998**, *58*, 3579.
[286] M. Kartalou, J. M. Essigmann, *Mut. Res-Fund. Mol. M.* **2001**, *478*, 1.
[287] M. A. Fuertes, C. Alonso, J. M. Perez, *Chem. Rev.* **2003**, *103*, 645.
[288] G. D. Kruh, *Oncogene* **2003**, *22*, 7262.
[289] R. P. Wernyj, P. J. Morin, *Drug Res. Update* **2004**, *7*, 227.
[290] D. B. Longley, P. G. Johnston, *J. Pathology* **2005**, *205*, 275.
[291] V. Brabec, J. Kasparkova, *Drug Res. Update* **2002**, *5*, 147.
[292] D. M. Townsend, K. D. Tew, *Oncogene* **2003**, *22*, 7369.
[293] R. Rosell, R. V. N. Lord, M. Taron, N. Reguart, *Lung Cancer* **2002**, *38*, 217.
[294] P. Karran, *Carcinogenesis* **2001**, *22*, 1931.
[295] S. H. Kaufmann, D. L. Vaux, *Oncogene* **2003**, *22*, 7414.
[296] H. Niedner, R. Christen, X. Lin, A. Kondo, S. B. Howell, *Mol. Pharmacol.* **2001**, *60*, 1153.
[297] M. Schuijer, E. Berns, *Hum. Mut.* **2003**, *21*, 285.
[298] L. A. Doyle, D. D. Ross, *Oncogene* **2003**, *22*, 7340.
[299] K. Zhu, I. Fukasawa, M. Fujinoki, M. Furuno, F. Inaba, T. Yamazaki, T. Kamemori, N. Kousaka, Y. Ota, M. Hayashi, T. Maehama, N. Inaba, *Int. J. Gyn.* **2005**, *15*, 747.
[300] M. J. Cleare, J. D. Hoeschele, *Bioinorg. Chem.* **1973**, *2*, 187.

[301] P. D. Braddock, T. A. Connors, M. Jones, A. R. Khokhar, D. H. Melzack, M. L. Tobe, *Chem-Biol. Interact.* **1975**, *11*, 145.
[302] M. S. Highley, A. H. Calvert, in *Platinum-Based Drugs in Cancer Therapy* (Eds.: L. R. Kelland, N. Farrell), Humana Press Inc., Totowa, **2000**, pp. 171.
[303] O. Rixe, W. Ortuzar, M. Alvarez, R. Parker, E. Reed, K. Paull, T. Fojo, *Biochem. Pharmacol.* **1996**, *52*, 1855.
[304] J. L. Misset, H. Bleiberg, W. Sutherland, M. Bekradda, E. Cvitkovic, *Crit. Rev. Oncol. Hematol.* **2000**, *35*, 75.
[305] J. D. Page, I. Husain, A. Sancar, S. G. Chaney, *Biochemistry* **1990**, *29*, 1016.
[306] M. M. Jennerwein, A. Eastman, A. Khokhar, *Chem-Biol. Interact.* **1989**, *70*, 39.
[307] J. M. Woynarowski, W. G. Chapman, C. Napier, M. C. S. Herzig, P. Juniewicz, *Mol. Pharmacol.* **1998**, *54*, 770.
[308] E. Raymond, S. Faivre, S. Chaney, J. Woynarowski, E. Cvitkovic, *Mol. Cancer Ther.* **2002**, *1*, 227.
[309] A. Ibrahim, S. Hirschfeld, M. H. Cohen, D. J. Griebel, G. A. Williams, R. Pazdur, *Oncologist* **2004**, *9*, 8.
[310] N. Farrell, in *Platinum-Based Drugs in Cancer Therapy* (Eds.: L. R. Kelland, N. Farrell), Humana Press Inc., Totowa, **2000**, pp. 321.
[311] N. Farrell, in *Metal Ions In Biolgical Systems, Vol 42: Metal Complexes In Tumor Diagnosis And As Anticancer Agents, Vol. 42*, **2004**, pp. 251.
[312] V. Brabec, J. Kasparkova, O. Vrana, O. Novakova, J. W. Cox, Y. Qu, N. Farrell, *Biochemistry* **1999**, *38*, 6781.
[313] J. Zehnulova, J. Kasparkova, N. Farrell, V. Brabec, *J. Biol. Chem.* **2001**, *276*, 22191.
[314] J. Kasparkova, J. Zehnulova, N. Farrell, V. Brabec, *J. Biol. Chem.* **2002**, *277*, 48076.
[315] J. D. Roberts, J. Peroutka, N. Farrell, *J. Inorg. Biochem.* **1999**, *77*, 51.
[316] A. L. Harris, X. Yang, A. Hegmans, L. Povrik, J. J. Ryan, L. R. Kelland, N. Farrell, *Inorg. Chem.* **2005**, *44*, 95989600.
[317] M. J. McKeage, P. Mistry, J. Ward, F. E. Boxall, S. Loh, C. Oneill, P. Ellis, L. R. Kelland, S. E. Morgan, B. Murrer, P. Santabarbara, K. R. Harrap, I. R. Judson, *Cancer Chemoth. Pharm.* **1995**, *36*, 451.
[318] J. Holford, F. Raynaud, B. A. Murrer, K. Grimaldi, J. A. Hartley, M. Abrams, L. R. Kelland, *Anticancer Drug Des.* **1998**, *13*, 1.
[319] S. Y. Sharp, C. F. O'Neill, P. Rogers, F. E. Boxall, L. R. Kelland, *Eur. J. Cancer* **2002**, *38*, 2309.
[320] Y. Kawamura-Akiyama, H. Kusaba, F. Kanzawa, T. Tamura, N. Saijo, K. Nishio, *Lung Cancer* **2002**, *38*, 43.
[321] F. I. Raynaud, F. E. Boxall, P. M. Goddard, M. Valenti, M. Jones, B. A. Murrer, M. Abrams, L. R. Kelland, *Clin. Cancer Res.* **1997**, *3*, 2063.
[322] NeoRX, *Vol. 2005*, Seattle, **2005**.
[323] G. Natile, M. Coluccia, in *Metal Ions In Biolgical Systems, Vol 42: Metal Complexes In Tumor Diagnosis And As Anticancer Agents, Vol. 42*, **2004**, pp. 209.
[324] S. Radulovic, Z. Tesic, S. Manic, *Curr. Med. Chem.* **2002**, *9*, 1611.
[325] J. M. Perez, M. A. Fuertes, C. Alonso, C. Navarro-Ranninger, *Crit. Rev. Oncol. Hematol.* **2000**, *35*, 109.
[326] N. Farrell, T. T. B. Ha, J. P. Souchard, F. L. Wimmer, S. Cros, N. P. Johnson, *J. Med. Chem.* **1989**, *32*, 2240.
[327] N. Farrell, L. R. Kelland, J. D. Roberts, M. Vanbeusichem, *Cancer Res.* **1992**, *52*, 5065.
[328] M. Vanbeusichem, N. Farrell, *Inorg. Chem.* **1992**, *31*, 634.
[329] E. I. Montero, S. Diaz, A. M. Gonzalez-Vadillo, J. M. Perez, C. Alonso, C. Navarro-Ranninger, *J. Med. Chem.* **1999**, *42*, 4264.
[330] E. Khazanov, Y. Barenholz, D. Gibson, Y. Najajreh, *J. Med. Chem.* **2002**, *45*, 5196.

[331] M. Coluccia, A. Nassi, F. Loseto, A. Boccarelli, M. A. Mariggio, D. Giordano, F. P. Intini, P. Caputo, G. Natile, *J. Med. Chem.* **1993**, *36*, 510.
[332] L. S. Hollis, A. R. Amundsen, E. W. Stern, *J. Med. Chem.* **1989**, *32*, 128.
[333] L. S. Hollis, W. I. Sundquist, J. N. Burstyn, W. J. Heigerbernays, S. F. Bellon, K. J. Ahmed, A. R. Amundsen, E. W. Stern, S. J. Lippard, *Cancer Res.* **1991**, *51*, 1866.
[334] V. Perron, D. Rabouin, E. Asselin, S. Parent, R. C. Gaudreault, G. Berube, *Bioorg. Chem.* **2005**, *33*, 1.
[335] V. Gagnon, M. E. St-Germain, C. Descoteaux, J. Provencher-Mandeville, S. Parent, S. K. Mandal, E. Asselin, G. Berube, *Bioorg. Med. Chem. Lett.* **2004**, *14*, 5919.
[336] J. J. Isola, *J. Pathology* **1993**, *170*, 31.
[337] V. Kuenenboumeester, T. H. Vanderkwast, W. L. J. Vanputten, C. Claassen, B. Vanooijen, S. C. Henzenlogmans, *Int. J. Cancer* **1992**, *52*, 581.
[338] O. A. Lea, S. Kvinnsland, T. Thorsen, *Cancer Res.* **1989**, *49*, 7162.
[339] F. Zunino, G. Pratesi, F. Formelli, A. Pasini, *Invest. New Drugs* **1990**, *8*, 341.
[340] A. Pasini, G. Pratesi, G. Savi, F. Zunino, *Inorg. Chim. A-Bioinorg.* **1987**, *137*, 123.
[341] K. F. Gean, R. Benshoshan, A. Ramu, I. Ringel, J. Katzhendler, D. Gibson, *Eur. J. Med. Chem.* **1991**, *26*, 593.
[342] D. Gibson, K. F. Gean, R. Benshoshan, A. Ramu, I. Ringel, J. Katzhendler, *J. Med. Chem.* **1991**, *34*, 414.
[343] R. A. Alderden, H. R. Mellor, S. Modok, T. W. Hambley, R. Callaghan, *Biochem. Pharmacol.* **2006**, *71*, 1136.
[344] W. I. Sundquist, D. P. Bancroft, S. J. Lippard, *Abst. Amer. Chem. Soc.* **1988**, *196*, 90.
[345] W. I. Sundquist, D. P. Bancroft, S. J. Lippard, *J. Am. Chem. Soc.* **1990**, *112*, 1590.
[346] B. E. Bowler, K. J. Ahmed, W. I. Sundquist, L. S. Hollis, E. E. Whang, S. J. Lippard, *J. Am. Chem. Soc.* **1989**, *111*, 1299.
[347] H. H. Lee, B. D. Palmer, B. C. Baguley, M. Chin, W. D. McFadyen, G. Wickham, D. Thorsbournepalmer, L. P. G. Wakelin, W. A. Denny, *J. Med. Chem.* **1992**, *35*, 2983.
[348] B. D. Palmer, H. H. Lee, P. Johnson, B. C. Baguley, G. Wickham, L. P. G. Wakelin, W. D. McFadyen, W. A. Denny, *J. Med. Chem.* **1990**, *33*, 3008.
[349] N. D. Sachinvala, H. Chen, W. P. Niemczura, E. Furusawa, R. E. Cramer, J. J. Rupp, I. Ganjian, *J. Med. Chem.* **1993**, *36*, 1791.
[350] H. C. Apfelbaum, J. Blum, F. Mandelbaumshavit, *Inorg. Chim. Acta* **1991**, *186*, 243.
[351] I. Niculesu-Ducaz, A. Cambanis, E. Taranauceanu, *J. Med. Chem.* **1967**, *10*, 172.
[352] M. E. Wall, G. S. Abernethy, F. I. Carroll, D. J. Taylor, *J. Med. Chem.* **1969**, *12*, 810.
[353] E. O. R. T. C. B. C. C. Group, *Eur. J. Cancer* **1969**, *5*, 1.
[354] G. Leclercq, N. Devleeschouwer, A. Danguy, A. Verrijdt, J. C. Heuson, *J. Steroid Biochem.* **1985**, *23*, 1111.
[355] M. Vilkas, R. Epsztein, J. Sainton, G. Leclercq, *Eur. J. Med. Chem.* **1982**, *17*, 191.
[356] M. Vilkas, L. Masamba, S. Makani, G. Leclercq, *Eur. J. Med. Chem.* **1987**, *22*, 27.
[357] K. Krohn, K. Kulikowski, G. Leclercq, *J. Med. Chem.* **1989**, *32*, 1532.
[358] H. Kohle, K. Krohn, G. Leclercq, *J. Med. Chem.* **1989**, *32*, 1538.
[359] R. K. Hom, D. Y. Chi, J. A. Katzenellenbogen, *J. Org. Chem.* **1996**, *61*, 2624.
[360] Y. Sugano, J. A. Katzenellenbogen, *Bioorg. Med. Chem. Lett.* **1996**, *6*, 361.
[361] R. K. Hom, J. A. Katzenellenbogen, *J. Org. Chem.* **1997**, *62*, 6290.
[362] M. B. Skaddan, J. A. Katzenellenbogen, *Bioconjugate Chem.* **1999**, *10*, 119.
[363] D. Y. Chi, J. P. Oneil, C. J. Anderson, M. J. Welch, J. A. Katzenellenbogen, *J. Med. Chem.* **1994**, *37*, 928.
[364] F. Wust, K. E. Carlson, J. A. Katzenellenbogen, H. Spies, B. Johannsen, *Steroids* **1998**, *63*, 665.

[365] M. Reisgys, F. Wust, R. Alberto, R. Schibli, P. A. Schubiger, H. J. Pietzsch, H. Spies, B. Johannsen, *Bioorg. Med. Chem. Lett.* **1997**, *7*, 2243.
[366] F. Wust, H. Spies, B. Johannsen, *Tet. Lett.* **1997**, *38*, 2931.
[367] F. Wust, H. Spies, B. Johannsen, *Bioorg. Med. Chem. Lett.* **1996**, *6*, 2729.
[368] J. P. Dizio, K. E. Carlson, C. J. Bannochie, M. J. Welch, E. Vonangerer, J. A. Katzenellenbogen, *J. Steroid Biochem.* **1992**, *42*, 363.
[369] M. B. Skaddan, F. R. Wust, J. A. Katzenellenbogen, *J. Org. Chem.* **1999**, *64*, 8108.
[370] H. M. Bigott, E. Parent, L. G. Luyt, J. A. Katzenellenbogen, M. J. Welch, *Bioconjugate Chem.* **2005**, *16*, 255.
[371] M. M. Mashaly, *Syn. React. Inorg. Metal-Org. Chem.* **2004**, *34*, 115.
[372] L. G. Luyt, H. M. Bigott, M. J. Welch, J. A. Katzenellenbogen, *Biorg. Med. Chem.* **2003**, *11*, 4977.
[373] J. B. Arterburn, C. Corona, K. V. Rao, K. E. Carlson, J. A. Katzenellenbogen, *J. Org. Chem.* **2003**, *68*, 7063.
[374] H. Enginar, P. Unak, F. Yurt, F. Z. Biber, *J. Radio. Nuc. Chem.* **2002**, *251*, 473.
[375] E. S. Mull, V. J. Sattigeri, A. L. Rodriguez, J. A. Katzenellenbogen, *Biorg. Med. Chem.* **2002**, *10*, 1381.
[376] M. B. Skadden, F. R. Wust, S. Jonson, R. Syhre, M. J. Welch, H. Spies, J. A. Katzenellenbogen, *Nuc. Med. Biol.* **2000**, *27*, 269.
[377] F. Wust, M. B. Skaddan, P. Leibnitz, H. Spies, J. A. Katzenellenbogen, B. Johannsen, *Biorg. Med. Chem.* **1999**, *7*, 1827.
[378] J. P. Dizio, C. J. Anderson, A. Davison, G. J. Ehrhardt, K. E. Carlson, M. J. Welch, J. A. Katzenellenbogen, *J. Nuc. Med.* **1992**, *33*, 558.
[379] J. P. Dizio, R. Fiaschi, A. Davison, A. G. Jones, J. A. Katzenellenbogen, *Bioconjugate Chem.* **1991**, *2*, 353.
[380] F. Wust, D. Scheller, H. Spies, B. Johannsen, *Eur. J. Inorg. Chem.* **1998**, 789.
[381] D. Vichard, M. Gruselle, H. Elamouri, G. Jaouen, J. Vaissermann, *Organometallics* **1992**, *11*, 2952.
[382] P. Pigeon, S. Top, A. Vessieres, M. Huche, E. A. Hillard, E. Salomon, G. Jaouen, *J. Med. Chem.* **2005**, *48*, 2814.
[383] D. Vichard, M. Gruselle, H. Elamouri, G. Jaouen, *J. Chem. Soc. Chem. Comm.* **1991**, 46.
[384] H. Elamouri, A. Vessieres, D. Vichard, S. Top, M. Gruselle, G. Jaouen, *J. Med. Chem.* **1992**, *35*, 3130.
[385] A. Vessieres, S. Top, P. Pigeon, E. Hillard, L. Boubeker, D. Spera, G. Jaouen, *J. Med. Chem.* **2005**, *48*, 3937.
[386] K. Kowalski, A. Vessieres, S. Top, G. Jaouen, J. Zakrzewski, *Tet. Lett.* **2003**, *44*, 2749.
[387] S. Top, A. Vessieres, G. Leclercq, J. Quivy, J. Tang, J. Vaissermann, M. Huche, G. Jaouen, *Chem. Eur. J.* **2003**, *9*, 5223.
[388] S. Top, A. Vessieres, C. Cabestaing, I. Laios, G. Leclercq, C. Provot, G. Jaouen, *J. Organomet. Chem.* **2001**, *637*, 500.
[389] D. Osella, C. Nervi, F. Galeotti, G. Cavigiolio, A. Vessieres, G. Jaouen, *Hel. Chim. Acta* **2001**, *84*, 3289.
[390] D. Osella, G. Dutto, C. Nervi, M. J. McGlinchey, A. Vessieres, G. Jaouen, *J. Organomet. Chem.* **1997**, *533*, 97.
[391] S. Top, B. Dauer, J. Vaissermann, G. Jaouen, *J. Organomet. Chem.* **1997**, *541*, 355.
[392] A. Vessieres, C. Vaillant, M. Gruselle, D. Vichard, G. Jaouen, *J. Chem. Soc. Chem. Comm.* **1990**, 837.
[393] C. Cassino, E. Gabano, M. Ravera, G. Cravotto, G. Palmisano, A. Vessieres, G. Jaouen, S. Mundwiler, R. Alberto, D. Osella, *Inorg. Chim. Acta* **2004**, *357*, 2157.
[394] G. Jaouen, S. Top, A. Vessieres, P. Pigeon, G. Leclercq, I. Laios, *Chem. Comm.* **2001**, 383.

[395] F. Le Bideau, A. Perez-Luna, J. Marrot, M. N. Rager, E. Stephan, S. Top, G. Jaouen, *Tetrahedron* **2001**, *57*, 3939.
[396] D. Osella, C. Nervi, L. Milone, F. Galeotti, A. Vessieres, G. Jaouen, *J. Organomet. Chem.* **2000**, *594*, 232.
[397] S. Top, C. Lescop, J. S. Lehn, G. Jaouen, *J. Organomet. Chem.* **2000**, *594*, 167.
[398] F. Le Bideau, E. B. Kaloum, P. Haquette, U. Kernbach, J. Marrot, E. Stephan, S. Top, A. Vessieres, G. Jaouen, *Chem. Comm.* **2000**, 211.
[399] S. Top, H. Elhafa, A. Vessieres, J. Quivy, J. Vaissermann, D. W. Hughes, M. J. McGlinchey, J. P. Mornon, E. Thoreau, G. Jaouen, *J. Am. Chem. Soc.* **1995**, *117*, 8372.
[400] S. Top, M. Gunn, G. Jaouen, J. Vaissermann, J. C. Daran, M. J. McGlinchey, *Organometallics* **1992**, *11*, 1201.
[401] G. Jaouen, A. Vessieres, *Pure App. Chem.* **1989**, *61*, 565.
[402] A. Vessieres, G. Jaouen, M. Gruselle, J. L. Rossignol, M. Savignac, S. Top, S. Greenfield, *J. Steroid Biochem.* **1988**, *30*, 301.
[403] A. Vessieres, S. Top, A. A. Ismail, I. S. Butler, M. Louer, G. Jaouen, *Biochemistry* **1988**, *27*, 6659.
[404] B. Elmouatassim, H. Elamouri, M. Salmain, G. Jaouen, *J. Organomet. Chem.* **1994**, *479*, C18.
[405] V. Philomin, A. Vessieres, M. Gruselle, G. Jaouen, *Bioconjugate Chem.* **1993**, *4*, 419.
[406] M. Salmain, A. Vessieres, I. S. Butler, G. Jaouen, *Bioconjugate Chem.* **1991**, *2*, 13.
[407] M. Gruselle, P. Deprez, A. Vessieres, S. Greenfield, G. Jaouen, J. P. Larue, D. Thouvenot, *J. Organomet. Chem.* **1989**, *359*, C53.
[408] G. Jaouen, J. A. S. Howell, M. C. Tirvengadum, P. McArdle, D. Cunningham, *J. Organomet. Chem.* **1989**, *370*, 51.
[409] A. A. Ismail, I. S. Butler, G. Jaouen, R. J. Angelici, G. N. Glavee, *Inorg. Syn.* **1989**, *26*, 31.
[410] A. Vessieres, S. Tondu, G. Jaouen, S. Top, A. A. Ismail, G. Teutsch, M. Moguilewsky, *Inorg. Chem.* **1988**, *27*, 1850.
[411] G. Jaouen, A. Vessieres, S. Top, M. Savignac, A. A. Ismail, I. S. Butler, *Organometallics* **1987**, *6*, 1985.
[412] S. Top, A. Vessieres, G. Jaouen, *J. Label. Comp. Radiopharmaceuticals.* **1987**, *24*, 1257.
[413] S. Tondu, S. Top, A. Vessieres, G. Jaouen, *J. Chem. Soc. Chem. Comm.* **1985**, 326.
[414] M. Mlekuz, P. Bougeard, B. G. Sayer, S. Peng, M. J. McGlinchey, A. Marinetti, J. Y. Saillard, J. B. Naceur, B. Mentzen, G. Jaouen, *Organometallics* **1985**, *4*, 1123.
[415] G. Jaouen, A. Vessieres, *Pure App. Chem.* **1985**, *57*, 1865.
[416] G. Jaouen, *Abstr. Am. Chem. Soc.* **1985**, *189*, 80.
[417] S. Top, G. Jaouen, A. Vessieres, J. P. Abjean, D. Davoust, C. A. Rodger, B. G. Sayer, M. J. McGlinchey, *Organometallics* **1985**, *4*, 2143.
[418] A. Jackson, J. Davis, R. J. Pither, A. Rodger, M. J. Hannon, *Inorg. Chem.* **2001**, *40*, 3964.
[419] G. M. Anstead, K. E. Carlson, J. A. Katzenellenbogen, *Steroids* **1997**, *62*, 268.
[420] C. Chesne, G. Leclercq, P. Pointeau, H. Patin, *Eur. J. Med. Chem.* **1986**, *21*, 321.
[421] M. P. Georgiadis, S. A. Haroutounian, K. P. Chondros, *Inorg. Chim. A-Bioinorg.* **1987**, *138*, 249.
[422] D. M. Spyriounis, V. J. Demopoulos, P. N. Kourounakis, D. Kouretas, A. Kortsaris, O. Antonoglou, *Eur. J. Med. Chem.* **1992**, *27*, 301.
[423] C. Descoteaux, J. Provencher-Mandeville, I. Mathieu, V. Perron, S. K. Mandal, E. Asselin, G. Berube, *Bioorg. Med. Chem. Lett.* **2003**, *13*, 3927.
[424] P. J. Bednarski, R. Gust, T. Spruss, N. Knebel, A. Otto, M. Earbel, R. Koop, E. Holler, E. Vonangerer, H. Schonenberger, *Cancer Treat. Rev.* **1990**, *17*, 221.

[425] N. Knebel, C. D. Schiller, M. R. Schneider, H. Schonenberger, E. Vonangerer, *Eur. J. Caner Clin. On.* **1989**, *25*, 293.
[426] N. Knebel, E. Vonangerer, *J. Med. Chem.* **1988**, *31*, 1675.
[427] N. G. Knebel, E. Vonangerer, *J. Med. Chem.* **1991**, *34*, 2145.
[428] S. Top, E. B. Kaloun, A. Vessieres, G. Leclercq, I. Laios, M. Ourevitch, C. Deuschel, M. J. McGlinchey, G. Jaouen, *Chembiochem* **2003**, *4*, 754.
[429] Katzenel.Ja, H. J. Johnson, H. N. Myers, *Biochemistry* **1973**, *12*, 4085.
[430] P. Kaspar, H. Witzel, *J. Steroid Biochem.* **1985**, *23*, 259.
[431] J. A. Katzellenbogen, B. A. Katzellenbogen, *Breast Cancer. Res. Tr.* **1982**, *2*, 347.
[432] M. Salman, B. R. Reddy, P. Delgado, P. L. Stotter, L. C. Fulcher, G. C. Chamness, *Steroids* **1991**, *56*, 375.
[433] M. Salman, B. R. Reddy, S. Ray, P. L. Stotter, G. C. Chamness, *J. Steroid Biochem.* **1986**, *24*, 539.
[434] D. B. Gower, in *Biochemistry of Steroid Hormones* (Ed.: H. L. J. Makin), Blackwell Scientific Publications, Oxford, **1984**, pp. 170.
[435] M. J. Wheeler, *Ann. Clin. Biochem.* **1995**, *32*, 345.
[436] G. Pelletier, *Histol. Histopath.* **2000**, *15*, 1261.
[437] D. B. Lubahn, D. R. Joseph, P. M. Sullivan, H. F. Willard, F. S. French, E. M. Wilson, *Science* **1988**, *240*, 327.
[438] H. Sleddens, B. A. Oostra, A. O. Brinkmann, J. Trapman, *Hum. Mol. Gen.* **1993**, *2*, 493.
[439] R. M. Evans, *Science* **1988**, *240*, 889.
[440] D. J. Mangelsdorf, C. Thummel, M. Beato, P. Herrlich, G. Schutz, K. Umesono, B. Blumberg, P. Kastner, M. Mark, P. Chambon, R. M. Evans, *Cell* **1995**, *83*, 835.
[441] L. P. Freedman, *Endocrin. Rev.* **1992**, *13*, 129.
[442] J. A. Simental, M. Sar, M. V. Lane, F. S. French, E. M. Wilson, *J. Biol. Chem.* **1991**, *266*, 510.
[443] G. Jenster, J. Trapman, A. O. Brinkmann, *Biochem. J.* **1993**, *293*, 761.
[444] W. Bourguet, M. Ruff, P. Chambon, H. Gronemeyer, D. Moras, *Nature* **1995**, *375*, 377.
[445] J. M. Wurtz, W. Bourguet, J. P. Renaud, V. Vivat, P. Chambon, D. Moras, H. Gronemeyer, *Nat. Struct. Biol.* **1996**, *3*, 87.
[446] P. M. Matias, P. Donner, R. Coelho, M. Thomaz, C. Peixoto, S. Macedo, N. Otto, S. Joschko, P. Scholz, A. Wegg, S. Basler, M. Schafer, U. Egner, M. A. Carrondo, *J. Biol. Chem.* **2000**, *275*, 26164.
[447] J. S. Sack, K. F. Kish, C. H. Wang, R. M. Attar, S. E. Kiefer, Y. M. An, G. Y. Wu, J. E. Scheffler, M. E. Salvati, S. R. Krystek, R. Weinmann, H. M. Einspahr, *P. Natl. Acad. Sci. U.S.A.*. **2001**, *98*, 4904.
[448] C. Y. Chang, D. P. McDonnell, *Mol. Endocrin.* **2002**, *16*, 647.
[449] A. Chadli, I. Bouhouche, W. Sullivan, B. Stensgard, N. McMahon, M. G. Catelli, D. O. Toft, *P. Natl. Acad. Sci. U.S.A.*. **2000**, *97*, 12524.
[450] D. K. Lee, C. S. Chang, *J. Clin. Endocrin. Metab.* **2003**, *88*, 4043.
[451] H. J. Lee, C. Chang, *Cell Mol. Life Sci.* **2003**, *60*, 1613.
[452] D. K. Lee, C. Chang, *J. Steroid Biochem.* **2003**, *84*, 41.
[453] Y. F. Shang, M. Myers, M. Brown, *Mol. Cell* **2002**, *9*, 601.
[454] M. R. Cardillo, E. Petrangeli, N. Aliotta, L. Salvatori, L. Ravenna, C. Chang, G. Castagna, *J. Exp. Clin. Cancer Res.* **1998**, *17*, 231.
[455] B. J. Slotman, B. R. Rao, *AntiCancer Res.* **1988**, *8*, 417.
[456] R. Kuhnel, J. Degraaff, B. R. Rao, J. G. Stolk, *J. Steroid Biochem.* **1987**, *26*, 393.
[457] J. V. Ilekis, J. P. Conner, C. S. Prins, K. Ferrer, C. Niederberger, B. Scoccia, *Gynecol. Oncol.* **1997**, *66*, 250.
[458] I. Leav, K. M. Lau, J. Y. Adams, J. E. McNeal, M. E. Taplin, J. F. Wang, H. Singh, S. M. Ho, *Am. J. Pathol.* **2001**, *159*, 79.

[459] A. Hobisch, Z. Culig, C. Radmayr, G. Bartsch, H. Klocker, A. Hittmair, *Cancer Res.* **1995**, *55*, 3068.
[460] J. A. R. Dewinter, P. J. A. Janssen, M. C. T. Verleunmooijman, J. Trapman, A. O. Brinkmann, A. B. Santerse, F. H. Schroder, T. H. Vanderkwast, *Am. J. Pathol.* **1994**, *144*, 735.
[461] I. Ochiai, K. I. Matsuda, M. Nishi, H. Ozawa, M. Kawata, *Mol. Endocrin.* **2004**, *18*, 26.
[462] R. J. Santen, *J. Clin. Endocrin. Metab.* **1992**, *75*, 685.
[463] T. Gilligan, P. W. Kantoff, *Urology* **2002**, *60*, 94.
[464] C. L. Bevan, *Trends Endocrin. Metab.* **2005**, *16*, 395.
[465] J. Javidan, A. D. Deitch, X. B. Shi, R. W. D. White, *Cancer Invest.* **2005**, *23*, 520.
[466] B. J. Feldman, D. Feldman, *Nat. Rev. Cancer* **2001**, *1*, 34.
[467] J. D. Debes, D. J. Tindall, *Cancer Lett.* **2002**, *187*, 1.
[468] P. Westin, A. Bergh, *Cancer Detect. Prev.* **1998**, *22*, 476.
[469] R. Montironi, M. Scarpelli, A. L. Beltran, *Virchows Archiv* **2004**, *444*, 503.
[470] M. Rahman, H. Miyamoto, C. S. Chang, *Clin. Cancer Res.* **2004**, *10*, 2208.
[471] I. V. Litvinov, A. M. De Marzo, J. T. Isaacs, *J. Clin. Endocrin. Metab.* **2003**, *88*, 2972.
[472] D. J. Liao, R. B. Dickson, *J. Steroid Biochem.* **2002**, *80*, 175.
[473] S. Brys, *Med. Sci. Mon.* **2000**, *6*, 433.
[474] C. Dimitrakakis, J. Zhou, C. A. Bondy, *Fertil. Steril.* **2002**, *77*, S26.
[475] S. Cos, A. Gonzalez, A. Guezmes, M. D. Mediavilla, C. Martinez-Campa, C. Alonso-Gonzalez, E. J. Sanchez-Barcelo, *Int. J. Cancer* **2006**, *118*, 274.
[476] K. Sonne-Hansen, A. E. Lykkesfeldt, *J. Steroid Biochem.* **2005**, *93*, 25.
[477] R. Schiff, G. C. Chamness, P. H. Brown, *Breast Cancer Res.* **2003**, *5*, 228.
[478] J. Geisler, P. E. Lonning, *Clin. Cancer Res.* **2005**, *11*, 2809.
[479] J. P. Crown, *Semin. Oncol.* **2001**, *28*, 28.
[480] M. P. Decatris, S. Sundar, K. J. O'Byrne, *Cancer Treat. Rev.* **2004**, *30*, 53.
[481] R. Edmondson, J. M. Monaghan, B. R. Davies, *Brit. J. Cancer* **2002**, *86*, 879.
[482] K. M. Lau, S. C. Mok, S. M. Ho, *P. Natl. Acad. Sci. U.S.A.*. **1999**, *96*, 5722.
[483] K. L. Terry, I. De Vivo, L. Titus-Ernstoff, M. C. Shih, D. W. Cramer, *Cancer Res.* **2005**, *65*, 5974.
[484] P. H. Wang, C. Chang, *Eur. J. Gynaecol. Oncol.* **2004**, *25*, 157.
[485] P. V. Nantermet, P. Masarachia, M. A. Gentile, B. Pennypacker, J. Xu, D. Holder, D. Gerhold, D. Towler, A. Schmidt, D. B. Kimmel, L. P. Freedman, S. Harada, W. J. Ray, *Endocrinology* **2005**, *146*, 564.
[486] A. Latorre, M. De Lena, A. Catino, E. Crucitta, D. Sambiasi, M. Guida, A. Misino, V. Lorusso, *In.. J. Oncol.* **2002**, *21*, 179.
[487] D. S. Dizon, *Onco. Special Ed.* **2002**, *5*, 79.
[488] W. C. Zeise, *Pog. Ann. Phys.* **1827**, *9*, 632.
[489] W. C. Zeise, *Maz. Pharma.* **1830**, *35*, 105.
[490] W. C. Zeise, *Pog. Ann. Phy.* **1831**, *21*, 497.
[491] F. R. Hartley, *The Chemistry of Platinum and Palladium*, Applied Science Publishers, London, **1973**.
[492] P. K. Byers, *Coord. Chem. Rev.* **1995**, *146*, A431.
[493] P. K. Byers, *Coord. Chem. Rev.* **1995**, *142*, 123.
[494] P. A. Chaloner, *Coord. Chem. Rev.* **1990**, *101*, 1.
[495] P. A. Chaloner, *Coord. Chem. Rev.* **1988**, *89*, 1.
[496] P. A. Chaloner, *Coord. Chem. Rev.* **1986**, *72*, 1.
[497] P. A. Chaloner, *Coord. Chem. Rev.* **1986**, *71*, 235.
[498] F. R. Hartley, *Coord. Chem. Rev.* **1985**, *67*, 1.
[499] F. R. Hartley, *Coord. Chem. Rev.* **1982**, *41*, 319.
[500] J. A. Davies, F. R. Hartley, *Chem. Rev.* **1981**, *81*, 79.
[501] F. R. Hartley, *Coord. Chem. Rev.* **1981**, *35*, 143.

[502] G. Albertin, S. Antoniutti, C. Busato, J. Castro, S. Garcia-Fontan, *Dalt. Trans.* **2005**, 2641.
[503] P. Bruggeller, *Inorg. Chem.* **1990**, *29*, 1742.
[504] J. A. Winter, F. T. A. Lin, R. E. Shepherd, *Inorg. Chim. Acta* **1989**, *155*, 155.
[505] J. H. Nelson, N. W. Alcock, *Inorg. Chem.* **1982**, *21*, 1196.
[506] C. V. Senoff, *Inorg. Chem.* **1978**, *17*, 2320.
[507] C. M. Harris, R. S. Nyholm, D. J. Phillips, *J. Chem. Soc.* **1960**, 4379.
[508] N. C. Stephenson, *J. Inorg. Nucl. Chem.* **1962**, *24*, 791.
[509] R. Makiura, I. Nagasawa, N. Kimura, S. Ishimaru, H. Kitagawa, R. Ikeda, *Chem. Comm.* **2001**, 1642.
[510] R. L. DeKock, H. B. Gray, *Chemical Structure and Bonding*, Menlo Park, **1980**.
[511] A. Werner, *Zeit. An. Allgemei. Chemie* **1893**, *3*, 267.
[512] K. Sonogashira, Y. Tohda, N. Hagihara, *Tet. Lett.* **1975**, 4467.
[513] P. Siemsen, R. C. Livingston, F. Diederich, *Angew. Chem-Int. Ed.* **2000**, *39*, 2633.
[514] F. Diederich, P. J. Stang, *Metal-Catalysed Cross-coupling Reactions*, Wiley-VCH, Weinheim, Germany, **1998**.
[515] H. A. Dieck, F. R. Heck, *J. Organomet. Chem.* **1975**, *93*, 259.
[516] L. Cassar, *J. Organomet. Chem.* **1975**, *93*, 253.
[517] M. J. Abrams, C. M. Giandomenico, J. F. Vollano, D. A. Schwartz, *Inorg. Chim. Acta* **1987**, *131*, 3.
[518] P. D. Braddock, R. Romeo, M. L. Tobe, *Inorg. Chem.* **1974**, *13*, 1170.
[519] N. Farrell, *J. Chem. Soc. Chem. Comm.* **1982**, 331.
[520] N. Farrell, *Acs Symposium Series* **1983**, *209*, 279.
[521] S. G. Dealmeida, J. L. Hubbard, N. Farrell, *Inorg. Chim. Acta* **1992**, *193*, 149.
[522] A. P. S. Fontes, Y. Zou, N. Farrell, *J. Inorg. Biochem.* **1994**, *55*, 79.
[523] F. A. Cotton, R. Francis, W. D. Horrocks, *J. Phys. Chem.* **1960**, *64*, 1534.
[524] S. C. Dhara, *Ind. J. Chem.* **1970**, *8*, 193.
[525] G. B. Kauffman, D. O. Cowan, *Inorg. Syn.* **1963**, *7*, 239.
[526] J. H. Price, A. N. Williamson, R. F. Schramm, B. B. Wayland, *Inorg. Chem.* **1972**, *11*, 1280.
[527] M. Lederer, E. LeipzigPagani, *Anal. Chim. Acta* **1997**, *350*, 203.
[528] S. T. Elleman, J. W. Reishus, D. S. Martin, *J. Am. Chem. Soc.* **1957**, *80*, 536.
[529] M. Lederer, E. Leipzig-Pagani, T. Lumini, *Anal. Chim. Acta* **1998**, *371*, 279.
[530] S. E. Miller, D. A. House, *Inorg. Chim. Acta* **1989**, *161*, 131.
[531] S. E. Miller, D. A. House, *Inorg. Chim. Acta* **1989**, *166*, 189.
[532] S. E. Miller, D. A. House, *Inorg. Chim. Acta* **1990**, *173*, 53.
[533] S. E. Miller, K. J. Gerard, D. A. House, *Inorg. Chim. Acta* **1991**, *190*, 135.
[534] S. E. Miller, D. A. House, *Inorg. Chim. Acta* **1991**, *187*, 125.
[535] S. E. Miller, H. Wen, D. A. House, W. T. Robinson, *Inorg. Chim. Acta* **1991**, *184*, 111.
[536] M. El-Khateeb, T. G. Appleton, B. G. Charles, L. R. Gahan, *J. Pharm. Sci.* **1999**, *88*, 319.
[537] M. Lederer, E. Leipzig-Pagani, *Ann. Chim. Acta* **1998**, *358*, 61.
[538] R. W. Hay, S. Miller, *Polyhedron* **1998**, *17*, 2337.
[539] S. J. Lippard, *Science* **1982**, *218*, 1075.
[540] R. Faggiani, B. Lippert, C. J. L. Lock, B. Rosenberg, *J. Am. Chem. Soc.* **1977**, *99*, 777.
[541] R. Faggiani, B. Lippert, C. J. L. Lock, B. Rosenberg, *Inorg. Chem.* **1977**, *16*, 1192.
[542] M. C. Lim, R. B. Martin, *J. Inorg. Nucl. Chem.* **1976**, *38*, 1911.
[543] M. J. Browning, PhD Thesis, University of Warwick (Coventry), **2006**.
[544] B. Pitteri, G. Marangoni, L. Cattalini, T. Bobbo, *J. Chem. Soc. Dalt. Trans.* **1995**, *23*, 3853.
[545] R. Romeo, M. Cusumano, *Inorg. Chim. Acta* **1981**, *49*, 167.
[546] R. Rotondo, F. Cusmano Priolo, *Inorg. Chim. Acta* **1984**, *85*, 111.

[547] V. X. Jin, S. I. Tan, J. D. Ranford, *Inorg. Chim. Acta* **2005**, *358*, 677.
[548] N. Marti, G. Hui Bon Hoa, J. Kozelka, *Inorg. Chem. Comm.* **1998**, *1*, 439.
[549] R. Dahm, *Develop. Biol.* **2005**, *278*, 274.
[550] A. Kossel, *DuBois-Reymond's Arch* **1891**, *181*, 181.
[551] S. Zamenhof, G. Brawerman, E. Chargaff, *Biochim. Biophys. Acta* **1952**, *9*, 402.
[552] J. D. Watson, F. H. C. Crick, *Nature* **1953**, *171*, 373.
[553] S. F. Bellon, J. H. Coleman, S. J. Lippard, *Biochemistry* **1991**, *30*, 8026.
[554] M. V. Keck, S. J. Lippard, *J. Am. Chem. Soc.* **1992**, *114*, 3386.
[555] R. L. Jones, A. C. Lanier, R. A. Keel, W. D. Wilson, *Nucl. Acids Res.* **1980**, *8*, 1613.
[556] J. C. Wang, *J. Mol. Biol.* **1974**, *89*, 783.
[557] T. Mosmann, *J. Immunol. Meth.* **1983**, *65*, 55.
[558] A. Aigner, S. S. Hsieh, C. Malerczyk, F. Czubayko, *Toxicology* **2000**, *144*, 221.
[559] D. Pluim, R. van Waardenburg, J. H. Beijnen, J. H. M. Schellens, *Cancer Chemoth. Pharm.* **2004**, *54*, 71.
[560] S. Kodalí, M. Burkley, K. Nag, R. C. Taylor, V. K. Moudgil, *Biochem. Bioph. Res. Co.* **1994**, *202*, 1413.
[561] C. Sanchez-Cano, Unpublished Results, University of Birmingham, **2006**.
[562] B. Green, R. E. Leake, *Steroid Hormones: A Practical Approach*, IRL Press, Oxford, **1987**.
[563] B. S. Katzenellenbogen, Y. Berthois, Y. Y. Sheen, K. Kendra, J. A. Katzenellenbogen, *AntiCancer Res.* **1986**, *6*, 396.
[564] Q. He, C. H. Liang, S. J. Lippard, *P. Natl. Acad. Sci. U.S.A.*. **2000**, *97*, 5768.
[565] S. Schertl, R. W. Hartmann, C. Batzl-Hartmann, G. Bernhardt, T. Spruss, K. Beckenlehner, M. Koch, R. Krauser, R. Schlemmer, R. Gust, H. Schoenberger, *Archiv Der Pharmazie* **2004**, *337*, 335.
[566] S. M. Piver, D. F. Silver, (Ed.: U. S. P. Office), United States, **1999**.
[567] C. J. Vangarderen, H. Vandenelst, J. Hvanboom, J. Reedijk, L. P. A. Vanhoute, *J. Am. Chem. Soc.* **1989**, *111*, 4123.
[568] V. Brabec, V. Kleinwachter, J. L. Butour, N. P. Johnson, *Biophys. Chem.* **1990**, *35*, 129.
[569] V. Bursova, J. Kasparkova, C. Hofr, V. Brabec, *Biophys. J.* **2005**, *88*, 1207.
[570] J. P. Macquet, J. L. Butour, *Eur. J. Biochem.* **1978**, *83*, 375.
[571] T. Peleg-Shulman, J. Katzhendler, D. Gibson, *J. Inorg. Biochem.* **2000**, *81*, 313.
[572] M. J. Browning, PhD Thesis, University of Warwick (Coventry), **2006**.
[573] G. H. Zhao, H. K. Lin, P. Yu, H. W. Sun, S. R. Zhu, Y. T. Chen, *Chem-Biol. Interact.* **1998**, *116*, 19.
[574] M. J. Waring, S. M. Henley, *Nucl. Acids Res.* **1975**, *2*, 567.
[575] J. Tuma, C. Richert, *Biochemistry* **2003**, *42*, 8957.
[576] C. F. Bleczinski, C. Richert, *J. Am. Chem. Soc.* **1999**, *121*, 10889.
[577] J. G. Muller, M. M. P. Ng, C. J. Burrows, *J. Mol. Recog.* **1996**, *9*, 143.
[578] H. P. Hsieh, J. G. Muller, C. J. Burrows, *Bioorg. Med. Chem.* **1995**, *3*, 823.
[579] X. W. Hui, N. Gresh, B. Pullman, *Nucl. Acids Res.* **1989**, *17*, 4177.
[580] T. Kato, K. Yano, K. Ikebukuro, I. Karube, *Nucl. Acids Res.* **2000**, *28*, 1963.
[581] A. Rodger, B. Norden, *Circular and Linear Dichroism*, Oxford University Press,. Oxford, **1997**.
[582] R. Marrington, T. R. Dafforn, D. J. Halsall, A. Rodger, *Biophys. J.* **2004**, *87*, 2002.
[583] W. R. Bauer, *Ann. Rev. Biophy. Bioeng.* **1978**, *7*, 287.
[584] E. W. Thulstrup, J. Michl, J. H. Eggers, *J. Phys. Chem.* **1970**, *74*, 3868